Title
Identification and Characterization of Effector Proteins and Genomic Analysis of the Cucurbit Powdery Mildew Golovinomyces cichoracearum

Author
Scheibel, Kate Elizabeth

Publication Date
2018

Peer reviewed|Thesis/dissertation

Identification and Characterization of Effector Proteins and Genomic Analysis of the Cucurbit Powdery Mildew *Golovinomyces cichoracearum*

By

Katherine E. Scheibel

A dissertation submitted in partial satisfaction of the

requirements for the degree of

Doctor of Philosophy

in

Plant Biology

in the

Graduate Division

of the

University of California, Berkeley

Committee in charge:

Professor Shauna Somerville, Chair
Professor Jennifer Lewis
Professor Russell Vance

Spring 2018

Abstract

Identification and Characterization of Effector Proteins and Genomic Analysis of the Cucurbit Powdery Mildew *Golovinomyces cichoracearum*

by

Katherine E. Scheibel

Doctor of Philosophy in Plant Biology

University of California, Berkeley

Professor Shauna C. Somerville, Chair

Powdery mildew, a fungal disease of plants, is one of the most significant causes of crop disease and yield loss worldwide. Collectively, this group of pathogens infects a diverse set of plant hosts, including wheat, barley, grape, and ornamental species. One such mildew, *Golovinomyces cichoracearum,* is the causative agent of powdery mildew disease on susceptible cucurbit species. The ability of this mildew to infect the model plant *Arabidopsis thaliana* has allowed for the study of the biology of this important class of plant pathogens in a laboratory setting.

When exposed to a susceptible host, *G. cichoracearum* forms a feeding structure within the plant cell, known as a haustorium. The fungus initiates changes in plant cell structure, gene expression, and nutrient transport to allow for its survival and reproduction. Relatively little is known about the molecular and cellular mechanisms employed by the fungus to elicit these cellular changes and evade the plant immune response. This is partially due to the recalcitrance of the fungus to genetic manipulation, the large and complicated nature of the powdery mildew genome, and the lack of genetic and genomic tools that have been developed for the study of this class of organisms.

Here, we describe the development of an *Agrobacterium tumefaciens*-mediated tool for transiently silencing *G. cichoracearum* genes during infection of Arabidopsis. We demonstrate that this technique can be successfully employed at the early stages of powdery mildew infection, and that silencing an essential fungal gene, *GcCYP51,* results in reduced haustorial formation and subsequent fungal growth. We then use this technique to identify three *G. cichoracearum* effectors, GcEC8, GcEC10, and GcEC17, that are required for virulence on Arabidopsis.

We then describe efforts to characterize these effectors in terms of gene expression, sub-cellular localization, the identification of plant interacting partners, bioinformatic prediction, and their roles in the suppression of the plant immune response.

GcEC10 is characterized as an RNase-like protein and is localized in the plant cytosol and nucleus. GcEC10 may interact with Arabidopsis proteins AtEDR4 and AtPHOS32, two proteins implicated in the plant immune response to pathogens. We determined that GcEC10 expression

suppresses the hypersensitive response (HR) elicited by the plant resistance gene/effector pair Bs2/AvrBs2. We propose a potential model in which GcEC10 attenuates the plant immune response leading to the hypersensitive response and immunity to powdery mildew via interference with mitogen-activated protein kinase cascades associated with plant immunity.

GcEC8 shares no sequence or domain homology with any proteins outside of the powdery mildews, and may interact with the plant protein AXR3, an auxin-responsive transcription factor. We propose that GcEC8 may interfere with the plant auxin response, leading to increased disease resistance, although the specific mechanism is not yet known.

GcEC17 is a highly-conserved powdery mildew effector, and is also characterized as an RNase-like protein. GcEc17 is localized in the plant nucleus and cytosol. Two hypothetical Arabidopsis genes, At4g29905 and At3g32930, were predicted to interact with GcEC17 via yeast two-hybrid, however we have not yet conceived of a model for GcEC17 action during powdery mildew infection.

We further describe efforts towards transient plasmid transformation of *G. cichoracearum,* which we hope will eventually lead to the ability of researchers to introduce the Cas9 genome editing system into the fungus. This might allow for the creation of stable, targeted genetic mutants, which has not yet been achieved in any powdery mildew species. Our efforts were unsuccessful, and here we detail the attempted methodologies in the hopes that future researchers may find more success.

Finally, we describe a method developed to achieve the purification of high molecular weight genomic DNA from *G. cichoracearum* suitable for Pacific Biosciences Single Molecule Long-Read Sequencing, and the analysis of the genome sequence obtained using this method. We compare the genome of *G. cichoracearum* to the genomes of four other sequenced powdery mildew species, *Blumeria graminis f. sp. hordei, B. graminis f. sp. hordei, Erysiphe pisi,* and *Golovinomyces orontii*. We found that the genomes of the mildews are similar in size and gene content, however we found that each species encodes a large, unique repertoire of predicted effector proteins.

These experiments provide some of the first insights into the genome and effector biology of the enigmatic plant pathogen *G. cichoracearum*. By combining novel molecular techniques with next-generation sequencing approaches, we now have a more complete idea of the mechanisms by which this fungus causes disease on its host plants.

Table of Contents

List of Figures

List of Tables

Acknowledgments

Thank you to my advisor, Professor Shauna Somerville, for providing me with the support necessary to complete the work presented in this dissertation. Thank you for being my mentor and my teacher, and for allowing me the freedom to explore. Thank you for your frequent insight and belief in me and in this project.

Thank you to my dissertation committee members, Professors Jennifer Lewis and Russell Vance, and additionally my qualifying exam committee members Professors Patricia Zambryski and Mary Wildermuth for your insight and ideas. Particular thanks to Professor Lewis and the members of her lab for allowing me to attend and participate in lab meetings and journal club over the past year, and for providing feedback on my work.

Thank you to the former members of the Somerville Labs, especially Drs. Nadav Sorek, Trevor Yeats, Patricia Bubner, Tamara Vellosillo, Candice Cherk Lim, Heidi Szemenyei, Bill Underwood, to Joanna Feehan, and my rotation mentor Dr. Dawn Chiniquy. Thank you for your guidance and mentorship. Special thanks to Drs. Clarice Acevedo de Souza and Yu Geng, without whom I literally could not have completed this work.

Much of this work was supported by the work of talented undergraduate researchers, Gustavo Garcia Jr., Jonathan Hermel, and Lance Mendoza. Thank you for your hard work and dedication.

Thank you to all of the scientists who provided me with materials, including Drs. Vellosillo, Schreiber, Schultink, Perez-Garcia, and to Emma Kovak, for your generosity and kindness. Thank you to the scientists at the Joint Genome Institute, especially Dr. Igor Gregoriev and Kerrie Barry, for their work on the Powdery Mildew Genomics Community Sequencing Project.

Thank you to the PMB staff for handling the logistical aspects of the department and enabling the research therein. Special thanks to Rocio Sanchez, GSAO-extraordinaire.

Thank you to the 2012 PMB Graduate Cohort, an amazing group of inspirational scientists. Special thanks to Anna Josephson-Day and Drs. Riva Bruenn, Ben Endelman, Monika Fischer, Becky Mackelprang, and Carine Marshall for your friendship and love throughout the last 6 years. Your support, both scientific and emotional, has meant the world to me. Thank you to Drs. (or soon to be) Johnson, Sylvain, Gomez and Hernandez for being my first friends when I moved to California, knowing nobody, and yet making me feel immediately at home.

Thank you to my family. My mother, Barbara Scheibel, my first teacher in life and in plant biology, and an inspiration in every way. My father, Michael Scheibel, my biggest supporter and cheerleader. My siblings, Barbara Anne, Mat, and Maria, the only people who can possibly understand where we’re all coming from and some of the coolest and most interesting people on Earth. Thank you to my grandparents and cousins, aunts, and uncles who have helped me to learn and grow throughout my life.

Thank you to my dear friends, Jordan Hilliard, Hayley Stormon, Annie Preston, Katia Koziara, Liz Sutphen, Liz Soltan, Judah Bellin and Katie Wheeler, for supporting me, listening to me complain and for inspiring me with your amazing successes and accomplishments.

Thank you to Dr. Vincent Wu, for everything.

Chapter 1: General Introduction

Biology of powdery mildews

The agronomically important class of plant pathogens collectively known as the powdery mildews is made up of over 900 related species of fungi (Braun & Cook, 2012). While each individual species infects only a narrow range of host species, the group in total infects a wide-range of plants, including grains, fruit trees, and vegetable crop species. Powdery mildew infection results in billions of dollars in agricultural losses annually, and collectively, the powdery mildew pathogens are the most significant cause of plant disease worldwide (Agrios, 1969).

The powdery mildews belong to a group of plant pathogens known as the obligate biotrophic plant pathogens. The term obligate refers to the inability of the fungi to grow in any other condition than on a plant host. This is thought to be because the powdery mildews have lost the ability to synthesize compounds necessary for axenic growth, and rely on the plant host to provide them, although the exact mechanisms of biotrophy have not yet been determined (Spanu et al., 2010, Vela-Corcía et al., 2016). Powdery mildews can only grow and reproduce on a live plant host. This biotrophic trait is thought to have evolved prior to the speciation events in the powdery mildew fungi (Takamatsu 2013).

The powdery mildew fungi are taxonomically located in the *Leotiomycete* class of *Ascomycete* fungi, and are grouped into five tribes within the family *Erisyphaeles (*Wang et al., 2006). The *Erysiphales* is a monophyletic group, and all described extant members are obligate biotrophic plant pathogens (Takamatsu, 2013). All powdery mildews are described as haploid individuals that produce uni-nucleate conidia during the asexual phase of their life-cycle, which is the portion of the life-cycle that is studied in the laboratory setting (Braun et al., 2002). In nature, mildews have been observed to form chasmothecia, which contain pigmented ascospores that are better able to survive harsh conditions (Glawe, 2008).

Powdery mildew disease is characterized by the appearance of “powdery” conidia on the leaf surface of infected plants. These asexual spores land on the leaf surface, carried by wind, water, or vectored by animals, and germinate, producing a specialized hyphal structure called an appressorium within 24 hours post infection (hpi). The appressorial structure grows along the surface of the leaf and penetrates the plant cell wall, likely using a combination of mechanical pressure and the secretion of a minimal suite of cell wall degrading enzymes (Spanu 2010). Within 48 hpi, a haustorium is formed. To accommodate this structure, the plant cell membrane of infected epidermal cells invaginates, surrounding the fungal haustorium. The haustorium is a complex feeding structure that exists within the plant cell, but separated from the plant cytosol by an atypical plant plasma membrane, the fungal cell membrane, and the intervening space known as the extrahaustorial matrix (Hückelhoven & Panstruga, 2011). Canonically, the haustorium is believed to be the site of bidirectional exchange for the powdery mildew-host interaction, wherein sugars and amino acids are transported into the fungal body and effector proteins are delivered from the fungus to the plant to facilitate infection and to evade host defenses. The haustorium is involved in the uptake of carbohydrates and amino acids from the plant cell, driven by a proton gradient generated by fungal H^+-ATPases (Hahn & Mendgen, 2001, Panstruga & O'Connell, 2006). This compatible interaction requires plant susceptibility proteins, for instance the MLO or MLO2 proteins in barley and Arabidopsis, respectively. Without this host compatibility factor, haustorial establishment is compromised (Büschges et al., 1997, Hückelhoven & Panstruga, 2011).

Multiple cellular changes occur in the infected plant cell during powdery mildew infection, including the rearrangement of the actin cytoskeleton, recruitment of particular proteins and lipids to the extrahaustorial membrane, deposition of callose, and changes in gene expression relating to the nutritive content of the cell (Figure 1.1, Micali et al., 2011, Hückelhoven & Panstruga, 2011). Many of these changes are complex and the mechanisms underlying them are not well understood.

After the establishment of the haustorial structure, the fungus produces secondary hyphae from the appressorium or germ-tube that grow along the surface of the leaf and generate additional haustoria. Other changes occur in more distal, uninfected cells following infection, including endoreduplication in mesophyll cells below the epidermal cells containing haustoria, which has been observed in the related powdery mildew, *Golovinomyces orontii*. This endoreduplication is thought to be important for the production and transport of useful sugars to the mildew. Approximately 5-7 days post infection (dpi) the powdery mildew produces conidiophores, aerial hyphae that differentiate into the chains of genetically identical asexual spores. which represent the completion of the asexual life cycle of the mildew (Chandran et al., 2010, Chandran et al., 2013). These spores can initiate new infections on host plants, and are disseminated via wind, water, or mechanical means (reviewed in Green et al., 2002, Adam & Somerville, 1996).

The biology of the powdery mildew fungi has been an active area of plant pathological research for over 100 years. However, due to the unique challenges that the fungi present to researchers, much is still unknown about this important group of plant pathogens.

Effector biology

The field of plant pathology has identified many effectors from Oomycete, bacterial, and fungal plant pathogens. Most of the identified effectors are characterized by their small size, lack of sequence homology to described proteins, and delivery into the host cell via a dedicated secretion mechanism, such as the type-III secretion system in bacterial plant pathogens, or the RXLR-mediated pathway in oomycete plant pathogens. Many described effectors come from these bacterial and oomycete plant pathogens, and are involved with suppressing the defense responses of the host plant (Dodds & Rathjen, 2010). The mechanisms of these effectors vary, and are often involved in blocking the immune cascade that would result in a lethal immune response (Jones & Dangl, 2006). Many of these effectors interact with a small number of common host-proteins, indicating that pathways for disease and immunity may be well conserved across pathogen kingdoms (Weßling et al., 2014) The typical effector complement of bacterial plant pathogens, such as the well characterized *Pseudomonas syringae*, averages 30-50 effectors (Lindeberg 2012).

Many known effectors play a role in the well-described "zig-zag" model. In this model, effectors mediate two levels of plant defense response. The first, pathogen-associated molecular pattern (PAMP)-triggered immunity (PTI), in which the plant responds to highly conserved pathogen-associated molecular motifs, is characterized by a reactive oxygen species (ROS) burst, calcium signaling, and callose deposition, among other responses (Abramovitch et al., 2006, He et al., 2007, Aslam et al., 2008, Lehmann et al., 2014). A similar response takes place upon the detection of certain plant cell-wall fragments generated from cell damage or pathogen invasion, termed damage-associated molecular pattern (DAMP)-triggered immunity (Ferrari et al., 2013). The second, effector-triggered immunity (ETI), in which the plant responds to recognition of specific effector molecules, is characterized by the hypersensitive response (HR), a programmed cell-death response (Dodds & Rathjen, 2010). Both PTI and ETI often include the activation of pathogen response (PR) genes and mitogen-activated protein kinases (MAPKs, reviewed in Tena et al., 2011). Evasion of these defense responses is critical for pathogen success, and as such, suppression of these responses has been a major focus of plant pathology research.

In contrast to bacterial plant pathogens, the genomes of filamentous fungal pathogens encode a relatively large number of effectors. This is often correlated to the presence of a large repertoire of transposable elements (Raffaele et al., 2012, Wicker et al., 2014). The powdery mildews *Blumeria graminis f.sp. hordei, B. graminis f. sp. tritici*, *Erysiphe necator* and *Golovinomyces orontii* are predicted to encode 491, 602, 150 and 115 candidate secreted effectors, respectively (Wicker et al., 2013, Spanu et al., 2010, Jones et al., 2014, Pedersen et al., 2012, Weßling et al., 2014). This may be due to the relative complexity of the cellular changes required for successful infection in these obligate biotrophs, as compared to bacterial necrotrophic or hemi-biotrophic pathogens. Studies investigating the effector repertoire of various *formae specialis* of the powdery mildew *B. graminis* have demonstrated that the effector complement of these powdery mildews diverged rapidly due to rapid turnover and positive selection of mutations (Menardo, et al.2017).

Golovinomyces cichoracearum *as a model for powdery mildew effector biology*

In this dissertation, we attempt to address some of the fundamental questions of powdery mildew biology. Most of the following experiments were performed using the cucurbit powdery mildew *Golovinomyces cichoracearum* race UCSC1. Previously known as *Erysiphe cichoracearum*, *G. cichoracearum* race UCSC1 was isolated at the University of California, Santa Cruz. *G. cichoracearum* is especially suited for genetic studies, as it is able to infect the model plant *Arabidopsis thaliana* accession Columbia *(Col-0)* in addition to susceptible cucumber (*Cucumis sativa*) cultivars (Adam & Somerville, 1996).

In order to investigate the roles of individual fungal genes during the course of powdery mildew infection on plant hosts, we developed a technique to deliver small RNAs to the fungal cell. This technique, a modification of the common plant virus-induced gene silencing method, utilizes *Agrobacterium tumefaciens*-mediated plant transformation to produce small RNAs. When these small RNAs are designed to correspond to fungal transcripts, we were able to demonstrate effective silencing of individual fungal genes. This application of virus-induced gene silencing is known as host-induced gene silencing (HIGS). HIGS allows for the targeted study of powdery mildew genes-of-interest, an important tool that can be used to determine the roles of individual genes or gene clusters during infection (Tinoco et al, 2010, Nowara et al., 2010, Burch-Smith et al., 2006).

Using HIGS, we attempted to identify fungal genes with important roles during *G. cichoracearum* infection. We identified several genes which, when silenced, significantly reduced the ability of *G. cichoracearum* to establish functional haustorium in Arabidopsis epidermal cells. These genes are the first *G. cichoracearum* effectors to have been identified.

We then used various techniques to probe the functions of these effectors during powdery mildew infection. The results from these studies provide the first insight into the fungal factors that influence the cellular and immune changes that take place during *G. cichoracearum* infection.

While gene-silencing is a powerful tool for the study of powdery mildew biology, the technique has limited application. For instance, it cannot be used to study essential powdery mildew genes, nor can it be used to introduce marker genes or other foreign DNA into the powdery mildew genome. For these reasons, we sought to develop methods to induce stable genetic changes in the *G. cichoracearum* genome. Building on work from Vela-Corciá et al. (2015), we attempted to introduce DNA plasmids into the powdery mildew genome. Success in these experiments might allow for the incorporation of experimentally useful genes into the *G. cichoracearum* genome. For instance, it might allow for the tagging of genes of interest with fluorescent markers, which would enable researchers to identify subcellular localization. We were ultimately unsuccessful in these attempts, but present the work completed with the hope that future researchers may have more success.

In order to better answer questions about the unique biology of *G. cichoracearum*, we collaborated with the Department of Energy Joint Genome Institute to produce an annotated genome sequence for *G. cichoracearum*. This sequencing effort, which is a part of a larger project to sequence the genomes of 11 phylogenetically distinct powdery mildews, allows for insight into the biology of *G. cichoracearum* that had previously been hindered by experimental roadblocks. We developed a method to isolate high-quality genomic DNA from the mildew, which allowed for the use of long-read sequencing technology. This technology greatly improved the quality of the genome assembly, compared to previous powdery mildew genome sequencing efforts.

Using bioinformatics tools, we were able to predict the entire effector complement of the fungus, search for missing genes that may play a role in the establishment of obligate biotrophy, and compare the genome of *G. cichoracearum* to that of other published powdery mildew genomes. This data, which is publicly available via the Joint Genome Institute's 1000 Fungal Genomes Project (https://genome.jgi.doe.gov/programs/fungi/index.jsf) can be used by the larger powdery mildew community to gain new insight into the biology of these interesting and important plant pathogens.

Figures

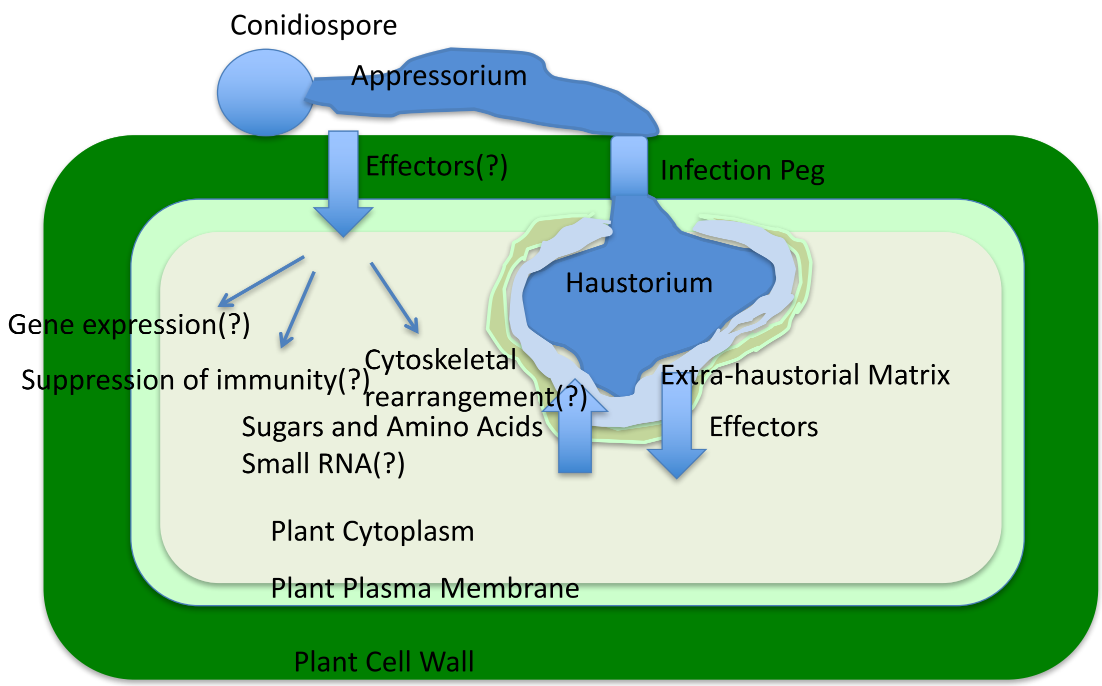

Figure 1.1 Cell biology of the host/powdery mildew interaction

When a powdery mildew conidium lands on the surface of the plant leaf, it germinates and produces an appressorium, a specialized hyphal structure. The appressorium grows across the surface of the plant cell, and a penetration peg is produced, which penetrates the plant cell wall. Once the cell wall has been breached, the haustorium is formed in an invagination of the plant plasma membrane. The space between the haustorium membrane and the plant cell membrane is the extra-haustorial matrix (EHM). Sugars, amino acids and other small molecules are delivered from the plant cell to the fungal cell across the EHM, and effectors are delivered from the haustorium to the plant cell. Effectors may be delivered before the formation of the haustorium via the appressorium or some other fungal structure. Once infected, the plant cell undergoes changes in gene expression, cytoskeletal rearrangement, and the immune response is suppressed (Adam & Somerville, 1996, Micali et al., 2011).

Chapter 2: Developing a Host-Induced Gene Silencing (HIGS) Strategy for Manipulation of Powdery Mildew Gene Expression

Introduction

Until recently, directed gene manipulation of the powdery mildews has not been described. Many aspects of the biology of the powdery mildew pathogens, therefore, have yet to be interrogated. The pathogen is thus far resistant to targeted stable genetic changes, and the curation of interesting mutants quickly becomes untenable due to the lack of efficient long-term storage methods.

Here, I describe a method for the transient silencing of targeted transcripts in *G. cichoracearum.* This method utilizes a modified version of virus-induced gene silencing (VIGS) known as host-induced gene silencing (HIGS) (Tinoco et al., 2010, Birch-Smith et al., 2006). The VIGS is a post-translational gene silencing technique takes advantage of the innate system of plant cells, which prevent viral proliferation and extracellular viral movement to induce silencing of native transcripts. Plant-specific RNA-fragments are cloned into the *Agrobacterium tumefaciens* Ti-plasmid, along with a modified viral genome. In this study, we used a Ti-plasmid containing a modified *Tobacco rattle virus* (TRV) (Burch-Smith et al., 2006).

Double-stranded RNAs are produced in the plant cell by RNA-dependent RNA polymerase enzymes. These RNAs are recognized by DICER-like proteins, which cleave the RNA into short interfering RNA, or siRNA. These siRNAs form complexes with the TRPB and ARGONAUT proteins to form the RISC body. The RISC body then cleaves mRNA containing complementary sequence to the siRNA, resulting in significantly reduced accumulation of the target RNA and protein. These siRNAs are trafficked throughout the plant, resulting in systematic VIGS in organs distal to the infiltrated leaves (Baulcome, 1999, Waterhouse & Fusaro, 2006, Kalantidis et al., 2008).

HIGS has been described in other plant pathogenic fungi, as well as nematodes, Oomycetes, parasitic plants, bacteria, and insects (reviewed by Koch & Kogel, 2014, Burch-Smith et al., 2006, Nowara et al., 2010, Panwar et al., 2013). Though the mechanism is not yet fully understood, it has been shown that the expression of small, double stranded RNAs targeting pathogen sequences in the plant cell can result in the silencing of pathogen transcripts (Figure 2.1, Nunes and Dean, 2012). These studies have used stably transformed plants and biolistic methods to express or deliver the small RNA. Here, I describe the first experiments using an *A. tumefaciens* system expressing TRV containing pathogen sequences to induce the transient reduction of powdery mildew transcripts.

HIGS target of purine biosynthesis results in red coloration in unsuccessful penetration attempts

The fungal gene *ADE2* encodes a phosphoribosylaminoimidazole carboxylase, which catalyzes a step in the biosynthesis of purine compounds. In *ade2* cells lacking a source of exogenous adenine, a red pigment accumulates, which results in an observable red coloration in *Saccharomyces cerevisiae* and purple coloration in *Neurospora crassa (*Rébora et al., 2001; Serres, 1960). Previous random mutagenesis experiments with *B. graminis f. sp. hordei* had resulted in red pigmentation of unknown origin, which were thought to potentially be due to an adenine biosynthesis deficiency (Sherwood et al., 1991). We designed primers based on the draft *G. orontii* genome sequence (https://gbrowse.mpipz.mpg.de/cgi-bin/gbrowse/Golovinomyces_orontii_V1_public/) and amplified and sequenced a fragment of the gene from purified *G. cichoracearum* cDNA.

We created silencing constructs containing 300 base pairs of homology to the *G. cichoracearum ADE2* (*GcADE2*) sequence in the pTRV2 vector used for VIGS in Arabidopsis (Figure 2.2A). This construct, along with the companion plasmid pTRV1, was delivered via *A. tumefaciens* infiltration, as was the positive VIGS positive control phytoene desaturase (*AtPDS*) and a VIGS negative control, GUS. Silencing of AtPDS results in a macroscopically visible white photobleaching phenotype. *GUS* encodes a β-glucuronidase and is commonly used as a negative control in VIGS studies (Burch-Smith et al., 2006).

Each silencing construct was expressed in *A. tumefaciens* and co-transformed into 10-day old Arabidopsis leaves along with the helper plasmid. Arabidopsis leaves were infected with *G. cichoracearum* 11 days after *A. tumefaciens* infiltration. Penetration success and hyphal growth were measured on the surface of infected leaves at 2 dpi. We observed a small number (<10%) of red fungal structures at 2 dpi, while most of the germinated conidia and associated hyphae were colorless (Figure 2.3A). No change in coloration was observed either macroscopically or microscopically at 7 dpi, in either hyphal growth or conidia for the majority of fungal propagules. No change in the ability of the fungus to successfully infect the plant was observed when *GcADE2* expression was reduced, as measured by comparing the ratio of successful penetration attempts in *GcAde2* silenced plants to that of plants expressing a silencing construct targeted at the *GUS* gene (Figure 2.3B). Successful penetration attempts were identified as germinated conidia that produced haustorial structures, as visualized via epifluorescence microscopy at 2 dpi. No significant changes were detected in the transcript abundance of *GcADE2*, as measured using qPCR. A fungal phosphate transporter gene, based on the sequence of Go_EST_c387, which is consistently expressed across the timecourse of infection, was used as a control gene for these transcript abundance experiments (Weßling & Panstruga, 2012, Weßling, 2013). *AtPDS*-silenced plants showed the characteristic bleaching phenotype at 11dpi, and plants expressing both *AtPDS* and *GUS* silencing constructs were unaffected in the penetration success of powdery mildew. These experiments were repeated twice with similar results. *GcAde2* was determined not to be a good indicator of silencing success for future HIGS experiments, as silencing could not be adequately measured either by observing the phenotype of silenced *G. cichoracearum* or via qRT-PCR quantification.

HIGS targeting of GcCyp5*1 results in reduced penetration success*

The fungal gene *CYP51* encodes a cytochrome p450 sterol 14 alpha-demethylase, an essential fungal ergosterol biosynthetic gene. It is the target of the azole class of fungicides (Aoyama et al., 1996, Délye et al., 1997). Reduction in *CYP51* transcript in the pathogenic fungus *Fusarium graminearum*, as well as in the powdery mildew *Blumeria graminis f. sp. hordei* resulted in reduced fungal growth (Koch et al.2014, Jones et al., 2014, Koch et al., 2013).

We created silencing constructs containing 300 base pairs of homology to the *G. cichoracearum CYP51* (*GcCYP51*) sequence in the pTRV2 vector used for VIGS in Arabidopsis (Figure 2.2B). This construct, along with the companion plasmid pTRV1, was delivered via *A. tumefaciens* infiltration.

Silencing and data collection were performed as described above. We observed a a decrease in penetration success at 2 dpi, with infected plants expressing *TRV2-GcCYP51* exhibiting 53% penetration success and plants expressing *TRV2-GcADE2* exhibiting 93% success (Figure 2.4B, C). At 7 dpi there was a significant reduction in powdery mildew growth on the leaves of infected plants expressing TRV2-GcCYP51 compared to plants expressing TRV2-GcADE2 (Figure 2.4A). Transcript levels of *GcCYP51* were reduced in GcCYP51-silenced infected leaves as measured using qPCR as described above (Figure 2.4D). These experiments were repeated twice with similar results. *GcCYP51* was determined to be a robust silencing control for future HIGS studies, and is required for survival of powdery mildew on Arabidopsis leaves.

Discussion

We demonstrated that it is possible to reduce the expression of *G. cichoracearum* genes by modifying the *A. tumefaciens*-mediated VIGS technique to target fungal transcripts, and that this reduction can have a significant impact on the ability of the powdery mildew to successfully infect the Arabidopsis leaves. While the exact mechanism of the transfer of the silencing constructs from the plant cell to the fungal cell is not known, this technique is an effective new tool to alter the expression of individual genes in this difficult to manipulate fungus. It is a useful technique as it builds on the widely-used Arabidopsis VIGS delivery mechanism, and requires very little optimization beyond that already described for that system.

We initially attempted to silence the expression of *GcADE2* to produce a non-lethal positive control for silencing in the *G. cichoracearum* Arabidopsis pathosystem. This control would have been useful to demonstrate the spatial and temporal extent of silencing. For instance, it would have indicated whether the targeted genes are silenced in the next generation of conidia produced by the mildew. While it was previously believed that powdery mildews are unable to synthesize purines, non-targeted mutagenesis experiments had produced red coloration in powdery mildews, and the transcript for *GoADE2* was detected in *G. orontii* transcriptomic studies. This result, along with data from other fungal systems, indicated that aspects of purine biosynthesis in powdery mildews could be experimentally disrupted, leading to a change in the mildew's color. Thus we concluded that this nonlethal phenotype might be a good candidate for a silencing control in powdery mildew.

The results of our silencing experiments indicate that the red coloration associated with disrupted powdery mildew purine biosynthesis may only accumulate in unsuccessful penetration attempts when *GcADE2*-targeted HIGS constructs are expressed in the host plant. This may be evidence of a starvation response in the powdery mildew. For example, the fungus may only attempt to synthesize purines if it is unable to obtain them from a host plant via a functional haustorium. While these experiments did not result in the production of a robust positive control, they did provide two interesting pieces of information. First, the silencing of fungal genes using the HIGS technique was possible, so the development of further constructs was prioritized. Second, the red coloration in fungi that were unable to successfully penetrate the host cells indicates that the HIGS-mediated silencing takes place before the successful establishment of a haustorial structure. This was of particular note, as it indicates that there is likely communication and exchange of compounds between the fungus and the plant before the establishment of the haustorial interface, challenging the canonical belief the haustorium is the only site of exchange.

The observation that *GcADE2*-silenced fungi were not deficient in penetration or conidiation indicates that the purine biosynthesis pathway is not necessary for the growth and reproduction of the fungus in this case. For these reasons, in future experiments, *GcAde2* silenced plants were used as a negative control for the effects of *A. tumefaciens* mediated expression of fungal-targeted silencing constructs, though we have minimal evidence that *GcAde2* is consistently and strongly silenced

Our second silencing target, *GcCYP51*, was a less optimal positive control as a successful silencing construct would result in a lethal phenotype for the fungus. We hoped to replicate the effect of popular fungicides by interfering with the action of the *GcCYP51* protein, in this case by reducing its expression. We were able to detect significant differences in the infection phenotypes of Arabidopsis expressing *GcCYP51* and *GcADE2* silencing constructs.

The penetration success at 2 dpi and macroscopic powdery mildew infection at 7 dpi of *GcCYP51*-silenced *G. cichoracearum* was significantly diminished compared to the *gcade2* control, and the *GcCYP51* transcript levels were significantly reduced in the silenced condition. Additionally, we noted that the efficiency of silencing was not uniform across the surface of the leaf. Rather, leaf areas around the midvein were significantly more likely to be silenced than the areas around the edges of the leaves. This is consistent with the silencing observed using the standard VIGS control *AtPDS*. Samples were taken from all areas of the leaf, however, so the penetration success and transcript levels in the *GcCYP51*-silenced conditions may be even more significant when taking silencing efficiency into account.

Because haustorial formation was reduced in *GcCYP51*-silenced leaves, once again these results indicate that silencing occurs before the establishment of a haustorial structure and is not dependent on the presence of this canonical site of communication between the plant and the fungus. The success of this technique, as well as the indication that silencing can occur at early stages of infection, suggest that this silencing method could be used to detect fungal factors involved in haustorial formation and penetration success of the pathogen.

Figures

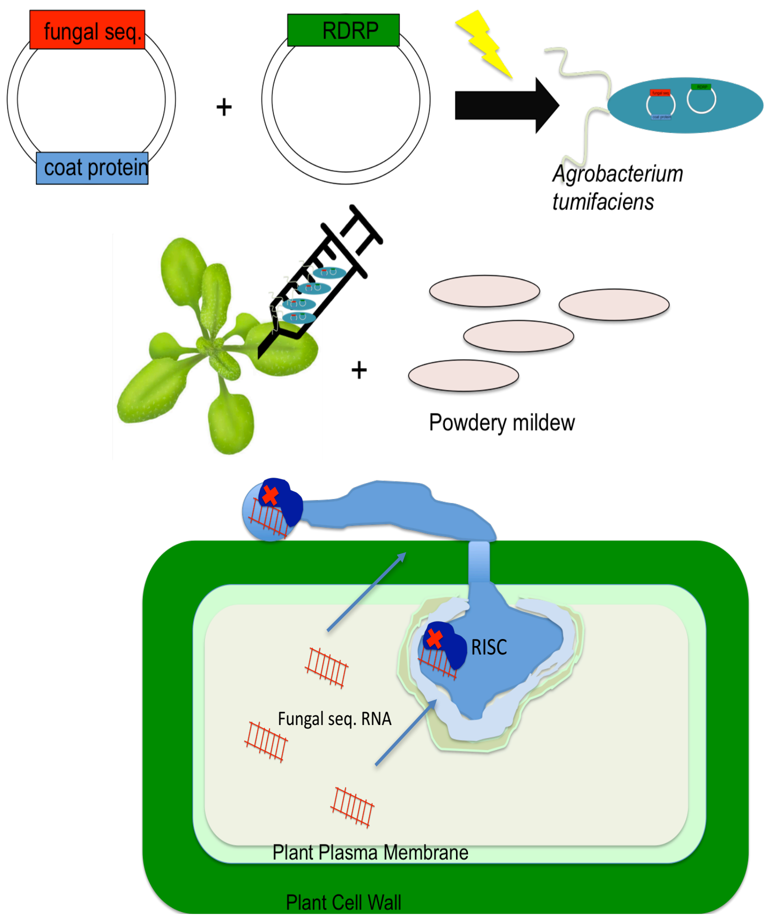

Figure 2.1 Host-induced gene silencing in powdery mildew fungi. 200-300 base pairs of a fungal-derived gene sequence is cloned into a virus-induced gene silencing vector, which contains a viral coat protein. This is co-transformed with a helper plasmid, containing RdRP, into *A. tumefaciens* and infiltrated into *Arabidopsis* leaves. The plant produces double-stranded RNA molecules corresponding to the fungal sequence. Nine days after infiltration, the leaves are infected with *G. cichoracearum*. The small RNAs are delivered from the plant cell to the fungal cell, and the RISC complex in the fungus silences transcripts with sequences corresponding to the double-stranded RNA.

A.

>GcAde2

ATGAATACAACTATCGGACTGCTTGGTGGCGGACAATTGGGACAAATGCTCTGTGAAGCTGCCAATCCG
TTAGGAGTAAGTGTGGTGGTTCTCGATGCCCCAAATTCTCCGGCAAAACAAGTTAATTCTAGAGTGTCAC
ACATCGATGGTTCATATACCGATCCAGAGAAGATCCGTGAGCTGGCTCGACGCGTAGACATATTAACTA
TTGAGACAGAACATGTCGACACCTACGTTCTGGAAGAGATCGCAGAGAAGGGAGTGGAGGTGCAACCA
AACTGGCGAACCATCCGCATCATTCAAGACAAATTTAAACAGAAGCAACATCTCATGGCTCACGGCGTTC
AAACAGTGATAGCAAAATCTGTTAAACCAGATCCCACAGATTTGAATGTCTTTGGATCGACGTTTGGTTT
TCCATTCATGCTGAAAACAAGAAAAAATGCATACGATGGAAGAGGTAATTTTATCGTCAAGACAAGTGT
TCATATTGAAAAGGCTCTGGAAGAATTCAGGACAAAAGACCTGTACGCAGAGAAGTGGGCAGACTTCA
AAATGGAACTAGCCGTGATGGTCGTTAAGTTTGAAGAAGGCTTGACTTCGGACGGACTAGGCACGGTG
GCCTACCCAGTCGTGGAGACTATCCACCAAGACAGCATTTGCCACTTGGTCTACGCACCCGCTCGTGGAA
TCTCCGACGATGTCCAGCAAAGAGCAAAAAAGATAGCACAGAAGGCAGTTGGCTGTCTCTGGGGTAGA
GGAGTTTTCGGGGTTGAACTATTTCTCCTGCAAGACGGAGAAATTGTGGTAAACGAGATTGCTCCTCGT
CCGCACAATTCGGGTCATTACACTATCGAAGCGTGTCCAACTTTCTCTCAATATAAGTCACAGCTTTTATC
GATTCTAGAAATAAGGCCTTATTTTCCAGAATCTGTAGTCCCGTTATTATCTCCAGCTATAATTATGCTCA
ATATCTTGGGAGGAGTAAACAAGAGATCACACGAGGCTTTAGTTGAAAAAGCTTTGCTCGTTCCATCTG
CTGCATTGCATCTGTATGGAAAAGAATCCAGGCCAGGTAGAAAGATAGGACATATCTCAATCATATCAA
GCACAATGTCGGAAGATACAGAAATTTGCAATTCTTAA

B.

>GcCyp51

ATGGGTGTCATCGAGACAGATTCTGAACCTTTTGCCCTACAAATCTCCAAGCGTGGGACATTTGTCGAGC
TACTGTGTATTTGTTGCTTATTTTTTCTACTGGCTGTGGTCGTCAATGTGCTGAAACAATTATTGTTTCGCA
ACCCTCATGAGCCACCAGTTGTATTTCACTGGTTTCCTGTGATTGGAAACGCCATTACGTACGGAATTGA
TCCCTACAGATTCTTCTTTGACTGTAAAGCCAAATATGGGGACATTTATACTTTCATCCTTTTTGGGAAGA
AGACGACGGTGTATTTGGGTCGACAAGGAAACAACTTCATACTGAACGGAAAGCTAAAAGATGTAAAC
GCTGAGATAGTATACAATGTATTGACAGGTCCGGTATTCGGGAAGGATGTAGTCTATGACTGTCCAAAC
TCAAAATTGATGGAGCAAAAGAAGTTCATGAAAACATGCCTTAGCACCGAAGCTTTCCGATCGTACGTG
CCCATAATACAAAACGAGGTAGAGACCTTCTTGAAGAAGTGTCCCAGCTTCAAAGGACAAAAAGGCACC
GTTGATATAACTGAAGTCATGGCTGAAATCACTATCTACACTGCTTCGCATGCTCTACAAGGAAAACAGG
TTCGTGACAAGTTTGATTCCTCTTTTGCGGCTCTCTATCATGACCTCGACATGGGGTTCTCCCCTATCAATT
TTATGCTGCCTTGGGCACCTCTTCCTCATAACCGGGCTCGTGACCATGCACAAAGAACCATAGCGAAAAT
TTATATGGATTTGATTAAGAGCCGTAGAGCAGAAAAAGAGAAATACGAGCAAGAGCACGATATAATGT
CGCACTTAATGCGATCGACATATAAAGATGGAACTCCAGTACCTGATCGAGAGATTGCACACATGTTGA
TTGCTCTCCTGATGGCTGGACAGCACTCTTCTTCCTCTACTAGTTCGTGGATTATGCTATGGTTGGCAGCT
CGTCCTGATATAATGGAAGAACTATACCAGGAACAGCTCGAAGTGTTCGGGTCGGACAAGACTCTCCCA
CCCCTGAAATATGAAGATCTCTCACAGCTTCGACTTCATCAAAATGTTCTCAAAGAAGTGCTTCGGCTTCA
TGCTCCCATCCACTCTATTATACGACAGGTCATGACCCCGATGCCTGTAGAAGGGACCAACTACGTCATC
CCAACGTCCCATTCTCTTCTCTCAGCTCCCGGATGTACTAGTCGTGATCCCGCGTATTTCCCTAATCCCCTT
CAATGGGACCCTCATCGTTGGGATCCAAAATCAGGAGGAGTCATCGTTCCAGATTTAAATGATGAGAAA
TTTGATTATGGATTTGGTCTAATCAGTACGGGCGCATCGAGTCCTTACCTGCCTTTTGGTGCTGGACGGC

ATCGCTGCATTGGCGAACAATTTGCAACTGTACAGTTGGTTACTATCATGGCAACTATGGTTCGCTTTTTC
AGATTTCATAATGTAGATGGGAGGAAAGGTGTTGTTGACACGGATTACTCAAGCCTTTTCTCACGACCG
CTGTCTCCAGCTGTGATTGGATGGGAAAAGAGGGAATAG

Figure 2.2 Sequences used for silencing construct design

A. Coding sequence of the *GcAde2* gene, with silencing sequence (red).
B. Coding sequence of the *GcCyp51* gene, with silencing sequence (red).

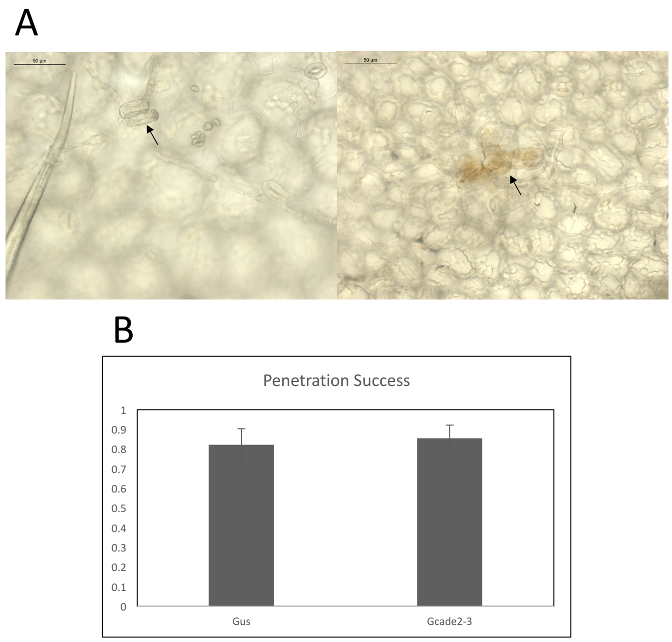

Figure 2.3 Silencing of GcAde2 *transcript can result in red coloration in failed penetration attempts*

A. Left: *Gus*-targeted control. Right: red coloration in *G. cichoracearum* conidia and hyphae in failed penetration attempt on *Arabidopsis* leaf surface. Arrows indicate conidia . Leaves were cleared with 70% ethanol.
B. Silencing of *GcAde2* does not result in a penetration defect. Penetration success was described by comparing the ratio of successful penetrations to the total number of penetration attempts at 2 dpi. Error bars indicate standard deviation. Eight biological replicates were measured per treatment. These experiments were repeated twice with similar results.

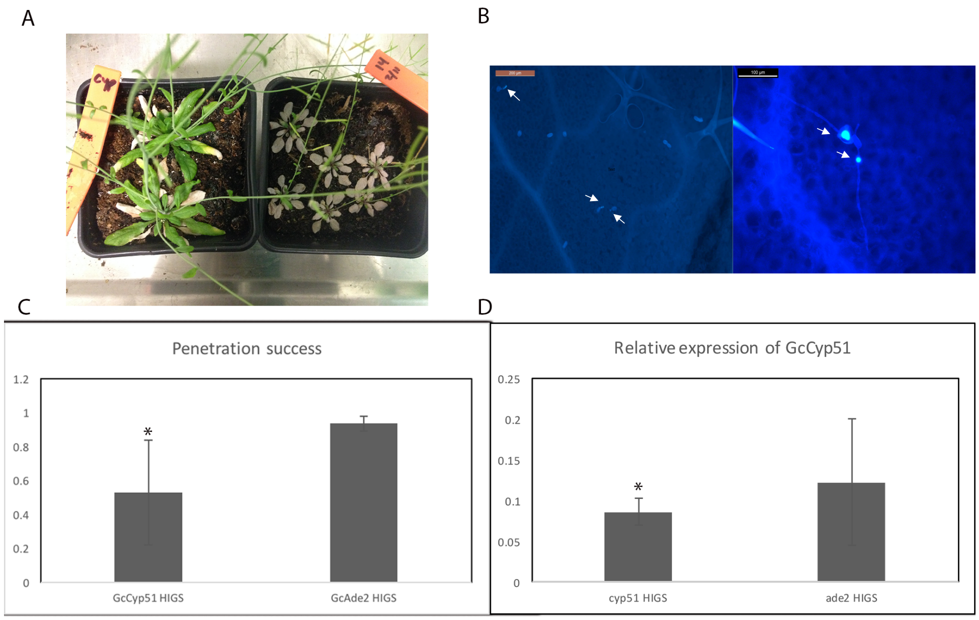

Fig 2.4 Silencing of GcCyp51 *transcript results in reduced penetration and disease symptoms*

A. *G. cichoracearum* infection is reduced on *GcCyp51* silenced plants. *GcCYP51-* (left) and *GcAde2*-silenced (right) plants are shown 7 dpi.
B. Control infection (right) and *GcCyp51*-silenced plants (left) at 2dpi. Leaves were collected at 2dpi, cleared with ethanol and stained with anline blue. Arrows indicate penetration attempts.
C. Penetration success is reduced at 2dpi. Penetration success was described by comparing the ratio of successful penetrations to the total number of penetration attempts. Bars indicate standard deviation. A student's t-test was performed on the data, and the asterisk indicates a p-value<0.01.
D. Quantitative real-time PCR of *GcAde2* transcript in control and GcAde2 silenced *G. cichoracearum* at 2 dpi. A student's t-test was performed on the data, and the asterisk indicates a p-value<0.01.

Tables

Table 2.1 Primers used in Chapter 2

ID	Name	Sequence	Purpose
KSO-101	GcADE2-1 F	taagcagaattcccgtcttgcaggagaaatag	For amplifying cDNA of Gc *ADE2* (based on *G. orontii* sequence) for cloning into pYL156
KSO-102	GcADE2-1 R	tgcttaggtaccggctctggaagaattcagga	
KSO-127	ade2qpcr-f	gaggagcaatctcgtttaccac	qPCR detection of *GoAde2*
KSO-128	ade2qpcr-r	tagaggagttttcggggttg	
KSO-131	GoCYP51 F	gtgagtaaggttaccgcaaaaaggcaccgtcaaaat	Gibson cloning of *GcCyp51* into pTRV2 cut by *EcoR1* and *KpnI*
KSO-132	GoCYP51 R	gcgtgagctcggtactgtgcaatctctcgatcagg	
KSO-247	GcPT_qPCR F	GGATCACAAGAGGAGCCAAA	qPCR detection of phosphate transporter (Weßling 2013)
KSO-248	GcPT_qPCR R	TTGCGACTTCAGAACCCTCT	
KSO-294	GcCyp51 qPCR F	CTCCCACCCCTGAAATATGAAG	qPCR detection of *GcCyp51*
KSO-295	GcCyp51 qPCR R	GATGACGTAGTTGGTCCCTTC	

Table 2.2 Plasmids used in Chapter 2

Glycerol Stock Number	Plasmid Name	Description	Source
13	GcADE2-pTRV2	Gene silencing construct, targeting GcAde2	Somerville -20 Plasmid stock
52	GcCYP51-pTRV2	Positive control for Gene silencing construct, targeting GcCyp51	Somerville -20 Plasmid stock
15	pYL192(p TRV1)	Tobacco rattle virus (TRV)-induced gene silencing vector containing TRV movement protein and replicase	Somerville -20 Plasmid stock
14	pYL156 (pTRV2)	TRV-induced gene silencing vector containing TRV coat protein and multiple cloning site for restriction digest/ligation cloning strategy	Somerville -20 Plasmid stock
14	TRV2-AtPDS	Positive control for TRV-induced gene silencing, silences of phytoene desaturase (PDS)	Somerville -20 Plasmid stock
16	TRV2-GUS	Negative control for TRV-induced gene silencing, silences GUS	This study
17	TRV2-empty	Negative control for TRV-induced gene silencing	Somerville -20 Plasmid stock

Chapter 3: Silencing of Three *G. cichoracearum* Effector Candidates

Introduction

The functions of the predicted powdery mildew effectors are largely unknown. A small subset of the large effector space of powdery mildews has been characterized. This is partially a consequence of the methods employed in effector identification, which exclude any secreted proteins with significant sequence homology to proteins outside of the powdery mildews. A significant subset powdery mildew effectors have been shown to contain domains with structural homology to fungal T1 RNase-like domains, however many are missing the key catalytic residues normally associated with RNase function (Spanu 2017).

Ridout et al., (2006) identified the two effector genes from *B. graminis f. sp. hordei*, *Avr_{k1} and Avr_{a10},* and showed that expression of both effectors in barley leaves resulted in enhanced infection in susceptible cultivars. These effectors had been previously predicted genetically, along with 23 additional candidate effector loci (Brown & Jessup, 1995). Recognition of these effectors by resistance-genes in resistant barley cultivars resulted in cell-death (Ridout et al., 2006). Aguilar et al. (2015) demonstrated that 8 candidate secreted *B. graminis f. sp. hordei* effectors (CSEP0007, CSEP0025, CSEP0128, CSEP0211, CSEP0247, CSEP0345, CSEP0420 and CSEP0422) were required for “normal aggressiveness” of the fungi at early time-points.

Schmidt (2015) found that several *B. graminis f. sp. hordei* effectors were differentially expressed over the course of infection, and encoded functional secretion signals including a cleavage site. These effector candidates were determined to localize to the plant cytosol and nucleus upon translocation, and did not suppress the barley cell-death response to BAX, a proapoptotic protein that induces cell death across plants, animals, and fungi (Schmidt, 2015). Two effector candidates interacted with and activate host proteins HvARF-GAP (an ADP-ribosylation factor (ARF)–GTPase-activating protein (GAP)) and HvTPMT (thiopurine-methyl-transferase), respectively. These interactions suggest that the effectors may be targeting host vesicle trafficking and volatile production, respectively (Schmidt, 2015). An additional *B. graminis f. sp. hordei* candidate effector, BEC1019, was shown to be required for powdery mildew infection, and to suppress *Xanthomonas*-induced cell death in barley (Whigham et al., 2015).

Pedersen et al. (2012) analyzed the *B. graminis* candidate secreted effector (CSEP) arsenal. They determined that the 491 CSEPs clustered into 72 families, and were largely preferentially expressed in the haustorium as compared to epiphytic fungal structures. A large subset of these predicted proteins (i.e. 72 CSEPS) contained ribonuclease-like domains. Additionally, Pedersen et al. (2012) found that the amino acid cysteine was overrepresented in the CSEPs, and predicted a high prevalence of disulfide bond formation. Also, many CSEP contained the conserved [YWF]xC domain within the first 30 amino acids of the mature protein sequence (Godfrey et al., 2010). It was also noted that the CSEPS often appeared in clusters in the *B. graminis* genome, indicating that the proliferation of CSEPs may have been due in part to gene duplication (Pedersen 2012).

There has been some characterization of powdery mildew effector protein function, both *in vitro* and in the context of powdery mildew infection. The *B. graminis f. sp. hordei* CSEP CSEP0105 was shown to inhibit the chaperone activity of a barley heat shock protein, HvHsp16.9, interfering with the ability of the protein to prevent heat-induced protein aggregation. CSEP0105 was demonstrated to be required for *B. graminis f. sp. hordei* virulence via HIGS in barley, and was shown to localize specifically to the cytosol of barley cells when co-expressed with *HvHSP16.9*. When not co-expressed with the heat-shock protein, CSEP0105 was observed in both the cytosol and nucleus of barley cells (Ahmed et al., 2016).

Another *B. graminis f. sp. hordei* CSEP, CSEP0064, was shown to interact with several barley proteins, including a glutathione-S-transferase, a malate dehydrogenase, a ribosome-associated protein, and a thaumatin-like protein. This effector is a RNase-like effector, and the researchers believed that it may target multiple proteins over the course of infection. The functional role of these interactions is not known (Pennington et al.2016).

In a study of the barley powdery mildew pathogen, *B. graminis f.sp. hordei*, it was shown that when effectors were targeted using HIGS, approximately one third of knockdowns resulted in a deficiency in penetration success (Pliego et al., 2013). This was particularly surprising, as the absence of single effector proteins in other systems rarely results in a significant defect in infection capability. These results were validated, and it was demonstrated that expression of a non-targeted version of the *Blumeria* effector candidates (BEC) in HIGS targeted cells resulted in the complementation of the infection phenotype. The effector BEC1011 was further characterized to be involved in cell-death suppression in infected barley cells (Pliego et al.2013).

We attempted to use the previously described *A. tumefaciens*-mediated HIGS technique to interrogate *G. cichoracearum* effector candidates. Because the genome sequence of the *G. cichoracearum* was not available, we attempted to amplify effectors based on the genome sequence of the related powdery mildew *G. orontii* (Panstruga et al., 2012). These *G. orontii* genes were identified as candidate effectors due to the presence of an amino (n)-terminal secretion signal, absence of a predicted transmembrane domain, and lack of significant sequence homology to other proteins outside of those found in other powdery mildews.

Forty-eight effector candidates were identified based on their high level of expression in *G. orontii*, acceptable length for the HIGS construct design, and predicted domain homology. Primers were designed to amplify these from *G. cichoracearum* cDNA. Twenty-two of those genes determined to be present and expressed in *G. cichoracearum*, referred to here as *G. cichoracearum* effector candidates (GcEC), were then used as templates for HIGS as described above, and the infection phenotype was determined. Three GcECs were determined to have effects on the early stages of *G. cichoracearum* infection, with two defective in penetration/haustorial formation and one with significantly reduced secondary hyphal growth following successful penetration.

Several G. orontii *effectors have a close homolog expressed in* G. cichoracearum

We identified our "Top 40" effector candidates from the predicted list of *G. orontii* effectors. These were prioritized based on three factors. First, the most highly expressed effector candidates in *G. orontii* were selected based on transcription data provided by Ralf Weßling from the Max Planck Institute for Plant Breeding Research (Weßling, personal communication). We reasoned that highly expressed effectors were most likely to be important for infection on the common host of *G. orontii* and *G. cichoracearum,* Arabidopsis. Our second criterion for selection was the presence of any predicted domains with homology to domains of known function. This was an attempt to simplify further analysis of these effector proteins. Finally, we eliminated effector candidates whose predicted *G. orontii* coding sequence was less than 250 base pairs, as the silencing protocol described above requires 200-300 base pairs of homology to be expressed by the VIGS vectors. After sorting by these three criteria, we selected the 40 best candidates as our "Top 40" predicted effectors and designed primers based on the published *G. orontii* genome and transcriptome data (Table 3.1). These selections were determined to have no significant targets within the Arabidopsis transcriptome using siRNA Scan (http://bioinfo2.noble.org/RNAiScan.htm), so as to minimize the effects of off-target host-silencing on our results. We then attempted to amplify 200-300 base pair silencing constructs of the "Top 40" effector candidates from *G. cichoracearum* cDNA. cDNA synthesized from RNA collected from heavily infected leaves at 10 dpi, in an attempt to include a broad range of life stages of the fungus, including both early, mid, and late infection. Of the "Top 40" candidates, we successfully amplified 22. This work was done with the assistance of an undergraduate research assistant, Gustavo Garcia.

HIGS of three G. cichoracearum *effector candidates results in difference in infection at 2dpi*

We then constructed HIGS silencing vectors as described previously from 21 of the *G. cichoracearum effector* candidates in the VIGS vector pTRV2, as described in the previous chapter. Penetration success and hyphal growth were measured on infected leaves at 2 dpi (Figure 3.1) We observed that the silencing of two effectors, *G. cichoracearum Effector Candidate (GcEC) 10* and *GcEC17*, resulted in reduced penetration success of 82% and 85%, relative to infected plants expressing the *GcAde2* targeted HIGS vector. Targeted silencing of a third effector, *GcEC8*, resulted in a 24% decrease in hyphal growth at 2 dpi, as calculated by measuring the length of the longest hyphal branch originating from the powdery mildew conidia, when compared infected plants expressing the *GcAde2* targeted HIGS vector (Figure 3.2). qPCR transcript detection showed a reproducible decrease in effector transcript levels in the silenced condition, however these results were not statistically significant. Silencing of *GcEc8*, *GcEc10* and *GcEC17* was repeated twice more with similar results.

Discussion

G. orontii genes were annotated as candidate secreted effector proteins (CSEP) by Ralf Weßling based on the presence of a secretion signal in the N-terminal region, absence of a predicted transmembrane domain, and lack of homology to previously described proteins (Weßling et al., 2014) We believe that these criteria likely eliminated some effectors. Because the mechanism of delivery from the fungal cell to the plant cell is not well described, there may be alternate secretion signals specific to delivery during infection that differ from the canonical secretion signal. A great number of vesicles have been observed in the extra-haustorial matrix, of unknown origin and contents (Micali et al., 2011). Finally, few described effectors are homologous to known proteins, however this may not be true in the biotrophic fungal plant pathogens (Spanu et al., 2010, Panstruga et al., 2012). Despite this, Weßling et al.(2014) identified 179 CSEPs in the *G. orontii* transcriptome, and these identifications were used to choose our "Top 40" *G. cichoracearum* effector candidates. Although these criteria may be overly restrictive, they provide a suitable starting point for the identification of effector candidates in powdery mildew systems.

We were somewhat surprised to find such a large overlap in the presence of predicted effector transcripts between the *G. orontii* and *G. cichoracearum* transcriptome. Very few predicted effectors are shared between *Bgh* and *G. orontii,* although the overlap between *G. orontii* and *E. pisi* is comparatively larger (Weßling at al, 2014). Even the closely related *B. graminis f. sp hordei* and *B. graminis f. sp. tritici* effector repertoires show evidence of extensive gene duplication and loss (Menardo et al., 2017). The fact that we were able to amplify 22 of 40 tested effector candidates from *G. cichoracearum* RNA, indicating that these effectors are not only present in the genome but expressed as well, may suggest that these effectors are important for the pathogens' abilities to infect their shared host plant, *Arabidopsis.* Overlap in predicted effector candidates between *G. cichoracearum* and other powdery mildews is discussed in more detail in Chapter 8.

HIGS constructs were used in infection assays as described in Chapter 2. The silencing of 2 of the 21 *G. cichoracearum* effector candidates was shown to significantly reduce the ability of the fungus to successfully penetrate the host cells and form haustoria. A third effector candidate's haustorial formation and penetration resembled the control constructs when silenced, however secondary hyphal growth was significantly reduced, indicating that the haustoria may not be functioning to deliver nutrients to the developing pathogen. None of these three candidates had an obvious effect on the growth of powdery mildew at 7dpi as observed macroscopically.

Our findings are consistent with those in HIGS studies of *B. graminis. f. sp. hordei* effectors, where the haustorial index, or the ability of the fungus to form haustoria, is compromised. These studies did not report an overall decrease in powdery mildew disease on the leaves of the barley studied, however this may be due to the logistics of HIGS in barley. In these experiments, researchers used biolistic bombardment to introduce silencing constructs into detached barley leaves, limiting the ability of researchers to observe later stages of infection (Pliego et al., 2013, Aguilar et al., 2015)

We believe that our HIGS technique may have underestimated the percentage of the "Top 40" effector candidates that reduce the ability of *G. cichoracearum* to infect *Arabidopsis*. Based on results in the barley powdery mildew *B. graminis f. sp. hordei* presented in Pedersen et al., (2011), we might have expected approximately 30% of the silenced effector candidates to result in a defect in haustorial formation. As previously discussed in Chapter 2, silencing efficiency was not uniform across the surface of the leaf, but rather was much more efficient near the midvein. Additionally, when visualized with *PDS*, not all leaves were silenced to the same degree, and some plants showed no signs of silencing at all. We believe that these factors may have contributed to false negative results for some of the predicted effector candidates, and our data should not eliminate these effector candidates from further study or characterization. It is also possible that these effector candidates resulted in a difference in pathogen virulence that was not detected using our measurement techniques. For instance, *GcEC8* was only detected because of a chance observation of its particularly short hyphal length, as its penetration success was not altered in our HIGS experiments. The silencing of other effector candidates could have resulted in similar, or different and unknown defects in the ability of *G. cichoracearum* to infect Arabidopsis.

It is also possible that the virulence impacts of these effectors may be redundant to other effectors, and therefore silencing only single effectors would not result in a virulence defect. This could be tested by silencing multiple effectors at a time. Silencing clusters of effectors based on genomic position or gene family may reveal pathogenicity islands or important, unknown classes of powdery mildew effectors. This analysis will become more accessible after the publication of a high-quality *G. cichoracearum* genome.

The lack of uniform silencing on individual leaves, between leaves on the same plant, and between plants likely eliminated the ability to detect significant reductions in the transcript levels for silenced effectors. Due to the biotrophic nature of the fungus, samples for RNA extraction were taken from whole leaves, and we estimate the fungal RNA percentage to be only a small proportion of total RNA, with the remainder being made up by plant RNA. This, combined with the noise introduced by silencing, likely makes it difficult to detect expression differences for our silenced effectors. Due to the significant difference in penetration success and hyphal length, however, we believe that silencing of the transcripts is, indeed, taking place.

Figures

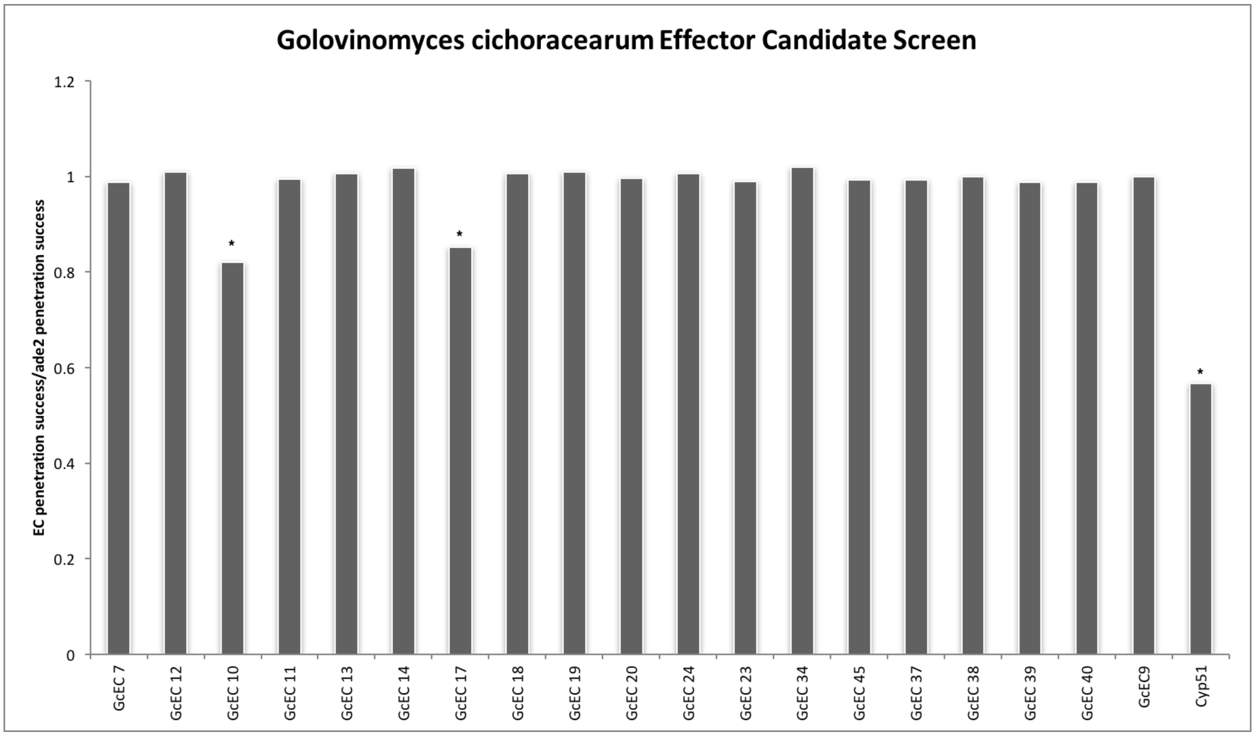

Figure 3.1 Penetration success measured at 2 dpi in Arabidopsis leaves infected with G. cichoracearum *expressing silencing constructs for candidate* G. cichoracearum *effectors.* Statistical analysis was performed on each individual dataset using student's t-test, with p-value < 0.01 indicated by (*).

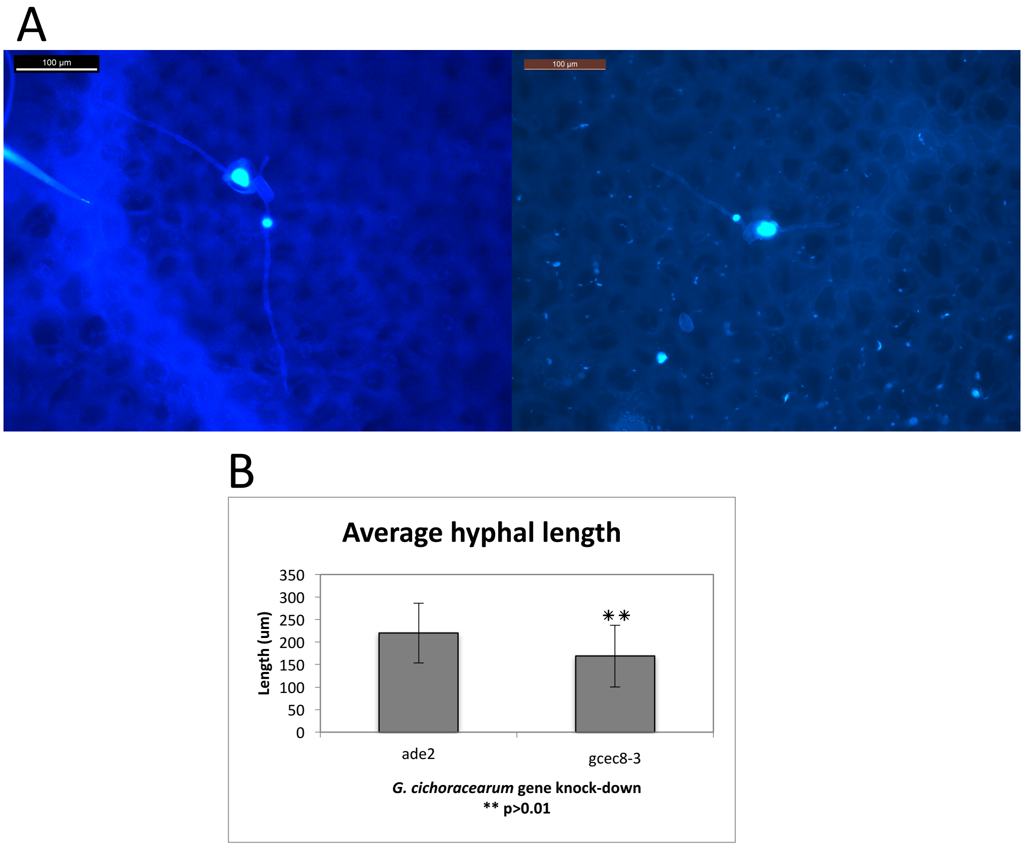

Figure 3.2: Silencing of GcEC8 *results in a hyphal elongation defect at 2 dpi*

A. Representative micrograph of *GcAde2* (right) and *GcEC8* (left) silenced leaves infected with *G. cichoracearum* at 2dpi.
B. Average hyphal length measured at 2 dpi in *GcAde2* (ade2) and GcEC8 (gcec8-1) silenced leaves. P-value < 0.01 was calculated using student's t-test.

Tables

Table 3.1 Top 40 G. orontii *effector candidates*

G. cichoracearum effector cadndiate (GcEC)	(Orontii Effector Candidate) OEC	Amplified from Gc cDNA?	Silencing infection phenotype	Hit in Bgh (tblastn) <0,00001	Hit in E. pisi (tblastn)
1	OEC72	n	N/A	Y	Y
2	OEC73	n	N/A	Y	Y
3	OEC31	n	N/A	N	Y
4	OEC70	n	N/A	N	N
5	OEC48	n	N/A	N	N
6	OEC33.2	n	N/A	N	N
7	OEC33	y	No phenotype observed	N	N
8	OEC33.1	y	Shorter hyphae at 2dpi	N	N
9	OEC28	y	No phenotype observed	N	N
10	OEC10	y	Reduced penetration	N	Y
11	OEC18	y	No phenotype observed	N	N
12	OEC1	y	Not cloned into silencing construct	N	N
13	OEC58	y	No phenotype observed	N	N
14	OEC19	y	No phenotype observed	N	N
15	OEC9	n	N/A	N	N
16	OEC34	n	N/A	N	N
17	OEC16	y	Reduced penetration	N	Y
18	OEC8	y	No phenotype observed	N	N
19	OEC12	y	No phenotype observed	N	N
20	OEC7	y	No phenotype observed	N	N
21	OEC36	y	Not cloned into silencing construct	N	N
22	OEC6	n	N/A	N	N
23	OEC45	y	No phenotype observed	N	N
24	OEC56	y	No phenotype observed	N	N
25	OEC71	n	N/A	N	N
26	OEC29	n	N/A	N	N
27	OEC5	y	Not cloned into silencing construct	N	N
28	OEC11	n	N/A	N	N
29	OEC27	n	N/A	N	N
30	OEC2	n	N/A	N	N
31	OEC65	n	N/A	N	N

G. cichoracearum effector cadndiate (GcEC)	(Orontii Effector Candidate) OEC	Amplified from Gc cDNA?	Silencing infection phenotype	Hit in Bgh (tblastn) <0,00001	Hit in E. pisi (tblastn)
32	OEC4	n	N/A	N	N
34	OEC21	y	No phenotype observed	N	Y
35	OEC40	y	No phenotype observed	N	Y
36	OEC51	n	N/A	N	N
37	OEC46	y	No phenotype observed	N	N
38	OEC15	y	No phenotype observed	N	Y
39	OEC13	y	No phenotype observed	N	N
40	OEC37	y	No phenotype observed	N	N

Table 3.2 Primers used in Chapter 3

ID	Name	Sequence	Purpose
KSO-156	GcEC1 Gibson F	gtgagtaaggttaccgTGCACGCCTTATTCTTCTC	Gibson cloning of GcEC into pTRV2 cut by EcoRI and KpnI
KSO-157	GcEC1 Gibson R	gcgtgagctcggtacGCGACTAAGCTCGCTACTG	
KSO-158	GcEC3 Gibson F	gtgagtaaggttaccgTGTCCAAACTGGTGCGATAG	Gibson cloning of GcEC into pTRV2 cut by EcoRI and KpnI
KSO-159	GcEC3 Gibson R	gcgtgagctcggtacGTATGCACCTCCCGTCAAC	
KSO-160	GcEC6 Gibson F	gtgagtaaggttaccgGGTCCTTTTTCGTGGTCAG	Gibson cloning of GcEC into pTRV2 cut by EcoRI and KpnI
KSO-161	GcEC6 Gibson R	gcgtgagctcggtacTCTTAGCCCGACGACCAT	
KSO-162	GcEC7 Gibson F	gtgagtaaggttaccgGGGCGAGATTGTAGAAGAC	Gibson cloning of GcEC into pTRV2 cut by EcoRI and KpnI
KSO-163	GcEC7 Gibson R	gcgtgagctcggtacGGAGTTTTTGAACGCAAAG	
KSO-164	GcCE8 Gibson F	gtgagtaaggttaccgCTTCCTCACAACAGCAAC	Gibson cloning of GcEC into pTRV2 cut by EcoRI and KpnI
KSO-165	GcEC8 Gibson R	gcgtgagctcggtacACCCTCTCCTCCTCCATTAC	
KSO-166	GcEC9 Gibson F	gtgagtaaggttaccgCTCCTCCATGAGCTTCGTTC	Gibson cloning of GcEC into pTRV2 cut by EcoRI and KpnI
KSO-167	GcEC9 Gibson R	gcgtgagctcggtacGCAAGTGCCTCTTTCAATC	
KSO-168	GcCE9 Gibson F	gtgagtaaggttaccgGCTTTACCATTCTGGTTC	Gibson cloning of GcEC into pTRV2 cut by EcoRI and KpnI
KSO-169	GcEC9 Gibson R	gcgtgagctcggtacTCGTCATCGGATTTCTCG	
KSO-170	GcEC10 Gibson F	gtgagtaaggttaccggctttaccattctggttctcg	Gibson cloning of GcEC into pTRV2 cut by EcoRI and KpnI
KSO-171	GcEC10 Gibson R	gcgtgagctcggtaccggatttctcgac	
KSO-172	GcEC 11 Gibson F	gtgagtaaggttaccgtcccttgcaaattcggttac	Gibson cloning of GcEC into pTRV2 cut by EcoRI and KpnI
KSO-173	GcEC 11 Gibson R	gcgtgagctcggtacttgttttgcatccatttcca	
KSO-174	GcEc12 Gibson F	gtgagtaaggttaccgtcgacactttccaccatgaa	Gibson cloning of GcEC into pTRV2 cut by EcoRI and KpnI
KSO-175	GcEC12 Gibson R	gcgtgagctcggtacttgttcgcagagatcaaacg	
KSO-176	GcEC13 Gibson F	gtgagtaaggttaccgtggtgtcaaggtcaaacgaa	Gibson cloning of GcEC into pTRV2 cut by EcoRI and KpnI
KSO-177	GcEC13 Gibson R	gcgtgagctcggtactgacgaaggtgcagtaccag	
KSO-178	GcEC14 Gibson F	gtgagtaaggttaccgcctacgacaatttggcacct	Gibson Cloning of GcEC into pTRV2 cut by EcoRI and KpnI
KSO-179	GcEC14 Gibson R	gtgagtaaggttaccgtcatcttaattcctcacatctcatc	
KSO-187	GcEC15 Gibson F	gtgagtaaggttaccggctaagaatggggcatcaaa	Gibson cloning of GcEC into pTRV2 cut by EcoRI and KpnI
KSO-188	GcEC15 Gibson R	gcgtgagctcggtacagtccttggtctcggaacct	
KSO-189	GcEc16 Gibson F	gtgagtaaggttaccgtgtagttgccgacctcagtg	Gibson cloning of GcEC into pTRV2 cut by EcoRI and KpnI
KSO-190	GcEC16 Gibson R	gcgtgagctcggtacgcgccagcattcttagagtc	
KSO-191	GcEC17 Gibson F	gtgagtaaggttaccgtcgcaggatgactagtgtcg	Gibson cloning of GcEC into pTRV2 cut by EcoRI and KpnI
KSO-192	GcEC17 Gibson R	gcgtgagctcggtactcacccaacatgtccaaaga	
KSO-193	GcEC18 Gibson F	gtgagtaaggttaccggtcggcattgaatcttggtt	Gibson cloning of GcEC into pTRV2 cut by EcoRI and KpnI
KSO-194	GcEC18 Gibson R	gcgtgagctcggtacttgacagtgctgaccctgag	
KSO-195	GcEC19 Gibson F	gtgagtaaggttaccgatgaatgaatgtgccacgaa	Gibson cloning of GcEC into pTRV2 cut by EcoRI and KpnI
KSO-196	GcEC19 Gibson R	gcgtgagctcggtacgccaataggaaatccgatca	
KSO-197	GcEC20 Gibson F	gtgagtaaggttaccgaatgagcttagcccagacga	Gibson cloning of GcEC into pTRV2 cut by EcoRI and KpnI
KSO-198	GcEC20 Gibson R	gcgtgagctcggtactgaattttgatgagcgcaaa	
KSO-199	GcEC21 Gibson F	gtgagtaaggttaccgcgtcattttgacgggtttct	Gibson cloning of GcEC into pTRV2 cut by EcoRI and KpnI
KSO-200	GcEC21 Gibson R	gcgtgagctcggtacttcttgcctctccctcagac	
KSO-201	GcEC22 Gibson F	gtgagtaaggttaccgtgcgactatctcatccgtca	Gibson cloning of GcEC into pTRV2 cut by EcoRI and KpnI
KSO-202	GcEC22 Gibson R	gcgtgagctcggtacaccagcgtgaggacttgact	
KSO-203	GcEC23 Gibson F	gtgagtaaggttaccgtccgacacgacgataaatca	Gibson cloning of GcEC into pTRV2 cut by EcoRI and KpnI
KSO-204	GcEC23 Gibson R	gcgtgagctcggtacggtttcacagtcagggcatt	
KSO-205	GcEC24 Gibson F	gtgagtaaggttaccgttccggatggtccagaatag	Gibson cloning of GcEC into pTRV2 cut by EcoRI and KpnI
KSO-206	GcEC 24 Gibson R	gcgtgagctcggtaccgaggttcgagatgagtggt	
KSO-207	GcEC 25 Gibson F	gtgagtaaggttaccgccggatcgttatcctcttca	Gibson cloning of GcEC into pTRV2 cut by EcoRI and KpnI
KSO-208	GcEC 25 Gibson R	gcgtgagctcggtactccgtatccactgccttctt	
KSO-209	GcEC 26 Gibson F	gtgagtaaggttaccgatgcccaagaaacgaagatg	Gibson cloning of GcEC into pTRV2 cut by EcoRI and KpnI
KSO-210	GcEC 26 Gibson R	gcgtgagctcggtacccccctcaaaccaggactgta	
KSO-211	GcEC 27 Gibson F	gtgagtaaggttaccgccttcgcccaatccatacta	Gibson cloning of GcEC into pTRV2 cut by EcoRI and KpnI
KSO-212	GcEC 27 Gibson R	gcgtgagctcggtaccacatcaaatttggcccttc	
KSO-213	GcEC 28 Gibson F	gtgagtaaggttaccgcctgctaagcaccgattctc	Gibson cloning of GcEC into pTRV2 cut by EcoRI and KpnI

ID	Name	Sequence	Purpose
KSO-214	GcEC 28 Gibson R	gcgtgagctcggtacaatacagccggagacacagg	
KSO-215	GcEC 29 Gibson F	gtgagtaaggttaccgggcagtagcgtagggcatta	Gibson cloning of GcEC into pTRV2 cut by EcoRI and KpnI
KSO-216	GcEC 29 Gibson R	gcgtgagctcggtacagacacgcatggcttcttct	
KSO-217	GcEC 34 Gibson F	gtgagtaaggttaccgcttcgttaaccgtctgggct	Gibson cloning of GcEC into pTRV2 cut by EcoRI and KpnI
KSO-218	GcEC 34 Gibson R	gcgtgagctcggtactcgttgcagctgatcttggt	
KSO-219	GcEC 35 Gibson F	gtgagtaaggttaccggggtcatcgctaaggagacg	Gibson cloning of GcEC into pTRV2 cut by EcoRI and KpnI
KSO-220	GcEC 35 Gibson R	gcgtgagctcggtacggtttgataccccccaaggca	
KSO-221	GcEC 36 Gibson F	gtgagtaaggttaccgcgggagggcaactaagctta	Gibson cloning of GcEC into pTRV2 cut by EcoRI and KpnI
KSO-222	GcEC 36 Gibson R	gcgtgagctcggtactccggtgaatcgatgtccac	
KSO-223	GcEC 37 Gibson F	gtgagtaaggttaccgagcatcctgagacctgggat	Gibson cloning of GcEC into pTRV2 cut by EcoRI and KpnI
KSO-224	GcEC 37 Gibson R	gcgtgagctcggtacgggtaacgtcccgacttgtt	
KSO-225	GcEC 38 Gibson F	gtgagtaaggttaccggatctcggcattctcccagg	Gibson cloning of GcEC into pTRV2 cut by EcoRI and KpnI
KSO-226	GcEC 38 Gibson R	gcgtgagctcggtacttcacttggatcacggctcc	
KSO-227	GcEC 39 Gibson F	gtgagtaaggttaccgtagaggccgtacgatttgct	Gibson cloning of GcEC into pTRV2 cut by EcoRI and KpnI
KSO-228	GcEC 39 Gibson R	gcgtgagctcggtactgttcagtctcgcagttgct	
KSO-229	GcEC 40 Gibson F	gtgagtaaggttaccggctctctgctgctcgctaaa	Gibson cloning of GcEC into pTRV2 cut by EcoRI and KpnI
KSO-230	GcEC 40 Gibson R	gcgtgagctcggtacggtgcggctgatggtataat	
KSO-386	8_qPCRF	TGCTAAAGCGTCAACGTAGG	qPCR detection of GcEC
KSO-387	8_qPCRR	CATTTCCGCGACCATTTCCT	
KSO-388	10_qPCRF	AATGCCGACTTGGACCATTC	qPCR detection of GcEC
KSO-389	10_qPCRR	TCTCGACCCGACATGTCTTC	
KSO-390	17_qPCRf	ATCGCTGTACGCAATGGATG	qPCR detection of GcEC
KSO-391	17_qPCRR	AACGGTGCAGTCCATAGTCA	

Table 3.3 Plasmids used in this study

Glycerol Stock Number	Plasmid Name	Description	Source
20	GcEC 8-pTRV2	Gene silencing construct, targeting GcEC8	This study
21	GcEC 10-pTRV2	Gene silencing construct, targeting GcEC10	This study
22	GcEC 12-pTRV2	Gene silencing construct, targeting GcEC12	This study
23	GcEC 13-pTRV2	Gene silencing construct, targeting GcEC13	This study
24	GcEC 14-pTRV2	Gene silencing construct, targeting GcEC14	This study
25	GcEC 7-pTRV2	Gene silencing construct, targeting GcEC7	This study
34	GcEC 18-pTRV2	Gene silencing construct, targeting GcEC18	This study
35	GcEc 19-pTRV2	Gene silencing construct, targeting GcEC819	This study
36	GcEC 20-pTRV2	Gene silencing construct, targeting GcEC20	This study
37	GcEC 21-pTRV2	Gene silencing construct, targeting GcEC21	This study
38	GcEC 23-pTRV2	Gene silencing construct, targeting GcEC23	This study
39	GcEC 24-pTRV2	Gene silencing construct, targeting GcEC34	This study
40	GcEC 34-pTRV2	Gene silencing construct, targeting GcEC34	This study
41	GcEC 35-pTRV2	Gene silencing construct, targeting GcEC35	This study
42	GcEC 37-pTRV2	Gene silencing construct, targeting GcEC37	This study
43	GcEC 38-pTRV2	Gene silencing construct, targeting GcEC38	This study
44	GcEC 40-pTRV2	Gene silencing construct, targeting GcEC40	This study
46	GcEC 11-pTRV2	Gene silencing construct, targeting GcEC11	This study
47	GcEC 17-pTRV2	Gene silencing construct, targeting GcEC17	This study
48	GcEC 39-pTRV2	Gene silencing construct, targeting GcEC39	This study
49	GcEC 41-pTRV2	Gene silencing construct, targeting GcEC41	This study
50	GcEC 27-pTRV2	Gene silencing construct, targeting GcEC27	This study
51	GcEC 9-pTRV2	Gene silencing construct, targeting GcEC9	This study

Chapter 4: Characterization of GcEC10

Introduction

Silencing of the putative *G. cichoracearum* effector *GcEC10* results in an 18% reduction in successful penetration attempts on the host plant Arabidopsis. This sequence and identity of this candidate were predicted based on *G. orontii* candidate effector *OEC10* from bioinformatic data obtained from Weßling et al. (2013). The *G. orontii* homolog of GcEC10 contains a predicted nuclear localization signal, and is closely related to *OEC40* and *OEC125*. *OEC40* is a close homolog of *GcEC35*, which was silenced as described in the previous chapter, however no *G. cichoracearum* infection phenotype was observed. *OEC125* was not included in the Top 40 *G. cichoracearum* effector candidates tested in these experiments. *OEC10* is homologous to a predicted gene in the *E. pisi* genome, as well, located on Contig 14629.1 (Spanu et al., 2010). Both OEC10 and GcEC10 contain an FxC motif in the N-terminal region of the mature protein sequence (Godfrey et al., 2010). No interactions between OEC10 and Arabidopsis proteins have been reported.

In his 2013 PhD thesis, Ralf Weßling demonstrated that several *G. orontii* effector candidates suppressed the cell-death response in *N. benthamiana* leaves when co-infiltrated with necrosis-inducing peptides derived from the *Colletotrichum higginsianum* and *Phytopthora* infestans, *Ch*NLP1 and *Pi*INF1, respectively. OEC 10 does not inhibit cell death in these assays. Although OEC10 was predicted to be localized in the plant nucleus, transient expression of OEC10 fused to citrine was observed in both the nucleus and the cytosol of transformed Arabidopsis epidermal cells.

We assessed the ability of GcEC10 to suppress *N. benthamiana* HR induced by the effector XeXopQ, as well as by the avirulence gene/resistance-gene pair *Bs2* and *AvrBs2.* XeXopQ is an effector derived from the bacterial plant pathogen *Xanthomonas spp.* and is homologous to the *P. syringae* effector HopQ (Teper et al., 2014). XeXopQ is recognized by *N. benthamiana,* and transient expression of XeXopQ in *N. benthaminia* leaves results in chlorotic or necrotic lesion formation 3-5 dpi (Adlung et al., 2016). AvrBs2 is a *Xanthamonas campestris pv. vesicatoria* effector recognized by the pepper protein Bs2 (Kearny & Staskawicz., 1990, Gassmann et al., 2010, Tai et al., 1999). When transiently coexpressed in *N. benthamiana* leaves, AvrBs2/Bs2 elicit an HR response characterized by cell-death at 3-5 dpi (Tai et al., 1999).

GcEC10 has a predicted length of 206 amino acids and no predicted homology to described proteins, though Phyre2.0 analysis suggests it may contain a ribonuclease-like domain (Kelley, et al.2015). When amplified from *G. cichoracearum* cDNA, it was found that GcEC10 is 78% identical at the amino acid level to OEC10 (Figure 4.1). In order to determine the role of this effector in the *G. cichoracearum* pathosystems, we performed a variety of *in vitro* and *in vivo* assays to determine characteristics such as subcellular localization, plant interacting-partners, and to characterize the response of the host plant to the presence of the effector protein. The results of these experiments have helped us to determine a model for the potential role of GcEC10 in the establishment of powdery mildew infection on Arabidopsis.

GcEC10 *encodes a predicted RNase-like domain and is targeted to the plant nucleus and cytosol*

The structure of GcEC10 excluding the signal peptide was predicted using Phyre2.0 and localization was predicted using Localizer (Figure 4.2A, Kelley, et al.2015, Sperschneider et al., 2017). The results from this analysis suggest that GcEC10 contains a nuclear localization signal (red) and a ribonuclease-like domain (cyan). The ribonuclease domain was identified by Phyre2.0 with ~90% confidence. As predicted by Localizer analysis, GcEC10 is most likely to localize in the plant nucleus and cytosol. Phosphorylation sites were predicted using NetPhos2.0 (http://www.cbs.dtu.dk/services/NetPhos/). Fifteen total phosphorylation sites were predicted outside of the signal-peptide region, including a single tyrosine, 11 serines, and 4 threonines (Figure 4.2B/C, Blom et al., 1999, Blom et al., 2004).

GcEC10-sp was cloned into the GFP-fusion vectors pMDC84 (N-terminal) and pMDC44 (carboxyl (c)-terminal). These constructs were expressed in *A. tumefaciens* and used to transiently transform *N. benthamiana* cells in an attempt to determine the subcellular localization of the predicted effector. These *N. benthamiana* leaves were observed using confocal microscopy. GcEC10-sp was observed to be localized in the cytosol and nucleus of the *N. benthamiana* epidermal cells. These experiments were repeated twice with similar results (Figure 4.3A). Transient expression of GcEC10-sp-GFP had no macroscopic effect on *N. benthamiana* leaf tissue at 3 dpi (Figure 4.3B).

Purification of recombinant GcEC10

GcEC10 lacking the N-terminal signal peptide (GcEC10-sp) was cloned fused to an N-terminal 6x-His tag in the pET28a(+) plasmid and expressed in BL21 Star *E. coli* under an IPTG inducible promoter. It was determined that the 17 kD GcEC10 protein was largely localized in the cytosolic fraction, which was used for further purification.

GcEC10-sp was then purified using a Ni-NTA column attached to an FPLC. Figure 4.4 shows combined data from two columns run under the same conditions. The purified GcEc10-sp-HIS fractions were combined from multiple columns for further analysis.

GcEC10 vs. Arabidopsis protein affinity pull-down

The purified GcEC10-sp was used as bait to pull-down prey host proteins from heavily infected Arabidopsis leaves. The reason for using heavily infected leaves as prey was twofold. First, we sought to identify interactions in the context of powdery mildew infection, which results in a great number of changes in gene-expression in the plant cell (Both et al., 2005). By using heavily infected leaves as the source of prey protein, interacting proteins that may be present in higher amounts in the infected condition would be more likely to be detected.

Additionally, heavily infected Arabidopsis leaves contain both plant and fungal proteins. Because this method does not necessarily bias the results towards plant proteins, we were interested in whether we would be able to identify fungal proteins that interact with GcEC10 during the course of infection, as well.

The eluted buffer containing GcEC10-sp and any potential interacting proteins was run on a polyacrylamide gel to determine whether GcEC10 co-precipitated with any Arabidopsis or *G. cichoracearum* proteins. No discernible bands were present only in the GcEC10 condition when stained with Coomasie Brilliant Blue (Figure 4.5A) or the more sensitive silver stain (Figure 4.5B). Bands of this nature would be indicative of a potential interaction between GcEC10-sp and a plant or fungal protein. This experiment was repeated with similar results.

GcEC10 interactors identified via mass-spectroscopy

To determine if any low abundance proteins were co-precipitated with GcEC10-sp that could not be visualized on the gel, the solution containing potential GcEc10-sp-bound proteins was sent to the QB3 mass spectroscopy lab for analysis (Table 4.1). No Arabidopsis proteins were found in all replicates. Two Arabidopsis proteins, AtPHOS32 and AtEDR4 (AT5G54430 and AT5G05190, respectively) were present only in the GcEC10 bait condition in sequence counts greater than one. These two proteins were selected for further study for direct interaction with GcEC10.

Bi-molecular fluorescence complementation of GcEC10 candidate interacting proteins

To determine whether GcEC10 could be observed to interact with either AtPhos32 or AtEDR4, we created bimolecular fluorescence complementation (BiFC) constructs.

GcEC10-sp fused to the N-terminus of YFP in pB7WGYn2 was observed to interact with AtPHOS32 fused to the C-terminus of YFP in pB7WGYc2 when transiently expressed in *N. benthamiana* cells, localized to a reticulated structure of unknown origin (Figure 4.6). No macroscopic change in the leaf morphology of the infiltrated *N. benthamiana* leaves was observed. This result was consistent across multiple *N. benthamiana* plants, but was not able to be replicated in subsequent experiments.

The N-terminus YFP of GcEC10-sp in pB7WGYn2 was not observed to interact with the C-terminus of YFP fused to AtEDR4 in pB7WGYc2 when transiently co-expressed in *N. benthamiana* leaves at 3dpi.

GcEC10 *expression is highest during the early stages of powdery mildew infection*

To determine the expression of *GcEC10* over the course of infection, qPCR was performed with primers designed based on the *GcE10* sequence. cDNA quantification was performed via qRT-PCR. Reads were normalized as previously described, and further normalized to 0 hpi expression levels. *GcEC10* expression was observed to increase by 401-fold at 48 hpi as compared to 0 hpi. The expression of GcEC10 at 5 dpi was 1.09-fold compared to 0 hpi, indicating that GcEC10 has a role in the early stages of powdery mildew infection, as indicated in Chapter 3.

Transient GcEC10 *expression suppresses effector-triggered* N. benthamiana *cell death*

To determine whether GcEC10 may play a role in the suppression of the plant immune response, we transiently co-expressed GcEC10-sp with XeXopQ and with both AvrBs2 and Bs2 in *N. benthamiana* leaves. AvrBs2/Bs2 transient expression resulted in necrotic lesions on the leaf surface at 2 dpi. Both XeXopQ and AvrBs2/Bs2 were observed to cause HR characterized by necrosis at 6 dpi, while GcEC10-sp does not cause a noticeable response when transiently expressed in this manner at any time-point (Figure 4.8B).

When GcEC10-sp was coexpressed with AvrBs2/Bs2, the formation of necrotic lesions was delayed. At 2 dpi, no observable HR occurred on the area of the leaf expressing all three constructs (Figure 4.8A). At 6 dpi the degree of HR was reduced in the leaf area expressing GcEC10-sp and AvrBs2/Bs2 compared to AvrBs2/Bs2 expressed with the empty vector control (Figure 4.8B).

Less HR was observed at 6 dpi when GcEC10-sp was coexpressed with XeXopQ, when compared to XeXopQ co-expressed with the empty vector control. No HR was observed in either of these conditions at 2 dpi (Figure 4.8A).

Discussion

Here, we further characterize the *G. cichoracearum* effector candidate GcEC10. As described in Chapter 2, reducing the transcript levels of *GcEC10* during *G. cichoracearum* infection on Arabidopsis results in an 18% reduction in penetration success and haustorial establishment. Our analysis indicated that GcEC10, like the *G. orontii* homolog OEC10, contains a predicted nuclear localization signal and an RNase-like domain.

Sub-cellular localization of the mature GcEc10 protein in plant cells was assayed by fusing GcEC10 without the signal peptide to GFP at both the N- and C-termini. In both cases, GFP fluorescence was observed in the nucleus and cytosol of *N. benthamiana* epidermal cells induced to transiently express the GcEC10 construct. This data corresponds with the results reported for the *G. orontii* homolog of GcEC10, OEC10, which was similarly observed in *N. benthamiana* cells. The presence of the protein in the cytosol, despite the predicted nuclear localization signal, may be due to the lack of interacting proteins, as described for the *B. graminis f. sp. hordei* effector, CSEP0105, which was observed in both the cytosol and nucleus when expressed alone, but was observed only in the nucleus when co-transformed with the interacting host-derived heat shock protein *Hv*HSP16.9.

In order to identify potential interactors of GcEC10, we attempted to express the mature protein (excluding the predicted signal peptide) in *E. coli*, followed by purification via FPLC. We predicted that GcEC10 would be amenable to this type of expression and purification, as it is a small, soluble protein. We was able to purify a 6x-His-tagged version of GcEC10 using the pET28a expression vector and a single NiNTA column. It was determined that GcEC10 was expressed in the soluble fraction of the *E. coli* cell lysate, and was largely excluded from the membrane fraction. Additional purification techniques, including a size-exclusion column and a MonoQ column did not result in significantly improved protein purification, and were therefore excluded from future purification efforts (data not shown).

Once we had purified GcEC10 protein, it was used as bait with total Arabidopsis purified protein as prey in a protein affinity pull-down experiment. While it was observed that the GcEC10 protein behaved as expected in these experiments, coming off the column when high concentrations of imidazole were applied, no bands co-occurring with GcEC10 when the co-IP was visualized on a gel with either Coomassie staining, or a more stringent silver staining procedure.

The fraction of the co-IP that was collected after the application of imidazole was trypsin-digested and sent for mass spectroscopy analysis, however, under the assumption that there may be low-abundance proteins that co-IP with GcEC10 that were not visualized on a gel. The results from the mass spectroscopy analysis supported this assumption, as fragments from two proteins were identified in small amounts, present only in the co-IP from the column containing GcEC10 and absent from the control columns. These two proteins, AtEDR4 and AtPHOS32, have both been implicated in previous plant pathology studies (Zhao et al., 2014, Wu et al., 2015, Merkouropoulos et al., 2008).

AtEDR4, Enhanced Disease Resistance 4, was identified in a screen for mutants with enhanced resistance to *G. cichoracearum* infection. *edr4* mutants display a relatively normal growth phenotype, however when infected with *G. cichoracearum*, the leaves of *edr4* plants display large necrotic regions and significantly reduced *G. cichoracearum* conidial proliferation in a salicylic-acid dependent manner. *edr4* mutants also display enhanced ROS accumulation and callose deposition at the sites of infection, and increased MPK activation. *edr4* mutants accumulate higher levels of defense-response genes *PR1*, *PR2* and *PR5* when infected with *G. cichoracearum*. Finally, EDR4 protein was shown to accumulate in the plasma membrane, *cis*-Golgi, and endoplasmic reticulum, as well as at the site of penetration in *G. cichoracearum* infected plants. This is potentially interesting, as recently it was determined that the extra-haustorial membrane, the origin of which is still not known, has similar markers to those found in the *cis*-Golgi and endoplasmic reticulum (Kwaaital et al., 2017). EDR4 is involved in the recruitment of EDR1, a Raf-like MAPK kinase kinase and negative regulator of salicylic acid-inducible defense, to the site of infection, and may have an impact on endocytosis and clathrin-mediated pathways (Wu et al., 2015). EDR4 has been shown to negatively affect the MAPK cascade (Zhao et al., 2014) The molecular function of AtEDR4 is not yet known (Wu et al., 2015).

AtPHOS32 was identified as a target of phosphorylation upon treatment with the bacterial PAMP peptide flg22. AtPHOS32 was determined to be a substrate for AtMPK3 and AtMPK6, mitogen-activated protein kinases involved in the plant defense and stress responses. Little else is known about AtPHOS32, however it is reported to share structural similarity with the bacterial universal stress protein A (USPA) (Merkouropoulos, et al. 2008).

The interaction between GcEC10 and AtEDR4 or AtPHOS32 could not be confirmed via yeast-2-hybrid interaction, as transformants of yeast expressing GcEC10 could not be obtained. It is possible that GcEC10 interferes with some crucial cellular process in yeast and therefore living transformed cells could not be recovered.

We then co-expressed GcEC10 fused to the N-terminus of YFP with AtEDR4 and AtPHOS32 fused to the C-terminus of YFP in *N. benthamiana* epidermal cells. If the two proteins interacted, the two YFP fragments would be brought close together and would be visible via fluorescence microscopy. No signal was observed when the effector was co-expressed with AtEDR4. When GcEC10-nYFP was co-expressed with AtPHOS32-cYFP, fluorescent signal was observed in reticulated structures in the *N. benthamiana* epidermal cells, indicating that GcEC10 and AtPHOS32 are able to interact *in planta*. It is possible that GcEC10 interferes with the ability of AtPHOS32 to be phosphorylated in an immune response, thereby increasing the susceptibility of the plant to infection. This interaction, however, was not robust, and was observed in only one of three co-expression experiments, though it was consistent across multiple biological replicates.

There are multiple reasons no or inconsistent interactions could have been observed between GcEC10 and AtEDR4 and AtPHOS32. it is possible that the interaction detected via co-immunoprecipitation and MS was not real, and the proteins do not interact in the context of infection. As *G. cichoracearum* is unable to infect *N. benthamiana*, it is also possible that additional plant or fungal components are necessary to initiate or stabilize this interaction.

The differential expression of GcEC10 over the course of *G. cichoracearum* infection corroborates the role of GcEC10 during the early stages of powdery mildew infection. GcEC10 was observed to be highly upregulated at 24hpi and even more highly upregulated at 48hpi, during the time of haustorial establishment and maturation. Our silencing results indicated that GcEC10 may be crucial for successful haustorial formation, and these results further confirm that hypothesis.

No cell death or chlorosis was observed in *N. benthamiana* plants transiently expressing any of the *GcEC10* constructs, the *AtEDR4* or *AtPHOS32* constructs, or any combination thereof, as might be expected if the interaction of these proteins resulted in recognition by the host plant.

To determine whether GcEC10 might be involved in the suppression of HR, the effector was co-expressed with XeXopQ, a necrosis-inducing effector, and with AvrBs2/Bs2, the combination of which induces HR. GcEC10 was determined to suppress the necrosis response associated with both of these effectors, indicating a potential role for the powdery mildew effector. The suppression of plant cell death in response to pathogen effectors characteristic of ETI is likely crucial for the success of the biotrophic powdery mildew pathogen. The importance of this is further underscored when considered with the knowledge that GcEC10 is important in the early stages of powdery mildew infection, as evidenced by the previously described HIGS results. If GcEC10 blocks the signaling cascade resulting in HR, the powdery mildew is able to remain invisible to the host, allowing for the establishment of a haustorium and the subsequent transfer of nutrients from the plant to the fungus. In order for the powdery mildew to elicit the extensive cellular changes in the plant cell architecture necessary for this transfer, many effectors may be transferred to the plant cell. Any of these effectors may be recognized by the plant cell, initiating the signaling-cascade resulting in ETI, and it follows that suppression of this response would be a beneficial role for a powdery mildew effector.

Given that the presence of a functional copy of AtEDR4 increases the susceptibility of Arabidopsis to *G. cichoracearum,* and that GcEC10 suppresses HR, one possibility may be that GcEC10 is involved in suppressing ETI during powdery mildew infection in an EDR4-dependent manner. As the recruitment of EDR4/EDR1 to the site of powdery mildew infection has been shown to be crucial for suppression of HR, GcEC10 may play a role in the stabilization or recruitment of EDR4 to the site of infection (Wu et al., 2015, Zhao et al., 2014). Future studies further probing this interaction could observe the localization of EDR4 in the absence of GcEC10. If this is the method of action of this effector, we would expect EDR4 localization to the site of infection to be compromised.

A separate model regarding the interaction between GcEC10 and AtPHOS32 may similarly involve inhibition of the HR response to infection. As AtPHOS32 is a substrate of MPK3 and MPK6 and may play a role in the immune cascade leading to HR, GcEC10 interference might block this cascade, resulting in an attenuated immune response. Future studies of the role of this effector might investigate the immune response of *phos32* mutant plants during powdery mildew in the presence and absence of GcEC10.

Figures

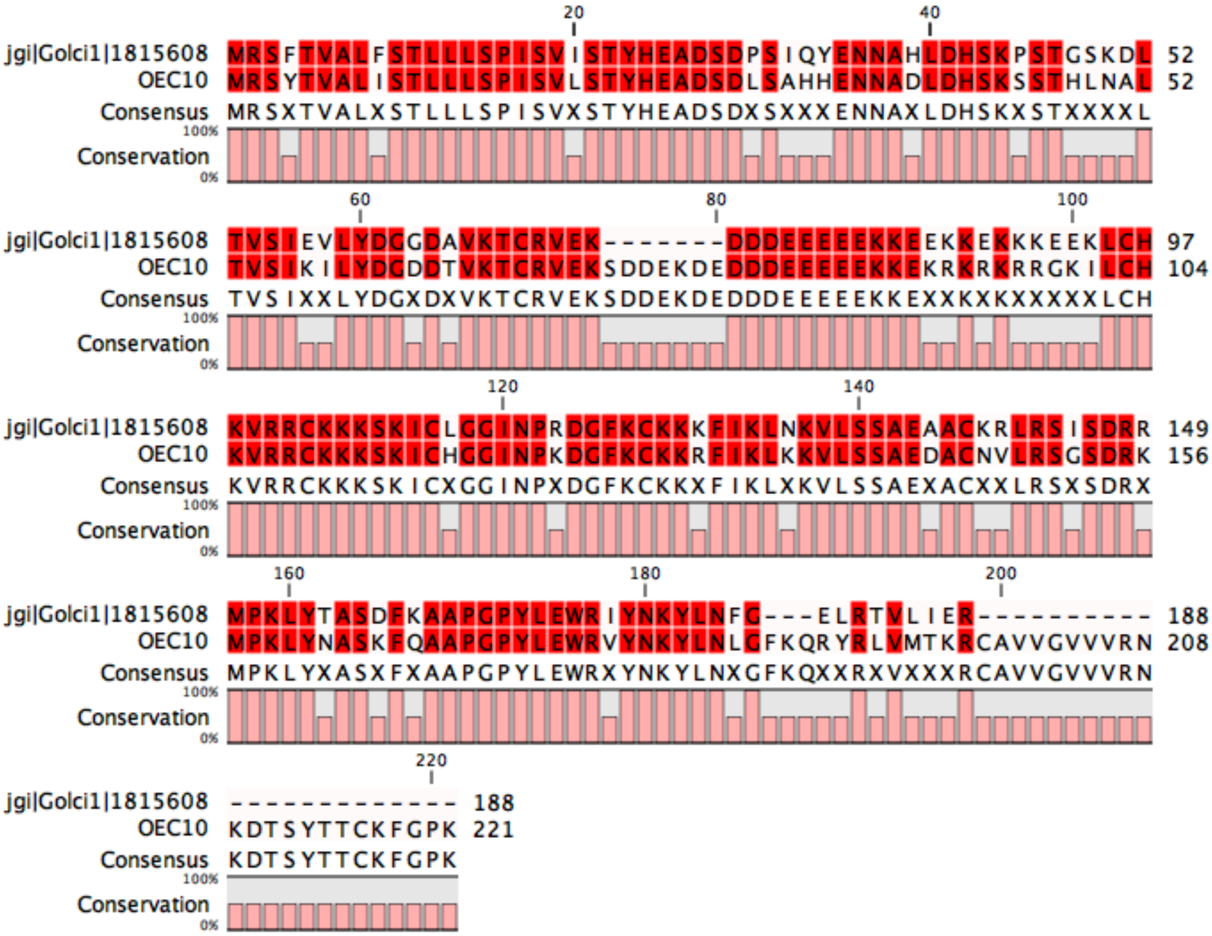

Figure 4.1 GcEC10 is 78% identical to OEC10. GcEC10 (jgi|Golci1|1815600|fgenesh1_kg.14_#_189_#_TRINITY_DN19994_c2_g1_i1, top) shares 78% amino acid sequence identity with the closest *G. orontii* homolog, OEC10 (bottom). Sequences were aligned using the Needleman-Wunsch algorithm (Needleman et al., 1970).

A

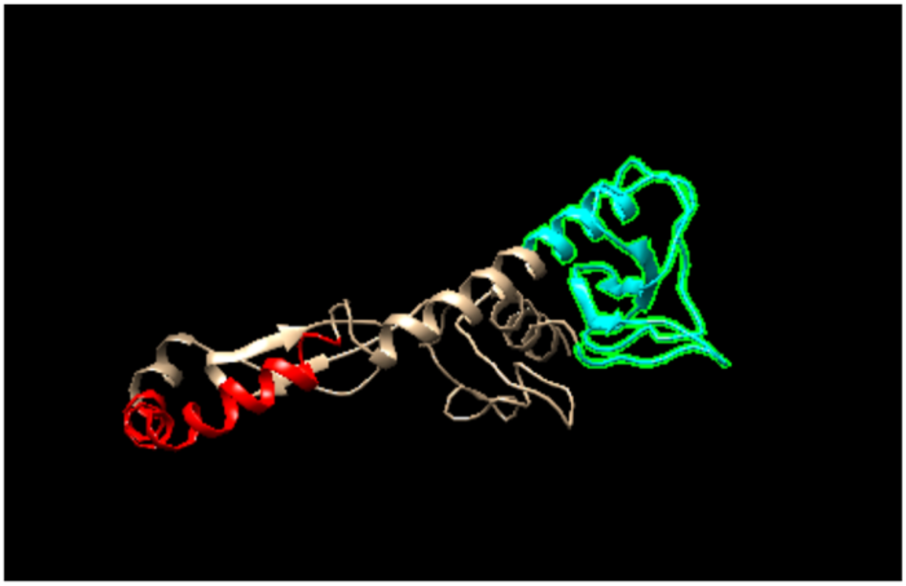

B

```
MRSFTVALFSTLLLSPISVLSTYHEADSDLSIHHENNADLDHSKSSTGSK   #    50
GLTVSIEVLYDGGDAVKTCRVRRCKKKSNICLGGINPRDGFKCKKKFIKL   #   100
SKVLSSAEAACKRLRSISDRRMPKLYTASDFKAAPGPYLEWRIYNKYLNF   #   150
GFKQHCRCSGPQQRHQLHPV                                 #   200
..S.T....S....S.....ST....................S.SST.S.   #    50
.................T.........S......................   #   100
S...SS.........S.S.........T..................Y...   #   150
........S...........
```

C

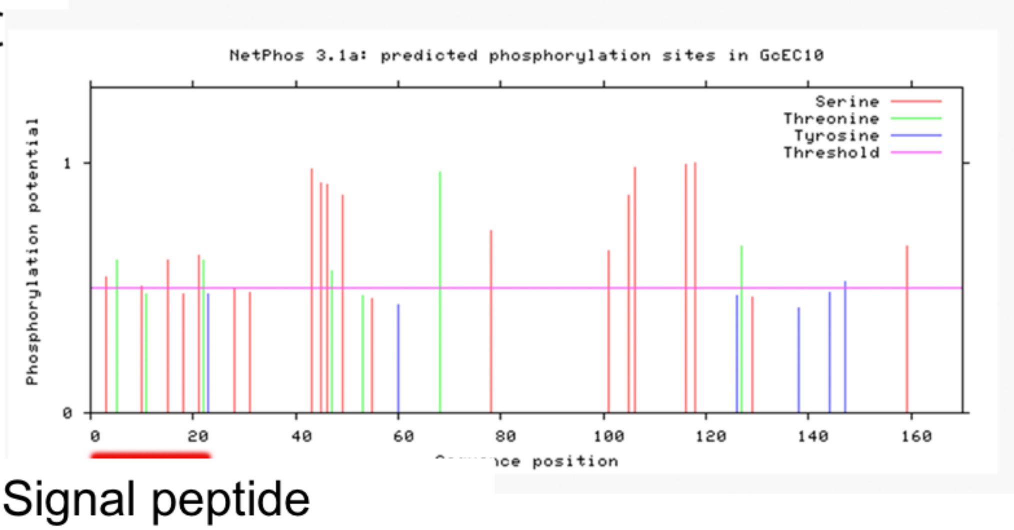

Figure 4.2 GcEC10 predicted structure

A. The amino acid sequence of GcEC10 was analyzed using Phyre 2.0 software and structure was predicted. The predicted RNase like domain (cyan) and the predicted nuclear localization signal (red) are indicated.
B. and C. Predicted phosphorylation sites of GcCE10 at serine, threonine and tyrosine residues, as predicted by NetPhos2.0. Threshold value of 0.5 phosphorylation is indicated. The signal peptide is indicated in red.

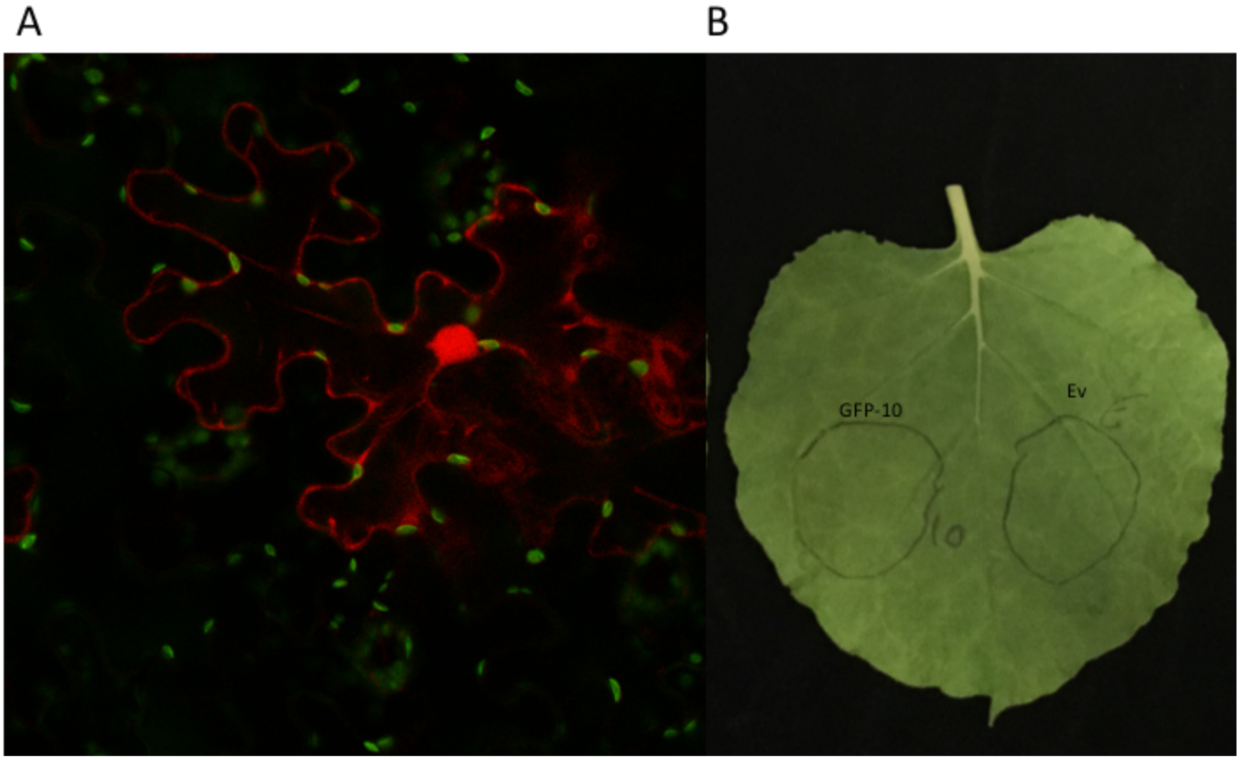

Figure 4.3 Transient expression of GcEC10-sp:GFP in N. benthamiana *leaves*

A. GFP fluorescence (red) was observed in the cytosol and nucleus 72 hours after infiltration when GcEC10-sp-GFP in pMDC44 was transiently expressed in *N. benthamiana* epidermal cells. Chlorophyll A autofluorescence is indicated in green.
B. Infiltrated *N. benthamiana* leaves 72 hours after infiltration, GcEC10-sp-GFP in pMDC44 right, Agrobacterium expressing pMDC44-EV, left. Expression of GcEC10-sp:GFP in *N. benthamiana* leaves does not elicit chlorotic or necrotic lesion formation.

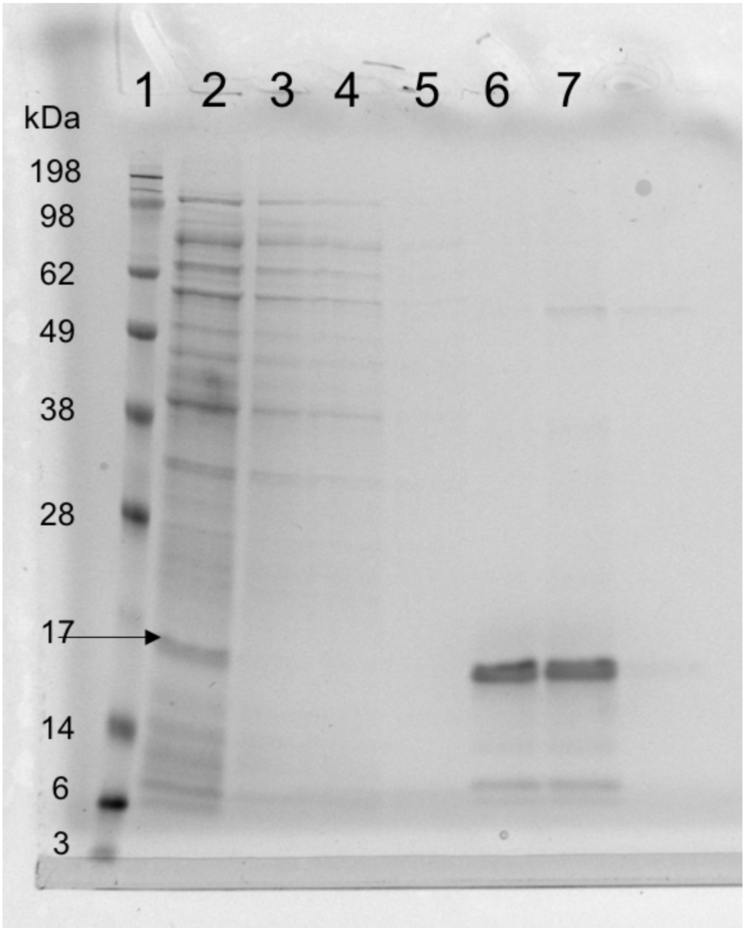

Figure 4.4 Purification of GcEC10-sp expressed in E. coli*.* Polyacrylamide gel showing the protein standard (See Blue2 Plus, lane 1), Total *E. coli protein* (lane 2), flow-through from two NiNTA columns (lanes 3 and 4), the final wash fractions (lane5) and the elution fractions (lanes 6 and 7). The band representing GcEC10-sp is indicated with an arrow.

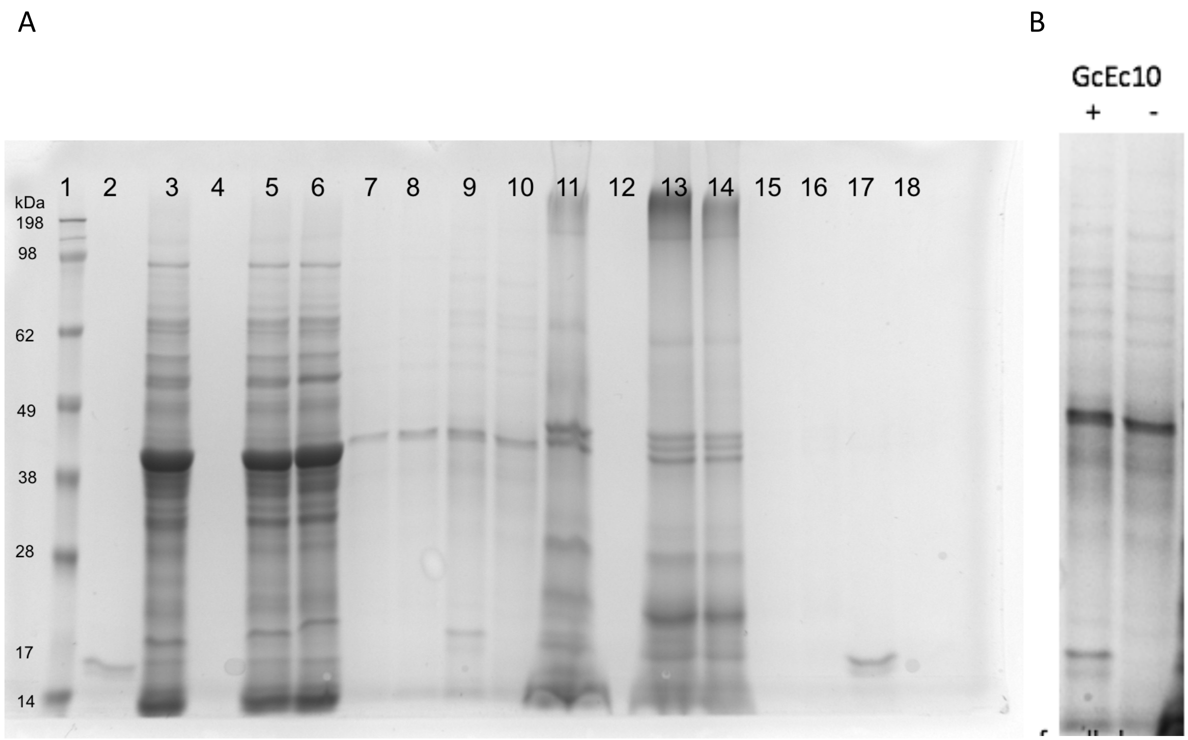

Figure 4.5 Protein affinity pull-down of Arabidopsis protein with GcEC10

A. Co-immunoprecipitation of GcEC10 with protein from *G. cichoracearum* infected Arabidopsis leaves visualized on 12% polyacrylamide gel with Coomassie Brilliant Blue. Polyacrylamide gel showing the protein standard (See Blue2 Plus, lane 1), Total purified GcEC10-sp protein (lane 2), total soluble plant protein (lane 3), flow-through for GcEC10-only column, experimental column and plant-only column (lanes 4-6), column wash for experimental and plant-only columns (lanes 7-8), and column elution for experimental and plant only columns (lanes 9-10). Lanes 2-10 were repeated with plant membrane protein as prey in lanes 11-18.
B. Co-immunoprecipitation of GcEC10 with protein from *G. cichoracearum* infected Arabidopsis leaves visualized on 12% polyacrylamide gel with silver stain. Total plant soluble protein as bait with (+) and without (-) GcEC10-sp as bait.

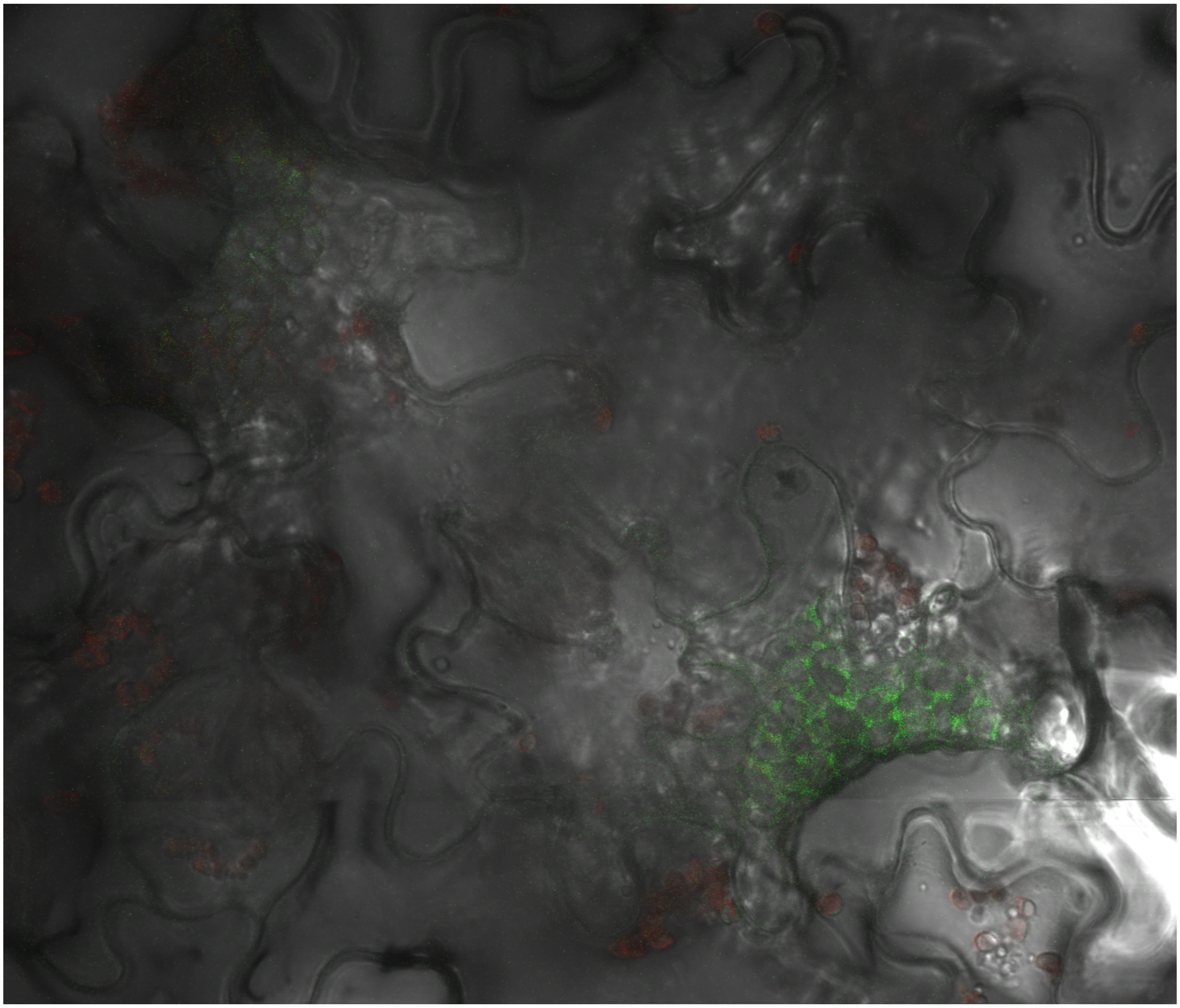

Figure 4.6 Bimolecular fluorescence complementation in GcEC10-sp and AtPHOS32. nYFP-GcEC10-sp in pB7WGYc2 transiently co-expressed with cYFP-AtPHOS32 in *N. benthamiana* leaf cells at 3dpi. YFP fluorescence indicated in green, chlorophyll-A autofluorescence indicated in red.

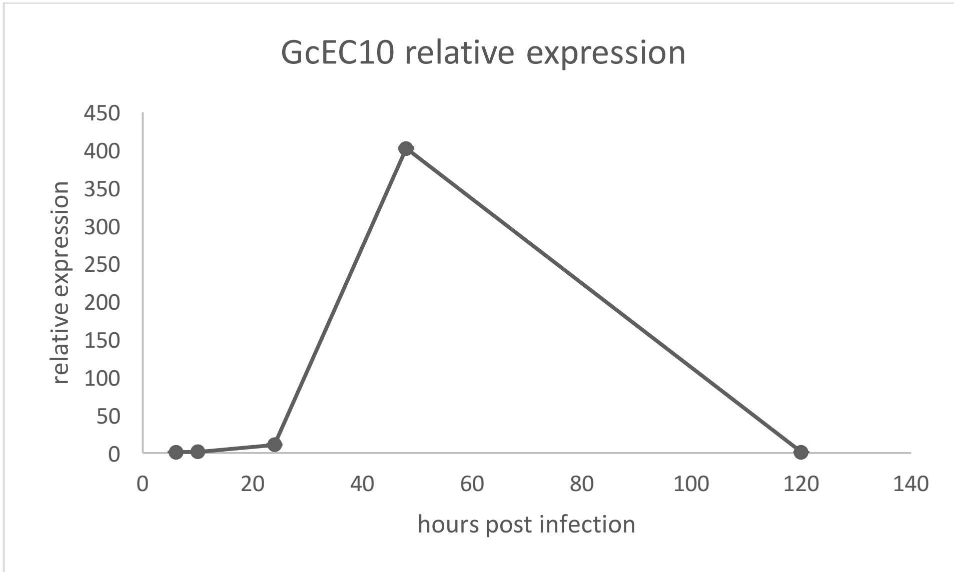

Figure 4.7 GcEC10 *expression timecourse via qPCR*
GcEC10 expression was quantified relative to the expression of *Go_EST_387*, a phosphate transporter, at 6 hpi, 10 hpi, 24 hpi, 48 hpi and 120 hpi. Results were normalized to 0 hpi expression. Data includes three biological replicates and two technical replicates per treatment. Error bars indicate standard deviation.

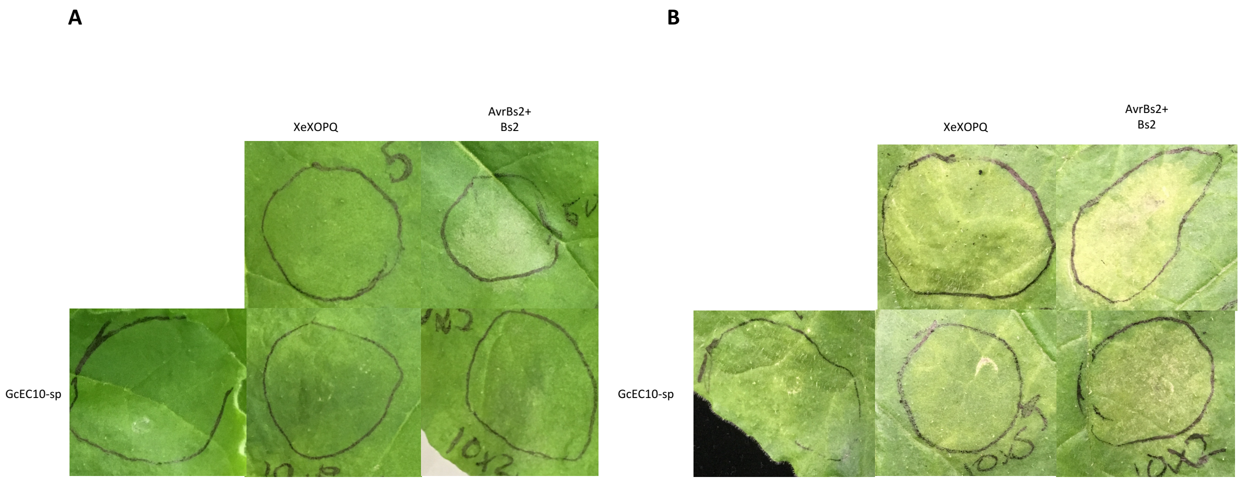

Figure 4.8 Transient GcEC10 *expression suppresses effector-triggered* N. benthamiana *cell death*

A. *GcEC10-sp* transiently expressed in *N. benthamiana* leaves imaged at 2 dpi. *GcEC10-sp* (bottom panels) was coexpressed with *XeXopQ* (middle column panels) or *AvrBs2/Bs2* (right column panels). Necrosis was observed in only the *AvrBs2/Bs2* condition.
B. *GcEC10-sp* transiently expressed in *N. benthamiana* leaves imaged at 6 dpi. *GcEC10-sp* (bottom panels) was coexpressed with *XeXopQ* (middle column panels) or *AvrBs2/Bs2* (right column panels). A reduction in necrosis was observed when *GcEC10-sp* was co-expressed with either *XeXopQ* or the *AvrBs2/Bs2* pair.

Tables

Table 4.1 Primers used in Chapter 4

ID	Name	Sequence	Purpose
KSO-347	10-spf	atgTCTACGTATCATGAGGCCG	For amplifying full length (fl) or mature (sp) GcEC10 from Gc cDNA
KSO-341(2)	10FLF	ATGCGTTCATACACTGTGGC	
KSO-342	10FLR	TTTCGGCCCGAATTTAC	
KSO-388	10_qPCRF	AATGCCGACTTGGACCATTC	For qPCR detection of GcEC10
KSO-389	10_qPCRR	TCTCGACCCGACATGTCTTC	
KSO-359	atedr4 f	atgACAATTTTCATGGCTTCTTGA	Amplification of AtEDR4
KSO-360	atedr4 r	CGTTCTTGGCTTGATAAT	
KSO-361	atphos32f	ATGAATCCAGCAGATTCCG	Amplification of AtPhos32
KSO-362	atphos32r	CTCATCTTTGATGTGTTCATGATG	
KSO-350	10-sp pet28 F	agcaaatgggtcgcgatgacctatcatgaggccg	Amplifcation of GcEC10-SP for Gibson Assembly into pET28
KSO-278	GcEC 10 Gibson R	cttgtcgacggagctCTATTTCGGCCCGAATTTAC	

Table 4.2 Plasmids used in Chapter 4

Plasmid Name	Description	Source
pET28-GcEC10-sp	GcEC10-sp in pET28a(-), under IPTG inducible promoter fused to 6x-His tag	This study
pMDC32-GcEC10-sp	GcEC10-sp in pMDC32 under 35x promoter	This study
pMDC84-GcEC10-sp	GcEC10-sp in pMDC84 under 35S promoter with C-terminal GFP fusion	This study
pMDC44-GcEC10-sp	GcEC10-sp in pMDC44 under 35S promoter with N-terminal GFP fusion	This study
pDONR207-GcEC10-sp	GcEC10-sp in pDONR207 entry plasmid	This study
pET28a(-)	IPTG-inducible expression vector with C-terminal his-tag	Somerville -20 Plasmid stocks
pMDC32	Plant expression construct	Somerville -20 Plasmid stocks
pMDC84	Plant expression construct	Somerville -20 Plasmid stocks
pMDC44	Plant expression construct	Somerville -20 Plasmid stocks
pB7WGYn2	BiFC vector 35S-HA-cYFP	Frank Harmon Lab
pK2GWYc9	BiFC vector 35s-myc-nyfp	Frank Harmon Lab
pK2GWYn9	BiFC vector 35s-ha-cyfp	Frank Harmon Lab
pB7WGYc2	BiFC vector 35s-myc-nYFP	Frank Harmon Lab
pB7WGYc2-EDR4	35S-HA-cYFP-AtEdr4	This study
pK2GWYn9-Phos32	35S-AtPhos32-Myc-nYFP	this study
pB7WGYn2-GcEC10-sp	35s-myc-nYFP-GcCe10-sp	this study
pB7WGYc2-Phos32	35S-myc-cYFP-AtPhos32	this study
pK2GWYc9-GcEC10-sp	35S-GcEc10-sp-HA-cYFP	this study
pK2GWYn9-EDR4	35S-AtEDR4-Myc-nYFP	this study

Chapter 5: Characterization of GcEC8 and GcEC17

Introduction

Silencing of the putative *G. cichoracearum* effector GcEC8 does not result in a decrease in successful penetration attempts on the host plant Arabidopsis, as described previously. However, the growth of hyphae after the haustorial establishment is significantly reduced. This sequence and identity of this candidate were predicted based on *G. orontii* candidate effector OEC33 from bioinformatic data presented in Weßling et al. (2013). *OEC8* is homologous to a predicted gene in the *E. pisi* genome, as well, located on Contig 7156.1. Neither OEC33 nor GcEC8 contain a [YWF]xC motif in the N-terminal region of the mature protein. No known interactions between OEC33 and Arabidopsis proteins have been tested (Weßling et al., 2013).

GcEC8 has a predicted length of 175 amino acids and no predicted homology to described proteins in the non-redundant protein database (https://www.ncbi.nlm.nih.gov/refseq/about/nonredundantproteins/). When amplified from *G. cichoracearum* cDNA, it was found that *GcEC8* is 94.5% identical at the nucleotide level and 100% identical at the amino acid level to OEC33 (Figure 5.1A). In order to determine the role of this effector in the *G. cichoracearum* pathosystems, we performed a variety of *in vitro* and *in vivo* assays to determine characteristics such as subcellular localization, plant interacting partners, and to characterize the response of the host plant to the presence of the effector protein. The results of these experiments have helped us to determine a model for the potential role of GcEC8 in the establishment of powdery mildew infection on Arabidopsis.

Silencing of the putative *G. cichoracearum* effector *GcEC17* results in a 15% reduction in successful penetration attempts on the host plant Arabidopsis, as described previously. This sequence and identity of this candidate were predicted based on *G. orontii* candidate effector OEC16 from bioinformatic data as described in Weßling et al., (2013). *OEC16* is homologous to a predicted gene in the *E. pisi* genome, as well, located on Contig 14629.1 and to a predicted *B. graminis f. sp. hordei* effector, CSEP0078. Both OEC16 and GcEC17 contain a predicted FxC motif in the N-terminal region of the mature protein sequence (Wessling et al.2014).

In his 2013 PhD thesis, Ralf Weßling demonstrated that several *G. orontii* effector candidates suppressed the cell-death response in *N. benthamiana* leaves when co-infiltrated with necrosis-inducing peptides derived from the *Colletotrichum higginsianum* and *Phytopthora* infestens, *Ch*NLP1 and *Pi*INF1, respectively. OEC16 was shown to inhibit cell death when transiently expressed in *N. benthamiana* leaves when co-infiltrated either *Ch*NLP1, but not when co-infiltrated with *Pi*INF1. In yeast-2-hybrid experiments, OEC16 was shown to interact with the Arabidopsis proteins AtTCP14 (AT3G47620), a transcription factor, and AtNAPRT2 (AT2G23420), a nicotinate phosphoribosyltransferase (Weßling et al., 2013).

GcEC17 has a predicted length of 194 amino acids and no predicted homology to described proteins, though Phyre2.0 analysis suggests it may contain a ribonuclease-like domain (Kelley et al., 2015). When amplified from *G. cichoracearum* cDNA, it was found that *GcEC17* is 93% identical at the amino acid level to OEC16 (Figure 5.1B). In order to determine the role of this effector in the *G. cichoracearum* pathosystems, we performed a variety of *in* *vitro* and *in vivo* assays to determine characteristics such as subcellular localization, plant interacting partners, and to characterize the response of the host plant to the presence of the effector protein. The results of these experiments have helped us to determine a model for the potential role of GcEC17 in the establishment of powdery mildew infection on Arabidopsis.

Protein structure prediction of GcEC8 and GcEC17

The structure of GcEC8 less the predicted signal peptide was predicted using Phyre2.0 and localization was predicted using Localizer (Kelley et al., 2015, Sperschneider et al., 2017). The results from this analysis suggest that GcEC8 contains no predicted domains, based on comparisons to proteins with described structure (Figure 5.2A). GcEC8 lacks any predicted transit or localization peptides. According to Localizer analysis, GcEC8 is most likely to localize in the plant nucleus and cytosol. Phosphorylation sites were predicted using NetPhos2.0 (http://www.cbs.dtu.dk/services/NetPhos/). Eleven total phosphorylation sites were predicted outside of the signal-peptide region, all of which were serine residues (Figure 5.2B/C, Blom et al., 1999, Blom et al., 2004).

The structure of GcEC17 missing the signal peptide was predicted using Phyre2.0 and localization was predicted using Localizer (Kelley et al., 2015, Sperschneider et al., 2017). The results from this analysis suggest that GcEC17 contains a nuclear localization signal (red) and a ribonuclease-like domain (cyan) (Figure 5.3A). The ribonuclease domain was identified with 96% confidence by Phyre2.0 analysis. According to Localizer analysis, GcEC17 is most likely to localize in the plant nucleus and cytosol. Phosphorylation sites were predicted using NetPhos2.0 (http://www.cbs.dtu.dk/services/NetPhos/). Twenty-one total phosphorylation sites were predicted outside of the signal-peptide region, including 4 tyrosines, 12 serines, and 5 threonines (Figure 5.3B/C, Blom et al., 1999, Blom et al., 2004).

GcEC17-sp was cloned into the GFP-fusion vectors pMDC84 (N-terminal) and pMDC44 (C-terminal). These constructs were expressed in *A. tumefaciens* and used to transiently transform *N. benthamiana* cells in an attempt to determine the subcellular localization of the predicted effector. These *N. benthamiana* leaves were observed using confocal microscopy. GcEC17-sp was observed to be localized in the cytosol and nucleus of the *N. benthamiana* epidermal cells (Figure 5.5A). No cell-death was noted in *N. benthamiana* expressing GcEC17-sp fusion protein (Figure 5.5B). These experiments were repeated twice with similar results.

Yeast 2-hybrid analysis of GcEC8 and GcEC17

To identify Arabidopsis proteins that interact with GcEC8 and GcEC17, Y2H analysis was performed using a construct containing GcEC8-SP and GcEC17-SP fused to the GAL4 DNA-binding domain in the pGBKT7 vector backbone in Y2H Gold yeast cells. The Arabidopsis normalized Mate and Plate Library, fused to the yeast GAL4-activation domain in the pGADT7 vector backbone in Y187 yeast cells was used as prey (Clontech).

Two positive GcEC8 interactors were identified in multiple independent yeast transformation events (Table 5.2, Figure 5.4A), AtAXR3 and AtXTH3 (At1g04250 and At3g25050, respectively) as the coexpression of these plasmids resulted in colonies with blue coloration of media lacking histidine, tryptophan, leucine, and adenine and containing auerobasidin A and X-a-gal. These interactions were confirmed by independently transforming the constructs into Y2H Gold yeast cells with the same results.

Two positive GcEC17 interactors were identified in multiple independent yeast transformation events (Figure 5.4B), a 6,7-dimethyl-8 ribityllumazine synthase (At3g32930), and a hypothetical protein (At4g29905) as the coexpression of these plasmids resulted in colonies with blue coloration of media lacking histidine, tryptophan, leucine, and adenine and containing auerobasidin A and x-a-gal. These interactions were confirmed by independently transforming the constructs into Y2H Gold yeast cells with the same results.

Expression of GcEC8 *and* GcEC17 *is highest during the early stages of* G. cichoracearum *infection*

To determine the expression patterns of *GcEC8* and *GcEC17* during the course of *G. cichoracearum* infection, qPCR was performed with primers designed based on the *GcE17* and *GcEC8* sequences at multiple time-points during infection. cDNA quantification was performed via qRT-PCR. Reads were normalized as described previously, and additionally to 0 hpi expression levels. Expression of GcEc17 was 1.5-2x higher at 6, 10, 24 and 48 hpi when compared to 0 hpi, and was reduced compared to 0 hpi at 120hpi. Expression of *GcEC8* increased from 5-fold higher than at 0 hpi to 726-fold higher than 0hpi at 48 hpi. The expression of *GcEC8* was not increased relative to the expression at 0 hpi at 5 dpi. Both of these results indicate a potential role at the early stages of infection for *GcEC8* and *GcEC17*, and are consistent with the data discussed in Chapter 3.

Transient expression of GcEC17 *does not suppress XeXopQ or AvrBs2/Bs2-induced HR in* N. benthamiana

To determine whether GcEC17 suppresses the plant immune response, we transiently co-expressed *GcEC17-sp* with *XeXopQ* and with both AvrBs2 and Bs2 in *N. benthamiana* leaves. *AvrBs2/Bs2* transient expression resulted in necrotic lesions on the leaf surface at 2 dpi. Both *XeXopQ* and *AvrBs2/Bs2* were observed to cause HR characterized by necrosis at 6 dpi, while *GcEC17-sp* does not cause a noticeable response when transiently expressed in this manner at any time-point. Co-expression of *GcEC17-sp* with either *XeXopQ* or *AvrBs2/Bs2* did not result in any change in the cell-death response of infiltrated *N. benthamiana* leaves at either 2 or 6 dpi (Figure 5.6).

Discussion

Here, we characterize two *G. cichoracearum* effector candidates identified in the HIGS experiments (Chapter 3), GcEC8 and GcEC17. These effectors are almost identical on the protein sequence level to two *G. orontii* effectors, OEC33 and OEC16, respectively. Little was previously known about the roles of these *G. orontii* effector candidates, though OEC16 had been determined to suppress the cell-death response induced by *Ch*NLP1 (Wessling, 2013). We attempted to characterize the *G. cichoracearum* versions of these effectors with respect to molecular structure, subcellular localization, plant-interacting proteins, expression over the course of infection, and the ability of these effector candidates to suppress the hypersensitive response induced by XeXopQ and AvrBs2/Bs2.

We determined that GcEC17 likely belongs to the class of powdery mildew effectors that encode an RNAse-like domain, which has been described elsewhere, and is likely to localize to the nucleus and cytosol once delivered into the plant cell (Pliego et al., 2013). This predicted localization was consistent with the observed subcellular localization of a transiently-expressed GcEC17 missing the signal peptide fused to GFP, which was observed in the nucleus and cytosol of *N. benthamiana* epidermal cells.

Structural analysis of GcEC8 was not informative, as no predicted domains could be inferred based on the sequence of the effector candidate. Localization prediction for this effector indicated that the GcEC8 is most likely localized in the nucleus and cytosol of the plant cell following translocation.

The expression of both *GcEC8* and *GcEC17* corroborate the predicted roles of the effectors at the early stages of powdery mildew infection. As described in Chapter 3. when the expression of either effector was reduced via HIGS, early infection events were compromised, with hyphal growth reduced in *GcEC8* HIGS experiments and penetration success reduced in *GcEC17* experiments. This is consistent with the observed expression levels, which peaked at 48 hpi for both *GcEC8* and *GcEC17*.

In comparison to both GcEc8 and GcEc10, the expression of GcEC17 is significantly less dynamic over the course of infection. The level of expression varied only between 0.8x and 2.4x that of the 0hpi expression, and it was the only effector candidate to show an expression level lower than that at 0 hpi (at 5 dpi). While HIGS data suggest an important role for GcEC17 in haustorial formation, it is not clear whether the protein is important during other phases of infection, which might account for its more tatic expression.

Yeast 2-hybrid analysis suggested two Arabidopsis proteins may interact with GcEC8-sp, AtAXR3 and AtXTH3. AtXTH3 has been characterized to have cellulose endotransglucosylase activity, cleaving the β-1,4-glucosidic bonds of cellulose and ligating the resulting reducing end to a non-reducing end of cellulosic or xyloglucan oligosaccharides. AtXTH3 is a member of the GH16 family of carbohydrate active enzymes, and is predicted to be secreted into the plant cell wall/extracellular space (Shinohara et al., 2017). We do not believe that it is likely that GcEC8 interacts with AXR3 in the plant cell, as the two are not likely to be localized in the same space, as GcEC8 was not predicted to be present in the apoplast.

AtAXR3 is a nuclear-localized transcription factor that inhibits auxin-inducible gene expression and has been implicated in the development of root hairs, leaf senescence and leaf growth (Rouse et al., 1998, Swarup et al., 2005, Ouellet et al., 2011, Knox et al., 2003, Perez-Perez et al., 2010). Auxin has been demonstrated to influence plant pathogen success in a number of ways, including weakening the plant cell wall, and repressing salicylic acid, another plant hormone that induces plant defense responses (reviewed in Fu & Wang., 2011). As GcEC8 may be localized in the plant nucleus, it may be interacting and potentially interfering with the activity of AtAXR3, blocking the inhibition of auxin-responsive genes, which could lead to enhanced susceptibility of the plant cell to the invading powdery mildew. These responses, including the loosening of the cell wall, may increase the ease by which the mildew can form haustoria undetected, and decrease the likelihood of an immune response by inhibiting salicylic acid-mediated immune responses. This could explain the observed *GcEC8* HIGS phenotype, which may have indicated recognition of the haustoria by the plant cell and an immune response that resulted in the death of the structure and a lack of further growth. Future experiments to confirm this role could include measurement of the auxin and salicylic acid content of leaves infected by *GcEC8*-silenced *G. cichoracearum*, and testing the phenotype of these mildew on auxin signaling mutants.

Two Arabidopsis interacting proteins were identified in yeast 2-hybrid studies using GcEc17-sp as bait, as well. Both of these, At4g29905 and At3g32930, are relatively poorly characterized genes. At4g29905 is a hypothetical protein and has been implicated as responsive to nitrate in roots (Vidal et al., 2013). Localizer prediction indicates that At4g29905 is localized in the plant nucleus, and as such could potentially interact with GcEC17 in the plant cell, as the effector was detected in the nucleus when fused to GFP and transiently expressed in *N. benthamiana* cells (Sperschneider et al., 2017).

Wang et al. (2017) demonstrated that At3g32930, which is similar to a bacterial 6,7-dimethyl-8 ribityllumazine synthase, is associated with the plant hypersensitive response to bacterial pathogens. While the role of this gene in defense response is not yet known, it is conceivable that if it is involved with the hypersensitive response, and is inhibited by interaction with GcEC17, this protein may be involved in mediating this response and thereby increasing the likelihood of *G. cichoracearum* infection. No cell-death suppressing phenotype was observed when GcEc17 was co-expressed with either AvrBs2/Bs2 or XeXopQ, however. This result does not preclude the role of GcEC17 in the suppression of the cell-death response, however, as it may require interaction with Arabidopsis-specific genes, or be a part of a multi-protein complex with other powdery mildew proteins. Future studies of this interaction might include co-expression of *GcEC17-sp* and *At3g32930* in *N. benthamiana* along with cell-death elicitors.

Figures

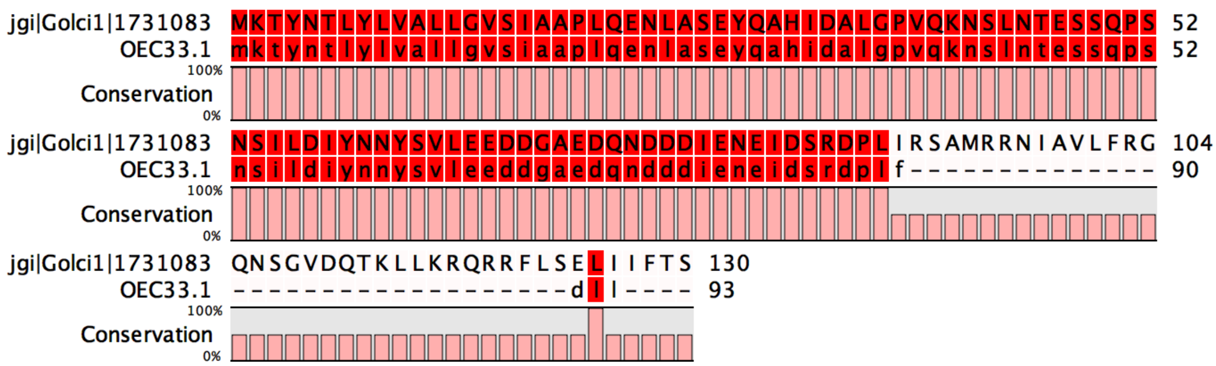

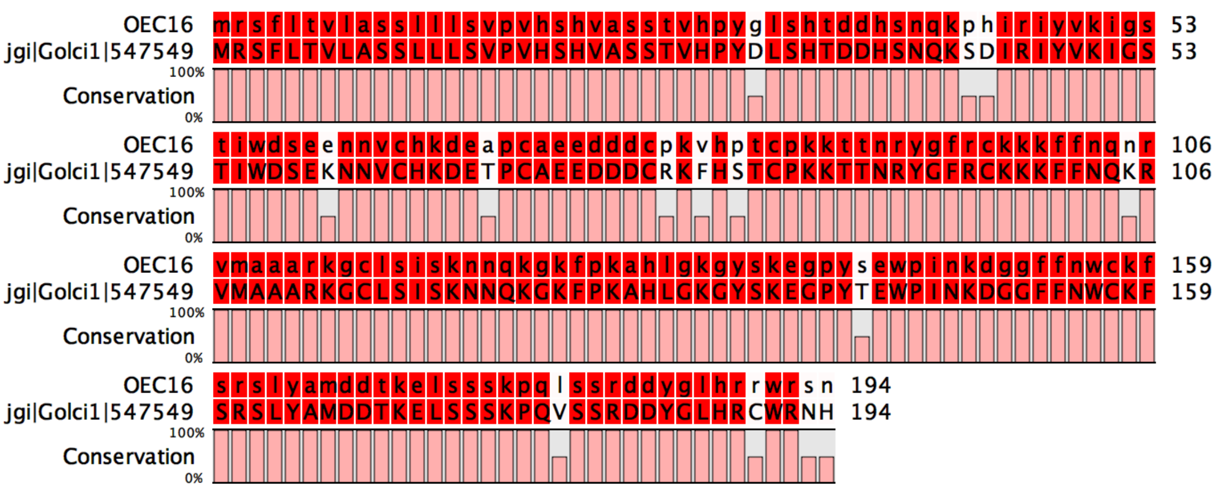

Figure 5.1 Comparisons of GcEC8 and GcEC17 to G. orontii *homologs*

A. GcEC8 is 100% identical to OEC33.1 GcEC8 (jgi|Golci1|1731083, top) shares 100% protein sequence identity with the closest *G. orontii* homolog, OEC33.1 (bottom), though GcEC8 continues beyond the expected end of OEC33.1. Sequences were aligned using the Needleman-Wunsch algorithm.
B. GcEc17 (jgi|Golci1|547549|CE547548_9241, bottom) shares 93% protein sequence identity with the closest *G. orontii* homolog, OEC16 (top), Sequences were aligned using the Needleman-Wunsch algorithm (Needleman et al., 1970).

A

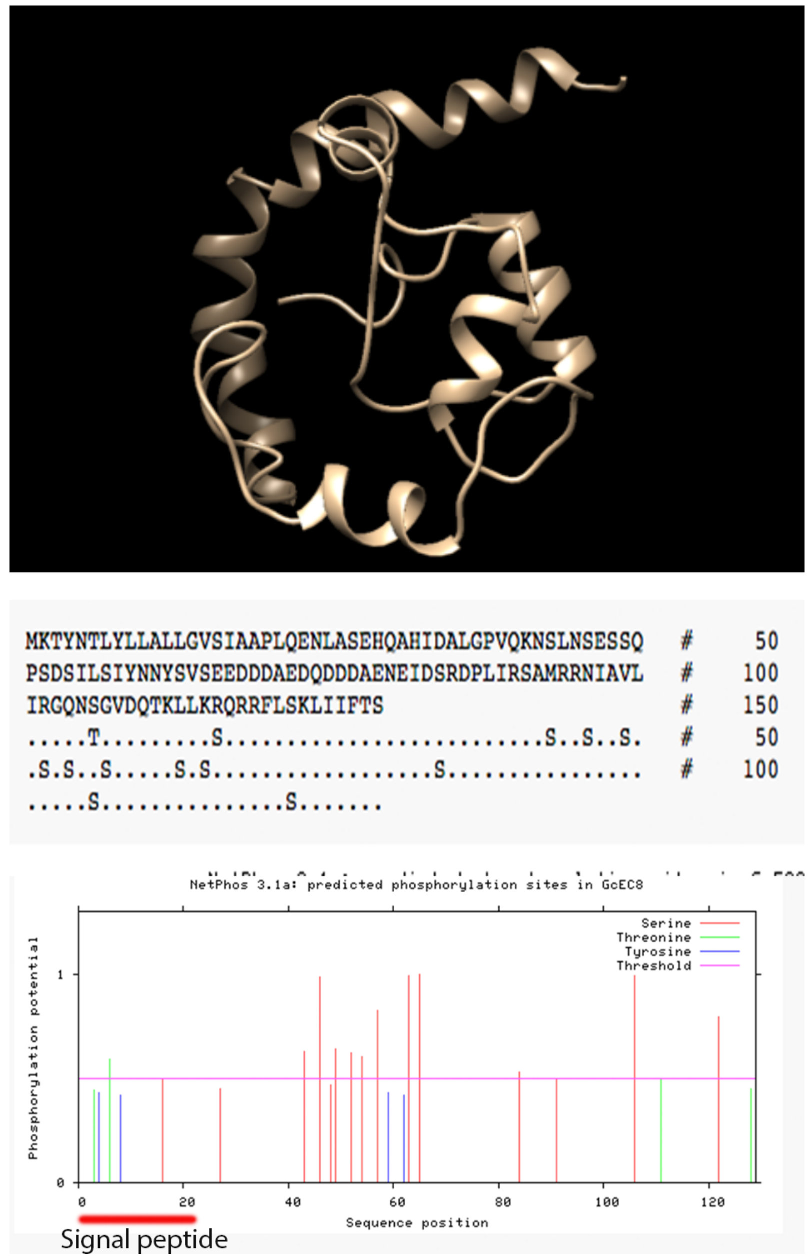

Figure 5.2 GcEC8 predicted structure

A. The amino acid sequence of GcEC8 was analyzed using Phyre 2.0 software and structure was predicted.
B. and C. Predicted phosphorylation sites of GcCE8 at serine, threonine and tyrosine residues, as predicted by NetPhos2.0. Threshold value of 0.5 phosphorylation is indicated. The signal peptide is indicated in red.

A

B

```
MRSFLTVLASSLLLSVPVHSHVASSTVHPYDLSHTDDHSNQKSDIRIYVK    #     50
IGSTIWDSEKNNVCHKDETPCAEEDDDCRKFHSTCPKKTTNRYGFRCKKK    #    100
FFNQKRVMAAARKGCLSISKNNQKGKFPKAHLGKGYSKEGPYTEWPINKD    #    150
GGFFNWCKFSRSLYAMDDTKELSSSKPQVSSRDDYGLHRCWRNH          #    200
..S..T........S....S....ST........T...............    #     50
..S....S..........T.............ST....TT..Y.......    #    100
................S.S.................S....Y........    #    150
.........S...Y........SSS....SS...Y.........
```

C

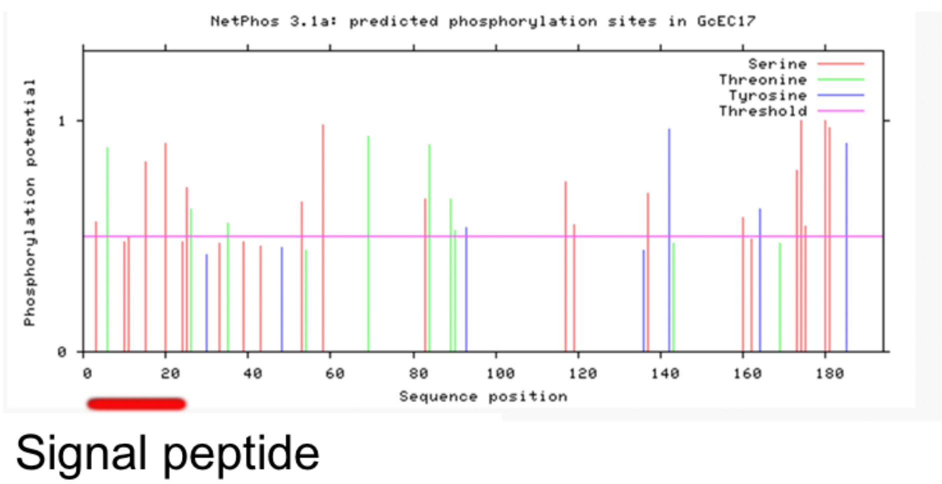

Figure 5.3 GcEC17 predicted structure

A. The amino acid sequence of GcEC17 was analyzed using Phyre 2.0 software and structure was predicted. The predicted RNase like domain (cyan) and the predicted nuclear localization signal (red) are indicated.
B. and C. Predicted phosphorylation sites of GcCE17 at serine, threonine and tyrosine residues, as predicted by NetPhos2.0. Threshold value of 0.5 phosphorylation is indicated. The signal peptide is indicated in red.

A

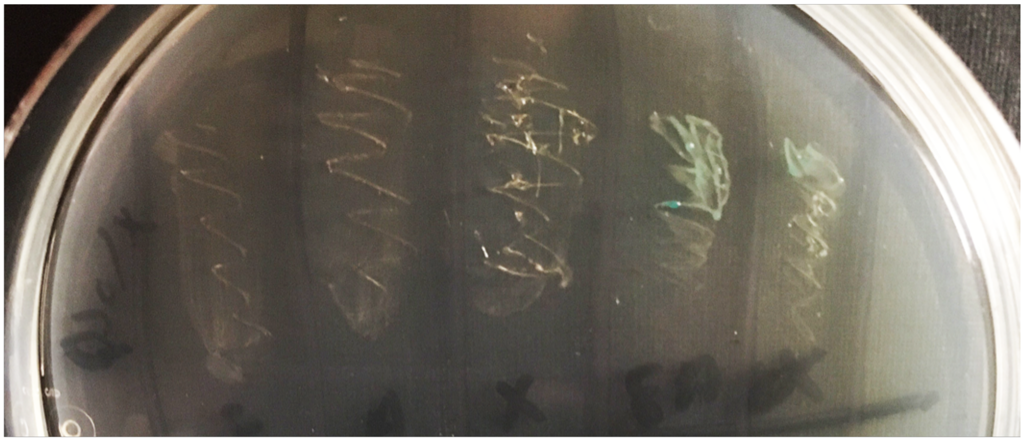

B

Figure 5.4 Identification of GcEC8 and GcEC17 interactors via yeast 2-hybrid analysis

A. GcEC8-sp interacts with AtAXR3 and AtXTH3 in Y2H. Yeast cells expressing GcEC8-sp-Gal4-DB, AtAXR3-Gal4-AD and AtXTH3-Gal4-AD in pGADT7, and co-expressing GcEC8-sp-Gal4-DB and atAXR3-Gal4-AD, GcEC8-sp-Gal4-DB and AtXTH3-Gal4-AD (bottom right) plated on synthetic defined media supplemented with amino acids missing histidine, adenine, tryptophan and leucine as well as x-a-gal and auerobasidin a.
B. GcEC17-sp interacts with At3g32930 and At4g29905 in Y2H. Yeast cells expressing GcEC17-sp-Gal4-DB, At4g29905-Gal4-AD and At3g32930-Gal4-AD in pGADT7and co-expressing GcEC17-sp-Gal4-DB and At4g29905-Gal4-AD or GcEC17-sp-Gal4-DB and At3g32930-Gal4-AD plated on synthetic defined media supplemented with amino acids missing histidine, adenine, tryptophan and leucine as well as x-a-gal and auerobasidin a.

A.

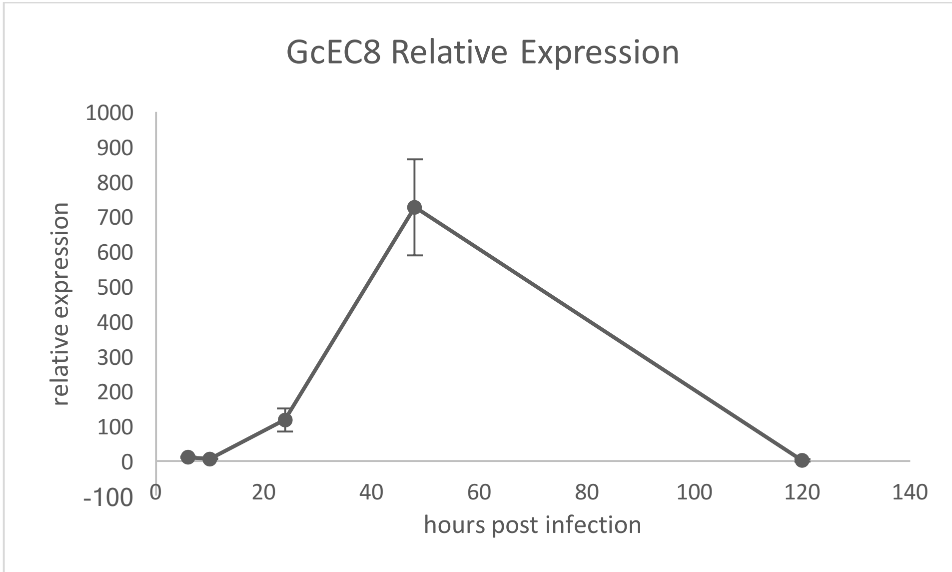

B.

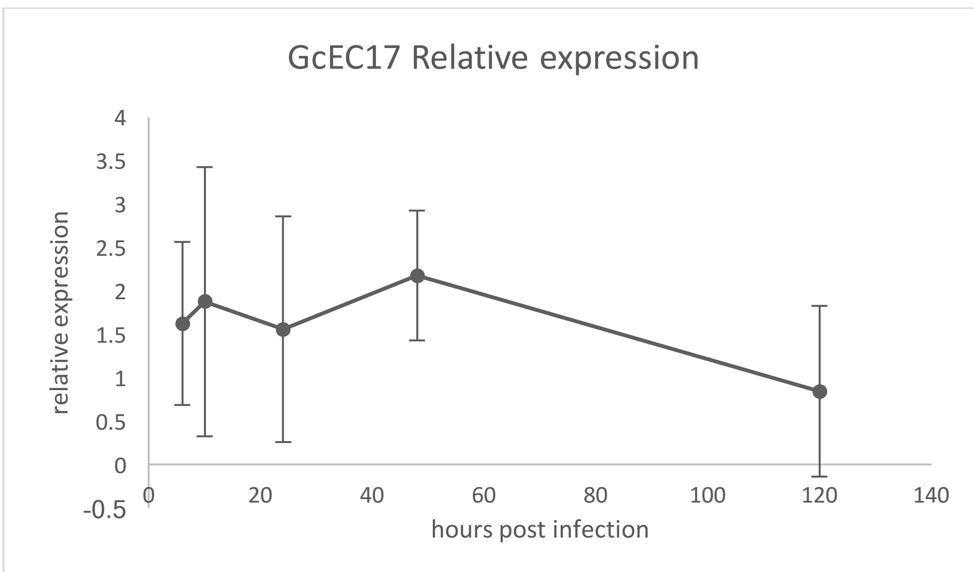

Figure 5.4 GcEC8 *and* GcEC17 *expression timecourse via qRT-PCR*

A. *GcEC8* expression was quantified relative to the expression of a *Go_EST_387* at 6 hpi, 10 hpi, 24 hpi, 48 hpi and 120 hpi. Results were normalized to 0hpi expression. Data includes three biological replicates and two technical replicates per treatment. Error bars indicate standard deviation.
B. *GcEC17* expression was quantified relative to the expression of *Go_EST_387* at 6hpi, 10 hpi, 24 hpi, 48 hpi and 120 hpi. Results were normalized to 0 hpi expression. Data includes three biological replicates and two technical replicates per treatment. Error bars indicate standard deviation.

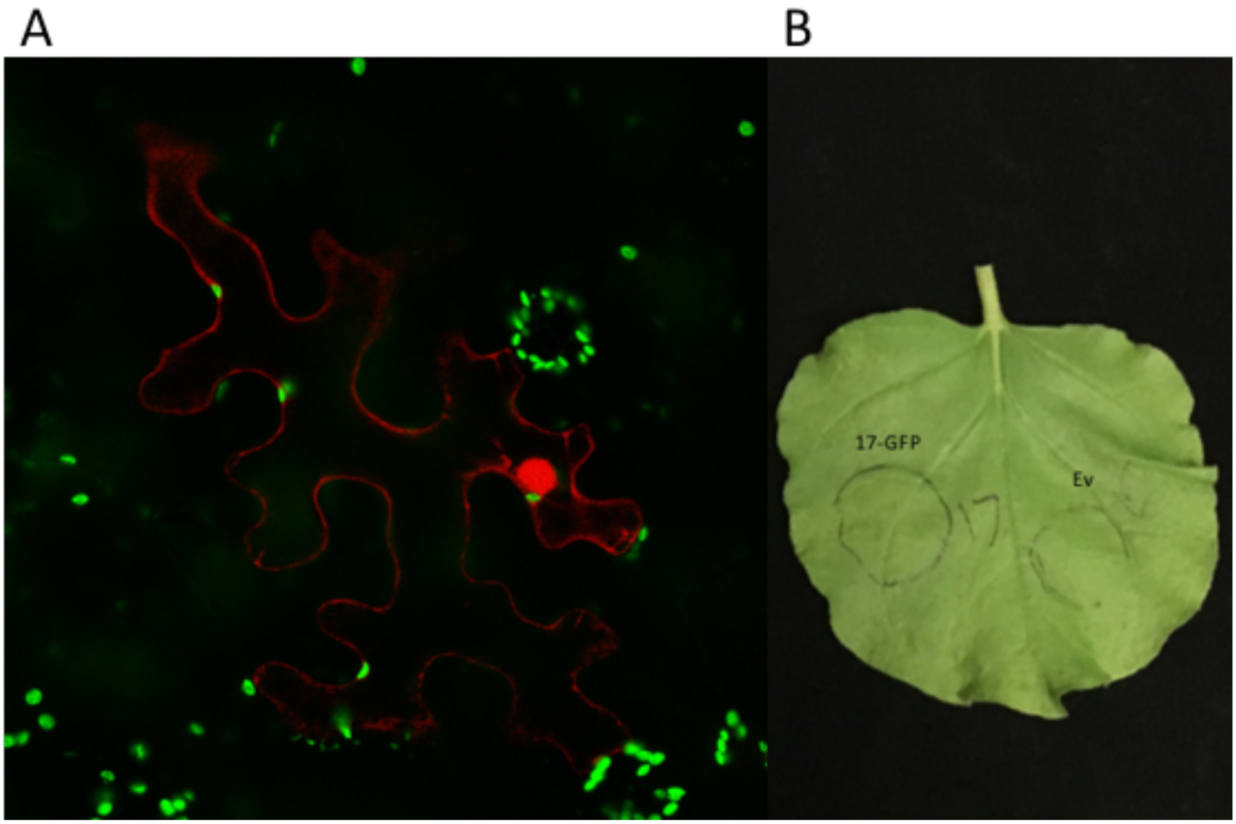

Figure 5.5 Transient expression of GcEc17-sp:GFP in N. benthamiana *leaves*

A. GFP fluorescence (red) was observed in the cytosol and nucleus 72 hours after infiltration when GcEC17-sp-GFP in pMDC84 was transiently expressed in *N. benthamiana* epidermal cells. Chlorophyll A autofluorescence (green) was observed as well.
B. Infiltrated *N. benthamiana* leaves 72 hours after *A. tumefaciens* infiltration, GcEC17-sp-GFP in pMDC84 (right) and pMDC84-EV (left). GcEC17-sp:GFP does not elicit any chlorotic or necrotic response in *N. benthamiana* leaves.

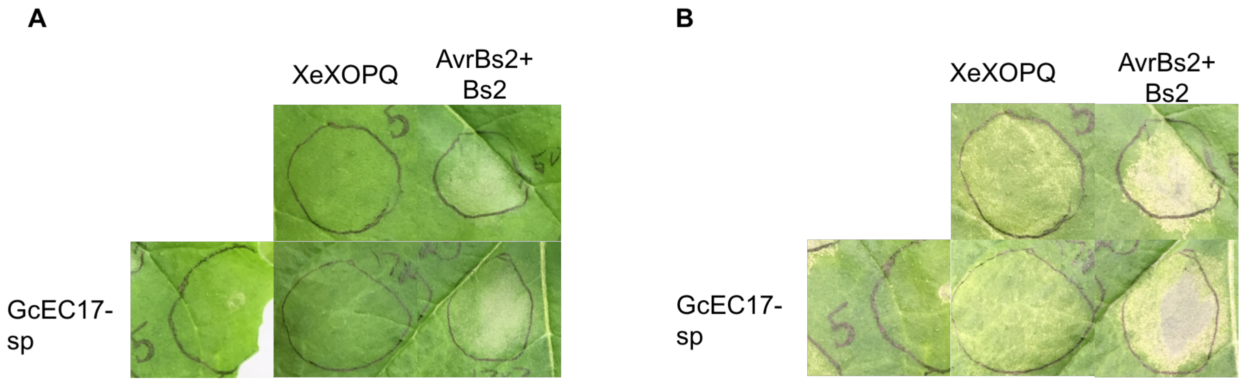

Figure 5.6 Transient GcEC17 *expression does not suppress effector-triggered* N. benthamiana *cell death*

A. GcEC17-sp transiently expressed in *N. benthamiana* leaves imaged at 2 dpi. GcEC17-sp (bottom panels) was coexpressed with XeXopQ (middle column panels) or AvrBs2/Bs2 (right column panels).
B. GcEC17-sp transiently expressed in *N. benthamiana* leaves imaged at 6 dpi. GcEC17-sp (bottom panels) was coexpressed with XeXopQ (middle column panels) or AvrBs2/Bs2 (right column panels).

Tables

Table 5.1 Primers used in Chapter 5

ID	Name	Sequence	Purpose
KSO-345	17flf	ATGCGATCTTTTCTCACTGTTTTG	For amplifying full length (fl) or mature (sp) GcEC17 from Gc cDNA
KSO-346	17flr	gttactgcgccaacgacg	
KSO-349	17-spf	atgcacgtcgcgtctagtacc	
KSO-343	8flf	atgaagacatacaacaccctgt	For amplifying full length (fl) or mature (sp) GcEC8 from Gc cDNA
KSO-344	8flr	TAGCAGATCGAATAAGGGA	
KSO-348	8-spf	ATGGCTCCCTTACAAGAAAA	
KSO-369	XTH3 F	ATGGACTATATGAGAATCTTTAGTGTTTTT	Amplification of AtXTH3
KSO-370	XTH3-NoStop R	ATAACATTCTCTAGGAGGAGTTTGGT	
KSO-371	AXR3 F	ATGATGGGCAGTGTCGAG	Amplification of AtAXR3
KSO-372	AXR3-NoStop R	AGCTCTGCTCTTGCACTT	
KSO-373	At3g32930 F	ATGCAACTCTCACTGGTTCAA	Amplification of At3g32930
KSO-374	At3g32930-NoStop R	AATGTTGGCGCCAGACC	
KSO-375	At4g29905 F	ATGTGTTTGGAAGTTGTGTATCAT	Amplification of At4g29905
KSO-376	At4g29905-NoStop R	TCAATAATACAAGACGAGATGACG	
KSO-281	T7 F	TAATACGACTCACTATAGGG	Sequencing confirmation of plasmids

Table 5.2 Plasmids used in Chapter 5

Plasmid Name	Description	Source
pMDC84-EV	Empty Vector	Somerville -20 Plasmid Stock
pGBKT7-p53	Y2H positive control	Jennifer Lewis Lab
pGBKT7-Lamin	Y2H negative control	Jennifer Lewis Lab
pGADT7-T-antigen	Y2H positive control	Jennifer Lewis Lab
pGBKT7-GcEC8-sp	GcEC8-sp-Gal4-DB in pGBKT7 for Y2H	This study
pGBKT7-GcEC17-sp	GcEC17-sp-Gal4-DB in pGBKT7 for Y2H	This study
pGADT7-XTH3	XTH3-Gal4-AD in pGADT7 for Y2H	Clontech Arabidopsis Normalized Mate & Plate library
pGADT7-AXR3	AXR3-Gal4-AD in pGADT7 for Y2H	Clontech Arabidopsis Normalized Mate & Plate library
pGADT7-At3g	At3g32930-Gal4-AD in pGADT7 for Y2H	Clontech Arabidopsis Normalized Mate & Plate library
pGADT7-At4g	At4g29905-Gal4-AD in pGADT7 for Y2H	Clontech Arabidopsis Normalized Mate & Plate library
pMDC32-GcEC8-sp	GcEC8-sp in pMDC32 under 35x promoter	This study
pMDC84-GcEC8-sp	GcEC8-sp in pMDC84 under 35S promoter with C-terminal GFP fusion	This study
pMDC44-GcEC8-sp	GcEC8-sp in pMDC44 under 35S promoter with N-terminal GFP fusion	This study
pDONR207-GcEC8-sp	GcEC8-sp in pDONR207 entry plasmid	This study
pMDC32-GcEC17-sp	GcEC17-sp in pMDC32 under 35x promoter	This study
pMDC84-GcEC17-sp	GcEC17-sp in pMDC84 under 35S promoter with C-terminal GFP fusion	This study
pMDC44-GcEC17-sp	GcEC17-sp in pMDC44 under 35S promoter with N-terminal GFP fusion	This study
pDONR207-GcEC17-sp	GcEC17-sp in pDONR207 entry plasmid	This study
pGBKT7GW	Gateway cloning vector for Gal4-DB fusion	Jennifer Lewis Lab
pGADT7	Cloning vector for Gal4-AD fusion	Jennifer Lewis Lab

Chapter 6: Developing a Method for the Generation of Stable Transformations of *G. cichoracearum*

Introduction

One aspect of *G. cichoracearum* biology that makes it a particularly difficult system to study is the lack of a reliable mechanism to genetically alter the fungus. A targeted system of changing, removing or adding genetic material has not yet been developed. The development of this type of system would allow for systematic study of potential effectors, elements required for biotrophy and host-specificity, and potentially the creation of a more experimental amenable system for studying this obligate biotrophic fungal pathogen.

Recently, a method for the transient plasmid transformation of *Podosphaera xanthii*, a powdery mildew that infects cucurbits, was described (Vela-Corcía et al., 2015). In this work, authors describe two methods of transferring a plasmid containing an antibiotic resistance marker and a GFP into the powdery mildew, which was then expressed. The researchers determined that the plasmid does not integrate into the fungal genome, nor does the plasmid replicate at the rate of the fungus, and as such it is diluted over the course of the fungal cell divisions and is not present in the next generation of powdery mildew. We thought to combine this transient transformation method with the developing CRISPR-Cas9 technology to potentially create a method to make stable, targeted changes in the *G. cichoracearum* genome.

The CRISPR-Cas9 system uses a bacterially-derived endonuclease, Cas9, to initiate the targeted mutagenesis of the Arabidopsis genome. The Cas9 protein forms a complex with a guide RNA molecule that contains a sequence targeted to a nucleotide sequence in the genome of the organism of interest. When recognized by the guide RNA, the Cas9 binds to the DNA and causes DNA damage. This damage initiates a double-stranded break repair response from the host, which often results in a single base pair insertion/deletion, causing a frame-shift mutation. This can be used to inactivate the gene of interest (Barrangou et al., 2007, Feng et al., 2013).

We thought to replace the GFP in the transiently expressed powdery mildew plasmid with Cas9 and a targeted guide RNA. We reasoned that, while the plasmid itself is not stably integrated into the genome, by expressing the Cas9 protein and guide RNA, we could induce a stable genetic change via a transiently expressed protein. We chose to attempt to silence non-lethal *G. cichoracearum* genes targeted by previously described silencing experiments (*GcAde1, GcAde2,* and *GcEC1)*

To achieve these ends, we first determined the success of the sgRNA pairs when incubated *in vitro* with purified Cas9 protein. We also attempted to optimize the transformation conditions for *G. cichoracearum*, based on those described by Vela-Corcía et al. (2015). In order to measure success, we first evaluated various artificial substrates as surfaces for the germination of *G. cichoracearum*. Identifying the optimal artificial germination surface would allow us to easily evaluation electroporation conditions in terms of conidial survival without introducing the confounding factor of the plant host. We also worked to evaluate various components of the transformation buffers described in the previous work. Although we were unable to achieve successful transient transformation of *G. cichoracearum*, we report the results of the optimization experiments here.

Cas9 can target G. cichoracearum *genomic DNA in vitro*

First, we assessed the viability of Cas9 targets in *G. cichoracearum in vitro*. We designed and synthesized guide RNAs that would target *GcAde1, GcAde2, and GcEC1 (*Table 6.1*).* These genes were chosen as they did not have obvious phenotypic affects when silenced in *G. cichoracearum* via HIGS, as described previously. This was a consideration as it was necessary for the mildew to survive without the genes targeted in these experiments, and the HIGS results indicated that silencing these genes may have little effect on the survival of the powdery mildew.

The Cas9 protein and amplified *G. cichoracearum* genomic DNA for each of the targets was incubated with and without the synthesized guide RNAs. We then determined whether the DNA had been cut via gel electrophoresis and visualization with ethidium bromide. We determined that all three genes were successfully targeted by the guide RNA/Cas9 combination *in vitro* to some extent*.*

The concentrations of all three full-length target sequences were reduced after incubation with Cas9 and the corresponding sgRNA when compared to incubation with Cas9 alone, as evidenced by the reduction of the intensity of the DNA bands (Figure 6.1). The band corresponding to the full-length *GcAde2* was completely absent, indicating efficient targeting by the Cas9/sgRNA complex. *GcEC1* was also targeted successfully, though not digested completely, as evidenced by the reduction in full-length amplified *GcEC1* and an accumulation of a smaller product, indicated by a red arrow. The concentration of *GcAde1* full length DNA was also reduced, though no smaller fragments were observed in this case.

These results indicate that the targeting of *G. cichoracearum* genes by the Cas9 protein with corresponding sgRNA is possible to varying degrees. For future experiments, this *GcAde2*-targeted sgRNA could be used, as it was determined to be the most efficient. This experiment was repeated 2 times with similar results.

Germination of G. cichoracearum *spores on artificial surfaces*

Artificial surfaces, including cellulose membrane, Teflon tape, and a glass slide, were prepared for use by washing three times in deionized water and blotted dry. The membrane and tape were placed on a 2% water-agar plate. Fresh *G. cichoracearum* spores were collected from heavily infected *C. sativa* leaves by tapping leaves over the surface of the glass slide, cellulose membrane, or Teflon tape. The glass slide was placed in an empty petri plate containing 1mL of diH_2O. The covers of all plates were applied and the plates were placed in darkness. 24 hours later, 200uL of water were washed over the surface to collect the spores, and the germination rate was measured via visualization using light microscopy. *B. graminis f. sp. hordei* spores were also germinated on a glass slide as a comparison in the same manner.

We found that the spores germinated on Teflon tape achieved an average germination rate of 22%. Spores germinated on cellulose membrane achieved an average germination rate of 21.25%. Spores germinated on a glass slide achieved an average germination rate of 26.875% (Figure 6.2). *B. graminis f. sp. hordei* spores germinated on a glass slide achieved a germination rate of 67.75%. These experiments were repeated twice with similar results.

Transient transformation of G. cichoracearum *and* P. neolycopersici *via electroporation*

We attempted to replicate the results of Vela-Corcía et al. (2015) in the *G. cichoracearum-C. sativa* system, as well as with the tomato powdery mildew *Pseudoidium neolycopersici* race *MF1*.

P. neolycopersici race *MF1* is a strain of *P. neolycopersici* isolated in Berkeley, CA in 2017. *P. neolycopersici* is able to infect susceptible tomato cultivars, and has been shown to infect Arabidopsis plants, as well. Compared to *G. cichoracearum*, *P. neolycopersici* produces spores that are more robust to submersion in water (G. Yu, personal communication).

The plasmid used to attempt to transform *G. cichoracearum, pCPXBteGFP,* was provided by Alejandro Pérez-Garcia, and is the plasmid which was used to successfully transform *P. xanthii*. The plasmid encodes the *P. xanthii* β-tubulin gene *PxTUB2* which confers resistance to the antibiotic Carbendazim under the native *P. xanthii* promoter, as well as *eGFP* controlled by the *A. nidulans gpd* promoter.

Initial attempts to follow the protocol produced no powdery mildew growth on *C. sativa* cotyledons or *Solanum lycopersicum* leaves. These conditions resulted in necrotic damage to the plant tissue thought to be related to the high concentration of mannitol in the recovery solution.

We performed experiments to optimize the recovery media to allow for the germination of our spores and to limit the damage to the leaf tissue. First, we measured the germination rate of spores on an artificial surface before and after electroporation, using the buffer conditions published in Vela-Corcía (2015). We found that electroporation itself did not seem to have a negative effect on conidial germination, however the germination rate of spores in both conditions was significant lower than that of spores that were transferred directly from infected leaves to the surface of the glass slide. 6 of 80 (7.5%) of spores germinated in the non-electroporated condition, while 9 of 97 (9.2%) of spores germinated in the electroporated condition (Figure 6.3A).

We then measured the germination rates of spores that were electroporated and rescued in varying concentrations of mannitol recovery buffer. We include the published concentration of 0.5M, as well as 0.1M, 0.01M and 0.05M mannitol. We found that no spores germinated in recovery buffer with low (0.01M and 0.05M) concentrations of mannitol, and that spores were able to germinate to similar levels in 0.5M and 0.1M mannitol recovery buffers, 5.5% and 7.2%, respectively (Figure 6.3B). This experiment was repeated with similar results.

We then determined that the spores were able to survive electroporation in both 0.1M sorbitol recovery media, as evidenced by propidium iodide staining, 6hr post electroporation, *(*Figure 6.4). This stain preferentially dyes dead cells, and was used to quantify the number of cells surviving the electroporation treatment*.* Electroporation of *G. cichoracearum* conidia and rescue in 0.1M sorbitol resulted in a decrease in average survival from 50% to 23%. This experiment was repeated twice with similar results.

We tested the ability of both mildews to infect detached cotyledon or leaf tissue when applied as a solution of conidia that had been transformed with the GFP-expressing plasmid used in Vela-Corcía et al. (2015). We tested recovery media ranging from 0.1M mannitol to 0.5M mannitol to test the effect of the recovery media on the leaves during the infection time-course. We also tested both 0.1M mannitol and 0.1M sorbitol, as sorbitol was thought to have less of a toxic effect for the plant tissue (Table 6.2).

At 15 days post inoculation, we observed the detached leaves for powdery mildew growth macroscopically and for GFP fluorescence using an epifluorescence microscope (Figure 6.5). No fungal growth was observed on the leaf surface on either cucumber or tomato leaves, and no GFP signal was detected at 15 days or at any earlier time-point. The condition of the leaves was noted for each condition, and it was determined that concentrations of 0.1M and 0.2M mannitol in the rescue buffer did not result in macroscopic lesion formation of the surfaces of detached leaves. These experiments were repeated twice with similar results.

Although the plasmid encodes a resistance gene to the antibiotic carbendazim, we did not apply this antibiotic to the surface of the leaves. Despite this, we did not observe any powdery mildew growth.

Direct delivery of Cas9 protein via electroporation

We attempted to deliver the Cas9 and guide RNA corresponding to the fungal *GcAde2* gene directly into fungal conidia via electroporation. Electroporated conidia were rescued in a solution of 0.1M sorbitol, and then sprayed onto cucumber leaves, as described above. We were unable to observe any powdery mildew growth from electroporated conidia using similar conditions to those described above.

Discussion

Here, we described initial attempts to develop a reliable, stable system to introduce targeted genetic modifications in the powdery mildew system. Once this system exists, researchers will be able to induce insertion/deletion mutations in targeted genes in the powdery mildew genome, allowing for the study of individual gene disruptions and functional characterization of interesting genetic elements of the pathogen. Additionally, it has been shown that co-expression of double-stranded DNA with the Cas9 and guide RNA can lead to integration of the DNA into the genome in yeast (Lee et al., 2015). This could lead to the ability to add genes to the powdery mildew genome, allowing for even better manipulation and study of the pathogen.

We provide *in vitro* evidence that Cas9 and guide RNA pairs can be used to target non-lethal *G. cichoracearum* genes. We found that the targeting efficiency for these genes varied, and further optimization could be performed in the future to ensure the best results. We hope that these targets, especially *GcAde2,* which was effectively targeted with the sgRNA used in this study, can be used in the future to verify the efficacy of Cas9 expression in the powdery mildew system.

While we could not introduce the protein-RNA complex to the powdery mildew conidia directly via electroporation, we believe that this still may be a possible mechanism for fungal transformation. The Cas9 protein, which is 168 kD, is likely too large to be delivered through the pores in the fungal cell wall. The introduction of cell wall degrading or loosening enzymes may enlarge the pore size and allow for the direct delivery of the protein in the future. It also may be possible to create and transform powdery mildew conidial sphaeroplasts, which are produced via the complete degradation of the fungal cell wall, though it is thus far unknown whether viable conidia could be regenerated from sphaeroplasts using this technique.

In order to evaluate the lethality of transformation methods, we determined the ability of *G. cichoracearum* to germinate on a variety of artificial substrates. We showed that *G. cichoracearum* is able to germinate to approximately the same level, 20-30% successful germination, on several surfaces, including a glass slide, a cellulose membrane, and Teflon tape. Glass slides were used for germination experiments, as they allowed for the easiest visualization and collection of germinated spores. Compared to the *B. graminis f. sp. graminis* rates of germination, which were measured to be 73%, *G. cichoracearum* spores have a low germination rate on artificial leaf surfaces. Additionally, germination rates of *G. cichoracearum* on leaf surfaces of Arabidopsis were observed to be significantly higher than that of spores on artificial surfaces, and was often as high as 80% in the previously described HIGS experiments. The mechanisms by which powdery mildew spores sense their environment are unknown, though these experiments hint at plant factors as being crucial at the earliest stages of powdery mildew growth.

We were unable to reproduce the published results described by Vela-Corcía (2015) to successfully transiently expressing plasmid-encoded proteins in the *P. xanthii* system in either *G. cichoracearum* or *P. neolycopersici*. We found the described conditions, including the use of 0.5M mannitol in the conidial electroporation recovery buffer, not conducive to the growth of powdery mildew. We describe here the attempted optimization of these conditions for *G. cichoracearum* and *P. neolycopersici.*

We were able to determine the optimal recovery buffer components for conidial germination and survival, however even these conditions did not allow for the growth of powdery mildew on the surface of plant leaves for either *G. cichoracearum* or *P. neolycopersici.* Further experimentation is needed to identify conditions that allow for both conidial survival and transformation in these systems. We determined that a recovery buffer with the concentration of 0.1M sorbitol or mannitol allows for the survival of a relatively small percentage of conidia, though we do not know what percentage, or even whether any of these conidia contain the plasmid of interest, as we were not able to observe growth that could be tested using the selection pressure of the encoded genetic resistance marker.

A larger proportion of conidia survived the electroporation than were observed to germinate on artificial substrates after this treatment, as evidenced by propidium iodide staining. It may be that a large proportion of *G. cichoracearum* spores are non-viable upon collection, however and this may be the bottleneck step for conidial survival and germination. It may be possible to increase this proportion by using only very fresh spores, which can be achieved by removing all of the older spores from the leaf surface 5 days before the experiment is to take place. We found that this drastically reduced the number of spores that were able to be collected. In order to balance the viability of spores collected from the leaf surface with the ability of researchers to collect an adequate number of spores for each experiment, further optimization of the timeline of infection and spore collection may be necessary.

We do not know the reasons for the failure of the described methods of transformation in *G. cichoracearum* and *P. neolycopersici* compared to *P. xanthii*. It is possible that *P. xanthii* spores are simply more robust than either the *G. cichoracearum* or *P. neolycopersici* spores, and as such are better able to survive after the application of electricity and suspension in the electroporation and recovery buffers. We hope that these results will lead to the eventual development of successful transformation efforts in many powdery mildew systems.

Figures

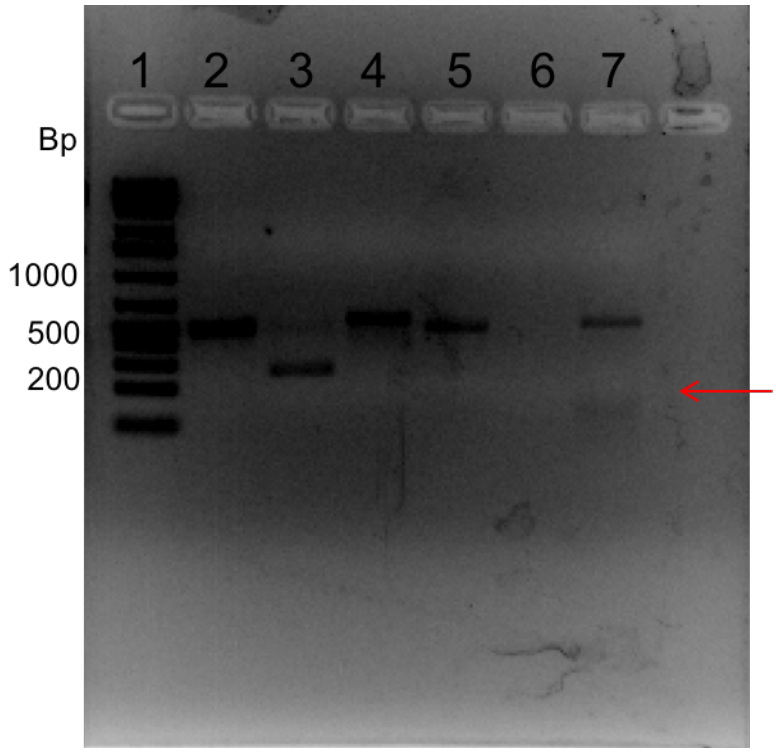

Figure 6.1 In vitro verification of Cas9 activity on G. cichoracearum *targets*. Amplified genomic DNA was incubated with purified Cas9 protein (lanes 2-4) and with Cas9+sgRNA (lanes 5-7) and run on 1% agarose gel with ethidium bromide and GeneRuler 1kb plus ladder (lane 1). Target genes GcAde1 (Lanes 2 and 5), GcAde2 (Lanes 3 and 6), and GcEC1 (Lanes 4 and 7). The red arrow indicates the presence of a faint band at approximately 200bp in Lane 7.

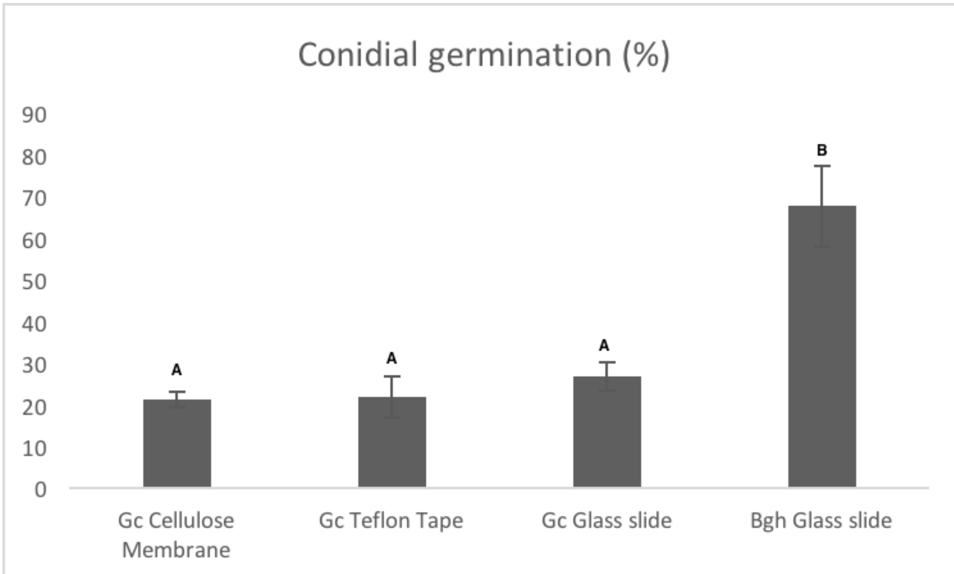

Figure 6.2 Germination rates of G. cichoracearum *and* B. graminis f. sp. hordei *spores on artificial substrates*

G. cichoracearum (Gc) spores were deposited on various artificial substrates (cellulose membrane, Teflon tape, and the surface of a glass slide) and germination was assessed via light microscopy at 6hpi. *B. graminis f. sp. hordei* (Bgh) spores were germinated on a glass slide under the same conditions and assessed in the same manner. One-way ANOVA with post-hoc Tukey HSD was performed on the results, with Bonferroni multiple comparison. No significant difference was determined between the *G. cichoracearum* spores in any treatment (A), while all three treatments differed significantly from the germination rate of *B. graminis f. sp. hordei* on the surface of a glass slide (B) with $p<0.01$.

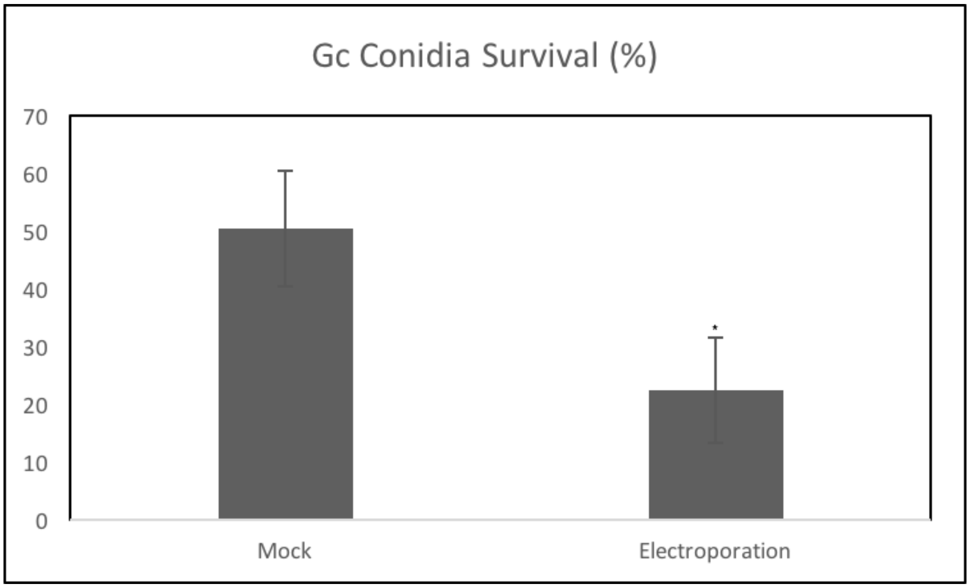

Figure 6.3: Cell death, as quantified by staining of electroporated conidia. ***G. cichoracearum*** conidia were stained with propidum iodide after electroporation and recovery in 0.1M sorbitol to determine the proportion of conidia that survived the treatment. Asterisk indicates p-value less than 0.05 as determined by student's t-test.

Figure 6.4 G. cichoracearum *transformation attempts on* C. sativa *cv. Bush Champion at 15 dpi in various recovery media.*
From right to left: 0.07M sorbitol without electroporation, 0.07M sorbitol with electroporation, 0.07M mannitol without electroporation, 0.07M mannitol with electroporation

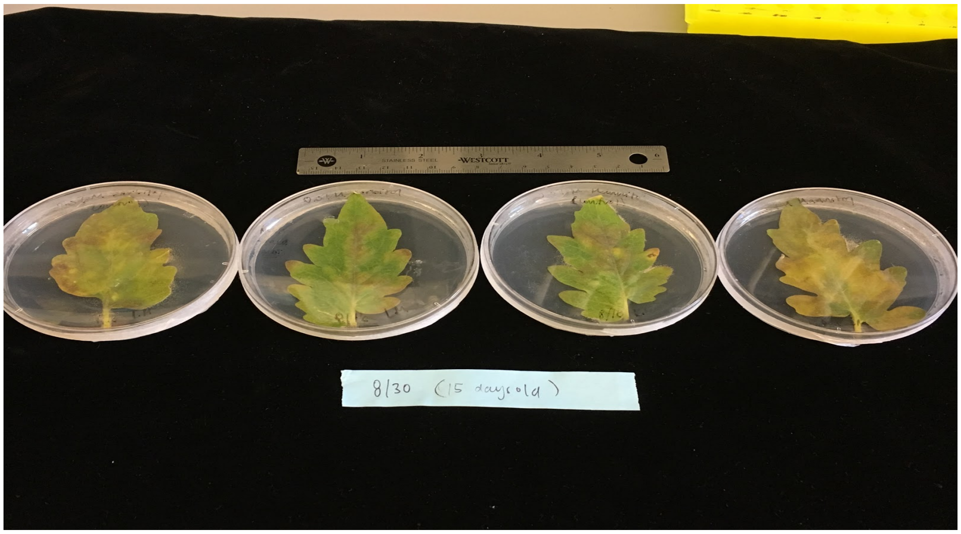

Figure 6.5 P. neolycopersici *transformation attempts on* S. lycopersicum *cv. Money Maker at 15 dpi.*
From right to left: 0.07M sorbitol without electroporation, 0.07M sorbitol with electroporation, 0.07M mannitol without electroporation, 0.07M mannitol with electroporation

Tables

Table 6.1 Guide RNA sequences used in Chapter 6

Target	sgRNA
GcAde1	GACCATGTAGATTTGAAGGG(CGG)
GcAde2	GAAGTGGGCAGACTTCAAAA(TGG)
GcEC1	GAGAAATCGTGTAAATGTTC(GGG)

Table 6.2 Conidial transformation conditions and results

Change	Rescue Buffer	Growth surface	Germination percentage	Leaf result	Transformation (GFP Fluorescence)
None (original)	0.5M Mannitol	Plant leaf	No fungal growth observed on plant leaves (crystalized sugar)	Toxic (necrotic spots observed)	None observed
Rescue Sugar	0.5M Sorbitol	Plant leaf	No fungal growth observed on plant leaves	Not toxic	None observed
None (original)	0.5M Mannitol	Glass slide	7%	n/a	n/a
No Electroporation	0.5M Mannitol	Glass slide	9%	n/a	n/a
Rescue Buffer	0.5M Mannitol	Glass slide	5%	n/a	n/a
Rescue Buffer	0.1M Mannitol	Glass slide	7%	n/a	n/a
Rescue Buffer	0.05M Mannitol	Glass slide	0%	n/a	n/a
Rescue Buffer	0.01M Mannitol	Glass slide	0%	n/a	n/a
Rescue Buffer	0.5M Mannitol	Plant leaf	No fungal growth observed on plant leaves	Toxic (necrotic spots observed)	None observed
Rescue Buffer	0.3M Mannitol	Plant leaf	No fungal growth observed on plant leaves	Semi-toxic (some necrosis observed)	None observed
Rescue Buffer	0.2M Mannitol	Plant leaf	No fungal growth observed on plant leaves	Not toxic	None observed
Rescue Buffer	0.1M Mannitol	Plant leaf	No fungal growth observed on plant leaves	Not toxic	None observed

Table 6.3 Primers used in Chapter 6

ID	Name	Sequence	Purpose
KSO-304	ade1 cc9 region F	cgattgtgcgtggttacatc	Amplification of GcAde1 region targted by sgRNA/Cas9
KSO-305	ade1 cc9 region R	cacaccgtcaactccttgaa	
KSO-306	ade2 cc9 region F	ctaccccagagacagccaac	Amplification of GcAde2 region targted by sgRNA/Cas9
KSO-307	ade2 cc9 region R	ggctctggaagaattcagga	
KSO-308	gcec1 cc9 region F	cctacgacaatttggcacct	Amplification of GcEC1 region targted by sgRNA/Cas9
KSO-309	gcec1 cc9 region R	gcgactaagctcgctactgc	
KSO-313	As-181 (in vitro cas9 activity reverse primer)	aaaagcaccgactcggtgccactttttcaagttgataacggactagccttatttAaact tgctaTGCTGtttcCAGCAtagctctTaaac	Reverse primer for synthesis of sgRNA
KSO-314	ade1 specific sgrna synth v 2.0	TAATACGACTCACTATAGGGAAGTTTAGATGTACCAGCGTgtttAa gagctaTGCTGgaa	Forward primer for GcAde1-targeted sgRNA synthesis
KSO-315	ade2 specific sgrna synth v 2.0	TAATACGACTCACTATAAGACCTGTACGCAGAGAAGTGGGgtttAa gagctaTGCTGgaa	Forward primer for GcAde2-targeted sgRNA synthesis
KSO-316	gcec1 specific sgrna v 2.0	TAATACGACTCACTATAGGGCTTGTAAATGTGCTAAAGAGgtttAa gagctaTGCTGgaa	Forward primer for GcEc1-targeted sgRNA synthesis

Table 6.4 Plasmids used in Chapter 6

Plasmid Name	Description	Source
pCPXBteGFP	GFP-expression plasmid from Vela-Corcía et al. (2015)	Perez-Garcia Lab

Chapter 7: Isolation of High Molecular Weight Genomic DNA and RNA from *G. cichoracearum* for High-Throughput Sequencing Applications

Preface

This chapter is taken in its entirety, with minor formatting adjustments, from a published research method, "Purification of High Molecular Weight Genomic DNA from Powdery Mildew for Long-Read Sequencing", which was published in 2017 in *The Journal of Visualized Experiments* (Feehan, Scheibel et al., 2017). This method was co-authored by Joanna Feehan, Salim Bourras, William Underwood, Beat Keller, Shauna Somerville, and myself. Joanna Feehan and I conducted the experiments leading to the development of this method, based on preliminary experiments by William Underwood. Beat Keller and Salim Bourras published an earlier protocol which was used as a reference. I composed the initial draft of the manuscript, and Joanna Feehan, Shauna Somerville and I produced the figures. All authors of this review worked together to edit the manuscript to produce the final published version.

Introduction

Powdery mildews are a group of obligate biotrophic fungal plant pathogens that, when taken together, are the largest cause of plant disease worldwide (Agrios, 1969). There are over 900 described species of powdery mildew, which have been taxonomically grouped into five tribes within the family *Erisyphaceae (*Braun & Cook, 2012). Due both to their economic importance and the intimate relationship they develop with their hosts, powdery mildew diseases have been the subject of research for >100 years. Upon infection, powdery mildews elicit drastic changes in the cellular structure, metabolism and molecular biology of their hosts, to benefit this pathogen. However, the study of powdery mildews is particularly challenging due to their obligate lifestyle, and growth of the fungus in pure culture has not yet been described (Both et al., 2005, Glawe et al., 2008, Fabro et al., 2008, Hückelhoven & Panstruga, 2011, Micali et al., 2011, Chandran et al., 2010). Reliable, stable genetic transformation of powdery mildews has also not yet been accomplished, although transient transformation has been reported in some species (Spanu & Panstruga, 2012, Vela-Corcía et al., 2015).

The sequencing and assembly of powdery mildew genomes has proven difficult due to a number of features of the genome itself. Powdery mildew genomes are large (120-180 kbp) relative to other fungal genomes, and consist of 60-90% evenly distributed repetitive elements (Hacquard, 2014). These elements include non-long terminal repeats, as well as uncategorized repetitive elements. Two formae specialis of a single powdery mildew species, *Blumeria graminis f. sp. hordei* and *f. sp. tritici* as well as the grape powdery mildew *Erysiphe necator,* have been sequenced, and draft genomes for several others have been completed (Spanu et al., 2010, Wicker et al., 2013, Jones et al., 2014). The repetitive nature of the genomes has made assembly difficult, and the completed Bgh genome was assembled into 6989 supercontigs with an L50 of 2 Mb (Spanu et al., 2010).

Despite the large genome, the powdery mildews appear to have a small number of protein coding genes, with 5,845 and 6,540 genes predicted in *B. graminis f. sp. hordei* and *B.*

graminis f. sp. tritici, respectively. The sequenced powdery mildews also appear to lack at least 99 core genes that are essential in other fungi, which is consistent with the dependence of the fungi on their host plant for survival (Hacquard et al., 2014, Spanu et al., 2010, Wicker et al., 2013, Jones et al., 2014).

Repetitive sequences near telomeres, centromeres, ribosomal RNA gene arrays and regions enriched in transposable elements are poorly assembled from short-read sequencing strategies and are often under-represented in genome assemblies (Thomma et al., 2016). Such regions are thought to be responsible for many of the gaps that occur in genome sequences, and this applies to the powdery mildews with their extensive expansion of repetitive elements (Parlange et al., 2011). Highly plastic genome regions are often found in such repetitive regions (Parlange et al., 2011). They serve as a site of chromosome rearrangements and often encode genes under strong selective pressure, such as the genes encoding effector proteins and the genes encoding enzymes of secondary metabolism. Advances in single-molecule long-read sequencing technologies provide a potential solution for sequencing across repetitive regions of genomes (Thomma et al., 2016). For example, Faino et al. (2015) found that including long-sequence read technologies and optical mapping allowed them to produce a gap-less genome sequence for two strains of the fungal plant pathogen *Verticillium dahlia*, tripling the proportion of repetitive DNA sequences in the genome, increasing the number of gene annotations (and reducing the number of partial or missing gene annotations) and revealing genome rearrangements (Faino et al., 2015).

To employ these long-read sequencing technologies, high concentrations of high quality genomic DNA, with minimal sizes >20 kbp, are needed. Here we describe our methods for conidial collection, purification of high molecular weight DNA from conidia and our quality control assessments using the powdery mildew species *Golovinomyces cichoracearum* grown on cucumber (Adam et al., 1999). This protocol is based on a protocol developed in the B. Keller laboratory group (University of Zürich, Zürich Switzerland) (Wicker et al., 2013, Bourras et al., 2015) and includes several modifications that led to increased DNA yields and a higher proportion of DNA >48.5 kbp in size. The protocol also includes quality control steps based on recommendations from the United States Department of Energy Joint Genome Institute (JGI, 2016).

Protocol:

1. Preparation of Fungal Material

1.1) Growing Powdery Mildew

Plants were grown in growth chambers with the following conditions: 22° C day temperature, 20°C night temperature, 80% relative humidity, 14-hr day-length and a light intensity of 125 µE/m2/sec provided by fluorescent lighting. Cucumber plants (*Cucumis sativa* variety Bush Champion) were infected with *Golovinomyces cichoracearum* strain UCSC1 as described (Adam et al., 1999, Wilson et al., 2001).

1.2) Harvesting Powdery Mildew Conidia

Harvest conidia from infected plants at 7-10 days after inoculation using a small vacuum with an in-line filter (11 µm) on which the conidia accumulate. Applying gentle pressure, run the vacuum nozzle along the surface of the leaf to collect the conidia. The average yield of *G. cichoracearum* is 20 mg of conidia from a heavily infected cucumber leaf of approximately 130 cm^2 in area. Brush about 150 mg of the conidia (approximately 375 µL volume) from the filter onto a sheet of clean paper. From here, transfer conidia into 2 mL cryovials with two 5/32-inch diameter steel milling balls that have been pre-chilled in liquid nitrogen. Immediately return tubes to liquid nitrogen. Store tubes at -80° C.

1.3) Breaking Open Conidia by Ball Milling

Flash freeze aluminum plates of ball mill in liquid nitrogen. Vigorously shake the cryovials with conidia and steel balls in the ball mill for 30 seconds at 30 cycles/sec. Immediately refreeze cryovials in liquid nitrogen.

Initially, a sample of conidia should be assessed by microscopy at 100X magnification for efficiency of cell wall rupture during grinding. If needed, grind for an additional 1-2 rounds of 30 sec for 30 cycles/sec but keep the number of rounds to a minimum. Routine assessment of conidial breakage by microscopy at this stage is unnecessary once optimal conditions have been established.

2. Genomic DNA Purification

2.1) Conidia Lysis

Working quickly to avoid thawing conidia, remove the steel balls from cryovials with a magnet. Add 700 µL 65° C lysis buffer (Table 7.1) and vortex 5-10 sec until a slurry is formed. At all subsequent steps, mix by gentle, slow inversion (1 inversion per 3 sec) and transfer DNA-containing solutions with wide-bore pipette tips. Add 300 µL pre-warmed (65° C) 5 % (v/v) sarcosyl, gently invert to mix five times. Incubate tubes for 30 min at 65° C; invert gently 3 times at 10, 20 and 30 min. Using wide-bore pipette tip, transfer entire solution to new 2 mL microcentrifuge tube.

2.2) DNA Extraction I

Add 1 volume of chloroform:isoamyl alcohol (24:1 v/v) to lysis solution, gently invert to mix five times. Incubate for 10 min at room temperature, gently inverting to mix five times at the halfway point and again at the end of the incubation. Centrifuge at room temperature for 15 min at 14,000 x g. Using wide-bore pipette tip, carefully transfer aqueous layer to new 2 mL microcentrifuge tube; avoid including material from the interface.

2.3) DNA Precipitation I

Add 1 volume room temperature 100% isopropanol (approximately 750 µL), gently invert to mix six times. Centrifuge at room temperature for 15 min at 14,000 x g. Carefully remove supernatant and discard. Add 450 µL pre-chilled (-20°C) 70% ethanol. Centrifuge for 5 min at room temperature at 14,000 x g. Carefully remove supernatant and discard. Centrifuge at 1,000 x g for 3 sec. Carefully remove supernatant with fine pipette tip and discard. Air-dry pellet for 15 min at room temperature. Do not dry for longer than 15 min. Resuspend pellet in

300 µL TE (10 mM Tris-Cl, 1 mM ethylene diamine tetra-acetic acid, pH 8.0). Incubate overnight at 4° C, or 1 hr at 65° C if necessary. Gently flick to resuspend any residual material that did not go into solution.

2.4) Remove RNA Contamination

Add 10 µL RNase A (10 mg/mL), gently invert to mix three times. Centrifuge at 1,000 x g for 3 sec. Incubate at 37° C for 2 hr.

2.5) DNA Extraction II

Add 300 µL phenol:chloroform:isoamyl alcohol (25:24:1 v/v), gently invert to mix five times. Incubate 10 min at room temperature, gently inverting to mix five times at the halfway mark and again at the end of the incubation. Centrifuge 15 min at room temperature at 14,000 x g. Using wide-bore pipette tip, transfer supernatant to new 1.5 mL microcentrifuge tube.

2.6) DNA Precipitation II

Add 0.01 volume 3 M sodium acetate pH 5.2 (approximately 3 µL), gently invert to mix five times. Add 2.5 volumes pre-chilled (-20° C) 100% ethanol (approximately 750 µL). Gently invert to mix five times. Incubate overnight at -20° C. Centrifuge 30 min at 4° C at 14,000 x g. Carefully remove the supernatant and discard. Add 450 µL pre-chilled (-20° C) 70% ethanol. Centrifuge for 5 min at 4° C at 14,000 x g. Carefully remove supernatant and discard. Centrifuge at 1,000 x g for 3 sec. Carefully remove supernatant with fine pipette tip and discard. Air-dry pellet for 30-60 min at room temperature. Resuspend pellet in 27.5 µL TE. Incubate overnight at 4° C, or 1 hr at 65° if necessary. Gently flick to resuspend any residual material that did not go into solution.

Aliquot 2.5 µL into 22.5 µL TE (final volume 25 µL) for quality control tests (see below). Take care when pipetting at this step as the high molecular weight genomic DNA can be difficult to pipette properly, and it is important to ensure that “QC Aliquot” is an accurate representation of genomic DNA sample.

Store DNA samples at 4° C until submission for sequencing. For long-term storage, store samples at -80°C and minimize freeze-thaw cycles to prevent shearing.

3. Quality Control

3.1) Sample Purity

Using a TE blank, assess the sample purity of the DNA by loading 1 µL of the QC Aliquot on a small-volume spectrophotometer. Record A260/A280 and A260/A230 readings. Pure DNA will have an A260/A280 ratio of approximately 1.8 and A260/A230 ratio between 1.8 and 2.2.

3.2) Quantification of Genomic DNA

Perform quantification of QC aliquot using a commercial double-stranded DNA quantification assay kit according to manufacturer instructions.

3.3) DNA Quality Assessment I

Load approximately 60 ng genomic DNA and a DNA ladder on an 0.7% agarose gel in 1X TAE (40 mM Tris, 20 mM acetic acid, and 1 mM EDTA, pH 8.0). Run gel apparatus until genomic DNA bands are 2 cm below the well and band, and separation in the ladder is apparent.

3.4) DNA Quality Assessment II

Load approximately 60 ng genomic DNA and a high molecular weight DNA ladder (suitable for pulsed-field gel electrophoresis) on a 1% agarose gel in 0.5X TBE (44.5 mM Tris, 44.5 mM boric acid, 1 mM EDTA, pH 8.3) and run in 0.5X TBE running buffer using a 5-80 kbp waveform pulsed-field gel electrophoresis protocol for 16 hr.

3.5) Assessment of Bacterial, Fungal, and Plant Contaminants

Perform polymerase chain reaction (PCR) to amplify the appropriate internal transcribed spacers (ITS) regions of the ribosomal genes using primers and amplification conditions listed in Table 7.2. Load 10 µL of the resultant reaction on a gel. A band representing the powdery mildew ITS region should be amplified with the fungal ITS primers. DNA from this amplicon and any amplicon generated with the bacterial, or plant primers should be sequenced to determine the origin of the contamination. Only powdery mildew ITS sequences should be found in the fungal amplicon.

Representative results:

A representative example of purified genomic DNA from *G. cichoracearum* run on an agarose gel using gel electrophoresis and using pulsed-field gel electrophoresis are shown in Figures 7.1 and 7.2, respectively. Genomic DNA preparations that pass, marginally pass and fail quality control are represented. Genomic DNA preparations that fully pass quality control are ideal for sequencing using long-read genome sequencing approaches. Preparations that marginally pass quality control are acceptable, but preparations that fully pass are preferred. Preparations that fail quality control are not acceptable for long-read genome sequencing approaches.

Discussion:

In order to obtain pure, high molecular weight genomic DNA from the obligate biotrophic powdery mildew fungi, a modified version of previously described methods was developed (Bourras et al., 2015). The average yield using this optimized protocol is 7 µg DNA per 150 mg conidia, a doubling of the yield obtained with a prior protocol. Also, the average size increased from approximately 20 kbp to over 48.5 kbp. This protocol was optimized in the cucumber-*G. cichoracearum* system. In order to obtain the best quality and highest purity DNA in other powdery mildew or obligate biotrophic fungi, additional modification of this protocol may be required.

Balancing high DNA yield and high molecular-weight of extracted DNA was a concern during the optimization of this protocol. Steps including vortexing were eliminated in order to minimize shearing of the DNA, and were replaced by gently mixing by inversion. This change increased the quality of the extracted DNA without significantly reducing the yield. Additionally, removal of the steel balls at the beginning the cell lysis step significantly increased DNA yield when compared to leaving the balls in the solution until the end of the lysis step.

No *G. cichoracearum* conidia remained intact after the ball milling procedure in step 1.3. To obtain good yields of high molecular weight genomic DNA, it is crucial that the fungal cell wall is disrupted during this step. Conidial integrity can be assessed microscopically, and additional ball milling or alternative methods of disruption may be required for other fungal species.

Some fungal conidia, notably the *Blumeria sp*., contain pigments that can contaminate DNA extraction and purification attempts. In these cases, we recommend including the DNA filtration step as outlined in the Bourras et al. (2015) protocol and an additional wash step with TE after the filtration step. The addition of the filtration step resulted in a small but significant increase in DNA degradation, and should only be included if excessive pigmentation remains after the second DNA precipitation step. These pigments, if allowed to remain in solution, may interfere with later analysis of quality and quantity of DNA and could potentially interfere with sequencing reactions.

This protocol includes both a traditional agarose gel electrophoresis step and a pulsed-field gel electrophoresis step. The first is an initial assessment of the fraction of DNA that is >20 kbp and the fraction that runs as a smear at <20 kbp. For the purpose of the downstream sequencing reactions required for powdery mildew genomes, the fraction of DNA <20 kbp should be minimal (see Figure 7.1, lane 2 versus lane 4). The pulsed-field gel electrophoresis assessment provides a better estimate of the size as DNA >20 kbp can be separated by size. DNA of >48.5 kbp is desirable for use in subsequent sequencing reactions (see Figure 7.2, lane 4).

The fungal material used in these experiments was propagated in growth chambers and contamination was limited using strict isolation protocols and personnel controls. Because of this, contamination with other, non-powdery mildew pathogens was minimal, and sequencing of the ITS region amplified using fungi-specific primers recovered only *G. cichoracearum* sequences. This may not be the case for powdery mildews collected from field sites or greenhouses lacking the same isolation controls, and contamination assessment in these cases will be critical for the assembly of high-quality genomes from the extracted DNA.

No one modification of the various fungal DNA isolation protocols was uniquely important. Rather slight modifications at many steps resulted in the relatively high yields of high molecular weight powdery mildew DNA reported here.

Figures

Figure 7.1 Agarose gel electrophoresis of purified genomic DNA. Lane 1: A DNA ladder, with bands ranging from 20 kbp to 75 bp; Lane 2: genomic DNA that passed quality control; Lane 3: genomic DNA that was considered marginal; and Lane 4: genomic DNA that failed quality control. Acceptable and marginal genomic DNA samples have a single band running above 20 kbp with minimal smearing at <20 kbp. Genomic DNA samples that fail quality control have smearing below 20 kbp, and may include low molecular weight fragments at approximately 100 bp (*). Pulsed-field gel electrophoresis is required to distinguish between acceptable and marginal DNA samples. Ethidium bromide was added to the gel prior to electrophoresis to visualize the genomic DNA. Samples were electrophoresed at 60V for 50 min. The gel was imaged under UV light using a gel documentation system.

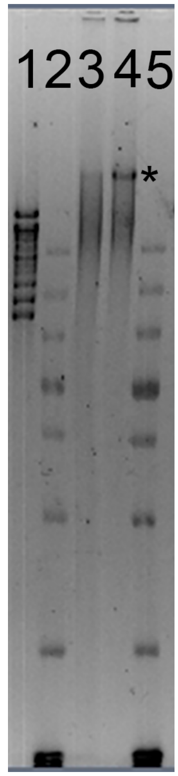

Figure 7.2 Pulsed-field gel electrophoresis (PFGE) of purified powdery mildew genomic DNA. Lane 1: molecular weight standards, with the highest band at 48.5 kbp and the lowest at 8.1 kbp. Lanes 2 and 5: molecular weight standards showing bands of 20, 10, 7, 5, 4, 3, 2 and 1.5 kbp (at the bottom of the gel image). Lane 3: a marginal DNA sample, with the majority of the DNA between 20 and 48.5 kbp in size. Lane 4: an acceptable DNA sample, with the majority of the DNA >48.5 kbp (*). Samples were run at 75V for 15 hours using a 5-80 kbp PFGE waveform program. DNA-staining dye was added to the gel after electrophoresis and the gel was imaged under UV light using a gel documentation system.

Tables

Table 7.1 Preparation of lysis buffer. Bring to a volume of 5ml with dH2O.

Reagent	**Final Concentration**
Potassium metabisulfite ($K_2S_2O_5$)	0.25M
Tris buffer pH 7.5	0.2M
Ethylenediaminetetraacetic acid (EDTA)	50mM
Sodium chloride (NaCl)	2M
Cetyltrimethyl ammonium bromide (CTAB)	2% v/v

Table 7.2 Primers for contamination assessment

Target	Primer Name	Primer Sequence	Tm (°C)	Expected Size (bp)
Fungal ITS2	FW (ITS9)	GAACGCAGCRAAIIGYGA	56-61.3	336
	RV (ITS4)	TCCTCCGCTTATTGATATGC	52.1	
Bacterial 16S V4	FW (515F)	GTGCCAGCMGCCGCGGTAA	63.8-66.5	331
	RV (805R)	GGACTACHVGGGTWTCTAAT	46.9-53.8	
Bacterial 16S V4-V5	FW (515F-Y)	GTGYCAGCMGCCGCGGTAA	60.8-66.5	450
	RV (926R)	CCGYCAATTYMTTTRAGTTT	43.9-53.8	
Fungal 18S V4	FW	CCAGCASCYGCGGTAATTCC	58.7-61.5	431
	RV	ACTTTCGTTCTTGATYRA	43.2-48.3	
Cucumis sativus PDS (LOC101204524)	CsPDS F	GTGAGTAAGGTTACCGTTTGGGGCTTATCCCAAT	63.8	750
	CsPDS R	GCGTGAGCTCGGTACTCTCATCCACTCTTGCAC	66.6	

Chapter 8: Genome Sequencing and Analysis of *G. cichoracearum*

Introduction

To date, the genomes of several powdery mildew species have been sequenced to varying depths. The recently sequenced barley powdery mildew, *B. graminis f. sp. hordei,* wheat powdery mildew, *B. graminis f. sp. tritici*, the grape powdery mildew, *E. necator*, and draft sequence assemblies of the Arabidopsis powdery mildew *G. orontii* and the pea powdery mildew *E. pisi*, along with the *de novo* sequenced transcriptome of the cucurbit powdery mildew *P. xanthii*, have provided the first pieces of information into the genomic structure and composition of these enigmatic pathogens (Spanu et al., 2010, Wicker et al., 2013,Vela-Corcía et al., 2016) .

In order to further study *Golovinomyces cichoracearum* and other powdery mildews*,* we were awarded a Department of Energy Joint Genome Institute Community Sequencing Project, which allowed for the sequencing of 11 powdery mildew species from each of the 5 tribes of the *Erysiphales (https://jgi.doe.gov/comparative-genomics-of-powdery-mildews/)*.

This project is valuable both in its breadth (including 11 diverse powdery mildew species) and in its depth. The use of PacBio long-read sequencing technology allows for significantly longer individual read-lengths, which is crucial for assembly of genomes as repetitive as the powdery mildew genomes.

There are several features of the published powdery mildew genomes that make the family particularly difficult to study on the genomic level. The mildew genomes are all large relative to related fungi, although the number of genes encoded by the genomes are fewer on average than those related fungi. The large, gene-poor genome is made up of many transposons that are thought to be evenly distributed throughout the genome. These elements are extremely numerous, and have made assembly using short-read sequencing data particularly challenging. It is believed that the expansion of repetitive elements relative to other fungi may be due to the absence of the repeat-induced point mutation (RIP) system found in other filamentous fungi, which is responsible for the removal of duplicated genes and is protective against transposon replication (Dean et al., 2005, Singer et al., 1995, Spanu et al., 2012). *B. graminis, G. orontii* and *P. xanthii* have all been shown to lack RIP-associated genes (Spanu et al., 2010, Vela-Corcía et al., 2016). Because of this, the sequences published to date have a large number of contigs, with many contigs containing only one or a few predicted genes (Spanu et al., 2010, Wicker et al., 2013). By using PacBio single-molecule real-time sequencing, we were able to achieve much longer reads. This allowed for higher quality better assembly, and a more complete view of the structure of the powdery mildew genomes.

Prior genome studies have shed light into the biology of the powdery mildew pathogen. Spanu (2010) found that the three powdery mildews sequenced at the time of publication, *B. graminis f. sp. hordei*, *G. orontii*, and *E. pisi* were each missing 99 genes that were determined to be core ascomycete genes. These missing genes may contribute the obligate biotrophy of the fungus, as their essential functions must be provided by the plant host, and were termed the missing ascomycete core genes (MACGs). For instance, the fungi are missing genes necessary for thiamine biosynthesis. This would indicate that the powdery mildews must necessarily receive the thiamine required for growth and development from the plant host, and may provide a partial explaination for the obligate biotrophic nature of the fungus (Spanu et al., 2010). Vela-Corcía et al. (2016) further determined that *P. xanthii* was also missing the majority of these MACGs using a *de novo* transcriptomic approach.

In the following studies, we compare the sequenced powdery mildew genomes to genomes of related *Leotiomycete* fungi *Sclerotinia sclerotiniorum* and *Meliniomyces variabilis*. *S. sclerotiniorum* is a necrotrophic plant pathogen with a broad host range, including over 400 plant species. It has been used as a model system for fungal pathogens. The sequencing of *S. sclerotiniorum* strain '1980' was published in 2011 (Amselem et al., 2011). *S. sclerotiniorum* is able to be grown axenically on defined media *in vitro*. *M. variabilis* is a plant endophyte which forms symbiotic associations with the roots of members of the plant family *Ericaceae*. *M. variabilis* association has beneficial impacts on plant growth*. M. variabilis* has been observed to grow axenicly on defined media. The genome of *M. variabilis* was published in 2018 (Martino et al., 2018).

Some surprising insights have been gleaned from the previously published genomes, as well. It was believed that powdery mildews penetrated the plant cell wall using a combination of turgor pressure and specialized enzymes, and had been hypothesized that the specificity of powdery mildews to their hosts may be due in part to the complement of cell wall degrading, carbohydrate-active enzymes (CAZYs) (Both et al., 2005, O'Connell & Panstruga, 2006). Potential targets for these enzymes might include cellulose, the main component of the plant primary cell wall, as well as components of pectin and hemicellulose. The powdery mildew hosts include both monocotyledonous and dicotyledonous plants, which vary widely in terms of cell wall composition. Surprisingly, very few CAZYs have been described in the powdery mildews (Spanu et al., 2010).

Additionally, the large number of effector proteins represented in powdery mildews has been predicted based on the sequenced powdery mildew genomes. Despite each sequenced mildew having a large complement of effectors, there is relatively little overlap among them (Weßling et al., 2014).

Here, I describe the results of the sequencing of the *G. cichoracearum* genome, and compare it to the previously sequenced powdery mildew genomes, both in quality and in composition.

Genome sequencing of G. cichoracearum *using PacBio long-read sequencing*

Genome sequencing and annotation was performed by the Joint Genome Institute (Grigoriev et al., 2012). The *G. cichoracearum* genome was sequenced using PacBio at 34.63x coverage. The genome was then assembled using Falcon for a total of 821 scaffolds with an N50 of 98 and an L50 of 0.44 Mbp (Chin et al., 2013). This assembly was annotated using the JGI Annotation Pipeline using RNA provided from a broad range of powdery mildew developmental stages, with a total of 129,021,646 expressed sequence tags (ESTs) mapped to the *G. cichoracearum* genome. The size of the *G. cichoracearum* genome is estimated to be 146.84 Mbp, encoding an estimated 6,782 genes.

The genome assembly and annotation statistics for *G. cichoracearum* are compared to those of the four other sequenced powdery mildews, *B. graminis f. sp. hordei, B. graminis f. sp. tritici, G. orontii* isolate MGH1, and *E. necator*, as well as to *S. sclerotiorum* and *M. mirabilis* in Table 8.1. The *G. orontii* genome was sequenced as a part of the same Community Sequencing Project with similar analysis and materials provided by the Wildermuth group at UC Berkeley. All data was downloaded from the JGI genome portal (https://genome.jgi.doe.gov/portal/)

Functional classification of annotated genes

Predicted *G. cichoracearum* proteins were grouped into functional categories according gene ontology (GO) terms during automated annotation. These GO terms were further reduced to GOSlim using AgBase GOSlimViewer (http://agbase.msstate.edu/cgi-bin/tools/goslimviewer_select.pl), with GO terms generated from yeast biological processes and cellular function (McCarthy et al., 2006).

We identified 3,218 biological GoSLIM terms for *G. cichoracearum* predicted proteins (Figure 8.1A). The largest fraction of these genes (51%) were grouped in the "biological processes" GOSlim group. Other large GOSlim groups included carbohydrate metabolic process (6.4% of annotated genes), and protein modification regulation and phosphorylation (5.9% each).

6,057 cellular function GoSLIM terms were identified for *G. cichoracearum* predicted proteins (Figure 8.1B). The largest fraction of these (30.4%) were classified only as molecular function, which indicates no specific function could be inferred. Ion binding, transferase, and hydrolase activities were also highly represented, containing 944, 516 and 406 predicted genes, respectively.

The G. cichoracearum *genome encodes a reduced set of carbohydrate-active enzymes*

We used the carbohydrate active enzyme (CAZY) prediction software dbCAN to predict the CAZYs present in the *G. cichoracearum* genome (Yin & Mao et al., 2012). We determined that the genome of *G. cichoracearum*, along with the genomes of the other sequenced powdery mildews *B. graminis f. sp. hordei, B. graminis f. sp. tritici*, and *E. necator* are significantly reduced in multiple CAZY families when compared to closely related fungi in the family *Leotiomycetes,* the plant pathogenic *S. sclerotiniorum* and the epiphytic *M. variabilis* (Figure 8.2, Appendix 7) (Spanu et al., 2010, Wicker et al., 2013, Amselem et al., 2011, Martino et al., 2018).

S. sclerotiniorum and *M. variabilis* have 569 and 1123 CAZYs, respectively. These CAZY-encoding genes represent 3.9% and 5.5% of the total genes encoded by those genomes. We determined that the *G. cichoracearum* genome encodes 183 CAZYs, consistent with those encoded in other powdery mildew genomes. These encoded CAZYs represent 2.6% of the total genes encoded in the *G. cichoracearum* genome.

The CAZYs are divided into 6 groups, auxiliary action (AA), carbohydrate-binding module (CBM), carbohydrate esterase (CE), glycoside hydrolase (GH), glycosyl transferase (GT), and polysaccharide lyase (PL). Of these, the GT group is largely associated with basal fungal activity, while the GH, CE, AA and PL groups contain members associated with plant-cell wall component degradation, host-microbe interactions, and biomass breakdown.

Compared to the related *S. sclerotiniorum* and *M. variabilis* fungi, all of the mildews, including *G. cichoracearum*, encode reduced numbers of CAZYs per group, with the exception of the GT group.

We further characterized the cell-wall degrading ability of the fungi by searching for enzymes with activity on pectin, cellulose and hemicellulose (Figure 8.3). Compared to *S. sclerotiniorum* and *M. variabilis*, all four mildews have severely reduced repertoires of enzymes active on plant cell wall components.

Identification of Ascomycete *core genes missing from* G. cichoracearum

We searched the *G. cichoracearum* genome for the presence of any of the previously identified missing Ascomycete core genes, which include both metabolic and regulatory proteins (Spanu et al., 2010, Vela-Corcía et al., 2016). The sequences of these genes were compiled and compared to a database containing a list of *G. cichoracearum* genes using the BLAST algorithm. Using an e-value cutoff of 10E-10, we determined that 9 of the 99 MACGs are present in the *G. cichoracearum* genome. With a less-stringent e-value cutoff of 10E-5, we identified an additional 9 MACGs in the *G. cichoracearum* genome. 81 MACGs were not found using either e-value cutoff. This data was added to data from Table S3 from Spanu (2010), and is presented in a modified form in Appendix 1.

Identification of G. cichoracearum *secreted proteins*

In order to identify *G. cichoracearum* candidate secreted effectors (ECs), we used SignalP4.1 (Petersen et al., 2007) to identify protein secretion signals combined with THMM transmembrane domain predictor to predict the *G. cichoracearum* proteins that are likely secreted by the fungus and not retained in the fungal plasma membrane. This analysis resulted in a list of 1227 proteins. We preformed the same analysis on *B. graminis f. sp. hordei, B. graminis f. sp. tritici, G. orontii* and *E. necator* as well, resulting in lists of 697, 534, 309, and 332 predicted secreted proteins, respectively (Appendix 2). Additionally, we searched for the EffectorP predicted *B. graminis f. sp. hordei* data for effectors with an experimentally validated role in promoting powdery mildew infection (Ahmed et al., 2015, Ahmed et al., 2016, Pliego et al., 2013, Aguilar et al., 2015, Whigham et al., 2015). Of 15 *B. graminis f. sp. hordei* effector candidates, 11 were represented in the EffectorP predicted data (Table 8.2).

Functional prediction of G. cichoracearum *secreted proteins*

We analyzed the list of GO terms associated with the *G. cichoracearum* SignalP predicted proteins again using the yeast GoSLIM groupings for biological processes (Figure 8.4A). The largest group, with 285 members, was again "biological process". The next three largest GoSLIM groups represented in the predicted *G. cichoracearum* secretome are associated with carbohydrate, amino acid, and nucleobase-containing small molecule metabolism, together including 62 genes, or 5% of the predicted secretome. Other highly represented GoSLIM groups included protein phosphorylation, cofactor metabolism, and DNA replication and repair.

1060 cellular function GoSLIM terms were identified for *G. cichoracearum* predicted secreted proteins (Figure 8.4B). The largest fraction of these (29.9%) were classified only as molecular function, which indicates no more specific function could be inferred. Ion binding, transferase, and hydrolase activities were also highly represented, containing 149, 89 and 82 predicted genes, respectively.

Identification of G. cichoracearum *candidate secreted effector proteins*

The predicted secreted proteins from all five powdery mildew genomes were then analyzed using the effector prediction software EffectorP (Sperschneider et al., 2015), which employs a machine learning approach to identify effector proteins based on experimentally validated fungal effectors. This analysis produced lists of candidate secreted effectors (Appendix 3). 229 candidate effectors were identified from the *G. cichoracearum* predicted secretome. 285, 184, 69, and 64 candidate effectors were identified from the *B. graminis f. sp. hordei*, *B. graminis f. sp. tritici, E. necator,* and *G. orontii* predicted secretomes, respectively. We used these predicted effectors for further analysis of the effector complements of these powdery mildews.

Functional prediction of G. cichoracearum *candidate secreted effectors*

We analyzed the list of GO terms associated with the *G. cichoracearum* SignalP predicted proteins again using the yeast GoSLIM groupings for both biological process (Figure 8.5A) and cellular function (Figure 8.5B). These results are presented in detail in Appendix 4.

The most common biological process GoSLIM group for candidate secreted *G. cichoracearum* effectors was again “biological process”, which contained 59.4% of annotated proteins, indicating an unknown functional role. Chromatin organization, carbohydrate metabolism contained 5.8% and 4.3% of annotated candidate secreted *G. cichoracearum* effectors, respectively.

The most common cellular function GoSLIM terms for the candidate secreted *G. cichoracearum* effectors was determined to be “molecular function”, indicating an unknown or undescribed function. 28.3% of candidate secreted *G. cichoracearum* effectors were grouped under the GoSLIM term molecular function. 14.1% of predicted effectors were grouped under the GoSLIM term structural constituent of ribosome, while 10.9% and 7.6% were grouped into ion binding and RNA binding, respectively.

Overlap in candidate secreted effectors between powdery mildew species

We used a reciprocal blastP to determine the overlap between the predicted effector complements of *G. cichoracearum, B. graminis f. sp. hordei, B. graminis f. sp. tritici* and *E. necator* (Figure 8.6A, Altschul et al., 1990). We found that the *B. graminis f. sp. hordei* and *B.*

graminis f. sp. tritici shared the largest effector overlap, including 151 candidate effector proteins. Six effector candidates were found in all four powdery mildew species.

Further analysis was conducted with the addition of effectors predicted in *G. orontii*, comparing the effector complement of *G. cichoracearum* to the four other powdery mildews (Figure 8.6B, Table 8.3). A total of four candidate secreted effectors were determined to be present in all five powdery mildews, including two which were tested in the HIGS experiments described in Chapter 3, GcEC13 and GcEC17. 21 effector candidates were found in both *G. cichoracearum* and *G. orontii*, the same number as were determined to be shared between *G. cichoracearum* and *E. necator*, though the 21 effectors are not the same between the two species. With an e-value cutoff of 10E-10, 194 *G. cichoracearum* effector candidates were determined to not be present in any other powdery mildew.

Using an e-value cutoff of 10E-10, GcEC8 and GcEC10 were determined to have a homologous effector candidate present in *G. orontii* and *E. necator*. GcEC17 was determined to be present in all of the examined powdery mildew genomes (Table 8.3).

Prediction of candidate secreted effector localization

We used the fungal effector localization predictor Localizer (Sperschneider et al., 2017A) along with the fungal apoplastic effector predictor ApoplastP (Sperschneider et al., 2017B) to predict the subcellular localization of the mature candidate secreted effectors from each of the mildews (Figure 8.7). In each of the mildews, the largest group of effectors lacked any predicted localization signal. In *G. cichoracearum*, the second largest group contained a nuclear localization signal without any other signal peptide, while the other mildews had a relatively larger number of apoplastic effectors. A relatively smaller number of effectors from each of the mildews was predicted to be targeted to either the chloroplast, the mitochondria, or both. This data is presented in detail in Appendix 5 (localization) and Appendix 6 (delivery to the apoplast).

Phylogenetic analysis of G. cichoracearum *effector candidates*

An unrooted tree of the 229 *G. cichoracearum* candidate effectors was constructed using the Maximum Likelihood method with bootstrap analysis (Figure 8.8, Table 8.3 Jones et al., 1992, Felsenstein et al., 1985). Based on this tree, most of the *G. cichoracearum* effectors do not cluster reliably into families, however 21 families containing 2 or more candidate effectors were determined using this analysis. The largest effector family contained 6 members.

G. cichoracearum effector candidates which demonstrated significant homology (e-value of 10E-10) to *B. graminis f. sp. hordei, B. graminis f. sp. tritici, E. necator,* and *G. orontii* candidate effectors were identified and marked on the tree, as were candidate effectors which were tested in Chapter 3. GcEC8 and GcEC17 were not determined to be members of effector families, while Gcec10 was determined to be a member of a 4-effector family, including 3 additional, untested *G. cichoracearum* effector candidates with significant homology to *E. necator* predicted effectors.

Discussion

Here, we performed an analysis of the newly sequenced *G. cichoracearum* genome. The sequencing of this genome was completed entirely using Pacific Biosciences sequencing technology, which had not yet been attempted for a powdery mildew.

Pacific Biosciences long-read sequencing was used in this case due to the predicted large size and high complexity of the *G. cichoracearum* genome. Analysis of previous genome sequencing efforts in powdery mildews had estimated genome sizes of over 100 MB, which is larger than most sequenced fungal genomes. This increased genome size is likely due to a genome composition of about 64% repetitive elements believed to be randomly dispersed throughout the genome. The size of many of these repetitive elements over 10kb in some cases, which would make assembly using Illumina short-read sequencing data challenging. This is supported by the large number of scaffolds which were produced from the analysis of the powdery mildew sequencing data (Spanu et al., 2010, Wicker et al., 2013).

Interestingly, these repetitive elements may be important for infection success for the powdery mildews. Effectors have been observed to associate with retrotransposon-rich regions (Menardo et al., 2017). Additionally, a recent study showed that ROPIP1, a peptide encoded in a non-long terminal repetitive element in the *B. graminis f. sp. hordei* genome, is implicated in the virulence of the pathogen (Nottensteiner et al., 2018). This further underscores the importance of accurate sequencing of these repetitive elements.

By using Pacific Biosciences long-read sequencing technology, which is able to achieve read-lengths up-to and above 20kb, we were able to assemble the *G. cichoracearum* genome to a number of scaffolds much lower than that which had been previously reported. For instance, the *B. graminis f. sp. hordei* genome analysis included 6843 scaffolds, while the *G. cichoracearum* genome contained 821 (Spanu et al., 2010, Wicker et al., 2013). This higher quality assembly allows for the analysis of the structure of the *G. cichoracearum* genome. For instance, it will be more possible to search for virulence gene clusters. It will also be possible to identify the hallmarks of evolution, such as gene clusters, which can provide further insight into the taxonomy of powdery mildews. As we found fewer similarities between *G. cichoracearum* and *G. orontii* as compared to other, less-related powdery mildews, than may have been expected, we may discover that the evolutionary history of the powdery mildews differs from what has been thus far predicted.

While the assembly statistics vary widely between the sequenced powdery mildew genomes, the predicted gene number for the sequenced powdery mildews is consistent between *G. cichoracearum*, *E. necator*, and both *B. graminis f. sp. hordei* and *f. sp. tritici.* Each of the mildews are predicted to encode ~6,500 genes. This is a significantly reduced gene set than is encoded by non-obligate fungi. The closely related Leotiomycete *S. sclerotiniorum* is predicted to encode 14,503 genes. Interestingly, the powdery mildew *G. orontii* genome annotation predicts a larger number of encoded proteins than was predicted in the other powdery mildews, though still fewer than either the *S. sclerotiniorum* or *M. variabilis*. This gene expansion does not seem to apply to either the predicted complement of secreted or effector proteins, however (Spanu et al., 2010, Wicker et al., 2013, Amselem et al., 2011).

It had previously been reported by Spanu (2010) that the powdery mildews contained a reduced arsenal of carbohydrate active enzymes (CAZY). In order to evaluate the CAZY complement of *G. cichoracearum*, we used the CAZY prediction tool dbCAN. We compared the genomes of the four sequenced powdery mildews, as well as *S. sclerotiniorum* and the Leotiomycete root endophyte *M. variabilis*. We determined that, compared to *S. sclerotiniorum* and *M. variabilis*, all four powdery mildews have reduced CAZY arsenals that are largely similar on the level of gene families.

Each powdery mildew genome encoded only 179-191 CAZYs, while the *S. sclerotiniorum* and *M. variabilis* genomes encoded 569 and 1123, respectively. The powdery mildew genomes contained similar levels of GT enzymes, which are largely associated with basal fungal metabolism, while they were significantly reduced in all other CAZY types. We further searched for protein families within the CAZY types that are associated with the degradation of plant cell wall components, including lignin, pectin, hemicellulose, and cellulose. Enzymes in these families were either severely reduced in number or entirely absent.

It had previously been believed that powdery mildews penetrated the plant cell wall using a combination of secreted CAZY proteins and turgor pressure (Both et al., 2005, O'Connell & Panstruga, 2006). While this still may be the case, it is interesting to note the severely reduced CAZY repertoire, especially in the families associated with plant cell wall degradation. All four of the examined mildews contained only a single enzyme predicated to be active on cellulose, the major constituent of the plant cell wall. Pectin- and hemicellulose-active enzymes were similarly reduced when compared to related fungi. It is possible that in order to avoid the immune response associated with the detection of cell-wall damage, the mildew uses only enzymes that produce very specific degradation products. What these products might be is an interesting avenue of inquiry, and now that the CAZY complement of the mildews has been identified, it can be studied in more detail. Another interesting question revolves around the differences in CAZY composition between mildews that are able to infect plants with varying cell-wall compositions.

For instance, both *G. cichoracearum* and *G. orontii* encode predicted pectate lyase proteins, which are absent in both *formae specialis* of *B. graminis.* This could be indicative of some dicot specialization, as the cell walls of dicotyledonous plants (such as Arabidopsis and *C. sativa*) contain significantly more pectin than those of monocotyledonous plants (such as wheat and barley) (reviewed by McCann & Roberts, 1991). This analysis does not perfectly describe the differences between the mildews studied here, however. *E. necator*, also a pathogen of dicots, encodes the smallest complement of pectin-active enzymes of all the mildews, and does not encode any enzymes in the pectate lyase family.

The severely reduced complement of cell wall degrading enzymes may be due to the biotrophic nature of the powdery mildew. In order to avoid the DAMP-triggered immune response, a careful and targeted breakdown of the plant cell wall is necessary, and may even employ non-canonical enzymes which allow the mildew to breach the cell wall of the plant without creating recognizable fragments that may result in the recognition of the pathogen.

Functional prediction of the biological processes annotation genes of *G. cichoracearum* revealed that a majority of the predicted genes are classified only broadly as involved in biological processes. Of the remaining annotated predicted genes, the largest groups were those containing carbohydrate metabolism, various protein modifications, and cell-cycle related proteins. Similar analysis of cellular function indicated that a majority of the predicted genes are classified only broadly as having a molecular function. Relatively large groups of ion binding, transferase and hydrolase functions were also predicted.

We used SignalP software to predict the identity of proteins that are likely to be secreted and not retained in the plasma membrane (Petersen et al., 2007). We found a relatively large range of the number of predicted secreted proteins among the powdery mildews. We predicted that the *G. cichoracearum* genome encodes 1227 secreted proteins, while the *B. graminis f. sp. hordei, G. orontii,* and *tritici* and *E. necator* genomes encode significantly fewer. The reasons for this discrepancy are not clear at this time, and further analysis of the genes encoded by the *G. cichoracearum* did not reveal similar differences.

Functional classification of the biological process and cellular function classifications of the SignalP predicted *G. cichoracearum* genes were similar to those of the total predicted protein complement of the powdery mildew. The majority of secreted proteins were also grouped under the biological process GoSLIM term, and although the next largest group encoded amino acid metabolism, DNA replication, and protein modification groups remained highly represented. Cellular function groups were identified in similar ration between the total predicted protein content of *G. cichoracearum* and the SignalP predicted secreted proteins.

In order to predict the candidate secreted effectors encoded by the *G. cichoracearum* genome, we used the fungal effector prediction tool EffectorP (Sperschneider et al., 2015). EffectorP is a machine-learning program that was trained to detect fungal secreted effector proteins using a dataset of experimentally validated fungal effectors. This dataset contained only a single powdery mildew effector, Avr10, which was identified from *B. graminis f. sp. hordei* (Ridout et al., 2006). EffectorP determined that the most discriminative features for effector prediction are protein size, net charge, and presence of cysteine, serine and tryptophan amino acids. An interesting validation of EffectorP occurred when testing the software on the *B. graminis f. sp. hordei* dataset of secreted proteins. Despite not being trained on the presence of an N-terminal [YWF]xC domain as an indicator of the identity of a protein as an effector, as discussed in Godfrey et al. (2010), 66% of predicted effectors contained the motif at the N-terminus of the protein. Additionally, 90% of the EffectorP predicted effectors were annotated as candidate secreted effector proteins in the *B. graminis f. sp. hordei* genome (Sperschneider et al., 2015).

This approach differs from previous powdery mildew effector prediction approaches. In previous publications, powdery mildew effectors were identified based on their secretion signal, lack of membrane retention, and lack of homology to known effectors (Weßling et al., 2013, Spanu et al., 2010, Wicker et al., 2013, Vela-Corcía et al., 2016). In order to compare the predicted effector complement of *G. cichoracearum* to that of other powdery mildews with sequenced genomes, we obtained the genome files of these mildews and reanalyzed them using the same techniques that were used for the *G. cichoracearum* genome. This has resulted in a different list of candidate secreted effector proteins used in this analysis compared to other published work.

We found that the predicted secreted effectors varied in number between the powdery mildew genomes we analyzed in this work. *B. graminis f. sp. hordei* encoded the largest number, 285, while *G. cichoracearum* and *B. graminis f. sp. tritici* encoded 184 and 179, respectively. *E. necator* was predicted to include the fewest secreted effectors, 69. Forty percent of the proteins predicted to be secreted by *B. graminis f. sp. hordei* were predicted to be effectors, while 34% of *B. graminis f. sp. tritici* and 22% of *E. necator.* Only 15% of the proteins from *G. cichoracearum* identified by SignalP as predicted secreted proteins were annotated as likely effectors.

We then used the fungal effector prediction programs Apoplast and Localizer to predict whether the effectors were likely to be located in the apoplast or within the plant cell, and if they were predicted to be present in the plant cell, where in the cell they were likely to be. Similar effector-localization profiles were predicted for each mildew, with a large number of effectors predicted to be transported into the plant cell but lacking any additional transit peptide. Many effectors were predicted to contain nuclear localization signals and chloroplast transit-peptides, as well as a large number of predicted apoplastic effectors.

We also compared the effector complements of the powdery mildews against one another. Previous work had reported very low overlap between the effector repertoires of powdery mildews. Our analysis showed that only six predicted effectors were shared between all four powdery mildew genomes. A small number of effectors were conserved between three of the mildews but excluded from the fourth. The largest overlap was found between the two *formae speciales* of *B. graminis*, which included 132 effector proteins.The large overlap between *B. graminis f. sp. hordei* and *B. graminis f. sp. tritici* is consistent with previously published work, and is unsurprising as the two are more closely related than to the other mildews. The majority of *G. cichoracearum* effectors were unique, while *E. necator* and both formae specialis of *B. graminis* shared more than half of their effector repertoire with at least one other powdery mildew.

As *E. necator* and *G. cichoracearum* infect dicotyledonous plant hosts while *B. graminis f. sp. hordei* and *f. sp.* tritici each infect monocotyledonous hosts, we hypothesized that there may be a larger overlap in the effector complement of these mildews than they might have with either *B. graminis*. This was not found to be the case. Rather, the overlap between *E. necator* was determined to be larger with the *B. graminis* mildews than with the *G. cichoracearum*.

The large difference in the number of predicted effectors between *G. cichoracearum* and *G. orontii* was particularly surprising, as the two mildews are believed to be closely related and infect an overlapping host range. Furthermore, that the two mildews did not share a more substantial overlap when compared to the more distantly related *E. necator* was another surprising result. Somewhat surprisingly, *G. cichoracearum* shares the same number of predicted effectors with *G. orontii* as with *E. necator*, although these effectors are not necessarily the same. Because *G. orontii* and *G. cichoracearum* are believed to be closely related and share an overlapping host range, it was expected that the overlap in predicted effectors might be larger than with the more distantly related *E. necator*, which is unable to infect Arabidopsis. GcEC8 and GcEC10 were both determined to contain homologs in the effector complement of *E. necator*, while GcEC17 was determined to be present in the effector complements of all studied powdery mildews.

We also analyzed the biological process and cellular function classifications of the *G. cichoracearum* candidate secreted effectors. The biological process of only 28 of the 179 predicted effectors were categorized more specifically than the biological process GoSLIM group. The second largest GoSLIM biological process categorization, chromatin organization, contained 4 candidate effectors. That these effectors are not obviously characterized by function is unsurprising, as this is true for plant pathogenic effectors across kingdoms (reviewed in Varden et al., 2017).

The cellular function GoSLIM characterization of the candidate secreted effector proteins differed from that of the SignalP predicted proteins and the total protein complement. Proteins annotated as structural constituent of the ribosome and RNA binding were overrepresented, relative to the total protein or predicted secreted proteins. This supports previous work to identify powdery mildew effectors, which have been demonstrated to contain large families of RNase-like proteins, although the roles of many of these proteins have not yet been described.

Phylogenetic analysis of the *G. cichoracearum* predicted effectors indicated that most effectors were likely not members of large protein families. Interestingly, few members of the most-expanded families were determined to have homologs among the effector candidates of other powdery mildews, indicating that unique effectors may have undergone gene-duplication after speciation. This was not the case for the family containing GcEC10, in which all 4 members were also found in *E. necator*. These effectors are likely part of the large group of effectors with RNase like domains, the importance of which remains unknown.

Planned future experiments as a part of the JGI CSP include an RNA-sequencing experiment that will include analysis of plant and fungal transcripts over the course of powdery mildew infection. This result will provide insight into the biology of the powdery mildew pathogen, and may offer clues as to when and how key events take place during infection. This data will be coupled with transcript profiling of the infected plant as well, and as such we may be able to interrogate direct relationships between fungal infection and plant response. This data will also allow for a more detailed annotation of the *G. cichoracearum* genome, and the large-scale clustering of potential effectors by their transcription patterns during infection.

Figures

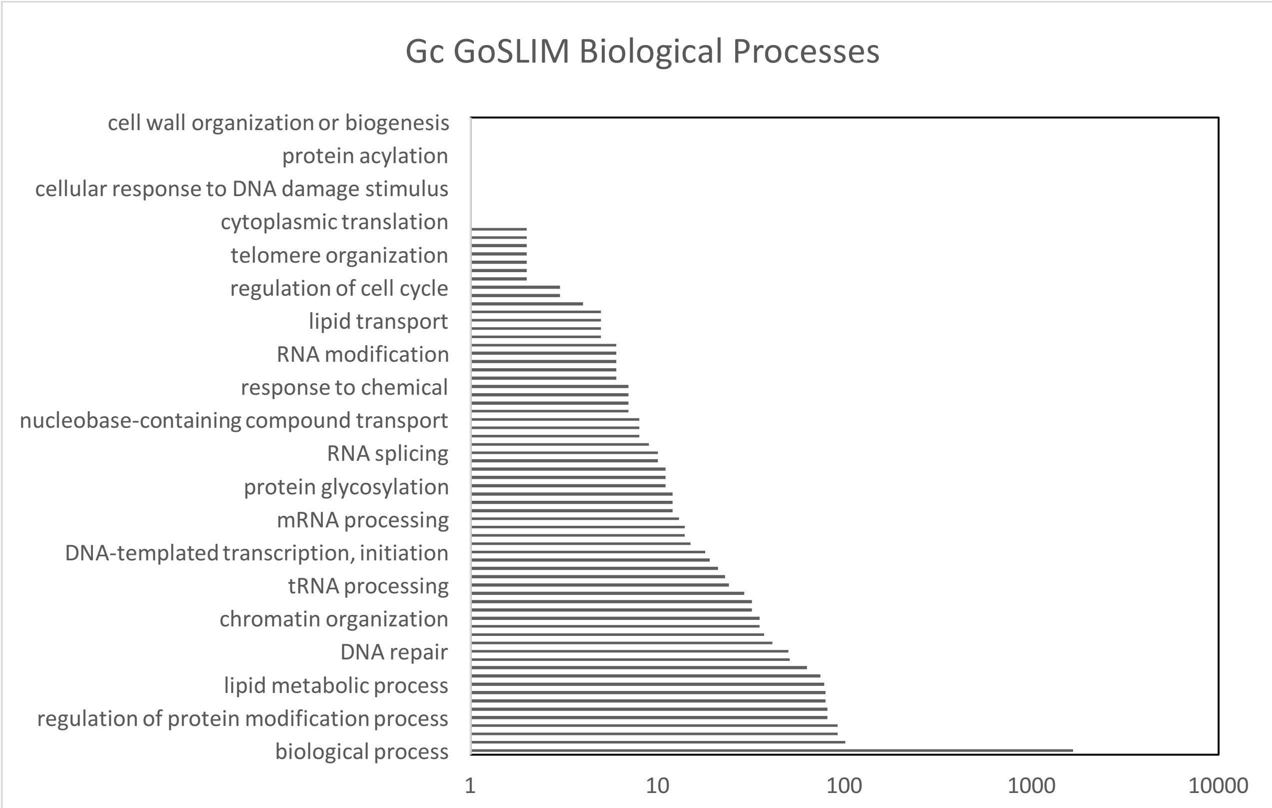
Gc GoSLIM Biological Processes
cell wall organization or biogenesis
protein acylation
cellular response to DNA damage stimulus
cytoplasmic translation
telomere organization
regulation of cell cycle
lipid transport
RNA modification
response to chemical
nucleobase-containing compound transport
RNA splicing
protein glycosylation
mRNA processing
DNA-templated transcription, initiation
tRNA processing
chromatin organization
DNA repair
lipid metabolic process
regulation of protein modification process
biological process
1
10
100
1000
10000

B.

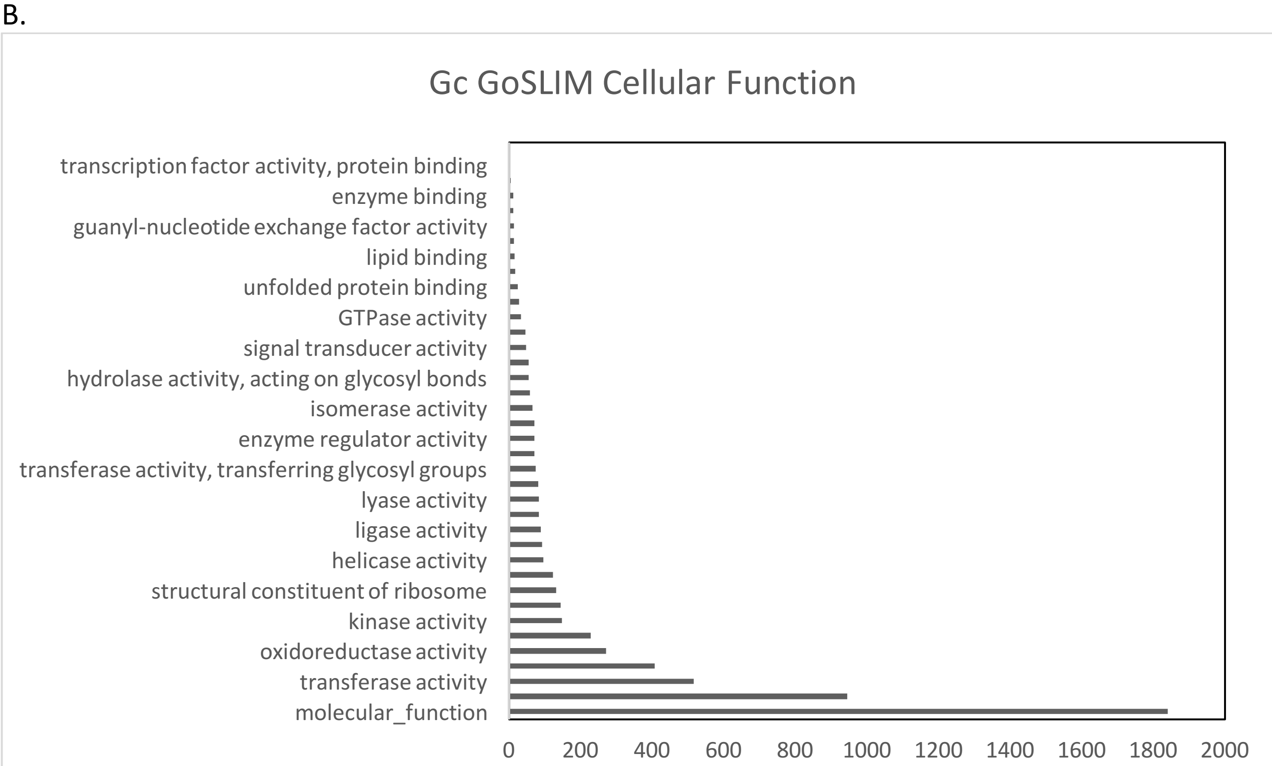
Gc GoSLIM Cellular Function
transcription factor activity, protein binding
enzyme binding
guanyl-nucleotide exchange factor activity
lipid binding
unfolded protein binding
GTPase activity
signal transducer activity
hydrolase activity, acting on glycosyl bonds
isomerase activity
enzyme regulator activity
transferase activity, transferring glycosyl groups
lyase activity
ligase activity
helicase activity
structural constituent of ribosome
kinase activity
oxidoreductase activity
transferase activity
molecular_function
0
200
400
600
800
1000
1200
1400
1600
1800
2000

Figure 8.1 Functional classification of annotated G. cichoracearum *genes*
GoSLIM classification of automated GO annotation of predicted *G. cichoracearum(Gc)* genes for (A) biological processes and (B) cellular function. The number of genes present in each category is indicated on the x-axis.

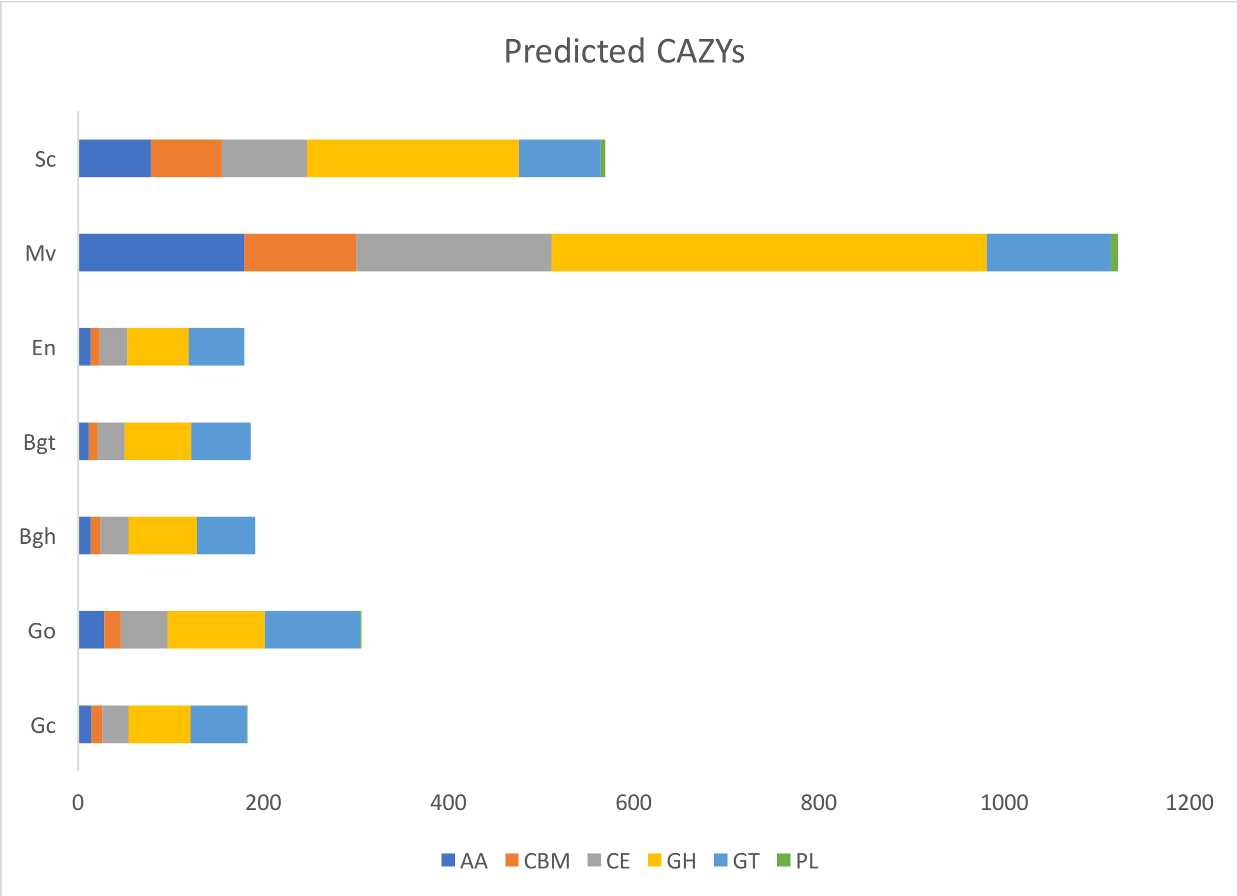

Figure 8.2 Comparison of the CAZY repertoires of select Leotiomycetes
dbCAN analysis was performed on *M. variabilis (Mv), S. sclerotinia (Sc)* *B. graminis f. sp. hordei (Bgh), B. graminis f. sp. tritici (Bgt), E. necator (En), G, orontii (Go),* and *G. cichoracearum (Gc).* CAZY were grouped into auxillary action (AA), carbohydrate-binding module (CBM), carbohydrate esterase (CE), glycoside hydrolase (GH), glycosyl transferase (GT), and polysaccharide lyase (PL).

A.

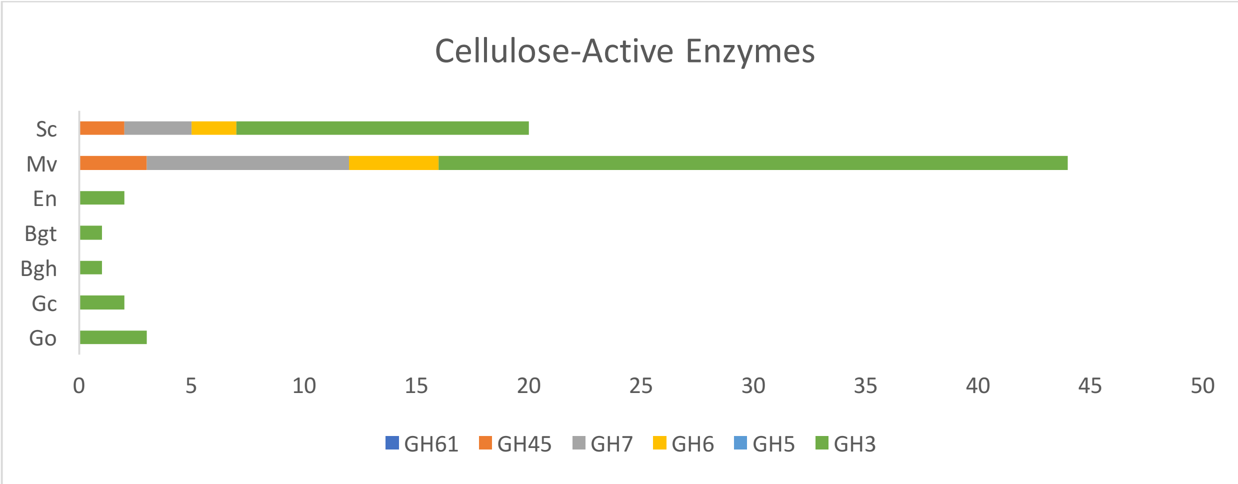
Cellulose-Active Enzymes
Sc
Mv
En
Bgt
Bgh
Gc
Go
0
5
10
15
20
25
30
35
40
45
50
GH61
GH45
GH7
GH6
GH5
GH3

B.

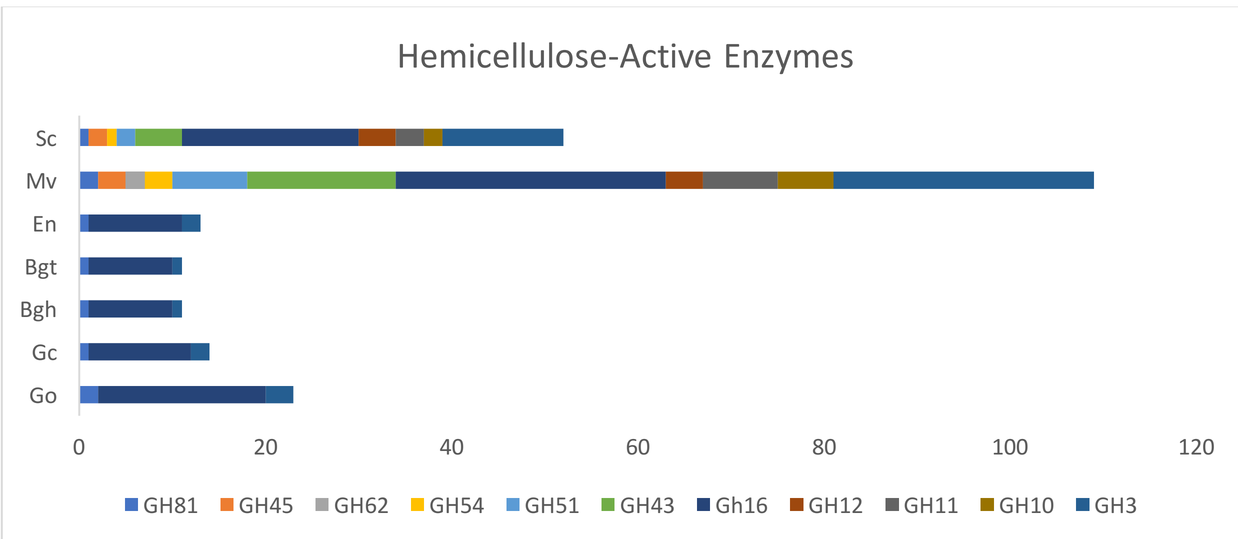
Hemicellulose-Active Enzymes
Sc
Mv
En
Bgt
Bgh
Gc
Go
0
20
40
60
80
100
120
GH81
GH45
GH62
GH54
GH51
GH43
Gh16
GH12
GH11
GH10
GH3

C.

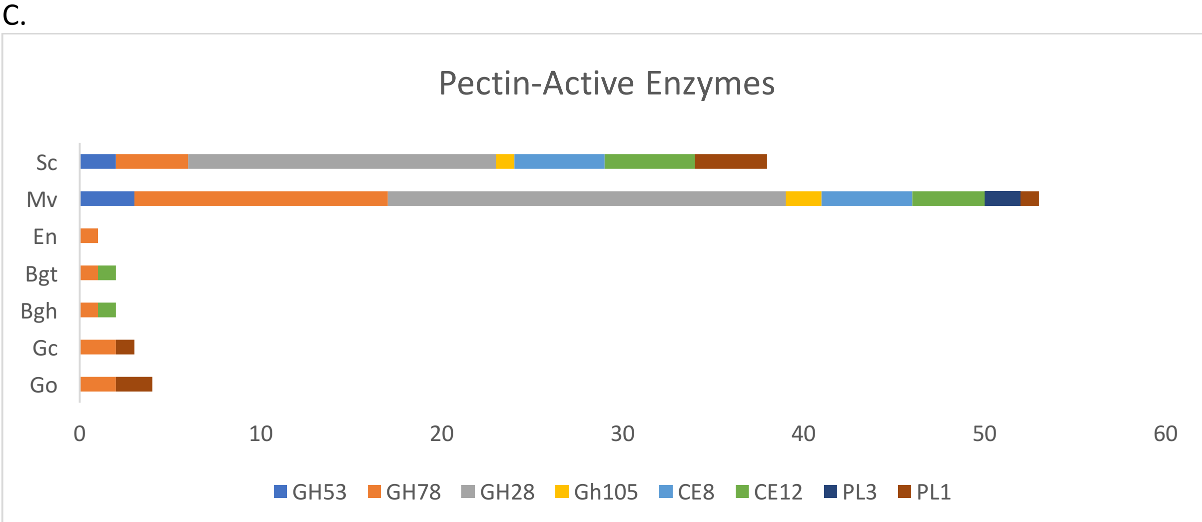
Pectin-Active Enzymes
Sc
Mv
En
Bgt
Bgh
Gc
Go
0
10
20
30
40
50
60
GH53
GH78
GH28
Gh105
CE8
CE12
PL3
PL1

Figure 8.3 Comparison of plant cell wall polymer active CAZY repertoires of select Leotiomycetes
dbCAN analysis was performed on *M. variabilis (Mv), S. sclerotinia (Sc)*
B. graminis f. sp. hordei (Bgh), B. graminis f. sp. tritici (Bgt), E. necator (En), G. orontii (Go) and G. cichoracearum (Gc). Enzymes predicted to have activity on plant cell wall polymers were identified (Cantarel et al., 2009).

A. Genes annotated as having cellulose-degrading activity in families glycosyl hydrolase (GH) 61, GH45, GH7, GH6, GH5 and GH3.
B. Genes annotated as having hemicellulose-degrading activity in families GH81, GH45, GH62, GH54, GH51, GH43, GH16, GH12, GH11, Gh10 and GH3.
C. Genes annotated as having pectin-degrading activity in families GH53, GH78, GH28, GH105, carbohydrate esterase (CE) 8, CE12, pectate lyase (PL) 3, and PL1.

A.

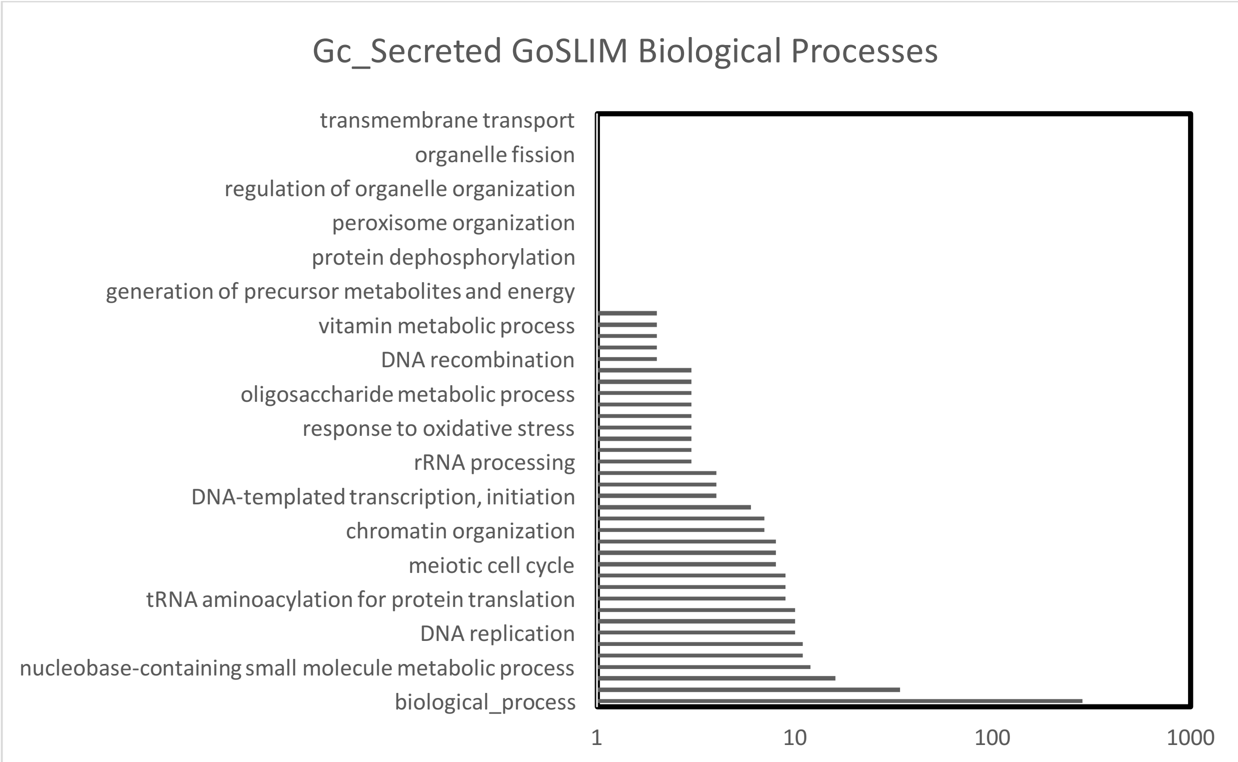
Gc_Secreted GoSLIM Biological Processes
transmembrane transport
organelle fission
regulation of organelle organization
peroxisome organization
protein dephosphorylation
generation of precursor metabolites and energy
vitamin metabolic process
DNA recombination
oligosaccharide metabolic process
response to oxidative stress
rRNA processing
DNA-templated transcription, initiation
chromatin organization
meiotic cell cycle
tRNA aminoacylation for protein translation
DNA replication
nucleobase-containing small molecule metabolic process
biological_process
1
10
100
1000

B.

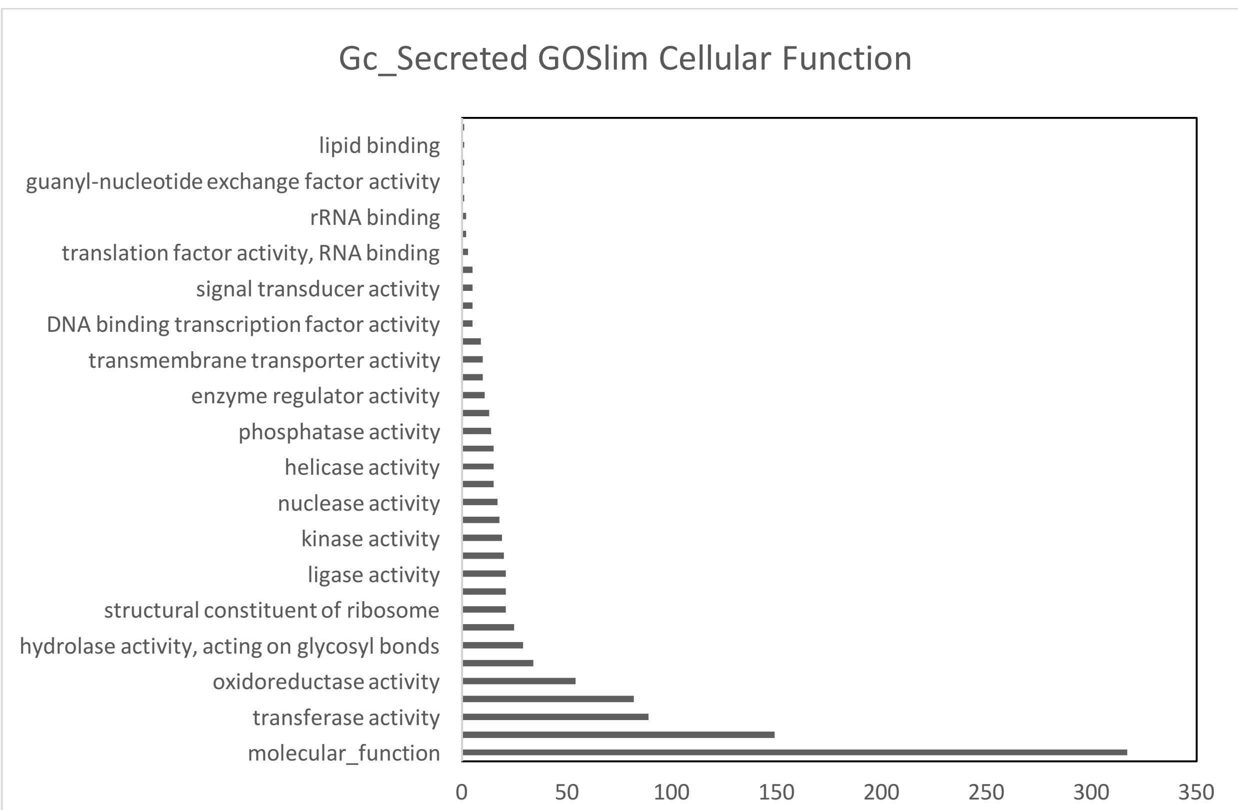
Gc_Secreted GOSlim Cellular Function
lipid binding
guanyl-nucleotide exchange factor activity
rRNA binding
translation factor activity, RNA binding
signal transducer activity
DNA binding transcription factor activity
transmembrane transporter activity
enzyme regulator activity
phosphatase activity
helicase activity
nuclease activity
kinase activity
ligase activity
structural constituent of ribosome
hydrolase activity, acting on glycosyl bonds
oxidoreductase activity
transferase activity
molecular_function
0
50
100
150
200
250
300
350

Figure 8.4 Functional Prediction of G. cichoracearum *secreted proteins*
GoSLIM classification of automated GO annotation of predicted *G. cichoracearum(Gc)* secreted proteins for (A) biological processes and (B) cellular function. The number of genes present in each category is indicated on the x-axis.

A.

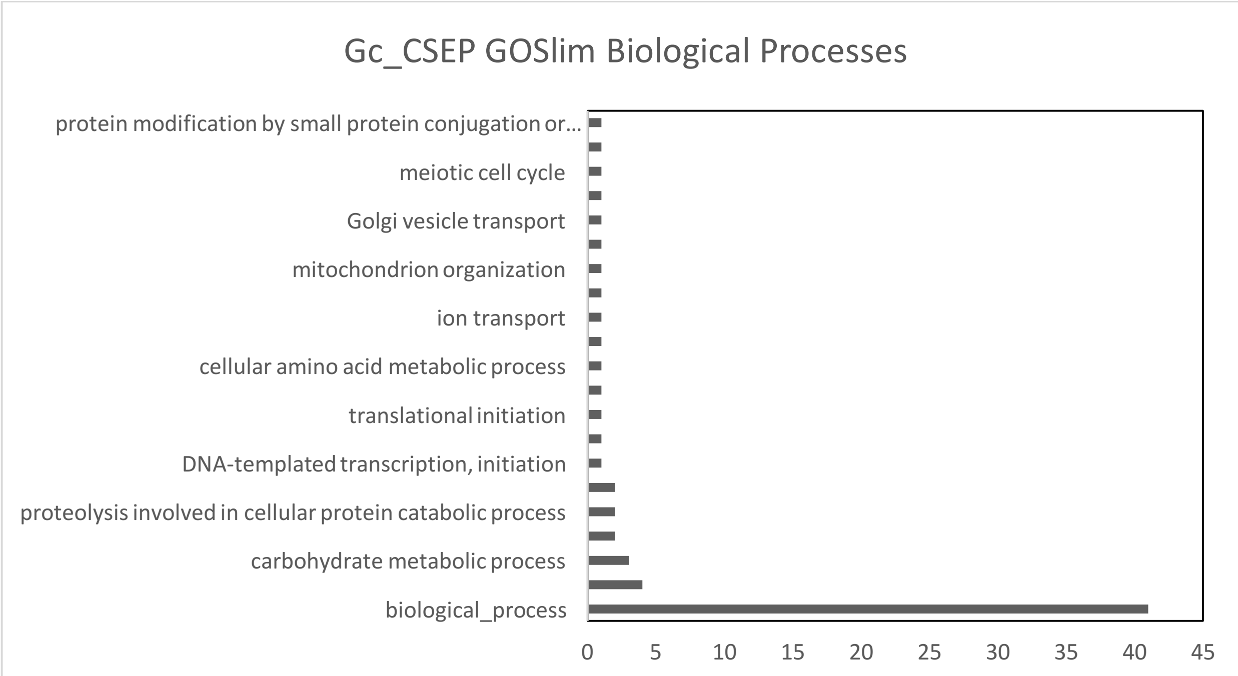
Gc_CSEP GOSlim Biological Processes
protein modification by small protein conjugation or...
meiotic cell cycle
Golgi vesicle transport
mitochondrion organization
ion transport
cellular amino acid metabolic process
translational initiation
DNA-templated transcription, initiation
proteolysis involved in cellular protein catabolic process
carbohydrate metabolic process
biological_process
0
5
10
15
20
25
30
35
40
45

B.

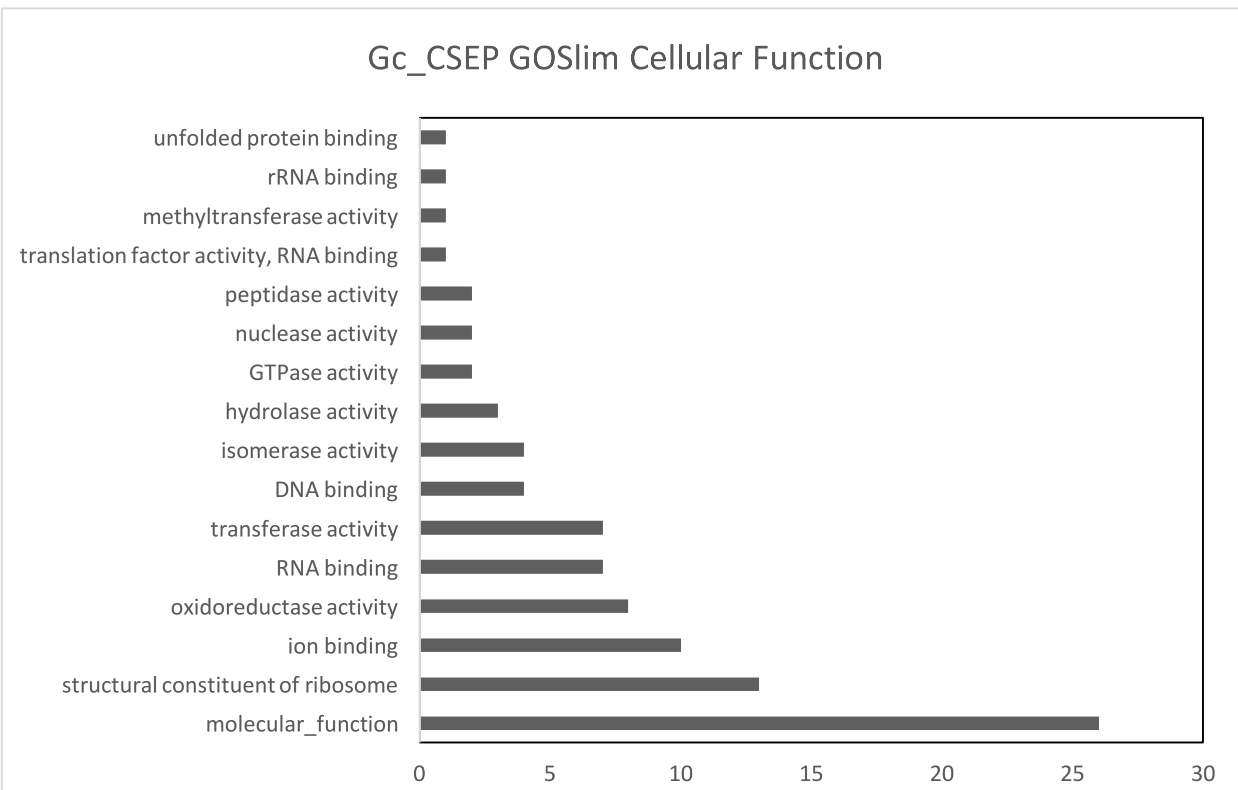
Gc_CSEP GOSlim Cellular Function
unfolded protein binding
rRNA binding
methyltransferase activity
translation factor activity, RNA binding
peptidase activity
nuclease activity
GTPase activity
hydrolase activity
isomerase activity
DNA binding
transferase activity
RNA binding
oxidoreductase activity
ion binding
structural constituent of ribosome
molecular_function
0
5
10
15
20
25
30

Figure 8.5 Functional prediction of G. cichoracearum *candidate secreted effector proteins (CSEP)*
GoSLIM classification of automated GO annotation of predicted *G. cichoracearum(Gc)* candidate secreted effector proteins for (A) biological processes and (B) cellular function. The number of genes present in each category is indicated on the x-axis.

A.

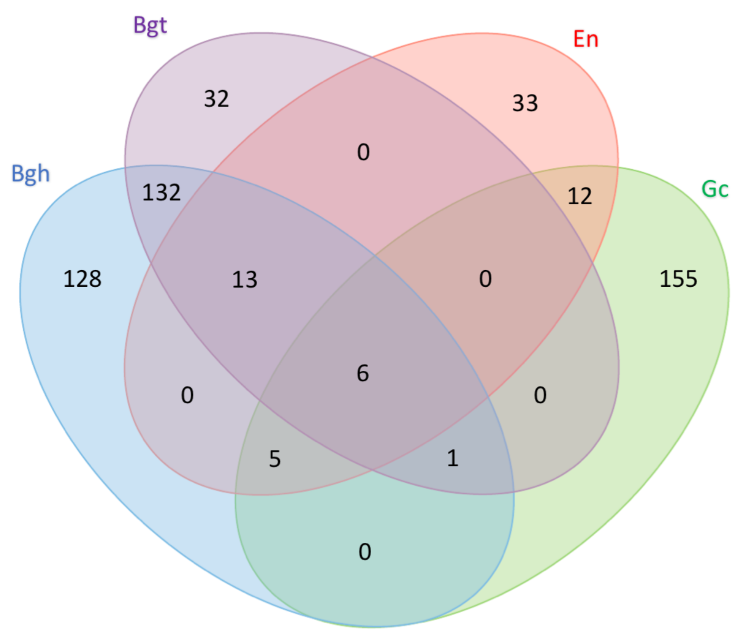
Bgt
En
Bgh
Gc
32
33
0
132
12
128
13
0
155
6
0
0
5
1
0

B.

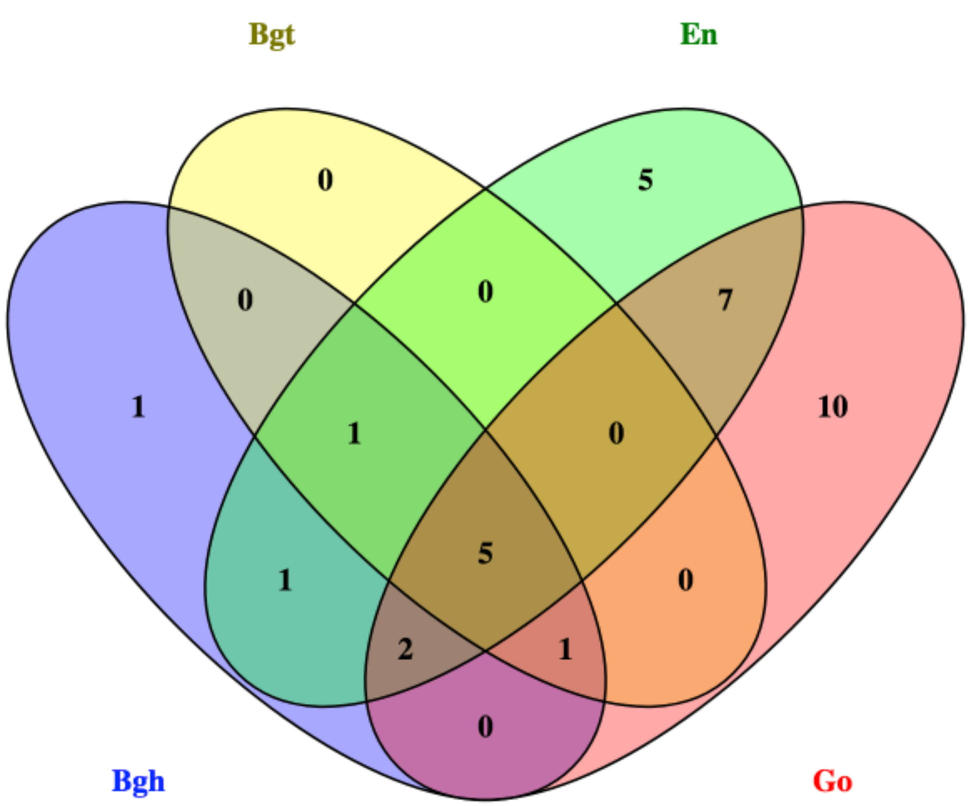
Bgt
En
0
5
0
0
7
1
1
0
10
5
1
0
2
1
0
Bgh
Go

Figure 8.6 Conserved effectors among powdery mildew isolates

A. Reciprocal blastP analysis was performed on *B. graminis f. sp. hordei (Bgh), B. graminis f. sp. tritici (Bgt), E. necator (En), and G. cichoracearum (Gc)* candidate secreted effectors with an e-value cutoff of 10E-10
B. Reciprocal blastP analysis was performed to compare the predicted effector complement of *G. cichoracearum* to that of Bgh, Bgt, En and Go with an e-value cutoff of 10E-10. All effector candidates in this graph are shared with *G. cichoracearum.*

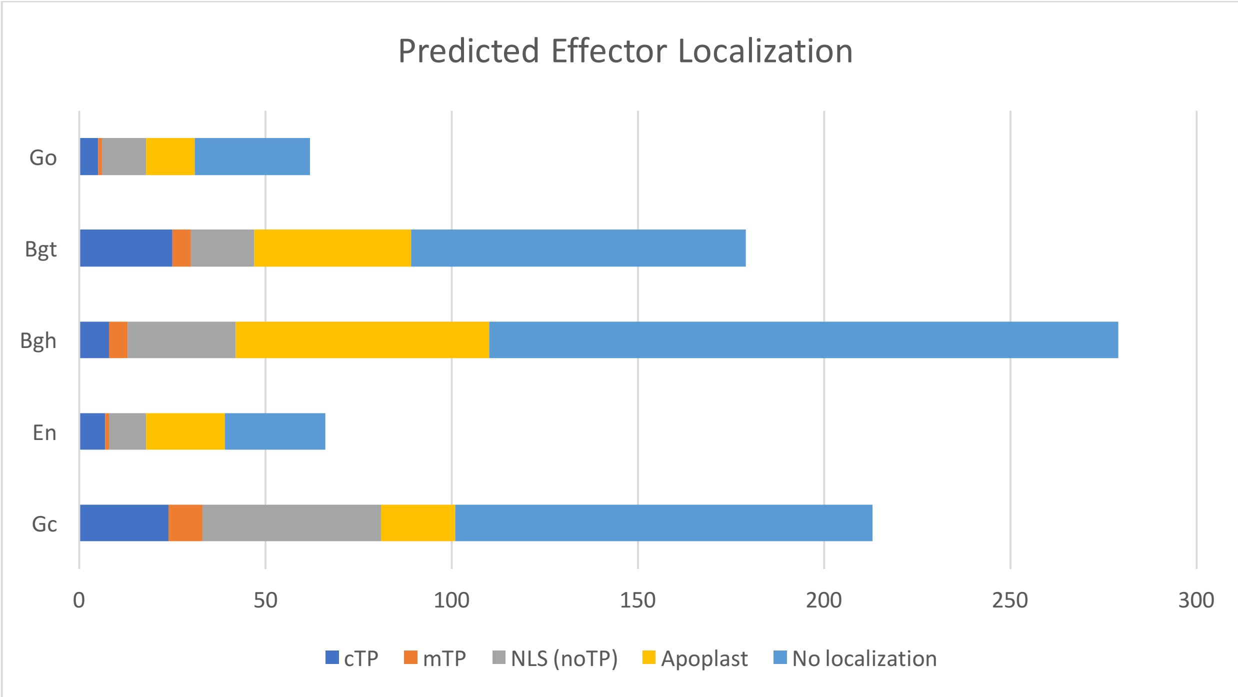

Figure 8.7 Predicted candidate secreted effector localization
Subcellular and apoplast targeting analysis was performed on *B. graminis f. sp. hordei (Bgh), B. graminis f. sp. tritici (Bgt), E. necator (En), G. orontii (Go), and G. cichoracearum (Gc)* using Localizer and Apoplast. Candidate secreted effectors are grouped by the presence of a chloroplast transit-peptide (cTP), mitochondria transit-peptide (mTP), nuclear localization signal without a signal peptide (NLS (noTP)), or likely apoplast localization.

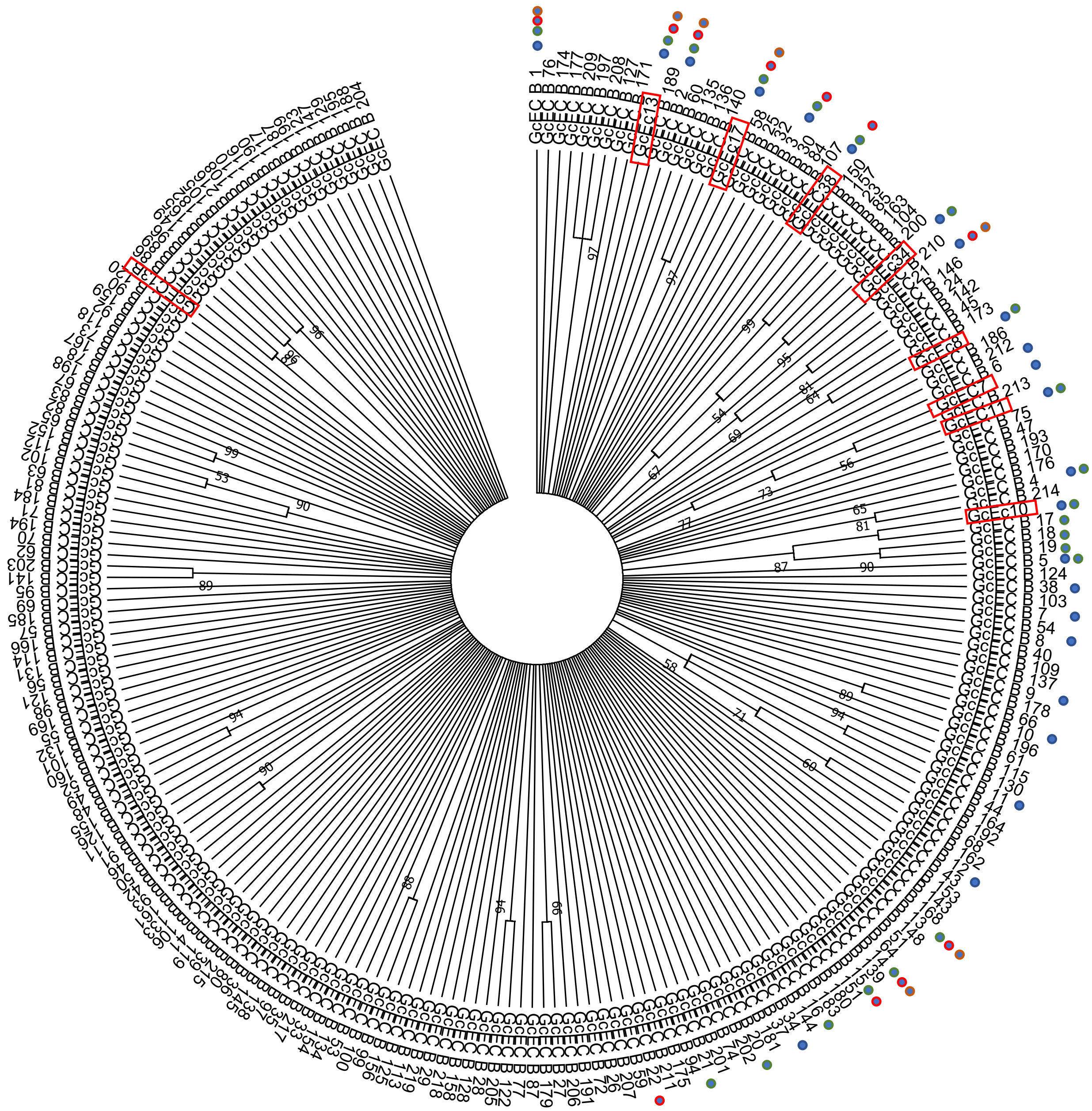

Figure 8.8. Molecular phylogenetic analysis by Maximum Likelihood method of G. cichoracearum *effector candidates*

Effector candidates with significant (E=value < 10E-5) homology to other powdery mildews are marked with blue (*G. orontii*), green *(E. necator*), red (*B. graminis f. sp. hordei)*, or orange (*B. graminis f. sp. tritici*) dots. HIGS-silenced effectors (Chapter II) are marked with red boxes.

Tables

Table 8.1: Genome sequencing statistics. Compiled publicly available data 1000 Fungal Genomes (https://genome.jgi.doe.gov/programs/fungi/index.jsf) Data from *B. graminis f. sp. hordei* (Bgh), *Erisyphe necator* (En), *B. graminis f. sp. tritici* (Bgt), *G. cichoracearum* (Gc), *S. sclerotiniorum* (Sc) and *G. orontii* (Go).

	Bgh	**En**	**Bgt**	**Gc**	**Sc**	**Go**
Genome Assembly size (Mbp)	118.73	52.51	158.94	146.84	38.33	211.31
Sequencing read coverage depth	5	76	13	34.63		16.46
# of contigs	11503	7919	21712	821	679	388
# of scaffolds	6843	5935	1867	821	37	388
# of scaffolds >= 2Kbp	989	3696	1867	821	37	387
Scaffold N50	18	710	58	98	9	65
Scaffold L50 (Mbp)	2.03	0.02	0.76	0.44	1.55	1.07
# of gaps	4660	1984	19845	0	642	0
% of scaffold length in gaps	25.90%	0.5	48.4	0	0.9	0
Three largest Scaffolds (Mbp)	9.69, 6.65, 5.19	0.19,0.16,0.13	5.2, 2.96, 2.57	2.35,2.10,2.07	2.78, 2.72, 2.63	4.15, 3.93, 3.13
Average length (bp) of:	***average***			***average***		
gene	1711	1558	1443	1680	1342	1584
transcript	1455	1419	1333	1483	1092	1413
exon	526	528	536	433	360	450
intron	70	84	75	83	141	82
description:						
protein length (aa)	485	473	444	436	363	415
exons per gene	2.77	2.69	2.49	3.43	2.8	3.14
# of gene models	6470	6484	6525	6782	14503	10830

Table 8.2: Representation of B. graminis f. sp. hordei *experimentally derived effectors in EffectorP predicted effectorome*. The EffectorP predicted proteome was searched for the experimentally validated *B. graminis f. sp. hordei* (Bgh) candidate secreted effector proteins (CSEP) as described in multiple studies (reference column).

Reference	**CSEP**	**Experimental phenotype?**	**Predicted by EffectorP?**
Ahmed et al., 2016	CSEP0254	Yes	Yes
Whigham et al., 2015	BEC1019	Yes	Yes
Ahmed et al., 2015	CSEP0105	Yes	No
Pliego et al., 2013	CSEP0064	Yes	Yes
Pliego et al., 2014	CSEP0264	Yes	Yes
Aguilar et al., 2015	CSEP0007	Yes	Yes
Aguilar et al., 2015	CSEP0128	Yes	Yes
Aguilar et al., 2015	CSEP0211	Yes	No
Aguilar et al., 2015	CSEP0247	Yes	No
Pliego et al., 2013	CSEP0191	Yes	Yes
Pliego et al., 2014	CSEP0491	Yes	Yes
Pliego et al., 2015	BEC1005	Yes	No
Pliego et al., 2016	BEC1019	Yes	Yes
Pliego et al., 2017	CSEP0135	Yes	Yes
Pliego et al., 2018	CSEP0196	Yes	Yes

Table 8.3: Predicted effector overlap between G. cichoracearum *and other powdery mildews.* ***G. cichoracearum*** (Gc) candidate effectors were compared to the EffectorP predicted effectorome of *G. orontii* (Go), *E. necator* (En), *B. graminis f. sp. hordei* (Bgh), and *B. graminis f. sp. tritici* (Bgt) with an e-value cutoff of 10E-10.

Gc effector	**Name used in this study**	**HIGS Phenotype ?**	**Homolog in Go?**	**Homolog in En?**	**Homolog in Bgh?**	**Homolog in Bgt?**
jgi|Golci1|1764386|e_gw1.76.44.1	GcEC_B_1		Y	Y	Y	Y
jgi|Golci1|1814346|fgenesh1_kg.11_#_19_#_TRINITY_DN16512_c0_g2_i3	GcEc13	No	Y	Y	Y	Y
jgi|Golci1|1817600|fgenesh1_kg.21_#_180_#_TRINITY_DN10989_c0_g3_i1	GcEC_B_2		Y	Y	Y	Y
jgi|Golci1|547549|CE547548_9241	GcEc17	Yes	Y	Y	Y	Y
jgi|Golci1|1731401|gm4.27226_g	GcEC_B_3		Y	Y	Y	N
jgi|Golci1|287936|CE287935_2773	GcEC38	No	Y	Y	Y	N
jgi|Golci1|1727806|gm4.23631_g	GcEc34	No	Y	Y	N	N
jgi|Golci1|1731083|gm4.26908_g	GcEc8	Yes	Y	Y	N	N
jgi|Golci1|1760570|e_gw1.6.10.1	GcEC11	No	Y	Y	N	N
jgi|Golci1|1815600|fgenesh1_kg.14_#_189_#_TRINITY_DN19994_c2_g1_i1	GcEc10	Yes	Y	Y	N	N
jgi|Golci1|585565|CE585564_4983	GcEC_B_4		Y	Y	N	N
jgi|Golci1|704175|CE704174_1109	GcEC_B_5		Y	Y	N	N
jgi|Golci1|1854454|fgenesh1_pm.2_#_22	GcEC21	No	Y	N	Y	Y
jgi|Golci1|1278290|CE1278289_2265	GcEC_B_6		Y	N	N	N
jgi|Golci1|1336305|CE1336304_824	GcEC_B_7		Y	N	N	N
jgi|Golci1|1714669|gm4.10494_g	GcEC_B_8		Y	N	N	N
jgi|Golci1|1798088|fgenesh1_pg.161_#_5	GcEC_B_9		Y	N	N	N
jgi|Golci1|1846658|fgenesh1_kg.263_#_45_#_TRINITY_DN20009_c7_g4_i2	GcEC_B_10		Y	N	N	N
jgi|Golci1|1847261|fgenesh1_kg.277_#_40_#_TRINITY_DN11115_c0_g1_i1	GcEC_B_11		Y	N	N	N
jgi|Golci1|1855481|fgenesh1_pm.35_#_8	GcEC_B_12		Y	N	N	N
jgi|Golci1|1867482|estExt_fgenesh1_pg.C_3960001	GcEC7	No	Y	N	N	N
jgi|Golci1|1799339|fgenesh1_pg.326_#_6	GcEC_B_13		N	Y	Y	Y
jgi|Golci1|1801984|estExt_Genemark4.C_260037	GcEC_B_14		N	Y	Y	Y
jgi|Golci1|1861191|estExt_fgenesh1_pm.C_1420008	GcEC_B_15		N	Y	Y	N
jgi|Golci1|1794491|fgenesh1_pg.4_#_48	GcEC_B_16		N	Y	N	N
jgi|Golci1|1815608|fgenesh1_kg.14_#_197_#_TRINITY_DN19994_c2_g1_i1	GcEC_B_17		N	Y	N	N
jgi|Golci1|1815611|fgenesh1_kg.14_#_200_#_TRINITY_DN19994_c2_g1_i1	GcEC_B_18		N	Y	N	N
jgi|Golci1|1815652|fgenesh1_kg.14_#_241_#_TRINITY_DN19994_c2_g1_i1	GcEC_B_19		N	Y	N	N
jgi|Golci1|528027|CE528026_1161	GcEC_B_20		N	Y	N	N
jgi|Golci1|686639|CE686638_4676	GcEC_B_21		N	Y	N	N

Gc effector	Name used in this study	HIGS Phenotype ?	Homolog in Go?	Homolog in En?	Homolog in Bgh?	Homolog in Bgt?
jgi|Golci1|1763298|e_gw1.52.7.1	GcEC_B_22		N	N	Y	N
jgi|Golci1|1017100|CE1017099_5758	GcEC_B_23		N	N	N	N
jgi|Golci1|1138219|CE1138218_188	GcEC_B_24		N	N	N	N
jgi|Golci1|1435786|CE1435785_986	GcEC_B_25		N	N	N	N
jgi|Golci1|1451405|CE1451404_11	GcEC_B_26		N	N	N	N
jgi|Golci1|1557851|CE1557850_1529	GcEC_B_27		N	N	N	N
jgi|Golci1|1727440|gm4.23265_g	GcEC_B_28		N	N	N	N
jgi|Golci1|1751675|gw1.355.9.1	GcEC_B_29		N	N	N	N
jgi|Golci1|1760131|e_gw1.3.125.1	GcEC_B_30		N	N	N	N
jgi|Golci1|1766399|e_gw1.133.69.1	GcEC_B_32		N	N	N	N
jgi|Golci1|1770009|e_gw1.406.3.1	GcEC_B_33		N	N	N	N
jgi|Golci1|1795608|fgenesh1_pg.32_#_27	GcEC_B_34		N	N	N	N
jgi|Golci1|1796298|fgenesh1_pg.60_#_3	GcEC_B_35		N	N	N	N
jgi|Golci1|1797699|fgenesh1_pg.133_#_3	GcEC_B_36		N	N	N	N
jgi|Golci1|1798567|fgenesh1_pg.205_#_5	GcEC_B_37		N	N	N	N
jgi|Golci1|1802261|estExt_Genemark4.C_310178	GcEC_B_38		N	N	N	N
jgi|Golci1|1805531|estExt_Genemark4.C_1270027	GcEC_B_39		N	N	N	N
jgi|Golci1|1809409|fgenesh1_kg.1_#_172_#_TRINITY_DN13694_c1_g3_i1	GcEC_B_40		N	N	N	N
jgi|Golci1|1809650|fgenesh1_kg.1_#_413_#_TRINITY_DN19368_c4_g24_i1	GcEC_B_41		N	N	N	N
jgi|Golci1|1809665|fgenesh1_kg.1_#_428_#_TRINITY_DN19413_c1_g1_i2	GcEC_B_42		N	N	N	N
jgi|Golci1|1809735|fgenesh1_kg.1_#_498_#_TRINITY_DN19133_c11_g6_i8	GcEC_B_43		N	N	N	N
jgi|Golci1|1809941|fgenesh1_kg.1_#_704_#_TRINITY_DN20914_c5_g6_i1	GcEC_B_44		N	N	N	N
jgi|Golci1|1809996|fgenesh1_kg.1_#_759_#_TRINITY_DN16679_c0_g2_i6	GcEC_B_45		N	N	N	N
jgi|Golci1|1810114|fgenesh1_kg.1_#_877_#_TRINITY_DN17764_c0_g1_i6	GcEC_B_46		N	N	N	N
jgi|Golci1|1810676|fgenesh1_kg.2_#_441_#_TRINITY_DN18692_c2_g2_i5	GcEC_B_47		N	N	N	N
jgi|Golci1|1810858|fgenesh1_kg.3_#_112_#_TRINITY_DN19285_c4_g1_i1	GcEC_B_48		N	N	N	N
jgi|Golci1|1810871|fgenesh1_kg.3_#_125_#_TRINITY_DN19285_c4_g1_i4	GcEC_B_49		N	N	N	N
jgi|Golci1|1810957|fgenesh1_kg.3_#_211_#_TRINITY_DN19413_c1_g1_i2	GcEC_B_50		N	N	N	N
jgi|Golci1|1810977|fgenesh1_kg.3_#_231_#_TRINITY_DN22998_c0_g1_i1	GcEC_B_51		N	N	N	N
jgi|Golci1|1811028|fgenesh1_kg.3_#_282_#_TRINITY_DN15396_c0_g1_i5	GcEC_B_52		N	N	N	N
jgi|Golci1|1811645|fgenesh1_kg.4_#_316_#_TRINITY_DN25802_c0_g1_i1	GcEC_B_53		N	N	N	N
jgi|Golci1|1811800|fgenesh1_kg.4_#_471_#_TRINITY_DN6084_c0_g2_i1	GcEC_B_54		N	N	N	N
jgi|Golci1|1811990|fgenesh1_kg.5_#_142_#_TRINITY_DN27152_c0_g1_i1	GcEC_B_55		N	N	N	N

Gc effector	Name used in this study	HIGS Phenotype ?	Homolog in Go?	Homolog in En?	Homolog in Bgh?	Homolog in Bgt?
jgi|Golci1|1812887|fgenesh1_kg.7_#_39_#_TRINITY_DN19367_c0_g4_i1	GcEC_B_56		N	N	N	N
jgi|Golci1|1812929|fgenesh1_kg.7_#_81_#_TRINITY_DN25097_c0_g1_i1	GcEC_B_57		N	N	N	N
jgi|Golci1|1813185|fgenesh1_kg.7_#_337_#_TRINITY_DN19205_c2_g3_i1	GcEC_B_58		N	N	N	N
jgi|Golci1|1813197|fgenesh1_kg.7_#_349_#_TRINITY_DN18565_c1_g4_i2	GcEC_B_59		N	N	N	N
jgi|Golci1|1813260|fgenesh1_kg.7_#_412_#_TRINITY_DN5562_c0_g2_i2	GcEC_B_60		N	N	N	N
jgi|Golci1|1813329|fgenesh1_kg.7_#_481_#_TRINITY_DN17658_c1_g2_i1	GcEC_B_61		N	N	N	N
jgi|Golci1|1813332|fgenesh1_kg.8_#_1_#_TRINITY_DN14936_c0_g3_i1	GcEC_B_62		N	N	N	N
jgi|Golci1|1813651|fgenesh1_kg.9_#_15_#_TRINITY_DN13887_c0_g1_i5	GcEC_B_63		N	N	N	N
jgi|Golci1|1813697|fgenesh1_kg.9_#_61_#_TRINITY_DN10177_c0_g2_i1	GcEC_B_64		N	N	N	N
jgi|Golci1|1813993|fgenesh1_kg.9_#_357_#_TRINITY_DN18756_c0_g2_i1	GcEC_B_65		N	N	N	N
jgi|Golci1|1814547|fgenesh1_kg.11_#_220_#_TRINITY_DN17012_c1_g1_i13	GcEC_B_66		N	N	N	N
jgi|Golci1|1814618|fgenesh1_kg.11_#_291_#_TRINITY_DN18841_c3_g2_i3	GcEC_B_67		N	N	N	N
jgi|Golci1|1814645|fgenesh1_kg.11_#_318_#_TRINITY_DN20914_c5_g5_i2	GcEC_B_68		N	N	N	N
jgi|Golci1|1814776|fgenesh1_kg.12_#_79_#_TRINITY_DN15444_c0_g1_i4	GcEC_B_69		N	N	N	N
jgi|Golci1|1814870|fgenesh1_kg.12_#_173_#_TRINITY_DN12092_c0_g1_i6	GcEC_B_70		N	N	N	N
jgi|Golci1|1814966|fgenesh1_kg.12_#_269_#_TRINITY_DN5415_c0_g2_i1	GcEC_B_71		N	N	N	N
jgi|Golci1|1816348|fgenesh1_kg.17_#_89_#_TRINITY_DN15392_c1_g1_i3	GcEC_B_72		N	N	N	N
jgi|Golci1|1817113|fgenesh1_kg.19_#_258_#_TRINITY_DN17941_c0_g1_i1	GcEC_B_73		N	N	N	N
jgi|Golci1|1817364|fgenesh1_kg.20_#_242_#_TRINITY_DN20960_c5_g6_i1	GcEC_B_74		N	N	N	N
jgi|Golci1|1817609|fgenesh1_kg.21_#_189_#_TRINITY_DN1116_c0_g1_i1	GcEC_B_75		N	N	N	N
jgi|Golci1|1817793|fgenesh1_kg.22_#_74_#_TRINITY_DN1718_c0_g1_i1	GcEC_B_76		N	N	N	N
jgi|Golci1|1819209|fgenesh1_kg.28_#_27_#_TRINITY_DN19263_c7_g1_i2	GcEC_B_77		N	N	N	N
jgi|Golci1|1819382|fgenesh1_kg.28_#_200_#_TRINITY_DN19374_c3_g2_i2	GcEC_B_78		N	N	N	N
jgi|Golci1|1819761|fgenesh1_kg.30_#_60_#_TRINITY_DN14005_c0_g2_i1	GcEC_B_80		N	N	N	N
jgi|Golci1|1820301|fgenesh1_kg.32_#_58_#_TRINITY_DN20727_c1_g8_i1	GcEC_B_81		N	N	N	N
jgi|Golci1|1820440|fgenesh1_kg.32_#_197_#_TRINITY_DN18957_c0_g4_i2	GcEC_B_82		N	N	N	N
jgi|Golci1|1820447|fgenesh1_kg.32_#_204_#_TRINITY_DN18957_c0_g4_i2	GcEC_B_83		N	N	N	N
jgi|Golci1|1820705|fgenesh1_kg.33_#_210_#_TRINITY_DN17726_c0_g3_i2	GcEC_B_84		N	N	N	N
jgi|Golci1|1821358|fgenesh1_kg.36_#_187_#_TRINITY_DN19282_c2_g3_i10	GcEC_B_85		N	N	N	N
jgi|Golci1|1821576|fgenesh1_kg.37_#_206_#_TRINITY_DN19375_c2_g5_i4	GcEC_B_86		N	N	N	N

<table>
<tr><th>Gc effector</th><th>Name used in this study</th><th>HIGS Phenotype ?</th><th>Homolog in Go?</th><th>Homolog in En?</th><th>Homolog in Bgh?</th><th>Homolog in Bgt?</th></tr>
<tr><td>jgi|Golci1|1821582|fgenesh1_kg.37_#_212_#_TRINITY_DN19375_c1_g1_i6</td><td>GcEC_B_87</td><td></td><td>N</td><td>N</td><td>N</td><td>N</td></tr>
<tr><td>jgi|Golci1|1821596|fgenesh1_kg.37_#_226_#_TRINITY_DN19375_c2_g5_i4</td><td>GcEC_B_89</td><td></td><td>N</td><td>N</td><td>N</td><td>N</td></tr>
<tr><td>jgi|Golci1|1821886|fgenesh1_kg.38_#_187_#_TRINITY_DN5411_c0_g1_i1</td><td>GcEC_B_90</td><td></td><td>N</td><td>N</td><td>N</td><td>N</td></tr>
<tr><td>jgi|Golci1|1822203|fgenesh1_kg.40_#_83_#_TRINITY_DN33122_c0_g1_i1</td><td>GcEC_B_91</td><td></td><td>N</td><td>N</td><td>N</td><td>N</td></tr>
<tr><td>jgi|Golci1|1822245|fgenesh1_kg.40_#_125_#_TRINITY_DN11647_c0_g1_i1</td><td>GcEC_B_92</td><td></td><td>N</td><td>N</td><td>N</td><td>N</td></tr>
<tr><td>jgi|Golci1|1822476|fgenesh1_kg.42_#_46_#_TRINITY_DN20617_c11_g9_i1</td><td>GcEC_B_93</td><td></td><td>N</td><td>N</td><td>N</td><td>N</td></tr>
<tr><td>jgi|Golci1|1822518|fgenesh1_kg.42_#_88_#_TRINITY_DN5281_c0_g2_i1</td><td>GcEC_B_94</td><td></td><td>N</td><td>N</td><td>N</td><td>N</td></tr>
<tr><td>jgi|Golci1|1823472|fgenesh1_kg.47_#_58_#_TRINITY_DN18948_c0_g1_i1</td><td>GcEC_B_95</td><td></td><td>N</td><td>N</td><td>N</td><td>N</td></tr>
<tr><td>jgi|Golci1|1823511|fgenesh1_kg.47_#_97_#_TRINITY_DN20795_c10_g1_i1</td><td>GcEC_B_96</td><td></td><td>N</td><td>N</td><td>N</td><td>N</td></tr>
<tr><td>jgi|Golci1|1824111|fgenesh1_kg.50_#_116_#_TRINITY_DN13688_c0_g1_i1</td><td>GcEC_B_97</td><td></td><td>N</td><td>N</td><td>N</td><td>N</td></tr>
<tr><td>jgi|Golci1|1824208|fgenesh1_kg.51_#_13_#_TRINITY_DN19964_c3_g10_i1</td><td>GcEC_B_98</td><td></td><td>N</td><td>N</td><td>N</td><td>N</td></tr>
<tr><td>jgi|Golci1|1824679|fgenesh1_kg.53_#_186_#_TRINITY_DN19325_c3_g9_i1</td><td>GcEC_B_99</td><td></td><td>N</td><td>N</td><td>N</td><td>N</td></tr>
<tr><td>jgi|Golci1|1824686|fgenesh1_kg.53_#_193_#_TRINITY_DN19325_c3_g26_i1</td><td colspan="2">GcEC_B_100</td><td>N</td><td>N</td><td>N</td><td>N</td></tr>
<tr><td>jgi|Golci1|1825223|fgenesh1_kg.56_#_61_#_TRINITY_DN9431_c0_g1_i1</td><td colspan="2">GcEC_B_101</td><td>N</td><td>N</td><td>N</td><td>N</td></tr>
<tr><td>jgi|Golci1|1825381|fgenesh1_kg.57_#_71_#_TRINITY_DN20841_c2_g2_i1</td><td colspan="2">GcEC_B_102</td><td>N</td><td>N</td><td>N</td><td>N</td></tr>
<tr><td>jgi|Golci1|1825635|fgenesh1_kg.59_#_51_#_TRINITY_DN10057_c0_g1_i2</td><td colspan="2">GcEC_B_103</td><td>N</td><td>N</td><td>N</td><td>N</td></tr>
<tr><td>jgi|Golci1|1826245|fgenesh1_kg.62_#_136_#_TRINITY_DN8979_c0_g1_i1</td><td colspan="2">GcEC_B_104</td><td>N</td><td>N</td><td>N</td><td>N</td></tr>
<tr><td>jgi|Golci1|1826621|fgenesh1_kg.63_#_330_#_TRINITY_DN15719_c1_g1_i7</td><td colspan="2">GcEC_B_105</td><td>N</td><td>N</td><td>N</td><td>N</td></tr>
<tr><td>jgi|Golci1|1826724|fgenesh1_kg.64_#_97_#_TRINITY_DN973_c0_g2_i1</td><td colspan="2">GcEC_B_106</td><td>N</td><td>N</td><td>N</td><td>N</td></tr>
<tr><td>jgi|Golci1|1826956|fgenesh1_kg.66_#_36_#_TRINITY_DN17222_c0_g2_i1</td><td colspan="2">GcEC_B_107</td><td>N</td><td>N</td><td>N</td><td>N</td></tr>
<tr><td>jgi|Golci1|1827166|fgenesh1_kg.67_#_111_#_TRINITY_DN17962_c2_g12_i1</td><td colspan="2">GcEC_B_108</td><td>N</td><td>N</td><td>N</td><td>N</td></tr>
<tr><td>jgi|Golci1|1827365|fgenesh1_kg.69_#_57_#_TRINITY_DN14533_c0_g1_i1</td><td colspan="2">GcEC_B_109</td><td>N</td><td>N</td><td>N</td><td>N</td></tr>
<tr><td>jgi|Golci1|1827755|fgenesh1_kg.72_#_6_#_TRINITY_DN26106_c0_g1_i1</td><td colspan="2">GcEC_B_110</td><td>N</td><td>N</td><td>N</td><td>N</td></tr>
<tr><td>jgi|Golci1|1828306|fgenesh1_kg.74_#_159_#_TRINITY_DN20841_c3_g1_i5</td><td colspan="2">GcEC_B_111</td><td>N</td><td>N</td><td>N</td><td>N</td></tr>
<tr><td>jgi|Golci1|1828308|fgenesh1_kg.74_#_161_#_TRINITY_DN20841_c2_g2_i1</td><td colspan="2">GcEC_B_112</td><td>N</td><td>N</td><td>N</td><td>N</td></tr>
<tr><td>jgi|Golci1|1829769|fgenesh1_kg.83_#_33_#_TRINITY_DN18986_c0_g1_i36</td><td colspan="2">GcEC_B_113</td><td>N</td><td>N</td><td>N</td><td>N</td></tr>
<tr><td>jgi|Golci1|1830139|fgenesh1_kg.86_#_78_#_TRINITY_DN12388_c0_g1_i4</td><td colspan="2">GcEC_B_114</td><td>N</td><td>N</td><td>N</td><td>N</td></tr>
<tr><td>jgi|Golci1|1830243|fgenesh1_kg.86_#_182_#_TRINITY_DN6911_c0_g1_i2</td><td colspan="2">GcEC_B_115</td><td>N</td><td>N</td><td>N</td><td>N</td></tr>
<tr><td>jgi|Golci1|1830255|fgenesh1_kg.87_#_10_#_TRINITY_DN11063_c0_g2_i1</td><td colspan="2">GcEC_B_116</td><td>N</td><td>N</td><td>N</td><td>N</td></tr>
<tr><td>jgi|Golci1|1830338|fgenesh1_kg.87_#_93_#_TRINITY_DN19091_c0_g1_i14</td><td colspan="2">GcEC_B_117</td><td>N</td><td>N</td><td>N</td><td>N</td></tr>
</table>

Gc effector	Name used in this study	HIGS Phenotype ?	Homolog in Go?	Homolog in En?	Homolog in Bgh?	Homolog in Bgt?
jgi|Golci1|1830648|fgenesh1_kg.89_#_47_#_TRINITY_DN19764_c2_g1_i2	GcEC_B_118		N	N	N	N
jgi|Golci1|1830679|fgenesh1_kg.89_#_78_#_TRINITY_DN13925_c0_g5_i1	GcEC_B_119		N	N	N	N
jgi|Golci1|1830926|fgenesh1_kg.91_#_30_#_TRINITY_DN19719_c2_g1_i12	GcEC_B_120		N	N	N	N
jgi|Golci1|1831039|fgenesh1_kg.91_#_143_#_TRINITY_DN18274_c2_g1_i1	GcEC_B_121		N	N	N	N
jgi|Golci1|1831419|fgenesh1_kg.95_#_88_#_TRINITY_DN17620_c0_g1_i1	GcEC_B_122		N	N	N	N
jgi|Golci1|1831692|fgenesh1_kg.98_#_27_#_TRINITY_DN14153_c0_g2_i1	GcEC_B_123		N	N	N	N
jgi|Golci1|1832687|fgenesh1_kg.106_#_4_#_TRINITY_DN4980_c0_g3_i1	GcEC_B_124		N	N	N	N
jgi|Golci1|1832789|fgenesh1_kg.106_#_106_#_TRINITY_DN12524_c0_g1_i3	GcEC_B_125		N	N	N	N
jgi|Golci1|1832791|fgenesh1_kg.106_#_108_#_TRINITY_DN18297_c0_g1_i1	GcEC_B_126		N	N	N	N
jgi|Golci1|1832953|fgenesh1_kg.107_#_159_#_TRINITY_DN17265_c0_g1_i1	GcEC_B_127		N	N	N	N
jgi|Golci1|1833160|fgenesh1_kg.109_#_37_#_TRINITY_DN17662_c0_g1_i2	GcEC_B_128		N	N	N	N
jgi|Golci1|1833347|fgenesh1_kg.110_#_126_#_TRINITY_DN20810_c8_g4_i3	GcEC_B_129		N	N	N	N
jgi|Golci1|1833918|fgenesh1_kg.114_#_101_#_TRINITY_DN17423_c0_g2_i3	GcEC_B_130		N	N	N	N
jgi|Golci1|1833976|fgenesh1_kg.115_#_43_#_TRINITY_DN14384_c0_g1_i5	GcEC_B_131		N	N	N	N
jgi|Golci1|1834689|fgenesh1_kg.119_#_126_#_TRINITY_DN2916_c0_g1_i2	GcEC_B_132		N	N	N	N
jgi|Golci1|1834832|fgenesh1_kg.120_#_67_#_TRINITY_DN16150_c0_g1_i5	GcEC_B_133		N	N	N	N
jgi|Golci1|1834873|fgenesh1_kg.120_#_108_#_TRINITY_DN17226_c0_g1_i30	GcEC_B_134		N	N	N	N
jgi|Golci1|1835113|fgenesh1_kg.121_#_151_#_TRINITY_DN20141_c1_g2_i5	GcEC_B_135		N	N	N	N
jgi|Golci1|1835397|fgenesh1_kg.124_#_42_#_TRINITY_DN19711_c3_g4_i7	GcEC_B_136		N	N	N	N
jgi|Golci1|1835924|fgenesh1_kg.129_#_77_#_TRINITY_DN14418_c0_g2_i1	GcEC_B_137		N	N	N	N
jgi|Golci1|1837153|fgenesh1_kg.140_#_51_#_TRINITY_DN17470_c0_g4_i1	GcEC_B_138		N	N	N	N
jgi|Golci1|1837446|fgenesh1_kg.142_#_1_#_TRINITY_DN1921_c0_g1_i1	GcEC_B_139		N	N	N	N
jgi|Golci1|1837499|fgenesh1_kg.142_#_54_#_TRINITY_DN19711_c3_g4_i7	GcEC_B_140		N	N	N	N
jgi|Golci1|1837602|fgenesh1_kg.143_#_67_#_TRINITY_DN19491_c6_g2_i1	GcEC_B_141		N	N	N	N
jgi|Golci1|1838023|fgenesh1_kg.147_#_17_#_TRINITY_DN5681_c0_g1_i2	GcEC_B_142		N	N	N	N
jgi|Golci1|1838171|fgenesh1_kg.148_#_35_#_TRINITY_DN33716_c0_g1_i1	GcEC_B_143		N	N	N	N
jgi|Golci1|1838207|fgenesh1_kg.148_#_71_#_TRINITY_DN17399_c1_g1_i2	GcEC_B_144		N	N	N	N
jgi|Golci1|1838249|fgenesh1_kg.148_#_113_#_TRINITY_DN19651_c1_g2_i1	GcEC_B_145		N	N	N	N
jgi|Golci1|1838285|fgenesh1_kg.149_#_36_#_TRINITY_DN8471_c0_g1_i1	GcEC_B_146		N	N	N	N
jgi|Golci1|1838867|fgenesh1_kg.153_#_112_#_TRINITY_DN2342_c0_g1_i1	GcEC_B_147		N	N	N	N

Gc effector	Name used in this study	HIGS Phenotype ?	Homolog in Go?	Homolog in En?	Homolog in Bgh?	Homolog in Bgt?
jgi|Golci1|1838928|fgenesh1_kg.153_#_173_#_TRINITY_DN17383_c0_g2_i3	GcEC_B_148		N	N	N	N
jgi|Golci1|1840128|fgenesh1_kg.168_#_82_#_TRINITY_DN20795_c10_g3_i1	GcEC_B_149		N	N	N	N
jgi|Golci1|1840186|fgenesh1_kg.168_#_140_#_TRINITY_DN2224_c0_g1_i1	GcEC_B_150		N	N	N	N
jgi|Golci1|1840418|fgenesh1_kg.170_#_29_#_TRINITY_DN15635_c0_g3_i1	GcEC_B_151		N	N	N	N
jgi|Golci1|1840524|fgenesh1_kg.171_#_72_#_TRINITY_DN20841_c2_g2_i1	GcEC_B_152		N	N	N	N
jgi|Golci1|1840959|fgenesh1_kg.175_#_99_#_TRINITY_DN25916_c0_g1_i1	GcEC_B_153		N	N	N	N
jgi|Golci1|1841438|fgenesh1_kg.180_#_47_#_TRINITY_DN18902_c1_g1_i1	GcEC_B_154		N	N	N	N
jgi|Golci1|1841637|fgenesh1_kg.182_#_71_#_TRINITY_DN19169_c0_g2_i1	GcEC_B_155		N	N	N	N
jgi|Golci1|1842294|fgenesh1_kg.191_#_31_#_TRINITY_DN21101_c2_g19_i1	GcEC_B_156		N	N	N	N
jgi|Golci1|1842411|fgenesh1_kg.193_#_25_#_TRINITY_DN28222_c0_g1_i1	GcEC_B_157		N	N	N	N
jgi|Golci1|1842557|fgenesh1_kg.196_#_25_#_TRINITY_DN20525_c2_g11_i1	GcEC_B_158		N	N	N	N
jgi|Golci1|1842817|fgenesh1_kg.200_#_72_#_TRINITY_DN18898_c3_g1_i2	GcEC_B_159		N	N	N	N
jgi|Golci1|1842879|fgenesh1_kg.201_#_57_#_TRINITY_DN12213_c0_g1_i3	GcEC_B_160		N	N	N	N
jgi|Golci1|1843169|fgenesh1_kg.205_#_18_#_TRINITY_DN16887_c0_g2_i5	GcEC_B_161		N	N	N	N
jgi|Golci1|1843408|fgenesh1_kg.208_#_37_#_TRINITY_DN20914_c5_g6_i1	GcEC_B_162		N	N	N	N
jgi|Golci1|1843633|fgenesh1_kg.211_#_33_#_TRINITY_DN20912_c5_g7_i3	GcEC_B_163		N	N	N	N
jgi|Golci1|1843635|fgenesh1_kg.211_#_35_#_TRINITY_DN20914_c5_g5_i2	GcEC_B_164		N	N	N	N
jgi|Golci1|1843848|fgenesh1_kg.215_#_6_#_TRINITY_DN21014_c8_g1_i1	GcEC_B_165		N	N	N	N
jgi|Golci1|1844611|fgenesh1_kg.224_#_22_#_TRINITY_DN19708_c1_g3_i14	GcEC_B_166		N	N	N	N
jgi|Golci1|1844841|fgenesh1_kg.230_#_14_#_TRINITY_DN31389_c0_g1_i1	GcEC_B_167		N	N	N	N
jgi|Golci1|1845265|fgenesh1_kg.239_#_6_#_TRINITY_DN21049_c5_g4_i1	GcEC_B_168		N	N	N	N
jgi|Golci1|1845359|fgenesh1_kg.240_#_40_#_TRINITY_DN11304_c0_g2_i1	GcEC_B_169		N	N	N	N
jgi|Golci1|1845481|fgenesh1_kg.242_#_49_#_TRINITY_DN19534_c2_g5_i1	GcEC_B_170		N	N	N	N
jgi|Golci1|1846209|fgenesh1_kg.255_#_12_#_TRINITY_DN18203_c6_g1_i1	GcEC_B_171		N	N	N	N
jgi|Golci1|1846232|fgenesh1_kg.255_#_35_#_TRINITY_DN17478_c2_g1_i8	GcEC_B_173		N	N	N	N
jgi|Golci1|1846577|fgenesh1_kg.261_#_83_#_TRINITY_DN1718_c0_g1_i1	GcEC_B_174		N	N	N	N
jgi|Golci1|1846680|fgenesh1_kg.264_#_20_#_TRINITY_DN12296_c0_g1_i1	GcEC_B_175		N	N	N	N
jgi|Golci1|1846764|fgenesh1_kg.266_#_9_#_TRINITY_DN12539_c0_g2_i1	GcEC_B_176		N	N	N	N
>jgi|Golci1|1846914|fgenesh1_kg.270_#_10_#_TRINITY_DN1718_c0_g1_i1	GcEC_B_177		N	N	N	N
jgi|Golci1|1847190|fgenesh1_kg.274_#_27_#_TRINITY_DN26142_c0_g1_i1	GcEC_B_178		N	N	N	N

Gc effector	Name used in this study	HIGS Phenotype ?	Homolog in Go?	Homolog in En?	Homolog in Bgh?	Homolog in Bgt?
jgi|Golci1|1847210|fgenesh1_kg.276_#_1_#_TRINITY_DN6029_c0_g1_i1	GcEC_B_179		N	N	N	N
jgi|Golci1|1847249|fgenesh1_kg.277_#_28_#_TRINITY_DN20914_c5_g6_i1	GcEC_B_180		N	N	N	N
jgi|Golci1|1847448|fgenesh1_kg.278_#_167_#_TRINITY_DN18781_c0_g4_i2	GcEC_B_181		N	N	N	N
jgi|Golci1|1847758|fgenesh1_kg.284_#_24_#_TRINITY_DN21014_c8_g1_i1	GcEC_B_182		N	N	N	N
jgi|Golci1|1847763|fgenesh1_kg.284_#_29_#_TRINITY_DN8542_c0_g1_i2	GcEC_B_183		N	N	N	N
jgi|Golci1|1847945|fgenesh1_kg.288_#_7_#_TRINITY_DN16904_c1_g1_i5	GcEC_B_184		N	N	N	N
jgi|Golci1|1847985|fgenesh1_kg.288_#_47_#_TRINITY_DN1467_c0_g2_i1	GcEC_B_185		N	N	N	N
jgi|Golci1|1848150|fgenesh1_kg.292_#_28_#_TRINITY_DN12002_c0_g1_i1	GcEC_B_186		N	N	N	N
jgi|Golci1|1848194|fgenesh1_kg.294_#_20_#_TRINITY_DN5720_c0_g4_i1	GcEC_B_187		N	N	N	N
jgi|Golci1|1848281|fgenesh1_kg.297_#_21_#_TRINITY_DN7952_c0_g2_i1	GcEC_B_188		N	N	N	N
jgi|Golci1|1848292|fgenesh1_kg.298_#_10_#_TRINITY_DN3024_c0_g1_i1	GcEC_B_189		N	N	N	N
jgi|Golci1|1848303|fgenesh1_kg.299_#_10_#_TRINITY_DN16800_c0_g2_i9	GcEC_B_190		N	N	N	N
jgi|Golci1|1848627|fgenesh1_kg.308_#_11_#_TRINITY_DN8353_c0_g1_i2	GcEC_B_191		N	N	N	N
jgi|Golci1|1849102|fgenesh1_kg.322_#_79_#_TRINITY_DN20914_c5_g5_i2	GcEC_B_192		N	N	N	N
jgi|Golci1|1849710|fgenesh1_kg.337_#_1_#_TRINITY_DN18943_c0_g1_i1	GcEC_B_193		N	N	N	N
jgi|Golci1|1849726|fgenesh1_kg.337_#_17_#_TRINITY_DN811_c0_g2_i1	GcEC_B_194		N	N	N	N
jgi|Golci1|1849957|fgenesh1_kg.343_#_17_#_TRINITY_DN21097_c4_g3_i1	GcEC_B_195		N	N	N	N
jgi|Golci1|1850082|fgenesh1_kg.346_#_43_#_TRINITY_DN20009_c7_g4_i2	GcEC_B_196		N	N	N	N
jgi|Golci1|1850536|fgenesh1_kg.359_#_2_#_TRINITY_DN5190_c0_g1_i1	GcEC_B_197		N	N	N	N
jgi|Golci1|1851023|fgenesh1_kg.372_#_38_#_TRINITY_DN2394_c0_g1_i1	GcEC_B_198		N	N	N	N
jgi|Golci1|1851523|fgenesh1_kg.387_#_14_#_TRINITY_DN19490_c1_g1_i2	GcEC_B_199		N	N	N	N
jgi|Golci1|1851917|fgenesh1_kg.397_#_37_#_TRINITY_DN19431_c1_g5_i1	GcEC_B_200		N	N	N	N
jgi|Golci1|1851977|fgenesh1_kg.398_#_14_#_TRINITY_DN6817_c0_g1_i4	GcEC_B_201		N	N	N	N
jgi|Golci1|1852279|fgenesh1_kg.411_#_1_#_TRINITY_DN18771_c1_g5_i1	GcEC_B_202		N	N	N	N
jgi|Golci1|1852292|fgenesh1_kg.411_#_14_#_TRINITY_DN19491_c6_g2_i1	GcEC_B_203		N	N	N	N
jgi|Golci1|1852783|fgenesh1_kg.439_#_8_#_TRINITY_DN16152_c0_g2_i1	GcEC_B_204		N	N	N	N
jgi|Golci1|1852935|fgenesh1_kg.454_#_3_#_TRINITY_DN8373_c0_g1_i1	GcEC_B_205		N	N	N	N
jgi|Golci1|1853106|fgenesh1_kg.470_#_8_#_TRINITY_DN19037_c3_g3_i9	GcEC_B_206		N	N	N	N
>jgi|Golci1|1853244|fgenesh1_kg.488_#_4_#_TRINITY_DN14750_c0_g1_i1	GcEC_B_207		N	n	n	n
jgi|Golci1|1853298|fgenesh1_kg.498_#_2_#_TRINITY_DN5190_c0_g1_i1	GcEC_B_208		N	N	N	N

Gc effector	**Name used in this study**	**HIGS Phenotype ?**	**Homolog in Go?**	**Homolog in En?**	**Homolog in Bgh?**	**Homolog in Bgt?**
jgi|Golci1|1853805|fgenesh1_kg.628_#_2_#_TRINITY_DN5190_c0_g1_i1	GcEC_B_209		N	N	N	N
jgi|Golci1|1854311|fgenesh1_kg.806_#_2_#_TRINITY_DN8471_c0_g3_i1	GcEC_B_210		N	N	N	N
jgi|Golci1|1854317|fgenesh1_kg.808_#_4_#_TRINITY_DN8471_c0_g2_i1	GcEC_B_211		N	N	N	N
jgi|Golci1|1867255|estExt_fgenesh1_pg.C_3340001	GcEC_B_212		N	N	N	N
jgi|Golci1|1910368|MIX42608_10_31	GcEC_B_213		N	N	N	N
jgi|Golci1|20843|CE20842_127	GcEC_B_214		N	N	N	N
jgi|Golci1|397334|CE397333_28	GcEC_B_215		N	N	N	N
jgi|Golci1|540405|CE540404_23	GcEC_B_216		N	N	N	N
jgi|Golci1|669736|CE669735_39518	GcEC13	No	N	N	N	N
jgi|Golci1|682040|CE682039_47	GcEC_B_217		N	N	N	N
jgi|Golci1|748233|CE748232_145	GcEC_B_218		N	N	N	N
jgi|Golci1|815078|CE815077_16	GcEC_B_219		N	N	N	N

Materials and Methods

Polymerase chain reaction (PCR)
For genotyping, reactions were performed with standard Taq polymerase (New England Biolabs, NEB), 10x Standard Taq buffer, 2.5µM dNTPs, and 10µM of each primer. For cloning, Phusion polymerase (NEB) was used with 5x HF buffer, 2.5µM dNTPs, and 10µM of each primer. Reaction conditions were as described in the manufacturer's instructions. Product visualization was performed by combining samples with 6x OrangeG loading dye and run on 1% agarose gels with ethidium bromide and imaged using UV light in a GelDoc XR bioimager (Bio-Rad).

Plasmid DNA preparation
3ml cultures of *Escherichia coli* containing the plasmid of interest were grown overnight at 37°C with the appropriate antibiotic in LB media. Cells were harvested and plasmids extracted using a Miniprep Kit (Qiagen) according to manufacturer's instructions.

Fungal RNA Isolation
Heavily infected Arabidopsis leaves were harvested 7 days post inoculation (dpi) and flash frozen in liquid nitrogen in tubes containing two 2mm steel balls. Leaves were then shaken 3 times in a ball mill (Retsch) at 250/second for 30 seconds. Plant RNeasy kit (Qiagen) was then used to isolate RNA according to manufacturer's instructions with on column DNaseI treatment.

Fungal cDNA Synthesis
cDNA was synthesized from 1µg fungal RNA using the M-MuLV kit (NEB) according to manufacturer's instructions.

Selection of initial silencing targets
50 highly-expressed effector candidates were identified from the predicted *Golovinomyces orontii* genome (Weßling et al., personal communication). Candidates were selected that were 1) at least 200 base pairs (bp) in length, 2) highly expressed compared to other candidates, 3) contained domains with predicted similarity to described domains.

Cloning strategies
Standard cloning methods were used to create constructs (modified from Sambrook et al., 1989). Constructs were sequenced to verify presence of expected sequence and to ensure that there were no unwanted mutations. Plasmids and primers used in this study are listed in Tables 2.2, 2.3, 3.1, 3.2, 4.1, 4.2, 5.1, 5.2, 6.3, 6.4, and 7.2.

Construction of HIGS plasmids
Primers were designed to amplify approximately 200 bp of each of the "Top 40" effector candidates, GcCyp51, or GcAde2, with 3' and 5' overhangs corresponding to the sequence of pYL156. Products that were successfully amplified were cloned into pYL156 (pTRV2) digested

with EcoRI and KpnI via Gibson Assembly using NEBuilder HiFi DNA Assembly Master Mix (NEB) to form HIGS constructs (Dong et al., 2007).

Construction of *E. coli* expression plasmids

Primers were designed to amplify the entire sequence of effector candidates GcEC8, GcEC10, and GcEC17 excluding the predicted signal peptide and stop codon with 3' and 5' overhangs corresponding to the sequence of pET28(+)α (Invitrogen). Products that were successfully amplified were cloned into pET28(+)α digested with SalI and BamHI via Gibson Assembly using NEBuilder HiFi DNA Assembly Master Mix (NEB).

Construction of GFP-Fusion, Yeast Expression, and Bimolecular Fluorescence Complementation Plasmids

Primers were designed to amplify the entire sequence of effector candidates GcEc8, GcEC10 and GcEC17 excluding the predicted signal peptide and stop codon. Constructs were synthesized by GeneArt (https://geneart.com/), amplified using PCR and cloned into pCR8 through the use of a TOPO cloning kit (Thermo Fisher Scientific). Primers were designed for Arabidopsis genes excluding stop codon and amplified from Arabidopsis cDNA and cloned into pCR8 in a similar fashion. Constructs were then cloned into pMDC 32, pMDC 44, pGBKT7-GW pB7WGYn2, pK2GWYc9, pK2GWYn9, pB7WGYc2and pMDC 84 using the Gateway LR Clonase II Enzyme mix kit (Thermo Fisher Scientific, Curtis et al., 2013, Karimi et al., 2002).

Arabidopsis thaliana Growth Conditions

Columbia-0 (Col-0) ecotype of *A. thaliana* seed were surface sterilized with 50% bleach and 0.5% SDS for 6 m prior to 3 water washes and resuspended in water. Seeds were stratified at 4°C for 48 hours. Seeds were then planted on the surface of soil and grown in Percival (14 h) growth chambers at 70% relative humidity with 14 h light at 100 $\mu E\ m^{-2}s^{-1}$ at 22°C day temperature and 20°C night temperature. Pots were covered with a transparent cover for 5 days after sowing. Plants were fertilized with Miracle Gro 5 days after sowing and bottom watered (modified from Weigel and Glazebrook, 2002).

Cucumis sativa Growth Conditions

C. sativa cv. Bush Champion (Burpee) seeds were planted 1" deep in soil, covered, and grown in Percival growth chamber at 70% relative humidity with 16h light at 100 $\mu E\ m^{-2}s^{-1}$ at 22°C day temperature and 20°C night temperature. Plants were fertilized with Miracle Grow 5 days after sowing and bottom watered.

Nicotiana benthamiana Growth Conditions

N. benthamiana seeds were placed on the surface of soil and grown in Percival (14 h) growth chambers at 70% relative humidity with 14 h light at 100 $\mu E\ m^{-2}s^{-1}$ at 22°C day temperature and 20°C night temperature. Plants were fertilized with Miracle Gro 5 days after sowing and bottom watered.

Powdery mildew growth and infections

Golovinomyces cichoracearum UCSC1 was maintained on cucumber plants under conditions described above. Three-week old plants were inoculated by placing a 1.3 m high settling tower over the flat and dispersing spores using compressed air from heavily infected cucumber leaves. After 5 minutes, the plants were moved to a growth chamber under 16 h light with a light intensity of 100µE m-2 s-1, 22°C day temperature and 20°C night temperature and 75% relative humidity.

Chemically competent *E. coli* transformation

25 µL chemically competent *E. coli* cells were incubated with 200 ng purified plasmid DNA for 30 minutes on ice, transferred to a 42°C water bath for 30 seconds and immediately returned to ice. Cells were rescued with 250 µL SOC media (Sigma-Aldrich) at 37°C for one hour and plated on appropriate antibiotics (modified from Sambrook et al., 1989).

Electrocompetent *Agrobacterium tumefaciens* transformation

25 µL electrocompetent *A. tumefaciens* cells were incubated with 200 ng purified plasmid DNA on ice and transferred to a pre-chilled 1mm electroporation cuvette. An electric pulse was delivered at 2 kV, 150 Ω, 50 µF. Cells were rescued in 1 mL Luria Broth (LB) at 28°C for 2 hours and plated on appropriate antibiotics (Weigel and Glazebrook, 2002).

Generation of transgenic *A. thaliana*

Overnight cultures of *A. tumefaciens* containing plasmids of interest were grown in appropriate antibiotic selective conditions. Plants were transformed via the floral dip method (Clough and Bent, 1998) and returned to growth chamber conditions until seed-set. Seeds were screened for resistance to relevant antibiotics and genotyped to confirm the presence of the transgene via PCR.

A. thaliana genomic DNA isolation

Leaf tissue was ground in DNA extraction buffer (200mM tris pH 7.5, 250 mM NaCl, 25 mM EDTA pH 8.0, 0.5% SDS) and centrifuged to separate the genomic DNA in the supernatant from the cell debris pellet. The supernatant was suspended in an equal volume of isopropanol, centrifuged, and the resultant pellet was washed with two volumes of 70% ethanol. The pellet was left to dry at room temperature and resuspended in water.

Host-Induced Gene Silencing

A modification of Virus-Induced Gene Silencing (Burch-Smith et al. 2006) was used in this study. Nine-day old *A. thaliana* seedlings with fully extended 1st but not 2nd leaves were selected for infiltration. *A. tumefaciens* containing modified Tobacco Rattle Virus (TRV) expressing 200 bp of a *G. cichoracearum* effector candidate, pTRV1 (pYL192) and pTRV2-PDS (phytoene desaturase, positive control) were grown overnight in LB media containing 25 µg/ml rifampicin, 25 µg/ml gentamycin, and 60 µg/ml kanamycin. 10mM MgCl2, 10mM MES, and 200 µM acetosyringone) to OD_{600} 1.5. Cultures were incubated at 30°C for two hours, and pTRV2 and pTRV1 cultures were combined at 1:1 immediately prior to syringe infiltration of the first true leaves. 10 days after infiltration, plants were infected with *G. cichoracearum*. Leaf tissue was collected 2 dpi and used for analysis.

SDS-PAGE and Western blot

SDS-PAGE was performed according to Laemmli (1970). Proteins were run on 12% Tris HCl pre-cast SDS-PAGE gels (Criterion) at 200V for 50 minutes. Gels were then either stained with GelCode Blue (Thermo Pierce) for 1 h and destained with water according to the manufacturer's protocol, stained with SYPRO Ruby (Bio-Rad) according to manufacturer's protocol, or transferred to a nitrocellulose membrane. Transfer occurred at 100V for 1h at 4°C. The membrane was then blocked with 5% milk in tris-buffered saline (TBS) for 1h at 4°C, followed by incubation with the primary antibody, three washes with TBS and 0.05% Tween 20 (TBST), and incubation with the second antibody (modified from Sambrook et al., 1989). The membrane was visualized with chemiluminescent substrate (Pierce) using the LAS4000 image reader (GE Healthcare Life Sciences).

Expression of GcEC10-sp in *E. coli*

GcEC10-sp in pET28(a) (Invitrogen) was transformed into BL21-Star(DE3) *E. coli* (Thermo Fisher Scientific) and overnight cultures were used to inoculate 1L of LB containing kanamycin to OD_{600} 0.5. The culture was induced with 0.3 mM IPTG and grown at 20°C for 6 hours. Cells were centrifuged at 10,000 xg for 15 minutes, washed with cold TBS and the pellet was stored at -80°C until used.

Purification of GcEC10-sp-HIS protein

A modified protocol from Sorek et al., (2007) was used in this study. *E. coli* culture pellets were homogenized in 50 mL lysis buffer (50 mM NaH2PO4 pH 7.6, 150 mM NaCl, 5 mM imidazole, 5% glycerol, 1 mM beta-mercaptoethanol) using the Avestin E3 Emulsiflex Homogenizer according to manufacturer's instructions. The resulting homogenate was then centrifuged at 20,000 rpm at 4°C for 1 hour. The effector candidates were purified from the supernatant using the fast-protein liquid chromatography AKTA Purifier 10 (GE) bound on a 1ml Ni-NTA column (Life Technologies) and eluted using 200 mM imidazole at a flow rate of 0.1-1ml per minute. The buffer was then exchanged using a Zeba Spin Desalting Column, 7K MWCO, 5mL (Thermo Scientific) according to manufacturer instructions and replaced with extraction buffer (50 mM NaH_2PO_4 pH 7, 300 mM NaCl, 40 mM imidazole, 5% glycerol, 1 mM beta-mercaptoethanol).

Extraction of infected *A. thaliana* protein

2.5 g of heavily infected *A. thaliana* leaves were ground to a fine powder in 8 mL extraction buffer on dry ice using a pre-chilled mortar and pestle. This was allowed to thaw and resuspended in 50 mL extraction buffer. The solution was then centrifuged at 100,000 xg for 1 hour. The supernatant containing soluble proteins was separated and frozen at -80°C until used. The pellet containing the membrane fraction was resuspended in extraction buffer with 0.5% Triton X100 and 0.1% SDS and centrifuged at 100,000 xg for 1 hour. The supernatant containing membrane proteins was removed and stored at -80°C until used.

Co-Immunoprecipitation of *G. cichoracearum* purified proteins with *A. thaliana* protein extract
300 µL NiNTA resin (Thermo Fisher Scientific) was added to a 5 mL column. 4 mL purified protein was added to the closed column and incubated with rotation at 4°C for one hour. 4 mL of extracted *A. thaliana* protein was added to the column and allowed to flow through. The column was then washed with 5 mL extraction buffer, which was allowed to run completely through the column. 0.5 mL elution buffer (50 mM NaH_2PO_4 pH 7.0, 300 mM NaCl, 200 mM imidazole, 5% glycerol, 1 mM beta-mercaptoethanol) was added to the closed column and incubated for 20 minutes at 4°C. The buffer was then allowed to run through the column and collected.

Protein quantification
Protein was quantified using a modified Bradford assay for 96-well plates following the manufacturer's Protein Assay protocol (Bio-Rad). 0.5, 1, 2, and 4µg BSA were used to create a standard curve. Samples were assayed in triplicate in a 96-well plate. 200µL of protein assay reagent was added and absorbance at 595nm was measured using Paradigm plate reader (Beckman-Coulter). Data from the standard curve was then compared to the sample and us ed to calculate protein concentration.

Confocal microscopy
Confocal imaging of *N. benthamiana* leaves was performed on a Leica ZS710 microscope with 488 nm and 510 nm lasers controlled by Zeiss software. Z series were collected with a 200-300 nm step size and reassembled in ImageJ.

Epifluorescence microscopy of Arabidopsis leaves
Images of aniline blue stained *A. thaliana* leaves were collected on a Leica DMI 5000 B microscope equipped with a 5x objective under bright field and fluorescence illumination at 488 nm (Eschrich and Currier, 1964, Adam and Somerville., 1996).

Image analysis
ImageJ (http://rsb.info.nih.gov/ij/) was used to analyze images obtained using microscopy. Aniline blue stained hyphae were measured by tracing the length of the hyphae after training the software using the scale bar included in the micrographs. Propidium iodide stained conidia were counted using the "Cell Counter" plugin.

Tryptic digestion of protein samples
Tryptic digestion was performed according to the protocols obtained from the QB3 Chemistry Mass Spectrometry Facility (http://qb3.berkeley.edu/msf/sample-preparation-guidelines) 10 µM protein samples were treated with dithiothreotol (DTT) and iodoacetamide to reduce and alkylate cysteines. Proteins were then digested overnight with 500 ng trypsin.

1-Dimensional liquid-chromatography mass-spectroscopy/mass-spectroscopy
The following method was provided by Lori Kohlstaedt, Coates Proteomics Facility, QB3, UC Berkeley.

Mass spectrometry was performed by the Proteomics/Mass Spectrometry Laboratory at UC Berkeley. Proteins were digested with trypsin, and the resulting peptides were desalted, dried and resuspended in buffer A. A nano LC column was packed in a 100 μm inner diameter glass capillary with an emitter tip. The column consisted of 10 cm of Polaris c18 5 μm packing material (Varian). The column was loaded by use of a pressure bomb and washed extensively with buffer A (see below). The column was then directly coupled to an electrospray ionization source mounted on a Thermo-Fisher LTQ XL linear ion trap mass spectrometer. An Agilent 1200 HPLC equipped with a split line so as to deliver a flow rate of 300 nl/min was used for chromatography. Peptides were eluted using a 90 min. gradient from buffer A to 60% Buffer B. Buffer A was 5% acetonitrile/ 0.02% heptaflurobutyric acid (HBFA); buffer B was 80% acetonitrile/ 0.02% HBFA.

Protein identification and quantification were done with IntegratedProteomics Pipeline (IP2, Integrated Proteomics Applications, Inc. San Diego, CA) using ProLuCID/Sequest, DTASelect2 and Census [Xu et al., 2006, Corciorva et al., 2007, Tab et al., 2002, Park et al., 2008]. Tandem mass spectra were extracted into ms1 and ms2 files from raw files using RawExtractor (McDonald et al., 2004) and were searched against the Arabidopsis protein database (obtained from arabidopsis.org) plus sequences of common contaminants, concatenated to a decoy database in which the sequence for each entry in the original database was reversed (Peng et al., 2003). LTQ data was searched with 3000.0 milli-amu precursor tolerance and the fragment ions were restricted to a 600.0 ppm tolerance. All searches were parallelized and searched on the VJC proteomics cluster. Search space included all fully tryptic peptide candidates with no missed cleavage restrictions. Carbamidomethylation (+57.02146) of cysteine was considered a static modification. We required 1 peptide per protein and both trypitic termini for each peptide identification. The ProLuCID search results were assembled and filtered using the DTASelect program (Corciorva et al., 2007, Tabb et al., 2002) with a peptide false discovery rate (FDR) of 0.001 for single peptides and a peptide FDR of 0.005 for additional peptide s for the same protein. Under such filtering conditions, the estimated false discovery rate was zero for the datasets used.

Preparation of competent *S. cerivisiae* cells

Competent cells of *S. cerivициae* strain Y2HGold (Clontech) cells were made using a Yeast Transformation Kit according to manufacturer's protocol (Sigma-Aldrich).

Transformation of competent *S. cerivisae* cells

Relevant constructs were transformed into Y2HGold competent cells using a Yeast Transformation Kit (Sigma-Aldrich) according to manufacturer's protocol. Transformants were verified on yeast dropout media augmented with amino acids excepting tryptophan. Plasmids were isolated via Yeast Plasmid Miniprep Kit (Qiagen) and the presence of the correct insert was verified by sequencing.

E. coli growth conditions

Colonies of *E. coli* were propagated on Luria Broth (LB, Sigma-Aldrich) agar plates with appropriate antibiotic at 37°C . Liquid cultures of *E. coli* were grown in LB at 37°C with shaking at 250 rpm with appropriate antibiotic selection.

A. tumefaciens growth conditions

Colonies of *E. coli* were propagated on LB agar plates with appropriate antibiotic at 30°C. Liquid cultures of *A. tumefaciens* were grown in LB at 30°C with shaking at 250 rpm with appropriate antibiotic selection.

S. cerevisiae growth conditions

Colonies of *S. cerevisiae* were propagated on yeast peptone dextrose adenine (YPDA) or appropriate dropout media agar plates at 30°C (Clontech). Liquid cultures of *S. cerevisiae* were grown in YPDA or appropriate dropout media at 30°C with shaking at 250 rpm.

Transient gene expression in *N. benthamiana* and bi-molecular fluorescence complementation (BiFC)

Overnight cultures of *A. tumefaciens* containing BiFC constructs were resuspended individually in induction media (50mM MES, 0.5% glucose, 1.7mM NaH_2PO_4, 0.2mM acetosyringone and 5% 20X AB- mix (20X-AB mix comprised 373.9 mm NH_4Cl, 24.34 mm$MgSO_4$, 40.23 mm KCl, 1.36 mm$CaCl_2$, 0.18 mm$FeSO_4 \bullet 7H_2O$)). Cells were induced until OD_{600} reached 0.2 and syringe-infiltrated into the 3rd and 4th true leaves of 4 week old *N. benthamiana.* Leaves were observed for GFP- or YFP-fluorescence 48 hours post-infiltration.

Aniline blue staining

A. thaliana leaves were collected 2 dpi with *G. cichoracearum.* Leaves were cleared of chlorophyll in 70% ethanol overnight or at 65°C for 1 hour. Leaves were stained in Aniline blue solution (15mM K_2HPO_4 pH9, 0.2mg/ml Aniline blue) overnight and imaged using epifluorescence microscopy (Eschrich and Currier, 1964, Adam and Somerville, 1996).

Cas9 *In vitro* activity assay

Target DNA sequences were amplified from genomic DNA via PCR. Guide RNA were synthesized using the HiScribe T7 High yield RNA Synthesis Kit (NEB) according to manufacturer's instructions. Target DNA was purified using QiaQuick PCR Purification Kit (Qiagen) according to manufacturer's instructions. Purified Cas9 protein was generously provided by Dr. Michael Gomez. 0.5 µL of 1M Cas9 nuclease was incubated in Cas9 rection buffer with 1.5 µL of 10ng/µL sgRNA at for 10 minutes at 37°C. 100 ng substrate DNA was added and the reaction was incubated at 37°C overnight. Cas9 was denatured by incubation at 80°C for 10 minutes. Control reactions were run using the same protocol without sgRNA. 8 µL of each reation was mixed with loading dye and run at 120V for 25 minutes on a 1% agarose gel in 1X TAE with ethidium bromide and imaged under UV light using a GelDoc XR (Biorad).

Electroporation of powdery mildew conidia

Conidia from ~4 heavily infected cucumber or tomato leaves were collected and resuspended in electroporation buffer (1mM HEPES pH 7.0, 50 mM mannitol, 0.01% Tween-20) adjusted to 10^6 conidia/ml, as measured via haemocytometer. 120 µL of conidial suspension was mixed gently with 10 µg purified plasmid DNA or purified Cas9 protein and transferred to a pre-chilled 0.2cm electroporation cuvette. Two pulses of 1ms duration at 1.70 kV were applied at an interval of 5s. The conidia were immediately suspended in 1 ml of cold rescue buffer (see Table 7.1) and placed on ice for 10 minutes. Germination on an artificial surface was assayed by transferring 100 µL of conidial suspension to the surface of a glass slide.

Powdery mildew growth on detached leaves

Cucumber cotyledons or tomato leaves were detached and sterilized in 70% ethanol and left to dry. Leaves were then placed on the surface of water-agar plates. Conidial suspension was sprayed onto the leaf surface. Plants were incubated under 24 hr light conditions at 22°C for 15 days. Fungal growth was assayed using dissecting light microscopy or epifluorescence microscopy using 488 nm laser line.

Germination of conidia on artificial surface

The artificial surface (glass slide, Teflon tape, cellulose membrane) was washed 3x in diH_2O and blotted dry. Conidia were applied to the respective surfaces by either tapping heavily infected leaves over the surface or as described above. The glass slide was placed in a Petri plate containing 1mL of water and covered. The Teflon tape and cellulose membrane were placed on the surface of a water agar plate and covered. Plates were incubated at room temperature in the dark for 6 hours. 500 µL of water was used to wash the spores off of the surface and germination rate was observed and calculated via light microscopy.

Propidium Iodide Staining

Conidial solution was incubated for 60 seconds with propidium iodide at a final concentration of 1 ug/mL and imaged using a Leica DMI 5000 B microscope equipped with a 5x objective under bright field and 535nm fluorescence.

Genome and proteome data

Complete genomic, predicted protein, and gene ontology data was accessed and downloaded from the JGI (https://genome.jgi.doe.gov/portal/).

Phyre 2.0 protein fold recognition

Phyre 2.0 was accessed (http://www.sbg.bio.ic.ac.uk/phyre2/html/page.cgi?id=index). The mature amino acid sequence of GcEC8, GcEC10 and GcEC17 was input using the normal modeling mode perameters. PDB files were downloaded and visualized using Chimera (Pettersen et al., 2004)

SignalP analysis

SignalP analysis for complete predicted powdery mildew predicted proteomes was performed using local SignalP via a custom Python script, using default D-cutoff values. Proteins predicted to encode a signal peptide but lack a transmembrane domain were identified as the secreted protein complement of the powdery mildew.

BLAST-P analysis

Local BLAST analysis was performed using default parameters. Hits were determined by an e-value of 10E5 (Altschul et al., 1990).

EffectorP analysis

EffectorP was accessed (http://effectorp.csiro.au/). Proteins which had been identified via SignalP were entered and run using default parameters for EffectorP 1.0. Output was sorted and consolidated using a custom Python script (Sperschneider et al., 2015).

NetPhos Analysis

NetPhos3.1 was accessed (http://www.cbs.dtu.dk/services/NetPhos/). Full-length sequences of *G. cichoracearum* effector candidates were entered and run using parameters to identify serine, tyrosine and threonine phosphorylation sites, with a threshold of 0.5 (Blom et al., 1999, Blom et al., 2004).

ApoplastP Analysis

ApoplastP was accessed (http://apoplastp.csiro.au/) . Protein subsets which had been identified via EffectorP were entered and run using default parameters. Output was analyzed, sorted and consolidated using a custom Python script (Sperschneider et al., 2017).

Localizer Analysis

Localizer was accessed (http://localizer.csiro.au/) . Protein subsets which had been identified via EffectorP were entered and run using default parameters, and either full effector sequence or mature effector sequence options were selected as appropriate for the input data (Kelley et al., 2015). Output was analyzed, sorted and consolidated using a custom Python script. cTP, cTP+pmTP, cTP+NLS, and cTP+pmTP+NLS were consolidated under the term “cTP”. mTP, mTP+pcTP, mTP+pCTP+MLS, and mTP+NLS were consolidated under the term “mTP”.

GOSlim Analysis

Annotated GO terms associated with annotated powdery mildew genes was used as input for the AgBase GOSlimViewer (http://agbase.msstate.edu/cgi-bin/tools/goslimviewer_select.pl) with the Yeast GoSlim Set selected (McCarthy et al., 2006). Output was analyzed, sorted and consolidated using a custom Python script. This procedure was repeated with the GO terms associated with the subsets of powdery mildew proteins identified via SignalP and EffectorP.

CAZY prediction and analysis

The dbCAN annotation tool was accessed (http://csbl.bmb.uga.edu/dbCAN/annotate.php). Files containing predicted proteins from each powdery mildew was uploaded and run using default parameters (Yin et al., 2012). Output was analyzed, sorted and consolidated using a custom Python script.

Phylogeny of *G. cichoracearum* effectors

The evolutionary history was inferred by using the Maximum Likelihood method based on the JTT matrix-based model (Jones et al., 1992). The bootstrap consensus tree inferred from 500 replicates is taken to represent the evolutionary history of the taxa analyzed (Felsenstein, 1985). Branches corresponding to partitions reproduced in less than 50% bootstrap replicates are collapsed. Initial tree(s) for the heuristic search were obtained automatically by applying Neighbor-Join and BioNJ algorithms to a matrix of pairwise distances estimated using a JTT model, and then selecting the topology with superior log likelihood value. The analysis involved 225 amino acid sequences. All positions with less than 95% site coverage were eliminated. That is, fewer than 5% alignment gaps, missing data, and ambiguous bases were allowed at any position. There were a total of 24 positions in the final dataset. Evolutionary analyses were conducted in MEGA7 (Kumar et al., 2016).

Yeast 2-Hybrid

Yeast 2-hybrid analysis was performed using the Matchmaker Gold Yeast Two-Hybrid System (Clontech) according to manufacturer's instructions. Briefly, Y2H Gold cells containing effector candidate construct fused to Gal4 DNA-binding domain in pGBKT7 were mated with Y187 cells containing the Normalized Arabidopsis Library fused to the Gal4 activation domain in pGADT7 (Clontech) and plated on synthetic defined media lacking tryptophan and leucine supplemented with x-a-gal and aureobasidin A. Resultant blue colonies were further screened on more selective media, additionally missing adenine and histidine. Positive interactors were isolated and identified via sequencing, and co-transformed with the effector candidate in pGBKT7 to confirm the interaction.

qPCR

qPCR was performed on total RNA extracted from infected Arabidopsis leaves using the RNeasy Plant Mini kit (Qiagen) with the on-column DNaseI treatment according to the manufacturer's protocol. 2μg of RNA was used to synthesize cDNA using the RNA to cDNA EcoDry Premix kit (Clontech) according to manufacturer's instructions. qRT-PCR was performed using the SensiFast SYBR HiRox kit (Bioline) and the Roche Light Cycler 480 according to manufacturer's instructions. The amplification conditions were as follows: 50°C for 2 m, 95°C for 10 m; 40 cycles of 95°C for 15 s and 60°C for 60 s. Expression values were extracted using ΔΔCt method (Livak and Schmittgen, 2001), and normalized to that of the endogenous control tubulin (GcTUB2) and the expression of the gene at 0hpi. For all genes, three technical replicates and three biological replicates were performed. The absence of primer-dimer formation was confirmed by performing a melting- curve and specificity of the primers was verified by performing National Center for Biotechnology Information primer BLAST searches.

N. benthamiana cell death suppression

A modified version of the protocol described in Kleemann et al., (2012) was used to assess the ability of *G. cichoracearum* to suppress the hypersensitive response in *N. benthamiana* leaf cells. GFP-fusions of the effector candidates in the pMDC44 vector and XeXopQ or Bs2/AvrBs2 in pE1776 (kindly provided by Dr. A. Schultink, Integrated Genomics Institute, UC Berkeley) were grown overnight to the stationary phase in LB media and resuspended either to OD 0.5

(effector candidates) or 1 (HR-inducing constructs) in induction media (10 mM 2-(N-morpholino)ethanesulfonic acid (MES), pH 5.6; 10 mM $MgCl_2$; 200 µM Acetosyringone) and shaken at 28˚C for 4 hours. The constructs were then combined 1:10 effector candidate:HR-inducing construct and syringe infiltrated into the leaves of 5-week old *N. benthamiana* plants. Control infiltrations of the single constructs were included on the same leaves. Plants were placed back into the growth chamber and observed for macroscopic HR at 3-7 days post induction.

Works Cited

Abramovitch, R., Kim, Y., Chen, S., Dickman, M., & Martin, G. (2003). Pseudomonas type III effector AvrPtoB induces plant disease susceptibility by inhibition of host programmed cell death. *EMBO Journal*, *22*.

Adam, L., Ellwood, S., Wilson, I., Saenz, G., Xiao, S., Oliver, R. P., Turner, J. G., & Somerville, S. (1999). Comparison of Erysiphe cichoracearum and E. cruciferarum and a survey of 360 Arabidopsis thaliana accessions for resistance to these two powdery mildew pathogens. *Molecular Plant-Microbe Interactions : MPMI*, *12*(12), 1031–1043. https://doi.org/10.1094/MPMI.1999.12.12.1031

Adlung, N., Prochaska, H., Thieme, S. Banik, A., Blüher, D., John, P., Nagel, O., Schulze, S., Gantner, J., Delker, C., Stuttmann, J., & Bonas, U. (2016) Non-host resistanceinduced by the Xanthomonas effector XopQ is widespread within thegenus Nicotiana and functionally depends on EDS1. *Front. Plant Sci. 7,1796*

Agrios, G. (2005). *Plant Pathology*. (K. Sonnack, Ed.) (5th ed.). Burlington: Elsevier Academic Press.

Aguilar, G. B., Pedersen, C. and Thordal-Christensen, H. (2016), Identification of eight effector candidate genes involved in early aggressiveness of the barley powdery mildew fungus. *Plant Pathol, 65: 953-958. doi:10.1111/ppa.12476*

Altschul, S. F., Gish, W., Miller, W., Myers, E. W., & Lipman, D. J. (1990). Basic local alignment search tool. *Journal of Molecular Biology*, *215*, 403–410.

Amselem, J., Cuomo, C., van Kan, J., Viaud, M., Benito, E., Couloux, A., Coutinho, P., de Vries, R., Dyer, P., Fillinger, S., Fournier, E., Gout, L., Hahn, M., Kohn, L., Lapalu, N., Plummer, K., Pradier, J., Quevillon, E., Sharon, A., Simon, A., ten Have, A., Tudzynski, B., Tudzynski, P., & Win, D. M. (2011). Genomic analysis of the necrotrophic fungal pathogens Sclerotinia sclerotiorum and Botrytis cinerea. *PLoS Genetics*, *7*(8).

Aslam, S., Erbs, G., Morrissey, K., Newman, M.-A., Chinchilla, D., Boller, T., Molinaro, A., Jackson, R., & Cooper, R. (2009). Microbe-associated molecular pattern (MAMP) signatures , synergy , size and charge : influences on perception or mobility and host. *Molecular Plant Pathology*, *10*(3), 375–387. https://doi.org/10.1111/J.1364-3703.2009.00537.X

Aoyama, Y., Noshiro, M., Gotoh, O., Imaoka, S., Funae, Y., Kurosawa, N., Horiuchi, T., Yoshida, Y. (1996).Sterol 14-demethylase p450 (P45014DM*) is one of the most ancient and conserved p450 species. *Journal of Biochemistry, 119 (5), pp. 926-933.*

Barrangou, R., Fremaux, C., Deveau, C., Richards, M., Boyaval, P., Moineau, S., Romero, D., & Horvath, P. (2007). CRISPR Provides Acquired Resistance Against Viruses in Prokaryotes. *Science*, *315*(March), 1709–1712. https://doi.org/10.1126/science.1138140

Baulcombe, D. (1999). Fast forward genetics based on virus-induced gene silencing. *Curr Opin Plant Biol*.

Blom, N., Gammeltoft, S., and Brunak, S. (1999). Sequence- and structure-based prediction of eukaryotic protein phosphorylation sites. *Journal of Molecular Biology: 294(5): 1351-1362.*

Blom N, Sicheritz-Ponten T, Gupta R, Gammeltoft S, & Brunak S. (2004). Prediction of post-translational glycosylation and phosphorylation of proteins from the amino acid sequence. *Proteomics: Jun;4(6):1633-49, review*

Both, M., Csukai, M., Stumpf, M. P. H., & Spanu, P. D. (2005). Gene expression profiles of Blumeria graminis indicate dynamic changes to primary metabolism during development of an obligate biotrophic pathogen. *The Plant Cell*, *17*(July), 2107–2122. https://doi.org/10.1105/tpc.105.032631.1

Bourras, S., McNally, K. E., Ben-David, R., Parlange, F., Roffler, S., Praz, C. R., Oberhaensli, S., Menardo, F., Stirnweis, D., Frenkel, Z., Schaefer, L. K., Fluckiger, S., Treier, G., Herren, G., Korol, a B., Wicker, T., & Keller, B. (2015). Multiple avirulence loci and allele-specific effector fecognition control the Pm3 race-specific resistance of wheat to powdery mildew. *Plant Cell*, *27*(October), 2991–3012. https://doi.org/10.1105/tpc.15.00171

Braun, U., & Cook, R. (2012). *Taxonomic Manual of the Erysiphales (Powdery Mildews)*. Utrecht: CBS-KNAW Fungal Biodiversity Centre.

Brown, J.K.M., and Jessop, A.C. (1995). Genetics of avirulences in Erysiphe graminis f. sp. hordei. *Plant Pathol. 44 1039–1049.*

Burch-Smith, T. M., Schiff, M., Liu, Y., & Dinesh-Kumar, S. P. (2006). Efficient virus-induced gene silencing in Arabidopsis. *Plant Physiology*, *142*(1), 21–27. https://doi.org/10.1104/pp.106.084624

Büschges, R., Hollricher, K., Panstruga, R., Simons, G., Wolter, M., Frijters, A., van Daelen, R., van der Lee, T., Diergaarde, P., Groenendijk, J., Töpsch, S., Vos, P., Salamini, F., & Schulze-Lefert, P. (1997). The barley Mlo gene: a novel control element of plant pathogen resistance. *Cell*, *88*(5), 695–705. https://doi.org/http://dx.doi.org/10.1016/S0092-8674(00)81912-1

Cantarel, B. L., Coutinho, P. M., Rancurel, C., Bernard, T., Lombard, V., & Henrissat, B. (2009). The Carbohydrate-Active EnZymes database (CAZy): an expert resource for Glycogenomics.

Nucleic Acids Research, 37(Database issue), D233–D238. http://doi.org/10.1093/nar/gkn663

Chandran, D., Inada, N., Hather, G., Kleindt, C. K., & Wildermuth, M. C. (2010). Laser microdissection of Arabidopsis cells at the powdery mildew infection site reveals site-specific processes and regulators. *Proceedings of the National Academy of Sciences of the United States of America*, *107*(1), 460–465. https://doi.org/10.1073/pnas.0912492107

Chandran, D., Rickert, J., Cherk, C., Dotson, B. R., & Wildermuth, M. C. (2013). Host cell ploidy underlying the fungal feeding site is a determinant of powdery mildew growth and reproduction. *Molecular Plant-Microbe Interactions : MPMI*, *26*(5), 537–545. https://doi.org/10.1094/MPMI-10-12-0254-R

Chin, C.-S., Alexander, D. H., Marks, P., Klammer, A. A., Drake, J., Heiner, C., Clum, A., Copeland, A., Huddleston, J., Eichler, E. E., Turner, S. W., & Korlach, J. (2013). Nonhybrid, finished microbial genome assemblies from long-read SMRT sequencing data. *Nature Methods*, *10*(6), 563.

Clough, S. J. and Bent, A. F. (1998), Floral dip: a simplified method forAgrobacterium-mediated transformation ofArabidopsis thaliana. *The Plant Journal*, *16: 735–743.* doi:10.1046/j.1365-313x.1998.00343.x

Cociorva D, D LT, Yates JR (2007) Validation of tandem mass spectrometry database search results using DTASelect. *Current protocols in bioinformatics/editoral board, Andreas D Baxevanis [et al] Chapter 13: Unit 13 14.*

Curtis, M. D., & Grossniklaus, U. (2003). A Gateway Cloning Vector Set for High-Throughput Functional Analysis of Genes in Planta*. Plant Physiology, 133(2), 462–469.* http://doi.org/10.1104/pp.103.027979

Dean, R., Talbot, N., Ebbole, D., Farman, M., Mitchell, T., Orbach, M., Thon, M., Kulkarni, R., Xu, J., Pan, H., Read, N., Lee, Y., Carbone, I., Brown, D., Oh, Y., Donofrio, N., Jeong, J., Soanes, D., Djonovic, S., Kolomiets, E., Rehmeyer, C., Li, W., Harding, M., Kim, S., Lebrun, M., Bohne, & Birren, B. (2005). The genome sequence of the rice blast fungus Magnaporthe grisea. *Nature*, *434*(7036).

Délye, C., Laigret, F., Corio-Costet, M.-F. (1997). A mutation in the 14α-Demethylase gene of Uncinula necator that correlates with resistance to a sterol biosynthesis inhibitor. *Applied and Environmental Microbiology, 63 (8), pp. 2966-2970.*

Dong, Y., Burch-Smith, T. M., Liu, Y., Mamillapalli, P. and Dinesh-Kumar, S. P. (2007). A ligation-independent cloning tobacco rattle virus vector for high-throughput virus-induced gene silencing identifies roles for NbMADS4-1 and -2 in floral development. *Plant Physiol 145(4): 1161-1170*

Dodds, P. N., & Rathjen, J. P. (2010). Plant immunity: towards an integrated view of plant-pathogen interactions. *Nature Reviews. Genetics*, *11*(8), 539–548. https://doi.org/10.1038/nrg2812

Eschrich, W., and Currier, H.B. (1964) Identification of callose by its diachrome and fluorochrome reactions. *Stain Technol. 39, 303-307.*

Fabro, G., Di Rienzo, J. a, Voigt, C. a, Savchenko, T., Dehesh, K., Somerville, S., & Alvarez, M. E. (2008). Genome-wide expression profiling Arabidopsis at the stage of Golovinomyces cichoracearum haustorium formation. *Plant Physiology*, *146*(3), 1421–1439. https://doi.org/10.1104/pp.107.111286

Faino, L., Seidl, M. F., Datema, E., van den Berg, G., Janssen, A., Wittenberg, A., & Thomma, B. P. H. J. (2015). Single-Molecule Real-Time Sequencing Combined with Optical Mapping Yields Completely Finished Fungal Genome. *mBio*, *6*(4), 1–11. https://doi.org/10.1128/mBio.00936-15.Invited

Feehan, J. M., Scheibel, K. E., Bourras, S., Underwood, W., Keller, B., & Somerville, S. C. (2017) Purification of High Molecular Weight Genomic DNA from Powdery Mildew for Long-Read Sequencing. *J. Vis. Exp. (121), e55463, doi:10.3791/55463*

Feng, Z., Zhang, B., Ding, W., Liu, X., Yang, D. L., Wei, P., Cao, F., Zhu, S., Zhang, F., Mao, Y., & Zhu, J. K. (2013). Efficient genome editing in plants using a CRISPR/Cas system. *Cell Research*, *23*(10), 1229–1232. https://doi.org/10.1038/cr.2013.114

Ferrari, S. (2013). Oligogalacturonides: plant damage-associated molecular patterns and regulators of growth and development. *Frontiers in Plant Science*, *4*(March), 1–9. https://doi.org/10.3389/fpls.2013.00049

Fu, J., & Wang, S. (2011). Insights into Auxin Signaling in Plant–Pathogen Interactions. *Frontiers in Plant Science*, 2, 74. http://doi.org/10.3389/fpls.2011.00074

Gassmann, W., Dahlbeck, D., Chesnokova, O., Minsavage, G. V., Jones, J. B., and Staskawicz, B. J. 2000. Molecular evolution of virulence in natural field strains of Xanthomonas campestris pv. vesicatoria. *J. Bacteriol. 182:7053-7059*. 10.1128/JB.182.24.7053-7059.2000

Glawe, D. a. (2008). The powdery mildews: a review of the world’s most familiar (yet poorly known) plant pathogens. *Annual Review of Phytopathology*, *46*, 27–51. https://doi.org/10.1146/annurev.phyto.46.081407.104740

Godfrey, D., Böhlenius, H., Pedersen, C., Zhang, Z., Emmersen, J., & Thordal-Christensen, H. (2010). Powdery mildew fungal effector candidates share N-terminal Y/F/WxC-motif. *BMC Genomics*, *11*.

Grant, S. R., Fisher, E. J., Chang, J. H., Mole, B. M., & Dangl, J. L. (2006). Subterfuge and Manipulation: Type III Effector Proteins of Phytopathogenic Bacteria. *Annual Review of Microbiology*, *60*(1), 425–449. https://doi.org/10.1146/annurev.micro.60.080805.142251

Green, JR, Carver, TL, & Gurr, SJ. (2002) The Formation and Function of Infection and Feeding Structures. *The Powdery Mildews: A Comprehensiv Treatise.* The American Phytopathological Society, St. Paul, Minnesota.

Grigoriev IV, Nordberg H, Shabalov I, Aerts A, Cantor M, Goodstein D, Kuo A, Minovitsky S, Nikitin R, Ohm RA, Otillar R, Poliakov A, Ratnere I, Riley R, Smirnova T, Rokhsar D, Dubchak I. (2012) The Genome Portal of the Department of Energy Joint Genome Institute. *Nucleic Acids Res. Jan;40:D26-32.*

Hacquard, S. (2014). Chapter Four - the genomics of powdery mildew fungi: Past achievements, present status and future prospects. In M.M. Francis (Ed.), *Advances in Botanical Research* (pp. 109–142). Academic Press.

Hacquard, S., Kracher, B., Maekawa, T., Vernaldi, S., Schulze-Lefert, P., & Ver Loren van Themaat, E. (2013). Mosaic genome structure of the barley powdery mildew pathogen and conservation of transcriptional programs in divergent hosts. *Proceedings of the National Academy of Sciences of the United States of America*, *110*, E2219-28. https://doi.org/10.1073/pnas.1306807110

Hückelhoven, R. (2005). Powdery mildew susceptibility and biotrophic infection strategies. *FEMS Microbiology Letters*, *245*, 9–17. https://doi.org/10.1016/j.femsle.2005.03.001

Hückelhoven, R., & Panstruga, R. (2011). Cell biology of the plant-powdery mildew interaction. *Current Opinion in Plant Biology*, *14*(6), 738–461. Hückelhoven, R. & Panstruga, R. Cell biol. https://doi.org/10.1016/j.pbi.2011.08.002

Jones D.T., Taylor W.R., and Thornton J.M. (1992). The rapid generation of mutation data matrices from protein sequences. *Computer Applications in the Biosciences 8: 275-282.*

Jones, J. D. G., & Dangl, J. L. (2006). The plant immune system. *Nature*, *444*(7117), 323–329. https://doi.org/10.1038/nature05286

Jones, L., Riaz, S., Morales-Cruz, A., Amrine, K. C. H., McGuire, B., Gubler, W. D., Walker, M. A., & Cantu, D. (2014). Adaptive genomic structural variation in the grape powdery mildew pathogen, Erysiphe necator. *BMC Genomics*, *15*, 1081. https://doi.org/10.1186/1471-2164-15-1081

Kalantidis, K., Schumacher, H. T., Alexiadis, T., & Helm, J. M. (2008). RNA silencing movement in plants. *Biology of the Cell*.

M. Karimi, D. Inzé, A. Depicker, GATEWAY vectors for Agrobacterium-mediated plant transformation. *Trends Plant Sci. 7, 193 (2002). doi:10.1016/S1360-1385(02)02251-3 Medline*

Kearney, B., and Staskawicz, B. J. (1990). Widespread distribution and fitness contribution of Xanthomonas campestris avirulence gene avrBs2. *Nature 346:385-386*. doi 10.1038/346385a0

Kelly, L. A., Mezulis, S., Yates, C., Wass, M., & Sternberg, M. (2015). The Phyre2 web portal for protein modelling, prediction, and analysis. *Nature Protocols*, *10*(6), 845–858. https://doi.org/10.1038/nprot.2015-053

Kleemann J, Rincon-Rivera LJ, Takahara H, Neumann U, van Themaat EVL, van der Does, HC, Hacqurd S, Stüber, K, Will, I, Schmalenbach, W, Schmelzer, E, & O'Connell, RJ (2012) Sequential Delivery of Host-Induced Virulence Effectors by Appressoria and Intracellular Hyphae of the Phytopathogen Colletotrichum higginsianum. *PLOS Pathogens 8(4): e1002643.* https://doi.org/10.1371/journal.ppat.1002643

Koch, A., & Kogel, K.-H. (2014). New wind in the sails: improving the agronomic value of crop plants through RNAi-mediated gene silencing. *Plant Biotechnology Journal*, n/a-n/a. https://doi.org/10.1111/pbi.12226

Koch, A., Kumar, N., Weber, L., Keller, H., Imani, J., & Kogel, K.-H. (2013). Host-induced gene silencing of cytochrome P450 lanosterol C14α-demethylase-encoding genes confers strong resistance to Fusarium species. *Proceedings of the National Academy of Sciences of the United States of America*, *110*(48), 19324–19329. https://doi.org/10.1073/pnas.1306373110

Knox, K., Grierson, C. S., & Leyser, O. (2003). AXR3and SHY2 interact to regulate root hair development. *Development*, *130*(23), 5769 LP-5777. Retrieved from http://dev.biologists.org/content/130/23/5769.

Kumar S., Stecher G., and Tamura K. (2016). MEGA7: Molecular Evolutionary Genetics Analysis version 7.0 for bigger datasets. *Molecular Biology and Evolution 33:1870-1874.*

Kwaaitaal, M., Nielsen, M., Böhlenius, & H., Thordal-Christensen, H. (2017) The plant membrane surrounding powdery mildew haustoria shares properties with the endoplasmic reticulum membrane. *Journal of Experimental Botany, Volume 68, Issue 21-22* doi: 10.1093/jxb/erx403

Lee, M. E., DeLoache, W. C., Cervantes, B., & Dueber, J. E. (2015). A Highly Characterized Yeast Toolkit for Modular, Multipart Assembly. *ACS Synthetic Biology*, *4*(9), 975–986. https://doi.org/10.1021/sb500366v

Lehmann, S., Serrano, M., L'Haridon, F., Tjamos, S. E., & Metraux, J.-P. (2014). Reactive oxygen species and plant resistance to fungal pathogens. *Phytochemistry*. https://doi.org/10.1016/j.phytochem.2014.08.027

Livak, K. J., & Schmittgen, T. D. (2001). Analysis of Relative Gene Expression Data Using Real-Time Quantitative PCR and the 2−ΔΔCT Method. *Methods*, *25*(4), 402–408. https://doi.org/https://doi.org/10.1006/meth.2001.1262

Lynne Reuber, T., Plotnikova, J. M., Dewdney, J., Rogers, E. E., William Wood, B., & Ausubel, F. M. (1998). Correlation of defense gene induction defects with powdery mildew susceptibility in Arabidopsis enhanced disease susceptibility mutants. *Plant Journal*, *16*, 473–485. https://doi.org/10.1046/j.1365-313X.1998.00319.x

Martinez-Zapater, J., and Salinas, J. Arabidopsis Protocols. Methods in Molecular Biology, Vol. 82., Humana Press 1998.

Martino, E., Morin, E., Grelet, G., Kuo, A., Kohler, A., Daghino, S., Barry, K., Cichocki, N., Clum, A., Dockter, R., Hainaut, M., Kuo, R., LaButti, K., Lindahl, B., Lindquist, E., Lipzen, A., Khouja, H., Magnuson, J., Murat, C., Ohm, R., Singer, S., Spatafora, J., Wang, M., & Veneault-Fourre, P. S. (2018). Comparative genomics and transcriptomics depict ericoid mycorrhizal fungi as versatile saprotrophs and plant mutualists. *New Phytologist*.

McCann, M. C., K. Roberts. 1991. Architecture of the primary cell wall. In: The Cytoskeletal Basis of Plant Growth and Form (C. W. Lloyd, ed.). London: Academic Press, pp. 109-129

McCarthy, F. M., Wang, N., Magee, G. B., Nanduri, B., Lawrence, M. L., Camon, E. B., Barrell, D. G., Hill, D. P., Dolan, M. E., Williams, W. P., Luthe, D. S., Bridges, S. M., & Burgess, S. C. (2006). AgBase: A functional genomics resource for agriculture. *BMC Genomics*, *7*, 1–13. https://doi.org/10.1186/1471-2164-7-229

McDonald WH, Tabb DL, Sadygov RG, MacCoss MJ, Venable J, Graumann, J., Johnson, J., Corciorva, D., & Yates, JD.. (2004) MS1, MS2, and SQT-three unified, compact, and easily parsed file formats for the storage of shotgun proteomic spectra and identifications*. Rapid communications in mass spectrometry : RCM 18: 2162–2168.* doi: 10.1002/rcm.1603

Menardo, F., Praz, C. R., Wicker, T., & Keller, B. (2017). Rapid turnover of effectors in grass powdery mildew (Blumeria graminis). *BMC Evolutionary Biology*, *17*(1), 1–14. https://doi.org/10.1186/s12862-017-1064-2

Micali, C. O., Neumann, U., Grunewald, D., Panstruga, R., & O'Connell, R. (2011). Biogenesis of a specialized plant-fungal interface during host cell internalization of Golovinomyces orontii haustoria. *Cellular Microbiology*, *13*(2), 210–226. https://doi.org/10.1111/j.1462-5822.2010.01530.x

Needleman, Saul B. & Wunsch, Christian D. (1970). A general method applicable to the search for similarities in the amino acid sequence of two proteins. *Journal of Molecular Biology. 48 (3): 443–53.* doi:10.1016/0022-2836(70)90057-4

Nordahl Petersen, T., Brunak, S., von Heijne, G., & Nielsen, H. (2011). SignalP 4.0: discriminating signal peptides from transmembrane regions. *Thomas Nordahl Petersen, Søren Brunak, Gunnar von Heijne & Henrik Nielsen*, *8*, 785–786.

Nowara, D., Gay, A., Lacomme, C., Shaw, J., Ridout, C., Douchkov, D., Hensel, G., Kumlehn, J., & Schweizer, P. (2010). HIGS: host-induced gene silencing in the obligate biotrophic fungal pathogen Blumeria graminis. *The Plant Cell*, *22*(9), 3130–3141. https://doi.org/10.1105/tpc.110.077040

Nottensteiner, M., Zechmann, B., McCollum, C., & Huckelhoven, R. (2018). A Barley Powdery Mildew Fungus Non-Autonomous Retrotransposon Encodes a Peptide that Supports Penetration Success on Barley. *bioRxiv*. Retrieved from http://biorxiv.org/content/early/2018/01/03/242271

Nunes, C. C., & Dean, R. A. (2012). Micro-review Host-induced gene silencing : a tool for understanding fungal host interaction and for developing novel disease control strategies. *Molecular Plant Pathology*, *13*(5), 519–529. https://doi.org/10.1111/J.1364-3703.2011.00766.X

O'Connell, R. J., & Panstruga, R. (2006). Tête à tête inside a plant cell: establishing compatibility between plants and biotrophic fungi and oomycetes. *The New Phytologist*, *171*(4), 699–718. https://doi.org/10.1111/j.1469-8137.2006.01829.x

Ouellet, F., Overvoorde, P. J., & Theologis, A. (2001). IAA17/AXR3: Biochemical Insight into an Auxin Mutant Phenotype. *The Plant Cell*, *13*(4), 829 LP-841. Retrieved from http://www.plantcell.org/content/13/4/829

Park, S.K.,Venable, J.D., Xu, T., & Yates., JR. (2008) A quantitative analysis software tool for mass spectrometry-based proteomics. *Nature methods 5, 319-322*

Parlange, F., Oberhaensli, S., Breen, J., Platzer, M., Taudien, S., Šimková, H., Wicker, T., Doležel, J., & Keller, B. (2011). A major invasion of transposable elements accounts for the large size of the Blumeria graminis f.sp. tritici genome. *Functional and Integrative Genomics*, *11*, 671–677. https://doi.org/10.1007/s10142-011-0240-5

Pedersen, C., Ver, E., Themaat, L. Van, Mcguffin, L. J., Abbott, J. C., Burgis, T. A., Barton, G., Bindschedler, L. V, Lu, X., Maekawa, T., Weßling, R., Cramer, R., Thordal-christensen, H., Panstruga, R., & Spanu, P. D. (2012). Structure and evolution of barley powdery mildew effector candidates Structure and evolution of barley powdery mildew effector candidates. *BMC Genomics*, *13*(694).

Peng J, Elias JE, Thoreen CC, Licklider LJ, & Gygi SP (2003) Evaluation of multidimensional chromatography coupled with tandem mass spectrometry (LC/LC-MS/MS) for large-scale protein analysis: the yeast proteome. *Journal of proteome research 2: 43–50*. doi: 10.1021/pr025556v

Pennington, H. G., Gheorghe, D. M., Damerum, A., Pliego, C., Spanu, P. D., Cramer, R., & Bindschedler, L. V. (2016). Interactions between the Powdery Mildew Effector BEC1054 and Barley Proteins Identify Candidate Host Targets. *Journal of Proteome Research*, *15*(3), 826–839. https://doi.org/10.1021/acs.jproteome.5b00732

Pérez-Pérez, J. M., Candela, H., Robles, P., López-Torrejón, G., del Pozo, J. C., & Micol, J. L. (2010). A Role for AUXIN RESISTANT3 in the Coordination of Leaf Growth. *Plant and Cell Physiology*, *51*(10), 1661–1673. Retrieved from http://dx.doi.org/10.1093/pcp/pcq123

Pettersen, E., Goddard, T., Huang, C., GS, C., Greenblatt, D., Meng, E., & Ferrin, T. (2004). UCSF Chimera--a visualization system for exploratory research and analysis. *J Comput Chem*.

Pliego, C., Nowara, D., Bonciani, G., Gheorghe, D. M., Xu, R., Surana, P., Whigham, E., Nettleton, D., Bogdanove, A. J., Wise, R. P., Schweizer, P., Bindschedler, L. V, & Spanu, P. D. (2013). Host-induced gene silencing in barley powdery mildew reveals a class of ribonuclease-like effectors. *Molecular Plant-Microbe Interactions : MPMI*, *26*(6), 633–642. https://doi.org/10.1094/MPMI-01-13-0005-R

Raffaele, S., & Kamoun, S. (2012). Genome evolution in filamentous plant pathogens: Why bigger can be better. *Nature Reviews Microbiology*, *10*(6), 417–430. https://doi.org/10.1038/nrmicro2790

Rébora, K., Desmoucelles, C., Borne, F., Pinson, B., & Daignan-fornier, B. (2001). Yeast AMP Pathway Genes Respond to Adenine through Regulated Synthesis of a Metabolic Intermediate Yeast AMP Pathway Genes Respond to Adenine through Regulated Synthesis of a Metabolic Intermediate. https://doi.org/10.1128/MCB.21.23.7901

Ridout CJ, Skamnioti P, Porritt O, Sacristan S, Jones JDG, Brown JKM. (2006) Multiple avirulence paralogues in cereal powdery mildew fungi may contribute to parasite fitness and defeat of plant resistance. *Plant Cell*. 2006;18(9):2402–14.

Rouse, D., Mackay, P., Stirnberg, P., Estelle, M., & Leyser, O. (1998). Changes in Auxin Response from Mutations in an AUX/IAA Gene. *Science*, *279*(5355), 1371 LP-1373. Retrieved from http://science.sciencemag.org/content/279/5355/1371

Sambrook, J., Fritsch, E.F. and Maniatis, T. (1989) Molecular Cloning: A Laboratory Manual. Cold Spring Harbor, NY: Cold Spring Harbor Laboratory Press.

Schmidt, S. M., Kuhn, H., Micali, C., Liller, C., Kwaaitaal, M., & Panstruga, R. (2014). Interaction of a Blumeria graminis f. sp. hordei effector candidate with a barley ARF-GAP suggests that host vesicle trafficking is a fungal pathogenicity target. *Molecular Plant Pathology*, *15*(6), 535–549. https://doi.org/10.1111/mpp.12110

Science, S. (2008). User Manual: Pippin Pulse Electrophoresis Power Supply. Retrieved from http://www.sagescience.com/wp-content/uploads/2014/01/Pippin-Pulse-User-Manual-RevH.pdf

Serres, F. J. De. (1956). STUDIES WITH PURPLE ADENINE MUTANTS IN NEUROSPORA. *Genetics*.

Sherwood, J. E., Slutsky, B., & Somerville, S. C. (1991). Induced Morphological and Virulence Variants of the Obligate Barley Pathogen Erysiphe graminis f. sp. hordei.

Shinohara, N., Sunagawa, N., Tamura, S., Yokoyama, R., Ueda, M., Igarashi, K., & Nishitani, K. (2017). The plant cell-wall enzyme AtXTH3 catalyses covalent cross-linking between cellulose and cello-oligosaccharide. *Scientific Reports*, *7*, 46099. Retrieved from http://dx.doi.org/10.1038/srep46099

Singer, M., Marcotte, B., & Selker, E. (1995). DNA methylation associated with repeat-induced point mutation in Neurospora crassa. *Molecular and Cellular Biology.*, *15*(10).

Sorek, N., Poraty, L., Sternberg, H., Bar, E., Lewinsohn, E., & Yalovsky, S. (2007). Activation Status-Coupled Transient S Acylation Determines Membrane Partitioning of a Plant Rho-Related GTPase. *Molecular and Cellular Biology.*, *27*(6), 2144–2154.

Spanu, P. D., Abbott, J. C., Amselem, J., Burgis, T. a, Soanes, D. M., Stüber, K., Ver Loren van Themaat, E., Brown, J. K. M., Butcher, S. a, Gurr, S. J., Lebrun, M.-H., Ridout, C. J., Schulze-Lefert, P., Talbot, N. J., Ahmadinejad, N., Ametz, C., Barton, G. R., Benjdia, M., Bidzinski, P., Bindschedler, L. V, Both, M., Brewer, M. T., Cadle-Davidson, L., Cadle-Davidson, M. M., Collemare, J., Cramer, R., Frenkel, O., Godfrey, D., Harriman, J., Hoede, C., King, B. C., Klages, S., Kleemann, J., Knoll, D., Koti, P. S., Kreplak, J., López-Ruiz, F. J., Lu, X., Maekawa, T., Mahanil, S., Micali, C., Milgroom, M. G., Montana, G., Noir, S., O'Connell, R. J., Oberhaensli, S., Parlange, F., Pedersen, C., Quesneville, H., Reinhardt, R., Rott, M., Sacristán, S., Schmidt, S. M., Schön, M., Skamnioti, P., Sommer, H., Stephens, A., Takahara, H., Thordal-Christensen, H., Vigouroux, M., Wessling, R., Wicker, T., & Panstruga, R. (2010). Genome expansion and gene loss in powdery mildew fungi reveal tradeoffs in extreme parasitism. *Science (New York, N.Y.)*, *330*(6010), 1543–1546. https://doi.org/10.1126/science.1194573

Spanu, P. D. (2012). The Genomics of Obligate (and Nonobligate) Biotrophs. *Annual Review of Phytopathology*, *50*.

Spanu, P. D. (2015). RNA-protein interactions in plant disease: Hackers at the dinner table. *New Phytologist*, *207*(4), 991–995. https://doi.org/10.1111/nph.13495

Spanu, P. D., & Panstruga, R. (2012). Powdery mildew genomes in the crosshairs. *New Phytologist*, *195*, 20–22. https://doi.org/10.1111/j.1469-8137.2012.04173.x

Sperschneider, J., Gardiner, D., Dodds, P., Tini, F., Covarelli, L., Singh, K., Manners, J., & Taylor, J. (2015). EffectorP: Predicting Fungal Effector Proteins from Secretomes Using Machine Learning. *New Phytologist*.

Sperschneider, J., Catanzariti, A.-M., DeBoer, K., Petre, B., Gardiner, D. M., Singh, K. B., Dodds, P. N., & Taylor, J. M. (2017). LOCALIZER: subcellular localization prediction of both plant and effector proteins in the plant cell. *Scientific Reports*, *7*.

Sperschneider, J., Dodds, P. N., Singh, K. B., & Taylor, J. M. (2017). ApoplastP: prediction of effectors and plant proteins in the apoplast using machine learning. *New Phytologist*.

Swarup, R., Kramer, E. M., Perry, P., Knox, K., Leyser, H. M. O., Haseloff, J., Beemster, G. T. S., Bhalerao, R., & Bennett, M. J. (2005). Root gravitropism requires lateral root cap and epidermal cells for transport and response to a mobile auxin signal. *Nature Cell Biology*, *7*, 1057. Retrieved from http://dx.doi.org/10.1038/ncb1316

Tabb DL, McDonald WH, Yates JR 3rd (2002) DTASelect and Contrast: tools for assembling and comparing protein identifications from shotgun proteomics*. Journal of proteome research 1: 21–26.* doi: 10.1021/pr015504q

Tai, T. H., Dahlbeck, D., Clark, E. T., Gajiwala, P., Pasion, R., Whalen, M. C., Stall, R. E., and Staskawicz, B. J. 1999. Expression of the Bs2 pepper gene confers resistance to bacterial spot disease in tomato. *Proc. Natl. Acad. Sci. U.S.A. 96:14153-14158.* 10.1073/pnas.96.24.14153

Tena G., Boudsocq M., Sheen J. (2011). Protein kinase signaling networks in plant innate immunity. *Curr. Opin. Plant Biol. 14: 519–529.*

Teper, D., Salomon, D., Sunitha, S., Kim, J.G., Mudgett, M.B. and Sessa, G. (2014) Xanthomonas euvesicatoria type III effector XopQ interacts withtomato and pepper 14-3-3 isoforms to suppress effector-triggered immunity. *Plant J.77, 297–309.*

Thomma, B. P. H. J., Seidl, M. F., Shi-Kunne, X., Cook, D. E., Bolton, M. D., van Kan, J. a L., & Faino, L. (2016). Mind the gap; seven reasons to close fragmented genome assemblies. *Fungal Genetics and Biology*, *90*, 24–30. https://doi.org/10.1016/j.fgb.2015.08.010

Tinoco ML, Dias BB, Dall'Astta RC, Pamphile JA, Aragao FJ, et al. (2010) In vivo trans-specific gene silencing in fungal cells by in planta expression of a double-stranded RNA. *BMC Biol 31: 27.*

Varden, F. A., De la Concepcion, J. C., Maidment, J. H. R., & Banfield, M. J. (2017). Taking the stage: effectors in the spotlight. *Current Opinion in Plant Biology*, *38*, 25–33. https://doi.org/https://doi.org/10.1016/j.pbi.2017.04.013

Vela-Corcía, D., Bautista, R., De Vicente, A., Spanu, P. D., & Pérez-García, A. (2016). De novo analysis of the epiphytic transcriptome of the cucurbit powdery mildew fungus Podosphaera xanthii and identification of candidate secreted effector proteins. *PLoS ONE*, *11*(10), 1–21. https://doi.org/10.1371/journal.pone.0163379

Vela-Corcía, D., Romero, D., Torés, J., De Vicente, A., & Pérez-García, A. (2015). Transient transformation of Podosphaera xanthii by electroporation of conidia. *BMC Microbiology*, *15*, 20. https://doi.org/10.1186/s12866-014-0338-8

Vidal, E. A., Moyano, T. C., Krouk, G., Katari, M. S., Tanurdzic, M., McCombie, W. R., Coruzzi, G. M., & Gutiérrez, R. A. (2013). Integrated RNA-seq and sRNA-seq analysis identifies novel nitrate-responsive genes in Arabidopsis thaliana roots. *BMC Genomics*, *14*(1), 701. https://doi.org/10.1186/1471-2164-14-701

Wang, B., Li, Z., Xu, W., Feng, X., Wan, Q., Zan, Y., Sheng, S., & Shen, X. (2017). Bivariate genomic analysis identifies a hidden locus associated with bacteria hypersensitive response in Arabidopsis thaliana. *Scientific Reports*, *7*, 45281. Retrieved from http://dx.doi.org/10.1038/srep45281

Wang, W., & Wang, Z.-Y. (2014). At the intersection of plant growth and immunity. *Cell Host & Microbe, 15(4), 400–402*. http://doi.org/10.1016/j.chom.2014.03.014

Wang, Z., Johnston, P. R., Takamatsu, S., Spatafora, J. W., & Hibbett, D. S. (2006). Toward a phylogenetic classification of the Leotiomycetes based on rDNA data. *Mycologia*, *98*(6), 1065–1075. https://doi.org/10.3852/mycologia.98.6.1065

Waterhouse, P. M., & Fusaro, A. F. (2006). Viruses Face a Double Defense by Plant Small RNAs. *Science*.

Weigel, D. and Glazebrook, J. (2002) Arabidopsis: a laboratory manual. *Cold Spring Harbor Laboratory Press, New York.*

Weßling, R. (2013). Isolation and functional characterization of Arabidopsis powdery mildew effector proteins. *PhD*.

Weßling, R., Epple, P., Altmann, S., He, Y., Yang, L., Henz, S. R., McDonald, N., Wiley, K., Bader, K. C., Gläßer, C., Mukhtar, M. S., Haigis, S., Ghamsari, L., Stephens, A. E., Ecker, J. R., Vidal, M., Jones, J. D. G., Mayer, K. F. X., Ver Loren van Themaat, E., Weigel, D., Schulze-Lefert, P., Dangl, J. L., Panstruga, R., & Braun, P. (2014). Convergent Targeting of a Common Host Protein-Network by Pathogen Effectors from Three Kingdoms of Life. *Cell Host & Microbe*, *16*(3), 364–375. https://doi.org/10.1016/j.chom.2014.08.004

Weßling, R., Schmidt, S. M., Micali, C. O., Knaust, F., Reinhardt, R., Neumann, U., Ver Loren van Themaat, E., & Panstruga, R. (2012). Transcriptome analysis of enriched Golovinomyces orontii haustoria by deep 454 pyrosequencing. *Fungal Genetics and Biology : FG & B*, *49*(6), 470–482. https://doi.org/10.1016/j.fgb.2012.04.00

Weßling, R., & Panstruga, R. (2012). Rapid quantification of plant-powdery mildew interactions by qPCR and conidiospore counts. *Plant Methods*, *8*(1), 35. https://doi.org/10.1186/1746-4811-8-35

Whigham, E., Qi, S., Mistry, D., Surana, P., Xu, R., Fuerst, G., Pliego, C., Bindschedler, L. V, Spanu, P. D., Dickerson, J. A., Innes, R. W., Nettleton, D., Bogdanove, A. J., & Wise, R. P. (2015). Broadly Conserved Fungal Effector BEC1019 Suppresses Host Cell Death and Enhances Pathogen Virulence in Powdery Mildew of Barley (*Hordeum vulgare* L.). *Molecular Plant-Microbe Interactions*, *28*(9), 968–983. https://doi.org/10.1094/MPMI-02-15-0027-FI

Wicker, T., Oberhaensli, S., Parlange, F., Buchmann, J. P., Shatalina, M., Roffler, S., Ben-David, R., Doležel, J., Šimková, H., Schulze-Lefert, P., Spanu, P. D., Bruggmann, R., Amselem, J., Quesneville, H., Ver Loren van Themaat, E., Paape, T., Shimizu, K. K., & Keller, B. (2013). The wheat powdery mildew genome shows the unique evolution of an obligate biotroph. *Nature Genetics*, *45*(9), 1092–1096. https://doi.org/10.1038/ng.2704

Wilson, I. W., Schiff, C. L., Hughes, D. E., & Somerville, S. C. (2001). Quantitative trait loci analysis of powdery mildew disease resistance in the Arbidopsis thaliana accession Kashmir-1. *Genetics*, *158*, 1301–1309.

Xu, T., Venable, J.D., Park, S.K., Cociorva, D., Lu, B., Liao, L., Wohlschlegel, J., Hewel, J. & Yates, J. (2006). ProLuCID, a fast and sensitive tandem mass spectra-based protein identification program. *Mol Cell Proteomics.5(10):S174–S174.*

Yin, N., Mao, X., Yang, J., Chen, X., Mao, F., & Xu, Y. (2012). dbCAN: a web resource for automated carbohydrate-active enzyme annotation,. *Nucleic Acids Research*, *40*.

Zhao C., Nie H., Shen Q., Zhang S., Lukowitz W., Tang D. (2014). EDR1 physically interacts with MKK4/MKK5 and negatively regulates a MAP kinase cascade to modulate plant innate immunity. *PLoS Genet. 10: e1004389*.

iTag sample amplification quality control. (2016). Retrieved August 8, 2016, from http://1ofdmq2n8tc36m6i46scovo2e.wpengine.netdna-cdn.com/wp-content/uploads/2015/02/iTag-Sample-Amplification-QC-v1.1.pdf

DNA sample submission guidelines. (2016). Retrieved August 8, 2016, from http://1ofdmq2n8tc36m6i46scovo2e.wpengine.netdna-cdn.com/wp-content/uploads/2016/04/DNA-Preparation-Requirements-1.pdf

Genomic DNA sample quality control. (2016). Retrieved August 8, 2016, from http://jgi.doe.gov/wp-content/uploads/2013/11/Genomic-DNA-Sample-QC.pdf

Appendices

Appendix 1*: Missing Ascomycete Core Genes*

This table has been modified from Table S3 (Spanu et al., 2010).

This table contains data modified from Table S3 (Spanu et al., 2010) Colums A-Q contain data collected from that table, Column R contains new analysis

Systematic name [1]	Gene name	SGDID	*S. cerevisiae* (proteome) [2]	*S. sclerotiorum* (genome) [3]	*M. grisea* (genome) [4]	*C. higginsianum* (genome) [5]	*B. graminis* (genome) [6]	*E. pisi* (genome) [7]	*G. orontii* (genome) [8]	*B. graminis* (ESTs, mixed) [9]	*E. pisi* (ESTs, conidia) [10]	*G. orontii* (ESTs, haustoria) [11]	*E. necator* (ESTs, sporulating mycelium) [12]	*P. graminis* f.sp. *tritici* (genome) [13]	*P. triticina* 1-1 BBBD Race 1 (genome) [14]	*Hyaloperonospora arabidopsidis* Emoy 2 (genome) [15]	G. cichoracearum race UCSC 1^16
thiamine metabolism/transport																	
YGR144W	THI4	SGDID: S000003376	+	3.00E-46	3.00E-85	1.00E-98	-	-	-	-	-	-	-	1.00E-35	3.00E-51	-	
YPL214C	THI6	SGDID: S000006135	+	7.00E-41	1.00E-65	2.00E-44	-	-	-	-	-	-	-	4.00E-24	2.00E-26	-	
YLR237W	THI7	SGDID: S000004227	+	2.00E-36	1.00E-85	4.00E-90	-	-	-	-	-	-	-	-	-	-	
YOL055C	THI20	SGDID: S000005416	+	6.00E-20	5.00E-28	7.00E-33	-	-	-	-	-	-	-	6.00E-16	3.00E-14	-	
YPL258C	THI21	SGDID: S000006179	+	3.00E-19	5.00E-27	2.00E-36	-	-	-	-	-	-	-	1.00E-14	1.00E-14	-	
YPR121W	THI22	SGDID: S000006325	+	4.00E-15	2.00E-21	2.00E-21	-	-	-	-	-	-	-	8.00E-13	5.00E-16	-	
YOR192C	THI72	SGDID: S000005718	+	1.00E-39	2.00E-91	5.00E-95	-	-	-	-	-	-	-	-	-	-	
YOR071C	NRT1	SGDID: S000005597	+	2.00E-42	4.00E-93	2.00E-89	-	-	-	-	-	-	-	-	-	-	
allantoine metabolism/transport																	
YIR0	DAL1	SGDID: S0000	+	7.00E-	1.00E-	1.00E-82	-	-	-	-	-	-	-	8.00E-40	1.00E-	7.00E-09	

27C		01466		116	105										30		
YIR029W	DAL2	SGDID: S000001468	+	7.00E-91	8.00E-93	2.00E-93	-	-	-	-	-	-	-	2.00E-27	9.00E-29	6.00E-45	
YIR028W	DAL4	SGDID: S000001467	+	2.00E-123	4.00E-120	5.00E-84	-	-	-	-	-	-	-	-	-	-	
YIR023W	DAL81	SGDID: S000001462	+	1.00E-88	9.00E-90	5.00E-91	-	-	-	-	-	-	-	-	-	-	6.86E-06
YHL016C	DUR3	SGDID: S000001008	+	4.00E-150	4.00E-119	1.00E-127	-	-	-	-	-	-	-	-	-	-	3.04E-05
methionine metabolism and (siro-)heme biosynthesis																	
YKR069W	MET1	SGDID: S000001777	+	6.00E-110	1.00E-100	1.00E-29	-	-	-	-	-	-	-	-	-	7.00E-17	-
YJR010W	MET3	SGDID: S000003771	+	3.00E-128	3.00E-161	3.00E-108	-	-	-	-	-	-	-	-	-	5.00E-25	-
YBR213W	MET8	SGDID: S000000417	+	9.00E-16	3.00E-16	4.00E-14	-	-	-	-	-	-	-	-	-	-	-
YKL001C	MET14	SGDID: S000001484	+	1.00E-77	1.00E-76	1.00E-74	-	-	-	-	-	-	-	-	-	3.00E-57	-
YPR167C	MET16	SGDID: S000006371	+	4.00E-78	1.00E-76	6.00E-77	-	-	-	-	2.00E-06	-	-	-	-	4.00E-18	1.43E-05
YOR278W	HEM4	SGDID: S000005804	+	3.00E-12	2.00E-11	3.00E-16	-	-	-	-	-	-	-	-	-	5.00E-09	1.89E-13
alcohol metabolism/fermentation																	
YGL256W	ADH4	SGDID: S000003225	+	2.00E-12	7.00E-14	3.00E-16	-	-	-	-	-	-	1.00E-09	-	-	1.00E-27	-
YCR107W	AAD3	SGDID: S000000704	+	2.00E-89	9.00E-54	2.00E-137	-	-	-	-	-	-	-	-	-	5.00E-11	-
YDL243C	AAD4	SGDID: S000002402	+	4.00E-89	1.00E-58	5.00E-142	-	-	-	-	-	-	-	-	-	4.00E-12	-
YFL056	AAD6	SGDID: S0000	+	2.00E-42	3.00E-	3.00E-74	-	-	-	-	-	-	-	-	-	-	-

C		01838			14												
YJR155W	AAD10	SGDID: S000003916	+	4.00E-75	4.00E-59	6.00E-122	-	-	-	-	-	-	-	-	-	7.00E-12	-
YNL331C	AAD14	SGDID: S000005275	+	1.00E-96	9.00E-59	6.00E-161	-	-	-	-	-	-	-	-	-	1.00E-12	-
YOL165C	AAD15	SGDID: S000005525	+	1.00E-21	2.00E-17	3.00E-46	-	-	-	-	-	-	-	-	-	-	-
YFL057C	AAD16	SGDID: S000001837	+	2.00E-26	2.00E-22	3.00E-57	-	-	-	-	-	-	-	-	-	-	-
YPL088W	YPL088W	SGDID: S000006009	+	1.00E-72	1.00E-85	1.00E-87	-	-	-	-	-	-	-	6.00E-15	1.00E-15	5.00E-22	-
YLR044C	PDC1	SGDID: S000004034	+	3.00E-144	2.00E-75	1.00E-132	1.00E-07	7.00E-10	1.00E-19	-	-	4.00E-10	2.00E-15	5.00E-11	1.00E-10	7.00E-08	1.01E-21
YOL086C	ADH1	SGDID: S000005446	+	4.00E-84	9.00E-90	4.00E-98	-	-	2.00E-19	-	-	5.00E-08	-	-	-	2.00E-58	6.26E-20
glutamate metabolism																	
YOR375C	GDH1	SGDID: S000005902	+	8.00E-117	6.00E-137	3.00E-117	-	-	-	-	-	-	-	-	-	5.00E-60	-
YAL062W	GDH3	SGDID: S000000058	+	4.00E-113	9.00E-127	3.00E-114	-	-	-	-	-	-	-	-	-	1.00E-63	-
uracil metabolism/transport																	
YBL042C	FUI1	SGDID: S000000138	+	3.00E-123	1.00E-115	6.00E-83	-	-	-	-	-	-	-	-	-	-	-
YBR021W	FUR4	SGDID: S000000225	+	4.00E-121	2.00E-116	3.00E-86	-	-	-	-	-	-	-	-	-	-	-
YKL216W	URA1	SGDID: S000001699	+	5.00E-19	2.00E-16	2.00E-13	-	-	-	-	-	-	-	-	-	3.00E-13	-
glutathione metabolism																	
YGR154C	GTO1	SGDID: S000003386	+	3.00E-43	3.00E-48	1.00E-17	-	-	-	-	-	-	-	-	-	3.00E-32	-
YMR251	GTO3	SGDID: S0000	+	4.00E-59	2.00E-	2.00E-47	-	-	-	-	-	-	-	-	-	6.00E-37	-

W		04863			68												
YKR076W	ECM4	SGDID: S000001784	+	5.00E-68	1.00E-79	4.00E-35	-	-	-	-	-	-	-	-	-	1.00E-50	-
YLR299W	ECM38	SGDID: S000004290	+	1.00E-39	2.00E-40	1.00E-50	-	-	-	-	-	-	-	3.00E-54	7.00E-50	-	6.93E-09
detoxification/stress response																	
YER185W	PUG1	SGDID: S000000987	+	1.00E-18	4.00E-13	4.00E-14	-	-	-	-	-	-	-	-	-	-	-
YGR213C	RTA1	SGDID: S000003445	+	5.00E-34	3.00E-34	2.00E-37	-	-	-	-	-	-	-	2.00E-09	9.00E-19	-	-
YLR046C	YLR046C	SGDID: S000004036	+	4.00E-20	5.00E-16	3.00E-21	-	-	-	-	-	-	-	-	3.00E-14	-	-
YJR104C	SOD1	SGDID: S000003865	+	2.00E-47	2.00E-43	8.00E-47	-	-	-	-	-	-	-	-	-	1.00E-28	-
YGR234W	YHB1	SGDID: S000003466	+	1.00E-48	2.00E-56	4.00E-50	-	-	-	-	-	-	-	-	-	1.00E-31	-
YIL053W	RHR2	SGDID: S000001315	+	6.00E-13	4.00E-17	3.00E-19	-	-	-	-	-	-	-	-	-	-	-
YPR201W	ARR3	SGDID: S000006405	+	1.00E-42	2.00E-57	3.00E-52	-	-	-	-	-	-	-	-	-	7.00E-22	-
YGL196W	DSD1	SGDID: S000003164	+	6.00E-16	4.00E-38	9.00E-37	-	-	-	-	-	-	-	-	-	-	-
YHR044C	DOG1	SGDID: S000001086	+	6.00E-16	2.00E-15	5.00E-16	-	-	-	-	-	-	-	-	-	-	-
YHR043C	DOG2	SGDID: S000001085	+	1.00E-16	3.00E-15	4.00E-16	-	-	-	-	-	-	-	-	-	-	-
arabinono-1,4-lactone biosynthesis																	
YML086C	ALO1	SGDID: S000004551	+	2.00E-87	1.00E-83	2.00E-74	-	-	-	-	-	-	-	4.00E-24	4.00E-17	2.00E-21	
YMR041C	ARA2	SGDID: S000004644	+	5.00E-52	1.00E-45	5.00E-47	-	-	-	-	-	-	-	-	-	-	
proteins of unknown function																	
YDL144C	YDL144C	SGDID: S000002303	+	4.00E-23	1.00E-16	4.00E-26	-	-	-	-	-	-	-	5.00E-07	9.00E-06	-	3.41

																	E-12
YDR132C	YDR132C	SGDID:S000002539	+	2.00E-39	5.00E-36	2.00E-31	-	-	-	-	-	-	-	-	-	-	-
YIL067C	YIL067C	SGDID:S000001329	+	9.00E-56	6.00E-51	3.00E-53	-	-	-	-	-	-	-	3.00E-22	4.00E-18	-	-
YJR124C	YJR124C	SGDID:S000003885	+	9.00E-69	7.00E-70	7.00E-67	-	-	-	-	-	-	4.00E-11	-	-	-	-
YLR108C	YLR108C	SGDID:S000004098	+	3.00E-21	8.00E-20	3.00E-15	-	-	-	-	-	-	-	-	-	-	-
YOL137W	BSC6	SGDID:S000005497	+	4.00E-14	6.00E-17	2.00E-19	-	-	-	-	-	-	-	-	-	-	-
YPR127W	YPR127W	SGDID:S000006331	+	9.00E-43	3.00E-46	5.00E-51	-	-	-	-	-	-	-	2.00E-08	-	-	-
YPL103C	FMP30	SGDID:S000006024	+	3.00E-24	9.00E-30	1.00E-30	-	-	-	-	-	-	-	-	-	-	-
YPL277C	YPL277C	SGDID:S000006198	+	5.00E-21	9.00E-17	2.00E-24	-	-	-	-	3.00E-14	-	1.00E-10	1.00E-19	3.00E-17	-	-
YPR022C	YPR022C	SGDID:S000006226	+	8.00E-30	3.00E-41	4.00E-39	-	-	-	2.00E-06	2.00E-07	3.00E-06	4.00E-07	-	-	-	2.50E-08
chaperones																	
YBR227C	MCX1	SGDID:S000000431	+	1.00E-59	8.00E-64	7.00E-66	-	-	-	-	-	-	-	3.00E-24	2.00E-52	1.00E-54	-
YMR038C	CCS1	SGDID:S000004641	+	1.00E-32	3.00E-29	2.00E-29	-	-	-	-	-	-	-	-	-	-	-
nitrate metabolism																	
XP_752655			-	2.00E-151	2.00E-130	4.00E-143	-	-	-	-	-	-	-	-	-	8.00E-56	-
CAD28426			-	0.00E+00	0.00E+00	0.00E+00	-	-	-	-	-	-	-	-	-	-	2.00E-10
AAL85636			-	0.00E+00	0.00E+00	0.00E+00	4.00E-22	2.00E-25	2.00E-12	2.00E-11	2.00E-31	4.00E-11	2.00E-31	2.00E-10	5.00E-19	8.00E-41	6.00E-38
proteases/peptidases																	

YBR286W	APE3	SGDID:S000000490	+	5.00E-114	5.00E-108	2.00E-103	-	-	-	-	-	-	-	-	-	-	-
YHR132C	ECM14	SGDID:S000001174	+	7.00E-83	3.00E-79	4.00E-78	-	-	-	-	-	-	-	-	-	1.00E-23	-
YIL108W	YIL108W	SGDID:S000001370	+	5.00E-84	7.00E-79	2.00E-96	-	-	-	-	-	-	-	-	-	-	-
aromatic amino acid metabolism																	
YGL202W	ARO8	SGDID:S000003170	+	1.00E-98	2.00E-96	5.00E-96	-	-	-	-	-	-	4.00E-10	-	-	7.00E-19	-
YHR137W	ARO9	SGDID:S000001179	+	2.00E-47	8.00E-46	1.00E-44	-	-	-	-	-	-	-	-	-	1.00E-17	-
YER152C	YER152C	SGDID:S000000954	+	3.00E-44	4.00E-26	7.00E-55	-	-	-	-	-	-	-	-	-	9.00E-28	-
channels/transporters																	
YJL093C	TOK1	SGDID:S000003629	+	3.00E-53	6.00E-37	4.00E-38	-	-	-	-	-	-	-	-	-	-	-
YBR296C	PHO89	SGDID:S000000500	+	3.00E-74	1.00E-86	4.00E-76	-	-	-	-	-	-	-	-	-	8.00E-08	-
YIL023C	YKE4	SGDID:S000001285	+	9.00E-27	5.00E-25	6.00E-26	-	-	-	-	-	-	-	-	-	4.00E-21	-
YKL221W	MCH2	SGDID:S000001704	+	2.00E-58	1.00E-33	5.00E-25	-	-	-	-	-	-	5.00E-08	-	-	-	1.03E-15
YOL162W	YOL162W	SGDID:S000005522	+	3.00E-49	1.00E-35	3.00E-47	-	-	-	-	-	-	-	-	-	-	4.89E-05
repeat-induced point mutation (RIP)																	
gi|154296783	ref|XP_001548821.1		-	0.00E+00	4.00E-67	2.00E-63	-	-	-	-	-	-	-	-	-	-	-
gi|154322765	ref|XP_001560697.1		-	2.00E-127	1.00E-56	7.00E-60	-	-	-	-	-	-	-	-	-	-	-
gi|2906004	gb|AAC03766.1		-	2.00E-66	4.00E-32	3.00E-22	-	-	-	-	-	-	-	1.00E-10	4.00E-09	-	-
mating type/cell cycle/buddin																	

g																
YBR276C	PPS1	SGDID: S000000480	+	2.00E-43	9.00E-21	2.00E-37	-	-	-	-	-	-	-	2.00E-35	6.00E-31	2.00E-08	-
YGL056C	SDS23	SGDID: S000003024	+	5.00E-56	1.00E-41	3.00E-47	-	-	-	-	-	-	-	-	-	-	-
YBR214W	SDS24	SGDID: S000000418	+	4.00E-56	7.00E-40	2.00E-45	-	-	-	-	-	-	-	-	-	-	-
YIL140W	AXL2	SGDID: S000001402	+	1.00E-37	2.00E-29	2.00E-36	-	-	-	-	-	-	-	1.00E-21	5.00E-25	-	-
ER quality control																
YPL096W	PNG1	SGDID: S000006017	+	7.00E-53	1.00E-51	1.00E-47	-	-	-	-	-	-	-	-	-	1.00E-54	-
YHR176W	FMO1	SGDID: S000001219	+	2.00E-38	2.00E-37	4.00E-34	-	-	-	-	-	-	-	-	-	7.00E-11	2.45E-12
YBR015C	MNN2	SGDID: S000000219	+	5.00E-23	2.00E-38	8.00E-39	-	-	-	-	-	-	-	-	-	1.00E-18	-
YJL186W	MNN5	SGDID: S000003722	+	2.00E-17	2.00E-34	3.00E-37	-	-	-	-	-	-	-	-	-	6.00E-17	-
other																
YLL057C	JLP1	SGDID: S000003980	+	1.00E-72	2.00E-17	2.00E-81	-	-	-	-	-	-	-	-	-	-	-
YDR465C	RMT2	SGDID: S000002873	+	2.00E-48	4.00E-44	6.00E-50	-	-	-	-	-	-	-	1.00E-30	8.00E-25	-	-
YNL229C	URE2	SGDID: S000005173	+	3.00E-28	2.00E-28	3.00E-18	-	-	-	-	2.00E-06	-	-	-	-	1.00E-07	-
YOR388C	FDH1	SGDID: S000005915	+	5.00E-57	1.00E-112	3.00E-104	3.00E-14	2.00E-13	1.00E-08	1.00E-06	1.00E-13	2.00E-09	8.00E-16	1.00E-20	5.00E-23	6.00E-19	3.21E-20
YDR242W	AMD2	SGDID: S000002650	+	5.00E-44	2.00E-30	6.00E-50	-	-	-	-	-	-	-	-	-	2.00E-07	7.05E-06
YMR302	YME2	SGDID: S0000	+	2.00E-	4.00E-	3.00E-	-	-	-	-	-	-	-	-	-	-	-

C		04917		109	115	113											
YJL145W	SFH5	SGDID: S000003681	+	3.00E-27	9.00E-24	5.00E-24	-	-	-	-	-	-	-	-	-	-	-
YLR047C	FRE8	SGDID: S000004037	+	1.00E-12	3.00E-11	3.00E-12	-	-	-	-	-	-	-	-	-	-	8.65E-08
YLR278C	YLR278C	SGDID: S000004268	+	4.00E-11	1.00E-19	2.00E-38	-	-	-	-	-	-	-	-	-	-	-
YIL162W	SUC2	SGDID: S000001424	+	3.00E-83	1.00E-79	7.00E-28	-	-	-	-	-	-	-	-	-	3.00E-15	-
YDR030C	RAD28	SGDID: S000002437	+	5.00E-14	2.00E-18	1.00E-18	-	-	-	-	-	-	-	-	-	-	3.46E-08

[1] manually added proteins are highlighted in light blue

This data taken directly from Spanu et al., 2010 Table S3

[2] ftp://genome-ftp.stanford.edu/yeast/data_download/sequence/genomic_sequence/orf_protein
+ (highlighted in green) indicates presence, - (highlighted in red) absence of the gene in the yeast genome

[3] http://www.broadinstitute.org/annotation/genome/sclerotinia_sclerotiorum (version 1); numbers indicate e-values of TBLASTN search

[4] http://www.broadinstitute.org/annotation/genome/magnaporthe_grisea (version MG6) ; numbers indicate e-values of TBLASTN search

[5] http://www.mpipz.mpg.de/english/research/pmi-dpt/Fungal_genomes/ (version 1); numbers indicate e-values of TBLASTN search

[6] http://www.blugen.org/ (CABOG assembly); - (highlighted in red) indicates absence (e-value >1E-05) in this genome; e-values <1E-05 are indicated and highlighted in red when best reciprocal BLASTX hit against a protein different from the query protein and highlighted in green when best reciprocal BLASTX hit against the query protein

[7] http://www.mpipz.mpg.de/english/research/pmi-dpt/Fungal_genomes/ (version 2) - (highlighted in red) indicates absence (e-value >1E-05) in this genome; e-values <1E-05 are indicated and highlighted in red when best reciprocal BLASTX hit against a protein different from the query protein and highlighted in green when best reciprocal BLASTX hit against the query protein

[8] http://www.mpipz.mpg.de/english/research/pmi-dpt/Fungal_genomes/ (version 1) - (highlighted in red) indicates absence (e-value >1E-05) in this EST set; e-values <1E-05 are indicated and highlighted in red when best reciprocal BLASTX hit against a protein different from the query protein and highlighted in green when best reciprocal BLASTX hit against the query protein; the BLAST hit against ADH1 (YOL086C) likely results from the contaminating *Penicillium olsonii* (best BLAST hit is against *Penicillium chrysogenum*)

[9] http://www.blugen.org/ - (highlighted in red) indicates absence (e-value >1E-05) in this EST set; e-values <1E-05 are indicated and highlighted in red when best reciprocal BLASTX hit against a protein different from the query protein and highlighted in green when best reciprocal BLASTX hit against the query protein

[10] http://www.mpipz.mpg.de/english/research/pmi-dpt/Fungal_genomes/ - (highlighted in red) indicates absence (e-value >1E-05) in this EST set; e-values <1E-05 are indicated and highlighted in red when best reciprocal BLASTX hit against a protein different from the query protein and highlighted in green when best reciprocal BLASTX hit against the query protein

[11] http://www.mpipz.mpg.de/english/research/pmi-dpt/Fungal_genomes/ - (highlighted in red) indicates absence (e-value >1E-05) in this EST set; e-values <1E-05 are indicated and highlighted in red when best reciprocal BLASTX hit against a protein different from the query protein and highlighted in green when best reciprocal BLASTX hit against the query protein

[12] personal communication, L. Cadle-Davidson and M.G. Milgroom - (highlighted in red) indicates absence (e-value >1E-05) in this EST set; e-values <1E-05 are indicated and highlighted in red when best reciprocal BLASTX hit against a protein different from the query protein and highlighted in green when best reciprocal BLASTX hit against the query protein; positive BLAST hits (highlighted in green - typically against 1-2 EST reads) may either result from contaminations in the EST library or they may represent species-specific exceptions of the gene losses

[13] http://www.broadinstitute.org/annotation/genome/puccinia_group/ - (highlighted in red) indicates absence (e-value >1E-05) in this genome; e-values <1E-05 and >1E-010 are indicated in yellow and e-values <E-010 are highlighted in green

[14] http://www.broadinstitute.org/annotation/genome/puccinia_group/ - (highlighted in red) indicates absence (e-value >1E-05) in this genome; e-values <1E-05 and >1E-010 are indicated in yellow and e-values <E-010 are highlighted in green

15 http://www.ncbi.nlm.nih.gov/Traces/wgs/?val=ABWE01 - (highlighted in red) indicates absence (e-value >1E-05) in this genome; e-values <1E-05 and >1E-010 are indicated in yellow and e-values <E-010 are highlighted in green

16 http://genome.jgi.doe.gov/Golci1/Golci1.info.html - (highlighted in red) indicates absence (e-value >1E-05) in this genome; e-values <1E-05 and >1E-010 are indicated in yellow and e-values <E-010 are highlighted in green

Appendix 2*: Predicted secreted powdery mildew proteins*

Proteins predicted to be secreted and not retained in the plasma membrane encoded by the genomes of *G. cichoracearum (Gc), G. orontii (Go) B. graminis f. sp. hordei (Bgh), B. graminis f. sp. tritici (Bgt),* and *E. necator (En)*

Gc	**Bgh**	**Bgt**	**En**	**Go**
jgi|Golci1|101053|CE101052_5734	jgi|Blugr1|23228|BGHDH14_bghG007168000001001	jgi|Blugra1|3393|BGT96224_3563T0	jgi|Erynec1|3754|EV44_g0424T0	jgi|Golor2|4273758|e_gw1.44.867.1
jgi|Golci1|1014842|CE1014841_8231	jgi|Blugr1|23214|BGHDH14_bghG007158000001001	jgi|Blugra1|3416|BGT96224_E4403T0	jgi|Erynec1|3772|EV44_g0202T0	jgi|Golor2|4275160|e_gw1.46.294.1
jgi|Golci1|1017100|CE1017099_5758	jgi|Blugr1|23213|BGHDH14_bghG007156000001001	jgi|Blugra1|3429|BGT96224_ASP21079T0	jgi|Erynec1|3778|EV44_g0064T0	jgi|Golor2|4275660|e_gw1.47.1176.1
jgi|Golci1|1025653|CE1025652_28070	jgi|Blugr1|23201|BGHDH14_bgh03194	jgi|Blugra1|3451|BGT96224_222T0	jgi|Erynec1|3788|EV44_g0577T0	jgi|Golor2|4275886|e_gw1.48.1012.1
jgi|Golci1|1026988|CE1026987_15331	jgi|Blugr1|23193|BGHDH14_bgh02161	jgi|Blugra1|3470|BGT96224_AcSP30848T0	jgi|Erynec1|37|EV44_g0607T0	jgi|Golor2|42782|gm4.42782_g
jgi|Golci1|1039618|CE1039617_4885	jgi|Blugr1|23154|BGHDH14_bgh06756	jgi|Blugra1|3475|BGT96224_2588T0	jgi|Erynec1|3846|EV44_g0581T0	jgi|Golor2|4278404|e_gw1.53.42.1
jgi|Golci1|1043184|CE1043183_26608	jgi|Blugr1|23145|BGHDH14_bgh00016	jgi|Blugra1|3481|BGT96224_2816T0	jgi|Erynec1|385|EV44_g0592T0	jgi|Golor2|4280634|e_gw1.57.478.1
jgi|Golci1|105783|CE105782_5644	jgi|Blugr1|23143|BGHDH14_bghG003669000001001	jgi|Blugra1|3493|BGT96224_3806T0	jgi|Erynec1|3862|EV44_g0400T0	jgi|Golor2|4280651|e_gw1.57.704.1
jgi|Golci1|1138219|CE1138218_188	jgi|Blugr1|23130|BGHDH14_bgh05640	jgi|Blugra1|3511|BGT96224_1476T0	jgi|Erynec1|3863|EV44_g0269T0	jgi|Golor2|4281035|e_gw1.58.519.1
jgi|Golci1|1138350|CE1138349_3452	jgi|Blugr1|23112|BGHDH14_bgh06883	jgi|Blugra1|3519|BGT96224_E5891T0	jgi|Erynec1|3884|EV44_g0435T0	jgi|Golor2|4282550|e_gw1.61.800.1
jgi|Golci1|1169626|CE1169625_3316	jgi|Blugr1|23046|BGHDH14_bgh04274	jgi|Blugra1|3528|BGT96224_ASP20468T0	jgi|Erynec1|3897|EV44_g0430T0	jgi|Golor2|4283035|e_gw1.62.268.1
jgi|Golci1|1170146|CE1170145_986	jgi|Blugr1|23045|BGHDH14_bghG003574000001001	jgi|Blugra1|352|BGT96224_AcSP30555T0	jgi|Erynec1|38|EV44_g0321T0	jgi|Golor2|4284120|e_gw1.64.981.1
jgi|Golci1|123527|CE123526_500	jgi|Blugr1|23012|BGHDH14_bgh02951	jgi|Blugra1|3537|BGT96224_E10116T0	jgi|Erynec1|3909|EV44_g0285T0	jgi|Golor2|4284144|e_gw1.64.528.1
jgi|Golci1|1278290|CE1278289_2265	jgi|Blugr1|22999|BGHDH14_bgh05162	jgi|Blugra1|3566|BGT96224_ASP20548T0	jgi|Erynec1|3977|EV44_g0122T0	jgi|Golor2|4284289|e_gw1.64.469.1
jgi|Golci1|1285880|CE1285879_22103	jgi|Blugr1|22993|BGHDH14_bgh00680	jgi|Blugra1|3567|BGT96224_ASP21418T0	jgi|Erynec1|3984|EV44_g0043T0	jgi|Golor2|4284710|e_gw1.65.721.1
jgi|Golci1|1336305|CE1336304_824	jgi|Blugr1|22992|BGHDH14_bgh02727	jgi|Blugra1|3572|BGT96224_E5973T0	jgi|Erynec1|4034|EV44_g0573T0	jgi|Golor2|4284733|e_gw1.65.420.1
jgi|Golci1|137118|CE137117_1626	jgi|Blugr1|22979|BGHDH14_bgh04522	jgi|Blugra1|3575|BGT96224_1598T0	jgi|Erynec1|4050|EV44_g0404T0	jgi|Golor2|4288055|e_gw1.72.323.1
jgi|Golci1|1420455|CE1420454_10133	jgi|Blugr1|22969|BGHDH14_bgh06570	jgi|Blugra1|3584|BGT96224_E5965T0	jgi|Erynec1|4107|EV44_g0376T0	jgi|Golor2|4288203|e_gw1.72.634.1

Gc	Bgh	Bgt	En	Go
jgi|Golci1|1426233|CE1426232_69532	jgi|Blugr1|22949|BGHDH14_bgh05764	jgi|Blugra1|3585|BGT96224_E5539T0	jgi|Erynec1|4108|EV44_g0179T0	jgi|Golor2|4290009|e_gw1.76.505.1
jgi|Golci1|1435786|CE1435785_986	jgi|Blugr1|22946|BGHDH14_bgh00768	jgi|Blugra1|3587|BGT96224_E5538T0	jgi|Erynec1|415|EV44_g0455T0	jgi|Golor2|4290599|e_gw1.77.121.1
jgi|Golci1|1451405|CE1451404_11	jgi|Blugr1|22942|BGHDH14_bgh00086	jgi|Blugra1|3621|BGT96224_E10140T0	jgi|Erynec1|4188|EV44_g0106T0	jgi|Golor2|4290714|e_gw1.78.63.1
jgi|Golci1|1494519|CE1494518_4910	jgi|Blugr1|22935|BGHDH14_bgh00979	jgi|Blugra1|3628|BGT96224_E10128T0	jgi|Erynec1|4210|EV44_g0008T0	jgi|Golor2|4291356|e_gw1.79.285.1
jgi|Golci1|1500538|CE1500537_9279	jgi|Blugr1|22917|BGHDH14_bgh06445	jgi|Blugra1|365|BGT96224_2483T0	jgi|Erynec1|4250|EV44_g0108T0	jgi|Golor2|4294330|e_gw1.85.130.1
jgi|Golci1|1538307|CE1538306_42	jgi|Blugr1|22913|BGHDH14_bghG005039000001001	jgi|Blugra1|3667|BGT96224_959T0	jgi|Erynec1|4269|EV44_g0032T0	jgi|Golor2|4296132|e_gw1.89.422.1
jgi|Golci1|1544616|CE1544615_5324	jgi|Blugr1|22911|BGHDH14_bgh05102	jgi|Blugra1|3686|BGT96224_E5963T0	jgi|Erynec1|427|EV44_g0419T0	jgi|Golor2|4300322|e_gw1.100.145.1
jgi|Golci1|1557851|CE1557850_1529	jgi|Blugr1|22900|BGHDH14_bgh03739	jgi|Blugra1|3687|BGT96224_AcSP30748T0	jgi|Erynec1|4281|EV44_g0092T0	jgi|Golor2|4300671|e_gw1.101.199.1
jgi|Golci1|1595752|CE1595751_699	jgi|Blugr1|22898|BGHDH14_bgh03703	jgi|Blugra1|3689|BGT96224_E10108T0	jgi|Erynec1|4299|EV44_g0496T0	jgi|Golor2|4302905|e_gw1.107.371.1
jgi|Golci1|1601726|CE1601725_2959	jgi|Blugr1|22891|BGHDH14_bgh02974	jgi|Blugra1|3707|BGT96224_5078T0	jgi|Erynec1|4304|EV44_g0499T0	jgi|Golor2|4302926|e_gw1.107.491.1
jgi|Golci1|160524|CE160523_124457	jgi|Blugr1|22866|BGHDH14_bgh05397	jgi|Blugra1|3729|BGT96224_4159T0	jgi|Erynec1|4312|EV44_g0584T0	jgi|Golor2|4304457|e_gw1.112.248.1
jgi|Golci1|1704974|gm4.799_g	jgi|Blugr1|22788|BGHDH14_bgh02969	jgi|Blugra1|3735|BGT96224_1288T0	jgi|Erynec1|4331|EV44_g0411T0	jgi|Golor2|4304659|e_gw1.112.98.1
jgi|Golci1|1705548|gm4.1373_g	jgi|Blugr1|22777|BGHDH14_bgh03179	jgi|Blugra1|3744|BGT96224_E5670T0	jgi|Erynec1|4332|EV44_g0203T0	jgi|Golor2|4305152|e_gw1.114.433.1
jgi|Golci1|1709034|gm4.4859_g	jgi|Blugr1|22760|BGHDH14_bgh00779	jgi|Blugra1|3803|BGT96224_ASP20071T0	jgi|Erynec1|4347|EV44_g0103T0	jgi|Golor2|4307194|e_gw1.120.185.1
jgi|Golci1|1709244|gm4.5069_g	jgi|Blugr1|22752|BGHDH14_bgh00427	jgi|Blugra1|382|BGT96224_E40004T0	jgi|Erynec1|4352|EV44_g0353T0	jgi|Golor2|4307349|e_gw1.120.640.1
jgi|Golci1|1709326|gm4.5151_g	jgi|Blugr1|22729|BGHDH14_bgh03308	jgi|Blugra1|3851|BGT96224_AcSP30091T0	jgi|Erynec1|4366|EV44_g0412T0	jgi|Golor2|4307455|e_gw1.121.373.1
jgi|Golci1|1709785|gm4.5610_g	jgi|Blugr1|22703|BGHDH14_bgh00934	jgi|Blugra1|3854|BGT96224_87T0	jgi|Erynec1|4385|EV44_g0027T0	jgi|Golor2|4307982|e_gw1.122.178.1
jgi|Golci1|1709839|gm4.5664_g	jgi|Blugr1|22691|BGHDH14_bghG002926000001001	jgi|Blugra1|385|BGT96224_1299T0	jgi|Erynec1|4410|EV44_g0102T0	jgi|Golor2|4311515|e_gw1.133.186.1
jgi|Golci1|1713506|gm4.9331_g	jgi|Blugr1|22675|BGHDH14_bghG002914000001001	jgi|Blugra1|387|BGT96224_ASP20465T0	jgi|Erynec1|4422|EV44_g0144T0	jgi|Golor2|4316130|e_gw1.148.163.1
jgi|Golci1|1714669|gm4.10494_g	jgi|Blugr1|22674|BGHDH14_bghG002912000002001	jgi|Blugra1|3905|BGT96224_4344T0	jgi|Erynec1|4464|EV44_g0059T0	jgi|Golor2|4317995|e_gw1.155.332.1
jgi|Golci1|1717257|gm4.13082_g	jgi|Blugr1|22658|BGHDH14_bghG002872000001001	jgi|Blugra1|390|BGT96224_E5559T0	jgi|Erynec1|4472|EV44_g0488T0	jgi|Golor2|4318208|e_gw1.156.346.1

Gc	Bgh	Bgt	En	Go
jgi|Golci1|1718372|gm4.14197_g	jgi|Blugr1|22648|BGHDH14_bgh04272	jgi|Blugra1|3937|BGT96224_553T0	jgi|Erynec1|4475|EV44_g0555T0	jgi|Golor2|4324591|e_gw1.189.49.1
jgi|Golci1|1719518|gm4.15343_g	jgi|Blugr1|22643|BGHDH14_bgh06362	jgi|Blugra1|3950|BGT96224_1305T0	jgi|Erynec1|4481|EV44_g0323T0	jgi|Golor2|4325126|e_gw1.192.388.1
jgi|Golci1|1720076|gm4.15901_g	jgi|Blugr1|22634|BGHDH14_bghG002861000001001	jgi|Blugra1|3956|BGT96224_AcSP30161T0	jgi|Erynec1|4482|EV44_g0444T0	jgi|Golor2|4325526|e_gw1.194.236.1
jgi|Golci1|1720758|gm4.16583_g	jgi|Blugr1|22633|BGHDH14_bghG002857000001001	jgi|Blugra1|3957|BGT96224_4399T0	jgi|Erynec1|4486|EV44_g0225T0	jgi|Golor2|4326017|e_gw1.197.147.1
jgi|Golci1|1727440|gm4.23265_g	jgi|Blugr1|22626|BGHDH14_bgh05828	jgi|Blugra1|3958|BGT96224_2905T0	jgi|Erynec1|4489|EV44_g0416T0	jgi|Golor2|4326660|e_gw1.200.202.1
jgi|Golci1|1727806|gm4.23631_g	jgi|Blugr1|22603|BGHDH14_bghG002826000002001	jgi|Blugra1|3973|BGT96224_5460T0	jgi|Erynec1|4492|EV44_g0357T0	jgi|Golor2|4327645|e_gw1.207.172.1
jgi|Golci1|1728935|gm4.24760_g	jgi|Blugr1|22599|BGHDH14_bghG002822000002001	jgi|Blugra1|3980|BGT96224_AcSP30691T0	jgi|Erynec1|4520|EV44_g0209T0	jgi|Golor2|4327941|e_gw1.209.111.1
jgi|Golci1|1730890|gm4.26715_g	jgi|Blugr1|22594|BGHDH14_bgh06271	jgi|Blugra1|4006|BGT96224_5017T0	jgi|Erynec1|4553|EV44_g0291T0	jgi|Golor2|4328241|e_gw1.211.24.1
jgi|Golci1|1731083|gm4.26908_g	jgi|Blugr1|22583|BGHDH14_bghG002809000001001	jgi|Blugra1|4012|BGT96224_1307T0	jgi|Erynec1|4564|EV44_g0326T0	jgi|Golor2|4334278|estExt_Genewise1.C_1_t20298
jgi|Golci1|1731401|gm4.27226_g	jgi|Blugr1|22579|BGHDH14_bgh05325	jgi|Blugra1|4013|BGT96224_E5764T0	jgi|Erynec1|456|EV44_g0586T0	jgi|Golor2|4345403|estExt_Genewise1.C_54_t10240
jgi|Golci1|1734399|gm4.30224_g	jgi|Blugr1|22577|BGHDH14_bghG002806000001001	jgi|Blugra1|4036|BGT96224_E5763T0	jgi|Erynec1|4579|EV44_g0597T0	jgi|Golor2|4345719|estExt_Genewise1.C_560268
jgi|Golci1|1736136|gm4.31961_g	jgi|Blugr1|22574|BGHDH14_bgh04220	jgi|Blugra1|4044|BGT96224_E6038T0	jgi|Erynec1|4580|EV44_g0364T0	jgi|Golor2|4353779|estExt_Genewise1.C_1300080
jgi|Golci1|1738069|gm4.33894_g	jgi|Blugr1|22570|BGHDH14_bgh01295	jgi|Blugra1|4050|BGT96224_AcSP30310T0	jgi|Erynec1|4679|EV44_g0081T0	jgi|Golor2|4362462|estExt_Genewise1Plus.C_8_t10061
jgi|Golci1|1738175|gm4.34000_g	jgi|Blugr1|22556|BGHDH14_bghG002783000001001	jgi|Blugra1|4077|BGT96224_5373T0	jgi|Erynec1|4681|EV44_g0110T0	jgi|Golor2|4364265|estExt_Genewise1Plus.C_14_t20048
jgi|Golci1|1738519|gm4.34344_g	jgi|Blugr1|22548|BGHDH14_bgh03816	jgi|Blugra1|408|BGT96224_3778T0	jgi|Erynec1|4693|EV44_g0315T0	jgi|Golor2|4366513|estExt_Genewise1Plus.C_24_t20045
jgi|Golci1|1751675|gw1.355.9.1	jgi|Blugr1|22538|BGHDH14_bghG002765000001001	jgi|Blugra1|4092|BGT96224_4804T0	jgi|Erynec1|4713|EV44_g0473T0	jgi|Golor2|4385556|fgenesh1_pg.1_#_36
jgi|Golci1|1760131|e_gw1.3.125.1	jgi|Blugr1|22533|BGHDH14_bghG002745000001001	jgi|Blugra1|4097|BGT96224_AcSP30056T0	jgi|Erynec1|4717|EV44_g0441T0	jgi|Golor2|4385645|fgenesh1_pg.1_#_125
jgi|Golci1|1760176|e_gw1.3.48.1	jgi|Blugr1|22529|BGHDH14_bghG002737000001001	jgi|Blugra1|4113|BGT96224_901T0	jgi|Erynec1|4729|EV44_g0288T0	jgi|Golor2|4385702|fgenesh1_pg.1_#_182
jgi|Golci1|1760284|e_gw1.4.153.1	jgi|Blugr1|22521|BGHDH14_bgh00804	jgi|Blugra1|4114|BGT96224_E3602T0	jgi|Erynec1|4747|EV44_g0325T0	jgi|Golor2|4385767|fgenesh1_pg.2_#_41
jgi|Golci1|1760291|e_gw1.4.122.1	jgi|Blugr1|22515|BGHDH14_bgh00588	jgi|Blugra1|4133|BGT96224_2380T0	jgi|Erynec1|4762|EV44_g0451T0	jgi|Golor2|4385974|fgenesh1_pg.3_#_33
jgi|Golci1|1760570|e_gw1.6.10.1	jgi|Blugr1|22499|BGHDH14_bgh04526	jgi|Blugra1|4144|BGT96224_E5845T0	jgi|Erynec1|4768|EV44_g0533T0	jgi|Golor2|4385996|fgenesh1_pg.3_#_55

<table>
<tr><th>Gc</th><th>Bgh</th><th>Bgt</th><th>En</th><th>Go</th></tr>
<tr><td>jgi|Golci1|1760966|e_gw1.11.4.1</td><td>jgi|Blugr1|22487|BGHDH14_bgh01555</td><td>jgi|Blugra1|4145|BGT96224_E5843T0</td><td>jgi|Erynec1|4836|EV44_g0017T0</td><td>jgi|Golor2|4386015|fgenesh1_pg.3_#_74</td></tr>
<tr><td>jgi|Golci1|1761429|e_gw1.17.42.1</td><td>jgi|Blugr1|22465|BGHDH14_bgh00729</td><td>jgi|Blugra1|4146|BGT96224_E5846T0</td><td>jgi|Erynec1|4839|EV44_g0349T0</td><td>jgi|Golor2|4386022|fgenesh1_pg.3_#_81</td></tr>
<tr><td>jgi|Golci1|1761486|e_gw1.18.47.1</td><td>jgi|Blugr1|22452|BGHDH14_bghG002294000001001</td><td>jgi|Blugra1|4163|BGT96224_E3962T0</td><td>jgi|Erynec1|483|EV44_g0324T0</td><td>jgi|Golor2|4386068|fgenesh1_pg.4_#_5</td></tr>
<tr><td>jgi|Golci1|1761500|e_gw1.18.11.1</td><td>jgi|Blugr1|22425|BGHDH14_bghG002265000001001</td><td>jgi|Blugra1|4167|BGT96224_4096T0</td><td>jgi|Erynec1|484|EV44_g0508T0</td><td>jgi|Golor2|4386072|fgenesh1_pg.4_#_9</td></tr>
<tr><td>jgi|Golci1|1762318|e_gw1.31.9.1</td><td>jgi|Blugr1|22424|BGHDH14_bgh01178</td><td>jgi|Blugra1|4174|BGT96224_3118T0</td><td>jgi|Erynec1|4851|EV44_g0456T0</td><td>jgi|Golor2|4386379|fgenesh1_pg.6_#_29</td></tr>
<tr><td>jgi|Golci1|1762457|e_gw1.34.55.1</td><td>jgi|Blugr1|22423|BGHDH14_bghG002260000001001</td><td>jgi|Blugra1|4196|BGT96224_E5543T0</td><td>jgi|Erynec1|4862|EV44_g0164T0</td><td>jgi|Golor2|4386386|fgenesh1_pg.6_#_36</td></tr>
<tr><td>jgi|Golci1|1762806|e_gw1.41.34.1</td><td>jgi|Blugr1|22406|BGHDH14_bgh06353</td><td>jgi|Blugra1|4197|BGT96224_E5634T0</td><td>jgi|Erynec1|4887|EV44_g0350T0</td><td>jgi|Golor2|4386436|fgenesh1_pg.6_#_86</td></tr>
<tr><td>jgi|Golci1|1762868|e_gw1.42.61.1</td><td>jgi|Blugr1|22405|BGHDH14_bgh02076</td><td>jgi|Blugra1|4203|BGT96224_1348T0</td><td>jgi|Erynec1|4895|EV44_g0341T0</td><td>jgi|Golor2|4386558|fgenesh1_pg.7_#_82</td></tr>
<tr><td>jgi|Golci1|1762967|e_gw1.43.33.1</td><td>jgi|Blugr1|22401|BGHDH14_bghG002254000001001</td><td>jgi|Blugra1|4222|BGT96224_1276T0</td><td>jgi|Erynec1|4898|EV44_g0549T0</td><td>jgi|Golor2|4386747|fgenesh1_pg.8_#_117</td></tr>
<tr><td>jgi|Golci1|1763023|e_gw1.44.13.1</td><td>jgi|Blugr1|22389|BGHDH14_bgh06118</td><td>jgi|Blugra1|4235|BGT96224_4102T0</td><td>jgi|Erynec1|4916|EV44_g0184T0</td><td>jgi|Golor2|4386813|fgenesh1_pg.9_#_39</td></tr>
<tr><td>jgi|Golci1|1763090|e_gw1.46.31.1</td><td>jgi|Blugr1|22372|BGHDH14_bghG002234000001001</td><td>jgi|Blugra1|4243|BGT96224_ASP20572T0</td><td>jgi|Erynec1|4937|EV44_g0216T0</td><td>jgi|Golor2|4386860|fgenesh1_pg.9_#_86</td></tr>
<tr><td>jgi|Golci1|1763156|e_gw1.47.40.1</td><td>jgi|Blugr1|22323|BGHDH14_bgh00584</td><td>jgi|Blugra1|4253|BGT96224_E5888T0</td><td>jgi|Erynec1|4939|EV44_g0335T0</td><td>jgi|Golor2|4386995|fgenesh1_pg.11_#_41</td></tr>
<tr><td>jgi|Golci1|1763209|e_gw1.48.20.1</td><td>jgi|Blugr1|22309|BGHDH14_bghG002170000001001</td><td>jgi|Blugra1|4258|BGT96224_ASP21259T0</td><td>jgi|Erynec1|4985|EV44_g0446T0</td><td>jgi|Golor2|4387034|fgenesh1_pg.11_#_80</td></tr>
<tr><td>jgi|Golci1|1763298|e_gw1.52.7.1</td><td>jgi|Blugr1|22308|BGHDH14_bgh03686</td><td>jgi|Blugra1|425|BGT96224_E10002T0</td><td>jgi|Erynec1|5020|EV44_g0256T0</td><td>jgi|Golor2|4387045|fgenesh1_pg.11_#_91</td></tr>
<tr><td>jgi|Golci1|1763717|e_gw1.61.11.1</td><td>jgi|Blugr1|22305|BGHDH14_bghG002161000001001</td><td>jgi|Blugra1|4267|BGT96224_1302T0</td><td>jgi|Erynec1|5025|EV44_g0361T0</td><td>jgi|Golor2|4387243|fgenesh1_pg.13_#_61</td></tr>
<tr><td>jgi|Golci1|1764052|e_gw1.69.22.1</td><td>jgi|Blugr1|22300|BGHDH14_bgh03689</td><td>jgi|Blugra1|4273|BGT96224_ASP21069T0</td><td>jgi|Erynec1|5063|EV44_g0039T0</td><td>jgi|Golor2|4387853|fgenesh1_pg.20_#_20</td></tr>
<tr><td>jgi|Golci1|1764359|e_gw1.76.55.1</td><td>jgi|Blugr1|22285|BGHDH14_bgh03087</td><td>jgi|Blugra1|4289|BGT96224_5074T0</td><td>jgi|Erynec1|5088|EV44_g0113T0</td><td>jgi|Golor2|4387976|fgenesh1_pg.21_#_56</td></tr>
<tr><td>jgi|Golci1|1764386|e_gw1.76.44.1</td><td>jgi|Blugr1|22277|BGHDH14_bgh02259</td><td>jgi|Blugra1|4291|BGT96224_ASP20861T0</td><td>jgi|Erynec1|509|EV44_g0527T0</td><td>jgi|Golor2|4387978|fgenesh1_pg.21_#_58</td></tr>
<tr><td>jgi|Golci1|1764870|e_gw1.89.51.1</td><td>jgi|Blugr1|22270|BGHDH14_bghG002084000001001</td><td>jgi|Blugra1|4301|BGT96224_BCGB2T0</td><td>jgi|Erynec1|5106|EV44_g0246T0</td><td>jgi|Golor2|4387986|fgenesh1_pg.21_#_66</td></tr>
<tr><td>jgi|Golci1|1765076|e_gw1.95.16.1</td><td>jgi|Blugr1|22269|BGHDH14_bgh04534</td><td>jgi|Blugra1|4302|BGT96224_AcSP30622T0</td><td>jgi|Erynec1|512|EV44_g0601T0</td><td>jgi|Golor2|4387991|fgenesh1_pg.21_#_71</td></tr>
<tr><td>jgi|Golci1|1765437|e_gw1.105.48.1</td><td>jgi|Blugr1|22264|BGHDH14_bgh01411</td><td>jgi|Blugra1|4315|BGT96224_AcSP31262T0</td><td>jgi|Erynec1|5135|EV44_g0391T0</td><td>jgi|Golor2|4388268|fgenesh1_pg.24_#_87</td></tr>
</table>

Gc	Bgh	Bgt	En	Go
jgi|Golci1|1765905|e_gw1.119.51.1	jgi|Blugr1|22249|BGHDH14_bgh04018	jgi|Blugra1|4320|BGT96224_E5545T0	jgi|Erynec1|5150|EV44_g0559T0	jgi|Golor2|4388615|fgenesh1_pg.29_#_34
jgi|Golci1|1766135|e_gw1.124.8.1	jgi|Blugr1|22247|BGHDH14_bgh00778	jgi|Blugra1|4328|BGT96224_ASP20446T0	jgi|Erynec1|5183|EV44_g0307T0	jgi|Golor2|4388800|fgenesh1_pg.31_#_28
jgi|Golci1|1766162|e_gw1.124.64.1	jgi|Blugr1|22236|BGHDH14_bghG004010000002001	jgi|Blugra1|4335|BGT96224_249T0	jgi|Erynec1|5214|EV44_g0255T0	jgi|Golor2|4389219|fgenesh1_pg.37_#_29
jgi|Golci1|1766399|e_gw1.133.69.1	jgi|Blugr1|22229|BGHDH14_bgh01296	jgi|Blugra1|4341|BGT96224_1536T0	jgi|Erynec1|5228|EV44_g0505T0	jgi|Golor2|4389238|fgenesh1_pg.37_#_48
jgi|Golci1|1766476|e_gw1.136.39.1	jgi|Blugr1|22221|BGHDH14_bgh01315	jgi|Blugra1|4346|BGT96224_AcSP30434T0	jgi|Erynec1|5250|EV44_g0482T0	jgi|Golor2|4389252|fgenesh1_pg.38_#_8
jgi|Golci1|1767091|e_gw1.160.12.1	jgi|Blugr1|22218|BGHDH14_bgh01281	jgi|Blugra1|4351|BGT96224_3046T0	jgi|Erynec1|5258|EV44_g0252T0	jgi|Golor2|4389417|fgenesh1_pg.41_#_10
jgi|Golci1|1767356|e_gw1.174.34.1	jgi|Blugr1|22185|BGHDH14_bgh04235	jgi|Blugra1|435|BGT96224_3280T0	jgi|Erynec1|5262|EV44_g0379T0	jgi|Golor2|4390161|fgenesh1_pg.53_#_59
jgi|Golci1|1767366|e_gw1.174.5.1	jgi|Blugr1|22176|BGHDH14_bgh05321	jgi|Blugra1|4361|BGT96224_AcSP30616T0	jgi|Erynec1|5274|EV44_g0521T0	jgi|Golor2|4390393|fgenesh1_pg.57_#_38
jgi|Golci1|1767728|e_gw1.190.6.1	jgi|Blugr1|22132|BGHDH14_bghG003972000001001	jgi|Blugra1|4362|BGT96224_ASP20617T0	jgi|Erynec1|5275|EV44_g0466T0	jgi|Golor2|4390417|fgenesh1_pg.58_#_1
jgi|Golci1|1767876|e_gw1.199.31.1	jgi|Blugr1|22115|BGHDH14_bgh04921	jgi|Blugra1|4364|BGT96224_E6054T0	jgi|Erynec1|5287|EV44_g0149T0	jgi|Golor2|4390418|fgenesh1_pg.58_#_2
jgi|Golci1|1767966|e_gw1.205.18.1	jgi|Blugr1|22106|BGHDH14_bgh00780	jgi|Blugra1|4387|BGT96224_ASP20929T0	jgi|Erynec1|5288|EV44_g0569T0	jgi|Golor2|4390616|fgenesh1_pg.61_#_17
jgi|Golci1|1768065|e_gw1.212.3.1	jgi|Blugr1|22092|BGHDH14_bgh06712	jgi|Blugra1|4404|BGT96224_E5838T0	jgi|Erynec1|5301|EV44_g0512T0	jgi|Golor2|4390630|fgenesh1_pg.61_#_31
jgi|Golci1|1768565|e_gw1.254.14.1	jgi|Blugr1|22068|BGHDH14_bgh04181	jgi|Blugra1|4405|BGT96224_E5839T0	jgi|Erynec1|5307|EV44_g0140T0	jgi|Golor2|4390783|fgenesh1_pg.64_#_20
jgi|Golci1|1768784|e_gw1.271.13.1	jgi|Blugr1|22064|BGHDH14_bghG003936000001001	jgi|Blugra1|4407|BGT96224_AcSP31175T0	jgi|Erynec1|5316|EV44_g0228T0	jgi|Golor2|4390806|fgenesh1_pg.64_#_43
jgi|Golci1|1769015|e_gw1.287.6.1	jgi|Blugr1|22053|BGHDH14_bgh04847	jgi|Blugra1|441|BGT96224_5394T0	jgi|Erynec1|5377|EV44_g0395T0	jgi|Golor2|4390911|fgenesh1_pg.66_#_42
jgi|Golci1|1769315|e_gw1.320.15.1	jgi|Blugr1|22034|BGHDH14_bgh03696	jgi|Blugra1|4428|BGT96224_AcSP31269T0	jgi|Erynec1|5385|EV44_g0230T0	jgi|Golor2|4391091|fgenesh1_pg.70_#_6
jgi|Golci1|1769635|e_gw1.353.1.1	jgi|Blugr1|22033|BGHDH14_bgh02979	jgi|Blugra1|4431|BGT96224_E10117T0	jgi|Erynec1|5407|EV44_g0413T0	jgi|Golor2|4391232|fgenesh1_pg.73_#_9
jgi|Golci1|1770009|e_gw1.406.3.1	jgi|Blugr1|22032|BGHDH14_bgh03474	jgi|Blugra1|4436|BGT96224_2810T0	jgi|Erynec1|5409|EV44_g0242T0	jgi|Golor2|4391578|fgenesh1_pg.79_#_10
jgi|Golci1|1770174|e_gw1.442.5.1	jgi|Blugr1|22028|BGHDH14_bgh04095	jgi|Blugra1|444|BGT96224_3113T0	jgi|Erynec1|5440|EV44_g0083T0	jgi|Golor2|4391584|fgenesh1_pg.79_#_16
jgi|Golci1|1770256|e_gw1.486.1.1	jgi|Blugr1|22026|BGHDH14_bgh04093	jgi|Blugra1|4476|BGT96224_ASP20303T0	jgi|Erynec1|5474|EV44_g0265T0	jgi|Golor2|4391585|fgenesh1_pg.79_#_17
jgi|Golci1|1781399|estExt_Genewise1Plus.C_120046	jgi|Blugr1|22023|BGHDH14_bgh06602	jgi|Blugra1|4493|BGT96224_3948T0	jgi|Erynec1|5479|EV44_g0244T0	jgi|Golor2|4391587|fgenesh1_pg.79_#_19

Gc	Bgh	Bgt	En	Go
jgi|Golci1|1794248|fgenesh1_pg.1_#_94	jgi|Blugr1|22018|BGHDH14_bgh04554	jgi|Blugra1|4505|BGT96224_4772T0	jgi|Erynec1|5481|EV44_g0532T0	jgi|Golor2|4391594|fgenesh1_pg.79_#_26
jgi|Golci1|1794491|fgenesh1_pg.4_#_48	jgi|Blugr1|22015|BGHDH14_bgh02707	jgi|Blugra1|4558|BGT96224_AcSP30639T0	jgi|Erynec1|548|EV44_g0069T0	jgi|Golor2|4391815|fgenesh1_pg.84_#_5
jgi|Golci1|1794556|fgenesh1_pg.5_#_31	jgi|Blugr1|22014|BGHDH14_bgh01659	jgi|Blugra1|4560|BGT96224_AcSP30641T0	jgi|Erynec1|5499|EV44_g3855T0	jgi|Golor2|4391816|fgenesh1_pg.84_#_6
jgi|Golci1|1794745|fgenesh1_pg.8_#_42	jgi|Blugr1|22010|BGHDH14_bgh05787	jgi|Blugra1|4564|BGT96224_AcSP30643T0	jgi|Erynec1|5533|EV44_g0534T0	jgi|Golor2|4391818|fgenesh1_pg.84_#_8
jgi|Golci1|1794866|fgenesh1_pg.11_#_40	jgi|Blugr1|22009|BGHDH14_bgh04864	jgi|Blugra1|4613|BGT96224_E5862T0	jgi|Erynec1|5601|EV44_g0503T0	jgi|Golor2|4392063|fgenesh1_pg.89_#_3
jgi|Golci1|1794901|fgenesh1_pg.12_#_20	jgi|Blugr1|21988|BGHDH14_bghG003125000001001	jgi|Blugra1|4617|BGT96224_E5992T0	jgi|Erynec1|5621|EV44_g0429T0	jgi|Golor2|4392186|fgenesh1_pg.91_#_25
jgi|Golci1|1794939|fgenesh1_pg.13_#_7	jgi|Blugr1|21987|BGHDH14_bgh03693	jgi|Blugra1|4646|BGT96224_E5745T0	jgi|Erynec1|5622|EV44_g0380T0	jgi|Golor2|4392585|fgenesh1_pg.100_#_37
jgi|Golci1|1794940|fgenesh1_pg.13_#_8	jgi|Blugr1|21986|BGHDH14_bgh02835	jgi|Blugra1|4649|BGT96224_E5694T0	jgi|Erynec1|5625|EV44_g0115T0	jgi|Golor2|4392604|fgenesh1_pg.101_#_19
jgi|Golci1|1795608|fgenesh1_pg.32_#_27	jgi|Blugr1|21971|BGHDH14_bgh04744	jgi|Blugra1|4653|BGT96224_E5743T0	jgi|Erynec1|5645|EV44_g0116T0	jgi|Golor2|4392990|fgenesh1_pg.110_#_22
jgi|Golci1|1795610|fgenesh1_pg.32_#_29	jgi|Blugr1|21969|BGHDH14_bgh04143	jgi|Blugra1|4658|BGT96224_E10112T0	jgi|Erynec1|5671|EV44_g0363T0	jgi|Golor2|4393061|fgenesh1_pg.112_#_24
jgi|Golci1|1795776|fgenesh1_pg.38_#_9	jgi|Blugr1|21961|BGHDH14_bgh03602	jgi|Blugra1|467|BGT96224_ASP21338T0	jgi|Erynec1|5708|EV44_g0090T0	jgi|Golor2|4393337|fgenesh1_pg.120_#_7
jgi|Golci1|1795965|fgenesh1_pg.45_#_19	jgi|Blugr1|21947|BGHDH14_bgh01776	jgi|Blugra1|4680|BGT96224_E6002T0	jgi|Erynec1|5713|EV44_g0449T0	jgi|Golor2|4393399|fgenesh1_pg.122_#_2
jgi|Golci1|1795983|fgenesh1_pg.46_#_16	jgi|Blugr1|21946|BGHDH14_bgh00857	jgi|Blugra1|4681|BGT96224_E5699T0	jgi|Erynec1|5719|EV44_g0279T0	jgi|Golor2|4393521|fgenesh1_pg.124_#_29
jgi|Golci1|1796043|fgenesh1_pg.48_#_16	jgi|Blugr1|21942|BGHDH14_bgh03596	jgi|Blugra1|4683|BGT96224_E5698T0	jgi|Erynec1|5722|EV44_g0019T0	jgi|Golor2|4393664|fgenesh1_pg.129_#_1
jgi|Golci1|1796074|fgenesh1_pg.49_#_21	jgi|Blugr1|21938|BGHDH14_bghG003075000001001	jgi|Blugra1|4690|BGT96224_4619T0	jgi|Erynec1|5727|EV44_g0594T0	jgi|Golor2|4393688|fgenesh1_pg.130_#_7
jgi|Golci1|1796288|fgenesh1_pg.59_#_10	jgi|Blugr1|21935|BGHDH14_bgh00848	jgi|Blugra1|4714|BGT96224_1719T0	jgi|Erynec1|5739|EV44_g0029T0	jgi|Golor2|4393802|fgenesh1_pg.133_#_5
jgi|Golci1|1796298|fgenesh1_pg.60_#_3	jgi|Blugr1|21927|BGHDH14_bgh02178	jgi|Blugra1|4727|BGT96224_1763T0	jgi|Erynec1|5744|EV44_g0388T0	jgi|Golor2|4393973|fgenesh1_pg.138_#_7
jgi|Golci1|1796466|fgenesh1_pg.67_#_3	jgi|Blugr1|21884|BGHDH14_bgh02776	jgi|Blugra1|4735|BGT96224_1744T0	jgi|Erynec1|5747|EV44_g0231T0	jgi|Golor2|4394446|fgenesh1_pg.154_#_14
jgi|Golci1|1796522|fgenesh1_pg.69_#_21	jgi|Blugr1|21863|BGHDH14_bgh00507	jgi|Blugra1|4742|BGT96224_E5689T0	jgi|Erynec1|5773|EV44_g0076T0	jgi|Golor2|4394460|fgenesh1_pg.154_#_28
jgi|Golci1|1796590|fgenesh1_pg.72_#_9	jgi|Blugr1|21857|BGHDH14_bgh02534	jgi|Blugra1|4748|BGT96224_E10141T0	jgi|Erynec1|5776|EV44_g0089T0	jgi|Golor2|4394836|fgenesh1_pg.170_#_14
jgi|Golci1|1796709|fgenesh1_pg.78_#_6	jgi|Blugr1|21850|BGHDH14_bgh00503	jgi|Blugra1|4764|BGT96224_E10114T0	jgi|Erynec1|5781|EV44_g0034T0	jgi|Golor2|4394912|fgenesh1_pg.174_#_14

Gc	Bgh	Bgt	En	Go
jgi|Golci1|1796800|fgenesh1_pg.82_#_3	jgi|Blugr1|21830|BGHDH14_bgh05372	jgi|Blugra1|4781|BGT96224_3292T0	jgi|Erynec1|5790|EV44_g0596T0	jgi|Golor2|4394970|fgenesh1_pg.177_#_2
jgi|Golci1|1797000|fgenesh1_pg.92_#_2	jgi|Blugr1|21820|BGHDH14_bgh01390	jgi|Blugra1|4785|BGT96224_E10142T0	jgi|Erynec1|5843|EV44_g0264T0	jgi|Golor2|4395264|fgenesh1_pg.190_#_3
jgi|Golci1|1797621|fgenesh1_pg.127_#_7	jgi|Blugr1|21813|BGHDH14_bgh00059	jgi|Blugra1|479|BGT96224_ASP20359T0	jgi|Erynec1|5853|EV44_g0156T0	jgi|Golor2|4395331|fgenesh1_pg.194_#_8
jgi|Golci1|1797699|fgenesh1_pg.133_#_3	jgi|Blugr1|21808|BGHDH14_bgh00122	jgi|Blugra1|4806|BGT96224_2103T0	jgi|Erynec1|5860|EV44_g0530T0	jgi|Golor2|4395703|fgenesh1_pg.217_#_7
jgi|Golci1|1797784|fgenesh1_pg.138_#_16	jgi|Blugr1|21805|BGHDH14_bgh04889	jgi|Blugra1|4809|BGT96224_3216T0	jgi|Erynec1|5864|EV44_g0491T0	jgi|Golor2|4395799|fgenesh1_pg.224_#_10
jgi|Golci1|1797846|fgenesh1_pg.143_#_2	jgi|Blugr1|21803|BGHDH14_bgh03709	jgi|Blugra1|4835|BGT96224_5123T0	jgi|Erynec1|58|EV44_g0107T0	jgi|Golor2|4395813|fgenesh1_pg.225_#_7
jgi|Golci1|1797996|fgenesh1_pg.153_#_16	jgi|Blugr1|21790|BGHDH14_bgh04888	jgi|Blugra1|4857|BGT96224_312T0	jgi|Erynec1|5919|EV44_g0037T0	jgi|Golor2|4395825|fgenesh1_pg.226_#_8
jgi|Golci1|1798088|fgenesh1_pg.161_#_5	jgi|Blugr1|21786|BGHDH14_bgh02945	jgi|Blugra1|4865|BGT96224_E5630T0	jgi|Erynec1|5929|EV44_g0571T0	jgi|Golor2|4395946|fgenesh1_pg.240_#_3
jgi|Golci1|1798567|fgenesh1_pg.205_#_5	jgi|Blugr1|21765|BGHDH14_bghG004450000001001	jgi|Blugra1|4876|BGT96224_E2438T0	jgi|Erynec1|5938|EV44_g0486T0	jgi|Golor2|4395949|fgenesh1_pg.240_#_6
jgi|Golci1|1798623|fgenesh1_pg.212_#_4	jgi|Blugr1|21763|BGHDH14_bgh03037	jgi|Blugra1|4881|BGT96224_5153T0	jgi|Erynec1|5942|EV44_g0096T0	jgi|Golor2|4399842|estExt_Genemark4.C_250170
jgi|Golci1|1798650|fgenesh1_pg.216_#_2	jgi|Blugr1|21762|BGHDH14_bghG004439000001001	jgi|Blugra1|4884|BGT96224_E6004T0	jgi|Erynec1|5980|EV44_g0506T0	jgi|Golor2|4400545|estExt_Genemark4.C_320084
jgi|Golci1|1798850|fgenesh1_pg.242_#_8	jgi|Blugr1|21761|BGHDH14_bgh03028	jgi|Blugra1|4907|BGT96224_E5582T0	jgi|Erynec1|6011|EV44_g0593T0	jgi|Golor2|4405080|estExt_Genemark4.C_950004
jgi|Golci1|1798871|fgenesh1_pg.246_#_3	jgi|Blugr1|21760|BGHDH14_bgh03042	jgi|Blugra1|4928|BGT96224_2870T0	jgi|Erynec1|6032|EV44_g0182T0	jgi|Golor2|4409105|estExt_Genemark4.C_1990054
jgi|Golci1|1798916|fgenesh1_pg.250_#_7	jgi|Blugr1|21759|BGHDH14_bgh03046	jgi|Blugra1|494|BGT96224_2867T0	jgi|Erynec1|6058|EV44_g0525T0	jgi|Golor2|5505766|fgenesh1_pm.76_#_14
jgi|Golci1|1799339|fgenesh1_pg.326_#_6	jgi|Blugr1|21756|BGHDH14_bgh00950	jgi|Blugra1|495|BGT96224_118T0	jgi|Erynec1|6061|EV44_g0562T0	jgi|Golor2|5506571|fgenesh1_pm.96_#_19
jgi|Golci1|1799506|fgenesh1_pg.360_#_6	jgi|Blugr1|21746|BGHDH14_bgh04094	jgi|Blugra1|4977|BGT96224_1280T0	jgi|Erynec1|6062|EV44_g0564T0	jgi|Golor2|5506572|fgenesh1_pm.96_#_20
jgi|Golci1|1799537|fgenesh1_pg.368_#_3	jgi|Blugr1|21743|BGHDH14_bghG004392000002001	jgi|Blugra1|4978|BGT96224_AcSP30986T0	jgi|Erynec1|6064|EV44_g0542T0	jgi|Golor2|5506693|fgenesh1_pm.100_#_11
jgi|Golci1|1800421|estExt_Genemark4.C_3_t10476	jgi|Blugr1|21739|BGHDH14_bghG004378000001001	jgi|Blugra1|4998|BGT96224_ASP20209T0	jgi|Erynec1|6069|EV44_g0346T0	jgi|Golor2|5506880|fgenesh1_pm.105_#_21
jgi|Golci1|1801984|estExt_Genemark4.C_260037	jgi|Blugr1|21738|BGHDH14_bgh00947	jgi|Blugra1|5001|BGT96224_AcSP30210T0	jgi|Erynec1|6071|EV44_g0558T0	jgi|Golor2|5507195|fgenesh1_pm.115_#_18
jgi|Golci1|1802261|estExt_Genemark4.C_310178	jgi|Blugr1|21736|BGHDH14_bghG004376000001001	jgi|Blugra1|5018|BGT96224_AcSP30464T0	jgi|Erynec1|6076|EV44_g0598T0	jgi|Golor2|5507239|fgenesh1_pm.117_#_2
jgi|Golci1|1803082|estExt_Genemark4.C_500077	jgi|Blugr1|21733|BGHDH14_bghG004373000002001	jgi|Blugra1|5032|BGT96224_ASP20735T0	jgi|Erynec1|6091|EV44_g0016T0	jgi|Golor2|5507366|fgenesh1_pm.121_#_14

Gc	Bgh	Bgt	En	Go
jgi|Golci1|1805531|estExt_Genemark4.C_1270027	jgi|Blugr1|21715|BGHDH14_bghG003905000001001	jgi|Blugra1|5033|BGT96224_E5660T0	jgi|Erynec1|6103|EV44_g0372T0	jgi|Golor2|5507450|fgenesh1_pm.123_#_45
jgi|Golci1|1807836|estExt_Genemark4.C_2750051	jgi|Blugr1|21712|BGHDH14_bgh03377	jgi|Blugra1|5034|BGT96224_E10129T0	jgi|Erynec1|6108|EV44_g0476T0	jgi|Golor2|5507483|fgenesh1_pm.125_#_8
jgi|Golci1|1808700|estExt_Genemark4.C_3920006	jgi|Blugr1|21705|BGHDH14_bgh05140	jgi|Blugra1|5082|BGT96224_535T0	jgi|Erynec1|6114|EV44_g0283T0	jgi|Golor2|5507560|fgenesh1_pm.127_#_17
jgi|Golci1|1809407|fgenesh1_kg.1_#_170_#_TRINITY_DN7173	jgi|Blugr1|21699|BGHDH14_bghG003896000001001	jgi|Blugra1|5084|BGT96224_1296T0	jgi|Erynec1|6120|EV44_g0155T0	jgi|Golor2|5507847|fgenesh1_pm.138_#_6
jgi|Golci1|1809409|fgenesh1_kg.1_#_172_#_TRINITY_DN1369	jgi|Blugr1|21694|BGHDH14_bgh05118	jgi|Blugra1|5098|BGT96224_E5996T0	jgi|Erynec1|619|EV44_g0408T0	jgi|Golor2|5508073|fgenesh1_pm.148_#_6
jgi|Golci1|1809450|fgenesh1_kg.1_#_213_#_TRINITY_DN1818	jgi|Blugr1|21691|BGHDH14_bgh00824	jgi|Blugra1|5099|BGT96224_178T0	jgi|Erynec1|6201|EV44_g0458T0	jgi|Golor2|5508904|fgenesh1_pm.189_#_8
jgi|Golci1|1809647|fgenesh1_kg.1_#_410_#_TRINITY_DN1260	jgi|Blugr1|21688|BGHDH14_bgh05116	jgi|Blugra1|5106|BGT96224_AcSP30696T0	jgi|Erynec1|6210|EV44_g0206T0	jgi|Golor2|5509024|fgenesh1_pm.198_#_4
jgi|Golci1|1809650|fgenesh1_kg.1_#_413_#_TRINITY_DN1936	jgi|Blugr1|21672|BGHDH14_bgh02337	jgi|Blugra1|5129|BGT96224_E5563T0	jgi|Erynec1|6287|EV44_g0465T0	jgi|Golor2|5527435|MIX17811_2159_39
jgi|Golci1|1809665|fgenesh1_kg.1_#_428_#_TRINITY_DN1941	jgi|Blugr1|21671|BGHDH14_bgh03855	jgi|Blugra1|5162|BGT96224_E5883T0	jgi|Erynec1|6321|EV44_g0605T0	jgi|Golor2|5538213|MIX28589_1597_91
jgi|Golci1|1809706|fgenesh1_kg.1_#_469_#_TRINITY_DN1164	jgi|Blugr1|21662|BGHDH14_bgh05117	jgi|Blugra1|5176|BGT96224_194T0	jgi|Erynec1|6322|EV44_g0526T0	jgi|Golor2|5549432|MIX39808_49710_55
jgi|Golci1|1809735|fgenesh1_kg.1_#_498_#_TRINITY_DN1913	jgi|Blugr1|21622|BGHDH14_bgh01337	jgi|Blugra1|5189|BGT96224_E5665T0	jgi|Erynec1|6368|EV44_g0396T0	jgi|Golor2|5549786|MIX40162_2277_93
jgi|Golci1|1809801|fgenesh1_kg.1_#_564_#_TRINITY_DN1904	jgi|Blugr1|21620|BGHDH14_bghG003813000001001	jgi|Blugra1|51|BGT96224_E5918T0	jgi|Erynec1|6418|EV44_g0229T0	jgi|Golor2|5574177|MIX64553_1218_76
jgi|Golci1|1809870|fgenesh1_kg.1_#_633_#_TRINITY_DN1637	jgi|Blugr1|21608|BGHDH14_bghG003803000001001	jgi|Blugra1|5202|BGT96224_E5979T0	jgi|Erynec1|641|EV44_g0383T0	jgi|Golor2|5620848|MIX111224_9898_70
jgi|Golci1|1809941|fgenesh1_kg.1_#_704_#_TRINITY_DN2091	jgi|Blugr1|21607|BGHDH14_bghG003801000001001	jgi|Blugra1|5223|BGT96224_4589T0	jgi|Erynec1|6467|EV44_g0472T0	jgi|Golor2|5656176|MIX146552_1573_95
jgi|Golci1|1809996|fgenesh1_kg.1_#_759_#_TRINITY_DN1667	jgi|Blugr1|21605|BGHDH14_bghG003798000001001	jgi|Blugra1|5231|BGT96224_4783T0	jgi|Erynec1|651|EV44_g0053T0	jgi|Golor2|5714216|MIX204592_419_59
jgi|Golci1|1810049|fgenesh1_kg.1_#_812_#_TRINITY_DN1818	jgi|Blugr1|21604|BGHDH14_bgh04984	jgi|Blugra1|5245|BGT96224_2234T0	jgi|Erynec1|662|EV44_g0226T0	jgi|Golor2|5724564|MIX214940_4712_22
jgi|Golci1|1810114|fgenesh1_kg.1_#_877_#_TRINITY_DN1776	jgi|Blugr1|21602|BGHDH14_bgh06022	jgi|Blugra1|5269|BGT96224_AcSP31200T0	jgi|Erynec1|664|EV44_g0214T0	jgi|Golor2|5818307|estExt_fgenesh1_pg.C_400026
jgi|Golci1|1810171|fgenesh1_kg.1_#_934_#_TRINITY_DN1794	jgi|Blugr1|21592|BGHDH14_bgh01722	jgi|Blugra1|5272|BGT96224_E5659T0	jgi|Erynec1|698|EV44_g0134T0	jgi|Golor2|5819261|estExt_fgenesh1_pg.C_590001
jgi|Golci1|1810243|fgenesh1_kg.2_#_8_#_TRINITY_DN2032_c	jgi|Blugr1|21589|BGHDH14_bgh03094	jgi|Blugra1|5275|BGT96224_652T0	jgi|Erynec1|715|EV44_g0319T0	jgi|Golor2|5820476|estExt_fgenesh1_pg.C_840010
jgi|Golci1|1810265|fgenesh1_kg.2_#_30_#_TRINITY_DN16713	jgi|Blugr1|21576|BGHDH14_bgh03967	jgi|Blugra1|5289|BGT96224_E6030T0	jgi|Erynec1|721|EV44_g0570T0	jgi|Golor2|5820477|estExt_fgenesh1_pg.C_840011
jgi|Golci1|1810304|fgenesh1_kg.2_#_69_#_TRINITY_DN16046	jgi|Blugr1|21562|BGHDH14_bgh02580	jgi|Blugra1|5292|BGT96224_ASP21188T0	jgi|Erynec1|724|EV44_g0061T0	jgi|Golor2|5821145|estExt_fgenesh1_pg.C_1000010

Gc	Bgh	Bgt	En	Go
jgi|Golci1|1810423|fgenesh1_kg.2_#_188_#_TRINITY_DN1384	jgi|Blugr1|21520|BGHDH14_bgh01379	jgi|Blugra1|5316|BGT96224_E3523T0	jgi|Erynec1|728|EV44_g0303T0	jgi|Golor2|5821715|estExt_fgenesh1_pg.C_1160023
jgi|Golci1|1810435|fgenesh1_kg.2_#_200_#_TRINITY_DN1971	jgi|Blugr1|21515|BGHDH14_bgh06674	jgi|Blugra1|5319|BGT96224_E5858T0	jgi|Erynec1|739|EV44_g0351T0	jgi|Golor2|5823087|estExt_fgenesh1_pg.C_1650005
jgi|Golci1|1810514|fgenesh1_kg.2_#_279_#_TRINITY_DN5994	jgi|Blugr1|21479|BGHDH14_bgh02206	jgi|Blugra1|5320|BGT96224_E4932T0	jgi|Erynec1|745|EV44_g0333T0	jgi|Golor2|5824170|estExt_fgenesh1_pg.C_2390009
jgi|Golci1|1810532|fgenesh1_kg.2_#_297_#_TRINITY_DN1840	jgi|Blugr1|21435|BGHDH14_bghG003355000001001	jgi|Blugra1|5323|BGT96224_E10119T0	jgi|Erynec1|764|EV44_g0606T0	jgi|Golor2|5824174|estExt_fgenesh1_pg.C_2400001
jgi|Golci1|1810628|fgenesh1_kg.2_#_393_#_TRINITY_DN1939	jgi|Blugr1|21434|BGHDH14_bghG003347000001001	jgi|Blugra1|5326|BGT96224_1209T0	jgi|Erynec1|841|EV44_g0080T0	jgi|Golor2|5824175|estExt_fgenesh1_pg.C_2400002
jgi|Golci1|1810653|fgenesh1_kg.2_#_418_#_TRINITY_DN5646	jgi|Blugr1|21427|BGHDH14_bghG003337000001001	jgi|Blugra1|5328|BGT96224_E5995T0	jgi|Erynec1|898|EV44_g0186T0	jgi|Golor2|5829115|estExt_fgenesh1_pm.C_810030
jgi|Golci1|1810662|fgenesh1_kg.2_#_427_#_TRINITY_DN1815	jgi|Blugr1|21424|BGHDH14_bgh02916	jgi|Blugra1|5332|BGT96224_E6035T0	jgi|Erynec1|907|EV44_g0131T0	jgi|Golor2|5831497|estExt_fgenesh1_pm.C_1710008
jgi|Golci1|1810676|fgenesh1_kg.2_#_441_#_TRINITY_DN1869	jgi|Blugr1|21422|BGHDH14_bgh05042	jgi|Blugra1|5336|BGT96224_E3888T0	jgi|Erynec1|913|EV44_g0320T0	jgi|Golor2|5832179|estExt_fgenesh1_pm.C_2280002
jgi|Golci1|1810719|fgenesh1_kg.2_#_484_#_TRINITY_DN1775	jgi|Blugr1|21420|BGHDH14_bgh02917	jgi|Blugra1|5372|BGT96224_E5638T0	jgi|Erynec1|914|EV44_g0538T0	jgi|Golor2|583252|CE539873_399
jgi|Golci1|1810810|fgenesh1_kg.3_#_64_#_TRINITY_DN19285	jgi|Blugr1|21404|BGHDH14_bgh01198	jgi|Blugra1|5377|BGT96224_BCGB1T0	jgi|Erynec1|925|EV44_g0516T0	jgi|Golor2|632048|CE588669_11379
jgi|Golci1|1810858|fgenesh1_kg.3_#_112_#_TRINITY_DN1928	jgi|Blugr1|21401|BGHDH14_bgh04923	jgi|Blugra1|5378|BGT96224_2749T0	jgi|Erynec1|929|EV44_g0143T0	jgi|Golor2|635348|CE591969_64
jgi|Golci1|1810871|fgenesh1_kg.3_#_125_#_TRINITY_DN1928	jgi|Blugr1|21400|BGHDH14_bgh04924	jgi|Blugra1|5388|BGT96224_ASP20408T0	jgi|Erynec1|936|EV44_g0362T0	jgi|Golor2|636606|CE593227_1576
jgi|Golci1|1810908|fgenesh1_kg.3_#_162_#_TRINITY_DN1932	jgi|Blugr1|21399|BGHDH14_bgh03212	jgi|Blugra1|5391|BGT96224_E5738T0	jgi|Erynec1|943|EV44_g0489T0	jgi|Golor2|6765|gm4.6765_g
jgi|Golci1|1810915|fgenesh1_kg.3_#_169_#_TRINITY_DN1932	jgi|Blugr1|21395|BGHDH14_bgh01232	jgi|Blugra1|5399|BGT96224_ASP20389T0	jgi|Erynec1|1001|EV44_g0172T0	jgi|Golor2|6825|gm4.6825_g
jgi|Golci1|1810957|fgenesh1_kg.3_#_211_#_TRINITY_DN1941	jgi|Blugr1|21393|BGHDH14_bghG003307000001001	jgi|Blugra1|5413|BGT96224_3750T0	jgi|Erynec1|1051|EV44_g0513T0	jgi|Golor2|697252|CE653873_12337
jgi|Golci1|1810977|fgenesh1_kg.3_#_231_#_TRINITY_DN2299	jgi|Blugr1|21382|BGHDH14_bgh00242	jgi|Blugra1|5440|BGT96224_697T0	jgi|Erynec1|1056|EV44_g0547T0	jgi|Golor2|710617|CE667238_383
jgi|Golci1|1811008|fgenesh1_kg.3_#_262_#_TRINITY_DN1737	jgi|Blugr1|21377|BGHDH14_bgh01944	jgi|Blugra1|5442|BGT96224_ASP21248T0	jgi|Erynec1|105|EV44_g0427T0	jgi|Golor2|922974|CE879595_225
jgi|Golci1|1811028|fgenesh1_kg.3_#_282_#_TRINITY_DN1539	jgi|Blugr1|21322|BGHDH14_bgh00373	jgi|Blugra1|5490|BGT96224_ASP20340T0	jgi|Erynec1|109|EV44_g0334T0	jgi|Golor2|936621|CE893242_11734
jgi|Golci1|1811100|fgenesh1_kg.3_#_354_#_TRINITY_DN3174	jgi|Blugr1|21287|BGHDH14_bgh04219	jgi|Blugra1|5492|BGT96224_E10014T0	jgi|Erynec1|1121|EV44_g0405T0	jgi|Golor2|951457|CE908078_2841
jgi|Golci1|1811131|fgenesh1_kg.3_#_385_#_TRINITY_DN1355	jgi|Blugr1|21280|BGHDH14_bgh06323	jgi|Blugra1|5493|BGT96224_ASP20811T0	jgi|Erynec1|1124|EV44_g0183T0	jgi|Golor2|97205|CE53826_15
jgi|Golci1|1811137|fgenesh1_kg.3_#_391_#_TRINITY_DN9646	jgi|Blugr1|21253|BGHDH14_bgh02650	jgi|Blugra1|5500|BGT96224_E5610T0	jgi|Erynec1|1153|EV44_g0467T0	jgi|Golor2|9850|gm4.9850_g

Gc	Bgh	Bgt	En	Go
jgi|Golci1|1811139|fgenesh1_kg.3_#_393_#_TRINITY_DN9646	jgi|Blugr1|21251|BGHDH14_bgh03006	jgi|Blugra1|5501|BGT96224_ASP20337T0	jgi|Erynec1|1161|EV44_g0257T0	jgi|Golor2|1005179|CE961800_33617
jgi|Golci1|1811175|fgenesh1_kg.3_#_429_#_TRINITY_DN3536	jgi|Blugr1|21246|BGHDH14_bgh04257	jgi|Blugra1|5508|BGT96224_717T0	jgi|Erynec1|1162|EV44_g0187T0	jgi|Golor2|1017800|CE974421_2764
jgi|Golci1|1811180|fgenesh1_kg.3_#_434_#_TRINITY_DN1907	jgi|Blugr1|21242|BGHDH14_bgh03290	jgi|Blugra1|550|BGT96224_396T0	jgi|Erynec1|1163|EV44_g0524T0	jgi|Golor2|1083367|CE1039988_3283
jgi|Golci1|1811186|fgenesh1_kg.3_#_440_#_TRINITY_DN1601	jgi|Blugr1|21240|BGHDH14_bgh03293	jgi|Blugra1|5540|BGT96224_E5993T0	jgi|Erynec1|1182|EV44_g0009T0	jgi|Golor2|1097308|CE1053929_13977
jgi|Golci1|1811228|fgenesh1_kg.3_#_482_#_TRINITY_DN5980	jgi|Blugr1|21238|BGHDH14_bgh03986	jgi|Blugra1|5541|BGT96224_E5924T0	jgi|Erynec1|1188|EV44_g0348T0	jgi|Golor2|1128132|CE1084753_4368
jgi|Golci1|1811230|fgenesh1_kg.3_#_484_#_TRINITY_DN1360	jgi|Blugr1|21231|BGHDH14_bgh06505	jgi|Blugra1|5549|BGT96224_3107T0	jgi|Erynec1|1227|EV44_g0104T0	jgi|Golor2|1134729|CE1091350_19869
jgi|Golci1|1811290|fgenesh1_kg.3_#_544_#_TRINITY_DN1838	jgi|Blugr1|21206|BGHDH14_bgh01362	jgi|Blugra1|5550|BGT96224_AcSP30282T0	jgi|Erynec1|1236|EV44_g0322T0	jgi|Golor2|1144947|CE1101568_210
jgi|Golci1|1811291|fgenesh1_kg.3_#_545_#_TRINITY_DN1970	jgi|Blugr1|21167|BGHDH14_bgh05144	jgi|Blugra1|5554|BGT96224_ASP20281T0	jgi|Erynec1|1292|EV44_g0468T0	jgi|Golor2|1152413|CE1109034_16
jgi|Golci1|1811313|fgenesh1_kg.3_#_567_#_TRINITY_DN1917	jgi|Blugr1|21159|BGHDH14_bghG004322000001001	jgi|Blugra1|5559|BGT96224_ASP20794T0	jgi|Erynec1|133|EV44_g0078T0	jgi|Golor2|1211497|CE1168118_111
jgi|Golci1|1811314|fgenesh1_kg.3_#_568_#_TRINITY_DN5958	jgi|Blugr1|21146|BGHDH14_bgh01237	jgi|Blugra1|5561|BGT96224_E5998T0	jgi|Erynec1|1340|EV44_g0540T0	jgi|Golor2|12934|gm4.12934_g
jgi|Golci1|1811324|fgenesh1_kg.3_#_578_#_TRINITY_DN1932	jgi|Blugr1|21117|BGHDH14_bgh04771	jgi|Blugra1|5566|BGT96224_E5872T0	jgi|Erynec1|1343|EV44_g0345T0	jgi|Golor2|1334857|CE1291478_6518
jgi|Golci1|1811327|fgenesh1_kg.3_#_581_#_TRINITY_DN1758	jgi|Blugr1|21109|BGHDH14_bgh04998	jgi|Blugra1|5570|BGT96224_3222T0	jgi|Erynec1|1405|EV44_g0537T0	jgi|Golor2|1342176|CE1298797_13848
jgi|Golci1|1811333|fgenesh1_kg.4_#_4_#_TRINITY_DN19575_	jgi|Blugr1|21108|BGHDH14_bghG004252000002001	jgi|Blugra1|5575|BGT96224_E10102T0	jgi|Erynec1|1421|EV44_g0014T0	jgi|Golor2|1344606|CE1301227_3070
jgi|Golci1|1811438|fgenesh1_kg.4_#_109_#_TRINITY_DN1853	jgi|Blugr1|21098|BGHDH14_bgh05195	jgi|Blugra1|5587|BGT96224_3240T0	jgi|Erynec1|1443|EV44_g0276T0	jgi|Golor2|13449|gm4.13449_g
jgi|Golci1|1811474|fgenesh1_kg.4_#_145_#_TRINITY_DN1276	jgi|Blugr1|21095|BGHDH14_bghG004239000001001	jgi|Blugra1|5593|BGT96224_E5936T0	jgi|Erynec1|1448|EV44_g0437T0	jgi|Golor2|13502|gm4.13502_g
jgi|Golci1|1811591|fgenesh1_kg.4_#_262_#_TRINITY_DN1096	jgi|Blugr1|21071|BGHDH14_bghG004221000001001	jgi|Blugra1|559|BGT96224_3481T0	jgi|Erynec1|1501|EV44_g0305T0	jgi|Golor2|1358472|CE1315093_2729
jgi|Golci1|1811600|fgenesh1_kg.4_#_271_#_TRINITY_DN1953	jgi|Blugr1|21066|BGHDH14_bghG004219000001001	jgi|Blugra1|55|BGT96224_4376T0	jgi|Erynec1|1511|EV44_g0425T0	jgi|Golor2|1379604|CE1336225_3260
jgi|Golci1|1811645|fgenesh1_kg.4_#_316_#_TRINITY_DN2580	jgi|Blugr1|21065|BGHDH14_bgh05281	jgi|Blugra1|5625|BGT96224_E5667T0	jgi|Erynec1|153|EV44_g0565T0	jgi|Golor2|1400643|CE1357264_19966
jgi|Golci1|1811657|fgenesh1_kg.4_#_328_#_TRINITY_DN2079	jgi|Blugr1|21062|BGHDH14_bghG004216000001001	jgi|Blugra1|5626|BGT96224_AcSP31411T0	jgi|Erynec1|1543|EV44_g0208T0	jgi|Golor2|1426835|CE1383456_50
jgi|Golci1|1811678|fgenesh1_kg.4_#_349_#_TRINITY_DN1797	jgi|Blugr1|21025|BGHDH14_bghG006760000001001	jgi|Blugra1|5627|BGT96224_E5664T0	jgi|Erynec1|1587|EV44_g0572T0	jgi|Golor2|1456249|CE1412870_15500
jgi|Golci1|1811709|fgenesh1_kg.4_#_380_#_TRINITY_DN1932	jgi|Blugr1|21018|BGHDH14_bgh00896	jgi|Blugra1|564|BGT96224_E5567T0	jgi|Erynec1|1639|EV44_g0332T0	jgi|Golor2|1473392|CE1430013_12

<table>
<tr><th>Gc</th><th>Bgh</th><th>Bgt</th><th>En</th><th>Go</th></tr>
<tr><td>jgi|Golci1|1811714|fgenesh1_kg.4_#_385_#_TRINITY_DN1932</td><td>jgi|Blugr1|20999|BGHDH14_bghG004983000002001</td><td>jgi|Blugra1|5655|BGT96224_4984T0</td><td>jgi|Erynec1|1644|EV44_g0127T0</td><td>jgi|Golor2|14865|gm4.14865_g</td></tr>
<tr><td>jgi|Golci1|1811771|fgenesh1_kg.4_#_442_#_TRINITY_DN1951</td><td>jgi|Blugr1|20997|BGHDH14_bgh02065</td><td>jgi|Blugra1|5697|BGT96224_1166T0</td><td>jgi|Erynec1|1647|EV44_g0551T0</td><td>jgi|Golor2|15422|gm4.15422_g</td></tr>
<tr><td>jgi|Golci1|1811800|fgenesh1_kg.4_#_471_#_TRINITY_DN6084</td><td>jgi|Blugr1|20973|BGHDH14_bgh05886</td><td>jgi|Blugra1|5725|BGT96224_E5653T0</td><td>jgi|Erynec1|1669|EV44_g0174T0</td><td>jgi|Golor2|155207|CE111828_31</td></tr>
<tr><td>jgi|Golci1|1811814|fgenesh1_kg.4_#_485_#_TRINITY_DN1816</td><td>jgi|Blugr1|20953|BGHDH14_bgh03962</td><td>jgi|Blugra1|5735|BGT96224_E5625T0</td><td>jgi|Erynec1|169|EV44_g0330T0</td><td>jgi|Golor2|1582311|CE1538932_9410</td></tr>
<tr><td>jgi|Golci1|1811819|fgenesh1_kg.4_#_490_#_TRINITY_DN1511</td><td>jgi|Blugr1|20932|BGHDH14_bghG004934000002001</td><td>jgi|Blugra1|5736|BGT96224_E5906T0</td><td>jgi|Erynec1|1713|EV44_g2331T0</td><td>jgi|Golor2|160610|CE117231_1849</td></tr>
<tr><td>jgi|Golci1|1811854|fgenesh1_kg.5_#_6_#_TRINITY_DN14063_</td><td>jgi|Blugr1|20931|BGHDH14_bgh00673</td><td>jgi|Blugra1|575|BGT96224_E5867T0</td><td>jgi|Erynec1|1730|EV44_g0415T0</td><td>jgi|Golor2|16886|gm4.16886_g</td></tr>
<tr><td>jgi|Golci1|1811858|fgenesh1_kg.5_#_10_#_TRINITY_DN17145</td><td>jgi|Blugr1|20930|BGHDH14_bgh04025</td><td>jgi|Blugra1|5762|BGT96224_AcSP31344T0</td><td>jgi|Erynec1|1749|EV44_g0082T0</td><td>jgi|Golor2|16958|gm4.16958_g</td></tr>
<tr><td>jgi|Golci1|1811880|fgenesh1_kg.5_#_32_#_TRINITY_DN16301</td><td>jgi|Blugr1|20928|BGHDH14_bghG004931000001001</td><td>jgi|Blugra1|5765|BGT96224_3809T0</td><td>jgi|Erynec1|1751|EV44_g0355T0</td><td>jgi|Golor2|1758586|CE1715207_130</td></tr>
<tr><td>jgi|Golci1|1811891|fgenesh1_kg.5_#_43_#_TRINITY_DN4903_</td><td>jgi|Blugr1|20878|BGHDH14_bghG004910000002001</td><td>jgi|Blugra1|5769|BGT96224_E5728T0</td><td>jgi|Erynec1|1752|EV44_g0591T0</td><td>jgi|Golor2|1833915|CE1790536_3334</td></tr>
<tr><td>jgi|Golci1|1811990|fgenesh1_kg.5_#_142_#_TRINITY_DN2715</td><td>jgi|Blugr1|25613|BGHDH14_bgh04082</td><td>jgi|Blugra1|5778|BGT96224_E5901T0</td><td>jgi|Erynec1|1785|EV44_g0120T0</td><td>jgi|Golor2|1847098|CE1803719_35</td></tr>
<tr><td>jgi|Golci1|1812023|fgenesh1_kg.5_#_175_#_TRINITY_DN1903</td><td>jgi|Blugr1|25612|BGHDH14_bgh05803</td><td>jgi|Blugra1|5789|BGT96224_AcSP31356T0</td><td>jgi|Erynec1|1825|EV44_g0130T0</td><td>jgi|Golor2|1861011|CE1817632_11511</td></tr>
<tr><td>jgi|Golci1|1812026|fgenesh1_kg.5_#_178_#_TRINITY_DN1689</td><td>jgi|Blugr1|25610|BGHDH14_bgh03695</td><td>jgi|Blugra1|5795|BGT96224_E5850T0</td><td>jgi|Erynec1|1888|EV44_g0301T0</td><td>jgi|Golor2|1868945|CE1825566_9174</td></tr>
<tr><td>jgi|Golci1|1812054|fgenesh1_kg.5_#_206_#_TRINITY_DN1932</td><td>jgi|Blugr1|25608|BGHDH14_bghG011456000001001</td><td>jgi|Blugra1|5797|BGT96224_4507T0</td><td>jgi|Erynec1|1899|EV44_g0352T0</td><td>jgi|Golor2|187528|CE144149_16188</td></tr>
<tr><td>jgi|Golci1|1812060|fgenesh1_kg.5_#_212_#_TRINITY_DN1932</td><td>jgi|Blugr1|25592|BGHDH14_bgh00034</td><td>jgi|Blugra1|5804|BGT96224_AcSP31373T0</td><td>jgi|Erynec1|189|EV44_g0181T0</td><td>jgi|Golor2|18866|gm4.18866_g</td></tr>
<tr><td>jgi|Golci1|1812163|fgenesh1_kg.5_#_315_#_TRINITY_DN1614</td><td>jgi|Blugr1|25588|BGHDH14_bgh02531</td><td>jgi|Blugra1|5807|BGT96224_848T0</td><td>jgi|Erynec1|18|EV44_g0086T0</td><td>jgi|Golor2|19307|gm4.19307_g</td></tr>
<tr><td>jgi|Golci1|1812245|fgenesh1_kg.5_#_397_#_TRINITY_DN9002</td><td>jgi|Blugr1|25574|BGHDH14_bgh00353</td><td>jgi|Blugra1|5826|BGT96224_E5990T0</td><td>jgi|Erynec1|1901|EV44_g0007T0</td><td>jgi|Golor2|1964933|CE1921554_25494</td></tr>
<tr><td>jgi|Golci1|1812316|fgenesh1_kg.5_#_468_#_TRINITY_DN1755</td><td>jgi|Blugr1|25544|BGHDH14_bgh02057</td><td>jgi|Blugra1|5828|BGT96224_ASP21390T0</td><td>jgi|Erynec1|1922|EV44_g0414T0</td><td>jgi|Golor2|1976834|CE1933455_632</td></tr>
<tr><td>jgi|Golci1|1812325|fgenesh1_kg.6_#_9_#_TRINITY_DN1331_c</td><td>jgi|Blugr1|25522|BGHDH14_bgh03706</td><td>jgi|Blugra1|5830|BGT96224_E5690T0</td><td>jgi|Erynec1|1925|EV44_g0233T0</td><td>jgi|Golor2|2011771|CE1968392_572</td></tr>
<tr><td>jgi|Golci1|1812487|fgenesh1_kg.6_#_171_#_TRINITY_DN1932</td><td>jgi|Blugr1|25516|BGHDH14_bghG000281000002001</td><td>jgi|Blugra1|5833|BGT96224_E5693T0</td><td>jgi|Erynec1|1933|EV44_g0595T0</td><td>jgi|Golor2|2014664|CE1971285_16355</td></tr>
<tr><td>jgi|Golci1|1812505|fgenesh1_kg.6_#_189_#_TRINITY_DN1137</td><td>jgi|Blugr1|25511|BGHDH14_bgh00773</td><td>jgi|Blugra1|5835|BGT96224_3194T0</td><td>jgi|Erynec1|1934|EV44_g0137T0</td><td>jgi|Golor2|2024408|CE1981029_4222</td></tr>
<tr><td>jgi|Golci1|1812514|fgenesh1_kg.6_#_198_#_TRINITY_DN1930</td><td>jgi|Blugr1|25508|BGHDH14_bghG000280000001001</td><td>jgi|Blugra1|5840|BGT96224_E5673T0</td><td>jgi|Erynec1|1960|EV44_g0356T0</td><td>jgi|Golor2|2115243|CE2071864_9318</td></tr>
</table>

Gc	Bgh	Bgt	En	Go
jgi|Golci1|1812539|fgenesh1_kg.6_#_223_#_TRINITY_DN1766	jgi|Blugr1|25470|BGHDH14_bgh06635	jgi|Blugra1|5846|BGT96224_E10003T0	jgi|Erynec1|1971|EV44_g0119T0	jgi|Golor2|2196081|CE2152702_4483
jgi|Golci1|1812653|fgenesh1_kg.6_#_337_#_TRINITY_DN1124	jgi|Blugr1|25468|BGHDH14_bgh03742	jgi|Blugra1|5849|BGT96224_E5820T0	jgi|Erynec1|1991|EV44_g0148T0	jgi|Golor2|2211938|CE2168559_198692
jgi|Golci1|1812735|fgenesh1_kg.6_#_419_#_TRINITY_DN1908	jgi|Blugr1|25462|BGHDH14_bgh03746	jgi|Blugra1|5850|BGT96224_E6034T0	jgi|Erynec1|2019|EV44_g0221T0	jgi|Golor2|2216701|CE2173322_14703
jgi|Golci1|1812760|fgenesh1_kg.6_#_444_#_TRINITY_DN1626	jgi|Blugr1|25453|BGHDH14_bgh03747	jgi|Blugra1|5864|BGT96224_E5754T0	jgi|Erynec1|202|EV44_g0448T0	jgi|Golor2|2273013|CE2229634_5661
jgi|Golci1|1812772|fgenesh1_kg.6_#_456_#_TRINITY_DN1427	jgi|Blugr1|25445|BGHDH14_bghG000207000002001	jgi|Blugra1|5867|BGT96224_E5974T0	jgi|Erynec1|2030|EV44_g0100T0	jgi|Golor2|2310198|CE2266819_9543
jgi|Golci1|1812791|fgenesh1_kg.6_#_475_#_TRINITY_DN1779	jgi|Blugr1|25444|BGHDH14_bghG000207000001001	jgi|Blugra1|5898|BGT96224_AcSP31400T0	jgi|Erynec1|2050|EV44_g0313T0	jgi|Golor2|2357526|CE2314147_186
jgi|Golci1|1812818|fgenesh1_kg.6_#_502_#_TRINITY_DN1437	jgi|Blugr1|25442|BGHDH14_bgh03749	jgi|Blugra1|5899|BGT96224_974T0	jgi|Erynec1|2064|EV44_g0519T0	jgi|Golor2|2363518|CE2320139_7091
jgi|Golci1|1812823|fgenesh1_kg.6_#_507_#_TRINITY_DN6654	jgi|Blugr1|25435|BGHDH14_bgh00693	jgi|Blugra1|5900|BGT96224_AcSP30411T0	jgi|Erynec1|2080|EV44_g0331T0	jgi|Golor2|2456219|CE2412840_146
jgi|Golci1|1812887|fgenesh1_kg.7_#_39_#_TRINITY_DN19367	jgi|Blugr1|25402|BGHDH14_bgh03744	jgi|Blugra1|5907|BGT96224_E5822T0	jgi|Erynec1|2081|EV44_g0443T0	jgi|Golor2|2457092|CE2413713_2657
jgi|Golci1|1812929|fgenesh1_kg.7_#_81_#_TRINITY_DN25097	jgi|Blugr1|25401|BGHDH14_bgh03459	jgi|Blugra1|5919|BGT96224_3593T0	jgi|Erynec1|2146|EV44_g0369T0	jgi|Golor2|246500|CE203121_322
jgi|Golci1|1812953|fgenesh1_kg.7_#_105_#_TRINITY_DN1438	jgi|Blugr1|25386|BGHDH14_bgh03443	jgi|Blugra1|5935|BGT96224_3484T0	jgi|Erynec1|2200|EV44_g0602T0	jgi|Golor2|2487786|CE2444407_119
jgi|Golci1|1813061|fgenesh1_kg.7_#_213_#_TRINITY_DN1578	jgi|Blugr1|25385|BGHDH14_bghG000122000001001	jgi|Blugra1|594|BGT96224_E5710T0	jgi|Erynec1|2213|EV44_g0205T0	jgi|Golor2|24931|gm4.24931_g
jgi|Golci1|1813120|fgenesh1_kg.7_#_272_#_TRINITY_DN1047	jgi|Blugr1|25382|BGHDH14_bghG000107000003001	jgi|Blugra1|595|BGT96224_E5713T0	jgi|Erynec1|2251|EV44_g0194T0	jgi|Golor2|25168|gm4.25168_g
jgi|Golci1|1813185|fgenesh1_kg.7_#_337_#_TRINITY_DN1920	jgi|Blugr1|25370|BGHDH14_bgh00843	jgi|Blugra1|5968|BGT96224_1946T0	jgi|Erynec1|2252|EV44_g0426T0	jgi|Golor2|2531858|CE2488479_830
jgi|Golci1|1813194|fgenesh1_kg.7_#_346_#_TRINITY_DN9616	jgi|Blugr1|25364|BGHDH14_bghG000103000002001	jgi|Blugra1|5982|BGT96224_E5600T0	jgi|Erynec1|2265|EV44_g0147T0	jgi|Golor2|2606300|CE2562921_8603
jgi|Golci1|1813197|fgenesh1_kg.7_#_349_#_TRINITY_DN1856	jgi|Blugr1|25363|BGHDH14_bgh00021	jgi|Blugra1|6000|BGT96224_E5721T0	jgi|Erynec1|227|EV44_g0133T0	jgi|Golor2|2674892|CE2631513_232
jgi|Golci1|1813221|fgenesh1_kg.7_#_373_#_TRINITY_DN2011	jgi|Blugr1|25349|BGHDH14_bgh00227	jgi|Blugra1|6002|BGT96224_E5701T0	jgi|Erynec1|2302|EV44_g0502T0	jgi|Golor2|2701140|CE2657761_105
jgi|Golci1|1813231|fgenesh1_kg.7_#_383_#_TRINITY_DN1018	jgi|Blugr1|25344|BGHDH14_bgh04209	jgi|Blugra1|6005|BGT96224_AcSP31429T0	jgi|Erynec1|2324|EV44_g0378T0	jgi|Golor2|2718593|CE2675214_4362
jgi|Golci1|1813260|fgenesh1_kg.7_#_412_#_TRINITY_DN5562	jgi|Blugr1|25333|BGHDH14_bghG000059000001001	jgi|Blugra1|6011|BGT96224_AcSP31430T0	jgi|Erynec1|2372|EV44_g0599T0	jgi|Golor2|28190|gm4.28190_g
jgi|Golci1|1813291|fgenesh1_kg.7_#_443_#_TRINITY_DN1305	jgi|Blugr1|25311|BGHDH14_bgh02080	jgi|Blugra1|6013|BGT96224_123T0	jgi|Erynec1|2375|EV44_g0575T0	jgi|Golor2|28715|gm4.28715_g
jgi|Golci1|1813310|fgenesh1_kg.7_#_462_#_TRINITY_DN1490	jgi|Blugr1|25299|BGHDH14_bghG000032000001001	jgi|Blugra1|6019|BGT96224_1694T0	jgi|Erynec1|237|EV44_g0152T0	jgi|Golor2|296044|CE252665_7144

Gc	Bgh	Bgt	En	Go
jgi|Golci1|1813322|fgenesh1_kg.7_#_474_#_TRINITY_DN2000	jgi|Blugr1|25294|BGHDH14_bghG000026000002001	jgi|Blugra1|6042|BGT96224_1611T0	jgi|Erynec1|2403|EV44_g0366T0	jgi|Golor2|30362|gm4.30362_g
jgi|Golci1|1813329|fgenesh1_kg.7_#_481_#_TRINITY_DN1765	jgi|Blugr1|25293|BGHDH14_bgh04206	jgi|Blugra1|6046|BGT96224_ASP21455T0	jgi|Erynec1|2412|EV44_g0178T0	jgi|Golor2|343951|CE300572_3457
jgi|Golci1|1813332|fgenesh1_kg.8_#_1_#_TRINITY_DN14936_	jgi|Blugr1|25292|BGHDH14_bghG000026000001001	jgi|Blugra1|6054|BGT96224_BCG6T0	jgi|Erynec1|2442|EV44_g0484T0	jgi|Golor2|365352|CE321973_6279
jgi|Golci1|1813410|fgenesh1_kg.8_#_79_#_TRINITY_DN17420	jgi|Blugr1|25290|BGHDH14_bghG000024000001001	jgi|Blugra1|6055|BGT96224_ASP20978T0	jgi|Erynec1|2444|EV44_g0052T0	jgi|Golor2|36947|gm4.36947_g
jgi|Golci1|1813447|fgenesh1_kg.8_#_116_#_TRINITY_DN1248	jgi|Blugr1|25283|BGHDH14_bghG000012000002001	jgi|Blugra1|6061|BGT96224_2700T0	jgi|Erynec1|2466|EV44_g0274T0	jgi|Golor2|37474|gm4.37474_g
jgi|Golci1|1813479|fgenesh1_kg.8_#_148_#_TRINITY_DN1953	jgi|Blugr1|25275|BGHDH14_bgh00763	jgi|Blugra1|6066|BGT96224_2775T0	jgi|Erynec1|2504|EV44_g0567T0	jgi|Golor2|37702|gm4.37702_g
jgi|Golci1|1813570|fgenesh1_kg.8_#_239_#_TRINITY_DN9112	jgi|Blugr1|25228|BGHDH14_bghG005233000001001	jgi|Blugra1|6076|BGT96224_1691T0	jgi|Erynec1|2510|EV44_g0295T0	jgi|Golor2|389091|CE345712_19534
jgi|Golci1|1813599|fgenesh1_kg.8_#_268_#_TRINITY_DN1982	jgi|Blugr1|25213|BGHDH14_bgh04134	jgi|Blugra1|6081|BGT96224_E5816T0	jgi|Erynec1|2519|EV44_g0523T0	jgi|Golor2|3903|gm4.3903_g
jgi|Golci1|1813604|fgenesh1_kg.8_#_273_#_TRINITY_DN1091	jgi|Blugr1|25201|BGHDH14_bgh05085	jgi|Blugra1|6092|BGT96224_1828T0	jgi|Erynec1|2562|EV44_g0234T0	jgi|Golor2|3933|gm4.3933_g
jgi|Golci1|1813651|fgenesh1_kg.9_#_15_#_TRINITY_DN13887	jgi|Blugr1|25192|BGHDH14_bgh05154	jgi|Blugra1|6121|BGT96224_2599T0	jgi|Erynec1|2619|EV44_g0254T0	jgi|Golor2|3958|gm4.3958_g
jgi|Golci1|1813686|fgenesh1_kg.9_#_50_#_TRINITY_DN15098	jgi|Blugr1|25186|BGHDH14_bgh01263	jgi|Blugra1|6174|BGT96224_E5966T0	jgi|Erynec1|2628|EV44_g0447T0	jgi|Golor2|39603|gm4.39603_g
jgi|Golci1|1813697|fgenesh1_kg.9_#_61_#_TRINITY_DN10177	jgi|Blugr1|25164|BGHDH14_bgh02116	jgi|Blugra1|6178|BGT96224_ASP21056T0	jgi|Erynec1|2642|EV44_g0485T0	jgi|Golor2|4042552|gw1.37.111.1
jgi|Golci1|1813698|fgenesh1_kg.9_#_62_#_TRINITY_DN6913_	jgi|Blugr1|25153|BGHDH14_bgh00429	jgi|Blugra1|617|BGT96224_385T0	jgi|Erynec1|2657|EV44_g0304T0	jgi|Golor2|4062083|gw1.105.176.1
jgi|Golci1|1813702|fgenesh1_kg.9_#_66_#_TRINITY_DN14619	jgi|Blugr1|25148|BGHDH14_bgh00240	jgi|Blugra1|6206|BGT96224_E5570T0	jgi|Erynec1|267|EV44_g0500T0	jgi|Golor2|40714|gm4.40714_g
jgi|Golci1|1813803|fgenesh1_kg.9_#_167_#_TRINITY_DN1869	jgi|Blugr1|25145|BGHDH14_bghG006060000001001	jgi|Blugra1|6207|BGT96224_2846T0	jgi|Erynec1|269|EV44_g0431T0	jgi|Golor2|4087852|gw1.24.443.1
jgi|Golci1|1813843|fgenesh1_kg.9_#_207_#_TRINITY_DN1859	jgi|Blugr1|25144|BGHDH14_bghG006049000001001	jgi|Blugra1|6215|BGT96224_ASP21508T0	jgi|Erynec1|2702|EV44_g0585T0	jgi|Golor2|4152597|gw1.1.2549.1
jgi|Golci1|1813876|fgenesh1_kg.9_#_240_#_TRINITY_DN1932	jgi|Blugr1|25140|BGHDH14_bgh00413	jgi|Blugra1|6222|BGT96224_E5675T0	jgi|Erynec1|2706|EV44_g0004T0	jgi|Golor2|4173372|gw1.1.2905.1
jgi|Golci1|1813882|fgenesh1_kg.9_#_246_#_TRINITY_DN1932	jgi|Blugr1|25131|BGHDH14_bgh03625	jgi|Blugra1|6226|BGT96224_E40006T0	jgi|Erynec1|2752|EV44_g0464T0	jgi|Golor2|41914|gm4.41914_g
jgi|Golci1|1813929|fgenesh1_kg.9_#_293_#_TRINITY_DN2107	jgi|Blugr1|25115|BGHDH14_bgh03452	jgi|Blugra1|6228|BGT96224_BCG7T0	jgi|Erynec1|2807|EV44_g0218T0	jgi|Golor2|420515|CE377136_17003
jgi|Golci1|1813993|fgenesh1_kg.9_#_357_#_TRINITY_DN1875	jgi|Blugr1|25114|BGHDH14_bghG006029000001001	jgi|Blugra1|6241|BGT96224_BCG1T0	jgi|Erynec1|2844|EV44_g0317T0	jgi|Golor2|4207247|gw1.197.314.1
jgi|Golci1|1814044|fgenesh1_kg.9_#_408_#_TRINITY_DN1930	jgi|Blugr1|25113|BGHDH14_bghG006028000001001	jgi|Blugra1|6247|BGT96224_ASP20484T0	jgi|Erynec1|2860|EV44_g0018T0	jgi|Golor2|4210000|gw1.17.1541.1

Gc	Bgh	Bgt	En	Go
jgi|Golci1|1814045|fgenesh1_kg.9_#_409_#_TRINITY_DN1497	jgi|Blugr1|25110|BGHDH14_bghG006021000001001	jgi|Blugra1|6272|BGT96224_2440T0	jgi|Erynec1|2863|EV44_g0044T0	jgi|Golor2|422356|CE378977_6406
jgi|Golci1|1814300|fgenesh1_kg.10_#_241_#_TRINITY_DN146	jgi|Blugr1|25085|BGHDH14_bgh06230	jgi|Blugra1|6293|BGT96224_E5889T0	jgi|Erynec1|2884|EV44_g0237T0	jgi|Golor2|42264|gm4.42264_g
jgi|Golci1|1814316|fgenesh1_kg.10_#_257_#_TRINITY_DN157	jgi|Blugr1|25083|BGHDH14_bghG006299000001001	jgi|Blugra1|6301|BGT96224_E5912T0	jgi|Erynec1|2943|EV44_g0071T0	jgi|Golor2|423555|CE380176_87023
jgi|Golci1|1814326|fgenesh1_kg.10_#_267_#_TRINITY_DN148	jgi|Blugr1|25082|BGHDH14_bgh03818	jgi|Blugra1|6308|BGT96224_1257T0	jgi|Erynec1|295|EV44_g0185T0	jgi|Golor2|4238170|e_gw1.1.722.1
jgi|Golci1|1814346|fgenesh1_kg.11_#_19_#_TRINITY_DN1651	jgi|Blugr1|25081|BGHDH14_bghG006297000001001	jgi|Blugra1|6317|BGT96224_E5550T0	jgi|Erynec1|2992|EV44_g0528T0	jgi|Golor2|4240845|e_gw1.3.1431.1
jgi|Golci1|1814349|fgenesh1_kg.11_#_22_#_TRINITY_DN1174	jgi|Blugr1|25080|BGHDH14_bghG006289000001001	jgi|Blugra1|6320|BGT96224_E10120T0	jgi|Erynec1|2999|EV44_g0101T0	jgi|Golor2|4241060|e_gw1.3.1521.1
jgi|Golci1|1814366|fgenesh1_kg.11_#_39_#_TRINITY_DN1930	jgi|Blugr1|25079|BGHDH14_bghG006278000001001	jgi|Blugra1|6331|BGT96224_3765T0	jgi|Erynec1|3001|EV44_g0552T0	jgi|Golor2|4241368|e_gw1.3.722.1
jgi|Golci1|1814367|fgenesh1_kg.11_#_40_#_TRINITY_DN1819	jgi|Blugr1|25075|BGHDH14_bghG006273000001001	jgi|Blugra1|6338|BGT96224_5370T0	jgi|Erynec1|3007|EV44_g0583T0	jgi|Golor2|4241957|e_gw1.4.1399.1
jgi|Golci1|1814397|fgenesh1_kg.11_#_70_#_TRINITY_DN8644	jgi|Blugr1|25073|BGHDH14_bgh06951	jgi|Blugra1|6344|BGT96224_3684T0	jgi|Erynec1|3021|EV44_g0065T0	jgi|Golor2|4243857|e_gw1.5.1569.1
jgi|Golci1|1814408|fgenesh1_kg.11_#_81_#_TRINITY_DN2004	jgi|Blugr1|25072|BGHDH14_bgh04105	jgi|Blugra1|6371|BGT96224_E3419T0	jgi|Erynec1|3035|EV44_g0536T0	jgi|Golor2|4244020|e_gw1.5.1536.1
jgi|Golci1|1814547|fgenesh1_kg.11_#_220_#_TRINITY_DN170	jgi|Blugr1|25070|BGHDH14_bgh04343	jgi|Blugra1|637|BGT96224_E5607T0	jgi|Erynec1|3046|EV44_g0463T0	jgi|Golor2|4244566|e_gw1.6.827.1
jgi|Golci1|1814600|fgenesh1_kg.11_#_273_#_TRINITY_DN653	jgi|Blugr1|25062|BGHDH14_bgh06546	jgi|Blugra1|6388|BGT96224_3979T0	jgi|Erynec1|3054|EV44_g0582T0	jgi|Golor2|4245519|e_gw1.6.760.1
jgi|Golci1|1814604|fgenesh1_kg.11_#_277_#_TRINITY_DN181	jgi|Blugr1|25058|BGHDH14_bgh04130	jgi|Blugra1|640|BGT96224_5608T0	jgi|Erynec1|3059|EV44_g0544T0	jgi|Golor2|4246892|e_gw1.8.1524.1
jgi|Golci1|1814618|fgenesh1_kg.11_#_291_#_TRINITY_DN188	jgi|Blugr1|25055|BGHDH14_bgh02875	jgi|Blugra1|6473|BGT96224_E5981T0	jgi|Erynec1|3081|EV44_g0282T0	jgi|Golor2|4246948|e_gw1.8.663.1
jgi|Golci1|1814645|fgenesh1_kg.11_#_318_#_TRINITY_DN209	jgi|Blugr1|25053|BGHDH14_bgh03277	jgi|Blugra1|649|BGT96224_AcSP30305T0	jgi|Erynec1|3098|EV44_g0169T0	jgi|Golor2|4247566|e_gw1.8.1974.1
jgi|Golci1|1814663|fgenesh1_kg.11_#_336_#_TRINITY_DN594	jgi|Blugr1|25051|BGHDH14_bgh03273	jgi|Blugra1|6504|BGT96224_2053T0	jgi|Erynec1|3099|EV44_g0329T0	jgi|Golor2|4248106|e_gw1.9.56.1
jgi|Golci1|1814676|fgenesh1_kg.11_#_349_#_TRINITY_DN466	jgi|Blugr1|25050|BGHDH14_bgh03275	jgi|Blugra1|661|BGT96224_4961T0	jgi|Erynec1|3115|EV44_g0126T0	jgi|Golor2|4249866|e_gw1.10.1182.1
jgi|Golci1|1814712|fgenesh1_kg.12_#_15_#_TRINITY_DN1932	jgi|Blugr1|25043|BGHDH14_bgh03650	jgi|Blugra1|673|BGT96224_3534T0	jgi|Erynec1|3117|EV44_g0136T0	jgi|Golor2|4249978|e_gw1.10.568.1
jgi|Golci1|1814717|fgenesh1_kg.12_#_20_#_TRINITY_DN1932	jgi|Blugr1|25041|BGHDH14_bgh01420	jgi|Blugra1|687|BGT96224_1362T0	jgi|Erynec1|3146|EV44_g0433T0	jgi|Golor2|4251885|e_gw1.12.161.1
jgi|Golci1|1814745|fgenesh1_kg.12_#_48_#_TRINITY_DN3029	jgi|Blugr1|25030|BGHDH14_bghG001082000003001	jgi|Blugra1|688|BGT96224_E5818T0	jgi|Erynec1|3159|EV44_g0215T0	jgi|Golor2|4253923|e_gw1.15.454.1
jgi|Golci1|1814776|fgenesh1_kg.12_#_79_#_TRINITY_DN1544	jgi|Blugr1|25029|BGHDH14_bghG001082000002001	jgi|Blugra1|696|BGT96224_2525T0	jgi|Erynec1|3212|EV44_g0578T0	jgi|Golor2|4254214|e_gw1.15.476.1

Gc	Bgh	Bgt	En	Go
jgi|Golci1|1814833|fgenesh1_kg.12_#_136_#_TRINITY_DN176	jgi|Blugr1|25022|BGHDH14_bgh04352	jgi|Blugra1|710|BGT96224_1573T0	jgi|Erynec1|3219|EV44_g0293T0	jgi|Golor2|4255070|e_gw1.16.1229.1
jgi|Golci1|1814840|fgenesh1_kg.12_#_143_#_TRINITY_DN184	jgi|Blugr1|25016|BGHDH14_bghG001078000001001	jgi|Blugra1|727|BGT96224_E5717T0	jgi|Erynec1|321|EV44_g0150T0	jgi|Golor2|4256316|e_gw1.18.939.1
jgi|Golci1|1814870|fgenesh1_kg.12_#_173_#_TRINITY_DN120	jgi|Blugr1|25014|BGHDH14_bghG001077000001001	jgi|Blugra1|733|BGT96224_AcSP30729T0	jgi|Erynec1|3258|EV44_g0153T0	jgi|Golor2|4256428|e_gw1.18.185.1
jgi|Golci1|1814908|fgenesh1_kg.12_#_211_#_TRINITY_DN171	jgi|Blugr1|24978|BGHDH14_bgh04277	jgi|Blugra1|742|BGT96224_AcSP30730T0	jgi|Erynec1|3271|EV44_g0314T0	jgi|Golor2|4257895|e_gw1.20.173.1
jgi|Golci1|1814966|fgenesh1_kg.12_#_269_#_TRINITY_DN541	jgi|Blugr1|24976|BGHDH14_bgh03765	jgi|Blugra1|743|BGT96224_5168T0	jgi|Erynec1|3287|EV44_g0600T0	jgi|Golor2|4259517|e_gw1.22.482.1
jgi|Golci1|1815040|fgenesh1_kg.12_#_343_#_TRINITY_DN192	jgi|Blugr1|24951|BGHDH14_bghG001016000001001	jgi|Blugra1|757|BGT96224_1711T0	jgi|Erynec1|3302|EV44_g0401T0	jgi|Golor2|4260419|e_gw1.23.677.1
jgi|Golci1|1815079|fgenesh1_kg.12_#_382_#_TRINITY_DN181	jgi|Blugr1|24922|BGHDH14_bgh04920	jgi|Blugra1|776|BGT96224_E10132T0	jgi|Erynec1|3309|EV44_g0132T0	jgi|Golor2|4260459|e_gw1.23.667.1
jgi|Golci1|1815209|fgenesh1_kg.13_#_66_#_TRINITY_DN1368	jgi|Blugr1|24896|BGHDH14_bgh00473	jgi|Blugra1|811|BGT96224_1300T0	jgi|Erynec1|3370|EV44_g0590T0	jgi|Golor2|4266151|e_gw1.31.304.1
jgi|Golci1|1815227|fgenesh1_kg.13_#_84_#_TRINITY_DN1780	jgi|Blugr1|24878|BGHDH14_bgh00770	jgi|Blugra1|815|BGT96224_AcSP31310T0	jgi|Erynec1|3372|EV44_g0436T0	jgi|Golor2|4268365|e_gw1.35.342.1
jgi|Golci1|1815252|fgenesh1_kg.13_#_109_#_TRINITY_DN209	jgi|Blugr1|24876|BGHDH14_bgh06673	jgi|Blugra1|819|BGT96224_ASP20100T0	jgi|Erynec1|3377|EV44_g0036T0	jgi|Golor2|4268766|e_gw1.36.210.1
jgi|Golci1|1815350|fgenesh1_kg.13_#_207_#_TRINITY_DN152	jgi|Blugr1|24870|BGHDH14_bgh04817	jgi|Blugra1|832|BGT96224_5324T0	jgi|Erynec1|3386|EV44_g0518T0	jgi|Golor2|4268955|e_gw1.36.607.1
jgi|Golci1|1815378|fgenesh1_kg.13_#_235_#_TRINITY_DN207	jgi|Blugr1|24845|BGHDH14_bghG000925000001001	jgi|Blugra1|844|BGT96224_E5829T0	jgi|Erynec1|3422|EV44_g0003T0	jgi|Golor2|4269205|e_gw1.36.1073.1
jgi|Golci1|1815403|fgenesh1_kg.13_#_260_#_TRINITY_DN202	jgi|Blugr1|24843|BGHDH14_bghG000924000001001	jgi|Blugra1|855|BGT96224_4990T0	jgi|Erynec1|3446|EV44_g0344T0	jgi|Golor2|4269220|e_gw1.36.342.1
jgi|Golci1|1815416|fgenesh1_kg.14_#_5_#_TRINITY_DN18093	jgi|Blugr1|24838|BGHDH14_bghG000918000003001	jgi|Blugra1|879|BGT96224_E5639T0	jgi|Erynec1|3457|EV44_g0219T0	jgi|Golor2|426930|CE383551_11476
jgi|Golci1|1815595|fgenesh1_kg.14_#_184_#_TRINITY_DN199	jgi|Blugr1|24837|BGHDH14_bgh01194	jgi|Blugra1|881|BGT96224_1032T0	jgi|Erynec1|345|EV44_g0192T0	jgi|Golor2|4270499|e_gw1.38.1020.1
jgi|Golci1|1815600|fgenesh1_kg.14_#_189_#_TRINITY_DN199	jgi|Blugr1|24835|BGHDH14_bghG000898000005001	jgi|Blugra1|90|BGT96224_E10104T0	jgi|Erynec1|3471|EV44_g0312T0	jgi|Golor2|4270579|e_gw1.39.130.1
jgi|Golci1|1815605|fgenesh1_kg.14_#_194_#_TRINITY_DN190	jgi|Blugr1|24833|BGHDH14_bgh05143	jgi|Blugra1|948|BGT96224_2806T0	jgi|Erynec1|3475|EV44_g0403T0	jgi|Golor2|4270647|e_gw1.39.167.1
jgi|Golci1|1815608|fgenesh1_kg.14_#_197_#_TRINITY_DN199	jgi|Blugr1|24830|BGHDH14_bgh01044	jgi|Blugra1|955|BGT96224_AcSP30002T0	jgi|Erynec1|3480|EV44_g0165T0	jgi|Golor2|4271700|e_gw1.40.266.1
jgi|Golci1|1815611|fgenesh1_kg.14_#_200_#_TRINITY_DN199	jgi|Blugr1|24829|BGHDH14_bgh00065	jgi|Blugra1|956|BGT96224_E3893T0	jgi|Erynec1|3525|EV44_g0579T0	
jgi|Golci1|1815628|fgenesh1_kg.14_#_217_#_TRINITY_DN211	jgi|Blugr1|24828|BGHDH14_bgh01043	jgi|Blugra1|977|BGT96224_E10127T0	jgi|Erynec1|3550|EV44_g0145T0	
jgi|Golci1|1815652|fgenesh1_kg.14_#_241_#_TRINITY_DN199	jgi|Blugr1|24827|BGHDH14_bghG000860000001001	jgi|Blugra1|97|BGT96224_AcSP31216T0	jgi|Erynec1|3574|EV44_g0157T0	

Gc	Bgh	Bgt	En	Go
jgi|Golci1|1815655|fgenesh1_kg.14_#_244_#_TRINITY_DN207	jgi|Blugr1|24824|BGHDH14_bgh06766	jgi|Blugra1|987|BGT96224_31T0	jgi|Erynec1|3575|EV44_g0243T0	
jgi|Golci1|1815682|fgenesh1_kg.14_#_271_#_TRINITY_DN197	jgi|Blugr1|24823|BGHDH14_bgh01007	jgi|Blugra1|999|BGT96224_3269T0	jgi|Erynec1|3600|EV44_g0554T0	
jgi|Golci1|1815744|fgenesh1_kg.15_#_16_#_TRINITY_DN7387	jgi|Blugr1|24821|BGHDH14_bghG000833000001001	jgi|Blugra1|1008|BGT96224_1964T0	jgi|Erynec1|3611|EV44_g0196T0	
jgi|Golci1|1815788|fgenesh1_kg.15_#_60_#_TRINITY_DN2030	jgi|Blugr1|24820|BGHDH14_bgh00044	jgi|Blugra1|1023|BGT96224_4070T0	jgi|Erynec1|3648|EV44_g0539T0	
jgi|Golci1|1815917|fgenesh1_kg.15_#_189_#_TRINITY_DN176	jgi|Blugr1|24819|BGHDH14_bgh01193	jgi|Blugra1|1031|BGT96224_E5632T0	jgi|Erynec1|3671|EV44_g0407T0	
jgi|Golci1|1815920|fgenesh1_kg.15_#_192_#_TRINITY_DN176	jgi|Blugr1|24818|BGHDH14_bgh06734	jgi|Blugra1|103|BGT96224_4280T0	jgi|Erynec1|369|EV44_g0481T0	
jgi|Golci1|1815930|fgenesh1_kg.15_#_202_#_TRINITY_DN176	jgi|Blugr1|24816|BGHDH14_bgh00014	jgi|Blugra1|1045|BGT96224_489T0	jgi|Erynec1|372|EV44_g0387T0	
jgi|Golci1|1815933|fgenesh1_kg.15_#_205_#_TRINITY_DN176	jgi|Blugr1|24813|BGHDH14_bgh01006	jgi|Blugra1|1049|BGT96224_1259T0	jgi|Erynec1|3738|EV44_g0418T0	
jgi|Golci1|1816031|fgenesh1_kg.16_#_47_#_TRINITY_DN1727	jgi|Blugr1|24811|BGHDH14_bghG000801000001001	jgi|Blugra1|104|BGT96224_BCG4T0	jgi|Erynec1|3744|EV44_g0541T0	
jgi|Golci1|1816038|fgenesh1_kg.16_#_54_#_TRINITY_DN2007	jgi|Blugr1|24809|BGHDH14_bghG000799000001001	jgi|Blugra1|1057|BGT96224_40012T0	jgi|Erynec1|3745|EV44_g0604T0	
jgi|Golci1|1816103|fgenesh1_kg.16_#_119_#_TRINITY_DN121	jgi|Blugr1|24808|BGHDH14_bghG000792000001001	jgi|Blugra1|1058|BGT96224_AcSP31098T0		
jgi|Golci1|1816129|fgenesh1_kg.16_#_145_#_TRINITY_DN178	jgi|Blugr1|24807|BGHDH14_bgh01055	jgi|Blugra1|1066|BGT96224_E5686T0		
jgi|Golci1|1816137|fgenesh1_kg.16_#_153_#_TRINITY_DN178	jgi|Blugr1|24806|BGHDH14_bghG000778000001001	jgi|Blugra1|1067|BGT96224_E5685T0		
jgi|Golci1|1816265|fgenesh1_kg.17_#_6_#_TRINITY_DN19233	jgi|Blugr1|24805|BGHDH14_bghG000776000001001	jgi|Blugra1|107|BGT96224_E10109T0		
jgi|Golci1|1816348|fgenesh1_kg.17_#_89_#_TRINITY_DN1539	jgi|Blugr1|24803|BGHDH14_bghG000775000001001	jgi|Blugra1|1108|BGT96224_E10101T0		
jgi|Golci1|1816485|fgenesh1_kg.17_#_226_#_TRINITY_DN305	jgi|Blugr1|24798|BGHDH14_bgh00209	jgi|Blugra1|1141|BGT96224_3807T0		
jgi|Golci1|1816508|fgenesh1_kg.17_#_249_#_TRINITY_DN133	jgi|Blugr1|24788|BGHDH14_bghG000770000002001	jgi|Blugra1|1146|BGT96224_450T0		
jgi|Golci1|1816571|fgenesh1_kg.18_#_41_#_TRINITY_DN1923	jgi|Blugr1|24784|BGHDH14_bgh00303	jgi|Blugra1|1147|BGT96224_4375T0		
jgi|Golci1|1816801|fgenesh1_kg.18_#_271_#_TRINITY_DN504	jgi|Blugr1|24757|BGHDH14_bgh05108	jgi|Blugra1|1149|BGT96224_33BT0		
jgi|Golci1|1816866|fgenesh1_kg.19_#_11_#_TRINITY_DN1875	jgi|Blugr1|24750|BGHDH14_bgh02963	jgi|Blugra1|1160|BGT96224_ASP21173T0		
jgi|Golci1|1816870|fgenesh1_kg.19_#_15_#_TRINITY_DN1875	jgi|Blugr1|24738|BGHDH14_bghG000733000001001	jgi|Blugra1|1172|BGT96224_5431T0		

<table>
<tr><th>Gc</th><th>Bgh</th><th>Bgt</th><th>En</th><th>Go</th></tr>
<tr><td>jgi|Golci1|1816877|fgenesh1_kg.19_#_22_#_TRINITY_DN2828</td><td>jgi|Blugr1|24736|BGHDH14_bgh04942</td><td>jgi|Blugra1|1188|BGT96224_E5980T0</td><td></td><td></td></tr>
<tr><td>jgi|Golci1|1816886|fgenesh1_kg.19_#_31_#_TRINITY_DN1599</td><td>jgi|Blugr1|24729|BGHDH14_bgh03113</td><td>jgi|Blugra1|1193|BGT96224_AcSP30107T0</td><td></td><td></td></tr>
<tr><td>jgi|Golci1|1816942|fgenesh1_kg.19_#_87_#_TRINITY_DN1696</td><td>jgi|Blugr1|24725|BGHDH14_bgh03103</td><td>jgi|Blugra1|1201|BGT96224_E5777T0</td><td></td><td></td></tr>
<tr><td>jgi|Golci1|1817059|fgenesh1_kg.19_#_204_#_TRINITY_DN157</td><td>jgi|Blugr1|24721|BGHDH14_bgh01928</td><td>jgi|Blugra1|1211|BGT96224_E40000T0</td><td></td><td></td></tr>
<tr><td>jgi|Golci1|1817080|fgenesh1_kg.19_#_225_#_TRINITY_DN696</td><td>jgi|Blugr1|24719|BGHDH14_bghG000714000001001</td><td>jgi|Blugra1|1230|BGT96224_AcSP30749T0</td><td></td><td></td></tr>
<tr><td>jgi|Golci1|1817113|fgenesh1_kg.19_#_258_#_TRINITY_DN179</td><td>jgi|Blugr1|24709|BGHDH14_bgh03067</td><td>jgi|Blugra1|1231|BGT96224_AcSP31145T0</td><td></td><td></td></tr>
<tr><td>jgi|Golci1|1817180|fgenesh1_kg.20_#_58_#_TRINITY_DN1888</td><td>jgi|Blugr1|24671|BGHDH14_bgh05315</td><td>jgi|Blugra1|1235|BGT96224_2778T0</td><td></td><td></td></tr>
<tr><td>jgi|Golci1|1817218|fgenesh1_kg.20_#_96_#_TRINITY_DN2042</td><td>jgi|Blugr1|24659|BGHDH14_bghG000684000001001</td><td>jgi|Blugra1|123|BGT96224_E40011T0</td><td></td><td></td></tr>
<tr><td>jgi|Golci1|1817224|fgenesh1_kg.20_#_102_#_TRINITY_DN303</td><td>jgi|Blugr1|24656|BGHDH14_bghG000684000003001</td><td>jgi|Blugra1|1249|BGT96224_2900BT0</td><td></td><td></td></tr>
<tr><td>jgi|Golci1|1817334|fgenesh1_kg.20_#_212_#_TRINITY_DN192</td><td>jgi|Blugr1|24654|BGHDH14_bgh01923</td><td>jgi|Blugra1|124|BGT96224_E10121T0</td><td></td><td></td></tr>
<tr><td>jgi|Golci1|1817353|fgenesh1_kg.20_#_231_#_TRINITY_DN676</td><td>jgi|Blugr1|24637|BGHDH14_bghG000673000001001</td><td>jgi|Blugra1|1251|BGT96224_57BT0</td><td></td><td></td></tr>
<tr><td>jgi|Golci1|1817364|fgenesh1_kg.20_#_242_#_TRINITY_DN209</td><td>jgi|Blugr1|24625|BGHDH14_bghG000653000001001</td><td>jgi|Blugra1|1265|BGT96224_2970T0</td><td></td><td></td></tr>
<tr><td>jgi|Golci1|1817377|fgenesh1_kg.20_#_255_#_TRINITY_DN917</td><td>jgi|Blugr1|24611|BGHDH14_bgh01048</td><td>jgi|Blugra1|1266|BGT96224_4702T0</td><td></td><td></td></tr>
<tr><td>jgi|Golci1|1817397|fgenesh1_kg.20_#_275_#_TRINITY_DN277</td><td>jgi|Blugr1|24605|BGHDH14_bgh05956</td><td>jgi|Blugra1|1269|BGT96224_AcSP30152T0</td><td></td><td></td></tr>
<tr><td>jgi|Golci1|1817510|fgenesh1_kg.21_#_90_#_TRINITY_DN1460</td><td>jgi|Blugr1|24596|BGHDH14_bghG000619000001001</td><td>jgi|Blugra1|1307|BGT96224_E5723T0</td><td></td><td></td></tr>
<tr><td>jgi|Golci1|1817600|fgenesh1_kg.21_#_180_#_TRINITY_DN109</td><td>jgi|Blugr1|24572|BGHDH14_bghG000602000001001</td><td>jgi|Blugra1|1308|BGT96224_1212T0</td><td></td><td></td></tr>
<tr><td>jgi|Golci1|1817609|fgenesh1_kg.21_#_189_#_TRINITY_DN111</td><td>jgi|Blugr1|24569|BGHDH14_bgh05755</td><td>jgi|Blugra1|1309|BGT96224_E5724T0</td><td></td><td></td></tr>
<tr><td>jgi|Golci1|1817661|fgenesh1_kg.21_#_241_#_TRINITY_DN116</td><td>jgi|Blugr1|24565|BGHDH14_bgh04226</td><td>jgi|Blugra1|1312|BGT96224_E5722T0</td><td></td><td></td></tr>
<tr><td>jgi|Golci1|1817713|fgenesh1_kg.21_#_293_#_TRINITY_DN166</td><td>jgi|Blugr1|24526|BGHDH14_bghG000556000001001</td><td>jgi|Blugra1|1314|BGT96224_E5591T0</td><td></td><td></td></tr>
<tr><td>jgi|Golci1|1817728|fgenesh1_kg.22_#_9_#_TRINITY_DN19289</td><td>jgi|Blugr1|24494|BGHDH14_bgh04885</td><td>jgi|Blugra1|1326|BGT96224_1289T0</td><td></td><td></td></tr>
<tr><td>jgi|Golci1|1817765|fgenesh1_kg.22_#_46_#_TRINITY_DN1856</td><td>jgi|Blugr1|24484|BGHDH14_bgh04794</td><td>jgi|Blugra1|132|BGT96224_1850T0</td><td></td><td></td></tr>
</table>

Gc	Bgh	Bgt	En	Go
jgi|Golci1|1817767|fgenesh1_kg.22_#_48_#_TRINITY_DN2099	jgi|Blugr1|24462|BGHDH14_bgh02536	jgi|Blugra1|1330|BGT96224_E5731T0		
jgi|Golci1|1817793|fgenesh1_kg.22_#_74_#_TRINITY_DN1718	jgi|Blugr1|24461|BGHDH14_bghG000481000001001	jgi|Blugra1|1338|BGT96224_AcSP30530T0		
jgi|Golci1|1817797|fgenesh1_kg.22_#_78_#_TRINITY_DN1653	jgi|Blugr1|24457|BGHDH14_bgh00494	jgi|Blugra1|1346|BGT96224_3894T0		
jgi|Golci1|1817840|fgenesh1_kg.22_#_121_#_TRINITY_DN212	jgi|Blugr1|24440|BGHDH14_bgh03531	jgi|Blugra1|1358|BGT96224_ASP20145T0		
jgi|Golci1|1817931|fgenesh1_kg.22_#_212_#_TRINITY_DN141	jgi|Blugr1|24435|BGHDH14_bghG000464000001001	jgi|Blugra1|1375|BGT96224_2940T0		
jgi|Golci1|1817979|fgenesh1_kg.22_#_260_#_TRINITY_DN720	jgi|Blugr1|24423|BGHDH14_bghG000458000002001	jgi|Blugra1|1392|BGT96224_E5564T0		
jgi|Golci1|1818050|fgenesh1_kg.23_#_39_#_TRINITY_DN1536	jgi|Blugr1|24422|BGHDH14_bghG000457000001001	jgi|Blugra1|1419|BGT96224_2143T0		
jgi|Golci1|1818095|fgenesh1_kg.23_#_84_#_TRINITY_DN9020	jgi|Blugr1|24419|BGHDH14_bghG000456000001001	jgi|Blugra1|1427|BGT96224_2135T0		
jgi|Golci1|1818104|fgenesh1_kg.23_#_93_#_TRINITY_DN1931	jgi|Blugr1|24416|BGHDH14_bghG000452000001001	jgi|Blugra1|1436|BGT96224_E5704T0		
jgi|Golci1|1818267|fgenesh1_kg.23_#_256_#_TRINITY_DN147	jgi|Blugr1|24411|BGHDH14_bgh03838	jgi|Blugra1|1437|BGT96224_E5703T0		
jgi|Golci1|1818350|fgenesh1_kg.24_#_57_#_TRINITY_DN1148	jgi|Blugr1|24403|BGHDH14_bgh03841	jgi|Blugra1|1441|BGT96224_1442T0		
jgi|Golci1|1818421|fgenesh1_kg.24_#_128_#_TRINITY_DN199	jgi|Blugr1|24387|BGHDH14_bgh03043	jgi|Blugra1|1442|BGT96224_E5709T0		
jgi|Golci1|1818422|fgenesh1_kg.24_#_129_#_TRINITY_DN167	jgi|Blugr1|24374|BGHDH14_bgh02741	jgi|Blugra1|1446|BGT96224_E5707T0		
jgi|Golci1|1818457|fgenesh1_kg.24_#_164_#_TRINITY_DN162	jgi|Blugr1|24373|BGHDH14_bgh04954	jgi|Blugra1|1453|BGT96224_AcSP31496T0		
jgi|Golci1|1818483|fgenesh1_kg.24_#_190_#_TRINITY_DN193	jgi|Blugr1|24361|BGHDH14_bghG000425000003001	jgi|Blugra1|1478|BGT96224_19T0		
jgi|Golci1|1818491|fgenesh1_kg.24_#_198_#_TRINITY_DN193	jgi|Blugr1|24333|BGHDH14_bghG000417000001001	jgi|Blugra1|148|BGT96224_2708T0		
jgi|Golci1|1818609|fgenesh1_kg.25_#_105_#_TRINITY_DN197	jgi|Blugr1|24331|BGHDH14_bghG000417000002001	jgi|Blugra1|1490|BGT96224_ASP20508T0		
jgi|Golci1|1818619|fgenesh1_kg.25_#_115_#_TRINITY_DN188	jgi|Blugr1|24314|BGHDH14_bgh04026	jgi|Blugra1|1509|BGT96224_AcSP30038T0		
jgi|Golci1|1818653|fgenesh1_kg.25_#_149_#_TRINITY_DN197	jgi|Blugr1|24313|BGHDH14_bgh02942	jgi|Blugra1|1513|BGT96224_E5909T0		
jgi|Golci1|1818754|fgenesh1_kg.25_#_250_#_TRINITY_DN190	jgi|Blugr1|24304|BGHDH14_bgh03015	jgi|Blugra1|1541|BGT96224_2274T0		
jgi|Golci1|1818784|fgenesh1_kg.26_#_29_#_TRINITY_DN1825	jgi|Blugr1|24298|BGHDH14_bgh03375	jgi|Blugra1|1542|BGT96224_5013T0		

Gc	Bgh	Bgt	En	Go
jgi|Golci1|1818791|fgenesh1_kg.26_#_36_#_TRINITY_DN5969	jgi|Blugr1|24297|BGHDH14_bgh02998	jgi|Blugra1|1546|BGT96224_4859T0		
jgi|Golci1|1818839|fgenesh1_kg.26_#_84_#_TRINITY_DN1074	jgi|Blugr1|24296|BGHDH14_bghG000389000001001	jgi|Blugra1|1550|BGT96224_E6031T0		
jgi|Golci1|1819106|fgenesh1_kg.27_#_177_#_TRINITY_DN967	jgi|Blugr1|24294|BGHDH14_bgh06578	jgi|Blugra1|1564|BGT96224_3175T0		
jgi|Golci1|1819158|fgenesh1_kg.27_#_229_#_TRINITY_DN193	jgi|Blugr1|24293|BGHDH14_bgh03730	jgi|Blugra1|1569|BGT96224_E5984T0		
jgi|Golci1|1819163|fgenesh1_kg.27_#_234_#_TRINITY_DN193	jgi|Blugr1|24254|BGHDH14_bgh02825	jgi|Blugra1|158|BGT96224_E5560T0		
jgi|Golci1|1819209|fgenesh1_kg.28_#_27_#_TRINITY_DN1926	jgi|Blugr1|24253|BGHDH14_bgh02420	jgi|Blugra1|1606|BGT96224_1231T0		
jgi|Golci1|1819230|fgenesh1_kg.28_#_48_#_TRINITY_DN1210	jgi|Blugr1|24241|BGHDH14_bgh02262	jgi|Blugra1|163|BGT96224_1508T0		
jgi|Golci1|1819323|fgenesh1_kg.28_#_141_#_TRINITY_DN253	jgi|Blugr1|24240|BGHDH14_bgh02836	jgi|Blugra1|165|BGT96224_ASP20866T0		
jgi|Golci1|1819347|fgenesh1_kg.28_#_165_#_TRINITY_DN306	jgi|Blugr1|24239|BGHDH14_bgh02778	jgi|Blugra1|1662|BGT96224_852T0		
jgi|Golci1|1819382|fgenesh1_kg.28_#_200_#_TRINITY_DN193	jgi|Blugr1|24238|BGHDH14_bgh03466	jgi|Blugra1|1680|BGT96224_E5540T0		
jgi|Golci1|1819494|fgenesh1_kg.29_#_82_#_TRINITY_DN1907	jgi|Blugr1|24237|BGHDH14_bgh03464	jgi|Blugra1|170|BGT96224_ASP20702T0		
jgi|Golci1|1819590|fgenesh1_kg.29_#_178_#_TRINITY_DN304	jgi|Blugr1|24236|BGHDH14_bgh03568	jgi|Blugra1|1711|BGT96224_E5627T0		
jgi|Golci1|1819629|fgenesh1_kg.29_#_217_#_TRINITY_DN193	jgi|Blugr1|24235|BGHDH14_bghG001947000001001	jgi|Blugra1|1724|BGT96224_E10122T0		
jgi|Golci1|1819759|fgenesh1_kg.30_#_58_#_TRINITY_DN1400	jgi|Blugr1|24233|BGHDH14_bghG001944000001001	jgi|Blugra1|1733|BGT96224_4583T0		
jgi|Golci1|1819761|fgenesh1_kg.30_#_60_#_TRINITY_DN1400	jgi|Blugr1|24210|BGHDH14_bgh00720	jgi|Blugra1|1742|BGT96224_E6018T0		
jgi|Golci1|1819813|fgenesh1_kg.30_#_112_#_TRINITY_DN596	jgi|Blugr1|24179|BGHDH14_bgh00973	jgi|Blugra1|1747|BGT96224_E10005T0		
jgi|Golci1|1819815|fgenesh1_kg.30_#_114_#_TRINITY_DN453	jgi|Blugr1|24178|BGHDH14_bgh00226	jgi|Blugra1|1749|BGT96224_4496BT0		
jgi|Golci1|1819849|fgenesh1_kg.30_#_148_#_TRINITY_DN123	jgi|Blugr1|24147|BGHDH14_bgh00747	jgi|Blugra1|1751|BGT96224_1333T0		
jgi|Golci1|1819987|fgenesh1_kg.30_#_286_#_TRINITY_DN839	jgi|Blugr1|24122|BGHDH14_bgh05105	jgi|Blugra1|1754|BGT96224_ASP20287T0		
jgi|Golci1|1819990|fgenesh1_kg.30_#_289_#_TRINITY_DN195	jgi|Blugr1|24121|BGHDH14_bgh05104	jgi|Blugra1|1756|BGT96224_E10137T0		
jgi|Golci1|1820003|fgenesh1_kg.30_#_302_#_TRINITY_DN193	jgi|Blugr1|24118|BGHDH14_bgh05917	jgi|Blugra1|1805|BGT96224_AcSP31194T0		

<table>
<tr><th>Gc</th><th>Bgh</th><th>Bgt</th><th>En</th><th>Go</th></tr>
<tr><td>jgi|Golci1|1820012|fgenesh1_kg.30_#_311_#_TRINITY_DN193</td><td>jgi|Blugr1|24117|BGHDH14_bgh05106</td><td>jgi|Blugra1|1831|BGT96224_4300T0</td><td></td><td></td></tr>
<tr><td>jgi|Golci1|1820034|fgenesh1_kg.30_#_333_#_TRINITY_DN197</td><td>jgi|Blugr1|24114|BGHDH14_bgh03692</td><td>jgi|Blugra1|184|BGT96224_E5929T0</td><td></td><td></td></tr>
<tr><td>jgi|Golci1|1820045|fgenesh1_kg.30_#_344_#_TRINITY_DN155</td><td>jgi|Blugr1|24109|BGHDH14_bgh03481</td><td>jgi|Blugra1|1863|BGT96224_1473T0</td><td></td><td></td></tr>
<tr><td>jgi|Golci1|1820050|fgenesh1_kg.30_#_349_#_TRINITY_DN207</td><td>jgi|Blugr1|24107|BGHDH14_bgh00767</td><td>jgi|Blugra1|1871|BGT96224_721T0</td><td></td><td></td></tr>
<tr><td>jgi|Golci1|1820124|fgenesh1_kg.31_#_69_#_TRINITY_DN1776</td><td>jgi|Blugr1|24084|BGHDH14_bgh03457</td><td>jgi|Blugra1|188|BGT96224_E5861T0</td><td></td><td></td></tr>
<tr><td>jgi|Golci1|1820130|fgenesh1_kg.31_#_75_#_TRINITY_DN5959</td><td>jgi|Blugr1|24083|BGHDH14_bgh02774</td><td>jgi|Blugra1|18|BGT96224_4851T0</td><td></td><td></td></tr>
<tr><td>jgi|Golci1|1820255|fgenesh1_kg.32_#_12_#_TRINITY_DN1473</td><td>jgi|Blugr1|24082|BGHDH14_bghG001721000001001</td><td>jgi|Blugra1|1904|BGT96224_E5836T0</td><td></td><td></td></tr>
<tr><td>jgi|Golci1|1820281|fgenesh1_kg.32_#_38_#_TRINITY_DN5010</td><td>jgi|Blugr1|24081|BGHDH14_bgh05751</td><td>jgi|Blugra1|1906|BGT96224_ASP21312T0</td><td></td><td></td></tr>
<tr><td>jgi|Golci1|1820301|fgenesh1_kg.32_#_58_#_TRINITY_DN2072</td><td>jgi|Blugr1|24073|BGHDH14_bgh03794</td><td>jgi|Blugra1|1910|BGT96224_AcSP30824T0</td><td></td><td></td></tr>
<tr><td>jgi|Golci1|1820316|fgenesh1_kg.32_#_73_#_TRINITY_DN1472</td><td>jgi|Blugr1|24071|BGHDH14_bgh03995</td><td>jgi|Blugra1|1914|BGT96224_1306T0</td><td></td><td></td></tr>
<tr><td>jgi|Golci1|1820341|fgenesh1_kg.32_#_98_#_TRINITY_DN1749</td><td>jgi|Blugr1|24069|BGHDH14_bgh03922</td><td>jgi|Blugra1|1926|BGT96224_4746T0</td><td></td><td></td></tr>
<tr><td>jgi|Golci1|1820368|fgenesh1_kg.32_#_125_#_TRINITY_DN193</td><td>jgi|Blugr1|24068|BGHDH14_bghG001682000001001</td><td>jgi|Blugra1|1929|BGT96224_E5982T0</td><td></td><td></td></tr>
<tr><td>jgi|Golci1|1820372|fgenesh1_kg.32_#_129_#_TRINITY_DN183</td><td>jgi|Blugr1|24066|BGHDH14_bgh04159</td><td>jgi|Blugra1|194|BGT96224_BCG8T0</td><td></td><td></td></tr>
<tr><td>jgi|Golci1|1820440|fgenesh1_kg.32_#_197_#_TRINITY_DN189</td><td>jgi|Blugr1|24060|BGHDH14_bgh03857</td><td>jgi|Blugra1|1966|BGT96224_E10024T0</td><td></td><td></td></tr>
<tr><td>jgi|Golci1|1820442|fgenesh1_kg.32_#_199_#_TRINITY_DN553</td><td>jgi|Blugr1|23984|BGHDH14_bgh06200</td><td>jgi|Blugra1|196|BGT96224_E5985T0</td><td></td><td></td></tr>
<tr><td>jgi|Golci1|1820447|fgenesh1_kg.32_#_204_#_TRINITY_DN189</td><td>jgi|Blugr1|23981|BGHDH14_bgh04334</td><td>jgi|Blugra1|1982|BGT96224_1269T0</td><td></td><td></td></tr>
<tr><td>jgi|Golci1|1820485|fgenesh1_kg.32_#_242_#_TRINITY_DN455</td><td>jgi|Blugr1|23950|BGHDH14_bghG001597000001001</td><td>jgi|Blugra1|1988|BGT96224_E10118T0</td><td></td><td></td></tr>
<tr><td>jgi|Golci1|1820556|fgenesh1_kg.33_#_61_#_TRINITY_DN3026</td><td>jgi|Blugr1|23889|BGHDH14_bghG002664000001001</td><td>jgi|Blugra1|1989|BGT96224_E5547T0</td><td></td><td></td></tr>
<tr><td>jgi|Golci1|1820561|fgenesh1_kg.33_#_66_#_TRINITY_DN1765</td><td>jgi|Blugr1|23888|BGHDH14_bghG002653000001001</td><td>jgi|Blugra1|1990|BGT96224_AcSP30782T0</td><td></td><td></td></tr>
<tr><td>jgi|Golci1|1820603|fgenesh1_kg.33_#_108_#_TRINITY_DN162</td><td>jgi|Blugr1|23871|BGHDH14_bghG002637000001001</td><td>jgi|Blugra1|2002|BGT96224_3753T0</td><td></td><td></td></tr>
<tr><td>jgi|Golci1|1820705|fgenesh1_kg.33_#_210_#_TRINITY_DN177</td><td>jgi|Blugr1|23870|BGHDH14_bgh03059</td><td>jgi|Blugra1|201|BGT96224_E5842T0</td><td></td><td></td></tr>
</table>

Gc	Bgh	Bgt	En	Go
jgi|Golci1|1820751|fgenesh1_kg.34_#_14_#_TRINITY_DN1044	jgi|Blugr1|23844|BGHDH14_bghG002599000002001	jgi|Blugra1|202|BGT96224_ASP21585T0		
jgi|Golci1|1820803|fgenesh1_kg.34_#_66_#_TRINITY_DN1679	jgi|Blugr1|23843|BGHDH14_bghG002599000001001	jgi|Blugra1|204|BGT96224_3378T0		
jgi|Golci1|1820854|fgenesh1_kg.34_#_117_#_TRINITY_DN121	jgi|Blugr1|23842|BGHDH14_bgh04769	jgi|Blugra1|205|BGT96224_AcSP31586T0		
jgi|Golci1|1820941|fgenesh1_kg.35_#_14_#_TRINITY_DN1646	jgi|Blugr1|23841|BGHDH14_bgh05096	jgi|Blugra1|2094|BGT96224_E5923T0		
jgi|Golci1|1820972|fgenesh1_kg.35_#_45_#_TRINITY_DN1932	jgi|Blugr1|23840|BGHDH14_bghG002596000001001	jgi|Blugra1|209|BGT96224_E5913T0		
jgi|Golci1|1820980|fgenesh1_kg.35_#_53_#_TRINITY_DN1932	jgi|Blugr1|23839|BGHDH14_bgh05069	jgi|Blugra1|2104|BGT96224_AcSP31023T0		
jgi|Golci1|1821001|fgenesh1_kg.35_#_74_#_TRINITY_DN4833	jgi|Blugr1|23838|BGHDH14_bghG002593000001001	jgi|Blugra1|2122|BGT96224_AcSP31267T0		
jgi|Golci1|1821185|fgenesh1_kg.36_#_14_#_TRINITY_DN1889	jgi|Blugr1|23836|BGHDH14_bghG002593000004001	jgi|Blugra1|2124|BGT96224_AcSP31292T0		
jgi|Golci1|1821220|fgenesh1_kg.36_#_49_#_TRINITY_DN1865	jgi|Blugr1|23835|BGHDH14_bghG002593000003001	jgi|Blugra1|2152|BGT96224_1298T0		
jgi|Golci1|1821237|fgenesh1_kg.36_#_66_#_TRINITY_DN1934	jgi|Blugr1|23834|BGHDH14_bgh00377	jgi|Blugra1|2167|BGT96224_E10131T0		
jgi|Golci1|1821262|fgenesh1_kg.36_#_91_#_TRINITY_DN1932	jgi|Blugr1|23831|BGHDH14_bghG002591000003001	jgi|Blugra1|2168|BGT96224_2931T0		
jgi|Golci1|1821267|fgenesh1_kg.36_#_96_#_TRINITY_DN1932	jgi|Blugr1|23829|BGHDH14_bgh00381	jgi|Blugra1|2169|BGT96224_1215T0		
jgi|Golci1|1821296|fgenesh1_kg.36_#_125_#_TRINITY_DN170	jgi|Blugr1|23828|BGHDH14_bghG002591000002001	jgi|Blugra1|2187|BGT96224_E10100T0		
jgi|Golci1|1821358|fgenesh1_kg.36_#_187_#_TRINITY_DN192	jgi|Blugr1|23827|BGHDH14_bghG002591000001001	jgi|Blugra1|219|BGT96224_E5781T0		
jgi|Golci1|1821368|fgenesh1_kg.36_#_197_#_TRINITY_DN695	jgi|Blugr1|23825|BGHDH14_bghG002588000001001	jgi|Blugra1|2220|BGT96224_851T0		
jgi|Golci1|1821410|fgenesh1_kg.37_#_40_#_TRINITY_DN1494	jgi|Blugr1|23817|BGHDH14_bgh03318	jgi|Blugra1|2222|BGT96224_ASP21007T0		
jgi|Golci1|1821437|fgenesh1_kg.37_#_67_#_TRINITY_DN1932	jgi|Blugr1|23813|BGHDH14_bgh02924	jgi|Blugra1|2225|BGT96224_E5780T0		
jgi|Golci1|1821449|fgenesh1_kg.37_#_79_#_TRINITY_DN1932	jgi|Blugr1|23811|BGHDH14_bghG002559000001001	jgi|Blugra1|223|BGT96224_E5877T0		
jgi|Golci1|1821562|fgenesh1_kg.37_#_192_#_TRINITY_DN464	jgi|Blugr1|23810|BGHDH14_bgh04089	jgi|Blugra1|2243|BGT96224_5308T0		
jgi|Golci1|1821576|fgenesh1_kg.37_#_206_#_TRINITY_DN193	jgi|Blugr1|23806|BGHDH14_bgh04088	jgi|Blugra1|2252|BGT96224_E5732T0		
jgi|Golci1|1821582|fgenesh1_kg.37_#_212_#_TRINITY_DN193	jgi|Blugr1|23803|BGHDH14_bgh02922	jgi|Blugra1|225|BGT96224_E5880T0		

Gc	Bgh	Bgt	En	Go
jgi|Golci1|1821590|fgenesh1_kg.37_#_220_#_TRINITY_DN193	jgi|Blugr1|23802|BGHDH14_bgh02918	jgi|Blugra1|2268|BGT96224_2589T0		
jgi|Golci1|1821596|fgenesh1_kg.37_#_226_#_TRINITY_DN193	jgi|Blugr1|23801|BGHDH14_bgh00739	jgi|Blugra1|2277|BGT96224_E5769T0		
jgi|Golci1|1821701|fgenesh1_kg.38_#_2_#_TRINITY_DN16882	jgi|Blugr1|23795|BGHDH14_bgh06709	jgi|Blugra1|2292|BGT96224_1089T0		
jgi|Golci1|1821777|fgenesh1_kg.38_#_78_#_TRINITY_DN1785	jgi|Blugr1|23794|BGHDH14_bgh01406	jgi|Blugra1|2294|BGT96224_E5692T0		
jgi|Golci1|1821806|fgenesh1_kg.38_#_107_#_TRINITY_DN167	jgi|Blugr1|23792|BGHDH14_bgh01369	jgi|Blugra1|2295|BGT96224_E5645T0		
jgi|Golci1|1821863|fgenesh1_kg.38_#_164_#_TRINITY_DN177	jgi|Blugr1|23791|BGHDH14_bgh01407	jgi|Blugra1|2299|BGT96224_E6032T0		
jgi|Golci1|1821866|fgenesh1_kg.38_#_167_#_TRINITY_DN177	jgi|Blugr1|23790|BGHDH14_bgh02923	jgi|Blugra1|229|BGT96224_E5783T0		
jgi|Golci1|1821884|fgenesh1_kg.38_#_185_#_TRINITY_DN130	jgi|Blugr1|23789|BGHDH14_bgh01405	jgi|Blugra1|22|BGT96224_E5967T0		
jgi|Golci1|1821886|fgenesh1_kg.38_#_187_#_TRINITY_DN541	jgi|Blugr1|23786|BGHDH14_bgh01404	jgi|Blugra1|230|BGT96224_E5953T0		
jgi|Golci1|1821942|fgenesh1_kg.38_#_243_#_TRINITY_DN185	jgi|Blugr1|23779|BGHDH14_bgh01628	jgi|Blugra1|2318|BGT96224_E5681T0		
jgi|Golci1|1822142|fgenesh1_kg.40_#_22_#_TRINITY_DN9087	jgi|Blugr1|23778|BGHDH14_bgh04266	jgi|Blugra1|2331|BGT96224_E5682T0		
jgi|Golci1|1822184|fgenesh1_kg.40_#_64_#_TRINITY_DN117_	jgi|Blugr1|23777|BGHDH14_bgh04023	jgi|Blugra1|2353|BGT96224_574T0		
jgi|Golci1|1822203|fgenesh1_kg.40_#_83_#_TRINITY_DN3312	jgi|Blugr1|23776|BGHDH14_bgh03058	jgi|Blugra1|2367|BGT96224_E5679T0		
jgi|Golci1|1822245|fgenesh1_kg.40_#_125_#_TRINITY_DN116	jgi|Blugr1|23775|BGHDH14_bgh04024	jgi|Blugra1|2386|BGT96224_1161T0		
jgi|Golci1|1822276|fgenesh1_kg.41_#_26_#_TRINITY_DN1706	jgi|Blugr1|23773|BGHDH14_bgh06515	jgi|Blugra1|2407|BGT96224_65T0		
jgi|Golci1|1822313|fgenesh1_kg.41_#_63_#_TRINITY_DN1973	jgi|Blugr1|23772|BGHDH14_bghG002439000001001	jgi|Blugra1|2423|BGT96224_E5668T0		
jgi|Golci1|1822329|fgenesh1_kg.41_#_79_#_TRINITY_DN1875	jgi|Blugr1|23770|BGHDH14_bgh01629	jgi|Blugra1|2430|BGT96224_ASP21313T0		
jgi|Golci1|1822337|fgenesh1_kg.41_#_87_#_TRINITY_DN1825	jgi|Blugr1|23769|BGHDH14_bgh00225	jgi|Blugra1|2467|BGT96224_A20644T0		
jgi|Golci1|1822476|fgenesh1_kg.42_#_46_#_TRINITY_DN2061	jgi|Blugr1|23768|BGHDH14_bgh00020	jgi|Blugra1|2469|BGT96224_E5677T0		
jgi|Golci1|1822492|fgenesh1_kg.42_#_62_#_TRINITY_DN1869	jgi|Blugr1|23766|BGHDH14_bgh01412	jgi|Blugra1|246|BGT96224_E5765T0		
jgi|Golci1|1822518|fgenesh1_kg.42_#_88_#_TRINITY_DN5281	jgi|Blugr1|23765|BGHDH14_bgh01408	jgi|Blugra1|2477|BGT96224_2197T0		

Gc	Bgh	Bgt	En	Go
jgi|Golci1|1822678|fgenesh1_kg.42_#_248_#_TRINITY_DN125	jgi|Blugr1|23764|BGHDH14_bgh04281	jgi|Blugra1|2506|BGT96224_1560BT0		
jgi|Golci1|1822843|fgenesh1_kg.43_#_159_#_TRINITY_DN186	jgi|Blugr1|23749|BGHDH14_bghG002404000001001	jgi|Blugra1|2527|BGT96224_3821T0		
jgi|Golci1|1822870|fgenesh1_kg.43_#_186_#_TRINITY_DN193	jgi|Blugr1|23745|BGHDH14_bgh02500	jgi|Blugra1|2554|BGT96224_2013T0		
jgi|Golci1|1822879|fgenesh1_kg.43_#_195_#_TRINITY_DN203	jgi|Blugr1|23743|BGHDH14_bghG002403000001001	jgi|Blugra1|2558|BGT96224_AcSP31556T0		
jgi|Golci1|1822884|fgenesh1_kg.43_#_200_#_TRINITY_DN210	jgi|Blugr1|23736|BGHDH14_bghG002392000001001	jgi|Blugra1|2563|BGT96224_1254T0		
jgi|Golci1|1822931|fgenesh1_kg.44_#_37_#_TRINITY_DN1392	jgi|Blugr1|23731|BGHDH14_bgh02376	jgi|Blugra1|257|BGT96224_E5597T0		
jgi|Golci1|1822934|fgenesh1_kg.44_#_40_#_TRINITY_DN5014	jgi|Blugr1|23682|BGHDH14_bgh04927	jgi|Blugra1|2590|BGT96224_4877T0		
jgi|Golci1|1822967|fgenesh1_kg.44_#_73_#_TRINITY_DN1246	jgi|Blugr1|23665|BGHDH14_bgh03652	jgi|Blugra1|2602|BGT96224_273BT0		
jgi|Golci1|1822992|fgenesh1_kg.44_#_98_#_TRINITY_DN1877	jgi|Blugr1|23648|BGHDH14_bgh03528	jgi|Blugra1|260|BGT96224_E5561T0		
jgi|Golci1|1823018|fgenesh1_kg.44_#_124_#_TRINITY_DN190	jgi|Blugr1|23591|BGHDH14_bgh05283	jgi|Blugra1|2642|BGT96224_3115T0		
jgi|Golci1|1823029|fgenesh1_kg.44_#_135_#_TRINITY_DN190	jgi|Blugr1|23587|BGHDH14_bgh02390	jgi|Blugra1|2645|BGT96224_1213T0		
jgi|Golci1|1823051|fgenesh1_kg.45_#_13_#_TRINITY_DN1864	jgi|Blugr1|23570|BGHDH14_bghG001460000002001	jgi|Blugra1|2650|BGT96224_2318T0		
jgi|Golci1|1823054|fgenesh1_kg.45_#_16_#_TRINITY_DN1585	jgi|Blugr1|23567|BGHDH14_bgh06328	jgi|Blugra1|2667|BGT96224_E5964T0		
jgi|Golci1|1823078|fgenesh1_kg.45_#_40_#_TRINITY_DN2015	jgi|Blugr1|23534|BGHDH14_bghG001400000002001	jgi|Blugra1|2676|BGT96224_3472T0		
jgi|Golci1|1823080|fgenesh1_kg.45_#_42_#_TRINITY_DN2665	jgi|Blugr1|23510|BGHDH14_bgh06275	jgi|Blugra1|2692|BGT96224_2673T0		
jgi|Golci1|1823095|fgenesh1_kg.45_#_57_#_TRINITY_DN1253	jgi|Blugr1|23493|BGHDH14_bgh02285	jgi|Blugra1|2698|BGT96224_ASP20650T0		
jgi|Golci1|1823125|fgenesh1_kg.45_#_87_#_TRINITY_DN1523	jgi|Blugr1|23488|BGHDH14_bgh02588	jgi|Blugra1|2710|BGT96224_2403T0		
jgi|Golci1|1823252|fgenesh1_kg.46_#_7_#_TRINITY_DN8553_	jgi|Blugr1|23463|BGHDH14_bgh00838	jgi|Blugra1|2711|BGT96224_5010T0		
jgi|Golci1|1823258|fgenesh1_kg.46_#_13_#_TRINITY_DN5203	jgi|Blugr1|23460|BGHDH14_bgh01832	jgi|Blugra1|274|BGT96224_E5585T0		
jgi|Golci1|1823396|fgenesh1_kg.46_#_151_#_TRINITY_DN538	jgi|Blugr1|23457|BGHDH14_bghG001346000001001	jgi|Blugra1|2756|BGT96224_E5991T0		
jgi|Golci1|1823418|fgenesh1_kg.47_#_4_#_TRINITY_DN20795	jgi|Blugr1|23443|BGHDH14_bgh00082	jgi|Blugra1|2766|BGT96224_501T0		

<table>
<tr><th>Gc</th><th>Bgh</th><th>Bgt</th><th>En</th><th>Go</th></tr>
<tr><td>jgi|Golci1|1823464|fgenesh1_kg.47_#_50_#_TRINITY_DN1894</td><td>jgi|Blugr1|23439|BGHDH14_bgh00594</td><td>jgi|Blugra1|276|BGT96224_E5548T0</td><td></td><td></td></tr>
<tr><td>jgi|Golci1|1823469|fgenesh1_kg.47_#_55_#_TRINITY_DN1894</td><td>jgi|Blugr1|23438|BGHDH14_bghG001319000001001</td><td>jgi|Blugra1|2774|BGT96224_AcSP30596T0</td><td></td><td></td></tr>
<tr><td>jgi|Golci1|1823472|fgenesh1_kg.47_#_58_#_TRINITY_DN1894</td><td>jgi|Blugr1|23416|BGHDH14_bgh04781</td><td>jgi|Blugra1|278|BGT96224_E5782T0</td><td></td><td></td></tr>
<tr><td>jgi|Golci1|1823478|fgenesh1_kg.47_#_64_#_TRINITY_DN912_</td><td>jgi|Blugr1|23415|BGHDH14_bgh03734</td><td>jgi|Blugra1|2823|BGT96224_979T0</td><td></td><td></td></tr>
<tr><td>jgi|Golci1|1823511|fgenesh1_kg.47_#_97_#_TRINITY_DN2079</td><td>jgi|Blugr1|23414|BGHDH14_bgh03735</td><td>jgi|Blugra1|2852|BGT96224_4373T0</td><td></td><td></td></tr>
<tr><td>jgi|Golci1|1823524|fgenesh1_kg.47_#_110_#_TRINITY_DN190</td><td>jgi|Blugr1|23393|BGHDH14_bgh03731</td><td>jgi|Blugra1|2872|BGT96224_AcSP30775T0</td><td></td><td></td></tr>
<tr><td>jgi|Golci1|1823649|fgenesh1_kg.48_#_1_#_TRINITY_DN5190_</td><td>jgi|Blugr1|23392|BGHDH14_bghG001282000001001</td><td>jgi|Blugra1|2873|BGT96224_E5604T0</td><td></td><td></td></tr>
<tr><td>jgi|Golci1|1823703|fgenesh1_kg.48_#_55_#_TRINITY_DN1736</td><td>jgi|Blugr1|23377|BGHDH14_bgh00027</td><td>jgi|Blugra1|2874|BGT96224_E5603T0</td><td></td><td></td></tr>
<tr><td>jgi|Golci1|1823926|fgenesh1_kg.49_#_83_#_TRINITY_DN1168</td><td>jgi|Blugr1|23372|BGHDH14_bgh04121</td><td>jgi|Blugra1|2875|BGT96224_AcSP30893T0</td><td></td><td></td></tr>
<tr><td>jgi|Golci1|1824018|fgenesh1_kg.50_#_23_#_TRINITY_DN2270</td><td>jgi|Blugr1|23363|BGHDH14_bghG001240000001001</td><td>jgi|Blugra1|2878|BGT96224_E6037T0</td><td></td><td></td></tr>
<tr><td>jgi|Golci1|1824066|fgenesh1_kg.50_#_71_#_TRINITY_DN9515</td><td>jgi|Blugr1|23359|BGHDH14_bghG001226000001001</td><td>jgi|Blugra1|2891|BGT96224_3097T0</td><td></td><td></td></tr>
<tr><td>jgi|Golci1|1824075|fgenesh1_kg.50_#_80_#_TRINITY_DN1932</td><td>jgi|Blugr1|23356|BGHDH14_bghG001225000001001</td><td>jgi|Blugra1|2936|BGT96224_2286BT0</td><td></td><td></td></tr>
<tr><td>jgi|Golci1|1824080|fgenesh1_kg.50_#_85_#_TRINITY_DN1932</td><td>jgi|Blugr1|23349|BGHDH14_bghG001219000002001</td><td>jgi|Blugra1|2942|BGT96224_5451T0</td><td></td><td></td></tr>
<tr><td>jgi|Golci1|1824111|fgenesh1_kg.50_#_116_#_TRINITY_DN136</td><td>jgi|Blugr1|23339|BGHDH14_bgh04006</td><td>jgi|Blugra1|2973|BGT96224_2362T0</td><td></td><td></td></tr>
<tr><td>jgi|Golci1|1824198|fgenesh1_kg.51_#_3_#_TRINITY_DN933_c</td><td>jgi|Blugr1|23297|BGHDH14_bghG001169000001001</td><td>jgi|Blugra1|2985|BGT96224_4797T0</td><td></td><td></td></tr>
<tr><td>jgi|Golci1|1824201|fgenesh1_kg.51_#_6_#_TRINITY_DN6142_</td><td>jgi|Blugr1|23284|BGHDH14_bghG001154000002001</td><td>jgi|Blugra1|299|BGT96224_E10001T0</td><td></td><td></td></tr>
<tr><td>jgi|Golci1|1824208|fgenesh1_kg.51_#_13_#_TRINITY_DN1996</td><td>jgi|Blugr1|23253|BGHDH14_bgh04510</td><td>jgi|Blugra1|301|BGT96224_3843T0</td><td></td><td></td></tr>
<tr><td>jgi|Golci1|1824252|fgenesh1_kg.51_#_57_#_TRINITY_DN1932</td><td>jgi|Blugr1|23252|BGHDH14_bghG001105000001001</td><td>jgi|Blugra1|3022|BGT96224_E3136T0</td><td></td><td></td></tr>
<tr><td>jgi|Golci1|1824284|fgenesh1_kg.51_#_89_#_TRINITY_DN2075</td><td>jgi|Blugr1|23250|BGHDH14_bgh04512</td><td>jgi|Blugra1|3023|BGT96224_E5921T0</td><td></td><td></td></tr>
<tr><td>jgi|Golci1|1824360|fgenesh1_kg.52_#_36_#_TRINITY_DN1934</td><td>jgi|Blugr1|23245|BGHDH14_bgh06777</td><td>jgi|Blugra1|3024|BGT96224_E5922T0</td><td></td><td></td></tr>
<tr><td>jgi|Golci1|1824386|fgenesh1_kg.52_#_62_#_TRINITY_DN1625</td><td>jgi|Blugr1|23238|BGHDH14_bghG007171000001001</td><td>jgi|Blugra1|3030|BGT96224_E10124T0</td><td></td><td></td></tr>
</table>

<table>
<tr><th>Gc</th><th>Bgh</th><th>Bgt</th><th>En</th><th>Go</th></tr>
<tr><td>jgi|Golci1|1824409|fgenesh1_kg.52_#_85_#_TRINITY_DN8503</td><td>jgi|Blugr1|20867|BGHDH14_bgh01761</td><td>jgi|Blugra1|3046|BGT96224_1066T0</td><td></td><td></td></tr>
<tr><td>jgi|Golci1|1824452|fgenesh1_kg.52_#_128_#_TRINITY_DN519</td><td>jgi|Blugr1|20859|BGHDH14_bgh01769</td><td>jgi|Blugra1|304|BGT96224_E10103T0</td><td></td><td></td></tr>
<tr><td>jgi|Golci1|1824459|fgenesh1_kg.52_#_135_#_TRINITY_DN172</td><td>jgi|Blugr1|20822|BGHDH14_bgh03441</td><td>jgi|Blugra1|305|BGT96224_E6000T0</td><td></td><td></td></tr>
<tr><td>jgi|Golci1|1824471|fgenesh1_kg.52_#_147_#_TRINITY_DN130</td><td>jgi|Blugr1|20821|BGHDH14_bgh02083</td><td>jgi|Blugra1|3060|BGT96224_AcSP30632T0</td><td></td><td></td></tr>
<tr><td>jgi|Golci1|1824515|fgenesh1_kg.53_#_22_#_TRINITY_DN1238</td><td>jgi|Blugr1|20820|BGHDH14_bgh05730</td><td>jgi|Blugra1|3068|BGT96224_4602T0</td><td></td><td></td></tr>
<tr><td>jgi|Golci1|1824559|fgenesh1_kg.53_#_66_#_TRINITY_DN1203</td><td>jgi|Blugr1|20819|BGHDH14_bgh00589</td><td>jgi|Blugra1|307|BGT96224_4938T0</td><td></td><td></td></tr>
<tr><td>jgi|Golci1|1824589|fgenesh1_kg.53_#_96_#_TRINITY_DN1859</td><td>jgi|Blugr1|20818|BGHDH14_bghG003525000001001</td><td>jgi|Blugra1|30|BGT96224_5106T0</td><td></td><td></td></tr>
<tr><td>jgi|Golci1|1824679|fgenesh1_kg.53_#_186_#_TRINITY_DN193</td><td>jgi|Blugr1|20817|BGHDH14_bgh02087</td><td>jgi|Blugra1|3111|BGT96224_BCG9T0</td><td></td><td></td></tr>
<tr><td>jgi|Golci1|1824686|fgenesh1_kg.53_#_193_#_TRINITY_DN193</td><td>jgi|Blugr1|20816|BGHDH14_bgh06198</td><td>jgi|Blugra1|3112|BGT96224_BCG5T0</td><td></td><td></td></tr>
<tr><td>jgi|Golci1|1824714|fgenesh1_kg.53_#_221_#_TRINITY_DN134</td><td>jgi|Blugr1|20813|BGHDH14_bgh00774</td><td>jgi|Blugra1|3113|BGT96224_BCG2T0</td><td></td><td></td></tr>
<tr><td>jgi|Golci1|1824759|fgenesh1_kg.54_#_1_#_TRINITY_DN16220</td><td>jgi|Blugr1|20799|BGHDH14_bgh02653</td><td>jgi|Blugra1|3114|BGT96224_AcSP30403T0</td><td></td><td></td></tr>
<tr><td>jgi|Golci1|1824771|fgenesh1_kg.54_#_13_#_TRINITY_DN1834</td><td>jgi|Blugr1|20766|BGHDH14_bghG003462000001001</td><td>jgi|Blugra1|3115|BGT96224_BCG3T0</td><td></td><td></td></tr>
<tr><td>jgi|Golci1|1824862|fgenesh1_kg.54_#_104_#_TRINITY_DN849</td><td>jgi|Blugr1|20748|BGHDH14_bgh05174</td><td>jgi|Blugra1|3116|BGT96224_983T0</td><td></td><td></td></tr>
<tr><td>jgi|Golci1|1824938|fgenesh1_kg.54_#_180_#_TRINITY_DN153</td><td>jgi|Blugr1|20708|BGHDH14_bghG003444000001001</td><td>jgi|Blugra1|3118|BGT96224_E6051T0</td><td></td><td></td></tr>
<tr><td>jgi|Golci1|1824951|fgenesh1_kg.54_#_193_#_TRINITY_DN720</td><td>jgi|Blugr1|20693|BGHDH14_bgh02274</td><td>jgi|Blugra1|3119|BGT96224_E5613T0</td><td></td><td></td></tr>
<tr><td>jgi|Golci1|1824963|fgenesh1_kg.54_#_205_#_TRINITY_DN304</td><td>jgi|Blugr1|20659|BGHDH14_bgh00782</td><td>jgi|Blugra1|3120|BGT96224_E5583T0</td><td></td><td></td></tr>
<tr><td>jgi|Golci1|1824973|fgenesh1_kg.54_#_215_#_TRINITY_DN196</td><td>jgi|Blugr1|20643|BGHDH14_bgh02426</td><td>jgi|Blugra1|3122|BGT96224_E5584T0</td><td></td><td></td></tr>
<tr><td>jgi|Golci1|1825012|fgenesh1_kg.55_#_34_#_TRINITY_DN2079</td><td>jgi|Blugr1|20640|BGHDH14_bghG003379000001001</td><td>jgi|Blugra1|3123|BGT96224_E5553T0</td><td></td><td></td></tr>
<tr><td>jgi|Golci1|1825028|fgenesh1_kg.55_#_50_#_TRINITY_DN1932</td><td>jgi|Blugr1|20625|BGHDH14_bgh03052</td><td>jgi|Blugra1|3132|BGT96224_E5774T0</td><td></td><td></td></tr>
<tr><td>jgi|Golci1|1825055|fgenesh1_kg.55_#_77_#_TRINITY_DN1475</td><td>jgi|Blugr1|20619|BGHDH14_bgh04036</td><td>jgi|Blugra1|3135|BGT96224_1393T0</td><td></td><td></td></tr>
<tr><td>jgi|Golci1|1825125|fgenesh1_kg.55_#_147_#_TRINITY_DN202</td><td>jgi|Blugr1|20606|BGHDH14_bgh02050</td><td>jgi|Blugra1|3177|BGT96224_4078T0</td><td></td><td></td></tr>
</table>

<table>
<tr><th>Gc</th><th>Bgh</th><th>Bgt</th><th>En</th><th>Go</th></tr>
<tr><td>jgi|Golci1|1825139|fgenesh1_kg.55_#_161_#_TRINITY_DN877</td><td>jgi|Blugr1|20604|BGHDH14_bghG005990000002001</td><td colspan="2">jgi|Blugra1|3178|BGT96224_E5624T0</td><td></td></tr>
<tr><td>jgi|Golci1|1825166|fgenesh1_kg.56_#_4_#_TRINITY_DN19801</td><td>jgi|Blugr1|20599|BGHDH14_bgh03462</td><td colspan="2">jgi|Blugra1|3185|BGT96224_AcSP30120T0</td><td></td></tr>
<tr><td>jgi|Golci1|1825173|fgenesh1_kg.56_#_11_#_TRINITY_DN1980</td><td>jgi|Blugr1|20597|BGHDH14_bgh02701</td><td colspan="2">jgi|Blugra1|3186|BGT96224_ASP20119T0</td><td></td></tr>
<tr><td>jgi|Golci1|1825215|fgenesh1_kg.56_#_53_#_TRINITY_DN4291</td><td>jgi|Blugr1|20596|BGHDH14_bgh03470</td><td colspan="2">jgi|Blugra1|3187|BGT96224_AcSP30129T0</td><td></td></tr>
<tr><td>jgi|Golci1|1825223|fgenesh1_kg.56_#_61_#_TRINITY_DN9431</td><td>jgi|Blugr1|20595|BGHDH14_bgh05269</td><td colspan="2">jgi|Blugra1|3195|BGT96224_E5658T0</td><td></td></tr>
<tr><td>jgi|Golci1|1825290|fgenesh1_kg.56_#_128_#_TRINITY_DN202</td><td>jgi|Blugr1|20594|BGHDH14_bgh03736</td><td colspan="2">jgi|Blugra1|3208|BGT96224_ASP21198T0</td><td></td></tr>
<tr><td>jgi|Golci1|1825302|fgenesh1_kg.56_#_140_#_TRINITY_DN130</td><td>jgi|Blugr1|20592|BGHDH14_bghG005948000001001</td><td colspan="2">jgi|Blugra1|3211|BGT96224_E10110T0</td><td></td></tr>
<tr><td>jgi|Golci1|1825381|fgenesh1_kg.57_#_71_#_TRINITY_DN2084</td><td>jgi|Blugr1|20587|BGHDH14_bghG005940000001001</td><td colspan="2">jgi|Blugra1|3214|BGT96224_E10111T0</td><td></td></tr>
<tr><td>jgi|Golci1|1825384|fgenesh1_kg.57_#_74_#_TRINITY_DN7034</td><td>jgi|Blugr1|20577|BGHDH14_bgh03584</td><td colspan="2">jgi|Blugra1|3233|BGT96224_3880T0</td><td></td></tr>
<tr><td>jgi|Golci1|1825432|fgenesh1_kg.57_#_122_#_TRINITY_DN414</td><td>jgi|Blugr1|20576|BGHDH14_bghG005930000001001</td><td colspan="2">jgi|Blugra1|3275|BGT96224_E6023T0</td><td></td></tr>
<tr><td>jgi|Golci1|1825489|fgenesh1_kg.58_#_19_#_TRINITY_DN1493</td><td>jgi|Blugr1|20575|BGHDH14_bgh03571</td><td colspan="2">jgi|Blugra1|3309|BGT96224_AcSP30320T0</td><td></td></tr>
<tr><td>jgi|Golci1|1825588|fgenesh1_kg.59_#_4_#_TRINITY_DN20418</td><td>jgi|Blugr1|20572|BGHDH14_bgh02072</td><td colspan="2">jgi|Blugra1|3320|BGT96224_ASP20291T0</td><td></td></tr>
<tr><td>jgi|Golci1|1825613|fgenesh1_kg.59_#_29_#_TRINITY_DN1350</td><td>jgi|Blugr1|20570|BGHDH14_bgh03425</td><td colspan="2">jgi|Blugra1|3327|BGT96224_E5784T0</td><td></td></tr>
<tr><td>jgi|Golci1|1825634|fgenesh1_kg.59_#_50_#_TRINITY_DN1989</td><td colspan="2">jgi|Blugr1|20538|BGHDH14_bghG005862000001001</td><td></td><td></td></tr>
<tr><td>jgi|Golci1|1825635|fgenesh1_kg.59_#_51_#_TRINITY_DN1005</td><td colspan="2">jgi|Blugr1|20531|BGHDH14_bgh05066</td><td></td><td></td></tr>
<tr><td>jgi|Golci1|1825678|fgenesh1_kg.59_#_94_#_TRINITY_DN1661</td><td colspan="2">jgi|Blugr1|20525|BGHDH14_bgh02114</td><td></td><td></td></tr>
<tr><td>jgi|Golci1|1825706|fgenesh1_kg.59_#_122_#_TRINITY_DN184</td><td colspan="2">jgi|Blugr1|20521|BGHDH14_bgh04231</td><td></td><td></td></tr>
<tr><td>jgi|Golci1|1825720|fgenesh1_kg.60_#_4_#_TRINITY_DN19348</td><td colspan="2">jgi|Blugr1|20520|BGHDH14_bghG005853000001001</td><td></td><td></td></tr>
<tr><td>jgi|Golci1|1825741|fgenesh1_kg.60_#_25_#_TRINITY_DN1622</td><td colspan="2">jgi|Blugr1|20519|BGHDH14_bgh04113</td><td></td><td></td></tr>
<tr><td>jgi|Golci1|1825776|fgenesh1_kg.60_#_60_#_TRINITY_DN1189</td><td colspan="2">jgi|Blugr1|20513|BGHDH14_bghG006578000002001</td><td></td><td></td></tr>
<tr><td>jgi|Golci1|1825788|fgenesh1_kg.60_#_72_#_TRINITY_DN2102</td><td colspan="2">jgi|Blugr1|20512|BGHDH14_bghG006578000001001</td><td></td><td></td></tr>
</table>

<table>
<tr><th>Gc</th><th>Bgh</th><th>Bgt</th><th>En</th><th>Go</th></tr>
<tr><td>jgi|Golci1|1826058|fgenesh1_kg.61_#_165_#_TRINITY_DN193</td><td>jgi|Blugr1|20511|BGHDH14_bgh05270</td><td></td><td></td><td></td></tr>
<tr><td>jgi|Golci1|1826065|fgenesh1_kg.61_#_172_#_TRINITY_DN193</td><td>jgi|Blugr1|20510|BGHDH14_bgh01363</td><td></td><td></td><td></td></tr>
<tr><td>jgi|Golci1|1826208|fgenesh1_kg.62_#_99_#_TRINITY_DN2104</td><td>jgi|Blugr1|20509|BGHDH14_bgh02851</td><td></td><td></td><td></td></tr>
<tr><td>jgi|Golci1|1826212|fgenesh1_kg.62_#_103_#_TRINITY_DN210</td><td>jgi|Blugr1|20502|BGHDH14_bgh00670</td><td></td><td></td><td></td></tr>
<tr><td>jgi|Golci1|1826245|fgenesh1_kg.62_#_136_#_TRINITY_DN897</td><td>jgi|Blugr1|20500|BGHDH14_bgh04832</td><td></td><td></td><td></td></tr>
<tr><td>jgi|Golci1|1826267|fgenesh1_kg.62_#_158_#_TRINITY_DN192</td><td>jgi|Blugr1|20499|BGHDH14_bgh04830</td><td></td><td></td><td></td></tr>
<tr><td>jgi|Golci1|1826268|fgenesh1_kg.62_#_159_#_TRINITY_DN198</td><td>jgi|Blugr1|20498|BGHDH14_bgh01677</td><td></td><td></td><td></td></tr>
<tr><td>jgi|Golci1|1826276|fgenesh1_kg.62_#_167_#_TRINITY_DN103</td><td>jgi|Blugr1|20497|BGHDH14_bgh05925</td><td></td><td></td><td></td></tr>
<tr><td>jgi|Golci1|1826412|fgenesh1_kg.63_#_121_#_TRINITY_DN193</td><td>jgi|Blugr1|20494|BGHDH14_bgh02310</td><td></td><td></td><td></td></tr>
<tr><td>jgi|Golci1|1826584|fgenesh1_kg.63_#_293_#_TRINITY_DN172</td><td>jgi|Blugr1|20492|BGHDH14_bgh02939</td><td></td><td></td><td></td></tr>
<tr><td>jgi|Golci1|1826595|fgenesh1_kg.63_#_304_#_TRINITY_DN147</td><td>jgi|Blugr1|20488|BGHDH14_bgh02934</td><td></td><td></td><td></td></tr>
<tr><td>jgi|Golci1|1826621|fgenesh1_kg.63_#_330_#_TRINITY_DN157</td><td>jgi|Blugr1|20487|BGHDH14_bgh03694</td><td></td><td></td><td></td></tr>
<tr><td>jgi|Golci1|1826643|fgenesh1_kg.64_#_16_#_TRINITY_DN1935</td><td>jgi|Blugr1|20479|BGHDH14_bghG005814000001001</td><td></td><td></td><td></td></tr>
<tr><td>jgi|Golci1|1826689|fgenesh1_kg.64_#_62_#_TRINITY_DN1878</td><td>jgi|Blugr1|20467|BGHDH14_bgh01873</td><td></td><td></td><td></td></tr>
<tr><td>jgi|Golci1|1826693|fgenesh1_kg.64_#_66_#_TRINITY_DN1878</td><td>jgi|Blugr1|20452|BGHDH14_bgh04255</td><td></td><td></td><td></td></tr>
<tr><td>jgi|Golci1|1826709|fgenesh1_kg.64_#_82_#_TRINITY_DN1932</td><td>jgi|Blugr1|20446|BGHDH14_bgh03641</td><td></td><td></td><td></td></tr>
<tr><td>jgi|Golci1|1826714|fgenesh1_kg.64_#_87_#_TRINITY_DN1932</td><td>jgi|Blugr1|20431|BGHDH14_bgh02690</td><td></td><td></td><td></td></tr>
<tr><td>jgi|Golci1|1826724|fgenesh1_kg.64_#_97_#_TRINITY_DN973_</td><td>jgi|Blugr1|20429|BGHDH14_bgh02686</td><td></td><td></td><td></td></tr>
<tr><td>jgi|Golci1|1826761|fgenesh1_kg.64_#_134_#_TRINITY_DN202</td><td>jgi|Blugr1|20422|BGHDH14_bgh01863</td><td></td><td></td><td></td></tr>
<tr><td>jgi|Golci1|1826816|fgenesh1_kg.65_#_45_#_TRINITY_DN5650</td><td>jgi|Blugr1|20421|BGHDH14_bgh00012</td><td></td><td></td><td></td></tr>
<tr><td>jgi|Golci1|1826882|fgenesh1_kg.65_#_111_#_TRINITY_DN171</td><td>jgi|Blugr1|20386|BGHDH14_bghG005434000001001</td><td></td><td></td><td></td></tr>
</table>

Gc	Bgh	Bgt	En	Go
jgi|Golci1|1826886|fgenesh1_kg.65_#_115_#_TRINITY_DN136	jgi|Blugr1|20385|BGHDH14_bgh05145			
jgi|Golci1|1826953|fgenesh1_kg.66_#_33_#_TRINITY_DN1722	jgi|Blugr1|20384|BGHDH14_bgh05160			
jgi|Golci1|1826956|fgenesh1_kg.66_#_36_#_TRINITY_DN1722	jgi|Blugr1|20366|BGHDH14_bgh02386			
jgi|Golci1|1826980|fgenesh1_kg.66_#_60_#_TRINITY_DN1895	jgi|Blugr1|20327|BGHDH14_bgh06448			
jgi|Golci1|1827006|fgenesh1_kg.66_#_86_#_TRINITY_DN1797	jgi|Blugr1|20322|BGHDH14_bgh02452			
jgi|Golci1|1827107|fgenesh1_kg.67_#_52_#_TRINITY_DN1932	jgi|Blugr1|20301|BGHDH14_bgh04748			
jgi|Golci1|1827115|fgenesh1_kg.67_#_60_#_TRINITY_DN1932	jgi|Blugr1|20300|BGHDH14_bgh02977			
jgi|Golci1|1827147|fgenesh1_kg.67_#_92_#_TRINITY_DN1265	jgi|Blugr1|20293|BGHDH14_bghG005335000001001			
jgi|Golci1|1827166|fgenesh1_kg.67_#_111_#_TRINITY_DN179	jgi|Blugr1|20290|BGHDH14_bgh02435			
jgi|Golci1|1827208|fgenesh1_kg.68_#_39_#_TRINITY_DN1528	jgi|Blugr1|20289|BGHDH14_bghG005334000001001			
jgi|Golci1|1827269|fgenesh1_kg.68_#_100_#_TRINITY_DN172	jgi|Blugr1|20266|BGHDH14_bgh00674			
jgi|Golci1|1827271|fgenesh1_kg.68_#_102_#_TRINITY_DN103	jgi|Blugr1|20261|BGHDH14_bgh01978			
jgi|Golci1|1827281|fgenesh1_kg.68_#_112_#_TRINITY_DN282	jgi|Blugr1|20216|BGHDH14_bghG006918000001001			
jgi|Golci1|1827292|fgenesh1_kg.68_#_123_#_TRINITY_DN205	jgi|Blugr1|20195|BGHDH14_bgh03130			
jgi|Golci1|1827310|fgenesh1_kg.69_#_2_#_TRINITY_DN14903	jgi|Blugr1|20184|BGHDH14_bgh03812			
jgi|Golci1|1827317|fgenesh1_kg.69_#_9_#_TRINITY_DN20795	jgi|Blugr1|20181|BGHDH14_bgh04108			
jgi|Golci1|1827336|fgenesh1_kg.69_#_28_#_TRINITY_DN1932	jgi|Blugr1|20168|BGHDH14_bgh02218			
jgi|Golci1|1827365|fgenesh1_kg.69_#_57_#_TRINITY_DN1453	jgi|Blugr1|20159|BGHDH14_bgh00369			
jgi|Golci1|1827370|fgenesh1_kg.69_#_62_#_TRINITY_DN2680	jgi|Blugr1|20153|BGHDH14_bgh02245			
jgi|Golci1|1827382|fgenesh1_kg.69_#_74_#_TRINITY_DN2035	jgi|Blugr1|20131|BGHDH14_bghG005501000001001			
jgi|Golci1|1827442|fgenesh1_kg.69_#_134_#_TRINITY_DN131	jgi|Blugr1|20128|BGHDH14_bgh06046			

Gc	Bgh	Bgt	En	Go
jgi|Golci1|1827489|fgenesh1_kg.70_#_25_#_TRINITY_DN1723	jgi|Blugr1|20122|BGHDH14_bgh04629			
jgi|Golci1|1827502|fgenesh1_kg.70_#_38_#_TRINITY_DN1608	jgi|Blugr1|20101|BGHDH14_bghG005480000002001			
jgi|Golci1|1827505|fgenesh1_kg.70_#_41_#_TRINITY_DN3272	jgi|Blugr1|20085|BGHDH14_bghG005474000001001			
jgi|Golci1|1827670|fgenesh1_kg.71_#_72_#_TRINITY_DN1668	jgi|Blugr1|20077|BGHDH14_bgh06543			
jgi|Golci1|1827676|fgenesh1_kg.71_#_78_#_TRINITY_DN6168	jgi|Blugr1|20063|BGHDH14_bghG005458000001001			
jgi|Golci1|1827690|fgenesh1_kg.71_#_92_#_TRINITY_DN1855	jgi|Blugr1|20062|BGHDH14_bghG005457000001001			
jgi|Golci1|1827699|fgenesh1_kg.71_#_101_#_TRINITY_DN193	jgi|Blugr1|20049|BGHDH14_bgh02624			
jgi|Golci1|1827750|fgenesh1_kg.72_#_1_#_TRINITY_DN16946	jgi|Blugr1|20047|BGHDH14_bgh02857			
jgi|Golci1|1827755|fgenesh1_kg.72_#_6_#_TRINITY_DN26106	jgi|Blugr1|20046|BGHDH14_bgh02854			
jgi|Golci1|1827956|fgenesh1_kg.72_#_207_#_TRINITY_DN125	jgi|Blugr1|20012|BGHDH14_bghG006712000002001			
jgi|Golci1|1827986|fgenesh1_kg.73_#_5_#_TRINITY_DN7334_	jgi|Blugr1|20008|BGHDH14_bghG006712000001001			
jgi|Golci1|1827993|fgenesh1_kg.73_#_12_#_TRINITY_DN1604	jgi|Blugr1|20004|BGHDH14_bgh02031			
jgi|Golci1|1828131|fgenesh1_kg.73_#_150_#_TRINITY_DN198	jgi|Blugr1|20003|BGHDH14_bgh03636			
jgi|Golci1|1828209|fgenesh1_kg.74_#_62_#_TRINITY_DN1930	jgi|Blugr1|20002|BGHDH14_bgh04014			
jgi|Golci1|1828276|fgenesh1_kg.74_#_129_#_TRINITY_DN116	jgi|Blugr1|19998|BGHDH14_bgh04020			
jgi|Golci1|1828306|fgenesh1_kg.74_#_159_#_TRINITY_DN208	jgi|Blugr1|19997|BGHDH14_bgh03637			
jgi|Golci1|1828308|fgenesh1_kg.74_#_161_#_TRINITY_DN208	jgi|Blugr1|19996|BGHDH14_bghG006682000001001			
jgi|Golci1|1828321|fgenesh1_kg.75_#_12_#_TRINITY_DN1823	jgi|Blugr1|19976|BGHDH14_bgh05630			
jgi|Golci1|1828356|fgenesh1_kg.75_#_47_#_TRINITY_DN1932	jgi|Blugr1|19975|BGHDH14_bgh03613			
jgi|Golci1|1828361|fgenesh1_kg.75_#_52_#_TRINITY_DN1932	jgi|Blugr1|19974|BGHDH14_bgh02647			
jgi|Golci1|1828653|fgenesh1_kg.77_#_2_#_TRINITY_DN17238	jgi|Blugr1|19923|BGHDH14_bgh00755			

Gc	Bgh	Bgt	En	Go
jgi|Golci1|1828734|fgenesh1_kg.77_#_83_#_TRINITY_DN2110	jgi|Blugr1|19887|BGHDH14_bgh04081			
jgi|Golci1|1828806|fgenesh1_kg.78_#_2_#_TRINITY_DN8950_	jgi|Blugr1|19883|BGHDH14_bgh05093			
jgi|Golci1|1828938|fgenesh1_kg.78_#_134_#_TRINITY_DN108	jgi|Blugr1|19878|BGHDH14_bgh00783			
jgi|Golci1|1828996|fgenesh1_kg.78_#_192_#_TRINITY_DN281	jgi|Blugr1|19877|BGHDH14_bghG006408000001001			
jgi|Golci1|1829010|fgenesh1_kg.79_#_14_#_TRINITY_DN2076	jgi|Blugr1|19852|BGHDH14_bghG006402000004001			
jgi|Golci1|1829019|fgenesh1_kg.79_#_23_#_TRINITY_DN1932	jgi|Blugr1|19835|BGHDH14_bghG007473000001001			
jgi|Golci1|1829028|fgenesh1_kg.79_#_32_#_TRINITY_DN1932	jgi|Blugr1|19834|BGHDH14_bgh05844			
jgi|Golci1|1829067|fgenesh1_kg.79_#_71_#_TRINITY_DN1379	jgi|Blugr1|19803|BGHDH14_bgh00726			
jgi|Golci1|1829175|fgenesh1_kg.80_#_9_#_TRINITY_DN15403	jgi|Blugr1|19763|BGHDH14_bgh00029			
jgi|Golci1|1829297|fgenesh1_kg.80_#_131_#_TRINITY_DN142	jgi|Blugr1|19736|BGHDH14_bgh04292			
jgi|Golci1|1829371|fgenesh1_kg.81_#_26_#_TRINITY_DN1767	jgi|Blugr1|19723|BGHDH14_bgh04324			
jgi|Golci1|1829520|fgenesh1_kg.81_#_175_#_TRINITY_DN185	jgi|Blugr1|19714|BGHDH14_bgh06298			
jgi|Golci1|1829558|fgenesh1_kg.82_#_11_#_TRINITY_DN1698	jgi|Blugr1|19690|BGHDH14_bgh04262			
jgi|Golci1|1829603|fgenesh1_kg.82_#_56_#_TRINITY_DN1340	jgi|Blugr1|19689|BGHDH14_bgh03138			
jgi|Golci1|1829769|fgenesh1_kg.83_#_33_#_TRINITY_DN1898	jgi|Blugr1|19688|BGHDH14_bgh03786			
jgi|Golci1|1829777|fgenesh1_kg.83_#_41_#_TRINITY_DN2090	jgi|Blugr1|19687|BGHDH14_bgh06899			
jgi|Golci1|1829839|fgenesh1_kg.83_#_103_#_TRINITY_DN835	jgi|Blugr1|19686|BGHDH14_bgh04268			
jgi|Golci1|1829882|fgenesh1_kg.84_#_31_#_TRINITY_DN339_	jgi|Blugr1|19679|BGHDH14_bgh00982			
jgi|Golci1|1829896|fgenesh1_kg.84_#_45_#_TRINITY_DN1035	jgi|Blugr1|19677|BGHDH14_bgh03901			
jgi|Golci1|1829990|fgenesh1_kg.85_#_61_#_TRINITY_DN8485	jgi|Blugr1|19676|BGHDH14_bghG006623000001001			
jgi|Golci1|1830001|fgenesh1_kg.85_#_72_#_TRINITY_DN1470	jgi|Blugr1|19675|BGHDH14_bgh03874			

Gc	Bgh	Bgt	En	Go
jgi|Golci1|1830139|fgenesh1_kg.86_#_78_#_TRINITY_DN1238	jgi|Blugr1|19648|BGHDH14_bgh00406			
jgi|Golci1|1830203|fgenesh1_kg.86_#_142_#_TRINITY_DN184	jgi|Blugr1|19616|BGHDH14_bgh00772			
jgi|Golci1|1830243|fgenesh1_kg.86_#_182_#_TRINITY_DN691	jgi|Blugr1|19613|BGHDH14_bgh01675			
jgi|Golci1|1830255|fgenesh1_kg.87_#_10_#_TRINITY_DN1106	jgi|Blugr1|19603|BGHDH14_bgh01918			
jgi|Golci1|1830297|fgenesh1_kg.87_#_52_#_TRINITY_DN2116	jgi|Blugr1|19569|BGHDH14_bgh03691			
jgi|Golci1|1830300|fgenesh1_kg.87_#_55_#_TRINITY_DN7549	jgi|Blugr1|19566|BGHDH14_bgh00458			
jgi|Golci1|1830338|fgenesh1_kg.87_#_93_#_TRINITY_DN1909	jgi|Blugr1|19559|BGHDH14_bgh01537			
jgi|Golci1|1830432|fgenesh1_kg.88_#_78_#_TRINITY_DN1844	jgi|Blugr1|19532|BGHDH14_bghG004598000001001			
jgi|Golci1|1830436|fgenesh1_kg.88_#_82_#_TRINITY_DN5932	jgi|Blugr1|19525|BGHDH14_bgh06071			
jgi|Golci1|1830582|fgenesh1_kg.88_#_228_#_TRINITY_DN138	jgi|Blugr1|19505|BGHDH14_bgh01087			
jgi|Golci1|1830622|fgenesh1_kg.89_#_21_#_TRINITY_DN8497	jgi|Blugr1|19481|BGHDH14_bgh04366			
jgi|Golci1|1830648|fgenesh1_kg.89_#_47_#_TRINITY_DN1976	jgi|Blugr1|19456|BGHDH14_bgh06956			
jgi|Golci1|1830679|fgenesh1_kg.89_#_78_#_TRINITY_DN1392	jgi|Blugr1|19452|BGHDH14_bgh05314			
jgi|Golci1|1830686|fgenesh1_kg.89_#_85_#_TRINITY_DN9184	jgi|Blugr1|19427|BGHDH14_bgh03164			
jgi|Golci1|1830704|fgenesh1_kg.89_#_103_#_TRINITY_DN609	jgi|Blugr1|19424|BGHDH14_bgh05405			
jgi|Golci1|1830726|fgenesh1_kg.89_#_125_#_TRINITY_DN183	jgi|Blugr1|19397|BGHDH14_bgh03782			
jgi|Golci1|1830737|fgenesh1_kg.89_#_136_#_TRINITY_DN853	jgi|Blugr1|19387|BGHDH14_bgh02286			
jgi|Golci1|1830772|fgenesh1_kg.90_#_20_#_TRINITY_DN1510	jgi|Blugr1|19362|BGHDH14_bghG007601000001001			
jgi|Golci1|1830782|fgenesh1_kg.90_#_30_#_TRINITY_DN70_c	jgi|Blugr1|19350|BGHDH14_bgh00220			
jgi|Golci1|1830878|fgenesh1_kg.90_#_126_#_TRINITY_DN190	jgi|Blugr1|19348|BGHDH14_bgh03316			
jgi|Golci1|1830882|fgenesh1_kg.90_#_130_#_TRINITY_DN693	jgi|Blugr1|19341|BGHDH14_bgh02877			

Gc	Bgh	Bgt	En	Go
jgi|Golci1|1830887|fgenesh1_kg.90_#_135_#_TRINITY_DN973	jgi|Blugr1|19312|BGHDH14_bgh03534			
jgi|Golci1|1830890|fgenesh1_kg.90_#_138_#_TRINITY_DN210	jgi|Blugr1|19285|BGHDH14_bghG006513000001001			
jgi|Golci1|1830926|fgenesh1_kg.91_#_30_#_TRINITY_DN1971	jgi|Blugr1|19282|BGHDH14_bghG006513000002001			
jgi|Golci1|1830972|fgenesh1_kg.91_#_76_#_TRINITY_DN1314	jgi|Blugr1|19274|BGHDH14_bgh04078			
jgi|Golci1|1831018|fgenesh1_kg.91_#_122_#_TRINITY_DN193	jgi|Blugr1|19273|BGHDH14_bgh00249			
jgi|Golci1|1831023|fgenesh1_kg.91_#_127_#_TRINITY_DN193	jgi|Blugr1|19272|BGHDH14_bghG006508000001001			
jgi|Golci1|1831039|fgenesh1_kg.91_#_143_#_TRINITY_DN182	jgi|Blugr1|19271|BGHDH14_bgh04046			
jgi|Golci1|1831069|fgenesh1_kg.92_#_21_#_TRINITY_DN1388	jgi|Blugr1|19268|BGHDH14_bghG006495000001001			
jgi|Golci1|1831082|fgenesh1_kg.92_#_34_#_TRINITY_DN1934	jgi|Blugr1|19265|BGHDH14_bgh05412			
jgi|Golci1|1831087|fgenesh1_kg.92_#_39_#_TRINITY_DN7075	jgi|Blugr1|19263|BGHDH14_bgh04225			
jgi|Golci1|1831109|fgenesh1_kg.92_#_61_#_TRINITY_DN1218	jgi|Blugr1|19262|BGHDH14_bgh05491			
jgi|Golci1|1831116|fgenesh1_kg.92_#_68_#_TRINITY_DN2079	jgi|Blugr1|19261|BGHDH14_bgh05086			
jgi|Golci1|1831171|fgenesh1_kg.92_#_123_#_TRINITY_DN156	jgi|Blugr1|19260|BGHDH14_bgh04077			
jgi|Golci1|1831364|fgenesh1_kg.95_#_33_#_TRINITY_DN5530	jgi|Blugr1|19258|BGHDH14_bgh04027			
jgi|Golci1|1831374|fgenesh1_kg.95_#_43_#_TRINITY_DN1917	jgi|Blugr1|19256|BGHDH14_bgh06727			
jgi|Golci1|1831419|fgenesh1_kg.95_#_88_#_TRINITY_DN1762	jgi|Blugr1|19254|BGHDH14_bgh05609			
jgi|Golci1|1831455|fgenesh1_kg.96_#_14_#_TRINITY_DN1033	jgi|Blugr1|19253|BGHDH14_bghG009555000001001			
jgi|Golci1|1831497|fgenesh1_kg.96_#_56_#_TRINITY_DN2058	jgi|Blugr1|19250|BGHDH14_bghG009020000001001			
jgi|Golci1|1831570|fgenesh1_kg.96_#_129_#_TRINITY_DN113	jgi|Blugr1|19249|BGHDH14_bghG008908000001001			
jgi|Golci1|1831630|fgenesh1_kg.97_#_53_#_TRINITY_DN1865	jgi|Blugr1|19247|BGHDH14_bgh03579			
jgi|Golci1|1831687|fgenesh1_kg.98_#_22_#_TRINITY_DN2025	jgi|Blugr1|19246|BGHDH14_bgh03575			

Gc	Bgh	Bgt	En	Go
jgi|Golci1|1831692|fgenesh1_kg.98_#_27_#_TRINITY_DN1415	jgi|Blugr1|19245|BGHDH14_bgh03572			
jgi|Golci1|1831764|fgenesh1_kg.98_#_99_#_TRINITY_DN1552	jgi|Blugr1|19237|BGHDH14_bgh06532			
jgi|Golci1|1831767|fgenesh1_kg.98_#_102_#_TRINITY_DN155	jgi|Blugr1|19236|BGHDH14_bghG009249000001001			
jgi|Golci1|1831833|fgenesh1_kg.99_#_37_#_TRINITY_DN1760	jgi|Blugr1|19234|BGHDH14_bghG008002000002001			
jgi|Golci1|1831885|fgenesh1_kg.99_#_89_#_TRINITY_DN1912	jgi|Blugr1|19233|BGHDH14_bghG008885000001001			
jgi|Golci1|1831977|fgenesh1_kg.100_#_67_#_TRINITY_DN134	jgi|Blugr1|19222|BGHDH14_bgh00288			
jgi|Golci1|1832040|fgenesh1_kg.100_#_130_#_TRINITY_DN35	jgi|Blugr1|19220|BGHDH14_bgh03803			
jgi|Golci1|1832048|fgenesh1_kg.101_#_7_#_TRINITY_DN1854	jgi|Blugr1|19218|BGHDH14_bgh06169			
jgi|Golci1|1832286|fgenesh1_kg.103_#_1_#_TRINITY_DN1504	jgi|Blugr1|19215|BGHDH14_bgh02874			
jgi|Golci1|1832309|fgenesh1_kg.103_#_24_#_TRINITY_DN148	jgi|Blugr1|19212|BGHDH14_bgh06494			
jgi|Golci1|1832362|fgenesh1_kg.103_#_77_#_TRINITY_DN180	jgi|Blugr1|19211|BGHDH14_bghG008560000001001			
jgi|Golci1|1832388|fgenesh1_kg.103_#_103_#_TRINITY_DN17	jgi|Blugr1|19206|BGHDH14_bgh06518			
jgi|Golci1|1832463|fgenesh1_kg.104_#_40_#_TRINITY_DN182	jgi|Blugr1|19198|BGHDH14_bgh02928			
jgi|Golci1|1832485|fgenesh1_kg.104_#_62_#_TRINITY_DN196	jgi|Blugr1|19191|BGHDH14_bgh01613			
jgi|Golci1|1832539|fgenesh1_kg.104_#_116_#_TRINITY_DN11	jgi|Blugr1|19189|BGHDH14_bghG008117000001001			
jgi|Golci1|1832543|fgenesh1_kg.105_#_2_#_TRINITY_DN1187	jgi|Blugr1|19188|BGHDH14_bgh06517			
jgi|Golci1|1832582|fgenesh1_kg.105_#_41_#_TRINITY_DN190	jgi|Blugr1|19184|BGHDH14_bghG007788000001001			
jgi|Golci1|1832687|fgenesh1_kg.106_#_4_#_TRINITY_DN4980	jgi|Blugr1|19183|BGHDH14_bgh06413			
jgi|Golci1|1832704|fgenesh1_kg.106_#_21_#_TRINITY_DN164	jgi|Blugr1|19181|BGHDH14_bgh02925			
jgi|Golci1|1832789|fgenesh1_kg.106_#_106_#_TRINITY_DN12	jgi|Blugr1|19172|BGHDH14_bgh03582			
jgi|Golci1|1832791|fgenesh1_kg.106_#_108_#_TRINITY_DN18	jgi|Blugr1|19168|BGHDH14_bgh04083			

Gc	Bgh	Bgt	En	Go
jgi|Golci1|1832795|fgenesh1_kg.107_#_1_#_TRINITY_DN1298	jgi|Blugr1|19166|BGHDH14_bghG013624000001001			
jgi|Golci1|1832806|fgenesh1_kg.107_#_12_#_TRINITY_DN146	jgi|Blugr1|19165|BGHDH14_bgh03677			
jgi|Golci1|1832953|fgenesh1_kg.107_#_159_#_TRINITY_DN17	jgi|Blugr1|19163|BGHDH14_bgh05792			
jgi|Golci1|1833114|fgenesh1_kg.108_#_138_#_TRINITY_DN17	jgi|Blugr1|19159|BGHDH14_bghG009691000001001			
jgi|Golci1|1833117|fgenesh1_kg.108_#_141_#_TRINITY_DN75	jgi|Blugr1|19155|BGHDH14_bgh03376			
jgi|Golci1|1833119|fgenesh1_kg.108_#_143_#_TRINITY_DN18	jgi|Blugr1|19153|BGHDH14_bghG008575000001001			
jgi|Golci1|1833160|fgenesh1_kg.109_#_37_#_TRINITY_DN176	jgi|Blugr1|19149|BGHDH14_bghG008605000001001			
jgi|Golci1|1833231|fgenesh1_kg.110_#_10_#_TRINITY_DN193				
jgi|Golci1|1833286|fgenesh1_kg.110_#_65_#_TRINITY_DN136				
jgi|Golci1|1833288|fgenesh1_kg.110_#_67_#_TRINITY_DN157				
jgi|Golci1|1833347|fgenesh1_kg.110_#_126_#_TRINITY_DN20				
jgi|Golci1|1833351|fgenesh1_kg.110_#_130_#_TRINITY_DN18				
jgi|Golci1|1833530|fgenesh1_kg.112_#_10_#_TRINITY_DN125				
jgi|Golci1|1833555|fgenesh1_kg.112_#_35_#_TRINITY_DN112				
jgi|Golci1|1833577|fgenesh1_kg.112_#_57_#_TRINITY_DN193				
jgi|Golci1|1833586|fgenesh1_kg.112_#_66_#_TRINITY_DN176				
jgi|Golci1|1833599|fgenesh1_kg.112_#_79_#_TRINITY_DN185				
jgi|Golci1|1833673|fgenesh1_kg.112_#_153_#_TRINITY_DN21				
jgi|Golci1|1833683|fgenesh1_kg.113_#_10_#_TRINITY_DN104				
jgi|Golci1|1833918|fgenesh1_kg.114_#_101_#_TRINITY_DN17				
jgi|Golci1|1833941|fgenesh1_kg.115_#_8_#_TRINITY_DN1734				
jgi|Golci1|1833973|fgenesh1_kg.115_#_40_#_TRINITY_DN177				
jgi|Golci1|1833976|fgenesh1_kg.115_#_43_#_TRINITY_DN143				
jgi|Golci1|1833979|fgenesh1_kg.115_#_46_#_TRINITY_DN175				
jgi|Golci1|1833998|fgenesh1_kg.115_#_65_#_TRINITY_DN259				
jgi|Golci1|1834005|fgenesh1_kg.115_#_72_#_TRINITY_DN148				
jgi|Golci1|1834166|fgenesh1_kg.116_#_88_#_TRINITY_DN190				
jgi|Golci1|1834335|fgenesh1_kg.117_#_113_#_TRINITY_DN19				

Gc	Bgh	Bgt	En	Go
jgi|Golci1|1834385|fgenesh1_kg.118_#_16_#_TRINITY_DN168				
jgi|Golci1|1834403|fgenesh1_kg.118_#_34_#_TRINITY_DN207				
jgi|Golci1|1834502|fgenesh1_kg.118_#_133_#_TRINITY_DN55				
jgi|Golci1|1834526|fgenesh1_kg.118_#_157_#_TRINITY_DN19				
jgi|Golci1|1834596|fgenesh1_kg.119_#_33_#_TRINITY_DN190				
jgi|Golci1|1834599|fgenesh1_kg.119_#_36_#_TRINITY_DN773				
jgi|Golci1|1834637|fgenesh1_kg.119_#_74_#_TRINITY_DN187				
jgi|Golci1|1834689|fgenesh1_kg.119_#_126_#_TRINITY_DN29				
jgi|Golci1|1834832|fgenesh1_kg.120_#_67_#_TRINITY_DN161				
jgi|Golci1|1834873|fgenesh1_kg.120_#_108_#_TRINITY_DN17				
jgi|Golci1|1834874|fgenesh1_kg.120_#_109_#_TRINITY_DN10				
jgi|Golci1|1834906|fgenesh1_kg.120_#_141_#_TRINITY_DN59				
jgi|Golci1|1835013|fgenesh1_kg.121_#_51_#_TRINITY_DN135				
jgi|Golci1|1835113|fgenesh1_kg.121_#_151_#_TRINITY_DN20				
jgi|Golci1|1835118|fgenesh1_kg.121_#_156_#_TRINITY_DN20				
jgi|Golci1|1835122|fgenesh1_kg.121_#_160_#_TRINITY_DN10				
jgi|Golci1|1835287|fgenesh1_kg.123_#_24_#_TRINITY_DN190				
jgi|Golci1|1835309|fgenesh1_kg.123_#_46_#_TRINITY_DN204				
jgi|Golci1|1835369|fgenesh1_kg.124_#_14_#_TRINITY_DN939				
jgi|Golci1|1835397|fgenesh1_kg.124_#_42_#_TRINITY_DN197				
jgi|Golci1|1835483|fgenesh1_kg.125_#_25_#_TRINITY_DN189				
jgi|Golci1|1835510|fgenesh1_kg.125_#_52_#_TRINITY_DN175				
jgi|Golci1|1835582|fgenesh1_kg.125_#_124_#_TRINITY_DN16				
jgi|Golci1|1835615|fgenesh1_kg.125_#_157_#_TRINITY_DN13				
jgi|Golci1|1835666|fgenesh1_kg.126_#_50_#_TRINITY_DN843				
jgi|Golci1|1835797|fgenesh1_kg.128_#_66_#_TRINITY_DN177				
jgi|Golci1|1835855|fgenesh1_kg.129_#_8_#_TRINITY_DN1932				
jgi|Golci1|1835862|fgenesh1_kg.129_#_15_#_TRINITY_DN193				
jgi|Golci1|1835897|fgenesh1_kg.129_#_50_#_TRINITY_DN248				
jgi|Golci1|1835924|fgenesh1_kg.129_#_77_#_TRINITY_DN144				
jgi|Golci1|1836088|fgenesh1_kg.130_#_139_#_TRINITY_DN32				

<table>
<tr><th>Gc</th><th>Bgh</th><th>Bgt</th><th>En</th><th>Go</th></tr>
<tr><td colspan="2">jgi|Golci1|1836097|fgenesh1_kg.131_#_9_#_TRINITY_DN1659</td><td></td><td></td><td></td></tr>
<tr><td colspan="2">jgi|Golci1|1836117|fgenesh1_kg.131_#_29_#_TRINITY_DN105</td><td></td><td></td><td></td></tr>
<tr><td colspan="2">jgi|Golci1|1836148|fgenesh1_kg.131_#_60_#_TRINITY_DN154</td><td></td><td></td><td></td></tr>
<tr><td colspan="2">jgi|Golci1|1836170|fgenesh1_kg.131_#_82_#_TRINITY_DN138</td><td></td><td></td><td></td></tr>
<tr><td colspan="2">jgi|Golci1|1836343|fgenesh1_kg.133_#_97_#_TRINITY_DN453</td><td></td><td></td><td></td></tr>
<tr><td colspan="2">jgi|Golci1|1836364|fgenesh1_kg.133_#_118_#_TRINITY_DN18</td><td></td><td></td><td></td></tr>
<tr><td colspan="2">jgi|Golci1|1836526|fgenesh1_kg.134_#_122_#_TRINITY_DN11</td><td></td><td></td><td></td></tr>
<tr><td colspan="2">jgi|Golci1|1836585|fgenesh1_kg.135_#_56_#_TRINITY_DN106</td><td></td><td></td><td></td></tr>
<tr><td colspan="2">jgi|Golci1|1836696|fgenesh1_kg.136_#_60_#_TRINITY_DN145</td><td></td><td></td><td></td></tr>
<tr><td colspan="2">jgi|Golci1|1836757|fgenesh1_kg.137_#_11_#_TRINITY_DN108</td><td></td><td></td><td></td></tr>
<tr><td colspan="2">jgi|Golci1|1836876|fgenesh1_kg.137_#_130_#_TRINITY_DN19</td><td></td><td></td><td></td></tr>
<tr><td colspan="2">jgi|Golci1|1836930|fgenesh1_kg.137_#_184_#_TRINITY_DN20</td><td></td><td></td><td></td></tr>
<tr><td colspan="2">jgi|Golci1|1836950|fgenesh1_kg.138_#_16_#_TRINITY_DN115</td><td></td><td></td><td></td></tr>
<tr><td colspan="2">jgi|Golci1|1837005|fgenesh1_kg.138_#_71_#_TRINITY_DN195</td><td></td><td></td><td></td></tr>
<tr><td colspan="2">jgi|Golci1|1837054|fgenesh1_kg.139_#_17_#_TRINITY_DN537</td><td></td><td></td><td></td></tr>
<tr><td colspan="2">jgi|Golci1|1837070|fgenesh1_kg.139_#_33_#_TRINITY_DN170</td><td></td><td></td><td></td></tr>
<tr><td colspan="2">jgi|Golci1|1837096|fgenesh1_kg.139_#_59_#_TRINITY_DN151</td><td></td><td></td><td></td></tr>
<tr><td colspan="2">jgi|Golci1|1837148|fgenesh1_kg.140_#_46_#_TRINITY_DN187</td><td></td><td></td><td></td></tr>
<tr><td colspan="2">jgi|Golci1|1837153|fgenesh1_kg.140_#_51_#_TRINITY_DN174</td><td></td><td></td><td></td></tr>
<tr><td colspan="2">jgi|Golci1|1837171|fgenesh1_kg.140_#_69_#_TRINITY_DN125</td><td></td><td></td><td></td></tr>
<tr><td colspan="2">jgi|Golci1|1837183|fgenesh1_kg.140_#_81_#_TRINITY_DN329</td><td></td><td></td><td></td></tr>
<tr><td colspan="2">jgi|Golci1|1837223|fgenesh1_kg.140_#_121_#_TRINITY_DN77</td><td></td><td></td><td></td></tr>
<tr><td colspan="2">jgi|Golci1|1837265|fgenesh1_kg.141_#_40_#_TRINITY_DN116</td><td></td><td></td><td></td></tr>
<tr><td colspan="2">jgi|Golci1|1837351|fgenesh1_kg.141_#_126_#_TRINITY_DN18</td><td></td><td></td><td></td></tr>
<tr><td colspan="2">jgi|Golci1|1837353|fgenesh1_kg.141_#_128_#_TRINITY_DN42</td><td></td><td></td><td></td></tr>
<tr><td colspan="2">jgi|Golci1|1837379|fgenesh1_kg.141_#_154_#_TRINITY_DN20</td><td></td><td></td><td></td></tr>
<tr><td colspan="2">jgi|Golci1|1837446|fgenesh1_kg.142_#_1_#_TRINITY_DN1921</td><td></td><td></td><td></td></tr>
<tr><td colspan="2">jgi|Golci1|1837499|fgenesh1_kg.142_#_54_#_TRINITY_DN197</td><td></td><td></td><td></td></tr>
<tr><td colspan="2">jgi|Golci1|1837558|fgenesh1_kg.143_#_23_#_TRINITY_DN603</td><td></td><td></td><td></td></tr>
<tr><td colspan="2">jgi|Golci1|1837602|fgenesh1_kg.143_#_67_#_TRINITY_DN194</td><td></td><td></td><td></td></tr>
<tr><td colspan="2">jgi|Golci1|1837709|fgenesh1_kg.144_#_48_#_TRINITY_DN191</td><td></td><td></td><td></td></tr>
</table>

Gc	Bgh	Bgt	En	Go
jgi|Golci1|1837793|fgenesh1_kg.145_#_3_#_TRINITY_DN2001				
jgi|Golci1|1837888|fgenesh1_kg.145_#_98_#_TRINITY_DN280				
jgi|Golci1|1837890|fgenesh1_kg.145_#_100_#_TRINITY_DN17				
jgi|Golci1|1837896|fgenesh1_kg.145_#_106_#_TRINITY_DN10				
jgi|Golci1|1837960|fgenesh1_kg.146_#_45_#_TRINITY_DN148				
jgi|Golci1|1838023|fgenesh1_kg.147_#_17_#_TRINITY_DN568				
jgi|Golci1|1838064|fgenesh1_kg.147_#_58_#_TRINITY_DN148				
jgi|Golci1|1838164|fgenesh1_kg.148_#_28_#_TRINITY_DN175				
jgi|Golci1|1838171|fgenesh1_kg.148_#_35_#_TRINITY_DN337				
jgi|Golci1|1838207|fgenesh1_kg.148_#_71_#_TRINITY_DN173				
jgi|Golci1|1838249|fgenesh1_kg.148_#_113_#_TRINITY_DN19				
jgi|Golci1|1838285|fgenesh1_kg.149_#_36_#_TRINITY_DN847				
jgi|Golci1|1838347|fgenesh1_kg.149_#_98_#_TRINITY_DN235				
jgi|Golci1|1838489|fgenesh1_kg.150_#_104_#_TRINITY_DN26				
jgi|Golci1|1838643|fgenesh1_kg.152_#_29_#_TRINITY_DN203				
jgi|Golci1|1838667|fgenesh1_kg.152_#_53_#_TRINITY_DN177				
jgi|Golci1|1838796|fgenesh1_kg.153_#_41_#_TRINITY_DN195				
jgi|Golci1|1838867|fgenesh1_kg.153_#_112_#_TRINITY_DN23				
jgi|Golci1|1838907|fgenesh1_kg.153_#_152_#_TRINITY_DN18				
jgi|Golci1|1838919|fgenesh1_kg.153_#_164_#_TRINITY_DN18				
jgi|Golci1|1838928|fgenesh1_kg.153_#_173_#_TRINITY_DN17				
jgi|Golci1|1839011|fgenesh1_kg.154_#_77_#_TRINITY_DN175				
jgi|Golci1|1839035|fgenesh1_kg.154_#_101_#_TRINITY_DN91				
jgi|Golci1|1839044|fgenesh1_kg.155_#_9_#_TRINITY_DN1480				
jgi|Golci1|1839070|fgenesh1_kg.155_#_35_#_TRINITY_DN184				
jgi|Golci1|1839138|fgenesh1_kg.155_#_103_#_TRINITY_DN17				
jgi|Golci1|1839148|fgenesh1_kg.156_#_2_#_TRINITY_DN2045				
jgi|Golci1|1839149|fgenesh1_kg.156_#_3_#_TRINITY_DN2045				
jgi|Golci1|1839155|fgenesh1_kg.156_#_9_#_TRINITY_DN2045				
jgi|Golci1|1839190|fgenesh1_kg.156_#_44_#_TRINITY_DN171				
jgi|Golci1|1839208|fgenesh1_kg.157_#_4_#_TRINITY_DN1923				

Gc	Bgh	Bgt	En	Go
jgi|Golci1|1839235|fgenesh1_kg.157_#_31_#_TRINITY_DN179				
jgi|Golci1|1839296|fgenesh1_kg.158_#_20_#_TRINITY_DN111				
jgi|Golci1|1839349|fgenesh1_kg.158_#_73_#_TRINITY_DN180				
jgi|Golci1|1839432|fgenesh1_kg.159_#_73_#_TRINITY_DN399				
jgi|Golci1|1839497|fgenesh1_kg.160_#_59_#_TRINITY_DN183				
jgi|Golci1|1839576|fgenesh1_kg.161_#_48_#_TRINITY_DN121				
jgi|Golci1|1839648|fgenesh1_kg.162_#_28_#_TRINITY_DN554				
jgi|Golci1|1839735|fgenesh1_kg.163_#_18_#_TRINITY_DN189				
jgi|Golci1|1839762|fgenesh1_kg.163_#_45_#_TRINITY_DN445				
jgi|Golci1|1839766|fgenesh1_kg.163_#_49_#_TRINITY_DN116				
jgi|Golci1|1839855|fgenesh1_kg.165_#_2_#_TRINITY_DN1581				
jgi|Golci1|1839970|fgenesh1_kg.167_#_1_#_TRINITY_DN1517				
jgi|Golci1|1840047|fgenesh1_kg.168_#_1_#_TRINITY_DN1621				
jgi|Golci1|1840061|fgenesh1_kg.168_#_15_#_TRINITY_DN190				
jgi|Golci1|1840074|fgenesh1_kg.168_#_28_#_TRINITY_DN235				
jgi|Golci1|1840114|fgenesh1_kg.168_#_68_#_TRINITY_DN223				
jgi|Golci1|1840128|fgenesh1_kg.168_#_82_#_TRINITY_DN207				
jgi|Golci1|1840186|fgenesh1_kg.168_#_140_#_TRINITY_DN22				
jgi|Golci1|1840210|fgenesh1_kg.169_#_16_#_TRINITY_DN196				
jgi|Golci1|1840239|fgenesh1_kg.169_#_45_#_TRINITY_DN191				
jgi|Golci1|1840418|fgenesh1_kg.170_#_29_#_TRINITY_DN156				
jgi|Golci1|1840435|fgenesh1_kg.170_#_46_#_TRINITY_DN104				
jgi|Golci1|1840443|fgenesh1_kg.170_#_54_#_TRINITY_DN466				
jgi|Golci1|1840451|fgenesh1_kg.170_#_62_#_TRINITY_DN189				
jgi|Golci1|1840516|fgenesh1_kg.171_#_64_#_TRINITY_DN143				
jgi|Golci1|1840524|fgenesh1_kg.171_#_72_#_TRINITY_DN208				
jgi|Golci1|1840536|fgenesh1_kg.172_#_6_#_TRINITY_DN1254				
jgi|Golci1|1840564|fgenesh1_kg.172_#_34_#_TRINITY_DN203				
jgi|Golci1|1840591|fgenesh1_kg.172_#_61_#_TRINITY_DN176				
jgi|Golci1|1840741|fgenesh1_kg.174_#_5_#_TRINITY_DN1937				
jgi|Golci1|1840768|fgenesh1_kg.174_#_32_#_TRINITY_DN137				

Gc	Bgh	Bgt	En	Go
jgi|Golci1|1840828|fgenesh1_kg.174_#_92_#_TRINITY_DN193				
jgi|Golci1|1840834|fgenesh1_kg.174_#_98_#_TRINITY_DN193				
jgi|Golci1|1840902|fgenesh1_kg.175_#_42_#_TRINITY_DN323				
jgi|Golci1|1840959|fgenesh1_kg.175_#_99_#_TRINITY_DN259				
jgi|Golci1|1840974|fgenesh1_kg.175_#_114_#_TRINITY_DN21				
jgi|Golci1|1841031|fgenesh1_kg.175_#_171_#_TRINITY_DN14				
jgi|Golci1|1841183|fgenesh1_kg.177_#_21_#_TRINITY_DN749				
jgi|Golci1|1841221|fgenesh1_kg.177_#_59_#_TRINITY_DN193				
jgi|Golci1|1841226|fgenesh1_kg.177_#_64_#_TRINITY_DN193				
jgi|Golci1|1841297|fgenesh1_kg.178_#_34_#_TRINITY_DN171				
jgi|Golci1|1841404|fgenesh1_kg.180_#_13_#_TRINITY_DN188				
jgi|Golci1|1841415|fgenesh1_kg.180_#_24_#_TRINITY_DN137				
jgi|Golci1|1841438|fgenesh1_kg.180_#_47_#_TRINITY_DN189				
jgi|Golci1|1841551|fgenesh1_kg.181_#_65_#_TRINITY_DN164				
jgi|Golci1|1841637|fgenesh1_kg.182_#_71_#_TRINITY_DN191				
jgi|Golci1|1841639|fgenesh1_kg.182_#_73_#_TRINITY_DN191				
jgi|Golci1|1841646|fgenesh1_kg.182_#_80_#_TRINITY_DN169				
jgi|Golci1|1841779|fgenesh1_kg.182_#_213_#_TRINITY_DN18				
jgi|Golci1|1841783|fgenesh1_kg.182_#_217_#_TRINITY_DN18				
jgi|Golci1|1841809|fgenesh1_kg.183_#_26_#_TRINITY_DN172				
jgi|Golci1|1841843|fgenesh1_kg.184_#_30_#_TRINITY_DN257				
jgi|Golci1|1841845|fgenesh1_kg.184_#_32_#_TRINITY_DN337				
jgi|Golci1|1841881|fgenesh1_kg.185_#_1_#_TRINITY_DN9185				
jgi|Golci1|1841892|fgenesh1_kg.185_#_12_#_TRINITY_DN183				
jgi|Golci1|1841928|fgenesh1_kg.185_#_48_#_TRINITY_DN128				
jgi|Golci1|1841958|fgenesh1_kg.185_#_78_#_TRINITY_DN183				
jgi|Golci1|1842070|fgenesh1_kg.187_#_56_#_TRINITY_DN172				
jgi|Golci1|1842098|fgenesh1_kg.187_#_84_#_TRINITY_DN136				
jgi|Golci1|1842155|fgenesh1_kg.188_#_34_#_TRINITY_DN204				
jgi|Golci1|1842249|fgenesh1_kg.189_#_68_#_TRINITY_DN184				
jgi|Golci1|1842260|fgenesh1_kg.190_#_10_#_TRINITY_DN176				

Gc	Bgh	Bgt	En	Go
jgi|Golci1|1842294|fgenesh1_kg.191_#_31_#_TRINITY_DN211				
jgi|Golci1|1842347|fgenesh1_kg.192_#_11_#_TRINITY_DN211				
jgi|Golci1|1842371|fgenesh1_kg.192_#_35_#_TRINITY_DN162				
jgi|Golci1|1842389|fgenesh1_kg.193_#_3_#_TRINITY_DN9277				
jgi|Golci1|1842400|fgenesh1_kg.193_#_14_#_TRINITY_DN154				
jgi|Golci1|1842410|fgenesh1_kg.193_#_24_#_TRINITY_DN162				
jgi|Golci1|1842411|fgenesh1_kg.193_#_25_#_TRINITY_DN282				
jgi|Golci1|1842439|fgenesh1_kg.194_#_18_#_TRINITY_DN145				
jgi|Golci1|1842477|fgenesh1_kg.194_#_56_#_TRINITY_DN107				
jgi|Golci1|1842482|fgenesh1_kg.195_#_4_#_TRINITY_DN1843				
jgi|Golci1|1842485|fgenesh1_kg.195_#_7_#_TRINITY_DN1843				
jgi|Golci1|1842497|fgenesh1_kg.195_#_19_#_TRINITY_DN186				
jgi|Golci1|1842540|fgenesh1_kg.196_#_8_#_TRINITY_DN3297				
jgi|Golci1|1842557|fgenesh1_kg.196_#_25_#_TRINITY_DN205				
jgi|Golci1|1842659|fgenesh1_kg.198_#_40_#_TRINITY_DN121				
jgi|Golci1|1842744|fgenesh1_kg.199_#_57_#_TRINITY_DN111				
jgi|Golci1|1842752|fgenesh1_kg.200_#_7_#_TRINITY_DN1880				
jgi|Golci1|1842778|fgenesh1_kg.200_#_33_#_TRINITY_DN188				
jgi|Golci1|1842817|fgenesh1_kg.200_#_72_#_TRINITY_DN188				
jgi|Golci1|1842879|fgenesh1_kg.201_#_57_#_TRINITY_DN122				
jgi|Golci1|1842907|fgenesh1_kg.201_#_85_#_TRINITY_DN202				
jgi|Golci1|1843080|fgenesh1_kg.203_#_12_#_TRINITY_DN102				
jgi|Golci1|1843092|fgenesh1_kg.204_#_1_#_TRINITY_DN2370				
jgi|Golci1|1843153|fgenesh1_kg.205_#_2_#_TRINITY_DN3047				
jgi|Golci1|1843167|fgenesh1_kg.205_#_16_#_TRINITY_DN500				
jgi|Golci1|1843169|fgenesh1_kg.205_#_18_#_TRINITY_DN168				
jgi|Golci1|1843178|fgenesh1_kg.205_#_27_#_TRINITY_DN207				
jgi|Golci1|1843201|fgenesh1_kg.205_#_50_#_TRINITY_DN200				
jgi|Golci1|1843259|fgenesh1_kg.206_#_32_#_TRINITY_DN141				
jgi|Golci1|1843277|fgenesh1_kg.207_#_2_#_TRINITY_DN1964				
jgi|Golci1|1843364|fgenesh1_kg.207_#_89_#_TRINITY_DN125				

Gc	Bgh	Bgt	En	Go
jgi|Golci1|1843392|fgenesh1_kg.208_#_21_#_TRINITY_DN176				
jgi|Golci1|1843408|fgenesh1_kg.208_#_37_#_TRINITY_DN209				
jgi|Golci1|1843579|fgenesh1_kg.210_#_27_#_TRINITY_DN177				
jgi|Golci1|1843633|fgenesh1_kg.211_#_33_#_TRINITY_DN209				
jgi|Golci1|1843635|fgenesh1_kg.211_#_35_#_TRINITY_DN209				
jgi|Golci1|1843812|fgenesh1_kg.214_#_44_#_TRINITY_DN193				
jgi|Golci1|1843818|fgenesh1_kg.214_#_50_#_TRINITY_DN193				
jgi|Golci1|1843848|fgenesh1_kg.215_#_6_#_TRINITY_DN2101				
jgi|Golci1|1844001|fgenesh1_kg.217_#_35_#_TRINITY_DN172				
jgi|Golci1|1844155|fgenesh1_kg.219_#_55_#_TRINITY_DN155				
jgi|Golci1|1844288|fgenesh1_kg.221_#_72_#_TRINITY_DN167				
jgi|Golci1|1844441|fgenesh1_kg.222_#_44_#_TRINITY_DN193				
jgi|Golci1|1844448|fgenesh1_kg.222_#_51_#_TRINITY_DN193				
jgi|Golci1|1844611|fgenesh1_kg.224_#_22_#_TRINITY_DN197				
jgi|Golci1|1844652|fgenesh1_kg.225_#_1_#_TRINITY_DN1492				
jgi|Golci1|1844708|fgenesh1_kg.226_#_2_#_TRINITY_DN1942				
jgi|Golci1|1844712|fgenesh1_kg.226_#_6_#_TRINITY_DN1072				
jgi|Golci1|1844832|fgenesh1_kg.230_#_5_#_TRINITY_DN1760				
jgi|Golci1|1844841|fgenesh1_kg.230_#_14_#_TRINITY_DN313				
jgi|Golci1|1844856|fgenesh1_kg.230_#_29_#_TRINITY_DN102				
jgi|Golci1|1844978|fgenesh1_kg.232_#_46_#_TRINITY_DN112				
jgi|Golci1|1844981|fgenesh1_kg.232_#_49_#_TRINITY_DN138				
jgi|Golci1|1845012|fgenesh1_kg.233_#_17_#_TRINITY_DN495				
jgi|Golci1|1845017|fgenesh1_kg.233_#_22_#_TRINITY_DN699				
jgi|Golci1|1845050|fgenesh1_kg.234_#_4_#_TRINITY_DN1183				
jgi|Golci1|1845073|fgenesh1_kg.234_#_27_#_TRINITY_DN103				
jgi|Golci1|1845175|fgenesh1_kg.236_#_22_#_TRINITY_DN154				
jgi|Golci1|1845177|fgenesh1_kg.236_#_24_#_TRINITY_DN154				
jgi|Golci1|1845199|fgenesh1_kg.237_#_14_#_TRINITY_DN101				
jgi|Golci1|1845265|fgenesh1_kg.239_#_6_#_TRINITY_DN2104				
jgi|Golci1|1845283|fgenesh1_kg.239_#_24_#_TRINITY_DN164				

Gc	Bgh	Bgt	En	Go
jgi|Golci1|1845292|fgenesh1_kg.239_#_33_#_TRINITY_DN197				
jgi|Golci1|1845309|fgenesh1_kg.239_#_50_#_TRINITY_DN105				
jgi|Golci1|1845359|fgenesh1_kg.240_#_40_#_TRINITY_DN113				
jgi|Golci1|1845403|fgenesh1_kg.241_#_43_#_TRINITY_DN148				
jgi|Golci1|1845481|fgenesh1_kg.242_#_49_#_TRINITY_DN195				
jgi|Golci1|1845522|fgenesh1_kg.243_#_4_#_TRINITY_DN1220				
jgi|Golci1|1845528|fgenesh1_kg.243_#_10_#_TRINITY_DN170				
jgi|Golci1|1845583|fgenesh1_kg.244_#_35_#_TRINITY_DN164				
jgi|Golci1|1845730|fgenesh1_kg.246_#_47_#_TRINITY_DN139				
jgi|Golci1|1845899|fgenesh1_kg.249_#_22_#_TRINITY_DN193				
jgi|Golci1|1845905|fgenesh1_kg.249_#_28_#_TRINITY_DN193				
jgi|Golci1|1845963|fgenesh1_kg.250_#_58_#_TRINITY_DN911				
jgi|Golci1|1845971|fgenesh1_kg.250_#_66_#_TRINITY_DN188				
jgi|Golci1|1846062|fgenesh1_kg.252_#_38_#_TRINITY_DN183				
jgi|Golci1|1846104|fgenesh1_kg.253_#_41_#_TRINITY_DN156				
jgi|Golci1|1846209|fgenesh1_kg.255_#_12_#_TRINITY_DN182				
jgi|Golci1|1846220|fgenesh1_kg.255_#_23_#_TRINITY_DN182				
jgi|Golci1|1846232|fgenesh1_kg.255_#_35_#_TRINITY_DN174				
jgi|Golci1|1846264|fgenesh1_kg.256_#_28_#_TRINITY_DN753				
jgi|Golci1|1846266|fgenesh1_kg.256_#_30_#_TRINITY_DN112				
jgi|Golci1|1846350|fgenesh1_kg.257_#_8_#_TRINITY_DN1352				
jgi|Golci1|1846401|fgenesh1_kg.258_#_29_#_TRINITY_DN116				
jgi|Golci1|1846416|fgenesh1_kg.259_#_3_#_TRINITY_DN1187				
jgi|Golci1|1846531|fgenesh1_kg.261_#_37_#_TRINITY_DN209				
jgi|Golci1|1846577|fgenesh1_kg.261_#_83_#_TRINITY_DN171				
jgi|Golci1|1846592|fgenesh1_kg.262_#_12_#_TRINITY_DN415				
jgi|Golci1|1846658|fgenesh1_kg.263_#_45_#_TRINITY_DN200				
jgi|Golci1|1846680|fgenesh1_kg.264_#_20_#_TRINITY_DN122				
jgi|Golci1|1846757|fgenesh1_kg.266_#_2_#_TRINITY_DN1415				
jgi|Golci1|1846764|fgenesh1_kg.266_#_9_#_TRINITY_DN1253				
jgi|Golci1|1846843|fgenesh1_kg.268_#_23_#_TRINITY_DN182				

Gc	Bgh	Bgt	En	Go
jgi|Golci1|1846864|fgenesh1_kg.269_#_19_#_TRINITY_DN190				
jgi|Golci1|1846865|fgenesh1_kg.269_#_20_#_TRINITY_DN190				
jgi|Golci1|1846912|fgenesh1_kg.270_#_8_#_TRINITY_DN1193				
jgi|Golci1|1846914|fgenesh1_kg.270_#_10_#_TRINITY_DN171				
jgi|Golci1|1846916|fgenesh1_kg.270_#_12_#_TRINITY_DN134				
jgi|Golci1|1846931|fgenesh1_kg.270_#_27_#_TRINITY_DN110				
jgi|Golci1|1847069|fgenesh1_kg.271_#_136_#_TRINITY_DN16				
jgi|Golci1|1847070|fgenesh1_kg.271_#_137_#_TRINITY_DN16				
jgi|Golci1|1847104|fgenesh1_kg.272_#_2_#_TRINITY_DN6042				
jgi|Golci1|1847116|fgenesh1_kg.272_#_14_#_TRINITY_DN209				
jgi|Golci1|1847162|fgenesh1_kg.273_#_38_#_TRINITY_DN158				
jgi|Golci1|1847183|fgenesh1_kg.274_#_20_#_TRINITY_DN511				
jgi|Golci1|1847190|fgenesh1_kg.274_#_27_#_TRINITY_DN261				
jgi|Golci1|1847208|fgenesh1_kg.275_#_14_#_TRINITY_DN303				
jgi|Golci1|1847210|fgenesh1_kg.276_#_1_#_TRINITY_DN6029				
jgi|Golci1|1847221|fgenesh1_kg.276_#_12_#_TRINITY_DN202				
jgi|Golci1|1847249|fgenesh1_kg.277_#_28_#_TRINITY_DN209				
jgi|Golci1|1847261|fgenesh1_kg.277_#_40_#_TRINITY_DN111				
jgi|Golci1|1847448|fgenesh1_kg.278_#_167_#_TRINITY_DN18				
jgi|Golci1|1847481|fgenesh1_kg.279_#_3_#_TRINITY_DN1467				
jgi|Golci1|1847529|fgenesh1_kg.279_#_51_#_TRINITY_DN156				
jgi|Golci1|1847576|fgenesh1_kg.280_#_15_#_TRINITY_DN164				
jgi|Golci1|1847581|fgenesh1_kg.280_#_20_#_TRINITY_DN153				
jgi|Golci1|1847632|fgenesh1_kg.281_#_48_#_TRINITY_DN144				
jgi|Golci1|1847650|fgenesh1_kg.282_#_6_#_TRINITY_DN1470				
jgi|Golci1|1847758|fgenesh1_kg.284_#_24_#_TRINITY_DN210				
jgi|Golci1|1847763|fgenesh1_kg.284_#_29_#_TRINITY_DN854				
jgi|Golci1|1847783|fgenesh1_kg.285_#_16_#_TRINITY_DN176				
jgi|Golci1|1847856|fgenesh1_kg.286_#_52_#_TRINITY_DN200				
jgi|Golci1|1847945|fgenesh1_kg.288_#_7_#_TRINITY_DN1690				
jgi|Golci1|1847985|fgenesh1_kg.288_#_47_#_TRINITY_DN146				

Gc	Bgh	Bgt	En	Go
jgi|Golci1|1847989|fgenesh1_kg.288_#_51_#_TRINITY_DN105				
jgi|Golci1|1847992|fgenesh1_kg.288_#_54_#_TRINITY_DN306				
jgi|Golci1|1848042|fgenesh1_kg.289_#_38_#_TRINITY_DN164				
jgi|Golci1|1848088|fgenesh1_kg.290_#_39_#_TRINITY_DN915				
jgi|Golci1|1848138|fgenesh1_kg.292_#_16_#_TRINITY_DN202				
jgi|Golci1|1848150|fgenesh1_kg.292_#_28_#_TRINITY_DN120				
jgi|Golci1|1848194|fgenesh1_kg.294_#_20_#_TRINITY_DN572				
jgi|Golci1|1848251|fgenesh1_kg.296_#_8_#_TRINITY_DN6638				
jgi|Golci1|1848260|fgenesh1_kg.296_#_17_#_TRINITY_DN198				
jgi|Golci1|1848281|fgenesh1_kg.297_#_21_#_TRINITY_DN795				
jgi|Golci1|1848292|fgenesh1_kg.298_#_10_#_TRINITY_DN302				
jgi|Golci1|1848303|fgenesh1_kg.299_#_10_#_TRINITY_DN168				
jgi|Golci1|1848329|fgenesh1_kg.300_#_2_#_TRINITY_DN2154				
jgi|Golci1|1848340|fgenesh1_kg.300_#_13_#_TRINITY_DN577				
jgi|Golci1|1848476|fgenesh1_kg.304_#_24_#_TRINITY_DN161				
jgi|Golci1|1848543|fgenesh1_kg.306_#_14_#_TRINITY_DN194				
jgi|Golci1|1848595|fgenesh1_kg.307_#_8_#_TRINITY_DN1829				
jgi|Golci1|1848627|fgenesh1_kg.308_#_11_#_TRINITY_DN835				
jgi|Golci1|1848633|fgenesh1_kg.308_#_17_#_TRINITY_DN211				
jgi|Golci1|1848699|fgenesh1_kg.312_#_3_#_TRINITY_DN1654				
jgi|Golci1|1848744|fgenesh1_kg.312_#_48_#_TRINITY_DN969				
jgi|Golci1|1848747|fgenesh1_kg.312_#_51_#_TRINITY_DN197				
jgi|Golci1|1848766|fgenesh1_kg.313_#_18_#_TRINITY_DN133				
jgi|Golci1|1848769|fgenesh1_kg.313_#_21_#_TRINITY_DN505				
jgi|Golci1|1848805|fgenesh1_kg.314_#_12_#_TRINITY_DN840				
jgi|Golci1|1849005|fgenesh1_kg.321_#_3_#_TRINITY_DN1573				
jgi|Golci1|1849074|fgenesh1_kg.322_#_51_#_TRINITY_DN178				
jgi|Golci1|1849090|fgenesh1_kg.322_#_67_#_TRINITY_DN174				
jgi|Golci1|1849102|fgenesh1_kg.322_#_79_#_TRINITY_DN209				
jgi|Golci1|1849368|fgenesh1_kg.330_#_34_#_TRINITY_DN164				
jgi|Golci1|1849379|fgenesh1_kg.331_#_1_#_TRINITY_DN7063				

Gc	Bgh	Bgt	En	Go
jgi|Golci1|1849496|fgenesh1_kg.332_#_11_#_TRINITY_DN198				
jgi|Golci1|1849561|fgenesh1_kg.332_#_76_#_TRINITY_DN203				
jgi|Golci1|1849597|fgenesh1_kg.334_#_4_#_TRINITY_DN1902				
jgi|Golci1|1849605|fgenesh1_kg.334_#_12_#_TRINITY_DN182				
jgi|Golci1|1849666|fgenesh1_kg.335_#_9_#_TRINITY_DN1541				
jgi|Golci1|1849710|fgenesh1_kg.337_#_1_#_TRINITY_DN1894				
jgi|Golci1|1849726|fgenesh1_kg.337_#_17_#_TRINITY_DN811				
jgi|Golci1|1849758|fgenesh1_kg.338_#_32_#_TRINITY_DN178				
jgi|Golci1|1849766|fgenesh1_kg.338_#_40_#_TRINITY_DN182				
jgi|Golci1|1849779|fgenesh1_kg.338_#_53_#_TRINITY_DN126				
jgi|Golci1|1849911|fgenesh1_kg.342_#_12_#_TRINITY_DN192				
jgi|Golci1|1849932|fgenesh1_kg.342_#_33_#_TRINITY_DN171				
jgi|Golci1|1849957|fgenesh1_kg.343_#_17_#_TRINITY_DN210				
jgi|Golci1|1850056|fgenesh1_kg.346_#_17_#_TRINITY_DN193				
jgi|Golci1|1850082|fgenesh1_kg.346_#_43_#_TRINITY_DN200				
jgi|Golci1|1850167|fgenesh1_kg.347_#_85_#_TRINITY_DN103				
jgi|Golci1|1850263|fgenesh1_kg.350_#_32_#_TRINITY_DN519				
jgi|Golci1|1850265|fgenesh1_kg.350_#_34_#_TRINITY_DN519				
jgi|Golci1|1850311|fgenesh1_kg.352_#_1_#_TRINITY_DN1473				
jgi|Golci1|1850385|fgenesh1_kg.355_#_9_#_TRINITY_DN2079				
jgi|Golci1|1850415|fgenesh1_kg.355_#_39_#_TRINITY_DN210				
jgi|Golci1|1850482|fgenesh1_kg.358_#_1_#_TRINITY_DN4909				
jgi|Golci1|1850536|fgenesh1_kg.359_#_2_#_TRINITY_DN5190				
jgi|Golci1|1850537|fgenesh1_kg.359_#_3_#_TRINITY_DN5190				
jgi|Golci1|1850726|fgenesh1_kg.363_#_4_#_TRINITY_DN2357				
jgi|Golci1|1850756|fgenesh1_kg.364_#_17_#_TRINITY_DN186				
jgi|Golci1|1850769|fgenesh1_kg.364_#_30_#_TRINITY_DN496				
jgi|Golci1|1850991|fgenesh1_kg.372_#_6_#_TRINITY_DN1524				
jgi|Golci1|1851005|fgenesh1_kg.372_#_20_#_TRINITY_DN844				
jgi|Golci1|1851020|fgenesh1_kg.372_#_35_#_TRINITY_DN183				
jgi|Golci1|1851023|fgenesh1_kg.372_#_38_#_TRINITY_DN239				

Gc	Bgh	Bgt	En	Go
jgi|Golci1|1851033|fgenesh1_kg.373_#_6_#_TRINITY_DN1681				
jgi|Golci1|1851093|fgenesh1_kg.375_#_17_#_TRINITY_DN315				
jgi|Golci1|1851105|fgenesh1_kg.375_#_29_#_TRINITY_DN170				
jgi|Golci1|1851113|fgenesh1_kg.375_#_37_#_TRINITY_DN107				
jgi|Golci1|1851211|fgenesh1_kg.379_#_1_#_TRINITY_DN1841				
jgi|Golci1|1851228|fgenesh1_kg.379_#_18_#_TRINITY_DN193				
jgi|Golci1|1851234|fgenesh1_kg.379_#_24_#_TRINITY_DN193				
jgi|Golci1|1851440|fgenesh1_kg.385_#_13_#_TRINITY_DN171				
jgi|Golci1|1851523|fgenesh1_kg.387_#_14_#_TRINITY_DN194				
jgi|Golci1|1851553|fgenesh1_kg.387_#_44_#_TRINITY_DN169				
jgi|Golci1|1851767|fgenesh1_kg.392_#_56_#_TRINITY_DN169				
jgi|Golci1|1851858|fgenesh1_kg.395_#_2_#_TRINITY_DN1775				
jgi|Golci1|1851917|fgenesh1_kg.397_#_37_#_TRINITY_DN194				
jgi|Golci1|1851977|fgenesh1_kg.398_#_14_#_TRINITY_DN681				
jgi|Golci1|1851993|fgenesh1_kg.398_#_30_#_TRINITY_DN184				
jgi|Golci1|1852131|fgenesh1_kg.401_#_21_#_TRINITY_DN181				
jgi|Golci1|1852217|fgenesh1_kg.407_#_43_#_TRINITY_DN186				
jgi|Golci1|1852229|fgenesh1_kg.409_#_7_#_TRINITY_DN1425				
jgi|Golci1|1852279|fgenesh1_kg.411_#_1_#_TRINITY_DN1877				
jgi|Golci1|1852281|fgenesh1_kg.411_#_3_#_TRINITY_DN1877				
jgi|Golci1|1852286|fgenesh1_kg.411_#_8_#_TRINITY_DN1985				
jgi|Golci1|1852289|fgenesh1_kg.411_#_11_#_TRINITY_DN198				
jgi|Golci1|1852292|fgenesh1_kg.411_#_14_#_TRINITY_DN194				
jgi|Golci1|1852331|fgenesh1_kg.415_#_11_#_TRINITY_DN159				
jgi|Golci1|1852371|fgenesh1_kg.416_#_25_#_TRINITY_DN106				
jgi|Golci1|1852390|fgenesh1_kg.417_#_17_#_TRINITY_DN129				
jgi|Golci1|1852463|fgenesh1_kg.422_#_8_#_TRINITY_DN1047				
jgi|Golci1|1852550|fgenesh1_kg.427_#_10_#_TRINITY_DN193				
jgi|Golci1|1852555|fgenesh1_kg.427_#_15_#_TRINITY_DN193				
jgi|Golci1|1852656|fgenesh1_kg.432_#_37_#_TRINITY_DN190				
jgi|Golci1|1852723|fgenesh1_kg.437_#_34_#_TRINITY_DN167				

Gc	Bgh	Bgt	En	Go
jgi|Golci1|1852730|fgenesh1_kg.437_#_41_#_TRINITY_DN167				
jgi|Golci1|1852773|fgenesh1_kg.438_#_14_#_TRINITY_DN192				
jgi|Golci1|1852783|fgenesh1_kg.439_#_8_#_TRINITY_DN1615				
jgi|Golci1|1852792|fgenesh1_kg.440_#_4_#_TRINITY_DN1970				
jgi|Golci1|1852793|fgenesh1_kg.441_#_1_#_TRINITY_DN1198				
jgi|Golci1|1852831|fgenesh1_kg.444_#_8_#_TRINITY_DN3300				
jgi|Golci1|1852921|fgenesh1_kg.451_#_6_#_TRINITY_DN4492				
jgi|Golci1|1852935|fgenesh1_kg.454_#_3_#_TRINITY_DN8373				
jgi|Golci1|1852946|fgenesh1_kg.458_#_1_#_TRINITY_DN2023				
jgi|Golci1|1853106|fgenesh1_kg.470_#_8_#_TRINITY_DN1903				
jgi|Golci1|1853121|fgenesh1_kg.470_#_23_#_TRINITY_DN107				
jgi|Golci1|1853123|fgenesh1_kg.471_#_1_#_TRINITY_DN1760				
jgi|Golci1|1853134|fgenesh1_kg.471_#_12_#_TRINITY_DN176				
jgi|Golci1|1853205|fgenesh1_kg.485_#_2_#_TRINITY_DN1368				
jgi|Golci1|1853244|fgenesh1_kg.488_#_4_#_TRINITY_DN1475				
jgi|Golci1|1853259|fgenesh1_kg.489_#_4_#_TRINITY_DN1475				
jgi|Golci1|1853274|fgenesh1_kg.490_#_4_#_TRINITY_DN1475				
jgi|Golci1|1853296|fgenesh1_kg.497_#_1_#_TRINITY_DN306_				
jgi|Golci1|1853298|fgenesh1_kg.498_#_2_#_TRINITY_DN5190				
jgi|Golci1|1853401|fgenesh1_kg.525_#_12_#_TRINITY_DN192				
jgi|Golci1|1853422|fgenesh1_kg.543_#_1_#_TRINITY_DN1251				
jgi|Golci1|1853455|fgenesh1_kg.558_#_1_#_TRINITY_DN1255				
jgi|Golci1|1853536|fgenesh1_kg.574_#_2_#_TRINITY_DN1785				
jgi|Golci1|1853705|fgenesh1_kg.613_#_7_#_TRINITY_DN1509				
jgi|Golci1|1853718|fgenesh1_kg.614_#_7_#_TRINITY_DN1509				
jgi|Golci1|1853766|fgenesh1_kg.617_#_6_#_TRINITY_DN1166				
jgi|Golci1|1853772|fgenesh1_kg.618_#_5_#_TRINITY_DN1166				
jgi|Golci1|1853779|fgenesh1_kg.619_#_6_#_TRINITY_DN1166				
jgi|Golci1|1853786|fgenesh1_kg.620_#_6_#_TRINITY_DN1166				
jgi|Golci1|1853790|fgenesh1_kg.624_#_3_#_TRINITY_DN2608				
jgi|Golci1|1853795|fgenesh1_kg.627_#_1_#_TRINITY_DN1577				

Gc	Bgh	Bgt	En	Go
jgi|Golci1|1853805|fgenesh1_kg.628_#_2_#_TRINITY_DN5190				
jgi|Golci1|1853806|fgenesh1_kg.628_#_3_#_TRINITY_DN5190				
jgi|Golci1|1853956|fgenesh1_kg.643_#_2_#_TRINITY_DN5190				
jgi|Golci1|1854026|fgenesh1_kg.672_#_21_#_TRINITY_DN490				
jgi|Golci1|1854089|fgenesh1_kg.705_#_21_#_TRINITY_DN490				
jgi|Golci1|1854127|fgenesh1_kg.709_#_22_#_TRINITY_DN490				
jgi|Golci1|1854141|fgenesh1_kg.713_#_2_#_TRINITY_DN4958				
jgi|Golci1|1854265|fgenesh1_kg.754_#_1_#_TRINITY_DN1150				
jgi|Golci1|1854300|fgenesh1_kg.793_#_4_#_TRINITY_DN1705				
jgi|Golci1|1854310|fgenesh1_kg.806_#_1_#_TRINITY_DN8471				
jgi|Golci1|1854311|fgenesh1_kg.806_#_2_#_TRINITY_DN8471				
jgi|Golci1|1854314|fgenesh1_kg.808_#_1_#_TRINITY_DN8471				
jgi|Golci1|1854317|fgenesh1_kg.808_#_4_#_TRINITY_DN8471				
jgi|Golci1|1854324|fgenesh1_kg.812_#_2_#_TRINITY_DN1932				
jgi|Golci1|1854454|fgenesh1_pm.2_#_22				
jgi|Golci1|1854648|fgenesh1_pm.6_#_4				
jgi|Golci1|1854791|fgenesh1_pm.9_#_14				
jgi|Golci1|1855010|fgenesh1_pm.16_#_10				
jgi|Golci1|1855338|fgenesh1_pm.29_#_5				
jgi|Golci1|1855481|fgenesh1_pm.35_#_8				
jgi|Golci1|1855532|fgenesh1_pm.37_#_23				
jgi|Golci1|1855742|fgenesh1_pm.48_#_7				
jgi|Golci1|1855963|fgenesh1_pm.61_#_7				
jgi|Golci1|1856009|fgenesh1_pm.64_#_3				
jgi|Golci1|1856080|fgenesh1_pm.68_#_11				
jgi|Golci1|1856187|fgenesh1_pm.74_#_2				
jgi|Golci1|1856226|fgenesh1_pm.76_#_6				
jgi|Golci1|1856303|fgenesh1_pm.81_#_4				
jgi|Golci1|1856363|fgenesh1_pm.86_#_1				
jgi|Golci1|1856442|fgenesh1_pm.90_#_7				
jgi|Golci1|1856731|fgenesh1_pm.112_#_14				
jgi|Golci1|1856972|fgenesh1_pm.130_#_3				

Gc	Bgh	Bgt	En	Go
jgi|Golci1|1857217|fgenesh1_pm.153_#_1				
jgi|Golci1|1857226|fgenesh1_pm.153_#_10				
jgi|Golci1|1857509|fgenesh1_pm.187_#_2				
jgi|Golci1|1857594|fgenesh1_pm.200_#_1				
jgi|Golci1|1857804|fgenesh1_pm.241_#_3				
jgi|Golci1|1857807|fgenesh1_pm.241_#_6				
jgi|Golci1|1857858|fgenesh1_pm.251_#_1				
jgi|Golci1|1858120|fgenesh1_pm.313_#_4				
jgi|Golci1|1858224|fgenesh1_pm.342_#_1				
jgi|Golci1|1858239|fgenesh1_pm.347_#_1				
jgi|Golci1|1858343|fgenesh1_pm.377_#_1				
jgi|Golci1|1858354|fgenesh1_pm.381_#_3				
jgi|Golci1|1858405|fgenesh1_pm.400_#_1				
jgi|Golci1|1858528|fgenesh1_pm.480_#_1				
jgi|Golci1|1858548|fgenesh1_pm.514_#_1				
jgi|Golci1|1858564|fgenesh1_pm.559_#_1				
jgi|Golci1|1858619|fgenesh1_pm.702_#_1				
jgi|Golci1|1861191|estExt_fgenesh1_pm.C_1420008				
jgi|Golci1|1861267|estExt_fgenesh1_pm.C_1500006				
jgi|Golci1|1861770|estExt_fgenesh1_pm.C_2240004				
jgi|Golci1|1862138|estExt_fgenesh1_pm.C_3170006				
jgi|Golci1|1862248|estExt_fgenesh1_pm.C_3480004				
jgi|Golci1|1863488|estExt_fgenesh1_pg.C_190018				
jgi|Golci1|1866068|estExt_fgenesh1_pg.C_1570005				
jgi|Golci1|1867255|estExt_fgenesh1_pg.C_3340001				
jgi|Golci1|1867482|estExt_fgenesh1_pg.C_3960001				
jgi|Golci1|1873049|MIX5289_26051_51				
jgi|Golci1|1887904|MIX20144_7619_97				
jgi|Golci1|1899477|MIX31717_7039_38				
jgi|Golci1|1903926|MIX36166_2665_27				
jgi|Golci1|1906721|MIX38961_428_77				
jgi|Golci1|1910368|MIX42608_10_31				
jgi|Golci1|1914714|MIX46954_3892_46				
jgi|Golci1|1916674|MIX48914_5722_52				
jgi|Golci1|1923289|MIX55529_763_47				
jgi|Golci1|1924032|MIX56272_1987_15				

Gc	Bgh	Bgt	En	Go
jgi|Golci1|1928458|MIX60698_4315_56				
jgi|Golci1|1930962|MIX63202_5494_64				
jgi|Golci1|20843|CE20842_127				
jgi|Golci1|230424|CE230423_578				
jgi|Golci1|278543|CE278542_21829				
jgi|Golci1|284980|CE284979_111987				
jgi|Golci1|287936|CE287935_2773				
jgi|Golci1|289012|CE289011_5829				
jgi|Golci1|317059|CE317058_2449				
jgi|Golci1|397334|CE397333_28				
jgi|Golci1|409749|CE409748_119				
jgi|Golci1|419028|CE419027_458				
jgi|Golci1|435867|CE435866_14297				
jgi|Golci1|44936|CE44935_30				
jgi|Golci1|459810|CE459809_67626				
jgi|Golci1|513487|CE513486_2011				
jgi|Golci1|521573|CE521572_3884				
jgi|Golci1|528027|CE528026_1161				
jgi|Golci1|536469|CE536468_553796				
jgi|Golci1|540405|CE540404_23				
jgi|Golci1|547549|CE547548_9241				
jgi|Golci1|585565|CE585564_4983				
jgi|Golci1|619336|CE619335_102874				
jgi|Golci1|669736|CE669735_39518				
jgi|Golci1|682040|CE682039_47				
jgi|Golci1|686639|CE686638_4676				
jgi|Golci1|69422|CE69421_1502				
jgi|Golci1|699998|CE699997_2644				
jgi|Golci1|704175|CE704174_1109				
jgi|Golci1|748233|CE748232_145				
jgi|Golci1|752876|CE752875_583				

Gc	Bgh	Bgt	En	Go
jgi|Golci1|754101|CE754100_78741				
jgi|Golci1|775241|CE775240_4841				
jgi|Golci1|789767|CE789766_6051				
jgi|Golci1|812318|CE812317_5067				
jgi|Golci1|815078|CE815077_16				
jgi|Golci1|860795|CE860794_3344				
jgi|Golci1|971597|CE971596_72817				

Appendix 3: *Candidate secreted effector proteins*

Candidate secreted effector proteins predicted using EffectorP encoded by the genomes of *G. cichoracearum (Gc), G. orontii (Go) B. graminis f. sp. hordei (Bgh), B. graminis f. sp. tritici (Bgt),* and *E. necator (En)*

Gc	Bgh	Bgt	En	Go
jgi|Golci1|1017100|CE1017099_5758	jgi|Blugr1|25612|BGHDH14_bgh05803	jgi|Blugra1|1031|BGT96224_E5632T0	jgi|Erynec1|3754|EV44_g0424T0	jgi|Golor2|1128132|CE1084753_4368
jgi|Golci1|1138219|CE1138218_188	jgi|Blugr1|25610|BGHDH14_bgh03695	jgi|Blugra1|104|BGT96224_BCG4T0	jgi|Erynec1|3863|EV44_g0269T0	jgi|Golor2|1144947|CE1101568_210
jgi|Golci1|1278290|CE1278289_2265	jgi|Blugr1|25608|BGHDH14_bghG011456000001001	jgi|Blugra1|1057|BGT96224_40012T0	jgi|Erynec1|3884|EV44_g0435T0	jgi|Golor2|1211497|CE1168118_111
jgi|Golci1|1336305|CE1336304_824	jgi|Blugr1|25468|BGHDH14_bgh03742	jgi|Blugra1|1058|BGT96224_AcSP31098T0	jgi|Erynec1|3897|EV44_g0430T0	jgi|Golor2|1344606|CE1301227_3070
jgi|Golci1|1435786|CE1435785_986	jgi|Blugr1|25462|BGHDH14_bgh03746	jgi|Blugra1|1067|BGT96224_E5685T0	jgi|Erynec1|4034|EV44_g0573T0	jgi|Golor2|1379604|CE1336225_3260
jgi|Golci1|1451405|CE1451404_11	jgi|Blugr1|25453|BGHDH14_bgh03747	jgi|Blugra1|107|BGT96224_E10109T0	jgi|Erynec1|4332|EV44_g0203T0	jgi|Golor2|1426835|CE1383456_50
jgi|Golci1|1557851|CE1557850_1529	jgi|Blugr1|25445|BGHDH14_bghG000207000002001	jgi|Blugra1|1108|BGT96224_E10101T0	jgi|Erynec1|4482|EV44_g0444T0	jgi|Golor2|1473392|CE1430013_12
jgi|Golci1|1714669|gm4.10494_g	jgi|Blugr1|25442|BGHDH14_bgh03749	jgi|Blugra1|1188|BGT96224_E5980T0	jgi|Erynec1|4486|EV44_g0225T0	jgi|Golor2|155207|CE111828_31
jgi|Golci1|1727440|gm4.23265_g	jgi|Blugr1|25386|BGHDH14_bgh03443	jgi|Blugra1|1193|BGT96224_AcSP30107T0	jgi|Erynec1|4489|EV44_g0416T0	jgi|Golor2|2011771|CE1968392_572
jgi|Golci1|1727806|gm4.23631_g	jgi|Blugr1|25382|BGHDH14_bghG000107000003001	jgi|Blugra1|1231|BGT96224_AcSP31145T0	jgi|Erynec1|4492|EV44_g0357T0	jgi|Golor2|2310198|CE2266819_9543
jgi|Golci1|1731083|gm4.26908_g	jgi|Blugr1|25364|BGHDH14_bghG000103000002001	jgi|Blugra1|123|BGT96224_E40011T0	jgi|Erynec1|456|EV44_g0586T0	jgi|Golor2|2456219|CE2412840_146
jgi|Golci1|1731401|gm4.27226_g	jgi|Blugr1|25344|BGHDH14_bgh04209	jgi|Blugra1|1249|BGT96224_2900BT0	jgi|Erynec1|4579|EV44_g0597T0	jgi|Golor2|246500|CE203121_322
jgi|Golci1|1751675|gw1.355.9.1	jgi|Blugr1|25311|BGHDH14_bgh02080	jgi|Blugra1|1312|BGT96224_E5722T0	jgi|Erynec1|4713|EV44_g0473T0	jgi|Golor2|24931|gm4.24931_g
jgi|Golci1|1760131|e_gw1.3.125.1	jgi|Blugr1|25299|BGHDH14_bghG000032000001001	jgi|Blugra1|1326|BGT96224_1289T0	jgi|Erynec1|4768|EV44_g0533T0	jgi|Golor2|2531858|CE2488479_830
jgi|Golci1|1760176|e_gw1.3.48.1	jgi|Blugr1|25294|BGHDH14_bghG000026000002001	jgi|Blugra1|1330|BGT96224_E5731T0	jgi|Erynec1|4898|EV44_g0549T0	jgi|Golor2|2606300|CE2562921_8603
jgi|Golci1|1760570|e_gw1.6.10.1	jgi|Blugr1|25292|BGHDH14_bghG000026000001001	jgi|Blugra1|1338|BGT96224_AcSP30530T0	jgi|Erynec1|5106|EV44_g0246T0	jgi|Golor2|2674892|CE2631513_232
jgi|Golci1|1763298|e_gw1.52.7.1	jgi|Blugr1|25290|BGHDH14_bghG000024000001001	jgi|Blugra1|1427|BGT96224_2135T0	jgi|Erynec1|5150|EV44_g0559T0	jgi|Golor2|2701140|CE2657761_105
jgi|Golci1|1764386|e_gw1.76.44.1	jgi|Blugr1|25283|BGHDH14_bghG000012000002001	jgi|Blugra1|1436|BGT96224_E5704T0	jgi|Erynec1|5250|EV44_g0482T0	jgi|Golor2|343951|CE300572_3457

Gc	Bgh	Bgt	En	Go
jgi|Golci1|1766399|e_gw1.133.69.1	jgi|Blugr1|25131|BGHDH14_bgh03625	jgi|Blugra1|1442|BGT96224_E5709T0	jgi|Erynec1|5262|EV44_g0379T0	jgi|Golor2|365352|CE321973_6279
jgi|Golci1|1770009|e_gw1.406.3.1	jgi|Blugr1|25115|BGHDH14_bgh03452	jgi|Blugra1|1478|BGT96224_19T0	jgi|Erynec1|5288|EV44_g0569T0	jgi|Golor2|37702|gm4.37702_g
jgi|Golci1|1794491|fgenesh1_pg.4_#_48	jgi|Blugr1|25114|BGHDH14_bghG006029000001001	jgi|Blugra1|148|BGT96224_2708T0	jgi|Erynec1|5307|EV44_g0140T0	jgi|Golor2|3903|gm4.3903_g
jgi|Golci1|1795608|fgenesh1_pg.32_#_27	jgi|Blugr1|25113|BGHDH14_bghG006028000001001	jgi|Blugra1|1513|BGT96224_E5909T0	jgi|Erynec1|5385|EV44_g0230T0	jgi|Golor2|3933|gm4.3933_g
jgi|Golci1|1796298|fgenesh1_pg.60_#_3	jgi|Blugr1|25110|BGHDH14_bghG006021000001001	jgi|Blugra1|1541|BGT96224_2274T0	jgi|Erynec1|5409|EV44_g0242T0	jgi|Golor2|39603|gm4.39603_g
jgi|Golci1|1797699|fgenesh1_pg.133_#_3	jgi|Blugr1|25079|BGHDH14_bghG006278000001001	jgi|Blugra1|1550|BGT96224_E6031T0	jgi|Erynec1|5479|EV44_g0244T0	jgi|Golor2|4173372|gw1.1.2905.1
jgi|Golci1|1798088|fgenesh1_pg.161_#_5	jgi|Blugr1|25073|BGHDH14_bgh06951	jgi|Blugra1|158|BGT96224_E5560T0	jgi|Erynec1|5533|EV44_g0534T0	jgi|Golor2|4210000|gw1.17.1541.1
jgi|Golci1|1798567|fgenesh1_pg.205_#_5	jgi|Blugr1|25072|BGHDH14_bgh04105	jgi|Blugra1|165|BGT96224_ASP20866T0	jgi|Erynec1|5601|EV44_g0503T0	jgi|Golor2|4249978|e_gw1.10.568.1
jgi|Golci1|1799339|fgenesh1_pg.326_#_6	jgi|Blugr1|25070|BGHDH14_bgh04343	jgi|Blugra1|1711|BGT96224_E5627T0	jgi|Erynec1|5708|EV44_g0090T0	jgi|Golor2|4269205|e_gw1.36.1073.1
jgi|Golci1|1801984|estExt_Genemark4.C_260037	jgi|Blugr1|25058|BGHDH14_bgh04130	jgi|Blugra1|1742|BGT96224_E6018T0	jgi|Erynec1|5719|EV44_g0279T0	jgi|Golor2|4269220|e_gw1.36.342.1
jgi|Golci1|1802261|estExt_Genemark4.C_310178	jgi|Blugr1|25055|BGHDH14_bgh02875	jgi|Blugra1|1749|BGT96224_4496BT0	jgi|Erynec1|5744|EV44_g0388T0	jgi|Golor2|426930|CE383551_11476
jgi|Golci1|1805531|estExt_Genemark4.C_1270027	jgi|Blugr1|25053|BGHDH14_bgh03277	jgi|Blugra1|1756|BGT96224_E10137T0	jgi|Erynec1|5773|EV44_g0076T0	jgi|Golor2|4270647|e_gw1.39.167.1
jgi|Golci1|1809409|fgenesh1_kg.1_#_172_#_TRINITY_DN13694_c1_g3_i1	jgi|Blugr1|25051|BGHDH14_bgh03273	jgi|Blugra1|184|BGT96224_E5929T0	jgi|Erynec1|5790|EV44_g0596T0	jgi|Golor2|4278404|e_gw1.53.42.1
jgi|Golci1|1809650|fgenesh1_kg.1_#_413_#_TRINITY_DN19368_c4_g24_i1	jgi|Blugr1|25050|BGHDH14_bgh03275	jgi|Blugra1|1904|BGT96224_E5836T0	jgi|Erynec1|5929|EV44_g0571T0	jgi|Golor2|4280634|e_gw1.57.478.1
jgi|Golci1|1809665|fgenesh1_kg.1_#_428_#_TRINITY_DN19413_c1_g1_i2	jgi|Blugr1|25014|BGHDH14_bghG001077000001001	jgi|Blugra1|1910|BGT96224_AcSP30824T0	jgi|Erynec1|6058|EV44_g0525T0	jgi|Golor2|4280651|e_gw1.57.704.1
jgi|Golci1|1809735|fgenesh1_kg.1_#_498_#_TRINITY_DN19133_c11_g6_i8	jgi|Blugr1|24978|BGHDH14_bgh04277	jgi|Blugra1|1929|BGT96224_E5982T0	jgi|Erynec1|6064|EV44_g0542T0	jgi|Golor2|4296132|e_gw1.89.422.1
jgi|Golci1|1809941|fgenesh1_kg.1_#_704_#_TRINITY_DN20914_c5_g6_i1	jgi|Blugr1|24922|BGHDH14_bgh04920	jgi|Blugra1|194|BGT96224_BCG8T0	jgi|Erynec1|6114|EV44_g0283T0	jgi|Golor2|4307455|e_gw1.121.373.1
jgi|Golci1|1809996|fgenesh1_kg.1_#_759_#_TRINITY_DN16679_c0_g2_i6	jgi|Blugr1|24870|BGHDH14_bgh04817	jgi|Blugra1|1988|BGT96224_E10118T0	jgi|Erynec1|6210|EV44_g0206T0	jgi|Golor2|4386379|fgenesh1_pg.6_#_29
jgi|Golci1|1810114|fgenesh1_kg.1_#_877_#_TRINITY_DN17764_c0_g1_i6	jgi|Blugr1|24845|BGHDH14_bghG000925000001001	jgi|Blugra1|1989|BGT96224_E5547T0	jgi|Erynec1|6287|EV44_g0465T0	jgi|Golor2|4386813|fgenesh1_pg.9_#_39
jgi|Golci1|1810676|fgenesh1_kg.2_#_441_#_TRINITY_DN18692_c2_g2_i5	jgi|Blugr1|24821|BGHDH14_bghG000833000001001	jgi|Blugra1|1990|BGT96224_AcSP30782T0	jgi|Erynec1|6322|EV44_g0526T0	jgi|Golor2|4386995|fgenesh1_pg.11_#_41
jgi|Golci1|1810858|fgenesh1_kg.3_#_112_#_TRINITY_DN19285_c4_g1_i1	jgi|Blugr1|24809|BGHDH14_bghG000799000001001	jgi|Blugra1|201|BGT96224_E5842T0	jgi|Erynec1|641|EV44_g0383T0	jgi|Golor2|4388268|fgenesh1_pg.24_#_87

Gc	Bgh	Bgt	En	Go
jgi|Golci1|1810871|fgenesh1_kg.3_#_125_#_TRINITY_DN19285_c4_g1_i4	jgi|Blugr1|24788|BGHDH14_bghG000770000002001	jgi|Blugra1|202|BGT96224_ASP21585T0	jgi|Erynec1|898|EV44_g0186T0	jgi|Golor2|4389219|fgenesh1_pg.37_#_29
jgi|Golci1|1810957|fgenesh1_kg.3_#_211_#_TRINITY_DN19413_c1_g1_i2	jgi|Blugr1|24738|BGHDH14_bghG000733000001001	jgi|Blugra1|209|BGT96224_E5913T0	jgi|Erynec1|914|EV44_g0538T0	jgi|Golor2|4390161|fgenesh1_pg.53_#_59
jgi|Golci1|1810977|fgenesh1_kg.3_#_231_#_TRINITY_DN22998_c0_g1_i1	jgi|Blugr1|24719|BGHDH14_bghG000714000001001	jgi|Blugra1|2104|BGT96224_AcSP31023T0	jgi|Erynec1|1056|EV44_g0547T0	jgi|Golor2|4390630|fgenesh1_pg.61_#_31
jgi|Golci1|1811028|fgenesh1_kg.3_#_282_#_TRINITY_DN15396_c0_g1_i5	jgi|Blugr1|24709|BGHDH14_bgh03067	jgi|Blugra1|2187|BGT96224_E10100T0	jgi|Erynec1|1161|EV44_g0257T0	jgi|Golor2|4390806|fgenesh1_pg.64_#_43
jgi|Golci1|1811645|fgenesh1_kg.4_#_316_#_TRINITY_DN25802_c0_g1_i1	jgi|Blugr1|24654|BGHDH14_bgh01923	jgi|Blugra1|219|BGT96224_E5781T0	jgi|Erynec1|1405|EV44_g0537T0	jgi|Golor2|4391815|fgenesh1_pg.84_#_5
jgi|Golci1|1811800|fgenesh1_kg.4_#_471_#_TRINITY_DN6084_c0_g2_i1	jgi|Blugr1|24625|BGHDH14_bghG000653000001001	jgi|Blugra1|223|BGT96224_E5877T0	jgi|Erynec1|1421|EV44_g0014T0	jgi|Golor2|4391816|fgenesh1_pg.84_#_6
jgi|Golci1|1811990|fgenesh1_kg.5_#_142_#_TRINITY_DN27152_c0_g1_i1	jgi|Blugr1|24611|BGHDH14_bgh01048	jgi|Blugra1|2243|BGT96224_5308T0	jgi|Erynec1|1511|EV44_g0425T0	jgi|Golor2|4392990|fgenesh1_pg.110_#_22
jgi|Golci1|1812887|fgenesh1_kg.7_#_39_#_TRINITY_DN19367_c0_g4_i1	jgi|Blugr1|24569|BGHDH14_bgh05755	jgi|Blugra1|2252|BGT96224_E5732T0	jgi|Erynec1|1647|EV44_g0551T0	jgi|Golor2|4393061|fgenesh1_pg.112_#_24
jgi|Golci1|1812929|fgenesh1_kg.7_#_81_#_TRINITY_DN25097_c0_g1_i1	jgi|Blugr1|24565|BGHDH14_bgh04226	jgi|Blugra1|225|BGT96224_E5880T0	jgi|Erynec1|1730|EV44_g0415T0	jgi|Golor2|4393802|fgenesh1_pg.133_#_5
jgi|Golci1|1813185|fgenesh1_kg.7_#_337_#_TRINITY_DN19205_c2_g3_i1	jgi|Blugr1|24526|BGHDH14_bghG000556000001001	jgi|Blugra1|2299|BGT96224_E6032T0	jgi|Erynec1|1752|EV44_g0591T0	jgi|Golor2|4394446|fgenesh1_pg.154_#_14
jgi|Golci1|1813197|fgenesh1_kg.7_#_349_#_TRINITY_DN18565_c1_g4_i2	jgi|Blugr1|24494|BGHDH14_bgh04885	jgi|Blugra1|229|BGT96224_E5783T0	jgi|Erynec1|189|EV44_g0181T0	jgi|Golor2|4394460|fgenesh1_pg.154_#_28
jgi|Golci1|1813260|fgenesh1_kg.7_#_412_#_TRINITY_DN5562_c0_g2_i2	jgi|Blugr1|24462|BGHDH14_bgh02536	jgi|Blugra1|22|BGT96224_E5967T0	jgi|Erynec1|2050|EV44_g0313T0	jgi|Golor2|4395825|fgenesh1_pg.226_#_8
jgi|Golci1|1813329|fgenesh1_kg.7_#_481_#_TRINITY_DN17658_c1_g2_i1	jgi|Blugr1|24461|BGHDH14_bghG000481000001001	jgi|Blugra1|230|BGT96224_E5953T0	jgi|Erynec1|2064|EV44_g0519T0	jgi|Golor2|4395946|fgenesh1_pg.240_#_3
jgi|Golci1|1813332|fgenesh1_kg.8_#_1_#_TRINITY_DN14936_c0_g3_i1	jgi|Blugr1|24440|BGHDH14_bgh03531	jgi|Blugra1|2367|BGT96224_E5679T0	jgi|Erynec1|2200|EV44_g0602T0	jgi|Golor2|4409105|estExt_Genemark4.C_1990054
jgi|Golci1|1813651|fgenesh1_kg.9_#_15_#_TRINITY_DN13887_c0_g1_i5	jgi|Blugr1|24423|BGHDH14_bghG000458000002001	jgi|Blugra1|2423|BGT96224_E5668T0	jgi|Erynec1|2252|EV44_g0426T0	jgi|Golor2|5549786|MIX40162_2277_93
jgi|Golci1|1813697|fgenesh1_kg.9_#_61_#_TRINITY_DN10177_c0_g2_i1	jgi|Blugr1|24422|BGHDH14_bghG000457000001001	jgi|Blugra1|2430|BGT96224_ASP21313T0	jgi|Erynec1|2372|EV44_g0599T0	jgi|Golor2|5714216|MIX204592_419_59
jgi|Golci1|1813993|fgenesh1_kg.9_#_357_#_TRINITY_DN18756_c0_g2_i1	jgi|Blugr1|24419|BGHDH14_bghG000456000001001	jgi|Blugra1|2467|BGT96224_A20644T0	jgi|Erynec1|2412|EV44_g0178T0	jgi|Golor2|5820476|estExt_fgenesh1_pg.C_840010
jgi|Golci1|1814346|fgenesh1_kg.11_#_19_#_TRINITY_DN16512_c0_g2_i3	jgi|Blugr1|24416|BGHDH14_bghG000452000001001	jgi|Blugra1|2469|BGT96224_E5677T0	jgi|Erynec1|2444|EV44_g0052T0	jgi|Golor2|5824174|estExt_fgenesh1_pg.C_2400001
jgi|Golci1|1814547|fgenesh1_kg.11_#_220_#_TRINITY_DN17012_c1_g1_i13	jgi|Blugr1|24373|BGHDH14_bgh04954	jgi|Blugra1|2527|BGT96224_3821T0	jgi|Erynec1|2466|EV44_g0274T0	jgi|Golor2|5824175|estExt_fgenesh1_pg.C_2400002
jgi|Golci1|1814618|fgenesh1_kg.11_#_291_#_TRINITY_DN18841_c3_g2_i3	jgi|Blugr1|24361|BGHDH14_bghG000425000003001	jgi|Blugra1|2602|BGT96224_273BT0	jgi|Erynec1|2619|EV44_g0254T0	jgi|Golor2|635348|CE591969_64
jgi|Golci1|1814645|fgenesh1_kg.11_#_318_#_TRINITY_DN20914_c5_g5_i2	jgi|Blugr1|24333|BGHDH14_bghG000417000001001	jgi|Blugra1|2676|BGT96224_3472T0	jgi|Erynec1|2628|EV44_g0447T0	jgi|Golor2|636606|CE593227_1576

Gc	Bgh	Bgt	En	Go
jgi|Golci1|1814776|fgenesh1_kg.12_#_79_#_TRINITY_DN15444_c0_g1_i4	jgi|Blugr1|24331|BGHDH14_bghG000417000002001	jgi|Blugra1|2692|BGT96224_2673T0	jgi|Erynec1|3007|EV44_g0583T0	jgi|Golor2|710617|CE667238_383
jgi|Golci1|1814870|fgenesh1_kg.12_#_173_#_TRINITY_DN12092_c0_g1_i6	jgi|Blugr1|24314|BGHDH14_bgh04026	jgi|Blugra1|274|BGT96224_E5585T0	jgi|Erynec1|3081|EV44_g0282T0	jgi|Golor2|922974|CE879595_225
jgi|Golci1|1814966|fgenesh1_kg.12_#_269_#_TRINITY_DN5415_c0_g2_i1	jgi|Blugr1|24313|BGHDH14_bgh02942	jgi|Blugra1|2756|BGT96224_E5991T0	jgi|Erynec1|3117|EV44_g0136T0	jgi|Golor2|97205|CE53826_15
jgi|Golci1|1815600|fgenesh1_kg.14_#_189_#_TRINITY_DN19994_c2_g1_i1	jgi|Blugr1|24298|BGHDH14_bgh03375	jgi|Blugra1|2766|BGT96224_501T0	jgi|Erynec1|3159|EV44_g0215T0	jgi|Golor2|9850|gm4.9850_g
jgi|Golci1|1815608|fgenesh1_kg.14_#_197_#_TRINITY_DN19994_c2_g1_i1	jgi|Blugr1|24297|BGHDH14_bgh02998	jgi|Blugra1|276|BGT96224_E5548T0	jgi|Erynec1|3287|EV44_g0600T0	
jgi|Golci1|1815611|fgenesh1_kg.14_#_200_#_TRINITY_DN19994_c2_g1_i1	jgi|Blugr1|24294|BGHDH14_bgh06578	jgi|Blugra1|2852|BGT96224_4373T0	jgi|Erynec1|345|EV44_g0192T0	
jgi|Golci1|1815652|fgenesh1_kg.14_#_241_#_TRINITY_DN19994_c2_g1_i1	jgi|Blugr1|24293|BGHDH14_bgh03730	jgi|Blugra1|2873|BGT96224_E5604T0	jgi|Erynec1|3611|EV44_g0196T0	
jgi|Golci1|1816348|fgenesh1_kg.17_#_89_#_TRINITY_DN15392_c1_g1_i3	jgi|Blugr1|24254|BGHDH14_bgh02825	jgi|Blugra1|2875|BGT96224_AcSP30893T0	jgi|Erynec1|3648|EV44_g0539T0	
jgi|Golci1|1817113|fgenesh1_kg.19_#_258_#_TRINITY_DN17941_c0_g1_i1	jgi|Blugr1|24253|BGHDH14_bgh02420	jgi|Blugra1|2942|BGT96224_5451T0	jgi|Erynec1|369|EV44_g0481T0	
jgi|Golci1|1817364|fgenesh1_kg.20_#_242_#_TRINITY_DN20960_c5_g6_i1	jgi|Blugr1|24241|BGHDH14_bgh02262	jgi|Blugra1|3022|BGT96224_E3136T0		
jgi|Golci1|1817600|fgenesh1_kg.21_#_180_#_TRINITY_DN10989_c0_g3_i1	jgi|Blugr1|24239|BGHDH14_bgh02778	jgi|Blugra1|3023|BGT96224_E5921T0		
jgi|Golci1|1817609|fgenesh1_kg.21_#_189_#_TRINITY_DN1116_c0_g1_i1	jgi|Blugr1|24238|BGHDH14_bgh03466	jgi|Blugra1|3024|BGT96224_E5922T0		
jgi|Golci1|1817793|fgenesh1_kg.22_#_74_#_TRINITY_DN1718_c0_g1_i1	jgi|Blugr1|24237|BGHDH14_bgh03464	jgi|Blugra1|3030|BGT96224_E10124T0		
jgi|Golci1|1819209|fgenesh1_kg.28_#_27_#_TRINITY_DN19263_c7_g1_i2	jgi|Blugr1|24236|BGHDH14_bgh03568	jgi|Blugra1|3111|BGT96224_BCG9T0		
jgi|Golci1|1819382|fgenesh1_kg.28_#_200_#_TRINITY_DN19374_c3_g2_i2	jgi|Blugr1|24235|BGHDH14_bghG001947000001001	jgi|Blugra1|3112|BGT96224_BCG5T0		
jgi|Golci1|1819759|fgenesh1_kg.30_#_58_#_TRINITY_DN14005_c0_g3_i2	jgi|Blugr1|24114|BGHDH14_bgh03692	jgi|Blugra1|3113|BGT96224_BCG2T0		
jgi|Golci1|1819761|fgenesh1_kg.30_#_60_#_TRINITY_DN14005_c0_g2_i1	jgi|Blugr1|24084|BGHDH14_bgh03457	jgi|Blugra1|3115|BGT96224_BCG3T0		
jgi|Golci1|1820301|fgenesh1_kg.32_#_58_#_TRINITY_DN20727_c1_g8_i1	jgi|Blugr1|24083|BGHDH14_bgh02774	jgi|Blugra1|3123|BGT96224_E5553T0		
jgi|Golci1|1820440|fgenesh1_kg.32_#_197_#_TRINITY_DN18957_c0_g4_i2	jgi|Blugr1|24082|BGHDH14_bghG001721000001001	jgi|Blugra1|3132|BGT96224_E5774T0		
jgi|Golci1|1820447|fgenesh1_kg.32_#_204_#_TRINITY_DN18957_c0_g4_i2	jgi|Blugr1|24081|BGHDH14_bgh05751	jgi|Blugra1|3178|BGT96224_E5624T0		
jgi|Golci1|1820705|fgenesh1_kg.33_#_210_#_TRINITY_DN17726_c0_g3_i2	jgi|Blugr1|24073|BGHDH14_bgh03794	jgi|Blugra1|3187|BGT96224_AcSP30129T0		
jgi|Golci1|1821358|fgenesh1_kg.36_#_187_#_TRINITY_DN19282_c2_g3_i10	jgi|Blugr1|24071|BGHDH14_bgh03995	jgi|Blugra1|3195|BGT96224_E5658T0		
jgi|Golci1|1821576|fgenesh1_kg.37_#_206_#_TRINITY_DN19375_c2_g5_i4	jgi|Blugr1|24069|BGHDH14_bgh03922	jgi|Blugra1|3211|BGT96224_E10110T0		

Gc	Bgh	Bgt	En	Go
jgi|Golci1|1821582|fgenesh1_kg.37_#_212_#_TRINITY_DN19375_c1_g1_i6	jgi|Blugr1|24068|BGHDH14_bghG001682000001001	jgi|Blugra1|3214|BGT96224_E10111T0		
jgi|Golci1|1821590|fgenesh1_kg.37_#_220_#_TRINITY_DN19375_c1_g1_i6	jgi|Blugr1|24060|BGHDH14_bgh03857	jgi|Blugra1|3327|BGT96224_E5784T0		
jgi|Golci1|1821596|fgenesh1_kg.37_#_226_#_TRINITY_DN19375_c2_g5_i4	jgi|Blugr1|23984|BGHDH14_bgh06200	jgi|Blugra1|3416|BGT96224_E4403T0		
jgi|Golci1|1821886|fgenesh1_kg.38_#_187_#_TRINITY_DN5411_c0_g1_i1	jgi|Blugr1|23889|BGHDH14_bghG002664000001001	jgi|Blugra1|3470|BGT96224_AcSP30848T0		
jgi|Golci1|1822203|fgenesh1_kg.40_#_83_#_TRINITY_DN33122_c0_g1_i1	jgi|Blugr1|23888|BGHDH14_bghG002653000001001	jgi|Blugra1|3481|BGT96224_2816T0		
jgi|Golci1|1822245|fgenesh1_kg.40_#_125_#_TRINITY_DN11647_c0_g1_i1	jgi|Blugr1|23871|BGHDH14_bghG002637000001001	jgi|Blugra1|3537|BGT96224_E10116T0		
jgi|Golci1|1822476|fgenesh1_kg.42_#_46_#_TRINITY_DN20617_c11_g9_i1	jgi|Blugr1|23844|BGHDH14_bghG002599000002001	jgi|Blugra1|3572|BGT96224_E5973T0		
jgi|Golci1|1822518|fgenesh1_kg.42_#_88_#_TRINITY_DN5281_c0_g2_i1	jgi|Blugr1|23843|BGHDH14_bghG002599000001001	jgi|Blugra1|3584|BGT96224_E5965T0		
jgi|Golci1|1823472|fgenesh1_kg.47_#_58_#_TRINITY_DN18948_c0_g1_i1	jgi|Blugr1|23841|BGHDH14_bgh05096	jgi|Blugra1|3585|BGT96224_E5539T0		
jgi|Golci1|1823511|fgenesh1_kg.47_#_97_#_TRINITY_DN20795_c10_g1_i1	jgi|Blugr1|23839|BGHDH14_bgh05069	jgi|Blugra1|3587|BGT96224_E5538T0		
jgi|Golci1|1824111|fgenesh1_kg.50_#_116_#_TRINITY_DN13688_c0_g1_i1	jgi|Blugr1|23838|BGHDH14_bghG002593000001001	jgi|Blugra1|3667|BGT96224_959T0		
jgi|Golci1|1824208|fgenesh1_kg.51_#_13_#_TRINITY_DN19964_c3_g10_i1	jgi|Blugr1|23836|BGHDH14_bghG002593000004001	jgi|Blugra1|3686|BGT96224_E5963T0		
jgi|Golci1|1824679|fgenesh1_kg.53_#_186_#_TRINITY_DN19325_c3_g9_i1	jgi|Blugr1|23813|BGHDH14_bgh02924	jgi|Blugra1|3687|BGT96224_AcSP30748T0		
jgi|Golci1|1824686|fgenesh1_kg.53_#_193_#_TRINITY_DN19325_c3_g26_i1	jgi|Blugr1|23803|BGHDH14_bgh02922	jgi|Blugra1|3689|BGT96224_E10108T0		
jgi|Golci1|1825223|fgenesh1_kg.56_#_61_#_TRINITY_DN9431_c0_g1_i1	jgi|Blugr1|23802|BGHDH14_bgh02918	jgi|Blugra1|3851|BGT96224_AcSP30091T0		
jgi|Golci1|1825381|fgenesh1_kg.57_#_71_#_TRINITY_DN20841_c2_g2_i1	jgi|Blugr1|23795|BGHDH14_bgh06709	jgi|Blugra1|387|BGT96224_ASP20465T0		
jgi|Golci1|1825635|fgenesh1_kg.59_#_51_#_TRINITY_DN10057_c0_g1_i2	jgi|Blugr1|23794|BGHDH14_bgh01406	jgi|Blugra1|3980|BGT96224_AcSP30691T0		
jgi|Golci1|1826245|fgenesh1_kg.62_#_136_#_TRINITY_DN8979_c0_g1_i1	jgi|Blugr1|23792|BGHDH14_bgh01369	jgi|Blugra1|4036|BGT96224_E5763T0		
jgi|Golci1|1826621|fgenesh1_kg.63_#_330_#_TRINITY_DN15719_c1_g1_i7	jgi|Blugr1|23791|BGHDH14_bgh01407	jgi|Blugra1|4044|BGT96224_E6038T0		
jgi|Golci1|1826724|fgenesh1_kg.64_#_97_#_TRINITY_DN973_c0_g2_i1	jgi|Blugr1|23790|BGHDH14_bgh02923	jgi|Blugra1|4097|BGT96224_AcSP30056T0		
jgi|Golci1|1826956|fgenesh1_kg.66_#_36_#_TRINITY_DN17222_c0_g2_i1	jgi|Blugr1|23786|BGHDH14_bgh01404	jgi|Blugra1|4114|BGT96224_E3602T0		
jgi|Golci1|1827166|fgenesh1_kg.67_#_111_#_TRINITY_DN17962_c2_g12_i1	jgi|Blugr1|23779|BGHDH14_bgh01628	jgi|Blugra1|4144|BGT96224_E5845T0		

Gc	Bgh	Bgt	En	Go
jgi|Golci1|1827365|fgenesh1_kg.69_#_57_#_TRINITY_DN14533_c0_g1_i1	jgi|Blugr1|23778|BGHDH14_bgh04266	jgi|Blugra1|4163|BGT96224_E3962T0		
jgi|Golci1|1827755|fgenesh1_kg.72_#_6_#_TRINITY_DN26106_c0_g1_i1	jgi|Blugr1|23777|BGHDH14_bgh04023	jgi|Blugra1|4196|BGT96224_E5543T0		
jgi|Golci1|1828306|fgenesh1_kg.74_#_159_#_TRINITY_DN20841_c3_g1_i5	jgi|Blugr1|23776|BGHDH14_bgh03058	jgi|Blugra1|4243|BGT96224_ASP20572T0		
jgi|Golci1|1828308|fgenesh1_kg.74_#_161_#_TRINITY_DN20841_c2_g2_i1	jgi|Blugr1|23769|BGHDH14_bgh00225	jgi|Blugra1|4253|BGT96224_E5888T0		
jgi|Golci1|1829769|fgenesh1_kg.83_#_33_#_TRINITY_DN18986_c0_g1_i36	jgi|Blugr1|23768|BGHDH14_bgh00020	jgi|Blugra1|425|BGT96224_E10002T0		
jgi|Golci1|1830139|fgenesh1_kg.86_#_78_#_TRINITY_DN12388_c0_g1_i4	jgi|Blugr1|23766|BGHDH14_bgh01412	jgi|Blugra1|4267|BGT96224_1302T0		
jgi|Golci1|1830243|fgenesh1_kg.86_#_182_#_TRINITY_DN6911_c0_g1_i2	jgi|Blugr1|23765|BGHDH14_bgh01408	jgi|Blugra1|4302|BGT96224_AcSP30622T0		
jgi|Golci1|1830255|fgenesh1_kg.87_#_10_#_TRINITY_DN11063_c0_g2_i1	jgi|Blugr1|23743|BGHDH14_bghG002403000001001	jgi|Blugra1|4315|BGT96224_AcSP31262T0		
jgi|Golci1|1830338|fgenesh1_kg.87_#_93_#_TRINITY_DN19091_c0_g1_i14	jgi|Blugr1|23736|BGHDH14_bghG002392000001001	jgi|Blugra1|4320|BGT96224_E5545T0		
jgi|Golci1|1830648|fgenesh1_kg.89_#_47_#_TRINITY_DN19764_c2_g1_i2	jgi|Blugr1|23731|BGHDH14_bgh02376	jgi|Blugra1|4335|BGT96224_249T0		
jgi|Golci1|1830679|fgenesh1_kg.89_#_78_#_TRINITY_DN13925_c0_g5_i1	jgi|Blugr1|23682|BGHDH14_bgh04927	jgi|Blugra1|4341|BGT96224_1536T0		
jgi|Golci1|1830926|fgenesh1_kg.91_#_30_#_TRINITY_DN19719_c2_g1_i12	jgi|Blugr1|23488|BGHDH14_bgh02588	jgi|Blugra1|4364|BGT96224_E6054T0		
jgi|Golci1|1831039|fgenesh1_kg.91_#_143_#_TRINITY_DN18274_c2_g1_i1	jgi|Blugr1|23457|BGHDH14_bghG001346000001001	jgi|Blugra1|4405|BGT96224_E5839T0		
jgi|Golci1|1831419|fgenesh1_kg.95_#_88_#_TRINITY_DN17620_c0_g1_i1	jgi|Blugr1|23416|BGHDH14_bgh04781	jgi|Blugra1|4407|BGT96224_AcSP31175T0		
jgi|Golci1|1831692|fgenesh1_kg.98_#_27_#_TRINITY_DN14153_c0_g2_i1	jgi|Blugr1|23414|BGHDH14_bgh03735	jgi|Blugra1|4428|BGT96224_AcSP31269T0		
jgi|Golci1|1832687|fgenesh1_kg.106_#_4_#_TRINITY_DN4980_c0_g3_i1	jgi|Blugr1|23393|BGHDH14_bgh03731	jgi|Blugra1|467|BGT96224_ASP21338T0		
jgi|Golci1|1832789|fgenesh1_kg.106_#_106_#_TRINITY_DN12524_c0_g1_i3	jgi|Blugr1|23392|BGHDH14_bghG001282000001001	jgi|Blugra1|4690|BGT96224_4619T0		
jgi|Golci1|1832791|fgenesh1_kg.106_#_108_#_TRINITY_DN18297_c0_g1_i1	jgi|Blugr1|23377|BGHDH14_bgh00027	jgi|Blugra1|4742|BGT96224_E5689T0		
jgi|Golci1|1832953|fgenesh1_kg.107_#_159_#_TRINITY_DN17265_c0_g1_i1	jgi|Blugr1|23372|BGHDH14_bgh04121	jgi|Blugra1|4748|BGT96224_E10141T0		
jgi|Golci1|1833160|fgenesh1_kg.109_#_37_#_TRINITY_DN17662_c0_g1_i2	jgi|Blugr1|23363|BGHDH14_bghG001240000001001	jgi|Blugra1|4764|BGT96224_E10114T0		
jgi|Golci1|1833347|fgenesh1_kg.110_#_126_#_TRINITY_DN20810_c8_g4_i3	jgi|Blugr1|23359|BGHDH14_bghG001226000001001	jgi|Blugra1|4881|BGT96224_5153T0		
jgi|Golci1|1833918|fgenesh1_kg.114_#_101_#_TRINITY_DN17423_c0_g2_i3	jgi|Blugr1|23356|BGHDH14_bghG001225000001001	jgi|Blugra1|4907|BGT96224_E5582T0		

Gc	Bgh	Bgt	En	Go
jgi|Golci1|1833976|fgenesh1_kg.115_#_43_#_TRINITY_DN14384_c0_g1_i5	jgi|Blugr1|23250|BGHDH14_bgh04512	jgi|Blugra1|5001|BGT96224_AcSP30210T0		
jgi|Golci1|1834689|fgenesh1_kg.119_#_126_#_TRINITY_DN2916_c0_g1_i2	jgi|Blugr1|23214|BGHDH14_bghG007158000001001	jgi|Blugra1|5018|BGT96224_AcSP30464T0		
jgi|Golci1|1834832|fgenesh1_kg.120_#_67_#_TRINITY_DN16150_c0_g1_i5	jgi|Blugr1|23145|BGHDH14_bgh00016	jgi|Blugra1|5034|BGT96224_E10129T0		
jgi|Golci1|1834873|fgenesh1_kg.120_#_108_#_TRINITY_DN17226_c0_g1_i30	jgi|Blugr1|23143|BGHDH14_bghG003669000001001	jgi|Blugra1|5098|BGT96224_E5996T0		
jgi|Golci1|1835113|fgenesh1_kg.121_#_151_#_TRINITY_DN20141_c1_g2_i5	jgi|Blugr1|23046|BGHDH14_bgh04274	jgi|Blugra1|5162|BGT96224_E5883T0		
jgi|Golci1|1835397|fgenesh1_kg.124_#_42_#_TRINITY_DN19711_c3_g4_i7	jgi|Blugr1|22979|BGHDH14_bgh04522	jgi|Blugra1|5189|BGT96224_E5665T0		
jgi|Golci1|1835924|fgenesh1_kg.129_#_77_#_TRINITY_DN14418_c0_g2_i1	jgi|Blugr1|22969|BGHDH14_bgh06570	jgi|Blugra1|51|BGT96224_E5918T0		
jgi|Golci1|1837153|fgenesh1_kg.140_#_51_#_TRINITY_DN17470_c0_g4_i1	jgi|Blugr1|22911|BGHDH14_bgh05102	jgi|Blugra1|5272|BGT96224_E5659T0		
jgi|Golci1|1837446|fgenesh1_kg.142_#_1_#_TRINITY_DN1921_c0_g1_i1	jgi|Blugr1|22900|BGHDH14_bgh03739	jgi|Blugra1|5316|BGT96224_E3523T0		
jgi|Golci1|1837499|fgenesh1_kg.142_#_54_#_TRINITY_DN19711_c3_g4_i7	jgi|Blugr1|22898|BGHDH14_bgh03703	jgi|Blugra1|5332|BGT96224_E6035T0		
jgi|Golci1|1837602|fgenesh1_kg.143_#_67_#_TRINITY_DN19491_c6_g2_i1	jgi|Blugr1|22648|BGHDH14_bgh04272	jgi|Blugra1|5336|BGT96224_E3888T0		
jgi|Golci1|1838023|fgenesh1_kg.147_#_17_#_TRINITY_DN5681_c0_g1_i2	jgi|Blugr1|22634|BGHDH14_bghG002861000001001	jgi|Blugra1|5377|BGT96224_BCGB1T0		
jgi|Golci1|1838171|fgenesh1_kg.148_#_35_#_TRINITY_DN33716_c0_g1_i1	jgi|Blugr1|22633|BGHDH14_bghG002857000001001	jgi|Blugra1|5490|BGT96224_ASP20340T0		
jgi|Golci1|1838207|fgenesh1_kg.148_#_71_#_TRINITY_DN17399_c1_g1_i2	jgi|Blugr1|22603|BGHDH14_bghG002826000002001	jgi|Blugra1|5492|BGT96224_E10014T0		
jgi|Golci1|1838249|fgenesh1_kg.148_#_113_#_TRINITY_DN19651_c1_g2_i1	jgi|Blugr1|22599|BGHDH14_bghG002822000002001	jgi|Blugra1|5500|BGT96224_E5610T0		
jgi|Golci1|1838285|fgenesh1_kg.149_#_36_#_TRINITY_DN8471_c0_g1_i1	jgi|Blugr1|22577|BGHDH14_bghG002806000001001	jgi|Blugra1|5541|BGT96224_E5924T0		
jgi|Golci1|1838867|fgenesh1_kg.153_#_112_#_TRINITY_DN2342_c0_g1_i1	jgi|Blugr1|22574|BGHDH14_bgh04220	jgi|Blugra1|5550|BGT96224_AcSP30282T0		
jgi|Golci1|1838928|fgenesh1_kg.153_#_173_#_TRINITY_DN17383_c0_g2_i3	jgi|Blugr1|22556|BGHDH14_bghG002783000001001	jgi|Blugra1|5627|BGT96224_E5664T0		
jgi|Golci1|1840128|fgenesh1_kg.168_#_82_#_TRINITY_DN20795_c10_g3_i1	jgi|Blugr1|22548|BGHDH14_bgh03816	jgi|Blugra1|5735|BGT96224_E5625T0		
jgi|Golci1|1840186|fgenesh1_kg.168_#_140_#_TRINITY_DN2224_c0_g1_i1	jgi|Blugr1|22521|BGHDH14_bgh00804	jgi|Blugra1|5736|BGT96224_E5906T0		
jgi|Golci1|1840418|fgenesh1_kg.170_#_29_#_TRINITY_DN15635_c0_g3_i1	jgi|Blugr1|22452|BGHDH14_bghG002294000001001	jgi|Blugra1|575|BGT96224_E5867T0		

Gc	Bgh	Bgt	En	Go
jgi|Golci1|1840524|fgenesh1_kg.171_#_72_#_TRINITY_DN20841_c2_g2_i1	jgi|Blugr1|22425|BGHDH14_bghG002265000001001	jgi|Blugra1|5762|BGT96224_AcSP31344T0		
jgi|Golci1|1840959|fgenesh1_kg.175_#_99_#_TRINITY_DN25916_c0_g1_i1	jgi|Blugr1|22423|BGHDH14_bghG002260000001001	jgi|Blugra1|5795|BGT96224_E5850T0		
jgi|Golci1|1841438|fgenesh1_kg.180_#_47_#_TRINITY_DN18902_c1_g1_i1	jgi|Blugr1|22401|BGHDH14_bghG002254000001001	jgi|Blugra1|5804|BGT96224_AcSP31373T0		
jgi|Golci1|1841637|fgenesh1_kg.182_#_71_#_TRINITY_DN19169_c0_g2_i1	jgi|Blugr1|22309|BGHDH14_bghG002170000001001	jgi|Blugra1|5828|BGT96224_ASP21390T0		
jgi|Golci1|1842294|fgenesh1_kg.191_#_31_#_TRINITY_DN21101_c2_g19_i1	jgi|Blugr1|22308|BGHDH14_bgh03686	jgi|Blugra1|5835|BGT96224_3194T0		
jgi|Golci1|1842411|fgenesh1_kg.193_#_25_#_TRINITY_DN28222_c0_g1_i1	jgi|Blugr1|22305|BGHDH14_bghG002161000001001	jgi|Blugra1|5840|BGT96224_E5673T0		
jgi|Golci1|1842557|fgenesh1_kg.196_#_25_#_TRINITY_DN20525_c2_g11_i1	jgi|Blugr1|22300|BGHDH14_bgh03689	jgi|Blugra1|5850|BGT96224_E6034T0		
jgi|Golci1|1842817|fgenesh1_kg.200_#_72_#_TRINITY_DN18898_c3_g1_i2	jgi|Blugr1|22270|BGHDH14_bghG002084000001001	jgi|Blugra1|5867|BGT96224_E5974T0		
jgi|Golci1|1842879|fgenesh1_kg.201_#_57_#_TRINITY_DN12213_c0_g1_i3	jgi|Blugr1|22264|BGHDH14_bgh01411	jgi|Blugra1|5982|BGT96224_E5600T0		
jgi|Golci1|1843169|fgenesh1_kg.205_#_18_#_TRINITY_DN16887_c0_g2_i5	jgi|Blugr1|22249|BGHDH14_bgh04018	jgi|Blugra1|6005|BGT96224_AcSP31429T0		
jgi|Golci1|1843408|fgenesh1_kg.208_#_37_#_TRINITY_DN20914_c5_g6_i1	jgi|Blugr1|22176|BGHDH14_bgh05321	jgi|Blugra1|6046|BGT96224_ASP21455T0		
jgi|Golci1|1843633|fgenesh1_kg.211_#_33_#_TRINITY_DN20912_c5_g7_i3	jgi|Blugr1|22034|BGHDH14_bgh03696	jgi|Blugra1|6054|BGT96224_BCG6T0		
jgi|Golci1|1843635|fgenesh1_kg.211_#_35_#_TRINITY_DN20914_c5_g5_i2	jgi|Blugr1|22032|BGHDH14_bgh03474	jgi|Blugra1|6061|BGT96224_2700T0		
jgi|Golci1|1843848|fgenesh1_kg.215_#_6_#_TRINITY_DN21014_c8_g1_i1	jgi|Blugr1|22028|BGHDH14_bgh04095	jgi|Blugra1|6081|BGT96224_E5816T0		
jgi|Golci1|1844611|fgenesh1_kg.224_#_22_#_TRINITY_DN19708_c1_g3_i14	jgi|Blugr1|22026|BGHDH14_bgh04093	jgi|Blugra1|6174|BGT96224_E5966T0		
jgi|Golci1|1844841|fgenesh1_kg.230_#_14_#_TRINITY_DN31389_c0_g1_i1	jgi|Blugr1|22023|BGHDH14_bgh06602	jgi|Blugra1|6206|BGT96224_E5570T0		
jgi|Golci1|1845265|fgenesh1_kg.239_#_6_#_TRINITY_DN21049_c5_g4_i1	jgi|Blugr1|22009|BGHDH14_bgh04864	jgi|Blugra1|6207|BGT96224_2846T0		
jgi|Golci1|1845359|fgenesh1_kg.240_#_40_#_TRINITY_DN11304_c0_g2_i1	jgi|Blugr1|21987|BGHDH14_bgh03693	jgi|Blugra1|6215|BGT96224_ASP21508T0		
jgi|Golci1|1845481|fgenesh1_kg.242_#_49_#_TRINITY_DN19534_c2_g5_i1	jgi|Blugr1|21986|BGHDH14_bgh02835	jgi|Blugra1|6226|BGT96224_E40006T0		
jgi|Golci1|1846209|fgenesh1_kg.255_#_12_#_TRINITY_DN18203_c6_g1_i1	jgi|Blugr1|21942|BGHDH14_bgh03596	jgi|Blugra1|6228|BGT96224_BCG7T0		
jgi|Golci1|1846220|fgenesh1_kg.255_#_23_#_TRINITY_DN18203_c6_g1_i1	jgi|Blugr1|21938|BGHDH14_bghG003075000001001	jgi|Blugra1|6241|BGT96224_BCG1T0		
jgi|Golci1|1846232|fgenesh1_kg.255_#_35_#_TRINITY_DN17478_c2_g1_i8	jgi|Blugr1|21803|BGHDH14_bgh03709	jgi|Blugra1|6247|BGT96224_ASP20484T0		

Gc	Bgh	Bgt	En	Go
jgi|Golci1|1846577|fgenesh1_kg.261_#_83_#_TRINITY_DN1718_c0_g1_i1	jgi|Blugr1|21763|BGHDH14_bgh03037	jgi|Blugra1|6293|BGT96224_E5889T0		
jgi|Golci1|1846658|fgenesh1_kg.263_#_45_#_TRINITY_DN20009_c7_g4_i2	jgi|Blugr1|21762|BGHDH14_bghG004439000001001	jgi|Blugra1|6301|BGT96224_E5912T0		
jgi|Golci1|1846680|fgenesh1_kg.264_#_20_#_TRINITY_DN12296_c0_g1_i1	jgi|Blugr1|21761|BGHDH14_bgh03028	jgi|Blugra1|6317|BGT96224_E5550T0		
jgi|Golci1|1846764|fgenesh1_kg.266_#_9_#_TRINITY_DN12539_c0_g2_i1	jgi|Blugr1|21760|BGHDH14_bgh03042	jgi|Blugra1|6320|BGT96224_E10120T0		
jgi|Golci1|1846914|fgenesh1_kg.270_#_10_#_TRINITY_DN1718_c0_g1_i1	jgi|Blugr1|21733|BGHDH14_bghG004373000002001	jgi|Blugra1|6338|BGT96224_5370T0		
jgi|Golci1|1847190|fgenesh1_kg.274_#_27_#_TRINITY_DN26142_c0_g1_i1	jgi|Blugr1|21715|BGHDH14_bghG003905000001001	jgi|Blugra1|6371|BGT96224_E3419T0		
jgi|Golci1|1847210|fgenesh1_kg.276_#_1_#_TRINITY_DN6029_c0_g1_i1	jgi|Blugr1|21712|BGHDH14_bgh03377	jgi|Blugra1|637|BGT96224_E5607T0		
jgi|Golci1|1847249|fgenesh1_kg.277_#_28_#_TRINITY_DN20914_c5_g6_i1	jgi|Blugr1|21699|BGHDH14_bghG003896000001001	jgi|Blugra1|6473|BGT96224_E5981T0		
jgi|Golci1|1847261|fgenesh1_kg.277_#_40_#_TRINITY_DN11115_c0_g1_i1	jgi|Blugr1|21688|BGHDH14_bgh05116	jgi|Blugra1|649|BGT96224_AcSP30305T0		
jgi|Golci1|1847448|fgenesh1_kg.278_#_167_#_TRINITY_DN18781_c0_g4_i2	jgi|Blugr1|21672|BGHDH14_bgh02337	jgi|Blugra1|776|BGT96224_E10132T0		
jgi|Golci1|1847758|fgenesh1_kg.284_#_24_#_TRINITY_DN21014_c8_g1_i1	jgi|Blugr1|21671|BGHDH14_bgh03855	jgi|Blugra1|815|BGT96224_AcSP31310T0		
jgi|Golci1|1847763|fgenesh1_kg.284_#_29_#_TRINITY_DN8542_c0_g1_i2	jgi|Blugr1|21662|BGHDH14_bgh05117	jgi|Blugra1|844|BGT96224_E5829T0		
jgi|Golci1|1847945|fgenesh1_kg.288_#_7_#_TRINITY_DN16904_c1_g1_i5	jgi|Blugr1|21622|BGHDH14_bgh01337	jgi|Blugra1|955|BGT96224_AcSP30002T0		
jgi|Golci1|1847985|fgenesh1_kg.288_#_47_#_TRINITY_DN1467_c0_g2_i1	jgi|Blugr1|21515|BGHDH14_bgh06674	jgi|Blugra1|956|BGT96224_E3893T0		
jgi|Golci1|1848150|fgenesh1_kg.292_#_28_#_TRINITY_DN12002_c0_g1_i1	jgi|Blugr1|21435|BGHDH14_bghG003355000001001			
jgi|Golci1|1848194|fgenesh1_kg.294_#_20_#_TRINITY_DN5720_c0_g4_i1	jgi|Blugr1|21434|BGHDH14_bghG003347000001001			
jgi|Golci1|1848281|fgenesh1_kg.297_#_21_#_TRINITY_DN7952_c0_g2_i1	jgi|Blugr1|21424|BGHDH14_bgh02916			
jgi|Golci1|1848292|fgenesh1_kg.298_#_10_#_TRINITY_DN3024_c0_g1_i1	jgi|Blugr1|21382|BGHDH14_bgh00242			
jgi|Golci1|1848303|fgenesh1_kg.299_#_10_#_TRINITY_DN16800_c0_g2_i9	jgi|Blugr1|21287|BGHDH14_bgh04219			
jgi|Golci1|1848627|fgenesh1_kg.308_#_11_#_TRINITY_DN8353_c0_g1_i2	jgi|Blugr1|21246|BGHDH14_bgh04257			
jgi|Golci1|1849102|fgenesh1_kg.322_#_79_#_TRINITY_DN20914_c5_g5_i2	jgi|Blugr1|21240|BGHDH14_bgh03293			
jgi|Golci1|1849710|fgenesh1_kg.337_#_1_#_TRINITY_DN18943_c0_g1_i1	jgi|Blugr1|21206|BGHDH14_bgh01362			
jgi|Golci1|1849726|fgenesh1_kg.337_#_17_#_TRINITY_DN811_c0_g2_i1	jgi|Blugr1|21098|BGHDH14_bgh05195			
jgi|Golci1|1849957|fgenesh1_kg.343_#_17_#_TRINITY_DN21097_c4_g3_i1	jgi|Blugr1|21066|BGHDH14_bghG004219000001001			

Gc	Bgh	Bgt	En	Go
jgi|Golci1|1850082|fgenesh1_kg.346_#_43_#_TRINITY_DN20009_c7_g4_i2	jgi|Blugr1|21065|BGHDH14_bgh05281			
jgi|Golci1|1850536|fgenesh1_kg.359_#_2_#_TRINITY_DN5190_c0_g1_i1	jgi|Blugr1|21062|BGHDH14_bghG004216000001001			
jgi|Golci1|1851023|fgenesh1_kg.372_#_38_#_TRINITY_DN2394_c0_g1_i1	jgi|Blugr1|21025|BGHDH14_bghG006760000001001			
jgi|Golci1|1851523|fgenesh1_kg.387_#_14_#_TRINITY_DN19490_c1_g1_i2	jgi|Blugr1|20928|BGHDH14_bghG004931000001001			
jgi|Golci1|1851917|fgenesh1_kg.397_#_37_#_TRINITY_DN19431_c1_g5_i1	jgi|Blugr1|20867|BGHDH14_bgh01761			
jgi|Golci1|1851977|fgenesh1_kg.398_#_14_#_TRINITY_DN6817_c0_g1_i4	jgi|Blugr1|20822|BGHDH14_bgh03441			
jgi|Golci1|1852279|fgenesh1_kg.411_#_1_#_TRINITY_DN18771_c1_g5_i1	jgi|Blugr1|20821|BGHDH14_bgh02083			
jgi|Golci1|1852292|fgenesh1_kg.411_#_14_#_TRINITY_DN19491_c6_g2_i1	jgi|Blugr1|20818|BGHDH14_bghG003525000001001			
jgi|Golci1|1852783|fgenesh1_kg.439_#_8_#_TRINITY_DN16152_c0_g2_i1	jgi|Blugr1|20799|BGHDH14_bgh02653			
jgi|Golci1|1852935|fgenesh1_kg.454_#_3_#_TRINITY_DN8373_c0_g1_i1	jgi|Blugr1|20693|BGHDH14_bgh02274			
jgi|Golci1|1853106|fgenesh1_kg.470_#_8_#_TRINITY_DN19037_c3_g3_i9	jgi|Blugr1|20643|BGHDH14_bgh02426			
jgi|Golci1|1853244|fgenesh1_kg.488_#_4_#_TRINITY_DN14750_c0_g1_i1	jgi|Blugr1|20640|BGHDH14_bghG003379000001001			
jgi|Golci1|1853298|fgenesh1_kg.498_#_2_#_TRINITY_DN5190_c0_g1_i1	jgi|Blugr1|20599|BGHDH14_bgh03462			
jgi|Golci1|1853805|fgenesh1_kg.628_#_2_#_TRINITY_DN5190_c0_g1_i1	jgi|Blugr1|20597|BGHDH14_bgh02701			
jgi|Golci1|1854311|fgenesh1_kg.806_#_2_#_TRINITY_DN8471_c0_g3_i1	jgi|Blugr1|20595|BGHDH14_bgh05269			
jgi|Golci1|1854317|fgenesh1_kg.808_#_4_#_TRINITY_DN8471_c0_g2_i1	jgi|Blugr1|20594|BGHDH14_bgh03736			
jgi|Golci1|1854454|fgenesh1_pm.2_#_22	jgi|Blugr1|20592|BGHDH14_bghG005948000001001			
jgi|Golci1|1855481|fgenesh1_pm.35_#_8	jgi|Blugr1|20577|BGHDH14_bgh03584			
jgi|Golci1|1861191|estExt_fgenesh1_pm.C_1420008	jgi|Blugr1|20576|BGHDH14_bghG005930000001001			
jgi|Golci1|1867255|estExt_fgenesh1_pg.C_3340001	jgi|Blugr1|20575|BGHDH14_bgh03571			
jgi|Golci1|1867482|estExt_fgenesh1_pg.C_3960001	jgi|Blugr1|20572|BGHDH14_bgh02072			
jgi|Golci1|1910368|MIX42608_10_31	jgi|Blugr1|20570|BGHDH14_bgh03425			
jgi|Golci1|20843|CE20842_127	jgi|Blugr1|20521|BGHDH14_bgh04231			
jgi|Golci1|287936|CE287935_2773	jgi|Blugr1|20519|BGHDH14_bgh04113			
jgi|Golci1|397334|CE397333_28	jgi|Blugr1|20511|BGHDH14_bgh05270			
jgi|Golci1|528027|CE528026_1161	jgi|Blugr1|20510|BGHDH14_bgh01363			
jgi|Golci1|540405|CE540404_23	jgi|Blugr1|20488|BGHDH14_bgh02934			

Gc	Bgh	Bgt	En	Go
jgi|Golci1|547549|CE547548_9241	jgi|Blugr1|20487|BGHDH14_bgh03694			
jgi|Golci1|585565|CE585564_4983	jgi|Blugr1|20479|BGHDH14_bghG005814000001001			
jgi|Golci1|669736|CE669735_39518	jgi|Blugr1|20452|BGHDH14_bgh04255			
jgi|Golci1|682040|CE682039_47	jgi|Blugr1|20446|BGHDH14_bgh03641			
jgi|Golci1|686639|CE686638_4676	jgi|Blugr1|20421|BGHDH14_bgh00012			
jgi|Golci1|704175|CE704174_1109	jgi|Blugr1|20386|BGHDH14_bghG005434000001001			
jgi|Golci1|748233|CE748232_145	jgi|Blugr1|20293|BGHDH14_bghG005335000001001			
jgi|Golci1|815078|CE815077_16	jgi|Blugr1|20290|BGHDH14_bgh02435			
	jgi|Blugr1|20289|BGHDH14_bghG005334000001001			
	jgi|Blugr1|20181|BGHDH14_bgh04108			
	jgi|Blugr1|20131|BGHDH14_bghG005501000001001			
	jgi|Blugr1|20085|BGHDH14_bghG005474000001001			
	jgi|Blugr1|20077|BGHDH14_bgh06543			
	jgi|Blugr1|20063|BGHDH14_bghG005458000001001			
	jgi|Blugr1|20062|BGHDH14_bghG005457000001001			
	jgi|Blugr1|20049|BGHDH14_bgh02624			
	jgi|Blugr1|20047|BGHDH14_bgh02857			
	jgi|Blugr1|20046|BGHDH14_bgh02854			
	jgi|Blugr1|20003|BGHDH14_bgh03636			
	jgi|Blugr1|20002|BGHDH14_bgh04014			
	jgi|Blugr1|19998|BGHDH14_bgh04020			
	jgi|Blugr1|19997|BGHDH14_bgh03637			
	jgi|Blugr1|19996|BGHDH14_bghG006682000001001			
	jgi|Blugr1|19975|BGHDH14_bgh03613			
	jgi|Blugr1|19887|BGHDH14_bgh04081			
	jgi|Blugr1|19834|BGHDH14_bgh05844			
	jgi|Blugr1|19763|BGHDH14_bgh00029			

Gc	Bgh	Bgt	En	Go
	jgi|Blugr1|19690|BGHDH14_bgh04262			
	jgi|Blugr1|19689|BGHDH14_bgh03138			
	jgi|Blugr1|19688|BGHDH14_bgh03786			
	jgi|Blugr1|19687|BGHDH14_bgh06899			
	jgi|Blugr1|19686|BGHDH14_bgh04268			
	jgi|Blugr1|19677|BGHDH14_bgh03901			
	jgi|Blugr1|19676|BGHDH14_bghG006623000001001			
	jgi|Blugr1|19675|BGHDH14_bgh03874			
	jgi|Blugr1|19613|BGHDH14_bgh01675			
	jgi|Blugr1|19397|BGHDH14_bgh03782			
	jgi|Blugr1|19362|BGHDH14_bghG007601000001001			
	jgi|Blugr1|19348|BGHDH14_bgh03316			
	jgi|Blugr1|19262|BGHDH14_bgh05491			
	jgi|Blugr1|19260|BGHDH14_bgh04077			
	jgi|Blugr1|19258|BGHDH14_bgh04027			
	jgi|Blugr1|19254|BGHDH14_bgh05609			
	jgi|Blugr1|19253|BGHDH14_bghG009555000001001			
	jgi|Blugr1|19250|BGHDH14_bghG009020000001001			
	jgi|Blugr1|19249|BGHDH14_bghG008908000001001			
	jgi|Blugr1|19247|BGHDH14_bgh03579			
	jgi|Blugr1|19246|BGHDH14_bgh03575			
	jgi|Blugr1|19245|BGHDH14_bgh03572			
	jgi|Blugr1|19237|BGHDH14_bgh06532			
	jgi|Blugr1|19234|BGHDH14_bghG008002000002001			
	jgi|Blugr1|19233|BGHDH14_bghG008885000001001			
	jgi|Blugr1|19215|BGHDH14_bgh02874			
	jgi|Blugr1|19212|BGHDH14_bgh06494			

Gc	Bgh	Bgt	En	Go
	jgi|Blugr1|19211|BGHDH14_bghG008560000001001			
	jgi|Blugr1|19206|BGHDH14_bgh06518			
	jgi|Blugr1|19198|BGHDH14_bgh02928			
	jgi|Blugr1|19181|BGHDH14_bgh02925			
	jgi|Blugr1|19172|BGHDH14_bgh03582			
	jgi|Blugr1|19168|BGHDH14_bgh04083			
	jgi|Blugr1|19166|BGHDH14_bghG013624000001001			
	jgi|Blugr1|19163|BGHDH14_bgh05792			
	jgi|Blugr1|19155|BGHDH14_bgh03376			
	jgi|Blugr1|19153|BGHDH14_bghG008575000001001			

Appendix 4: *GoSLIM data for G. cichoracearum*

Whole Proteome			Predicted Secretome			Predicted Effectorome		
Biological Processes		**Number of genes**	**Biological Processes**		**Number of genes**	**Biological Process**		**Number of genes**
GO:0008150	biological process	1658	GO:0008150	biological_process	285	GO:0008150	biological_process	41
GO:0023052	signaling	101	GO:0005975	carbohydrate metabolic process	34	GO:0006325	chromatin organization	4
GO:0005975	carbohydrate metabolic process	92	GO:0006520	cellular amino acid metabolic process	16	GO:0005975	carbohydrate metabolic process	3
GO:0006468	protein phosphorylation	92	GO:0055086	nucleobase-containing small molecule metabolic process	12	GO:0023052	signaling	2
GO:0031399	regulation of protein modification process	81	GO:0006468	protein phosphorylation	11	GO:0051603	proteolysis involved in cellular protein catabolic process	2
GO:0055086	nucleobase-containing small molecule metabolic process	81	GO:0051186	cofactor metabolic process	11	GO:0055086	nucleobase-containing small molecule metabolic process	2
GO:0051321	meiotic cell cycle	79	GO:0006260	DNA replication	10	GO:0006352	DNA-templated transcription, initiation	1
GO:0070647	protein modification by small protein conjugation or removal	79	GO:0006281	DNA repair	10	GO:0006364	rRNA processing	1
GO:0006629	lipid metabolic process	78	GO:0006457	protein folding	10	GO:0006413	translational initiation	1
GO:0006520	cellular amino acid metabolic process	74	GO:0006418	tRNA aminoacylation for protein translation	9	GO:0006457	protein folding	1
GO:0006811	ion transport	63	GO:0006629	lipid metabolic process	9	GO:0006520	cellular amino acid metabolic process	1
GO:0051186	cofactor metabolic process	51	GO:0031399	regulation of protein modification process	9	GO:0006605	protein targeting	1
GO:0006281	DNA repair	50	GO:0051321	meiotic cell cycle	8	GO:0006811	ion transport	1
GO:0051603	proteolysis involved in cellular protein catabolic process	41	GO:0051603	proteolysis involved in cellular protein catabolic process	8	GO:000	response to oxidative stress	1

Whole Proteome			Predicted Secretome			Predicted Effectorome		
						6979		
GO:0006457	protein folding	37	GO:0070647	protein modification by small protein conjugation or removal	8	GO:0007005	mitochondrion organization	1
GO:0006260	DNA replication	35	GO:0006325	chromatin organization	7	GO:0031399	regulation of protein modification process	1
GO:0006325	chromatin organization	35	GO:0023052	signaling	7	GO:0048193	Golgi vesicle transport	1
GO:0006418	tRNA aminoacylation for protein translation	32	GO:0006811	ion transport	6	GO:0051186	cofactor metabolic process	1
GO:0070271	protein complex biogenesis	32	GO:0006352	DNA-templated transcription, initiation	4	GO:0051321	meiotic cell cycle	1
GO:0032787	monocarboxylic acid metabolic process	29	GO:0032787	monocarboxylic acid metabolic process	4	GO:0055085	transmembrane transport	1
GO:0008033	tRNA processing	24	GO:0070271	protein complex biogenesis	4	GO:0070647	protein modification by small protein conjugation or removal	1
GO:0055085	transmembrane transport	23	GO:0006364	rRNA processing	3	**Cellular Function**		
GO:0006091	generation of precursor metabolites and energy	21	GO:0006486	protein glycosylation	3	GO:0003674	molecular_function	26
GO:0006364	rRNA processing	19	GO:0006887	exocytosis	3	GO:0003735	structural constituent of ribosome	13
GO:0006352	DNA-templated transcription, initiation	18	GO:0006979	response to oxidative stress	3	GO:0043167	ion binding	10
GO:0007010	cytoskeleton organization	15	GO:0008033	tRNA processing	3	GO:0016491	oxidoreductase activity	8
GO:0006413	translational initiation	14	GO:0008380	RNA splicing	3	GO:0003723	RNA binding	7
GO:0045333	cellular respiration	14	GO:0009311	oligosaccharide metabolic process	3	GO:0016740	transferase activity	7
GO:0006397	mRNA processing	13	GO:0015931	nucleobase-containing compound transport	3	GO:0003677	DNA binding	4
GO:0006470	protein dephosphorylation	12	GO:0018193	peptidyl-amino acid modification	3	GO:0016853	isomerase activity	4

Whole Proteome			Predicted Secretome			Predicted Effectorome		
GO:0008643	carbohydrate transport	12	GO:0006310	DNA recombination	2	GO:0016787	hydrolase activity	3
GO:0018193	peptidyl-amino acid modification	12	GO:0006397	mRNA processing	2	GO:0003924	GTPase activity	2
GO:0006486	protein glycosylation	11	GO:0006413	translational initiation	2	GO:0004518	nuclease activity	2
GO:0006766	vitamin metabolic process	11	GO:0006766	vitamin metabolic process	2	GO:0008233	peptidase activity	2
GO:0048193	Golgi vesicle transport	11	GO:0007010	cytoskeleton organization	2	GO:0008135	translation factor activity, RNA binding	1
GO:0006605	protein targeting	10	GO:0000278	mitotic cell cycle	1	GO:0008168	methyltransferase activity	1
GO:0008380	RNA splicing	10	GO:0006091	generation of precursor metabolites and energy	1	GO:0019843	rRNA binding	1
GO:0006887	exocytosis	9	GO:0006414	translational elongation	1	GO:0051082	unfolded protein binding	1
GO:0006414	translational elongation	8	GO:0006417	regulation of translation	1			
GO:0006865	amino acid transport	8	GO:0006470	protein dephosphorylation	1			
GO:0015931	nucleobase-containing compound transport	8	GO:0006605	protein targeting	1			
GO:0006366	transcription by RNA polymerase II	7	GO:0007005	mitochondrion organization	1			
GO:0006979	response to oxidative stress	7	GO:0007031	peroxisome organization	1			
GO:0009311	oligosaccharide metabolic process	7	GO:0007059	chromosome segregation	1			
GO:0042221	response to chemical	7	GO:0032200	telomere organization	1			
GO:0006310	DNA recombination	6	GO:0033043	regulation of organelle organization	1			
GO:0007005	mitochondrion organization	6	GO:0042221	response to chemical	1			
GO:0007031	peroxisome organization	6	GO:0048193	Golgi vesicle transport	1			
GO:0009451	RNA modification	6	GO:0048285	organelle fission	1			
GO:0051604	protein maturation	6	GO:0051052	regulation of DNA metabolic process	1			
GO:0006417	regulation of translation	5	GO:0051726	regulation of cell cycle	1			
GO:0006497	protein lipidation	5	GO:0055085	transmembrane transport	1			
GO:0006869	lipid transport	5	**Cellular Processes**					

Whole Proteome			Predicted Secretome			Predicted Effectorome		
GO:0033043	regulation of organelle organization	5	GO:0003674	molecular_function	317			
GO:0048285	organelle fission	4	GO:0043167	ion binding	149			
GO:0007059	chromosome segregation	3	GO:0016740	transferase activity	89			
GO:0051726	regulation of cell cycle	3	GO:0016787	hydrolase activity	82			
GO:0000278	mitotic cell cycle	2	GO:0016491	oxidoreductase activity	54			
GO:0006897	endocytosis	2	GO:0003677	DNA binding	34			
GO:0008213	protein alkylation	2	GO:0016798	hydrolase activity, acting on glycosyl bonds	29			
GO:0032200	telomere organization	2	GO:0008233	peptidase activity	25			
GO:0042255	ribosome assembly	2	GO:0003735	structural constituent of ribosome	21			
GO:0051052	regulation of DNA metabolic process	2	GO:0016829	lyase activity	21			
GO:0070925	organelle assembly	2	GO:0016874	ligase activity	21			
GO:0002181	cytoplasmic translation	1	GO:0016853	isomerase activity	20			
GO:0006354	DNA-templated transcription, elongation	1	GO:0016301	kinase activity	19			
GO:0006383	transcription by RNA polymerase III	1	GO:0016887	ATPase activity	18			
GO:0006401	RNA catabolic process	1	GO:0004518	nuclease activity	17			
GO:0006974	cellular response to DNA damage stimulus	1	GO:0003723	RNA binding	15			
GO:0016050	vesicle organization	1	GO:0004386	helicase activity	15			
GO:0016197	endosomal transport	1	GO:0016779	nucleotidyltransferase activity	15			
GO:0016570	histone modification	1	GO:0016791	phosphatase activity	14			
GO:0043543	protein acylation	1	GO:0008168	methyltransferase activity	13			
GO:0048284	organelle fusion	1	GO:0030234	enzyme regulator activity	11			
GO:0051169	nuclear transport	1	GO:0016757	transferase activity, transferring glycosyl groups	10			
GO:0061025	membrane fusion	1	GO:0022857	transmembrane transporter activity	10			
GO:0071554	cell wall organization or biogenesis	1	GO:0051082	unfolded protein binding	9			
Cellular Function			GO:0003700	DNA binding transcription factor activity	5			
GO:0003674	molecular_function	1841	GO:0003924	GTPase activity	5			
GO:0043167	ion binding	944	GO:0004871	signal transducer activity	5			
GO:0016740	transferase activity	516	GO:0008565	protein transporter activity	5			
GO:0016787	hydrolase activity	406	GO:0008135	translation factor activity, RNA binding	3			

Whole Proteome			Predicted Secretome			Predicted Effectorome		
GO:0016491	oxidoreductase activity	270	GO:0008092	cytoskeletal protein binding	2			
GO:0003677	DNA binding	227	GO:0019843	rRNA binding	2			
GO:0016301	kinase activity	148	GO:0003682	chromatin binding	1			
GO:0016887	ATPase activity	143	GO:0005085	guanyl-nucleotide exchange factor activity	1			
GO:0003735	structural constituent of ribosome	131	GO:0005198	structural molecule activity	1			
GO:0022857	transmembrane transporter activity	123	GO:0008289	lipid binding	1			
GO:0004386	helicase activity	95	GO:0019899	enzyme binding	1			
GO:0003723	RNA binding	92						
GO:0016874	ligase activity	89						
GO:0008233	peptidase activity	83						
GO:0016829	lyase activity	83						
GO:0004518	nuclease activity	81						
GO:0016757	transferase activity, transferring glycosyl groups	74						
GO:0003700	DNA binding transcription factor activity	71						
GO:0030234	enzyme regulator activity	71						
GO:0016779	nucleotidyltransferase activity	70						
GO:0016853	isomerase activity	65						
GO:0016791	phosphatase activity	58						
GO:0016798	hydrolase activity, acting on glycosyl bonds	55						
GO:0008168	methyltransferase activity	54						
GO:0004871	signal transducer activity	47						
GO:0008565	protein transporter activity	45						
GO:0003924	GTPase activity	33						
GO:0008135	translation factor activity, RNA binding	28						
GO:0051082	unfolded protein binding	23						
GO:0003682	chromatin binding	16						
GO:0008289	lipid binding	15						
GO:0008092	cytoskeletal protein binding	14						
GO:0005085	guanyl-nucleotide exchange factor activity	13						
GO:0005198	structural molecule activity	12						

Whole Proteome			Predicted Secretome			Predicted Effectorome		
GO:0019899	enzyme binding	12						
GO:0019843	rRNA binding	5						
GO:0000988	transcription factor activity, protein binding	3						
GO:0008134	transcription factor binding	1						

Appendix 5*: Localizer Output for Powdery Mildew*

A. *G. cichoracearum* predicted effector candidate localization

Identifier	Chloroplast	Mitochondria	Nucleus
GcEC_B_1	-	-	-
GcEc13	-	-	-
GcEC_B_2	-	-	-
GcEc17	-	-	-
GcEC_B_3	-	-	-
GcEC38	-	-	-
GcEc34	-	-	-
GcEc8	-	-	Y (QRNGGGEGRGGGEGRGGNGRGNGRGNG)
GcEC11	-	-	-
GcEc10	Y (0.838 | 45-106)	Y (0.98 | 110-130)	-
GcEC_B_4	-	-	Y (KKTTNRYGFRCKKKFF)
GcEC_B_5	-	-	-
GcEC21	-	-	-
GcEC_B_6	-	-	-
GcEC_B_7	-	-	-
GcEC_B_8	-	-	-
GcEC_B_9	-	-	-
GcEC_B_10	-	-	-
GcEC_B_11	-	Y (0.997 | 53-76)	-
GcEC_B_12	-	-	-
GcEC7	-	-	-
GcEC_B_13	-	-	-
GcEC_B_14	-	-	-
GcEC_B_15	Y (0.977 | 49-74)	-	-
GcEC_B_16	-	-	-
GcEC_B_17	Y (0.853 | 45-95)	Y (0.98 | 101-121)	Y (RRCKKKSNICLGCKKKFIK)
GcEC_B_18	-	-	-
GcEC_B_19	-	-	-
GcEC_B_20	Y (0.996 | 52-89)	Y (0.983 | 73-93)	-
GcEC_B_21	-	-	-
GcEC_B_22	-	-	Y (KRHNGVGKFKYSPILSRRR)
GcEC_B_23	Y (0.999 | 68-88)	-	-
GcEC_B_24	-	-	-
GcEC_B_25	-	-	-
GcEC_B_26	-	-	-
GcEC_B_27	-	Y (0.972 | 74-95)	-
GcEC_B_28	-	-	-
GcEC_B_29	-	-	-
GcEC_B_30	-	-	-
GcEC_B_32	Y (0.947 | 59-86)	Y (0.998 | 53-73)	-
GcEC_B_33	-	-	-
GcEC_B_34	-	-	-
GcEC_B_35	-	-	-
GcEC_B_36	-	-	Y (RKYRKMNKLEAEVRKLKKK,RKMNKLEAEVRKLKKKQKA)
GcEC_B_37	-	-	Y (KKLKKSKKYKKRKHY,RSKKRKASKKFKIGKKLKKSKKYKKRKH)
GcEC_B_38	Y (0.997 | 23-61)	Y (1.0 | 35-60)	-
GcEC_B_39	-	Y (0.976 | 57-79)	-
GcEC_B_40	-	-	Y (KKSGKK,KKGKGPLNTGSQGIKKSGK)
GcEC_B_41	Y (0.998 | 64-84)	-	Y (RKAEMKATREERQKRW)
GcEC_B_42	-	-	-
GcEC_B_43	Y (0.989 | 41-75)	Y (0.993 | 33-56)	-

Identifier	Chloroplast	Mitochondria	Nucleus
GcEC_B_44	-	Y (0.971 | 60-80)	-
GcEC_B_45	-	-	Y (KRTNIPGMSRGRGRGGFRGRGYAGRGGYVPRGGGYRGGFRGGRGR)
GcEC_B_46	-	-	-
GcEC_B_47	-	Y (0.834 | 55-100)	-
GcEC_B_48	-	-	-
GcEC_B_49	Y (0.999 | 25-45)	-	-
GcEC_B_50	-	-	-
GcEC_B_51	-	-	Y (RKRR)
GcEC_B_52	-	-	-
GcEC_B_53	-	-	-
GcEC_B_54	-	-	Y (RKSAPSTGGVKKPHR,KKPHRYKPGTVALREIRR,KRVTIQSKDIQLARRLRG)
GcEC_B_55	-	-	-
GcEC_B_56	-	-	-
GcEC_B_57	-	-	-
GcEC_B_58	-	-	Y (KKIQNEDNSCQVRHETRRK)
GcEC_B_59	-	-	-
GcEC_B_60	-	-	-
GcEC_B_61	-	-	Y (RRNVEVTVEAILMLKTRKE)
GcEC_B_62	Y (0.969 | 43-84)	Y (0.979 | 70-101)	-
GcEC_B_63	-	-	-
GcEC_B_64	-	-	-
GcEC_B_65	-	-	-
GcEC_B_66	-	-	-
GcEC_B_67	-	-	-
GcEC_B_68	-	-	Y (RRRK)
GcEC_B_69	-	-	-
GcEC_B_70	-	-	-
GcEC_B_71	-	-	-
GcEC_B_72	-	Y (0.99 | 62-87)	-
GcEC_B_73	-	-	-
GcEC_B_74	-	-	-
GcEC_B_75	-	-	-
GcEC_B_76	-	-	-
GcEC_B_77	Y (0.819 | 25-45)	-	Y (KEPPRDRKKEKNIK)
GcEC_B_78	-	-	-
GcEC_B_80	-	-	Y (KRKTVTSLDVVYALKRQGR)
GcEC_B_81	-	-	-
GcEC_B_82	-	-	-
GcEC_B_83	-	-	-
GcEC_B_84	Y (0.999 | 63-130)	-	-
GcEC_B_85	Y (0.999 | 68-88)	-	Y (PKPS)
GcEC_B_86	-	-	-
GcEC_B_87	Y (0.968 | 45-86)	Y (0.965 | 62-102)	-
GcEC_B_89	-	-	-
GcEC_B_90	-	Y (0.999 | 28-48)	-
GcEC_B_91	-	-	-
GcEC_B_92	-	-	-
GcEC_B_93	-	-	-
GcEC_B_94	-	-	-
GcEC_B_95	-	Y (0.961 | 70-105)	-
GcEC_B_96	-	-	Y (RKGLSVQLAHYVTKKYKS)
GcEC_B_97	-	-	-
GcEC_B_98	-	-	Y (KKRNSGRLTKVLGCKKKGE)
GcEC_B_99	-	-	-
GcEC_B_100	-	-	-

Identifier	Chloroplast	Mitochondria	Nucleus
GcEC_B_101	-	Y (0.99 | 109-130)	Y (RRIRELTSLIQKRFKF)
GcEC_B_102	-	-	Y (KVKK,KKGKIMLVNPFVKYEKR)
GcEC_B_103	-	-	Y (KRVK)
GcEC_B_104	-	-	-
GcEC_B_105	Y (0.999 | 68-90)	-	-
GcEC_B_106	-	-	Y (RRFTIYNTLIRKKYT,KKNTLRIISKRNKER)
GcEC_B_107	-	-	-
GcEC_B_108	-	-	Y (RKCKPCGKDTHQRKRLSR)
GcEC_B_109	-	-	Y (KKKK)
GcEC_B_110	-	-	-
GcEC_B_111	-	-	Y (KKFIQKGFKNNKSKKIRS,LKPNSKKFIQKGFKNNKSKKI)
GcEC_B_112	-	-	Y (KVKK)
GcEC_B_113	-	-	Y (KKGRKN)
GcEC_B_114	-	-	Y (RRYNWFICKEKSCKKKAD)
GcEC_B_115	Y (0.926 | 58-81)	-	-
GcEC_B_116	-	-	-
GcEC_B_117	Y (0.98 | 44-64)	-	Y (RRERRNLDSMMKRMRFK)
GcEC_B_118	-	-	-
GcEC_B_119	-	-	Y (KRKPSLHFALGLGKKEKN,KRASIFDSFRYQFSKKDKV)
GcEC_B_120	Y (0.987 | 45-86)	Y (0.934 | 53-86)	Y (KRKKP)
GcEC_B_121	-	-	-
GcEC_B_122	-	-	Y (LKKIRAHRGLRHYWGLRVRGQHSKTTGRRGRTVGVSKKKGG)
GcEC_B_123	-	-	-
GcEC_B_124	-	-	Y (KRDMAYFARVTKKSDK)
GcEC_B_125	-	-	-
GcEC_B_126	-	-	-
GcEC_B_127	-	-	-
GcEC_B_128	-	-	-
GcEC_B_129	-	-	-
GcEC_B_130	-	-	-
GcEC_B_131	-	-	-
GcEC_B_132	-	-	-
GcEC_B_133	-	-	-
GcEC_B_134	-	Y (0.961 | 52-82)	-
GcEC_B_135	-	-	-
GcEC_B_136	-	-	-
GcEC_B_137	-	-	-
GcEC_B_138	-	-	-
GcEC_B_139	-	-	-
GcEC_B_140	-	-	-
GcEC_B_141	-	-	-
GcEC_B_142	-	-	-
GcEC_B_143	-	-	-
GcEC_B_144	-	-	-
GcEC_B_145	-	-	-
GcEC_B_146	-	-	-
GcEC_B_147	-	-	Y (RKRR)
GcEC_B_148	-	-	Y (RKFQIVNDAYYTLSDPRRR)
GcEC_B_149	-	-	Y (RKGLSVQSAHYVTKKYKS)
GcEC_B_150	Y (0.999 | 48-88)	-	-
GcEC_B_151	-	-	-
GcEC_B_152	-	-	Y (KVKK,KKGKLMLINPFVKYEKR)
GcEC_B_153	-	-	Y (KRKL)
GcEC_B_154	-	-	-
GcEC_B_155	-	-	Y (KSKRKKTNTRKESGKSKKKRIRNKNKKLN)

Identifier	Chloroplast	Mitochondria	Nucleus
GcEC_B_156	-	-	-
GcEC_B_157	-	-	-
GcEC_B_158	-	Y (0.958 | 77-97)	-
GcEC_B_159	Y (0.959 | 55-131)	-	-
GcEC_B_160	-	-	-
GcEC_B_161	-	Y (0.976 | 61-98)	-
GcEC_B_162	-	Y (0.991 | 60-83)	Y (RRRK,RRRR)
GcEC_B_163	-	-	Y (KRCGNSDDRSWSKKQRR)
GcEC_B_164	-	-	-
GcEC_B_165	Y (0.998 | 30-81)	-	Y (RRLKAKKNDK)
GcEC_B_166	-	Y (0.945 | 62-82)	-
GcEC_B_167	-	-	-
GcEC_B_168	-	Y (0.987 | 28-48)	-
GcEC_B_169	-	-	Y (KKPGKKNKLKI,KKNKLKITIRQFMKKWKL)
GcEC_B_170	-	-	-
GcEC_B_171	Y (0.988 | 73-103)	-	-
GcEC_B_173	-	-	Y (PKPKNKARKEVADKGLARGGRGRGGPRGRGGFRGGRGRGGRGF)
GcEC_B_174	-	-	-
GcEC_B_175	-	-	-
GcEC_B_176	-	-	-
GcEC_B_177	-	-	-
GcEC_B_178	-	-	-
GcEC_B_179	-	-	-
GcEC_B_180	-	-	Y (RRQKRKV,KKPFQVKKLEHERRREP)
GcEC_B_181	-	Y (0.961 | 33-56)	-
GcEC_B_182	Y (0.985 | 28-48)	-	Y (RRLKAKKNDK)
GcEC_B_183	-	-	Y (KKDRQSKGKNVRSKKS)
GcEC_B_184	-	-	Y (RRKDASSARIKRNKKT)
GcEC_B_185	-	-	-
GcEC_B_186	Y (0.795 | 59-94)	-	-
GcEC_B_187	-	-	Y (KKFLLISALSSRRSRA)
GcEC_B_188	-	Y (0.988 | 64-84)	Y (KRRK)
GcEC_B_189	Y (1.0 | 21-62)	-	-
GcEC_B_190	-	-	-
GcEC_B_191	-	-	-
GcEC_B_192	-	-	Y (RRRK)
GcEC_B_193	-	-	-
GcEC_B_194	Y (0.997 | 21-61)	-	-
GcEC_B_195	-	-	-
GcEC_B_196	-	-	-
GcEC_B_197	-	-	-
GcEC_B_198	-	-	-
GcEC_B_199	-	-	-
GcEC_B_200	-	Y (0.971 | 48-81)	-
GcEC_B_201	-	-	-
GcEC_B_202	Y (0.98 | 33-72)	-	-
GcEC_B_203	-	-	-
GcEC_B_204	-	-	-
GcEC_B_205	-	-	Y (LKKIRAHRGLRHYWGLRVRGQHSKTTGRRGRTVGVSKKKGG)
GcEC_B_206	-	-	-
GcEC_B_207	-	-	-
GcEC_B_208	-	-	-
GcEC_B_209	-	-	-
GcEC_B_210	-	-	-
GcEC_B_211	-	-	-

Identifier	Chloroplast	Mitochondria	Nucleus
GcEC_B_212	-	-	Y (KKRQGGGGGGGRGGGGGGRGGGGGGREGGGGGGGRNGGGRG)
GcEC_B_213	-	-	-
GcEC_B_214	-	-	-
GcEC_B_215	-	-	Y (KKKK)
GcEC_B_216	-	-	-
GcEC13	-	-	-
GcEC_B_217	-	-	Y (LGEV)
GcEC_B_218	-	-	Y (PDDKRMR)
GcEC_B_219	-	-	Y (RKIKRIR)

B. *G. orontii* predicted effector candidate localization

Identifier	Chloroplast	Mitochondria	Nucleus
jgi|Golor2|1128132|CE1084753_4368	-	-	-
jgi|Golor2|1144947|CE1101568_210	-	Y (0.97 | 39-108)	-
jgi|Golor2|1211497|CE1168118_111	-	Y (0.984 | 46-68)	-
jgi|Golor2|1344606|CE1301227_3070	-	-	-
jgi|Golor2|1379604|CE1336225_3260	Y (0.945 | 52-74)	-	-
jgi|Golor2|1426835|CE1383456_50	-	-	-
jgi|Golor2|1473392|CE1430013_12	-	-	-
jgi|Golor2|155207|CE111828_31	-	-	-
jgi|Golor2|2011771|CE1968392_572	-	-	-
jgi|Golor2|2310198|CE2266819_9543	Y (0.937 | 42-81)	Y (0.922 | 51-71)	-
jgi|Golor2|2456219|CE2412840_146	-	-	-
jgi|Golor2|246500|CE203121_322	-	-	-
jgi|Golor2|24931|gm4.24931_g	Y (0.957 | 60-100)	-	Y (RRNSASGRFHHKGNRR)
jgi|Golor2|2531858|CE2488479_830	-	-	Y (RRLYFEHLQDKPRVEKK)
jgi|Golor2|2606300|CE2562921_8603	-	-	-
jgi|Golor2|2674892|CE2631513_232	-	-	-
jgi|Golor2|2701140|CE2657761_105	-	-	-
jgi|Golor2|343951|CE300572_3457	Y (0.816 | 45-89)	-	-
jgi|Golor2|365352|CE321973_6279	-	-	Y (RKCQILGAVVIVKSKVKCK)
jgi|Golor2|37702|gm4.37702_g	-	-	Y (KKDAAKAGKKDAAKAGKK,KKDDDEDEKDDKNKLRRRR)
jgi|Golor2|3903|gm4.3903_g	-	-	-
jgi|Golor2|3933|gm4.3933_g	-	-	-
jgi|Golor2|39603|gm4.39603_g	-	-	-
jgi|Golor2|4173372|gw1.1.2905.1	-	-	-
jgi|Golor2|4210000|gw1.17.1541.1	-	-	-
jgi|Golor2|4249978|e_gw1.10.568.1	-	-	-
jgi|Golor2|4269205|e_gw1.36.1073.1	-	-	-
jgi|Golor2|4269220|e_gw1.36.342.1	-	-	-
jgi|Golor2|426930|CE383551_11476	-	-	-
jgi|Golor2|4270647|e_gw1.39.167.1	-	-	-
jgi|Golor2|4278404|e_gw1.53.42.1	-	-	-
jgi|Golor2|4280634|e_gw1.57.478.1	-	-	-
jgi|Golor2|4280651|e_gw1.57.704.1	-	-	Y (LGEV,RRRDKR)
jgi|Golor2|4296132|e_gw1.89.422.1	-	-	Y (RKRR)
jgi|Golor2|4307455|e_gw1.121.373.1	-	-	-
jgi|Golor2|4386379|fgenesh1_pg.6_#_29	-	Y (0.971 | 74-110)	Y (KLRRSISSVGKRAK)
jgi|Golor2|4386813|fgenesh1_pg.9_#_39	-	-	-
jgi|Golor2|4386995|fgenesh1_pg.11_#_41	-	-	-
jgi|Golor2|4388268|fgenesh1_pg.24_#_87	-	-	-
jgi|Golor2|4389219|fgenesh1_pg.37_#_29	-	-	-
jgi|Golor2|4390161|fgenesh1_pg.53_#_59	-	-	-
jgi|Golor2|4390630|fgenesh1_pg.61_#_31	-	-	Y (KKRQGGGGRE)
jgi|Golor2|4390806|fgenesh1_pg.64_#_43	-	-	-
jgi|Golor2|4391815|fgenesh1_pg.84_#_5	-	-	Y (RKGCIRISKNKQKGK)

Identifier	Chloroplast	Mitochondria	Nucleus
jgi|Golor2|4391816|fgenesh1_pg.84_#_6	-	-	Y (RKGCIRISKNKQKGK)
jgi|Golor2|4392990|fgenesh1_pg.110_#_22	-	-	-
jgi|Golor2|4393061|fgenesh1_pg.112_#_24	-	-	-
jgi|Golor2|4393802|fgenesh1_pg.133_#_5	-	-	-
jgi|Golor2|4394446|fgenesh1_pg.154_#_14	-	-	-
jgi|Golor2|4394460|fgenesh1_pg.154_#_28	-	-	-
jgi|Golor2|4395825|fgenesh1_pg.226_#_8	-	-	Y (KRTWGFTRWPKSYRPKDK)
jgi|Golor2|4395946|fgenesh1_pg.240_#_3	-	-	-
jgi|Golor2|4409105|estExt_Genemark4.C_1990054	-	-	-
jgi|Golor2|5549786|MIX40162_2277_93	-	-	-
jgi|Golor2|5714216|MIX204592_419_59	-	-	-
jgi|Golor2|5820476|estExt_fgenesh1_pg.C_840010	-	-	Y (KREKKKGKGK,KKFIKLSKVMNKAKKVCR)
jgi|Golor2|5824174|estExt_fgenesh1_pg.C_2400001	-	-	Y (KREKKKGKGKGK,KKFIKLSKVMNKAKKVCR)
jgi|Golor2|5824175|estExt_fgenesh1_pg.C_2400002	-	-	Y (KREKKKGKGKGK,KKFIKLSKVMNKAKKVCR)
jgi|Golor2|635348|CE591969_64	-	-	-
jgi|Golor2|636606|CE593227_1576	Y (0.927 | 64-86)	-	-
jgi|Golor2|710617|CE667238_383	-	-	-
jgi|Golor2|922974|CE879595_225	-	-	-
jgi|Golor2|97205|CE53826_15	-	-	-
jgi|Golor2|9850|gm4.9850_g	-	-	-

C. *Blumeria graminis f. sp. hordei* predicted effector candidate localization (effector probability assigned by EffectorP noted with effector name)

Identifier	Chloroplast	Mitochondria	Nucleus
jgi|Blugr1|25612|BGHDH14_bgh05803 | Effector probability: 0.722	-	-	-
jgi|Blugr1|25610|BGHDH14_bgh03695 | Effector probability: 0.98	-	-	-
jgi|Blugr1|25608|BGHDH14_bghG011456000001001 | Effector probability: 0.707	Y (0.892 | 34-72)	Y (0.968 | 92-113)	-
jgi|Blugr1|25468|BGHDH14_bgh03742 | Effector probability: 0.629	-	-	-
jgi|Blugr1|25462|BGHDH14_bgh03746 | Effector probability: 0.897	-	-	-
jgi|Blugr1|25453|BGHDH14_bgh03747 | Effector probability: 0.855	-	-	-
jgi|Blugr1|25445|BGHDH14_bghG000207000002001 | Effector probability: 0.998	-	-	-
jgi|Blugr1|25442|BGHDH14_bgh03749 | Effector probability: 0.921	-	-	-
jgi|Blugr1|25386|BGHDH14_bgh03443 | Effector probability: 0.979	-	-	-
jgi|Blugr1|25382|BGHDH14_bghG000107000003001 | Effector probability: 0.794	-	-	-
jgi|Blugr1|25364|BGHDH14_bghG000103000002001 | Effector probability: 0.765	-	-	-
jgi|Blugr1|25344|BGHDH14_bgh04209 | Effector probability: 0.962	-	-	-
jgi|Blugr1|25311|BGHDH14_bgh02080 | Effector probability: 0.575	-	-	-
jgi|Blugr1|25299|BGHDH14_bghG000032000001001 | Effector probability: 0.979	-	-	-
jgi|Blugr1|25294|BGHDH14_bghG000026000002001 | Effector probability: 0.609	-	-	-
jgi|Blugr1|25292|BGHDH14_bghG000026000001001 | Effector probability: 0.646	-	-	-
jgi|Blugr1|25290|BGHDH14_bghG000024000001001 | Effector probability: 0.998	-	-	-
jgi|Blugr1|25283|BGHDH14_bghG000012000002001 | Effector probability: 0.968	Y (0.963 | 57-86)	-	-
jgi|Blugr1|25131|BGHDH14_bgh03625 | Effector probability: 0.943	-	-	-
jgi|Blugr1|25115|BGHDH14_bgh03452 | Effector probability: 0.61	-	-	-
jgi|Blugr1|25114|BGHDH14_bghG006029000001001 | Effector probability: 0.959	-	-	-
jgi|Blugr1|25113|BGHDH14_bghG006028000001001 | Effector probability: 0.993	-	-	-
jgi|Blugr1|25110|BGHDH14_bghG006021000001001 | Effector probability: 0.926	-	-	-
jgi|Blugr1|25079|BGHDH14_bghG006278000001001 | Effector probability: 0.979	-	-	-
jgi|Blugr1|25073|BGHDH14_bgh06951 | Effector probability: 1.0	-	-	-
jgi|Blugr1|25072|BGHDH14_bgh04105 | Effector probability: 0.94	-	-	-
jgi|Blugr1|25070|BGHDH14_bgh04343 | Effector probability: 0.892	-	-	Y (RKKNFKIALYQGKYFKK)
jgi|Blugr1|25058|BGHDH14_bgh04130 | Effector probability: 0.999	-	-	-
jgi|Blugr1|25055|BGHDH14_bgh02875 | Effector probability: 0.58	-	-	-

Identifier	Chloroplast	Mitochondria	Nucleus
jgi|Blugr1|25053|BGHDH14_bgh03277 | Effector probability: 0.939	-	-	-
jgi|Blugr1|25051|BGHDH14_bgh03273 | Effector probability: 0.872	-	-	-
jgi|Blugr1|25050|BGHDH14_bgh03275 | Effector probability: 0.95	-	-	-
jgi|Blugr1|25014|BGHDH14_bghG001077000001001 | Effector probability: 0.939	-	-	-
jgi|Blugr1|24978|BGHDH14_bgh04277 | Effector probability: 0.991	-	-	-
jgi|Blugr1|24922|BGHDH14_bgh04920 | Effector probability: 0.969	-	-	Y (KIRKEIKK)
jgi|Blugr1|24870|BGHDH14_bgh04817 | Effector probability: 0.86	-	-	-
jgi|Blugr1|24845|BGHDH14_bghG000925000001001 | Effector probability: 0.902	-	-	-
jgi|Blugr1|24821|BGHDH14_bghG000833000001001 | Effector probability: 0.502	-	-	Y (KKGVEAFFYRKRPLK)
jgi|Blugr1|24809|BGHDH14_bghG000799000001001 | Effector probability: 0.911	-	-	Y (KKGVEAFFCTKKPLK)
jgi|Blugr1|24788|BGHDH14_bghG000770000002001 | Effector probability: 0.983	-	-	-
jgi|Blugr1|24738|BGHDH14_bghG000733000001001 | Effector probability: 0.949	-	-	-
jgi|Blugr1|24719|BGHDH14_bghG000714000001001 | Effector probability: 0.988	Y (0.97 | 21-58)	-	-
jgi|Blugr1|24709|BGHDH14_bgh03067 | Effector probability: 0.644	-	-	Y (KVKK)
jgi|Blugr1|24654|BGHDH14_bgh01923 | Effector probability: 0.606	-	-	Y (DKKAEAEKGKDGKDGKDGKDGKDGKQKR)
jgi|Blugr1|24625|BGHDH14_bghG000653000001001 | Effector probability: 0.976	-	-	-
jgi|Blugr1|24611|BGHDH14_bgh01048 | Effector probability: 0.987	-	-	-
jgi|Blugr1|24569|BGHDH14_bgh05755 | Effector probability: 0.695	-	Y (0.967 | 62-82)	Y (RKRK)
jgi|Blugr1|24565|BGHDH14_bgh04226 | Effector probability: 0.938	-	-	Y (RKRK)
jgi|Blugr1|24526|BGHDH14_bghG000556000001001 | Effector probability: 0.515	-	-	Y (PKKKRTK,RRGHFSKNTGYQCGSKKYK)
jgi|Blugr1|24494|BGHDH14_bgh04885 | Effector probability: 0.996	-	-	-
jgi|Blugr1|24462|BGHDH14_bgh02536 | Effector probability: 0.912	-	-	-
jgi|Blugr1|24461|BGHDH14_bghG000481000001001 | Effector probability: 0.896	-	-	-
jgi|Blugr1|24440|BGHDH14_bgh03531 | Effector probability: 0.573	-	-	-
jgi|Blugr1|24423|BGHDH14_bghG000458000002001 | Effector probability: 0.97	-	-	-
jgi|Blugr1|24422|BGHDH14_bghG000457000001001 | Effector probability: 0.872	-	-	Y (LRRPSVHRKP)
jgi|Blugr1|24419|BGHDH14_bghG000456000001001 | Effector probability: 0.983	-	-	-
jgi|Blugr1|24416|BGHDH14_bghG000452000001001 | Effector probability: 0.981	-	-	Y (RRPSVHRK)
jgi|Blugr1|24373|BGHDH14_bgh04954 | Effector probability: 0.901	-	-	-
jgi|Blugr1|24361|BGHDH14_bghG000425000003001 | Effector probability: 0.921	-	-	-

Identifier	Chloroplast	Mitochondria	Nucleus
jgi|Blugr1|24333|BGHDH14_bghG000417000001001 | Effector probability: 0.958	-	-	-
jgi|Blugr1|24331|BGHDH14_bghG000417000002001 | Effector probability: 0.998	-	-	-
jgi|Blugr1|24314|BGHDH14_bgh04026 | Effector probability: 0.853	-	-	-
jgi|Blugr1|24313|BGHDH14_bgh02942 | Effector probability: 0.993	-	-	-
jgi|Blugr1|24298|BGHDH14_bgh03375 | Effector probability: 0.954	-	-	-
jgi|Blugr1|24297|BGHDH14_bgh02998 | Effector probability: 0.973	-	-	-
jgi|Blugr1|24294|BGHDH14_bgh06578 | Effector probability: 0.989	-	-	-
jgi|Blugr1|24293|BGHDH14_bgh03730 | Effector probability: 0.555	-	-	-
jgi|Blugr1|24254|BGHDH14_bgh02825 | Effector probability: 0.997	-	-	-
jgi|Blugr1|24253|BGHDH14_bgh02420 | Effector probability: 0.947	-	-	-
jgi|Blugr1|24241|BGHDH14_bgh02262 | Effector probability: 0.975	-	-	-
jgi|Blugr1|24239|BGHDH14_bgh02778 | Effector probability: 0.96	-	-	-
jgi|Blugr1|24238|BGHDH14_bgh03466 | Effector probability: 0.944	-	-	-
jgi|Blugr1|24237|BGHDH14_bgh03464 | Effector probability: 0.671	-	-	-
jgi|Blugr1|24236|BGHDH14_bgh03568 | Effector probability: 0.972	-	-	-
jgi|Blugr1|24235|BGHDH14_bghG001947000001001 | Effector probability: 0.561	-	-	-
jgi|Blugr1|24114|BGHDH14_bgh03692 | Effector probability: 0.977	-	-	-
jgi|Blugr1|24084|BGHDH14_bgh03457 | Effector probability: 0.901	-	-	-
jgi|Blugr1|24083|BGHDH14_bgh02774 | Effector probability: 0.959	-	-	-
jgi|Blugr1|24082|BGHDH14_bghG001721000001001 | Effector probability: 0.96	-	-	-
jgi|Blugr1|24081|BGHDH14_bgh05751 | Effector probability: 0.977	-	-	-
jgi|Blugr1|24073|BGHDH14_bgh03794 | Effector probability: 0.826	-	-	-
jgi|Blugr1|24071|BGHDH14_bgh03995 | Effector probability: 0.786	-	-	-
jgi|Blugr1|24069|BGHDH14_bgh03922 | Effector probability: 0.893	-	-	-
jgi|Blugr1|24068|BGHDH14_bghG001682000001001 | Effector probability: 0.92	-	-	-
jgi|Blugr1|24060|BGHDH14_bgh03857 | Effector probability: 0.977	-	-	-
jgi|Blugr1|23984|BGHDH14_bgh06200 | Effector probability: 0.985	-	-	-
jgi|Blugr1|23889|BGHDH14_bghG002664000001001 | Effector probability: 0.978	-	-	-
jgi|Blugr1|23888|BGHDH14_bghG002653000001001 | Effector probability: 0.763	Y (0.993 | 42-64)	-	-
jgi|Blugr1|23871|BGHDH14_bghG002637000001001 | Effector probability: 0.729	-	-	-
jgi|Blugr1|23844|BGHDH14_bghG002599000002001 | Effector probability: 0.973	-	-	-

Identifier	Chloroplast	Mitochondria	Nucleus
jgi|Blugr1|23843|BGHDH14_bghG002599000001001 | Effector probability: 0.963	-	-	-
jgi|Blugr1|23841|BGHDH14_bgh05096 | Effector probability: 0.789	-	-	-
jgi|Blugr1|23839|BGHDH14_bgh05069 | Effector probability: 0.931	-	-	-
jgi|Blugr1|23838|BGHDH14_bghG002593000001001 | Effector probability: 0.978	-	-	-
jgi|Blugr1|23836|BGHDH14_bghG002593000004001 | Effector probability: 0.939	-	-	-
jgi|Blugr1|23813|BGHDH14_bgh02924 | Effector probability: 0.929	-	-	-
jgi|Blugr1|23803|BGHDH14_bgh02922 | Effector probability: 0.907	-	-	-
jgi|Blugr1|23802|BGHDH14_bgh02918 | Effector probability: 0.713	-	-	-
jgi|Blugr1|23795|BGHDH14_bgh06709 | Effector probability: 0.927	-	-	-
jgi|Blugr1|23794|BGHDH14_bgh01406 | Effector probability: 0.962	-	-	-
jgi|Blugr1|23792|BGHDH14_bgh01369 | Effector probability: 0.846	-	-	-
jgi|Blugr1|23791|BGHDH14_bgh01407 | Effector probability: 0.831	-	-	-
jgi|Blugr1|23790|BGHDH14_bgh02923 | Effector probability: 0.752	-	-	-
jgi|Blugr1|23786|BGHDH14_bgh01404 | Effector probability: 0.886	-	-	-
jgi|Blugr1|23779|BGHDH14_bgh01628 | Effector probability: 0.946	-	-	-
jgi|Blugr1|23778|BGHDH14_bgh04266 | Effector probability: 0.98	-	-	-
jgi|Blugr1|23777|BGHDH14_bgh04023 | Effector probability: 0.827	-	-	-
jgi|Blugr1|23776|BGHDH14_bgh03058 | Effector probability: 0.726	-	-	-
jgi|Blugr1|23769|BGHDH14_bgh00225 | Effector probability: 0.889	-	-	-
jgi|Blugr1|23768|BGHDH14_bgh00020 | Effector probability: 0.99	-	-	-
jgi|Blugr1|23766|BGHDH14_bgh01412 | Effector probability: 0.816	-	-	-
jgi|Blugr1|23765|BGHDH14_bgh01408 | Effector probability: 0.994	-	-	-
jgi|Blugr1|23743|BGHDH14_bghG002403000001001 | Effector probability: 0.974	-	-	-
jgi|Blugr1|23736|BGHDH14_bghG002392000001001 | Effector probability: 0.794	-	-	-
jgi|Blugr1|23731|BGHDH14_bgh02376 | Effector probability: 0.979	-	-	-
jgi|Blugr1|23682|BGHDH14_bgh04927 | Effector probability: 0.918	-	-	-
jgi|Blugr1|23488|BGHDH14_bgh02588 | Effector probability: 0.601	-	-	-
jgi|Blugr1|23457|BGHDH14_bghG001346000001001 | Effector probability: 0.999	-	-	-
jgi|Blugr1|23416|BGHDH14_bgh04781 | Effector probability: 0.673	-	-	Y (KRRR,KKKISCLKRWYIKHRKY)
jgi|Blugr1|23414|BGHDH14_bgh03735 | Effector probability: 0.555	-	Y (0.939 | 34-63)	-
jgi|Blugr1|23393|BGHDH14_bgh03731 | Effector probability: 0.533	-	-	-

Identifier	Chloroplast	Mitochondria	Nucleus
jgi|Blugr1|23392|BGHDH14_bghG001282000001001 | Effector probability: 0.949	-	-	-
jgi|Blugr1|23377|BGHDH14_bgh00027 | Effector probability: 0.532	-	Y (0.935 | 95-115)	-
jgi|Blugr1|23372|BGHDH14_bgh04121 | Effector probability: 0.678	-	-	-
jgi|Blugr1|23363|BGHDH14_bghG001240000001001 | Effector probability: 0.744	-	-	Y (FKVK)
jgi|Blugr1|23359|BGHDH14_bghG001226000001001 | Effector probability: 0.832	-	-	-
jgi|Blugr1|23356|BGHDH14_bghG001225000001001 | Effector probability: 0.869	Y (0.93 | 49-108)	-	-
jgi|Blugr1|23250|BGHDH14_bgh04512 | Effector probability: 0.611	-	-	Y (PCDKRKV)
jgi|Blugr1|23214|BGHDH14_bghG007158000001001 | Effector probability: 0.88	-	Y (0.93 | 98-118)	-
jgi|Blugr1|23145|BGHDH14_bgh00016 | Effector probability: 0.994	-	-	-
jgi|Blugr1|23143|BGHDH14_bghG003669000001001 | Effector probability: 0.855	-	-	-
jgi|Blugr1|23046|BGHDH14_bgh04274 | Effector probability: 0.954	-	-	-
jgi|Blugr1|22979|BGHDH14_bgh04522 | Effector probability: 1.0	-	-	-
jgi|Blugr1|22969|BGHDH14_bgh06570 | Effector probability: 0.964	-	-	-
jgi|Blugr1|22911|BGHDH14_bgh05102 | Effector probability: 0.977	-	-	-
jgi|Blugr1|22900|BGHDH14_bgh03739 | Effector probability: 0.902	-	-	-
jgi|Blugr1|22898|BGHDH14_bgh03703 | Effector probability: 0.979	-	-	-
jgi|Blugr1|22648|BGHDH14_bgh04272 | Effector probability: 0.87	-	-	Y (KRRP)
jgi|Blugr1|22634|BGHDH14_bghG002861000001001 | Effector probability: 0.869	-	-	-
jgi|Blugr1|22633|BGHDH14_bghG002857000001001 | Effector probability: 0.935	-	-	-
jgi|Blugr1|22603|BGHDH14_bghG002826000002001 | Effector probability: 0.66	Y (0.998 | 48-73)	-	Y (RRIRSAARSACKVIRKKKR)
jgi|Blugr1|22599|BGHDH14_bghG002822000002001 | Effector probability: 0.923	-	-	-
jgi|Blugr1|22577|BGHDH14_bghG002806000001001 | Effector probability: 0.999	-	-	-
jgi|Blugr1|22574|BGHDH14_bgh04220 | Effector probability: 0.652	-	-	-
jgi|Blugr1|22556|BGHDH14_bghG002783000001001 | Effector probability: 0.867	-	-	-
jgi|Blugr1|22548|BGHDH14_bgh03816 | Effector probability: 0.993	-	Y (0.987 | 27-49)	Y (RRSLTHCSVGKVYRRKGSR)
jgi|Blugr1|22521|BGHDH14_bgh00804 | Effector probability: 0.839	-	-	-
jgi|Blugr1|22452|BGHDH14_bghG002294000001001 | Effector probability: 0.834	-	-	-
jgi|Blugr1|22425|BGHDH14_bghG002265000001001 | Effector probability: 0.862	-	-	-
jgi|Blugr1|22423|BGHDH14_bghG002260000001001 | Effector probability: 0.956	-	-	-
jgi|Blugr1|22401|BGHDH14_bghG002254000001001 | Effector probability: 0.996	-	-	-
jgi|Blugr1|22309|BGHDH14_bghG002170000001001 | Effector probability: 0.947	Y (0.927 | 69-113)	-	-
jgi|Blugr1|22308|BGHDH14_bgh03686 | Effector probability: 0.973	-	-	-

Identifier	Chloroplast	Mitochondria	Nucleus
jgi|Blugr1|22305|BGHDH14_bghG002161000001001 | Effector probability: 0.974	-	-	-
jgi|Blugr1|22300|BGHDH14_bgh03689 | Effector probability: 0.973	-	-	-
jgi|Blugr1|22270|BGHDH14_bghG002084000001001 | Effector probability: 0.971	-	-	-
jgi|Blugr1|22264|BGHDH14_bgh01411 | Effector probability: 0.823	-	-	-
jgi|Blugr1|22249|BGHDH14_bgh04018 | Effector probability: 0.947	-	-	-
jgi|Blugr1|22176|BGHDH14_bgh05321 | Effector probability: 0.939	Y (0.99 | 84-108)	-	-
jgi|Blugr1|22034|BGHDH14_bgh03696 | Effector probability: 0.999	-	-	-
jgi|Blugr1|22032|BGHDH14_bgh03474 | Effector probability: 0.959	-	-	-
jgi|Blugr1|22028|BGHDH14_bgh04095 | Effector probability: 0.847	-	-	-
jgi|Blugr1|22026|BGHDH14_bgh04093 | Effector probability: 0.965	-	-	-
jgi|Blugr1|22023|BGHDH14_bgh06602 | Effector probability: 0.943	-	-	-
jgi|Blugr1|22009|BGHDH14_bgh04864 | Effector probability: 0.992	-	-	-
jgi|Blugr1|21987|BGHDH14_bgh03693 | Effector probability: 0.995	-	-	-
jgi|Blugr1|21986|BGHDH14_bgh02835 | Effector probability: 0.854	-	-	Y (SKGRTSKGRTSKGSPSRAARR)
jgi|Blugr1|21942|BGHDH14_bgh03596 | Effector probability: 0.952	-	-	-
jgi|Blugr1|21938|BGHDH14_bghG003075000001001 | Effector probability: 0.505	-	-	-
jgi|Blugr1|21803|BGHDH14_bgh03709 | Effector probability: 0.907	-	-	-
jgi|Blugr1|21763|BGHDH14_bgh03037 | Effector probability: 0.794	-	-	-
jgi|Blugr1|21762|BGHDH14_bghG004439000001001 | Effector probability: 0.62	-	-	Y (RRKR)
jgi|Blugr1|21761|BGHDH14_bgh03028 | Effector probability: 0.823	-	-	-
jgi|Blugr1|21760|BGHDH14_bgh03042 | Effector probability: 0.615	-	-	-
jgi|Blugr1|21733|BGHDH14_bghG004373000002001 | Effector probability: 0.955	Y (0.885 | 69-92)	Y (0.97 | 53-75)	-
jgi|Blugr1|21715|BGHDH14_bghG003905000001001 | Effector probability: 0.993	-	-	-
jgi|Blugr1|21712|BGHDH14_bgh03377 | Effector probability: 0.974	-	-	-
jgi|Blugr1|21699|BGHDH14_bghG003896000001001 | Effector probability: 0.931	-	-	-
jgi|Blugr1|21688|BGHDH14_bgh05116 | Effector probability: 0.898	-	-	Y (RRDLIEPIDVMKSLRK)
jgi|Blugr1|21672|BGHDH14_bgh02337 | Effector probability: 0.7	-	-	-
jgi|Blugr1|21671|BGHDH14_bgh03855 | Effector probability: 0.638	Y (0.982 | 23-64)	-	-
jgi|Blugr1|21662|BGHDH14_bgh05117 | Effector probability: 0.901	-	-	-
jgi|Blugr1|21622|BGHDH14_bgh01337 | Effector probability: 0.866	-	-	-
jgi|Blugr1|21515|BGHDH14_bgh06674 | Effector probability: 0.524	-	-	Y (RRNFGPDHKGYQCGKKKYI)
jgi|Blugr1|21435|BGHDH14_bghG003355000001001 | Effector probability: 0.701	-	-	-

Identifier	Chloroplast	Mitochondria	Nucleus
jgi|Blugr1|21434|BGHDH14_bghG003347000001001 | Effector probability: 0.789	-	-	Y (KRFSLDAAEEHARKARF)
jgi|Blugr1|21424|BGHDH14_bgh02916 | Effector probability: 0.702	-	-	-
jgi|Blugr1|21382|BGHDH14_bgh00242 | Effector probability: 0.958	-	-	-
jgi|Blugr1|21287|BGHDH14_bgh04219 | Effector probability: 0.893	-	-	-
jgi|Blugr1|21246|BGHDH14_bgh04257 | Effector probability: 0.957	-	-	-
jgi|Blugr1|21240|BGHDH14_bgh03293 | Effector probability: 0.959	-	-	Y (KHKR)
jgi|Blugr1|21206|BGHDH14_bgh01362 | Effector probability: 0.648	-	-	-
jgi|Blugr1|21098|BGHDH14_bgh05195 | Effector probability: 0.999	-	-	-
jgi|Blugr1|21066|BGHDH14_bghG004219000001001 | Effector probability: 0.947	-	-	-
jgi|Blugr1|21065|BGHDH14_bgh05281 | Effector probability: 0.744	-	-	Y (KKKPK,RKVVKQSCGIAKKRLKM)
jgi|Blugr1|21062|BGHDH14_bghG004216000001001 | Effector probability: 0.985	-	Y (0.988 | 57-78)	Y (RRRR)
jgi|Blugr1|21025|BGHDH14_bghG006760000001001 | Effector probability: 0.783	-	-	-
jgi|Blugr1|20928|BGHDH14_bghG004931000001001 | Effector probability: 0.933	-	-	Y (RRSSGPRHFGFECGSKKYK)
jgi|Blugr1|20867|BGHDH14_bgh01761 | Effector probability: 0.994	-	-	Y (KKAGGEKATKKVKAAAEKRAEK)
jgi|Blugr1|20822|BGHDH14_bgh03441 | Effector probability: 0.85	-	-	-
jgi|Blugr1|20821|BGHDH14_bgh02083 | Effector probability: 0.998	-	-	-
jgi|Blugr1|20818|BGHDH14_bghG003525000001001 | Effector probability: 0.968	-	-	-
jgi|Blugr1|20799|BGHDH14_bgh02653 | Effector probability: 0.649	-	-	-
jgi|Blugr1|20693|BGHDH14_bgh02274 | Effector probability: 0.949	-	-	-
jgi|Blugr1|20643|BGHDH14_bgh02426 | Effector probability: 0.855	-	-	-
jgi|Blugr1|20640|BGHDH14_bghG003379000001001 | Effector probability: 0.823	-	-	-
jgi|Blugr1|20599|BGHDH14_bgh03462 | Effector probability: 0.96	-	-	-
jgi|Blugr1|20597|BGHDH14_bgh02701 | Effector probability: 0.815	-	-	-
jgi|Blugr1|20595|BGHDH14_bgh05269 | Effector probability: 0.995	-	-	-
jgi|Blugr1|20594|BGHDH14_bgh03736 | Effector probability: 0.942	-	-	-
jgi|Blugr1|20592|BGHDH14_bghG005948000001001 | Effector probability: 0.998	-	-	-
jgi|Blugr1|20577|BGHDH14_bgh03584 | Effector probability: 0.808	-	-	-
jgi|Blugr1|20576|BGHDH14_bghG005930000001001 | Effector probability: 0.538	-	-	-
jgi|Blugr1|20575|BGHDH14_bgh03571 | Effector probability: 0.563	-	-	-
jgi|Blugr1|20572|BGHDH14_bgh02072 | Effector probability: 0.883	-	-	-
jgi|Blugr1|20570|BGHDH14_bgh03425 | Effector probability: 0.949	-	-	-

Identifier	Chloroplast	Mitochondria	Nucleus
jgi|Blugr1|20521|BGHDH14_bgh04231 | Effector probability: 0.941	-	-	Y (PKKKRTK,RRGYFSKNTGYECGSKKYK)
jgi|Blugr1|20519|BGHDH14_bgh04113 | Effector probability: 0.955	-	Y (0.964 | 62-82)	-
jgi|Blugr1|20511|BGHDH14_bgh05270 | Effector probability: 0.996	-	-	-
jgi|Blugr1|20510|BGHDH14_bgh01363 | Effector probability: 0.872	-	-	-
jgi|Blugr1|20488|BGHDH14_bgh02934 | Effector probability: 0.629	-	-	-
jgi|Blugr1|20487|BGHDH14_bgh03694 | Effector probability: 0.981	-	-	-
jgi|Blugr1|20479|BGHDH14_bghG005814000001001 | Effector probability: 0.888	-	-	-
jgi|Blugr1|20452|BGHDH14_bgh04255 | Effector probability: 0.999	-	-	-
jgi|Blugr1|20446|BGHDH14_bgh03641 | Effector probability: 0.911	-	-	-
jgi|Blugr1|20421|BGHDH14_bgh00012 | Effector probability: 0.815	-	-	-
jgi|Blugr1|20386|BGHDH14_bghG005434000001001 | Effector probability: 0.793	-	-	-
jgi|Blugr1|20293|BGHDH14_bghG005335000001001 | Effector probability: 0.625	-	-	-
jgi|Blugr1|20290|BGHDH14_bgh02435 | Effector probability: 0.834	-	-	-
jgi|Blugr1|20289|BGHDH14_bghG005334000001001 | Effector probability: 0.717	-	-	-
jgi|Blugr1|20181|BGHDH14_bgh04108 | Effector probability: 0.995	-	-	-
jgi|Blugr1|20131|BGHDH14_bghG005501000001001 | Effector probability: 0.779	-	-	-
jgi|Blugr1|20085|BGHDH14_bghG005474000001001 | Effector probability: 0.957	-	-	-
jgi|Blugr1|20077|BGHDH14_bgh06543 | Effector probability: 0.723	-	-	-
jgi|Blugr1|20063|BGHDH14_bghG005458000001001 | Effector probability: 0.536	-	Y (0.954 | 50-73)	-
jgi|Blugr1|20062|BGHDH14_bghG005457000001001 | Effector probability: 0.716	-	-	-
jgi|Blugr1|20049|BGHDH14_bgh02624 | Effector probability: 0.713	-	-	-
jgi|Blugr1|20047|BGHDH14_bgh02857 | Effector probability: 0.526	-	-	-
jgi|Blugr1|20046|BGHDH14_bgh02854 | Effector probability: 0.543	-	-	-
jgi|Blugr1|20003|BGHDH14_bgh03636 | Effector probability: 0.939	-	-	-
jgi|Blugr1|20002|BGHDH14_bgh04014 | Effector probability: 0.972	-	-	-
jgi|Blugr1|19998|BGHDH14_bgh04020 | Effector probability: 0.999	-	-	-
jgi|Blugr1|19997|BGHDH14_bgh03637 | Effector probability: 0.999	-	-	-
jgi|Blugr1|19996|BGHDH14_bghG006682000001001 | Effector probability: 0.986	-	-	-
jgi|Blugr1|19975|BGHDH14_bgh03613 | Effector probability: 0.505	-	-	-
jgi|Blugr1|19887|BGHDH14_bgh04081 | Effector probability: 0.974	-	-	-
jgi|Blugr1|19834|BGHDH14_bgh05844 | Effector probability: 0.942	-	Y (0.983 | 49-69)	-

Identifier	Chloroplast	Mitochondria	Nucleus
jgi|Blugr1|19763|BGHDH14_bgh00029 | Effector probability: 0.947	-	-	Y (KRVAVVYQQGYRNNRK)
jgi|Blugr1|19690|BGHDH14_bgh04262 | Effector probability: 0.893	-	-	-
jgi|Blugr1|19689|BGHDH14_bgh03138 | Effector probability: 0.88	-	-	-
jgi|Blugr1|19688|BGHDH14_bgh03786 | Effector probability: 0.9	-	-	-
jgi|Blugr1|19687|BGHDH14_bgh06899 | Effector probability: 0.978	-	-	-
jgi|Blugr1|19686|BGHDH14_bgh04268 | Effector probability: 0.872	-	-	Y (RRFSELITLWQRYLRR)
jgi|Blugr1|19677|BGHDH14_bgh03901 | Effector probability: 0.947	-	-	-
jgi|Blugr1|19676|BGHDH14_bghG006623000001001 | Effector probability: 0.923	-	-	-
jgi|Blugr1|19675|BGHDH14_bgh03874 | Effector probability: 0.854	-	-	-
jgi|Blugr1|19613|BGHDH14_bgh01675 | Effector probability: 0.841	-	-	-
jgi|Blugr1|19397|BGHDH14_bgh03782 | Effector probability: 0.996	-	-	-
jgi|Blugr1|19362|BGHDH14_bghG007601000001001 | Effector probability: 0.609	-	-	-
jgi|Blugr1|19348|BGHDH14_bgh03316 | Effector probability: 0.91	-	-	-
jgi|Blugr1|19262|BGHDH14_bgh05491 | Effector probability: 0.663	-	-	Y (KKPR)
jgi|Blugr1|19260|BGHDH14_bgh04077 | Effector probability: 0.674	-	-	Y (KKENDKKTSSEILSKKPRP)
jgi|Blugr1|19258|BGHDH14_bgh04027 | Effector probability: 0.996	-	-	-
jgi|Blugr1|19254|BGHDH14_bgh05609 | Effector probability: 0.56	-	-	-
jgi|Blugr1|19253|BGHDH14_bghG009555000001001 | Effector probability: 0.991	-	-	-
jgi|Blugr1|19250|BGHDH14_bghG009020000001001 | Effector probability: 0.952	-	-	-
jgi|Blugr1|19249|BGHDH14_bghG008908000001001 | Effector probability: 0.656	-	-	-
jgi|Blugr1|19247|BGHDH14_bgh03579 | Effector probability: 0.996	-	-	-
jgi|Blugr1|19246|BGHDH14_bgh03575 | Effector probability: 0.974	-	-	-
jgi|Blugr1|19245|BGHDH14_bgh03572 | Effector probability: 0.995	-	-	-
jgi|Blugr1|19237|BGHDH14_bgh06532 | Effector probability: 0.974	-	-	-
jgi|Blugr1|19234|BGHDH14_bghG008002000002001 | Effector probability: 0.969	-	-	Y (RRASGDPEPPNGDRHKTRK)
jgi|Blugr1|19233|BGHDH14_bghG008885000001001 | Effector probability: 0.757	-	-	-
jgi|Blugr1|19215|BGHDH14_bgh02874 | Effector probability: 0.935	-	-	-
jgi|Blugr1|19212|BGHDH14_bgh06494 | Effector probability: 1.0	-	-	-
jgi|Blugr1|19211|BGHDH14_bghG008560000001001 | Effector probability: 1.0	-	-	-
jgi|Blugr1|19206|BGHDH14_bgh06518 | Effector probability: 0.897	-	-	-
jgi|Blugr1|19198|BGHDH14_bgh02928 | Effector probability: 0.938	-	-	-
jgi|Blugr1|19181|BGHDH14_bgh02925 | Effector probability: 0.957	-	-	-

Identifier	Chloroplast	Mitochondria	Nucleus
jgi|Blugr1|19172|BGHDH14_bgh03582 | Effector probability: 0.995	-	-	-
jgi|Blugr1|19168|BGHDH14_bgh04083 | Effector probability: 0.523	-	-	-
jgi|Blugr1|19166|BGHDH14_bghG013624000001001 | Effector probability: 0.948	-	-	-
jgi|Blugr1|19163|BGHDH14_bgh05792 | Effector probability: 0.903	-	-	-
jgi|Blugr1|19155|BGHDH14_bgh03376 | Effector probability: 0.774	-	-	-
jgi|Blugr1|19153|BGHDH14_bghG008575000001001 | Effector probability: 0.974	-	-	-

D. *Blumeria graminis f. sp. tritici* predicted effector candidate localization (effector probability assigned by EffectorP noted with effector name)

Identifier	Chloroplast	Mitochondria	Nucleus
jgi|Blugra1|1031|BGT96224_E5632T0 | Effector probability: 0.724	-	-	-
jgi|Blugra1|104|BGT96224_BCG4T0 | Effector probability: 0.896	-	-	-
jgi|Blugra1|1057|BGT96224_40012T0 | Effector probability: 0.864	-	-	-
jgi|Blugra1|1058|BGT96224_AcSP31098T0 | Effector probability: 0.996	-	-	-
jgi|Blugra1|1067|BGT96224_E5685T0 | Effector probability: 0.947	-	-	-
jgi|Blugra1|107|BGT96224_E10109T0 | Effector probability: 0.954	-	-	-
jgi|Blugra1|1108|BGT96224_E10101T0 | Effector probability: 0.941	-	-	Y (KFAPGKKRWR)
jgi|Blugra1|1188|BGT96224_E5980T0 | Effector probability: 0.83	-	-	-
jgi|Blugra1|1193|BGT96224_AcSP30107T0 | Effector probability: 0.985	-	Y (0.959 | 21-47)	-
jgi|Blugra1|1231|BGT96224_AcSP31145T0 | Effector probability: 0.822	-	-	-
jgi|Blugra1|123|BGT96224_E40011T0 | Effector probability: 0.983	-	-	-
jgi|Blugra1|1249|BGT96224_2900BT0 | Effector probability: 0.937	-	-	-
jgi|Blugra1|1312|BGT96224_E5722T0 | Effector probability: 0.967	-	-	Y (KRNSDPRHFGFECGSRKYK)
jgi|Blugra1|1326|BGT96224_1289T0 | Effector probability: 0.979	-	-	-
jgi|Blugra1|1330|BGT96224_E5731T0 | Effector probability: 0.502	-	Y (0.892 | 87-107)	Y (KRKL)
jgi|Blugra1|1338|BGT96224_AcSP30530T0 | Effector probability: 0.902	-	-	-
jgi|Blugra1|1427|BGT96224_2135T0 | Effector probability: 0.993	-	-	Y (EKATKKAK,KKAKAEEVTEKRAEKR)
jgi|Blugra1|1436|BGT96224_E5704T0 | Effector probability: 0.943	Y (0.885 | 69-92)	Y (0.97 | 53-75)	-
jgi|Blugra1|1442|BGT96224_E5709T0 | Effector probability: 0.539	-	-	-
jgi|Blugra1|1478|BGT96224_19T0 | Effector probability: 0.902	-	-	-
jgi|Blugra1|148|BGT96224_2708T0 | Effector probability: 0.927	-	-	-
jgi|Blugra1|1513|BGT96224_E5909T0 | Effector probability: 0.552	-	-	-
jgi|Blugra1|1541|BGT96224_2274T0 | Effector probability: 0.512	-	-	Y (QDKKAEDGKDGKDGKDGKNGKQKR)
jgi|Blugra1|1550|BGT96224_E6031T0 | Effector probability: 0.815	-	-	-
jgi|Blugra1|158|BGT96224_E5560T0 | Effector probability: 0.826	-	-	-
jgi|Blugra1|165|BGT96224_ASP20866T0 | Effector probability: 0.984	-	-	Y (FKRR,LGEV)
jgi|Blugra1|1711|BGT96224_E5627T0 | Effector probability: 0.713	-	-	-
jgi|Blugra1|1742|BGT96224_E6018T0 | Effector probability: 0.971	-	-	-

Identifier	Chloroplast	Mitochondria	Nucleus
jgi|Blugra1|1749|BGT96224_4496BT0 | Effector probability: 0.758	-	-	-
jgi|Blugra1|1756|BGT96224_E10137T0 | Effector probability: 0.882	-	-	-
jgi|Blugra1|184|BGT96224_E5929T0 | Effector probability: 0.977	-	-	-
jgi|Blugra1|1904|BGT96224_E5836T0 | Effector probability: 0.856	-	-	-
jgi|Blugra1|1910|BGT96224_AcSP30824T0 | Effector probability: 0.807	-	-	-
jgi|Blugra1|1929|BGT96224_E5982T0 | Effector probability: 1.0	-	-	-
jgi|Blugra1|194|BGT96224_BCG8T0 | Effector probability: 0.936	-	-	-
jgi|Blugra1|1988|BGT96224_E10118T0 | Effector probability: 0.987	-	-	-
jgi|Blugra1|1989|BGT96224_E5547T0 | Effector probability: 0.893	-	-	-
jgi|Blugra1|1990|BGT96224_AcSP30782T0 | Effector probability: 0.795	-	-	-
jgi|Blugra1|201|BGT96224_E5842T0 | Effector probability: 0.7	-	-	-
jgi|Blugra1|202|BGT96224_ASP21585T0 | Effector probability: 0.708	-	-	-
jgi|Blugra1|209|BGT96224_E5913T0 | Effector probability: 0.996	-	-	-
jgi|Blugra1|2104|BGT96224_AcSP31023T0 | Effector probability: 0.979	-	-	-
jgi|Blugra1|2187|BGT96224_E10100T0 | Effector probability: 0.994	-	-	Y (RKSPNKFVQDRAKKF)
jgi|Blugra1|219|BGT96224_E5781T0 | Effector probability: 0.94	-	-	-
jgi|Blugra1|223|BGT96224_E5877T0 | Effector probability: 0.697	-	-	-
jgi|Blugra1|2243|BGT96224_5308T0 | Effector probability: 0.903	-	-	-
jgi|Blugra1|2252|BGT96224_E5732T0 | Effector probability: 0.938	-	Y (0.854 | 49-78)	Y (RELKRYK)
jgi|Blugra1|225|BGT96224_E5880T0 | Effector probability: 0.676	-	-	-
jgi|Blugra1|2299|BGT96224_E6032T0 | Effector probability: 0.99	-	-	-
jgi|Blugra1|229|BGT96224_E5783T0 | Effector probability: 0.913	-	-	Y (RKISNGPDVPYGQNHKTRK)
jgi|Blugra1|22|BGT96224_E5967T0 | Effector probability: 0.968	-	-	-
jgi|Blugra1|230|BGT96224_E5953T0 | Effector probability: 0.86	-	-	-
jgi|Blugra1|2367|BGT96224_E5679T0 | Effector probability: 0.598	-	-	-
jgi|Blugra1|2423|BGT96224_E5668T0 | Effector probability: 0.783	-	-	-
jgi|Blugra1|2430|BGT96224_ASP21313T0 | Effector probability: 0.793	-	-	Y (KKQDSDPIGRPVKNRKTRK)
jgi|Blugra1|2467|BGT96224_A20644T0 | Effector probability: 0.626	-	-	-
jgi|Blugra1|2469|BGT96224_E5677T0 | Effector probability: 0.96	-	-	-
jgi|Blugra1|2527|BGT96224_3821T0 | Effector probability: 0.602	-	-	-
jgi|Blugra1|2602|BGT96224_273BT0 | Effector probability: 0.661	-	-	-

Identifier	Chloroplast	Mitochondria	Nucleus
jgi|Blugra1|2676|BGT96224_3472T0 | Effector probability: 0.978	-	-	-
jgi|Blugra1|2692|BGT96224_2673T0 | Effector probability: 0.863	-	-	-
jgi|Blugra1|274|BGT96224_E5585T0 | Effector probability: 0.893	-	-	-
jgi|Blugra1|2756|BGT96224_E5991T0 | Effector probability: 1.0	-	-	-
jgi|Blugra1|2766|BGT96224_501T0 | Effector probability: 0.973	-	-	-
jgi|Blugra1|276|BGT96224_E5548T0 | Effector probability: 0.89	-	-	-
jgi|Blugra1|2852|BGT96224_4373T0 | Effector probability: 0.998	-	-	-
jgi|Blugra1|2873|BGT96224_E5604T0 | Effector probability: 0.953	-	-	-
jgi|Blugra1|2875|BGT96224_AcSP30893T0 | Effector probability: 0.999	-	-	-
jgi|Blugra1|2942|BGT96224_5451T0 | Effector probability: 0.968	-	-	-
jgi|Blugra1|3022|BGT96224_E3136T0 | Effector probability: 0.781	-	-	-
jgi|Blugra1|3023|BGT96224_E5921T0 | Effector probability: 0.998	-	-	-
jgi|Blugra1|3024|BGT96224_E5922T0 | Effector probability: 0.975	-	-	-
jgi|Blugra1|3030|BGT96224_E10124T0 | Effector probability: 0.98	-	-	-
jgi|Blugra1|3111|BGT96224_BCG9T0 | Effector probability: 0.875	-	Y (0.941 | 58-84)	-
jgi|Blugra1|3112|BGT96224_BCG5T0 | Effector probability: 0.964	-	-	-
jgi|Blugra1|3113|BGT96224_BCG2T0 | Effector probability: 0.933	-	-	-
jgi|Blugra1|3115|BGT96224_BCG3T0 | Effector probability: 0.902	-	-	-
jgi|Blugra1|3123|BGT96224_E5553T0 | Effector probability: 0.543	-	-	-
jgi|Blugra1|3132|BGT96224_E5774T0 | Effector probability: 0.865	-	-	-
jgi|Blugra1|3178|BGT96224_E5624T0 | Effector probability: 0.895	-	-	-
jgi|Blugra1|3187|BGT96224_AcSP30129T0 | Effector probability: 0.975	-	-	-
jgi|Blugra1|3195|BGT96224_E5658T0 | Effector probability: 0.745	-	-	-
jgi|Blugra1|3211|BGT96224_E10110T0 | Effector probability: 0.928	-	-	-
jgi|Blugra1|3214|BGT96224_E10111T0 | Effector probability: 0.972	-	-	-
jgi|Blugra1|3327|BGT96224_E5784T0 | Effector probability: 0.663	-	-	-
jgi|Blugra1|3416|BGT96224_E4403T0 | Effector probability: 0.911	-	-	-
jgi|Blugra1|3470|BGT96224_AcSP30848T0 | Effector probability: 0.951	-	-	-
jgi|Blugra1|3481|BGT96224_2816T0 | Effector probability: 0.741	-	-	-
jgi|Blugra1|3537|BGT96224_E10116T0 | Effector probability: 0.994	-	-	-
jgi|Blugra1|3572|BGT96224_E5973T0 | Effector probability: 0.974	-	-	-

Identifier	Chloroplast	Mitochondria	Nucleus
jgi|Blugra1|3584|BGT96224_E5965T0 | Effector probability: 0.861	-	-	Y (RRRK)
jgi|Blugra1|3585|BGT96224_E5539T0 | Effector probability: 0.76	-	-	-
jgi|Blugra1|3587|BGT96224_E5538T0 | Effector probability: 0.919	-	-	-
jgi|Blugra1|3667|BGT96224_959T0 | Effector probability: 0.533	-	-	-
jgi|Blugra1|3686|BGT96224_E5963T0 | Effector probability: 0.99	-	-	-
jgi|Blugra1|3687|BGT96224_AcSP30748T0 | Effector probability: 0.982	-	-	-
jgi|Blugra1|3689|BGT96224_E10108T0 | Effector probability: 0.801	-	-	-
jgi|Blugra1|3851|BGT96224_AcSP30091T0 | Effector probability: 0.89	-	-	-
jgi|Blugra1|387|BGT96224_ASP20465T0 | Effector probability: 0.846	-	-	-
jgi|Blugra1|3980|BGT96224_AcSP30691T0 | Effector probability: 0.986	-	-	Y (RKQSKQVKDYSNLRARKE)
jgi|Blugra1|4036|BGT96224_E5763T0 | Effector probability: 0.999	-	-	-
jgi|Blugra1|4044|BGT96224_E6038T0 | Effector probability: 0.746	-	-	-
jgi|Blugra1|4097|BGT96224_AcSP30056T0 | Effector probability: 0.703	-	-	Y (KHKR)
jgi|Blugra1|4114|BGT96224_E3602T0 | Effector probability: 0.946	-	-	-
jgi|Blugra1|4144|BGT96224_E5845T0 | Effector probability: 0.744	-	-	-
jgi|Blugra1|4163|BGT96224_E3962T0 | Effector probability: 0.99	-	-	Y (RKNKFKIALYQGRYFKR)
jgi|Blugra1|4196|BGT96224_E5543T0 | Effector probability: 0.92	-	-	-
jgi|Blugra1|4243|BGT96224_ASP20572T0 | Effector probability: 0.974	-	-	-
jgi|Blugra1|4253|BGT96224_E5888T0 | Effector probability: 0.962	-	-	-
jgi|Blugra1|425|BGT96224_E10002T0 | Effector probability: 0.813	-	-	-
jgi|Blugra1|4267|BGT96224_1302T0 | Effector probability: 0.868	-	-	-
jgi|Blugra1|4302|BGT96224_AcSP30622T0 | Effector probability: 0.988	-	-	-
jgi|Blugra1|4315|BGT96224_AcSP31262T0 | Effector probability: 0.657	-	-	-
jgi|Blugra1|4320|BGT96224_E5545T0 | Effector probability: 0.807	-	-	-
jgi|Blugra1|4335|BGT96224_249T0 | Effector probability: 0.661	-	-	-
jgi|Blugra1|4341|BGT96224_1536T0 | Effector probability: 0.981	-	-	-
jgi|Blugra1|4364|BGT96224_E6054T0 | Effector probability: 0.82	-	-	-
jgi|Blugra1|4405|BGT96224_E5839T0 | Effector probability: 0.855	-	-	-
jgi|Blugra1|4407|BGT96224_AcSP31175T0 | Effector probability: 0.961	-	-	-
jgi|Blugra1|4428|BGT96224_AcSP31269T0 | Effector probability: 0.948	-	-	Y (KRKEMQISMDRVARR)
jgi|Blugra1|467|BGT96224_ASP21338T0 | Effector probability: 0.973	-	-	-

Identifier	Chloroplast	Mitochondria	Nucleus
jgi|Blugra1|4690|BGT96224_4619T0 | Effector probability: 1.0	-	-	-
jgi|Blugra1|4742|BGT96224_E5689T0 | Effector probability: 0.793	-	-	-
jgi|Blugra1|4748|BGT96224_E10141T0 | Effector probability: 0.732	Y (0.998 | 67-96)	-	-
jgi|Blugra1|4764|BGT96224_E10114T0 | Effector probability: 0.753	-	Y (0.964 | 102-122)	-
jgi|Blugra1|4881|BGT96224_5153T0 | Effector probability: 0.99	-	-	-
jgi|Blugra1|4907|BGT96224_E5582T0 | Effector probability: 0.983	-	-	-
jgi|Blugra1|5001|BGT96224_AcSP30210T0 | Effector probability: 0.876	-	-	Y (KKDKERLKKNLERDKKT,KRKLSGLRAQAKKDKERLK,RKLSGLRAQAKKDKERLKKNLERDKK)
jgi|Blugra1|5018|BGT96224_AcSP30464T0 | Effector probability: 0.665	-	-	-
jgi|Blugra1|5034|BGT96224_E10129T0 | Effector probability: 0.976	-	-	-
jgi|Blugra1|5098|BGT96224_E5996T0 | Effector probability: 0.763	-	-	-
jgi|Blugra1|5162|BGT96224_E5883T0 | Effector probability: 0.973	-	-	-
jgi|Blugra1|5189|BGT96224_E5665T0 | Effector probability: 0.84	-	-	-
jgi|Blugra1|51|BGT96224_E5918T0 | Effector probability: 0.859	-	-	-
jgi|Blugra1|5272|BGT96224_E5659T0 | Effector probability: 0.978	Y (0.988 | 49-70)	Y (0.968 | 64-85)	-
jgi|Blugra1|5316|BGT96224_E3523T0 | Effector probability: 0.683	-	-	-
jgi|Blugra1|5332|BGT96224_E6035T0 | Effector probability: 0.681	-	Y (0.969 | 62-85)	Y (RKRK)
jgi|Blugra1|5336|BGT96224_E3888T0 | Effector probability: 0.596	Y (0.967 | 21-58)	Y (0.929 | 70-91)	-
jgi|Blugra1|5377|BGT96224_BCGB1T0 | Effector probability: 0.921	-	Y (0.98 | 51-80)	-
jgi|Blugra1|5490|BGT96224_ASP20340T0 | Effector probability: 0.98	-	-	-
jgi|Blugra1|5492|BGT96224_E10014T0 | Effector probability: 0.98	-	-	-
jgi|Blugra1|5500|BGT96224_E5610T0 | Effector probability: 1.0	-	-	-
jgi|Blugra1|5541|BGT96224_E5924T0 | Effector probability: 0.671	Y (0.982 | 51-71)	Y (0.993 | 93-121)	-
jgi|Blugra1|5550|BGT96224_AcSP30282T0 | Effector probability: 0.998	-	-	-
jgi|Blugra1|5627|BGT96224_E5664T0 | Effector probability: 0.898	-	-	-
jgi|Blugra1|5735|BGT96224_E5625T0 | Effector probability: 0.723	-	-	-
jgi|Blugra1|5736|BGT96224_E5906T0 | Effector probability: 0.995	-	-	-
jgi|Blugra1|575|BGT96224_E5867T0 | Effector probability: 0.681	-	-	-
jgi|Blugra1|5762|BGT96224_AcSP31344T0 | Effector probability: 0.936	-	-	-
jgi|Blugra1|5795|BGT96224_E5850T0 | Effector probability: 0.949	-	-	-
jgi|Blugra1|5804|BGT96224_AcSP31373T0 | Effector probability: 0.98	-	-	-

Identifier	Chloroplast	Mitochondria	Nucleus
jgi|Blugra1|5828|BGT96224_ASP21390T0 | Effector probability: 0.997	-	-	Y (KKDIEYSVDHAFKKRMQ)
jgi|Blugra1|5835|BGT96224_3194T0 | Effector probability: 0.791	Y (0.998 | 24-44)	-	Y (KVKK)
jgi|Blugra1|5840|BGT96224_E5673T0 | Effector probability: 0.984	-	-	-
jgi|Blugra1|5850|BGT96224_E6034T0 | Effector probability: 0.786	-	-	-
jgi|Blugra1|5867|BGT96224_E5974T0 | Effector probability: 0.995	-	-	-
jgi|Blugra1|5982|BGT96224_E5600T0 | Effector probability: 0.951	-	-	-
jgi|Blugra1|6005|BGT96224_AcSP31429T0 | Effector probability: 0.795	-	-	-
jgi|Blugra1|6046|BGT96224_ASP21455T0 | Effector probability: 0.592	-	-	-
jgi|Blugra1|6054|BGT96224_BCG6T0 | Effector probability: 0.964	-	-	-
jgi|Blugra1|6061|BGT96224_2700T0 | Effector probability: 0.865	-	-	-
jgi|Blugra1|6081|BGT96224_E5816T0 | Effector probability: 0.585	Y (0.876 | 51-102)	-	-
jgi|Blugra1|6174|BGT96224_E5966T0 | Effector probability: 0.97	-	-	-
jgi|Blugra1|6206|BGT96224_E5570T0 | Effector probability: 0.827	-	-	Y (PKNKRTK,RRGHFSKNTGYECGSKKYK)
jgi|Blugra1|6207|BGT96224_2846T0 | Effector probability: 0.506	-	-	-
jgi|Blugra1|6215|BGT96224_ASP21508T0 | Effector probability: 0.95	-	-	-
jgi|Blugra1|6226|BGT96224_E40006T0 | Effector probability: 0.914	-	Y (0.965 | 105-130)	-
jgi|Blugra1|6228|BGT96224_BCG7T0 | Effector probability: 0.988	-	-	-
jgi|Blugra1|6241|BGT96224_BCG1T0 | Effector probability: 0.971	-	-	-
jgi|Blugra1|6247|BGT96224_ASP20484T0 | Effector probability: 0.832	-	-	-
jgi|Blugra1|6293|BGT96224_E5889T0 | Effector probability: 0.768	-	-	-
jgi|Blugra1|6301|BGT96224_E5912T0 | Effector probability: 1.0	-	-	-
jgi|Blugra1|6317|BGT96224_E5550T0 | Effector probability: 0.963	-	-	-
jgi|Blugra1|6320|BGT96224_E10120T0 | Effector probability: 0.799	-	-	-
jgi|Blugra1|6338|BGT96224_5370T0 | Effector probability: 0.886	-	-	-
jgi|Blugra1|6371|BGT96224_E3419T0 | Effector probability: 0.913	-	-	-
jgi|Blugra1|637|BGT96224_E5607T0 | Effector probability: 0.831	-	-	Y (RRNLFKTSVPAKFRHRFK)
jgi|Blugra1|6473|BGT96224_E5981T0 | Effector probability: 0.987	-	-	-
jgi|Blugra1|649|BGT96224_AcSP30305T0 | Effector probability: 0.996	-	-	-
jgi|Blugra1|776|BGT96224_E10132T0 | Effector probability: 0.967	-	-	-
jgi|Blugra1|815|BGT96224_AcSP31310T0 | Effector probability: 0.97	-	-	-
jgi|Blugra1|844|BGT96224_E5829T0 | Effector probability: 0.848	-	-	-

Identifier	Chloroplast	Mitochondria	Nucleus
jgi|Blugra1|955|BGT96224_AcSP30002T0 | Effector probability: 0.729	-	-	-
jgi|Blugra1|956|BGT96224_E3893T0 | Effector probability: 0.986	-	-	-
#--------------------------------------			
#--------------------------------------			
# Proteins analyzed: 184			
# Number of proteins with cTP: 2 (1.1%)			
# Number of proteins with cTP & possible mTP: 2 (1.1%)			
# Number of proteins with cTP & NLS: 1 (0.5%)			
# Number of proteins with cTP & possible mTP & NLS: 0 (0.0%)			
# Number of proteins with mTP: 5 (2.7%)			
# Number of proteins with mTP & possible cTP: 2 (1.1%)			
# Number of proteins with mTP & NLS: 3 (1.6%)			
# Number of proteins with mTP & possible cTP & NLS: 0 (0.0%)			
# Number of proteins with NLS and no transit peptides: 17 (9.2%)			

E. *E. necator* predicted effector candidate localization (effector probability assigned by EffectorP noted with effector name)

Identifier	Chloroplast	Mitochondria	Nucleus
jgi|Erynec1|3754|EV44_g0424T0 | Effector probability: 1.0	-	-	-
jgi|Erynec1|3863|EV44_g0269T0 | Effector probability: 1.0	-	-	-
jgi|Erynec1|3884|EV44_g0435T0 | Effector probability: 0.969	-	-	-
jgi|Erynec1|3897|EV44_g0430T0 | Effector probability: 0.971	-	Y (0.979 | 30-52)	-
jgi|Erynec1|4034|EV44_g0573T0 | Effector probability: 0.591	-	Y (1.0 | 47-67)	Y (RILKRKS,RSRAKIRSLSLLRSRARILKR)
jgi|Erynec1|4332|EV44_g0203T0 | Effector probability: 0.926	-	-	Y (KPYKPYKP)
jgi|Erynec1|4482|EV44_g0444T0 | Effector probability: 0.718	-	-	-
jgi|Erynec1|4486|EV44_g0225T0 | Effector probability: 0.985	-	-	-
jgi|Erynec1|4489|EV44_g0416T0 | Effector probability: 0.702	Y (0.995 | 24-46)	-	-
jgi|Erynec1|4492|EV44_g0357T0 | Effector probability: 0.997	-	-	-
jgi|Erynec1|456|EV44_g0586T0 | Effector probability: 0.961	-	-	-
jgi|Erynec1|4579|EV44_g0597T0 | Effector probability: 0.924	-	-	-
jgi|Erynec1|4713|EV44_g0473T0 | Effector probability: 0.688	-	-	-
jgi|Erynec1|4768|EV44_g0533T0 | Effector probability: 0.644	-	-	-
jgi|Erynec1|4898|EV44_g0549T0 | Effector probability: 0.874	-	-	-
jgi|Erynec1|5106|EV44_g0246T0 | Effector probability: 0.993	-	-	-
jgi|Erynec1|5150|EV44_g0559T0 | Effector probability: 0.628	Y (0.996 | 50-79)	-	Y (KRFFLIPRGKNREQKR)
jgi|Erynec1|5250|EV44_g0482T0 | Effector probability: 0.88	-	-	-
jgi|Erynec1|5262|EV44_g0379T0 | Effector probability: 0.734	-	-	-
jgi|Erynec1|5288|EV44_g0569T0 | Effector probability: 0.92	-	-	Y (RKRFRKQHRKEAAEREAAERAAAEKAAAERKAAEKANQASGSGSKSRQKATKQRKGK)
jgi|Erynec1|5307|EV44_g0140T0 | Effector probability: 0.884	-	-	-
jgi|Erynec1|5385|EV44_g0230T0 | Effector probability: 0.832	-	-	-
jgi|Erynec1|5409|EV44_g0242T0 | Effector probability: 0.983	-	-	Y (KREIQNIFSKYINDISKKK)
jgi|Erynec1|5479|EV44_g0244T0 | Effector probability: 1.0	-	-	-
jgi|Erynec1|5533|EV44_g0534T0 | Effector probability: 0.972	-	-	-
jgi|Erynec1|5601|EV44_g0503T0 | Effector probability: 0.78	-	Y (0.978 | 67-106)	-
jgi|Erynec1|5708|EV44_g0090T0 | Effector probability: 0.758	-	-	-

Identifier	Chloroplast	Mitochondria	Nucleus
jgi|Erynec1|5719|EV44_g0279T0 | Effector probability: 0.982	-	-	-
jgi|Erynec1|5744|EV44_g0388T0 | Effector probability: 0.75	-	-	-
jgi|Erynec1|5773|EV44_g0076T0 | Effector probability: 0.656	-	-	-
jgi|Erynec1|5790|EV44_g0596T0 | Effector probability: 0.831	-	-	-
jgi|Erynec1|5929|EV44_g0571T0 | Effector probability: 1.0	-	-	-
jgi|Erynec1|6058|EV44_g0525T0 | Effector probability: 1.0	-	-	-
jgi|Erynec1|6064|EV44_g0542T0 | Effector probability: 0.625	-	-	-
jgi|Erynec1|6114|EV44_g0283T0 | Effector probability: 0.509	-	-	-
jgi|Erynec1|6210|EV44_g0206T0 | Effector probability: 0.984	-	-	-
jgi|Erynec1|6287|EV44_g0465T0 | Effector probability: 0.931	-	-	-
jgi|Erynec1|6322|EV44_g0526T0 | Effector probability: 0.994	-	-	-
jgi|Erynec1|641|EV44_g0383T0 | Effector probability: 0.959	Y (0.988 | 43-83)	-	-
jgi|Erynec1|898|EV44_g0186T0 | Effector probability: 0.787	-	-	Y (RKSK)
jgi|Erynec1|914|EV44_g0538T0 | Effector probability: 0.904	-	-	-
jgi|Erynec1|1056|EV44_g0547T0 | Effector probability: 0.996	-	-	-
jgi|Erynec1|1161|EV44_g0257T0 | Effector probability: 0.994	-	-	-
jgi|Erynec1|1405|EV44_g0537T0 | Effector probability: 0.978	Y (0.995 | 43-71)	Y (0.988 | 55-82)	Y (RHRR)
jgi|Erynec1|1421|EV44_g0014T0 | Effector probability: 0.9	-	-	-
jgi|Erynec1|1511|EV44_g0425T0 | Effector probability: 0.999	-	-	-
jgi|Erynec1|1647|EV44_g0551T0 | Effector probability: 1.0	-	-	-
jgi|Erynec1|1730|EV44_g0415T0 | Effector probability: 0.729	-	Y (0.989 | 50-72)	-
jgi|Erynec1|1752|EV44_g0591T0 | Effector probability: 0.947	-	-	-
jgi|Erynec1|189|EV44_g0181T0 | Effector probability: 0.777	-	-	-
jgi|Erynec1|2050|EV44_g0313T0 | Effector probability: 0.934	-	-	-
jgi|Erynec1|2064|EV44_g0519T0 | Effector probability: 0.738	-	-	Y (KRFCFRRGCKEEKLKRT)
jgi|Erynec1|2200|EV44_g0602T0 | Effector probability: 0.925	Y (0.995 | 52-81)	Y (0.938 | 63-92)	Y (KRLCFRRGCNKKSKH,KKSKHASGFQCKKKHF,KRNGRFWNNLRRGRYR,RRGCNKKSKHASGFQCKKK)
jgi|Erynec1|2252|EV44_g0426T0 | Effector probability: 0.939	-	-	Y (RIPKRRN)
jgi|Erynec1|2372|EV44_g0599T0 | Effector probability: 1.0	-	-	-
jgi|Erynec1|2412|EV44_g0178T0 | Effector probability: 0.901	-	-	-
jgi|Erynec1|2444|EV44_g0052T0 | Effector probability: 0.965	-	-	Y (LGEV)

Identifier	Chloroplast	Mitochondria	Nucleus
jgi|Erynec1|2466|EV44_g0274T0 | Effector probability: 0.999	-	-	-
jgi|Erynec1|2619|EV44_g0254T0 | Effector probability: 0.773	-	-	Y (RRRK)
jgi|Erynec1|2628|EV44_g0447T0 | Effector probability: 0.918	-	-	Y (KKRK,RGKHKKKLFAKKKKNK)
jgi|Erynec1|3007|EV44_g0583T0 | Effector probability: 0.755	Y (0.989 | 49-72)	-	Y (KRFCLKPGGCNKKYLKR,KKYLKRSSGFQCKKKYI)
jgi|Erynec1|3081|EV44_g0282T0 | Effector probability: 0.973	-	-	-
jgi|Erynec1|3117|EV44_g0136T0 | Effector probability: 0.86	-	-	-
jgi|Erynec1|3159|EV44_g0215T0 | Effector probability: 0.887	Y (0.986 | 84-104)	-	-
jgi|Erynec1|3287|EV44_g0600T0 | Effector probability: 0.849	-	-	Y (KKRP,KKYEIYSAAKRLCDVMKKR)
jgi|Erynec1|345|EV44_g0192T0 | Effector probability: 0.997	-	-	-
jgi|Erynec1|3611|EV44_g0196T0 | Effector probability: 0.954	-	-	-
jgi|Erynec1|3648|EV44_g0539T0 | Effector probability: 1.0	-	-	-
jgi|Erynec1|369|EV44_g0481T0 | Effector probability: 0.901	-	-	-

Appendix 6: ApoplastP Output for powdery mildew effector candidates

A. *G. cichoracearum* effector candidate apoplast localization prediction

#Identifier	Prediction	Probability
GcEC_B_1	Non-apoplastic	0.7
GcEc13	Non-apoplastic	0.91
GcEC_B_2	Apoplastic	0.55
GcEc17	Non-apoplastic	0.61
GcEC_B_3	Non-apoplastic	0.63
GcEC38	Apoplastic	0.55
GcEc34	Non-apoplastic	0.95
GcEc8	Non-apoplastic	0.79
GcEC11	Non-apoplastic	0.82
GcEc10	Non-apoplastic	0.73
GcEC_B_4	Non-apoplastic	0.67
GcEC_B_5	Apoplastic	0.75
GcEC21	Non-apoplastic	0.71
GcEC_B_6	Non-apoplastic	0.51
GcEC_B_7	Non-apoplastic	0.84
GcEC_B_8	Non-apoplastic	0.69
GcEC_B_9	Non-apoplastic	0.53
GcEC_B_10	Apoplastic	0.58
GcEC_B_11	Non-apoplastic	0.77
GcEC_B_12	Non-apoplastic	0.7
GcEC7	Non-apoplastic	0.79
GcEC_B_13	Non-apoplastic	0.94
GcEC_B_14	Apoplastic	0.72
GcEC_B_15	Non-apoplastic	0.63
GcEC_B_16	Non-apoplastic	0.81
GcEC_B_17	Non-apoplastic	0.76
GcEC_B_18	Non-apoplastic	0.76
GcEC_B_19	Non-apoplastic	0.81
GcEC_B_20	Non-apoplastic	0.62
GcEC_B_21	Non-apoplastic	0.57
GcEC_B_22	Non-apoplastic	0.91
GcEC_B_23	Non-apoplastic	0.63
GcEC_B_24	Non-apoplastic	0.79
GcEC_B_25	Non-apoplastic	0.61
GcEC_B_26	Apoplastic	0.6
GcEC_B_27	Non-apoplastic	0.56
GcEC_B_28	Non-apoplastic	0.76
GcEC_B_29	Non-apoplastic	0.92
GcEC_B_30	Non-apoplastic	0.55
GcEC_B_32	Non-apoplastic	0.97
GcEC_B_33	Apoplastic	0.89
GcEC_B_34	Non-apoplastic	0.8
GcEC_B_35	Non-apoplastic	0.53
GcEC_B_36	Non-apoplastic	0.94
GcEC_B_37	Non-apoplastic	0.68
GcEC_B_38	Non-apoplastic	0.95
GcEC_B_39	Non-apoplastic	0.94
GcEC_B_40	Non-apoplastic	0.52
GcEC_B_41	Non-apoplastic	0.98
GcEC_B_42	Non-apoplastic	0.84
GcEC_B_43	Non-apoplastic	0.95

#Identifier	Prediction	Probability
GcEC_B_44	Non-apoplastic	0.82
GcEC_B_45	Non-apoplastic	0.93
GcEC_B_46	Non-apoplastic	0.85
GcEC_B_47	Non-apoplastic	0.57
GcEC_B_48	Non-apoplastic	0.96
GcEC_B_49	Non-apoplastic	0.92
GcEC_B_50	Non-apoplastic	0.84
GcEC_B_51	Non-apoplastic	0.72
GcEC_B_52	Non-apoplastic	0.52
GcEC_B_53	Apoplastic	0.77
GcEC_B_54	Non-apoplastic	0.8
GcEC_B_55	Non-apoplastic	0.96
GcEC_B_56	Non-apoplastic	0.52
GcEC_B_57	Non-apoplastic	0.78
GcEC_B_58	Non-apoplastic	0.8
GcEC_B_59	Non-apoplastic	0.64
GcEC_B_60	Apoplastic	0.68
GcEC_B_61	Non-apoplastic	0.66
GcEC_B_62	Non-apoplastic	0.75
GcEC_B_63	Non-apoplastic	0.52
GcEC_B_64	Non-apoplastic	0.64
GcEC_B_65	Non-apoplastic	0.76
GcEC_B_66	Non-apoplastic	0.67
GcEC_B_67	Non-apoplastic	0.83
GcEC_B_68	Non-apoplastic	0.71
GcEC_B_69	Non-apoplastic	0.97
GcEC_B_70	Non-apoplastic	0.97
GcEC_B_71	Non-apoplastic	0.93
GcEC_B_72	Non-apoplastic	0.89
GcEC_B_73	Non-apoplastic	0.96
GcEC_B_74	Non-apoplastic	0.53
GcEC_B_75	Non-apoplastic	0.56
GcEC_B_76	Non-apoplastic	0.82
GcEC_B_77	Non-apoplastic	0.93
GcEC_B_78	Non-apoplastic	0.86
GcEC_B_80	Non-apoplastic	0.62
GcEC_B_81	Non-apoplastic	0.83
GcEC_B_82	Non-apoplastic	0.96
GcEC_B_83	Non-apoplastic	0.96
GcEC_B_84	Non-apoplastic	0.97
GcEC_B_85	Apoplastic	0.72
GcEC_B_86	Non-apoplastic	0.64
GcEC_B_87	Non-apoplastic	0.94
GcEC_B_89	Non-apoplastic	0.68
GcEC_B_90	Non-apoplastic	0.97
GcEC_B_91	Non-apoplastic	0.62
GcEC_B_92	Apoplastic	0.55
GcEC_B_93	Non-apoplastic	0.56
GcEC_B_94	Non-apoplastic	0.54
GcEC_B_95	Non-apoplastic	0.73
GcEC_B_96	Non-apoplastic	0.64
GcEC_B_97	Apoplastic	0.68
GcEC_B_98	Non-apoplastic	0.59
GcEC_B_99	Non-apoplastic	0.56
GcEC_B_100	Non-apoplastic	0.59

#Identifier	Prediction	Probability
GcEC_B_101	Non-apoplastic	0.95
GcEC_B_102	Non-apoplastic	0.86
GcEC_B_103	Non-apoplastic	0.77
GcEC_B_104	Non-apoplastic	0.59
GcEC_B_105	Non-apoplastic	0.76
GcEC_B_106	Non-apoplastic	0.86
GcEC_B_107	Non-apoplastic	0.59
GcEC_B_108	Non-apoplastic	0.75
GcEC_B_109	Non-apoplastic	0.95
GcEC_B_110	Non-apoplastic	0.94
GcEC_B_111	Non-apoplastic	0.78
GcEC_B_112	Non-apoplastic	0.91
GcEC_B_113	Non-apoplastic	0.75
GcEC_B_114	Non-apoplastic	0.8
GcEC_B_115	Non-apoplastic	0.65
GcEC_B_116	Non-apoplastic	0.78
GcEC_B_117	Non-apoplastic	1
GcEC_B_118	Non-apoplastic	1
GcEC_B_119	Non-apoplastic	0.77
GcEC_B_120	Non-apoplastic	0.72
GcEC_B_121	Non-apoplastic	0.6
GcEC_B_122	Non-apoplastic	0.65
GcEC_B_123	Non-apoplastic	0.65
GcEC_B_124	Non-apoplastic	0.89
GcEC_B_125	Non-apoplastic	0.61
GcEC_B_126	Non-apoplastic	0.96
GcEC_B_127	Non-apoplastic	0.93
GcEC_B_128	Non-apoplastic	0.62
GcEC_B_129	Non-apoplastic	0.67
GcEC_B_130	Non-apoplastic	0.83
GcEC_B_131	Non-apoplastic	0.96
GcEC_B_132	Non-apoplastic	0.66
GcEC_B_133	Non-apoplastic	0.54
GcEC_B_134	Non-apoplastic	0.76
GcEC_B_135	Non-apoplastic	0.81
GcEC_B_136	Non-apoplastic	0.95
GcEC_B_137	Non-apoplastic	0.61
GcEC_B_138	Apoplastic	0.55
GcEC_B_139	Non-apoplastic	0.86
GcEC_B_140	Non-apoplastic	0.94
GcEC_B_141	Non-apoplastic	0.91
GcEC_B_142	Non-apoplastic	0.73
GcEC_B_143	Non-apoplastic	0.97
GcEC_B_144	Non-apoplastic	0.51
GcEC_B_145	Apoplastic	0.56
GcEC_B_146	Non-apoplastic	0.89
GcEC_B_147	Non-apoplastic	0.85
GcEC_B_148	Non-apoplastic	0.99
GcEC_B_149	Non-apoplastic	0.77
GcEC_B_150	Non-apoplastic	0.72
GcEC_B_151	Non-apoplastic	0.63
GcEC_B_152	Non-apoplastic	0.99
GcEC_B_153	Non-apoplastic	0.78
GcEC_B_154	Non-apoplastic	0.56
GcEC_B_155	Non-apoplastic	0.82

#Identifier	Prediction	Probability
GcEC_B_156	Non-apoplastic	0.54
GcEC_B_157	Non-apoplastic	0.65
GcEC_B_158	Non-apoplastic	0.66
GcEC_B_159	Non-apoplastic	0.77
GcEC_B_160	Non-apoplastic	0.75
GcEC_B_161	Non-apoplastic	0.72
GcEC_B_162	Non-apoplastic	0.96
GcEC_B_163	Non-apoplastic	0.99
GcEC_B_164	Non-apoplastic	0.92
GcEC_B_165	Non-apoplastic	0.96
GcEC_B_166	Non-apoplastic	0.82
GcEC_B_167	Non-apoplastic	0.59
GcEC_B_168	Non-apoplastic	0.98
GcEC_B_169	Non-apoplastic	0.6
GcEC_B_170	Non-apoplastic	0.53
GcEC_B_171	Non-apoplastic	0.92
GcEC_B_173	Non-apoplastic	0.5
GcEC_B_174	Non-apoplastic	0.81
GcEC_B_175	Non-apoplastic	0.76
GcEC_B_176	Apoplastic	0.56
GcEC_B_177	Non-apoplastic	0.68
GcEC_B_178	Non-apoplastic	0.63
GcEC_B_179	Non-apoplastic	0.88
GcEC_B_180	Non-apoplastic	0.86
GcEC_B_181	Non-apoplastic	0.55
GcEC_B_182	Non-apoplastic	0.97
GcEC_B_183	Non-apoplastic	0.98
GcEC_B_184	Non-apoplastic	0.63
GcEC_B_185	Non-apoplastic	0.88
GcEC_B_186	Non-apoplastic	0.66
GcEC_B_187	Non-apoplastic	0.99
GcEC_B_188	Non-apoplastic	0.87
GcEC_B_189	Non-apoplastic	0.51
GcEC_B_190	Non-apoplastic	0.68
GcEC_B_191	Non-apoplastic	0.89
GcEC_B_192	Non-apoplastic	0.69
GcEC_B_193	Non-apoplastic	0.98
GcEC_B_194	Non-apoplastic	0.52
GcEC_B_195	Non-apoplastic	0.72
GcEC_B_196	Apoplastic	0.58
GcEC_B_197	Non-apoplastic	0.84
GcEC_B_198	Non-apoplastic	0.7
GcEC_B_199	Apoplastic	0.56
GcEC_B_200	Non-apoplastic	0.76
GcEC_B_201	Apoplastic	0.55
GcEC_B_202	Non-apoplastic	0.92
GcEC_B_203	Non-apoplastic	0.87
GcEC_B_204	Non-apoplastic	0.84
GcEC_B_205	Non-apoplastic	0.72
GcEC_B_206	Non-apoplastic	0.78
GcEC_B_207	Non-apoplastic	0.75
GcEC_B_208	Non-apoplastic	0.87
GcEC_B_209	Non-apoplastic	0.94
GcEC_B_210	Non-apoplastic	0.85
GcEC_B_211	Non-apoplastic	0.52

#Identifier	Prediction	Probability
GcEC_B_212	Apoplastic	0.56
GcEC_B_213	Non-apoplastic	0.82
GcEC_B_214	Non-apoplastic	0.97
GcEC_B_215	Non-apoplastic	0.76
GcEC_B_216	Non-apoplastic	0.81
GcEC13	Non-apoplastic	0.52
GcEC_B_217	Apoplastic	0.69
GcEC_B_218	Non-apoplastic	

B. *G. orontii* effector candidate apoplast localization prediction

#Identifier	Prediction	Probability
jgi|Golor2|1128132|CE1084753_4368 | Effector probability: 1.0	Non-apoplastic	0.78
jgi|Golor2|1144947|CE1101568_210 | Effector probability: 0.677	Non-apoplastic	0.74
jgi|Golor2|1211497|CE1168118_111 | Effector probability: 0.963	Non-apoplastic	0.74
jgi|Golor2|1344606|CE1301227_3070 | Effector probability: 0.505	Non-apoplastic	0.71
jgi|Golor2|1379604|CE1336225_3260 | Effector probability: 1.0	Non-apoplastic	0.72
jgi|Golor2|1426835|CE1383456_50 | Effector probability: 0.584	Non-apoplastic	0.56
jgi|Golor2|1473392|CE1430013_12 | Effector probability: 0.648	Non-apoplastic	0.56
jgi|Golor2|155207|CE111828_31 | Effector probability: 0.897	Non-apoplastic	0.68
jgi|Golor2|2011771|CE1968392_572 | Effector probability: 0.534	Apoplastic	0.56
jgi|Golor2|2310198|CE2266819_9543 | Effector probability: 0.999	Non-apoplastic	0.8
jgi|Golor2|2456219|CE2412840_146 | Effector probability: 1.0	Apoplastic	0.55
jgi|Golor2|246500|CE203121_322 | Effector probability: 0.653	Non-apoplastic	0.79
jgi|Golor2|24931|gm4.24931_g | Effector probability: 0.89	Non-apoplastic	0.81
jgi|Golor2|2531858|CE2488479_830 | Effector probability: 0.969	Non-apoplastic	0.94
jgi|Golor2|2606300|CE2562921_8603 | Effector probability: 0.947	Non-apoplastic	0.77
jgi|Golor2|2674892|CE2631513_232 | Effector probability: 1.0	Non-apoplastic	0.82
jgi|Golor2|2701140|CE2657761_105 | Effector probability: 0.999	Non-apoplastic	0.77
jgi|Golor2|343951|CE300572_3457 | Effector probability: 0.991	Apoplastic	0.58
jgi|Golor2|365352|CE321973_6279 | Effector probability: 0.531	Non-apoplastic	0.86
jgi|Golor2|37702|gm4.37702_g | Effector probability: 0.987	Non-apoplastic	0.57
jgi|Golor2|3903|gm4.3903_g | Effector probability: 0.987	Non-apoplastic	0.54
jgi|Golor2|3933|gm4.3933_g | Effector probability: 0.76	Non-apoplastic	0.5
jgi|Golor2|39603|gm4.39603_g | Effector probability: 0.731	Non-apoplastic	0.64
jgi|Golor2|4173372|gw1.1.2905.1 | Effector probability: 1.0	Apoplastic	0.84
jgi|Golor2|4210000|gw1.17.1541.1 | Effector probability: 0.903	Non-apoplastic	0.88
jgi|Golor2|4249978|e_gw1.10.568.1 | Effector probability: 0.963	Non-apoplastic	0.58
jgi|Golor2|4269205|e_gw1.36.1073.1 | Effector probability: 0.995	Non-apoplastic	0.8
jgi|Golor2|4269220|e_gw1.36.342.1 | Effector probability: 0.83	Non-apoplastic	0.6
jgi|Golor2|426930|CE383551_11476 | Effector probability: 0.94	Non-apoplastic	0.67
jgi|Golor2|4270647|e_gw1.39.167.1 | Effector probability: 0.92	Apoplastic	0.72
jgi|Golor2|4278404|e_gw1.53.42.1 | Effector probability: 0.554	Non-apoplastic	0.8
jgi|Golor2|4280634|e_gw1.57.478.1 | Effector probability: 0.792	Non-apoplastic	0.6
jgi|Golor2|4280651|e_gw1.57.704.1 | Effector probability: 0.993	Non-apoplastic	0.52
jgi|Golor2|4296132|e_gw1.89.422.1 | Effector probability: 0.97	Non-apoplastic	1
jgi|Golor2|4307455|e_gw1.121.373.1 | Effector probability: 0.726	Non-apoplastic	0.82

#Identifier	Prediction	Probability
jgi|Golor2|4386379|fgenesh1_pg.6_#_29 | Effector probability: 0.997	Non-apoplastic	0.8
jgi|Golor2|4386813|fgenesh1_pg.9_#_39 | Effector probability: 0.906	Apoplastic	0.7
jgi|Golor2|4386995|fgenesh1_pg.11_#_41 | Effector probability: 0.999	Non-apoplastic	0.5
jgi|Golor2|4388268|fgenesh1_pg.24_#_87 | Effector probability: 0.745	Non-apoplastic	0.87
jgi|Golor2|4389219|fgenesh1_pg.37_#_29 | Effector probability: 0.879	Apoplastic	0.67
jgi|Golor2|4390161|fgenesh1_pg.53_#_59 | Effector probability: 0.666	Non-apoplastic	0.69
jgi|Golor2|4390630|fgenesh1_pg.61_#_31 | Effector probability: 1.0	Non-apoplastic	0.79
jgi|Golor2|4390806|fgenesh1_pg.64_#_43 | Effector probability: 0.604	Non-apoplastic	0.83
jgi|Golor2|4391815|fgenesh1_pg.84_#_5 | Effector probability: 0.568	Non-apoplastic	0.6
jgi|Golor2|4391816|fgenesh1_pg.84_#_6 | Effector probability: 0.568	Non-apoplastic	0.6
jgi|Golor2|4392990|fgenesh1_pg.110_#_22 | Effector probability: 0.938	Non-apoplastic	0.99
jgi|Golor2|4393061|fgenesh1_pg.112_#_24 | Effector probability: 0.65	Non-apoplastic	0.85
jgi|Golor2|4393802|fgenesh1_pg.133_#_5 | Effector probability: 0.858	Non-apoplastic	0.51
jgi|Golor2|4394446|fgenesh1_pg.154_#_14 | Effector probability: 0.998	Non-apoplastic	0.5
jgi|Golor2|4394460|fgenesh1_pg.154_#_28 | Effector probability: 0.985	Apoplastic	0.67
jgi|Golor2|4395825|fgenesh1_pg.226_#_8 | Effector probability: 0.822	Non-apoplastic	0.75
jgi|Golor2|4395946|fgenesh1_pg.240_#_3 | Effector probability: 0.874	Non-apoplastic	0.85
jgi|Golor2|4409105|estExt_Genemark4.C_1990054 | Effector probability: 0.967	Apoplastic	0.56
jgi|Golor2|5549786|MIX40162_2277_93 | Effector probability: 0.518	Apoplastic	0.68
jgi|Golor2|5714216|MIX204592_419_59 | Effector probability: 0.869	Non-apoplastic	0.77
jgi|Golor2|5820476|estExt_fgenesh1_pg.C_840010 | Effector probability: 0.521	Non-apoplastic	0.91
jgi|Golor2|5824174|estExt_fgenesh1_pg.C_2400001 | Effector probability: 0.663	Non-apoplastic	0.99
jgi|Golor2|5824175|estExt_fgenesh1_pg.C_2400002 | Effector probability: 0.537	Non-apoplastic	0.99
jgi|Golor2|635348|CE591969_64 | Effector probability: 0.998	Apoplastic	0.57
jgi|Golor2|636606|CE593227_1576 | Effector probability: 0.506	Apoplastic	0.58
jgi|Golor2|710617|CE667238_383 | Effector probability: 0.897	Non-apoplastic	0.71
jgi|Golor2|922974|CE879595_225 | Effector probability: 0.533	Non-apoplastic	0.57
jgi|Golor2|97205|CE53826_15 | Effector probability: 0.992	Non-apoplastic	0.59
jgi|Golor2|9850|gm4.9850_g | Effector probability: 0.886	Apoplastic	0.63

C. *B. graminis f. sp. hordei* effector candidate apoplast localization prediction (EffectorP etermined effector probability noted after effector name)

#Identifier	Prediction	Probability
jgi|Blugr1|25612|BGHDH14_bgh05803 | Effector probability: 0.722	Apoplastic	0.78
jgi|Blugr1|25610|BGHDH14_bgh03695 | Effector probability: 0.98	Apoplastic	0.58
jgi|Blugr1|25608|BGHDH14_bghG011456000001001 | Effector probability: 0.707	Non-apoplastic	0.59
jgi|Blugr1|25468|BGHDH14_bgh03742 | Effector probability: 0.629	Non-apoplastic	0.61
jgi|Blugr1|25462|BGHDH14_bgh03746 | Effector probability: 0.897	Non-apoplastic	0.64
jgi|Blugr1|25453|BGHDH14_bgh03747 | Effector probability: 0.855	Non-apoplastic	0.65
jgi|Blugr1|25445|BGHDH14_bghG000207000002001 | Effector probability: 0.998	Apoplastic	0.74
jgi|Blugr1|25442|BGHDH14_bgh03749 | Effector probability: 0.921	Non-apoplastic	0.53
jgi|Blugr1|25386|BGHDH14_bgh03443 | Effector probability: 0.979	Apoplastic	0.76
jgi|Blugr1|25382|BGHDH14_bghG000107000003001 | Effector probability: 0.794	Non-apoplastic	0.64
jgi|Blugr1|25364|BGHDH14_bghG000103000002001 | Effector probability: 0.765	Non-apoplastic	0.64
jgi|Blugr1|25344|BGHDH14_bgh04209 | Effector probability: 0.962	Non-apoplastic	0.71
jgi|Blugr1|25311|BGHDH14_bgh02080 | Effector probability: 0.575	Non-apoplastic	0.78
jgi|Blugr1|25299|BGHDH14_bghG000032000001001 | Effector probability: 0.979	Non-apoplastic	0.55
jgi|Blugr1|25294|BGHDH14_bghG000026000002001 | Effector probability: 0.609	Non-apoplastic	0.51
jgi|Blugr1|25292|BGHDH14_bghG000026000001001 | Effector probability: 0.646	Non-apoplastic	0.5
jgi|Blugr1|25290|BGHDH14_bghG000024000001001 | Effector probability: 0.998	Apoplastic	0.66
jgi|Blugr1|25283|BGHDH14_bghG000012000002001 | Effector probability: 0.968	Apoplastic	0.65
jgi|Blugr1|25131|BGHDH14_bgh03625 | Effector probability: 0.943	Non-apoplastic	0.85
jgi|Blugr1|25115|BGHDH14_bgh03452 | Effector probability: 0.61	Non-apoplastic	0.79
jgi|Blugr1|25114|BGHDH14_bghG006029000001001 | Effector probability: 0.959	Non-apoplastic	0.79
jgi|Blugr1|25113|BGHDH14_bghG006028000001001 | Effector probability: 0.993	Apoplastic	0.77
jgi|Blugr1|25110|BGHDH14_bghG006021000001001 | Effector probability: 0.926	Non-apoplastic	0.53
jgi|Blugr1|25079|BGHDH14_bghG006278000001001 | Effector probability: 0.979	Apoplastic	0.83
jgi|Blugr1|25073|BGHDH14_bgh06951 | Effector probability: 1.0	Non-apoplastic	0.53
jgi|Blugr1|25072|BGHDH14_bgh04105 | Effector probability: 0.94	Non-apoplastic	0.63
jgi|Blugr1|25070|BGHDH14_bgh04343 | Effector probability: 0.892	Apoplastic	0.6
jgi|Blugr1|25058|BGHDH14_bgh04130 | Effector probability: 0.999	Non-apoplastic	0.61
jgi|Blugr1|25055|BGHDH14_bgh02875 | Effector probability: 0.58	Non-apoplastic	0.59
jgi|Blugr1|25053|BGHDH14_bgh03277 | Effector probability: 0.939	Non-apoplastic	0.54
jgi|Blugr1|25051|BGHDH14_bgh03273 | Effector probability: 0.872	Apoplastic	0.65
jgi|Blugr1|25050|BGHDH14_bgh03275 | Effector probability: 0.95	Apoplastic	0.67
jgi|Blugr1|25014|BGHDH14_bghG001077000001001 | Effector probability: 0.939	Non-apoplastic	0.66
jgi|Blugr1|24978|BGHDH14_bgh04277 | Effector probability: 0.991	Non-apoplastic	0.54

#Identifier	Prediction	Probability
jgi|Blugr1|24922|BGHDH14_bgh04920 | Effector probability: 0.969	Non-apoplastic	0.62
jgi|Blugr1|24870|BGHDH14_bgh04817 | Effector probability: 0.86	Non-apoplastic	0.97
jgi|Blugr1|24845|BGHDH14_bghG000925000001001 | Effector probability: 0.902	Non-apoplastic	0.66
jgi|Blugr1|24821|BGHDH14_bghG000833000001001 | Effector probability: 0.502	Apoplastic	0.6
jgi|Blugr1|24809|BGHDH14_bghG000799000001001 | Effector probability: 0.911	Non-apoplastic	0.52
jgi|Blugr1|24788|BGHDH14_bghG000770000002001 | Effector probability: 0.983	Non-apoplastic	0.93
jgi|Blugr1|24738|BGHDH14_bghG000733000001001 | Effector probability: 0.949	Apoplastic	0.69
jgi|Blugr1|24719|BGHDH14_bghG000714000001001 | Effector probability: 0.988	Apoplastic	0.65
jgi|Blugr1|24709|BGHDH14_bgh03067 | Effector probability: 0.644	Non-apoplastic	0.68
jgi|Blugr1|24654|BGHDH14_bgh01923 | Effector probability: 0.606	Apoplastic	0.81
jgi|Blugr1|24625|BGHDH14_bghG000653000001001 | Effector probability: 0.976	Non-apoplastic	0.68
jgi|Blugr1|24611|BGHDH14_bgh01048 | Effector probability: 0.987	Non-apoplastic	0.73
jgi|Blugr1|24569|BGHDH14_bgh05755 | Effector probability: 0.695	Non-apoplastic	0.91
jgi|Blugr1|24565|BGHDH14_bgh04226 | Effector probability: 0.938	Non-apoplastic	0.68
jgi|Blugr1|24526|BGHDH14_bghG000556000001001 | Effector probability: 0.515	Non-apoplastic	0.65
jgi|Blugr1|24494|BGHDH14_bgh04885 | Effector probability: 0.996	Non-apoplastic	0.75
jgi|Blugr1|24462|BGHDH14_bgh02536 | Effector probability: 0.912	Apoplastic	0.71
jgi|Blugr1|24461|BGHDH14_bghG000481000001001 | Effector probability: 0.896	Non-apoplastic	0.63
jgi|Blugr1|24440|BGHDH14_bgh03531 | Effector probability: 0.573	Apoplastic	0.61
jgi|Blugr1|24423|BGHDH14_bghG000458000002001 | Effector probability: 0.97	Non-apoplastic	0.67
jgi|Blugr1|24422|BGHDH14_bghG000457000001001 | Effector probability: 0.872	Non-apoplastic	0.72
jgi|Blugr1|24419|BGHDH14_bghG000456000001001 | Effector probability: 0.983	Non-apoplastic	0.53
jgi|Blugr1|24416|BGHDH14_bghG000452000001001 | Effector probability: 0.981	Non-apoplastic	0.58
jgi|Blugr1|24373|BGHDH14_bgh04954 | Effector probability: 0.901	Non-apoplastic	0.84
jgi|Blugr1|24361|BGHDH14_bghG000425000003001 | Effector probability: 0.921	Non-apoplastic	0.84
jgi|Blugr1|24333|BGHDH14_bghG000417000001001 | Effector probability: 0.958	Non-apoplastic	0.76
jgi|Blugr1|24331|BGHDH14_bghG000417000002001 | Effector probability: 0.998	Non-apoplastic	0.51
jgi|Blugr1|24314|BGHDH14_bgh04026 | Effector probability: 0.853	Apoplastic	0.78
jgi|Blugr1|24313|BGHDH14_bgh02942 | Effector probability: 0.993	Non-apoplastic	0.52
jgi|Blugr1|24298|BGHDH14_bgh03375 | Effector probability: 0.954	Non-apoplastic	0.55
jgi|Blugr1|24297|BGHDH14_bgh02998 | Effector probability: 0.973	Apoplastic	0.77
jgi|Blugr1|24294|BGHDH14_bgh06578 | Effector probability: 0.989	Non-apoplastic	0.61
jgi|Blugr1|24293|BGHDH14_bgh03730 | Effector probability: 0.555	Non-apoplastic	0.53
jgi|Blugr1|24254|BGHDH14_bgh02825 | Effector probability: 0.997	Non-apoplastic	0.73
jgi|Blugr1|24253|BGHDH14_bgh02420 | Effector probability: 0.947	Non-apoplastic	0.83
jgi|Blugr1|24241|BGHDH14_bgh02262 | Effector probability: 0.975	Non-apoplastic	0.52
jgi|Blugr1|24239|BGHDH14_bgh02778 | Effector probability: 0.96	Non-apoplastic	0.92
jgi|Blugr1|24238|BGHDH14_bgh03466 | Effector probability: 0.944	Non-apoplastic	0.64

#Identifier	Prediction	Probability
jgi|Blugr1|24237|BGHDH14_bgh03464 | Effector probability: 0.671	Non-apoplastic	0.8
jgi|Blugr1|24236|BGHDH14_bgh03568 | Effector probability: 0.972	Non-apoplastic	0.73
jgi|Blugr1|24235|BGHDH14_bghG001947000001001 | Effector probability: 0.561	Non-apoplastic	0.51
jgi|Blugr1|24114|BGHDH14_bgh03692 | Effector probability: 0.977	Non-apoplastic	0.56
jgi|Blugr1|24084|BGHDH14_bgh03457 | Effector probability: 0.901	Non-apoplastic	0.67
jgi|Blugr1|24083|BGHDH14_bgh02774 | Effector probability: 0.959	Non-apoplastic	0.88
jgi|Blugr1|24082|BGHDH14_bghG001721000001001 | Effector probability: 0.96	Non-apoplastic	0.56
jgi|Blugr1|24081|BGHDH14_bgh05751 | Effector probability: 0.977	Non-apoplastic	0.8
jgi|Blugr1|24073|BGHDH14_bgh03794 | Effector probability: 0.826	Non-apoplastic	0.89
jgi|Blugr1|24071|BGHDH14_bgh03995 | Effector probability: 0.786	Non-apoplastic	0.86
jgi|Blugr1|24069|BGHDH14_bgh03922 | Effector probability: 0.893	Non-apoplastic	0.9
jgi|Blugr1|24068|BGHDH14_bghG001682000001001 | Effector probability: 0.92	Non-apoplastic	0.89
jgi|Blugr1|24060|BGHDH14_bgh03857 | Effector probability: 0.977	Non-apoplastic	0.99
jgi|Blugr1|23984|BGHDH14_bgh06200 | Effector probability: 0.985	Apoplastic	0.75
jgi|Blugr1|23889|BGHDH14_bghG002664000001001 | Effector probability: 0.978	Non-apoplastic	0.52
jgi|Blugr1|23888|BGHDH14_bghG002653000001001 | Effector probability: 0.763	Apoplastic	0.64
jgi|Blugr1|23871|BGHDH14_bghG002637000001001 | Effector probability: 0.729	Non-apoplastic	0.91
jgi|Blugr1|23844|BGHDH14_bghG002599000002001 | Effector probability: 0.973	Non-apoplastic	0.72
jgi|Blugr1|23843|BGHDH14_bghG002599000001001 | Effector probability: 0.963	Apoplastic	0.59
jgi|Blugr1|23841|BGHDH14_bgh05096 | Effector probability: 0.789	Non-apoplastic	0.87
jgi|Blugr1|23839|BGHDH14_bgh05069 | Effector probability: 0.931	Apoplastic	0.6
jgi|Blugr1|23838|BGHDH14_bghG002593000001001 | Effector probability: 0.978	Non-apoplastic	0.67
jgi|Blugr1|23836|BGHDH14_bghG002593000004001 | Effector probability: 0.939	Apoplastic	0.57
jgi|Blugr1|23813|BGHDH14_bgh02924 | Effector probability: 0.929	Apoplastic	0.77
jgi|Blugr1|23803|BGHDH14_bgh02922 | Effector probability: 0.907	Apoplastic	0.58
jgi|Blugr1|23802|BGHDH14_bgh02918 | Effector probability: 0.713	Non-apoplastic	0.58
jgi|Blugr1|23795|BGHDH14_bgh06709 | Effector probability: 0.927	Non-apoplastic	0.77
jgi|Blugr1|23794|BGHDH14_bgh01406 | Effector probability: 0.962	Non-apoplastic	0.54
jgi|Blugr1|23792|BGHDH14_bgh01369 | Effector probability: 0.846	Non-apoplastic	0.87
jgi|Blugr1|23791|BGHDH14_bgh01407 | Effector probability: 0.831	Non-apoplastic	0.86
jgi|Blugr1|23790|BGHDH14_bgh02923 | Effector probability: 0.752	Non-apoplastic	0.56
jgi|Blugr1|23786|BGHDH14_bgh01404 | Effector probability: 0.886	Non-apoplastic	0.97
jgi|Blugr1|23779|BGHDH14_bgh01628 | Effector probability: 0.946	Non-apoplastic	0.58
jgi|Blugr1|23778|BGHDH14_bgh04266 | Effector probability: 0.98	Non-apoplastic	0.82
jgi|Blugr1|23777|BGHDH14_bgh04023 | Effector probability: 0.827	Non-apoplastic	0.63
jgi|Blugr1|23776|BGHDH14_bgh03058 | Effector probability: 0.726	Apoplastic	0.75
jgi|Blugr1|23769|BGHDH14_bgh00225 | Effector probability: 0.889	Non-apoplastic	0.6
jgi|Blugr1|23768|BGHDH14_bgh00020 | Effector probability: 0.99	Non-apoplastic	0.54

#Identifier	Prediction	Probability
jgi|Blugr1|23766|BGHDH14_bgh01412 | Effector probability: 0.816	Non-apoplastic	0.65
jgi|Blugr1|23765|BGHDH14_bgh01408 | Effector probability: 0.994	Non-apoplastic	0.77
jgi|Blugr1|23743|BGHDH14_bghG002403000001001 | Effector probability: 0.974	Non-apoplastic	0.92
jgi|Blugr1|23736|BGHDH14_bghG002392000001001 | Effector probability: 0.794	Non-apoplastic	0.58
jgi|Blugr1|23731|BGHDH14_bgh02376 | Effector probability: 0.979	Non-apoplastic	0.79
jgi|Blugr1|23682|BGHDH14_bgh04927 | Effector probability: 0.918	Non-apoplastic	0.86
jgi|Blugr1|23488|BGHDH14_bgh02588 | Effector probability: 0.601	Apoplastic	0.77
jgi|Blugr1|23457|BGHDH14_bghG001346000001001 | Effector probability: 0.999	Apoplastic	0.6
jgi|Blugr1|23416|BGHDH14_bgh04781 | Effector probability: 0.673	Non-apoplastic	0.68
jgi|Blugr1|23414|BGHDH14_bgh03735 | Effector probability: 0.555	Non-apoplastic	0.54
jgi|Blugr1|23393|BGHDH14_bgh03731 | Effector probability: 0.533	Non-apoplastic	0.63
jgi|Blugr1|23392|BGHDH14_bghG001282000001001 | Effector probability: 0.949	Apoplastic	0.63
jgi|Blugr1|23377|BGHDH14_bgh00027 | Effector probability: 0.532	Non-apoplastic	0.55
jgi|Blugr1|23372|BGHDH14_bgh04121 | Effector probability: 0.678	Apoplastic	0.76
jgi|Blugr1|23363|BGHDH14_bghG001240000001001 | Effector probability: 0.744	Non-apoplastic	0.7
jgi|Blugr1|23359|BGHDH14_bghG001226000001001 | Effector probability: 0.832	Non-apoplastic	0.6
jgi|Blugr1|23356|BGHDH14_bghG001225000001001 | Effector probability: 0.869	Non-apoplastic	0.51
jgi|Blugr1|23250|BGHDH14_bgh04512 | Effector probability: 0.611	Non-apoplastic	0.92
jgi|Blugr1|23214|BGHDH14_bghG007158000001001 | Effector probability: 0.88	Non-apoplastic	0.97
jgi|Blugr1|23145|BGHDH14_bgh00016 | Effector probability: 0.994	Non-apoplastic	0.53
jgi|Blugr1|23143|BGHDH14_bghG003669000001001 | Effector probability: 0.855	Non-apoplastic	0.53
jgi|Blugr1|23046|BGHDH14_bgh04274 | Effector probability: 0.954	Non-apoplastic	0.61
jgi|Blugr1|22979|BGHDH14_bgh04522 | Effector probability: 1.0	Apoplastic	0.74
jgi|Blugr1|22969|BGHDH14_bgh06570 | Effector probability: 0.964	Apoplastic	0.7
jgi|Blugr1|22911|BGHDH14_bgh05102 | Effector probability: 0.977	Apoplastic	0.68
jgi|Blugr1|22900|BGHDH14_bgh03739 | Effector probability: 0.902	Non-apoplastic	0.53
jgi|Blugr1|22898|BGHDH14_bgh03703 | Effector probability: 0.979	Non-apoplastic	0.83
jgi|Blugr1|22648|BGHDH14_bgh04272 | Effector probability: 0.87	Non-apoplastic	0.72
jgi|Blugr1|22634|BGHDH14_bghG002861000001001 | Effector probability: 0.869	Non-apoplastic	0.52
jgi|Blugr1|22633|BGHDH14_bghG002857000001001 | Effector probability: 0.935	Non-apoplastic	0.53
jgi|Blugr1|22603|BGHDH14_bghG002826000002001 | Effector probability: 0.66	Apoplastic	0.6
jgi|Blugr1|22599|BGHDH14_bghG002822000002001 | Effector probability: 0.923	Non-apoplastic	0.69
jgi|Blugr1|22577|BGHDH14_bghG002806000001001 | Effector probability: 0.999	Apoplastic	0.8
jgi|Blugr1|22574|BGHDH14_bgh04220 | Effector probability: 0.652	Non-apoplastic	0.93
jgi|Blugr1|22556|BGHDH14_bghG002783000001001 | Effector probability: 0.867	Non-apoplastic	0.86
jgi|Blugr1|22548|BGHDH14_bgh03816 | Effector probability: 0.993	Non-apoplastic	0.61
jgi|Blugr1|22521|BGHDH14_bgh00804 | Effector probability: 0.839	Non-apoplastic	0.54
jgi|Blugr1|22452|BGHDH14_bghG002294000001001 | Effector probability: 0.834	Non-apoplastic	0.8

#Identifier	Prediction	Probability
jgi|Blugr1|22425|BGHDH14_bghG002265000001001 | Effector probability: 0.862	Apoplastic	0.75
jgi|Blugr1|22423|BGHDH14_bghG002260000001001 | Effector probability: 0.956	Non-apoplastic	0.53
jgi|Blugr1|22401|BGHDH14_bghG002254000001001 | Effector probability: 0.996	Apoplastic	0.73
jgi|Blugr1|22309|BGHDH14_bghG002170000001001 | Effector probability: 0.947	Apoplastic	0.75
jgi|Blugr1|22308|BGHDH14_bgh03686 | Effector probability: 0.973	Apoplastic	0.58
jgi|Blugr1|22305|BGHDH14_bghG002161000001001 | Effector probability: 0.974	Apoplastic	0.72
jgi|Blugr1|22300|BGHDH14_bgh03689 | Effector probability: 0.973	Non-apoplastic	0.52
jgi|Blugr1|22270|BGHDH14_bghG002084000001001 | Effector probability: 0.971	Non-apoplastic	0.82
jgi|Blugr1|22264|BGHDH14_bgh01411 | Effector probability: 0.823	Non-apoplastic	0.8
jgi|Blugr1|22249|BGHDH14_bgh04018 | Effector probability: 0.947	Non-apoplastic	0.52
jgi|Blugr1|22176|BGHDH14_bgh05321 | Effector probability: 0.939	Non-apoplastic	0.72
jgi|Blugr1|22034|BGHDH14_bgh03696 | Effector probability: 0.999	Apoplastic	0.71
jgi|Blugr1|22032|BGHDH14_bgh03474 | Effector probability: 0.959	Non-apoplastic	0.9
jgi|Blugr1|22028|BGHDH14_bgh04095 | Effector probability: 0.847	Non-apoplastic	0.57
jgi|Blugr1|22026|BGHDH14_bgh04093 | Effector probability: 0.965	Non-apoplastic	0.82
jgi|Blugr1|22023|BGHDH14_bgh06602 | Effector probability: 0.943	Non-apoplastic	0.52
jgi|Blugr1|22009|BGHDH14_bgh04864 | Effector probability: 0.992	Apoplastic	0.56
jgi|Blugr1|21987|BGHDH14_bgh03693 | Effector probability: 0.995	Non-apoplastic	0.86
jgi|Blugr1|21986|BGHDH14_bgh02835 | Effector probability: 0.854	Non-apoplastic	0.93
jgi|Blugr1|21942|BGHDH14_bgh03596 | Effector probability: 0.952	Non-apoplastic	0.59
jgi|Blugr1|21938|BGHDH14_bghG003075000001001 | Effector probability: 0.505	Apoplastic	0.64
jgi|Blugr1|21803|BGHDH14_bgh03709 | Effector probability: 0.907	Non-apoplastic	0.87
jgi|Blugr1|21763|BGHDH14_bgh03037 | Effector probability: 0.794	Non-apoplastic	0.76
jgi|Blugr1|21762|BGHDH14_bghG004439000001001 | Effector probability: 0.62	Apoplastic	0.63
jgi|Blugr1|21761|BGHDH14_bgh03028 | Effector probability: 0.823	Non-apoplastic	0.74
jgi|Blugr1|21760|BGHDH14_bgh03042 | Effector probability: 0.615	Non-apoplastic	0.52
jgi|Blugr1|21733|BGHDH14_bghG004373000002001 | Effector probability: 0.955	Non-apoplastic	0.74
jgi|Blugr1|21715|BGHDH14_bghG003905000001001 | Effector probability: 0.993	Non-apoplastic	0.8
jgi|Blugr1|21712|BGHDH14_bgh03377 | Effector probability: 0.974	Non-apoplastic	0.8
jgi|Blugr1|21699|BGHDH14_bghG003896000001001 | Effector probability: 0.931	Non-apoplastic	0.85
jgi|Blugr1|21688|BGHDH14_bgh05116 | Effector probability: 0.898	Non-apoplastic	0.7
jgi|Blugr1|21672|BGHDH14_bgh02337 | Effector probability: 0.7	Non-apoplastic	0.67
jgi|Blugr1|21671|BGHDH14_bgh03855 | Effector probability: 0.638	Non-apoplastic	0.53
jgi|Blugr1|21662|BGHDH14_bgh05117 | Effector probability: 0.901	Non-apoplastic	0.59
jgi|Blugr1|21622|BGHDH14_bgh01337 | Effector probability: 0.866	Apoplastic	0.78
jgi|Blugr1|21515|BGHDH14_bgh06674 | Effector probability: 0.524	Non-apoplastic	0.55
jgi|Blugr1|21435|BGHDH14_bghG003355000001001 | Effector probability: 0.701	Non-apoplastic	0.61
jgi|Blugr1|21434|BGHDH14_bghG003347000001001 | Effector probability: 0.789	Non-apoplastic	0.74

#Identifier	Prediction	Probability
jgi|Blugr1|21424|BGHDH14_bgh02916 | Effector probability: 0.702	Non-apoplastic	0.62
jgi|Blugr1|21382|BGHDH14_bgh00242 | Effector probability: 0.958	Non-apoplastic	0.8
jgi|Blugr1|21287|BGHDH14_bgh04219 | Effector probability: 0.893	Non-apoplastic	0.52
jgi|Blugr1|21246|BGHDH14_bgh04257 | Effector probability: 0.957	Apoplastic	0.71
jgi|Blugr1|21240|BGHDH14_bgh03293 | Effector probability: 0.959	Non-apoplastic	0.54
jgi|Blugr1|21206|BGHDH14_bgh01362 | Effector probability: 0.648	Non-apoplastic	0.59
jgi|Blugr1|21098|BGHDH14_bgh05195 | Effector probability: 0.999	Non-apoplastic	0.63
jgi|Blugr1|21066|BGHDH14_bghG004219000001001 | Effector probability: 0.947	Non-apoplastic	0.59
jgi|Blugr1|21065|BGHDH14_bgh05281 | Effector probability: 0.744	Non-apoplastic	0.96
jgi|Blugr1|21062|BGHDH14_bghG004216000001001 | Effector probability: 0.985	Non-apoplastic	0.84
jgi|Blugr1|21025|BGHDH14_bghG006760000001001 | Effector probability: 0.783	Non-apoplastic	0.51
jgi|Blugr1|20928|BGHDH14_bghG004931000001001 | Effector probability: 0.933	Non-apoplastic	0.63
jgi|Blugr1|20867|BGHDH14_bgh01761 | Effector probability: 0.994	Non-apoplastic	0.54
jgi|Blugr1|20822|BGHDH14_bgh03441 | Effector probability: 0.85	Apoplastic	0.89
jgi|Blugr1|20821|BGHDH14_bgh02083 | Effector probability: 0.998	Apoplastic	0.64
jgi|Blugr1|20818|BGHDH14_bghG003525000001001 | Effector probability: 0.968	Non-apoplastic	0.61
jgi|Blugr1|20799|BGHDH14_bgh02653 | Effector probability: 0.649	Non-apoplastic	0.85
jgi|Blugr1|20693|BGHDH14_bgh02274 | Effector probability: 0.949	Non-apoplastic	0.88
jgi|Blugr1|20643|BGHDH14_bgh02426 | Effector probability: 0.855	Non-apoplastic	0.95
jgi|Blugr1|20640|BGHDH14_bghG003379000001001 | Effector probability: 0.823	Apoplastic	0.63
jgi|Blugr1|20599|BGHDH14_bgh03462 | Effector probability: 0.96	Apoplastic	0.63
jgi|Blugr1|20597|BGHDH14_bgh02701 | Effector probability: 0.815	Non-apoplastic	0.79
jgi|Blugr1|20595|BGHDH14_bgh05269 | Effector probability: 0.995	Non-apoplastic	0.8
jgi|Blugr1|20594|BGHDH14_bgh03736 | Effector probability: 0.942	Non-apoplastic	0.66
jgi|Blugr1|20592|BGHDH14_bghG005948000001001 | Effector probability: 0.998	Non-apoplastic	0.77
jgi|Blugr1|20577|BGHDH14_bgh03584 | Effector probability: 0.808	Non-apoplastic	0.77
jgi|Blugr1|20576|BGHDH14_bghG005930000001001 | Effector probability: 0.538	Non-apoplastic	0.77
jgi|Blugr1|20575|BGHDH14_bgh03571 | Effector probability: 0.563	Non-apoplastic	0.63
jgi|Blugr1|20572|BGHDH14_bgh02072 | Effector probability: 0.883	Non-apoplastic	0.77
jgi|Blugr1|20570|BGHDH14_bgh03425 | Effector probability: 0.949	Non-apoplastic	0.62
jgi|Blugr1|20521|BGHDH14_bgh04231 | Effector probability: 0.941	Non-apoplastic	0.59
jgi|Blugr1|20519|BGHDH14_bgh04113 | Effector probability: 0.955	Non-apoplastic	0.51
jgi|Blugr1|20511|BGHDH14_bgh05270 | Effector probability: 0.996	Non-apoplastic	0.87
jgi|Blugr1|20510|BGHDH14_bgh01363 | Effector probability: 0.872	Non-apoplastic	0.6
jgi|Blugr1|20488|BGHDH14_bgh02934 | Effector probability: 0.629	Non-apoplastic	0.67
jgi|Blugr1|20487|BGHDH14_bgh03694 | Effector probability: 0.981	Apoplastic	0.73
jgi|Blugr1|20479|BGHDH14_bghG005814000001001 | Effector probability: 0.888	Non-apoplastic	0.89
jgi|Blugr1|20452|BGHDH14_bgh04255 | Effector probability: 0.999	Non-apoplastic	0.6

#Identifier	Prediction	Probability
jgi|Blugr1|20446|BGHDH14_bgh03641 | Effector probability: 0.911	Non-apoplastic	0.95
jgi|Blugr1|20421|BGHDH14_bgh00012 | Effector probability: 0.815	Non-apoplastic	0.71
jgi|Blugr1|20386|BGHDH14_bghG005434000001001 | Effector probability: 0.793	Non-apoplastic	0.53
jgi|Blugr1|20293|BGHDH14_bghG005335000001001 | Effector probability: 0.625	Apoplastic	0.6
jgi|Blugr1|20290|BGHDH14_bgh02435 | Effector probability: 0.834	Non-apoplastic	0.54
jgi|Blugr1|20289|BGHDH14_bghG005334000001001 | Effector probability: 0.717	Apoplastic	0.61
jgi|Blugr1|20181|BGHDH14_bgh04108 | Effector probability: 0.995	Non-apoplastic	0.54
jgi|Blugr1|20131|BGHDH14_bghG005501000001001 | Effector probability: 0.779	Non-apoplastic	0.53
jgi|Blugr1|20085|BGHDH14_bghG005474000001001 | Effector probability: 0.957	Non-apoplastic	0.71
jgi|Blugr1|20077|BGHDH14_bgh06543 | Effector probability: 0.723	Non-apoplastic	0.57
jgi|Blugr1|20063|BGHDH14_bghG005458000001001 | Effector probability: 0.536	Non-apoplastic	0.84
jgi|Blugr1|20062|BGHDH14_bghG005457000001001 | Effector probability: 0.716	Non-apoplastic	0.62
jgi|Blugr1|20049|BGHDH14_bgh02624 | Effector probability: 0.713	Non-apoplastic	0.83
jgi|Blugr1|20047|BGHDH14_bgh02857 | Effector probability: 0.526	Apoplastic	0.59
jgi|Blugr1|20046|BGHDH14_bgh02854 | Effector probability: 0.543	Apoplastic	0.64
jgi|Blugr1|20003|BGHDH14_bgh03636 | Effector probability: 0.939	Apoplastic	0.71
jgi|Blugr1|20002|BGHDH14_bgh04014 | Effector probability: 0.972	Apoplastic	0.67
jgi|Blugr1|19998|BGHDH14_bgh04020 | Effector probability: 0.999	Non-apoplastic	0.51
jgi|Blugr1|19997|BGHDH14_bgh03637 | Effector probability: 0.999	Apoplastic	0.68
jgi|Blugr1|19996|BGHDH14_bghG006682000001001 | Effector probability: 0.986	Non-apoplastic	0.56
jgi|Blugr1|19975|BGHDH14_bgh03613 | Effector probability: 0.505	Non-apoplastic	0.71
jgi|Blugr1|19887|BGHDH14_bgh04081 | Effector probability: 0.974	Apoplastic	0.56
jgi|Blugr1|19834|BGHDH14_bgh05844 | Effector probability: 0.942	Non-apoplastic	0.81
jgi|Blugr1|19763|BGHDH14_bgh00029 | Effector probability: 0.947	Non-apoplastic	0.68
jgi|Blugr1|19690|BGHDH14_bgh04262 | Effector probability: 0.893	Non-apoplastic	0.91
jgi|Blugr1|19689|BGHDH14_bgh03138 | Effector probability: 0.88	Non-apoplastic	0.79
jgi|Blugr1|19688|BGHDH14_bgh03786 | Effector probability: 0.9	Non-apoplastic	0.84
jgi|Blugr1|19687|BGHDH14_bgh06899 | Effector probability: 0.978	Non-apoplastic	0.8
jgi|Blugr1|19686|BGHDH14_bgh04268 | Effector probability: 0.872	Non-apoplastic	0.87
jgi|Blugr1|19677|BGHDH14_bgh03901 | Effector probability: 0.947	Non-apoplastic	0.8
jgi|Blugr1|19676|BGHDH14_bghG006623000001001 | Effector probability: 0.923	Non-apoplastic	0.73
jgi|Blugr1|19675|BGHDH14_bgh03874 | Effector probability: 0.854	Non-apoplastic	0.85
jgi|Blugr1|19613|BGHDH14_bgh01675 | Effector probability: 0.841	Non-apoplastic	0.86
jgi|Blugr1|19397|BGHDH14_bgh03782 | Effector probability: 0.996	Non-apoplastic	0.71
jgi|Blugr1|19362|BGHDH14_bghG007601000001001 | Effector probability: 0.609	Non-apoplastic	0.51
jgi|Blugr1|19348|BGHDH14_bgh03316 | Effector probability: 0.91	Non-apoplastic	0.85
jgi|Blugr1|19262|BGHDH14_bgh05491 | Effector probability: 0.663	Non-apoplastic	0.71
jgi|Blugr1|19260|BGHDH14_bgh04077 | Effector probability: 0.674	Apoplastic	0.73

#Identifier	Prediction	Probability
jgi|Blugr1|19258|BGHDH14_bgh04027 | Effector probability: 0.996	Non-apoplastic	0.87
jgi|Blugr1|19254|BGHDH14_bgh05609 | Effector probability: 0.56	Non-apoplastic	0.52
jgi|Blugr1|19253|BGHDH14_bghG009555000001001 | Effector probability: 0.991	Non-apoplastic	0.62
jgi|Blugr1|19250|BGHDH14_bghG009020000001001 | Effector probability: 0.952	Apoplastic	0.66
jgi|Blugr1|19249|BGHDH14_bghG008908000001001 | Effector probability: 0.656	Apoplastic	0.55
jgi|Blugr1|19247|BGHDH14_bgh03579 | Effector probability: 0.996	Non-apoplastic	0.54
jgi|Blugr1|19246|BGHDH14_bgh03575 | Effector probability: 0.974	Apoplastic	0.55
jgi|Blugr1|19245|BGHDH14_bgh03572 | Effector probability: 0.995	Non-apoplastic	0.86
jgi|Blugr1|19237|BGHDH14_bgh06532 | Effector probability: 0.974	Non-apoplastic	0.55
jgi|Blugr1|19234|BGHDH14_bghG008002000002001 | Effector probability: 0.969	Non-apoplastic	0.57
jgi|Blugr1|19233|BGHDH14_bghG008885000001001 | Effector probability: 0.757	Non-apoplastic	0.62
jgi|Blugr1|19215|BGHDH14_bgh02874 | Effector probability: 0.935	Non-apoplastic	0.68
jgi|Blugr1|19212|BGHDH14_bgh06494 | Effector probability: 1.0	Apoplastic	0.6
jgi|Blugr1|19211|BGHDH14_bghG008560000001001 | Effector probability: 1.0	Apoplastic	0.6
jgi|Blugr1|19206|BGHDH14_bgh06518 | Effector probability: 0.897	Apoplastic	0.6
jgi|Blugr1|19198|BGHDH14_bgh02928 | Effector probability: 0.938	Non-apoplastic	0.69
jgi|Blugr1|19181|BGHDH14_bgh02925 | Effector probability: 0.957	Non-apoplastic	0.81
jgi|Blugr1|19172|BGHDH14_bgh03582 | Effector probability: 0.995	Non-apoplastic	0.53
jgi|Blugr1|19168|BGHDH14_bgh04083 | Effector probability: 0.523	Non-apoplastic	0.71
jgi|Blugr1|19166|BGHDH14_bghG013624000001001 | Effector probability: 0.948	Non-apoplastic	0.8
jgi|Blugr1|19163|BGHDH14_bgh05792 | Effector probability: 0.903	Non-apoplastic	0.69
jgi|Blugr1|19155|BGHDH14_bgh03376 | Effector probability: 0.774	Apoplastic	0.63
jgi|Blugr1|19153|BGHDH14_bghG008575000001001 | Effector probability: 0.974	Non-apoplastic	0.55

D. *B. graminis f. sp. tritici* effector candidate apoplast localization prediction (EffectorP etermined effector probability noted after effector name)

#Identifier	Prediction	Probability
jgi|Blugra1|1031|BGT96224_E5632T0 | Effector probability: 0.724	Non-apoplastic	0.85
jgi|Blugra1|104|BGT96224_BCG4T0 | Effector probability: 0.896	Non-apoplastic	0.52
jgi|Blugra1|1057|BGT96224_40012T0 | Effector probability: 0.864	Non-apoplastic	0.58
jgi|Blugra1|1058|BGT96224_AcSP31098T0 | Effector probability: 0.996	Non-apoplastic	0.9
jgi|Blugra1|1067|BGT96224_E5685T0 | Effector probability: 0.947	Non-apoplastic	0.88
jgi|Blugra1|107|BGT96224_E10109T0 | Effector probability: 0.954	Non-apoplastic	0.54
jgi|Blugra1|1108|BGT96224_E10101T0 | Effector probability: 0.941	Non-apoplastic	0.57
jgi|Blugra1|1188|BGT96224_E5980T0 | Effector probability: 0.83	Non-apoplastic	0.56
jgi|Blugra1|1193|BGT96224_AcSP30107T0 | Effector probability: 0.985	Non-apoplastic	0.94
jgi|Blugra1|1231|BGT96224_AcSP31145T0 | Effector probability: 0.822	Non-apoplastic	0.55
jgi|Blugra1|123|BGT96224_E40011T0 | Effector probability: 0.983	Non-apoplastic	0.66
jgi|Blugra1|1249|BGT96224_2900BT0 | Effector probability: 0.937	Non-apoplastic	0.75
jgi|Blugra1|1312|BGT96224_E5722T0 | Effector probability: 0.967	Non-apoplastic	0.61
jgi|Blugra1|1326|BGT96224_1289T0 | Effector probability: 0.979	Apoplastic	0.75
jgi|Blugra1|1330|BGT96224_E5731T0 | Effector probability: 0.502	Non-apoplastic	0.83
jgi|Blugra1|1338|BGT96224_AcSP30530T0 | Effector probability: 0.902	Non-apoplastic	0.69
jgi|Blugra1|1427|BGT96224_2135T0 | Effector probability: 0.993	Apoplastic	0.55
jgi|Blugra1|1436|BGT96224_E5704T0 | Effector probability: 0.943	Non-apoplastic	0.76
jgi|Blugra1|1442|BGT96224_E5709T0 | Effector probability: 0.539	Apoplastic	0.78
jgi|Blugra1|1478|BGT96224_19T0 | Effector probability: 0.902	Non-apoplastic	0.93
jgi|Blugra1|148|BGT96224_2708T0 | Effector probability: 0.927	Non-apoplastic	0.54
jgi|Blugra1|1513|BGT96224_E5909T0 | Effector probability: 0.552	Non-apoplastic	0.64
jgi|Blugra1|1541|BGT96224_2274T0 | Effector probability: 0.512	Apoplastic	0.8
jgi|Blugra1|1550|BGT96224_E6031T0 | Effector probability: 0.815	Non-apoplastic	0.51
jgi|Blugra1|158|BGT96224_E5560T0 | Effector probability: 0.826	Non-apoplastic	0.57
jgi|Blugra1|165|BGT96224_ASP20866T0 | Effector probability: 0.984	Non-apoplastic	0.73
jgi|Blugra1|1711|BGT96224_E5627T0 | Effector probability: 0.713	Apoplastic	0.6
jgi|Blugra1|1742|BGT96224_E6018T0 | Effector probability: 0.971	Non-apoplastic	0.71
jgi|Blugra1|1749|BGT96224_4496BT0 | Effector probability: 0.758	Non-apoplastic	0.91
jgi|Blugra1|1756|BGT96224_E10137T0 | Effector probability: 0.882	Apoplastic	0.71
jgi|Blugra1|184|BGT96224_E5929T0 | Effector probability: 0.977	Non-apoplastic	0.7
jgi|Blugra1|1904|BGT96224_E5836T0 | Effector probability: 0.856	Non-apoplastic	0.92
jgi|Blugra1|1910|BGT96224_AcSP30824T0 | Effector probability: 0.807	Non-apoplastic	0.72

#Identifier	Prediction	Probability
jgi|Blugra1|1929|BGT96224_E5982T0 | Effector probability: 1.0	Non-apoplastic	0.56
jgi|Blugra1|194|BGT96224_BCG8T0 | Effector probability: 0.936	Non-apoplastic	0.68
jgi|Blugra1|1988|BGT96224_E10118T0 | Effector probability: 0.987	Non-apoplastic	0.5
jgi|Blugra1|1989|BGT96224_E5547T0 | Effector probability: 0.893	Non-apoplastic	0.52
jgi|Blugra1|1990|BGT96224_AcSP30782T0 | Effector probability: 0.795	Non-apoplastic	1
jgi|Blugra1|201|BGT96224_E5842T0 | Effector probability: 0.7	Non-apoplastic	0.52
jgi|Blugra1|202|BGT96224_ASP21585T0 | Effector probability: 0.708	Apoplastic	0.62
jgi|Blugra1|209|BGT96224_E5913T0 | Effector probability: 0.996	Apoplastic	0.56
jgi|Blugra1|2104|BGT96224_AcSP31023T0 | Effector probability: 0.979	Non-apoplastic	0.52
jgi|Blugra1|2187|BGT96224_E10100T0 | Effector probability: 0.994	Non-apoplastic	0.54
jgi|Blugra1|219|BGT96224_E5781T0 | Effector probability: 0.94	Apoplastic	0.68
jgi|Blugra1|223|BGT96224_E5877T0 | Effector probability: 0.697	Apoplastic	0.69
jgi|Blugra1|2243|BGT96224_5308T0 | Effector probability: 0.903	Non-apoplastic	0.87
jgi|Blugra1|2252|BGT96224_E5732T0 | Effector probability: 0.938	Non-apoplastic	0.77
jgi|Blugra1|225|BGT96224_E5880T0 | Effector probability: 0.676	Non-apoplastic	0.59
jgi|Blugra1|2299|BGT96224_E6032T0 | Effector probability: 0.99	Non-apoplastic	0.53
jgi|Blugra1|229|BGT96224_E5783T0 | Effector probability: 0.913	Non-apoplastic	0.57
jgi|Blugra1|22|BGT96224_E5967T0 | Effector probability: 0.968	Non-apoplastic	0.62
jgi|Blugra1|230|BGT96224_E5953T0 | Effector probability: 0.86	Non-apoplastic	0.68
jgi|Blugra1|2367|BGT96224_E5679T0 | Effector probability: 0.598	Non-apoplastic	0.75
jgi|Blugra1|2423|BGT96224_E5668T0 | Effector probability: 0.783	Non-apoplastic	0.54
jgi|Blugra1|2430|BGT96224_ASP21313T0 | Effector probability: 0.793	Non-apoplastic	0.57
jgi|Blugra1|2467|BGT96224_A20644T0 | Effector probability: 0.626	Apoplastic	0.8
jgi|Blugra1|2469|BGT96224_E5677T0 | Effector probability: 0.96	Non-apoplastic	0.81
jgi|Blugra1|2527|BGT96224_3821T0 | Effector probability: 0.602	Apoplastic	0.78
jgi|Blugra1|2602|BGT96224_273BT0 | Effector probability: 0.661	Non-apoplastic	1
jgi|Blugra1|2676|BGT96224_3472T0 | Effector probability: 0.978	Apoplastic	0.57
jgi|Blugra1|2692|BGT96224_2673T0 | Effector probability: 0.863	Apoplastic	0.71
jgi|Blugra1|274|BGT96224_E5585T0 | Effector probability: 0.893	Non-apoplastic	0.5
jgi|Blugra1|2756|BGT96224_E5991T0 | Effector probability: 1.0	Apoplastic	0.77
jgi|Blugra1|2766|BGT96224_501T0 | Effector probability: 0.973	Apoplastic	0.69
jgi|Blugra1|276|BGT96224_E5548T0 | Effector probability: 0.89	Apoplastic	0.73
jgi|Blugra1|2852|BGT96224_4373T0 | Effector probability: 0.998	Non-apoplastic	0.76
jgi|Blugra1|2873|BGT96224_E5604T0 | Effector probability: 0.953	Non-apoplastic	0.56
jgi|Blugra1|2875|BGT96224_AcSP30893T0 | Effector probability: 0.999	Non-apoplastic	0.5
jgi|Blugra1|2942|BGT96224_5451T0 | Effector probability: 0.968	Apoplastic	0.55
jgi|Blugra1|3022|BGT96224_E3136T0 | Effector probability: 0.781	Non-apoplastic	0.81
jgi|Blugra1|3023|BGT96224_E5921T0 | Effector probability: 0.998	Apoplastic	0.55

#Identifier	Prediction	Probability
jgi|Blugra1|3024|BGT96224_E5922T0 | Effector probability: 0.975	Non-apoplastic	0.55
jgi|Blugra1|3030|BGT96224_E10124T0 | Effector probability: 0.98	Non-apoplastic	0.62
jgi|Blugra1|3111|BGT96224_BCG9T0 | Effector probability: 0.875	Non-apoplastic	0.62
jgi|Blugra1|3112|BGT96224_BCG5T0 | Effector probability: 0.964	Non-apoplastic	0.72
jgi|Blugra1|3113|BGT96224_BCG2T0 | Effector probability: 0.933	Non-apoplastic	0.54
jgi|Blugra1|3115|BGT96224_BCG3T0 | Effector probability: 0.902	Non-apoplastic	0.6
jgi|Blugra1|3123|BGT96224_E5553T0 | Effector probability: 0.543	Non-apoplastic	0.57
jgi|Blugra1|3132|BGT96224_E5774T0 | Effector probability: 0.865	Apoplastic	0.61
jgi|Blugra1|3178|BGT96224_E5624T0 | Effector probability: 0.895	Non-apoplastic	0.86
jgi|Blugra1|3187|BGT96224_AcSP30129T0 | Effector probability: 0.975	Non-apoplastic	0.67
jgi|Blugra1|3195|BGT96224_E5658T0 | Effector probability: 0.745	Non-apoplastic	0.87
jgi|Blugra1|3211|BGT96224_E10110T0 | Effector probability: 0.928	Non-apoplastic	0.51
jgi|Blugra1|3214|BGT96224_E10111T0 | Effector probability: 0.972	Apoplastic	0.62
jgi|Blugra1|3327|BGT96224_E5784T0 | Effector probability: 0.663	Non-apoplastic	0.66
jgi|Blugra1|3416|BGT96224_E4403T0 | Effector probability: 0.911	Non-apoplastic	0.93
jgi|Blugra1|3470|BGT96224_AcSP30848T0 | Effector probability: 0.951	Non-apoplastic	0.57
jgi|Blugra1|3481|BGT96224_2816T0 | Effector probability: 0.741	Apoplastic	0.85
jgi|Blugra1|3537|BGT96224_E10116T0 | Effector probability: 0.994	Non-apoplastic	0.6
jgi|Blugra1|3572|BGT96224_E5973T0 | Effector probability: 0.974	Non-apoplastic	0.71
jgi|Blugra1|3584|BGT96224_E5965T0 | Effector probability: 0.861	Non-apoplastic	0.92
jgi|Blugra1|3585|BGT96224_E5539T0 | Effector probability: 0.76	Non-apoplastic	0.51
jgi|Blugra1|3587|BGT96224_E5538T0 | Effector probability: 0.919	Apoplastic	0.66
jgi|Blugra1|3667|BGT96224_959T0 | Effector probability: 0.533	Non-apoplastic	0.5
jgi|Blugra1|3686|BGT96224_E5963T0 | Effector probability: 0.99	Non-apoplastic	0.54
jgi|Blugra1|3687|BGT96224_AcSP30748T0 | Effector probability: 0.982	Non-apoplastic	0.78
jgi|Blugra1|3689|BGT96224_E10108T0 | Effector probability: 0.801	Non-apoplastic	0.94
jgi|Blugra1|3851|BGT96224_AcSP30091T0 | Effector probability: 0.89	Non-apoplastic	0.67
jgi|Blugra1|387|BGT96224_ASP20465T0 | Effector probability: 0.846	Non-apoplastic	0.83
jgi|Blugra1|3980|BGT96224_AcSP30691T0 | Effector probability: 0.986	Non-apoplastic	0.77
jgi|Blugra1|4036|BGT96224_E5763T0 | Effector probability: 0.999	Non-apoplastic	0.64
jgi|Blugra1|4044|BGT96224_E6038T0 | Effector probability: 0.746	Non-apoplastic	0.85
jgi|Blugra1|4097|BGT96224_AcSP30056T0 | Effector probability: 0.703	Non-apoplastic	0.9
jgi|Blugra1|4114|BGT96224_E3602T0 | Effector probability: 0.946	Non-apoplastic	0.58
jgi|Blugra1|4144|BGT96224_E5845T0 | Effector probability: 0.744	Non-apoplastic	0.56
jgi|Blugra1|4163|BGT96224_E3962T0 | Effector probability: 0.99	Apoplastic	0.65
jgi|Blugra1|4196|BGT96224_E5543T0 | Effector probability: 0.92	Non-apoplastic	0.62
jgi|Blugra1|4243|BGT96224_ASP20572T0 | Effector probability: 0.974	Non-apoplastic	0.89
jgi|Blugra1|4253|BGT96224_E5888T0 | Effector probability: 0.962	Non-apoplastic	0.77

#Identifier	Prediction	Probability
jgi|Blugra1|425|BGT96224_E10002T0 | Effector probability: 0.813	Non-apoplastic	0.73
jgi|Blugra1|4267|BGT96224_1302T0 | Effector probability: 0.868	Apoplastic	0.75
jgi|Blugra1|4302|BGT96224_AcSP30622T0 | Effector probability: 0.988	Non-apoplastic	0.51
jgi|Blugra1|4315|BGT96224_AcSP31262T0 | Effector probability: 0.657	Non-apoplastic	0.65
jgi|Blugra1|4320|BGT96224_E5545T0 | Effector probability: 0.807	Non-apoplastic	0.76
jgi|Blugra1|4335|BGT96224_249T0 | Effector probability: 0.661	Non-apoplastic	0.75
jgi|Blugra1|4341|BGT96224_1536T0 | Effector probability: 0.981	Non-apoplastic	0.85
jgi|Blugra1|4364|BGT96224_E6054T0 | Effector probability: 0.82	Non-apoplastic	0.63
jgi|Blugra1|4405|BGT96224_E5839T0 | Effector probability: 0.855	Non-apoplastic	0.52
jgi|Blugra1|4407|BGT96224_AcSP31175T0 | Effector probability: 0.961	Non-apoplastic	0.53
jgi|Blugra1|4428|BGT96224_AcSP31269T0 | Effector probability: 0.948	Non-apoplastic	0.9
jgi|Blugra1|467|BGT96224_ASP21338T0 | Effector probability: 0.973	Non-apoplastic	0.51
jgi|Blugra1|4690|BGT96224_4619T0 | Effector probability: 1.0	Non-apoplastic	0.51
jgi|Blugra1|4742|BGT96224_E5689T0 | Effector probability: 0.793	Non-apoplastic	0.5
jgi|Blugra1|4748|BGT96224_E10141T0 | Effector probability: 0.732	Apoplastic	0.65
jgi|Blugra1|4764|BGT96224_E10114T0 | Effector probability: 0.753	Non-apoplastic	0.98
jgi|Blugra1|4881|BGT96224_5153T0 | Effector probability: 0.99	Apoplastic	0.56
jgi|Blugra1|4907|BGT96224_E5582T0 | Effector probability: 0.983	Non-apoplastic	0.85
jgi|Blugra1|5001|BGT96224_AcSP30210T0 | Effector probability: 0.876	Non-apoplastic	0.84
jgi|Blugra1|5018|BGT96224_AcSP30464T0 | Effector probability: 0.665	Non-apoplastic	0.76
jgi|Blugra1|5034|BGT96224_E10129T0 | Effector probability: 0.976	Apoplastic	0.74
jgi|Blugra1|5098|BGT96224_E5996T0 | Effector probability: 0.763	Apoplastic	0.61
jgi|Blugra1|5162|BGT96224_E5883T0 | Effector probability: 0.973	Non-apoplastic	0.57
jgi|Blugra1|5189|BGT96224_E5665T0 | Effector probability: 0.84	Non-apoplastic	0.71
jgi|Blugra1|51|BGT96224_E5918T0 | Effector probability: 0.859	Non-apoplastic	0.54
jgi|Blugra1|5272|BGT96224_E5659T0 | Effector probability: 0.978	Apoplastic	0.65
jgi|Blugra1|5316|BGT96224_E3523T0 | Effector probability: 0.683	Non-apoplastic	0.64
jgi|Blugra1|5332|BGT96224_E6035T0 | Effector probability: 0.681	Non-apoplastic	0.78
jgi|Blugra1|5336|BGT96224_E3888T0 | Effector probability: 0.596	Non-apoplastic	0.6
jgi|Blugra1|5377|BGT96224_BCGB1T0 | Effector probability: 0.921	Non-apoplastic	0.6
jgi|Blugra1|5490|BGT96224_ASP20340T0 | Effector probability: 0.98	Non-apoplastic	0.64
jgi|Blugra1|5492|BGT96224_E10014T0 | Effector probability: 0.98	Non-apoplastic	0.5
jgi|Blugra1|5500|BGT96224_E5610T0 | Effector probability: 1.0	Apoplastic	0.76
jgi|Blugra1|5541|BGT96224_E5924T0 | Effector probability: 0.671	Non-apoplastic	0.51
jgi|Blugra1|5550|BGT96224_AcSP30282T0 | Effector probability: 0.998	Apoplastic	0.64
jgi|Blugra1|5627|BGT96224_E5664T0 | Effector probability: 0.898	Apoplastic	0.55
jgi|Blugra1|5735|BGT96224_E5625T0 | Effector probability: 0.723	Non-apoplastic	0.54
jgi|Blugra1|5736|BGT96224_E5906T0 | Effector probability: 0.995	Non-apoplastic	0.54

#Identifier	Prediction	Probability
jgi|Blugra1|575|BGT96224_E5867T0 | Effector probability: 0.681	Non-apoplastic	0.53
jgi|Blugra1|5762|BGT96224_AcSP31344T0 | Effector probability: 0.936	Non-apoplastic	0.8
jgi|Blugra1|5795|BGT96224_E5850T0 | Effector probability: 0.949	Non-apoplastic	0.74
jgi|Blugra1|5804|BGT96224_AcSP31373T0 | Effector probability: 0.98	Non-apoplastic	0.69
jgi|Blugra1|5828|BGT96224_ASP21390T0 | Effector probability: 0.997	Non-apoplastic	0.72
jgi|Blugra1|5835|BGT96224_3194T0 | Effector probability: 0.791	Non-apoplastic	0.57
jgi|Blugra1|5840|BGT96224_E5673T0 | Effector probability: 0.984	Non-apoplastic	0.52
jgi|Blugra1|5850|BGT96224_E6034T0 | Effector probability: 0.786	Apoplastic	0.6
jgi|Blugra1|5867|BGT96224_E5974T0 | Effector probability: 0.995	Non-apoplastic	0.55
jgi|Blugra1|5982|BGT96224_E5600T0 | Effector probability: 0.951	Non-apoplastic	0.6
jgi|Blugra1|6005|BGT96224_AcSP31429T0 | Effector probability: 0.795	Non-apoplastic	0.88
jgi|Blugra1|6046|BGT96224_ASP21455T0 | Effector probability: 0.592	Non-apoplastic	0.99
jgi|Blugra1|6054|BGT96224_BCG6T0 | Effector probability: 0.964	Apoplastic	0.73
jgi|Blugra1|6061|BGT96224_2700T0 | Effector probability: 0.865	Non-apoplastic	0.94
jgi|Blugra1|6081|BGT96224_E5816T0 | Effector probability: 0.585	Non-apoplastic	0.83
jgi|Blugra1|6174|BGT96224_E5966T0 | Effector probability: 0.97	Non-apoplastic	0.74
jgi|Blugra1|6206|BGT96224_E5570T0 | Effector probability: 0.827	Non-apoplastic	0.74
jgi|Blugra1|6207|BGT96224_2846T0 | Effector probability: 0.506	Non-apoplastic	0.81
jgi|Blugra1|6215|BGT96224_ASP21508T0 | Effector probability: 0.95	Apoplastic	0.7
jgi|Blugra1|6226|BGT96224_E40006T0 | Effector probability: 0.914	Apoplastic	0.64
jgi|Blugra1|6228|BGT96224_BCG7T0 | Effector probability: 0.988	Apoplastic	0.73
jgi|Blugra1|6241|BGT96224_BCG1T0 | Effector probability: 0.971	Apoplastic	0.61
jgi|Blugra1|6247|BGT96224_ASP20484T0 | Effector probability: 0.832	Non-apoplastic	0.86
jgi|Blugra1|6293|BGT96224_E5889T0 | Effector probability: 0.768	Apoplastic	0.56
jgi|Blugra1|6301|BGT96224_E5912T0 | Effector probability: 1.0	Non-apoplastic	0.52
jgi|Blugra1|6317|BGT96224_E5550T0 | Effector probability: 0.963	Apoplastic	0.59
jgi|Blugra1|6320|BGT96224_E10120T0 | Effector probability: 0.799	Non-apoplastic	0.65
jgi|Blugra1|6338|BGT96224_5370T0 | Effector probability: 0.886	Non-apoplastic	0.79
jgi|Blugra1|6371|BGT96224_E3419T0 | Effector probability: 0.913	Non-apoplastic	0.6
jgi|Blugra1|637|BGT96224_E5607T0 | Effector probability: 0.831	Non-apoplastic	0.61
jgi|Blugra1|6473|BGT96224_E5981T0 | Effector probability: 0.987	Non-apoplastic	0.62
jgi|Blugra1|649|BGT96224_AcSP30305T0 | Effector probability: 0.996	Non-apoplastic	0.66
jgi|Blugra1|776|BGT96224_E10132T0 | Effector probability: 0.967	Non-apoplastic	0.88
jgi|Blugra1|815|BGT96224_AcSP31310T0 | Effector probability: 0.97	Non-apoplastic	0.7
jgi|Blugra1|844|BGT96224_E5829T0 | Effector probability: 0.848	Apoplastic	0.71
jgi|Blugra1|955|BGT96224_AcSP30002T0 | Effector probability: 0.729	Non-apoplastic	0.65
jgi|Blugra1|956|BGT96224_E3893T0 | Effector probability: 0.986	Non-apoplastic	0.61

E. *E. necator* effector candidate apoplast localization prediction (EffectorP etermined effector probability noted after effector name)

#Identifier	Prediction	Probability
jgi|Erynec1|3754|EV44_g0424T0 | Effector probability: 1.0	Apoplastic	0.66
jgi|Erynec1|3863|EV44_g0269T0 | Effector probability: 1.0	Non-apoplastic	0.66
jgi|Erynec1|3884|EV44_g0435T0 | Effector probability: 0.969	Non-apoplastic	0.61
jgi|Erynec1|3897|EV44_g0430T0 | Effector probability: 0.971	Non-apoplastic	0.55
jgi|Erynec1|4034|EV44_g0573T0 | Effector probability: 0.591	Non-apoplastic	0.81
jgi|Erynec1|4332|EV44_g0203T0 | Effector probability: 0.926	Apoplastic	0.59
jgi|Erynec1|4482|EV44_g0444T0 | Effector probability: 0.718	Non-apoplastic	0.65
jgi|Erynec1|4486|EV44_g0225T0 | Effector probability: 0.985	Non-apoplastic	0.64
jgi|Erynec1|4489|EV44_g0416T0 | Effector probability: 0.702	Non-apoplastic	0.83
jgi|Erynec1|4492|EV44_g0357T0 | Effector probability: 0.997	Apoplastic	0.69
jgi|Erynec1|456|EV44_g0586T0 | Effector probability: 0.961	Non-apoplastic	0.52
jgi|Erynec1|4579|EV44_g0597T0 | Effector probability: 0.924	Non-apoplastic	0.5
jgi|Erynec1|4713|EV44_g0473T0 | Effector probability: 0.688	Non-apoplastic	0.51
jgi|Erynec1|4768|EV44_g0533T0 | Effector probability: 0.644	Non-apoplastic	0.75
jgi|Erynec1|4898|EV44_g0549T0 | Effector probability: 0.874	Non-apoplastic	0.79
jgi|Erynec1|5106|EV44_g0246T0 | Effector probability: 0.993	Apoplastic	0.66
jgi|Erynec1|5150|EV44_g0559T0 | Effector probability: 0.628	Non-apoplastic	0.99
jgi|Erynec1|5250|EV44_g0482T0 | Effector probability: 0.88	Non-apoplastic	0.6
jgi|Erynec1|5262|EV44_g0379T0 | Effector probability: 0.734	Apoplastic	0.6
jgi|Erynec1|5288|EV44_g0569T0 | Effector probability: 0.92	Non-apoplastic	0.91
jgi|Erynec1|5307|EV44_g0140T0 | Effector probability: 0.884	Apoplastic	0.58
jgi|Erynec1|5385|EV44_g0230T0 | Effector probability: 0.832	Apoplastic	0.59
jgi|Erynec1|5409|EV44_g0242T0 | Effector probability: 0.983	Non-apoplastic	0.97
jgi|Erynec1|5479|EV44_g0244T0 | Effector probability: 1.0	Apoplastic	0.6
jgi|Erynec1|5533|EV44_g0534T0 | Effector probability: 0.972	Non-apoplastic	0.73
jgi|Erynec1|5601|EV44_g0503T0 | Effector probability: 0.78	Non-apoplastic	0.63
jgi|Erynec1|5708|EV44_g0090T0 | Effector probability: 0.758	Non-apoplastic	0.72
jgi|Erynec1|5719|EV44_g0279T0 | Effector probability: 0.982	Apoplastic	0.64
jgi|Erynec1|5744|EV44_g0388T0 | Effector probability: 0.75	Apoplastic	0.56
jgi|Erynec1|5773|EV44_g0076T0 | Effector probability: 0.656	Non-apoplastic	0.59
jgi|Erynec1|5790|EV44_g0596T0 | Effector probability: 0.831	Non-apoplastic	0.61
jgi|Erynec1|5929|EV44_g0571T0 | Effector probability: 1.0	Apoplastic	0.67
jgi|Erynec1|6058|EV44_g0525T0 | Effector probability: 1.0	Apoplastic	0.7
jgi|Erynec1|6064|EV44_g0542T0 | Effector probability: 0.625	Non-apoplastic	0.8

#Identifier	Prediction	Probability
jgi|Erynec1|6114|EV44_g0283T0 | Effector probability: 0.509	Non-apoplastic	0.91
jgi|Erynec1|6210|EV44_g0206T0 | Effector probability: 0.984	Non-apoplastic	0.77
jgi|Erynec1|6287|EV44_g0465T0 | Effector probability: 0.931	Non-apoplastic	0.61
jgi|Erynec1|6322|EV44_g0526T0 | Effector probability: 0.994	Apoplastic	0.79
jgi|Erynec1|641|EV44_g0383T0 | Effector probability: 0.959	Non-apoplastic	0.92
jgi|Erynec1|898|EV44_g0186T0 | Effector probability: 0.787	Non-apoplastic	0.93
jgi|Erynec1|914|EV44_g0538T0 | Effector probability: 0.904	Apoplastic	0.56
jgi|Erynec1|1056|EV44_g0547T0 | Effector probability: 0.996	Apoplastic	0.79
jgi|Erynec1|1161|EV44_g0257T0 | Effector probability: 0.994	Apoplastic	0.75
jgi|Erynec1|1405|EV44_g0537T0 | Effector probability: 0.978	Non-apoplastic	0.78
jgi|Erynec1|1421|EV44_g0014T0 | Effector probability: 0.9	Non-apoplastic	0.95
jgi|Erynec1|1511|EV44_g0425T0 | Effector probability: 0.999	Non-apoplastic	0.53
jgi|Erynec1|1647|EV44_g0551T0 | Effector probability: 1.0	Non-apoplastic	0.6
jgi|Erynec1|1730|EV44_g0415T0 | Effector probability: 0.729	Non-apoplastic	0.92
jgi|Erynec1|1752|EV44_g0591T0 | Effector probability: 0.947	Non-apoplastic	0.91
jgi|Erynec1|189|EV44_g0181T0 | Effector probability: 0.777	Non-apoplastic	0.89
jgi|Erynec1|2050|EV44_g0313T0 | Effector probability: 0.934	Non-apoplastic	0.61
jgi|Erynec1|2064|EV44_g0519T0 | Effector probability: 0.738	Non-apoplastic	1
jgi|Erynec1|2200|EV44_g0602T0 | Effector probability: 0.925	Non-apoplastic	0.92
jgi|Erynec1|2252|EV44_g0426T0 | Effector probability: 0.939	Non-apoplastic	0.67
jgi|Erynec1|2372|EV44_g0599T0 | Effector probability: 1.0	Non-apoplastic	0.64
jgi|Erynec1|2412|EV44_g0178T0 | Effector probability: 0.901	Non-apoplastic	0.84
jgi|Erynec1|2444|EV44_g0052T0 | Effector probability: 0.965	Apoplastic	0.72
jgi|Erynec1|2466|EV44_g0274T0 | Effector probability: 0.999	Apoplastic	0.6
jgi|Erynec1|2619|EV44_g0254T0 | Effector probability: 0.773	Non-apoplastic	0.78
jgi|Erynec1|2628|EV44_g0447T0 | Effector probability: 0.918	Non-apoplastic	0.58
jgi|Erynec1|3007|EV44_g0583T0 | Effector probability: 0.755	Non-apoplastic	0.99
jgi|Erynec1|3081|EV44_g0282T0 | Effector probability: 0.973	Apoplastic	0.57
jgi|Erynec1|3117|EV44_g0136T0 | Effector probability: 0.86	Apoplastic	0.87
jgi|Erynec1|3159|EV44_g0215T0 | Effector probability: 0.887	Non-apoplastic	0.65
jgi|Erynec1|3287|EV44_g0600T0 | Effector probability: 0.849	Non-apoplastic	0.88
jgi|Erynec1|345|EV44_g0192T0 | Effector probability: 0.997	Non-apoplastic	0.54
jgi|Erynec1|3611|EV44_g0196T0 | Effector probability: 0.954	Non-apoplastic	0.78
jgi|Erynec1|3648|EV44_g0539T0 | Effector probability: 1.0	Apoplastic	0.71
jgi|Erynec1|369|EV44_g0481T0 | Effector probability: 0.901	Non-apoplastic	0.82

Appendix 7: CAZY predictions for powdery mildew predicted genes

A. *G. cichoracearum* genes encoding predicted CAZY proteins

Query	Subject	E-value	Start	End	Covered Fraction
jgi|Golci1|1043184|CE1043183_26608	GH5_9.hmm	1.60E-119	2	306	0.993464052
jgi|Golci1|105783|CE105782_5644	AA11.hmm	1.40E-66	1	187	0.97382199
jgi|Golci1|105783|CE105782_5644	CBM18.hmm	0.00079	2	35	0.868421053
jgi|Golci1|1274390|CE1274389_3220	GT58.hmm	1.10E-123	30	364	0.917582418
jgi|Golci1|1285880|CE1285879_22103	GH16.hmm	1.20E-22	56	188	0.698412698
jgi|Golci1|1426233|CE1426232_69532	GH16.hmm	2.40E-20	33	185	0.804232804
jgi|Golci1|1449209|CE1449208_1547	GH81.hmm	7.50E-218	6	621	0.988745981
jgi|Golci1|1458582|CE1458581_7815	GT20.hmm	4.50E-198	10	475	0.978947368
jgi|Golci1|1461740|CE1461739_47777	GT2.hmm	2.10E-07	2	167	0.982142857
jgi|Golci1|1511718|CE1511717_8313	CE3.hmm	4.10E-54	1	194	0.994845361
jgi|Golci1|1705086|gm4.911_g	GT69.hmm	5.40E-56	1	238	0.991631799
jgi|Golci1|1707044|gm4.2869_g	AA1_3.hmm	9.90E-124	3	285	0.903846154
jgi|Golci1|1710373|gm4.6198_g	GH16.hmm	1.40E-22	35	189	0.814814815
jgi|Golci1|1714536|gm4.10361_g	GT15.hmm	3.90E-120	1	272	0.992673993
jgi|Golci1|1727097|gm4.22922_g	CE10.hmm	9.30E-18	71	319	0.727272727
jgi|Golci1|1730890|gm4.26715_g	CE10.hmm	2.10E-22	73	193	0.351906158
jgi|Golci1|1733541|gm4.29366_g	GT2.hmm	1.60E-32	1	110	0.648809524
jgi|Golci1|1738175|gm4.34000_g	GH3.hmm	1.80E-47	5	215	0.972222222
jgi|Golci1|1751925|gw1.4.113.1	GH132.hmm	1.10E-88	48	300	0.831683168
jgi|Golci1|1758734|gw1.116.48.1	CBM18.hmm	1.10E-05	8	36	0.736842105
jgi|Golci1|1758734|gw1.116.48.1	CE4.hmm	1.50E-28	7	125	0.907692308
jgi|Golci1|1760284|e_gw1.4.153.1	GH18.hmm	2.70E-76	3	287	0.959459459
jgi|Golci1|1760327|e_gw1.4.182.1	CE10.hmm	1.20E-24	95	233	0.404692082
jgi|Golci1|1760398|e_gw1.5.116.1	GT33.hmm	2.80E-110	4	333	0.774117647
jgi|Golci1|1760455|e_gw1.6.138.1	GH128.hmm	3.10E-69	4	224	0.982142857
jgi|Golci1|1761429|e_gw1.17.42.1	CE10.hmm	1.20E-29	73	187	0.33431085
jgi|Golci1|1761486|e_gw1.18.47.1	GH76.hmm	3.50E-77	10	345	0.93575419
jgi|Golci1|1762449|e_gw1.34.17.1	GT1.hmm	5.10E-55	85	368	0.740837696
jgi|Golci1|1762571|e_gw1.37.77.1	GT4.hmm	1.80E-34	11	146	0.84375

Query	Subject	E-value	Start	End	Covered Fraction
jgi|Golci1|1762877|e_gw1.42.81.1	GH16.hmm	2.40E-39	4	189	0.978835979
jgi|Golci1|1762967|e_gw1.43.33.1	GH16.hmm	9.80E-22	6	188	0.962962963
jgi|Golci1|1763023|e_gw1.44.13.1	AA1_3.hmm	5.90E-126	3	303	0.961538462
jgi|Golci1|1763179|e_gw1.48.39.1	CE16.hmm	3.20E-18	168	266	0.367041199
jgi|Golci1|1763354|e_gw1.52.82.1	GT15.hmm	5.00E-125	1	272	0.992673993
jgi|Golci1|1763433|e_gw1.54.19.1	GT20.hmm	2.70E-148	46	473	0.898947368
jgi|Golci1|1764298|e_gw1.74.32.1	GH17.hmm	2.20E-12	17	300	0.909967846
jgi|Golci1|1764490|e_gw1.79.78.1	CE5.hmm	3.80E-38	2	189	0.989417989
jgi|Golci1|1765261|e_gw1.100.37.1	GT2.hmm	1.40E-06	2	166	0.976190476
jgi|Golci1|1765278|e_gw1.101.2.1	GT1.hmm	3.70E-50	5	379	0.979057592
jgi|Golci1|1766162|e_gw1.124.64.1	AA9.hmm	1.50E-55	6	218	0.963636364
jgi|Golci1|1767100|e_gw1.161.9.1	GT59.hmm	1.70E-117	2	404	0.995049505
jgi|Golci1|1767392|e_gw1.175.9.1	GT34.hmm	5.10E-69	4	240	0.959349593
jgi|Golci1|1767728|e_gw1.190.6.1	GH47.hmm	2.40E-128	1	446	0.997757848
jgi|Golci1|1767966|e_gw1.205.18.1	CBM18.hmm	1.20E-07	2	35	0.868421053
jgi|Golci1|1767966|e_gw1.205.18.1	CE4.hmm	1.90E-29	8	125	0.9
jgi|Golci1|1768064|e_gw1.211.23.1	AA2.hmm	2.20E-62	4	254	0.980392157
jgi|Golci1|1768328|e_gw1.234.14.1	GT90.hmm	2.70E-85	3	248	0.98
jgi|Golci1|1768899|e_gw1.279.23.1	GT3.hmm	1.40E-304	1	637	0.998430141
jgi|Golci1|1769015|e_gw1.287.6.1	GH18.hmm	9.40E-59	3	283	0.945945946
jgi|Golci1|1769712|e_gw1.360.13.1	GH135.hmm	9.20E-76	1	235	0.987341772
jgi|Golci1|1769932|e_gw1.393.6.1	GT57.hmm	9.50E-171	3	479	0.98960499
jgi|Golci1|1769998|e_gw1.402.2.1	GT66.hmm	2.80E-191	8	597	0.84992785
jgi|Golci1|1770174|e_gw1.442.5.1	GH76.hmm	7.80E-111	10	349	0.946927374
jgi|Golci1|1770329|e_gw1.582.1.1	CE10.hmm	3.10E-08	83	207	0.363636364
jgi|Golci1|1781386|estExt_Genewise1Plus.C_120029	GH47.hmm	5.00E-165	1	446	0.997757848
jgi|Golci1|1794160|fgenesh1_pg.1_#_6	GT20.hmm	9.20E-159	32	475	0.932631579
jgi|Golci1|1794178|fgenesh1_pg.1_#_24	GT2.hmm	6.90E-40	1	167	0.988095238
jgi|Golci1|1794229|fgenesh1_pg.1_#_75	GT28.hmm	8.40E-14	29	126	0.617834395
jgi|Golci1|1794556|fgenesh1_pg.5_#_31	GH76.hmm	5.20E-101	9	344	0.93575419
jgi|Golci1|1794745|fgenesh1_pg.8_#_42	CE10.hmm	4.80E-29	66	214	0.434017595

Query	Subject	E-value	Start	End	Covered Fraction
jgi|Golci1|1794866|fgenesh1_pg.11_#_40	GH17.hmm	2.20E-14	46	311	0.852090032
jgi|Golci1|1795776|fgenesh1_pg.38_#_9	GH132.hmm	3.70E-93	11	300	0.95379538
jgi|Golci1|1797621|fgenesh1_pg.127_#_7	AA1_2.hmm	1.50E-152	2	338	0.988235294
jgi|Golci1|1797886|fgenesh1_pg.146_#_6	GH47.hmm	8.50E-140	1	444	0.993273543
jgi|Golci1|1798214|fgenesh1_pg.173_#_6	GH37.hmm	5.70E-148	5	490	0.987780041
jgi|Golci1|1798681|fgenesh1_pg.219_#_7	GT8.hmm	1.40E-39	29	255	0.879377432
jgi|Golci1|1798722|fgenesh1_pg.223_#_1	CE10.hmm	2.50E-46	76	335	0.759530792
jgi|Golci1|1798871|fgenesh1_pg.246_#_3	GH93.hmm	5.80E-64	2	272	0.879478827
jgi|Golci1|1799266|fgenesh1_pg.311_#_2	GT8.hmm	8.10E-44	30	254	0.871595331
jgi|Golci1|1799287|fgenesh1_pg.314_#_5	GT41.hmm	7.40E-50	299	518	0.310638298
jgi|Golci1|1805202|estExt_Genemark4.C_1150049	GT24.hmm	2.10E-133	1	248	0.995967742
jgi|Golci1|181019|CE181018_5253	GT62.hmm	8.80E-91	10	267	0.958955224
jgi|Golci1|1811175|fgenesh1_kg.3_#_429_#_TRINITY_DN3536_c0_g2_i1	AA2.hmm	8.20E-62	4	253	0.976470588
jgi|Golci1|1811289|fgenesh1_kg.3_#_543_#_TRINITY_DN10319_c0_g2_i1	GT39.hmm	2.20E-71	2	223	0.99103139
jgi|Golci1|1813310|fgenesh1_kg.7_#_462_#_TRINITY_DN14907_c0_g2_i1	GT76.hmm	3.30E-102	4	407	0.99017199
jgi|Golci1|1815943|fgenesh1_kg.15_#_215_#_TRINITY_DN16758_c0_g1_i2	GT22.hmm	2.70E-80	9	355	0.889460154
jgi|Golci1|1816934|fgenesh1_kg.19_#_79_#_TRINITY_DN18193_c0_g1_i2	GH31.hmm	4.50E-155	2	427	0.995316159
jgi|Golci1|1817510|fgenesh1_kg.21_#_90_#_TRINITY_DN14607_c0_g2_i4	AA7.hmm	1.50E-24	7	196	0.412663755
jgi|Golci1|1818350|fgenesh1_kg.24_#_57_#_TRINITY_DN11489_c0_g4_i1	GT2.hmm	5.50E-10	79	161	0.488095238
jgi|Golci1|1819894|fgenesh1_kg.30_#_193_#_TRINITY_DN15308_c0_g1_i4	GT32.hmm	2.40E-10	43	87	0.488888889
jgi|Golci1|1820130|fgenesh1_kg.31_#_75_#_TRINITY_DN5959_c0_g1_i3	GH17.hmm	4.00E-33	11	306	0.948553055
jgi|Golci1|1821185|fgenesh1_kg.36_#_14_#_TRINITY_DN18898_c11_g1_i6	GH5_9.hmm	7.20E-107	19	306	0.937908497
jgi|Golci1|1822313|fgenesh1_kg.41_#_63_#_TRINITY_DN1973_c0_g1_i1	GH18.hmm	2.30E-78	2	288	0.966216216
jgi|Golci1|1822673|fgenesh1_kg.42_#_243_#_TRINITY_DN2015_c0_g1_i1	GH3.hmm	5.30E-61	6	216	0.972222222
jgi|Golci1|1824198|fgenesh1_kg.51_#_3_#_TRINITY_DN933_c0_g1_i2	GH72.hmm	1.40E-133	3	312	0.990384615
jgi|Golci1|1824198|fgenesh1_kg.51_#_3_#_TRINITY_DN933_c0_g1_i2	CBM43.hmm	3.80E-19	1	82	0.975903614
jgi|Golci1|1825586|fgenesh1_kg.59_#_2_#_TRINITY_DN13388_c0_g2_i1	GT90.hmm	3.70E-73	3	248	0.98
jgi|Golci1|1826268|fgenesh1_kg.62_#_159_#_TRINITY_DN19881_c3_g1_i4	GH63.hmm	8.30E-29	318	565	0.433333333
jgi|Golci1|1826595|fgenesh1_kg.63_#_304_#_TRINITY_DN14780_c0_g1_i2	GH5_12.hmm	3.60E-158	2	357	0.65498155
jgi|Golci1|1827147|fgenesh1_kg.67_#_92_#_TRINITY_DN12656_c0_g2_i1	CBM18.hmm	0.0008	20	38	0.473684211
jgi|Golci1|1827147|fgenesh1_kg.67_#_92_#_TRINITY_DN12656_c0_g2_i1	AA5_1.hmm	3.00E-154	9	536	0.936056838

Query	Subject	E-value	Start	End	Covered Fraction
jgi|Golci1|1827442|fgenesh1_kg.69_#_134_#_TRINITY_DN13155_c0_g2_i2	AA5_1.hmm	1.20E-167	5	536	0.943161634
jgi|Golci1|1829882|fgenesh1_kg.84_#_31_#_TRINITY_DN339_c0_g1_i1	CBM18.hmm	8.00E-05	6	35	0.763157895
jgi|Golci1|1829882|fgenesh1_kg.84_#_31_#_TRINITY_DN339_c0_g1_i1	GH16.hmm	1.70E-24	12	185	0.915343915
jgi|Golci1|1832279|fgenesh1_kg.102_#_111_#_TRINITY_DN9069_c1_g2_i1	GT32.hmm	4.60E-08	5	76	0.788888889
jgi|Golci1|1835666|fgenesh1_kg.126_#_50_#_TRINITY_DN8437_c0_g1_i3	AA7.hmm	2.80E-75	5	454	0.980349345
jgi|Golci1|1836205|fgenesh1_kg.132_#_9_#_TRINITY_DN9378_c0_g1_i2	GT22.hmm	1.90E-91	1	389	0.997429306
jgi|Golci1|1839035|fgenesh1_kg.154_#_101_#_TRINITY_DN919_c0_g1_i1	GH20.hmm	3.00E-75	7	318	0.922848665
jgi|Golci1|1842347|fgenesh1_kg.192_#_11_#_TRINITY_DN21136_c82_g11_i1	GH78.hmm	7.60E-83	8	502	0.98015873
jgi|Golci1|1844832|fgenesh1_kg.230_#_5_#_TRINITY_DN17603_c0_g2_i5	GH92.hmm	2.00E-135	5	490	0.987780041
jgi|Golci1|1844856|fgenesh1_kg.230_#_29_#_TRINITY_DN10245_c0_g1_i4	CE10.hmm	1.90E-10	83	251	0.492668622
jgi|Golci1|1845199|fgenesh1_kg.237_#_14_#_TRINITY_DN10122_c0_g1_i1	GH38.hmm	2.50E-52	86	256	0.63197026
jgi|Golci1|1846121|fgenesh1_kg.254_#_2_#_TRINITY_DN19652_c2_g1_i1	GH16.hmm	1.50E-20	13	176	0.862433862
jgi|Golci1|1848633|fgenesh1_kg.308_#_17_#_TRINITY_DN21136_c82_g11_i1	GH78.hmm	2.40E-78	8	502	0.98015873
jgi|Golci1|1849646|fgenesh1_kg.334_#_53_#_TRINITY_DN15468_c0_g1_i13	CE1.hmm	2.10E-16	3	140	0.603524229
jgi|Golci1|1850265|fgenesh1_kg.350_#_34_#_TRINITY_DN5190_c1_g1_i1	CE16.hmm	5.20E-25	103	266	0.610486891
jgi|Golci1|1850537|fgenesh1_kg.359_#_3_#_TRINITY_DN5190_c1_g1_i1	CE16.hmm	2.20E-46	1	266	0.992509363
jgi|Golci1|1851993|fgenesh1_kg.398_#_30_#_TRINITY_DN18423_c0_g2_i2	GT35.hmm	1.20E-276	2	674	0.997032641
jgi|Golci1|1853806|fgenesh1_kg.628_#_3_#_TRINITY_DN5190_c1_g1_i1	CE16.hmm	2.70E-23	49	226	0.662921348
jgi|Golci1|1854359|fgenesh1_pm.1_#_25	GT31.hmm	2.70E-09	39	178	0.723958333
jgi|Golci1|1854381|fgenesh1_pm.1_#_47	GT62.hmm	2.30E-107	2	267	0.98880597
jgi|Golci1|1854569|fgenesh1_pm.4_#_18	CE14.hmm	8.50E-10	4	124	0.967741935
jgi|Golci1|1854687|fgenesh1_pm.6_#_43	CE1.hmm	2.50E-16	15	213	0.872246696
jgi|Golci1|1854793|fgenesh1_pm.9_#_16	GT62.hmm	2.70E-121	4	268	0.985074627
jgi|Golci1|1854834|fgenesh1_pm.10_#_21	CE1.hmm	1.10E-47	3	224	0.973568282
jgi|Golci1|1855028|fgenesh1_pm.16_#_28	GH13_40.hmm	1.20E-167	2	359	0.991666667
jgi|Golci1|1855058|fgenesh1_pm.18_#_3	GT4.hmm	6.00E-26	5	150	0.90625
jgi|Golci1|1855060|fgenesh1_pm.18_#_5	GT31.hmm	4.40E-06	75	163	0.458333333
jgi|Golci1|1855148|fgenesh1_pm.21_#_26	CBM21.hmm	1.20E-22	3	107	0.971962617
jgi|Golci1|1855219|fgenesh1_pm.24_#_13	GT2.hmm	9.10E-14	79	167	0.523809524
jgi|Golci1|1855338|fgenesh1_pm.29_#_5	GH125.hmm	3.50E-159	1	401	0.995024876
jgi|Golci1|1855479|fgenesh1_pm.35_#_6	GT4.hmm	5.40E-14	5	150	0.90625

Query	Subject	E-value	Start	End	Covered Fraction
jgi|Golci1|1855532|fgenesh1_pm.37_#_23	CE10.hmm	3.90E-39	69	187	0.346041056
jgi|Golci1|1855764|fgenesh1_pm.49_#_5	GT22.hmm	3.30E-99	3	388	0.989717224
jgi|Golci1|1855907|fgenesh1_pm.57_#_4	CE1.hmm	2.90E-06	82	207	0.550660793
jgi|Golci1|1856049|fgenesh1_pm.66_#_6	GT39.hmm	6.90E-73	2	223	0.99103139
jgi|Golci1|1856080|fgenesh1_pm.68_#_11	GH18.hmm	1.30E-58	3	287	0.959459459
jgi|Golci1|1856159|fgenesh1_pm.72_#_8	CE10.hmm	3.90E-24	69	190	0.35483871
jgi|Golci1|1856363|fgenesh1_pm.86_#_1	GH16.hmm	2.00E-22	11	176	0.873015873
jgi|Golci1|1856403|fgenesh1_pm.88_#_7	GH16.hmm	5.00E-30	10	176	0.878306878
jgi|Golci1|1856522|fgenesh1_pm.96_#_9	GH76.hmm	2.00E-56	69	332	0.734636872
jgi|Golci1|1856709|fgenesh1_pm.111_#_7	GH16.hmm	1.30E-19	4	189	0.978835979
jgi|Golci1|1856797|fgenesh1_pm.117_#_2	GT32.hmm	6.00E-13	40	88	0.533333333
jgi|Golci1|1856799|fgenesh1_pm.117_#_4	GH125.hmm	7.30E-68	1	198	0.490049751
jgi|Golci1|1856799|fgenesh1_pm.117_#_4	GH125.hmm	7.10E-71	230	402	0.427860697
jgi|Golci1|1857025|fgenesh1_pm.135_#_1	CBM47.hmm	0.00084	17	61	0.34375
jgi|Golci1|1857025|fgenesh1_pm.135_#_1	GH74.hmm	6.80E-06	31	110	0.339055794
jgi|Golci1|1857068|fgenesh1_pm.138_#_10	CE1.hmm	8.60E-07	8	140	0.581497797
jgi|Golci1|1857150|fgenesh1_pm.147_#_1	GH13_25.hmm	1.30E-201	3	448	0.993303571
jgi|Golci1|1857324|fgenesh1_pm.167_#_2	GH5_9.hmm	1.20E-87	2	305	0.990196078
jgi|Golci1|1857448|fgenesh1_pm.181_#_2	GT90.hmm	4.50E-70	24	248	0.896
jgi|Golci1|1857526|fgenesh1_pm.187_#_19	GT2.hmm	3.80E-18	1	64	0.375
jgi|Golci1|1857635|fgenesh1_pm.207_#_2	GT2.hmm	2.60E-09	2	166	0.976190476
jgi|Golci1|1857698|fgenesh1_pm.219_#_1	GH72.hmm	1.20E-49	119	311	0.615384615
jgi|Golci1|1857733|fgenesh1_pm.223_#_5	GT4.hmm	1.60E-34	8	150	0.8875
jgi|Golci1|1858004|fgenesh1_pm.281_#_3	GT15.hmm	3.00E-45	1	112	0.406593407
jgi|Golci1|1858004|fgenesh1_pm.281_#_3	GT15.hmm	4.80E-46	160	272	0.41025641
jgi|Golci1|1858287|fgenesh1_pm.359_#_5	GH76.hmm	1.30E-79	14	346	0.927374302
jgi|Golci1|1858294|fgenesh1_pm.360_#_3	GH114.hmm	2.40E-75	1	190	0.994736842
jgi|Golci1|1858564|fgenesh1_pm.559_#_1	GH72.hmm	1.10E-111	3	311	0.987179487
jgi|Golci1|1858619|fgenesh1_pm.702_#_1	GH92.hmm	9.70E-85	111	484	0.759674134
jgi|Golci1|1858924|estExt_fgenesh1_pm.C_60001	GT34.hmm	9.80E-71	54	245	0.776422764
jgi|Golci1|1859143|estExt_fgenesh1_pm.C_120001	GH13_40.hmm	1.40E-150	2	360	0.994444444

Query	Subject	E-value	Start	End	Covered Fraction
jgi|Golci1|1859261|estExt_fgenesh1_pm.C_160008	CE4.hmm	2.70E-20	6	124	0.907692308
jgi|Golci1|1860561|estExt_fgenesh1_pm.C_890006	GH92.hmm	2.40E-137	21	491	0.957230143
jgi|Golci1|1861986|estExt_fgenesh1_pm.C_2780001	GH15.hmm	3.50E-64	19	359	0.941828255
jgi|Golci1|1861986|estExt_fgenesh1_pm.C_2780001	CBM20.hmm	1.40E-24	1	88	0.966666667
jgi|Golci1|1862138|estExt_fgenesh1_pm.C_3170006	GT2.hmm	5.60E-23	2	79	0.458333333
jgi|Golci1|1864160|estExt_fgenesh1_pg.C_420043	GH92.hmm	5.20E-143	4	490	0.989816701
jgi|Golci1|1865285|estExt_fgenesh1_pg.C_1020007	GH18.hmm	4.80E-70	4	282	0.939189189
jgi|Golci1|1869437|MIX1677_1140_56	GT50.hmm	1.30E-94	1	261	0.992366412
jgi|Golci1|1873049|MIX5289_26051_51	CBM18.hmm	1.80E-06	9	36	0.710526316
jgi|Golci1|1873049|MIX5289_26051_51	CE4.hmm	1.80E-28	7	124	0.9
jgi|Golci1|1877178|MIX9418_7721_50	GT2.hmm	3.50E-15	79	164	0.505952381
jgi|Golci1|1880589|MIX12829_1811_23	CBM48.hmm	6.60E-09	2	45	0.565789474
jgi|Golci1|1880589|MIX12829_1811_23	GH13_8.hmm	3.90E-121	1	274	0.996350365
jgi|Golci1|1904573|MIX36813_7819_31	GT39.hmm	2.30E-70	2	222	0.986547085
jgi|Golci1|1905805|MIX38045_3490_60	AA3.hmm	6.70E-84	85	406	0.519417476
jgi|Golci1|1906721|MIX38961_428_77	GH18.hmm	2.00E-20	4	199	0.658783784
jgi|Golci1|1913054|MIX45294_5342_26	GH13_40.hmm	5.30E-171	2	360	0.994444444
jgi|Golci1|1917463|MIX49703_7875_17	GT48.hmm	5.10E-299	1	733	0.99052774
jgi|Golci1|284980|CE284979_111987	GH55.hmm	2.20E-298	6	739	0.990540541
jgi|Golci1|365755|CE365754_2291	GH131.hmm	1.50E-59	55	249	0.760784314
jgi|Golci1|536469|CE536468_553796	AA11.hmm	1.90E-71	1	187	0.97382199
jgi|Golci1|536469|CE536468_553796	CBM19.hmm	0.00075	6	44	0.844444444
jgi|Golci1|665770|CE665769_22024	CE1.hmm	9.60E-12	10	207	0.86784141
jgi|Golci1|667293|CE667292_849	PL1_10.hmm	4.70E-97	2	176	0.983050847
jgi|Golci1|686639|CE686638_4676	CE5.hmm	1.00E-41	1	188	0.989417989
jgi|Golci1|721307|CE721306_3713	GT90.hmm	1.30E-75	3	248	0.98
jgi|Golci1|752876|CE752875_583	AA7.hmm	3.50E-70	7	185	0.388646288
jgi|Golci1|754101|CE754100_78741	GH16.hmm	1.40E-16	21	176	0.82010582
jgi|Golci1|775241|CE775240_4841	GT22.hmm	2.10E-77	1	386	0.989717224
jgi|Golci1|825014|CE825013_5171	GT21.hmm	1.40E-87	1	233	0.995708155

B. *G. orontii* genes encoding predicted CAZY proteins

Query	Subject	E-value	Start	End	Covered Fraction
jgi|Golor2|1091039|CE1047660_15059	GT20.hmm	1.70E-154	56	474	0.88
jgi|Golor2|1093111|CE1049732_12660	GH16.hmm	3.20E-20	50	176	0.666666667
jgi|Golor2|10962|gm4.10962_g	CE10.hmm	3.80E-27	68	219	0.442815249
jgi|Golor2|1193207|CE1149828_6478	GT34.hmm	2.50E-69	3	243	0.975609756
jgi|Golor2|1358472|CE1315093_2729	AA1_3.hmm	4.90E-127	3	302	0.958333333
jgi|Golor2|1451813|CE1408434_39860	CE1.hmm	9.20E-12	24	208	0.810572687
jgi|Golor2|14865|gm4.14865_g	GH132.hmm	1.20E-65	116	300	0.607260726
jgi|Golor2|1526628|CE1483249_7699	GT62.hmm	4.20E-122	4	268	0.985074627
jgi|Golor2|1530710|CE1487331_7941	GT62.hmm	4.40E-122	4	268	0.985074627
jgi|Golor2|1582311|CE1538932_9410	GH92.hmm	4.30E-155	4	490	0.989816701
jgi|Golor2|160610|CE117231_1849	GH5_9.hmm	6.50E-105	2	305	0.990196078
jgi|Golor2|1852443|CE1809064_4746	GT50.hmm	5.40E-94	1	261	0.992366412
jgi|Golor2|1887081|CE1843702_6592	CE10.hmm	1.00E-30	59	207	0.434017595
jgi|Golor2|1948544|CE1905165_9878	GH47.hmm	1.40E-161	1	446	0.997757848
jgi|Golor2|1955492|CE1912113_6247	GT62.hmm	2.70E-92	5	267	0.97761194
jgi|Golor2|1993355|CE1949976_8195	AA3.hmm	3.30E-85	85	407	0.521035599
jgi|Golor2|1998393|CE1955014_31705	CE4.hmm	4.20E-17	6	117	0.853846154
jgi|Golor2|20989|gm4.20989_g	GT2.hmm	5.20E-41	1	168	0.994047619
jgi|Golor2|2115243|CE2071864_9318	GH18.hmm	1.40E-54	3	283	0.945945946
jgi|Golor2|2129325|CE2085946_12937	GH3.hmm	9.80E-48	5	215	0.972222222
jgi|Golor2|2169362|CE2125983_8030	CBM50.hmm	0.00072	1	39	0.95
jgi|Golor2|2211938|CE2168559_198692	AA11.hmm	7.30E-70	1	185	0.963350785
jgi|Golor2|2278186|CE2234807_10508	GH16.hmm	3.70E-29	9	187	0.941798942
jgi|Golor2|2315950|CE2272571_3681	GT58.hmm	1.40E-125	30	364	0.917582418
jgi|Golor2|2363518|CE2320139_7091	CE10.hmm	3.00E-27	64	219	0.454545455
jgi|Golor2|2615216|CE2571837_6282	GH13_40.hmm	1.20E-86	2	158	0.433333333
jgi|Golor2|2681763|CE2638384_27323	CE10.hmm	2.90E-45	76	335	0.759530792
jgi|Golor2|27213|gm4.27213_g	GT32.hmm	8.00E-05	5	65	0.666666667
jgi|Golor2|2735782|CE2692403_28739	CE10.hmm	1.10E-45	76	335	0.759530792

Query	Subject	E-value	Start	End	Covered Fraction
jgi|Golor2|28521|gm4.28521_g	GH47.hmm	8.30E-137	1	444	0.993273543
jgi|Golor2|2922698|CE2879319_13671	GH3.hmm	4.50E-48	5	215	0.972222222
jgi|Golor2|296044|CE252665_7144	CE10.hmm	8.40E-29	44	210	0.486803519
jgi|Golor2|3013|gm4.3013_g	GH18.hmm	2.60E-19	4	203	0.672297297
jgi|Golor2|30362|gm4.30362_g	AA1_2.hmm	4.10E-153	3	338	0.985294118
jgi|Golor2|35849|gm4.35849_g	GH47.hmm	6.60E-140	1	444	0.993273543
jgi|Golor2|39730|gm4.39730_g	AA2.hmm	1.90E-16	21	114	0.364705882
jgi|Golor2|39730|gm4.39730_g	AA2.hmm	2.80E-10	119	250	0.51372549
jgi|Golor2|39730|gm4.39730_g	AA2.hmm	7.50E-15	24	253	0.898039216
jgi|Golor2|39913|gm4.39913_g	GH13_40.hmm	6.40E-99	2	178	0.488888889
jgi|Golor2|4058420|gw1.66.155.1	AA11.hmm	1.40E-67	1	186	0.968586387
jgi|Golor2|4062083|gw1.105.176.1	AA11.hmm	4.80E-67	1	186	0.968586387
jgi|Golor2|4070742|gw1.100.164.1	GH76.hmm	1.30E-55	70	330	0.726256983
jgi|Golor2|4078966|gw1.110.249.1	GT69.hmm	8.80E-70	1	238	0.991631799
jgi|Golor2|4128169|gw1.276.28.1	GH128.hmm	9.00E-69	4	203	0.888392857
jgi|Golor2|4139178|gw1.36.664.1	GT39.hmm	4.20E-30	2	83	0.3632287
jgi|Golor2|4146951|gw1.93.496.1	GH16.hmm	2.20E-21	55	188	0.703703704
jgi|Golor2|4152597|gw1.1.2549.1	GT2.hmm	2.80E-09	2	166	0.976190476
jgi|Golor2|4171857|gw1.114.563.1	GT34.hmm	3.20E-84	3	245	0.983739837
jgi|Golor2|4172183|gw1.10.1464.1	CE1.hmm	3.40E-07	24	197	0.762114537
jgi|Golor2|4212047|gw1.174.325.1	GH93.hmm	1.30E-62	5	272	0.86970684
jgi|Golor2|42264|gm4.42264_g	GH76.hmm	4.90E-55	68	330	0.731843575
jgi|Golor2|4239109|e_gw1.2.601.1	GH128.hmm	0.00095	125	202	0.34375
jgi|Golor2|4241070|e_gw1.3.1542.1	GT20.hmm	6.50E-149	36	473	0.92
jgi|Golor2|4243768|e_gw1.5.662.1	GT4.hmm	1.80E-34	11	146	0.84375
jgi|Golor2|4244787|e_gw1.6.616.1	CBM21.hmm	6.10E-31	3	107	0.971962617
jgi|Golor2|4246892|e_gw1.8.1524.1	GH114.hmm	3.60E-76	1	189	0.989473684
jgi|Golor2|4247080|e_gw1.8.835.1	GH135.hmm	3.10E-75	1	236	0.991561181
jgi|Golor2|4247153|e_gw1.8.555.1	GH135.hmm	6.00E-75	1	236	0.991561181
jgi|Golor2|4247566|e_gw1.8.1974.1	GH114.hmm	3.10E-77	1	190	0.994736842
jgi|Golor2|4248106|e_gw1.9.56.1	GH125.hmm	7.10E-159	1	401	0.995024876

Query	Subject	E-value	Start	End	Covered Fraction
jgi|Golor2|4251885|e_gw1.12.161.1	GH15.hmm	5.10E-73	17	359	0.947368421
jgi|Golor2|4251885|e_gw1.12.161.1	CBM20.hmm	7.00E-24	1	88	0.966666667
jgi|Golor2|4255383|e_gw1.17.157.1	CE5.hmm	1.10E-42	1	188	0.989417989
jgi|Golor2|4255419|e_gw1.17.333.1	GT15.hmm	2.30E-125	1	272	0.992673993
jgi|Golor2|4255595|e_gw1.17.459.1	GT2.hmm	9.90E-14	79	167	0.523809524
jgi|Golor2|4255869|e_gw1.17.488.1	CE5.hmm	9.40E-43	2	189	0.989417989
jgi|Golor2|4257895|e_gw1.20.173.1	GT22.hmm	9.20E-76	1	386	0.989717224
jgi|Golor2|4258819|e_gw1.21.20.1	GT90.hmm	1.50E-73	3	248	0.98
jgi|Golor2|4260419|e_gw1.23.677.1	GH16.hmm	2.10E-24	24	188	0.867724868
jgi|Golor2|4260459|e_gw1.23.667.1	GH17.hmm	2.40E-23	25	311	0.919614148
jgi|Golor2|4261666|e_gw1.25.986.1	GT31.hmm	4.20E-06	75	163	0.458333333
jgi|Golor2|4263535|e_gw1.27.951.1	GT15.hmm	2.60E-125	1	272	0.992673993
jgi|Golor2|4264022|e_gw1.28.1189.1	GH18.hmm	1.30E-79	2	287	0.962837838
jgi|Golor2|4264543|e_gw1.29.423.1	GT21.hmm	1.10E-88	1	233	0.995708155
jgi|Golor2|4264560|e_gw1.29.1266.1	GT57.hmm	1.80E-172	3	479	0.98960499
jgi|Golor2|4264887|e_gw1.29.403.1	GH16.hmm	5.10E-40	5	189	0.973544974
jgi|Golor2|4265621|e_gw1.30.1071.1	GT20.hmm	9.50E-199	10	475	0.978947368
jgi|Golor2|4268365|e_gw1.35.342.1	GH16.hmm	6.10E-21	33	185	0.804232804
jgi|Golor2|4270199|e_gw1.38.863.1	GT2.hmm	2.00E-06	2	166	0.976190476
jgi|Golor2|4270256|e_gw1.38.5.1	CE1.hmm	5.00E-07	24	197	0.762114537
jgi|Golor2|4270499|e_gw1.38.1020.1	GH16.hmm	3.60E-16	21	176	0.82010582
jgi|Golor2|4272105|e_gw1.41.1019.1	GT2.hmm	9.20E-08	54	168	0.678571429
jgi|Golor2|4274344|e_gw1.45.367.1	GT90.hmm	3.80E-85	3	248	0.98
jgi|Golor2|4275660|e_gw1.47.1176.1	GH17.hmm	2.00E-13	46	311	0.852090032
jgi|Golor2|4275886|e_gw1.48.1012.1	CE10.hmm	6.50E-32	58	203	0.425219941
jgi|Golor2|4279732|e_gw1.55.765.1	GT3.hmm	1.70E-304	1	637	0.998430141
jgi|Golor2|4279744|e_gw1.55.664.1	GT15.hmm	5.90E-120	1	272	0.992673993
jgi|Golor2|4279850|e_gw1.55.589.1	CE1.hmm	2.70E-11	24	208	0.810572687
jgi|Golor2|4279948|e_gw1.56.424.1	CE10.hmm	1.20E-07	73	207	0.392961877
jgi|Golor2|4282550|e_gw1.61.800.1	CE1.hmm	1.70E-16	2	143	0.621145374
jgi|Golor2|4282901|e_gw1.61.167.1	AA5_1.hmm	1.90E-167	5	536	0.943161634

Query	Subject	E-value	Start	End	Covered Fraction
jgi|Golor2|4284674|e_gw1.65.649.1	GT4.hmm	1.50E-33	8	150	0.8875
jgi|Golor2|4284710|e_gw1.65.721.1	GH18.hmm	3.90E-75	3	287	0.959459459
jgi|Golor2|4284733|e_gw1.65.420.1	GH132.hmm	1.30E-90	47	300	0.834983498
jgi|Golor2|4288542|e_gw1.73.458.1	GT2.hmm	3.60E-15	79	164	0.505952381
jgi|Golor2|4290009|e_gw1.76.505.1	GT76.hmm	1.40E-100	4	407	0.99017199
jgi|Golor2|4290137|e_gw1.76.667.1	GH76.hmm	1.80E-106	25	349	0.905027933
jgi|Golor2|4290599|e_gw1.77.121.1	GH18.hmm	2.30E-75	3	287	0.959459459
jgi|Golor2|4291736|e_gw1.80.157.1	GT2.hmm	3.60E-15	79	164	0.505952381
jgi|Golor2|4292242|e_gw1.81.634.1	GT90.hmm	8.30E-70	15	248	0.932
jgi|Golor2|4293387|e_gw1.83.714.1	GH63.hmm	9.00E-32	318	565	0.433333333
jgi|Golor2|4295490|e_gw1.88.497.1	GH72.hmm	7.80E-101	84	312	0.730769231
jgi|Golor2|4295490|e_gw1.88.497.1	CBM43.hmm	5.20E-18	1	82	0.975903614
jgi|Golor2|4295841|e_gw1.89.77.1	GT39.hmm	6.50E-72	2	223	0.99103139
jgi|Golor2|4300053|e_gw1.99.750.1	GT15.hmm	7.30E-120	1	272	0.992673993
jgi|Golor2|4300671|e_gw1.101.199.1	CBM18.hmm	0.00014	6	35	0.763157895
jgi|Golor2|4300671|e_gw1.101.199.1	GH16.hmm	1.70E-23	24	185	0.851851852
jgi|Golor2|4302302|e_gw1.105.493.1	GH16.hmm	2.20E-20	12	176	0.867724868
jgi|Golor2|4305152|e_gw1.114.433.1	GH16.hmm	1.10E-22	36	189	0.80952381
jgi|Golor2|4307194|e_gw1.120.185.1	AA1_2.hmm	1.10E-152	3	338	0.985294118
jgi|Golor2|4307277|e_gw1.120.534.1	AA1_3.hmm	1.80E-125	3	302	0.958333333
jgi|Golor2|4308427|e_gw1.124.175.1	GT1.hmm	3.50E-54	86	368	0.738219895
jgi|Golor2|4309024|e_gw1.126.519.1	GT35.hmm	2.70E-276	2	674	0.997032641
jgi|Golor2|4309140|e_gw1.126.176.1	GT90.hmm	2.20E-76	3	248	0.98
jgi|Golor2|4309944|e_gw1.128.82.1	CE10.hmm	6.90E-08	80	207	0.372434018
jgi|Golor2|4310837|e_gw1.131.81.1	GH18.hmm	4.60E-19	4	201	0.665540541
jgi|Golor2|4311515|e_gw1.133.186.1	GH92.hmm	6.10E-157	13	490	0.971486762
jgi|Golor2|4314492|e_gw1.143.489.1	GT31.hmm	9.30E-09	39	178	0.723958333
jgi|Golor2|4315534|e_gw1.146.371.1	GT31.hmm	9.30E-09	39	178	0.723958333
jgi|Golor2|4316015|e_gw1.148.222.1	GH18.hmm	2.90E-55	3	287	0.959459459
jgi|Golor2|4316130|e_gw1.148.163.1	GH16.hmm	5.40E-21	33	185	0.804232804
jgi|Golor2|4317607|e_gw1.154.208.1	GT59.hmm	9.60E-121	2	404	0.995049505

Query	Subject	E-value	Start	End	Covered Fraction
jgi|Golor2|4319089|e_gw1.160.270.1	GH76.hmm	2.10E-106	25	349	0.905027933
jgi|Golor2|4320188|e_gw1.165.228.1	GT32.hmm	6.50E-21	5	89	0.933333333
jgi|Golor2|4326660|e_gw1.200.202.1	GH74.hmm	7.10E-06	30	110	0.343347639
jgi|Golor2|4327055|e_gw1.203.394.1	GT41.hmm	1.40E-49	298	518	0.312056738
jgi|Golor2|4327439|e_gw1.205.37.1	GH63.hmm	5.00E-32	318	565	0.433333333
jgi|Golor2|4327941|e_gw1.209.111.1	CE10.hmm	1.30E-28	66	203	0.401759531
jgi|Golor2|4328832|e_gw1.217.128.1	GT39.hmm	8.00E-72	2	223	0.99103139
jgi|Golor2|4331004|e_gw1.241.64.1	GT28.hmm	2.90E-13	29	123	0.598726115
jgi|Golor2|4340883|estExt_Genewise1.C_25_t10112	GH76.hmm	2.00E-77	6	341	0.93575419
jgi|Golor2|4345719|estExt_Genewise1.C_560268	GH72.hmm	1.40E-128	3	311	0.987179487
jgi|Golor2|4356063|estExt_Genewise1.C_1590195	CE10.hmm	5.40E-34	75	205	0.381231672
jgi|Golor2|4364265|estExt_Genewise1Plus.C_14_t20048	CE1.hmm	9.50E-17	2	142	0.616740088
jgi|Golor2|4365654|estExt_Genewise1Plus.C_20_t20158	CBM48.hmm	3.30E-05	16	69	0.697368421
jgi|Golor2|4366513|estExt_Genewise1Plus.C_24_t20045	CBM18.hmm	0.00014	6	35	0.763157895
jgi|Golor2|4366513|estExt_Genewise1Plus.C_24_t20045	GH16.hmm	8.60E-24	24	185	0.851851852
jgi|Golor2|4372464|estExt_Genewise1Plus.C_640065	GT33.hmm	3.80E-147	4	423	0.985882353
jgi|Golor2|4385556|fgenesh1_pg.1_#_36	CE10.hmm	2.40E-27	74	206	0.387096774
jgi|Golor2|4385597|fgenesh1_pg.1_#_77	GH92.hmm	4.60E-122	2	448	0.908350305
jgi|Golor2|4385702|fgenesh1_pg.1_#_182	GH17.hmm	1.20E-38	1	310	0.993569132
jgi|Golor2|4385853|fgenesh1_pg.2_#_127	CE1.hmm	9.00E-07	80	207	0.559471366
jgi|Golor2|4386558|fgenesh1_pg.7_#_82	AA9.hmm	3.90E-56	7	218	0.959090909
jgi|Golor2|4386660|fgenesh1_pg.8_#_30	CBM50.hmm	0.00073	1	39	0.95
jgi|Golor2|4387034|fgenesh1_pg.11_#_80	GH76.hmm	1.00E-100	11	346	0.93575419
jgi|Golor2|4387038|fgenesh1_pg.11_#_84	CE16.hmm	1.60E-65	1	266	0.992509363
jgi|Golor2|4387041|fgenesh1_pg.11_#_87	GT32.hmm	8.90E-22	3	87	0.933333333
jgi|Golor2|4387049|fgenesh1_pg.11_#_95	CE3.hmm	6.70E-55	1	194	0.994845361
jgi|Golor2|4387243|fgenesh1_pg.13_#_61	GH132.hmm	1.70E-90	34	294	0.858085809
jgi|Golor2|4387333|fgenesh1_pg.14_#_60	AA5_1.hmm	9.50E-169	5	536	0.943161634
jgi|Golor2|4387976|fgenesh1_pg.21_#_56	CBM18.hmm	5.40E-06	8	36	0.736842105
jgi|Golor2|4387976|fgenesh1_pg.21_#_56	CE4.hmm	1.80E-28	7	125	0.907692308
jgi|Golor2|4387978|fgenesh1_pg.21_#_58	CBM18.hmm	1.30E-05	8	36	0.736842105
jgi|Golor2|4387978|fgenesh1_pg.21_#_58	CE4.hmm	1.20E-28	7	126	0.915384615

Query	Subject	E-value	Start	End	Covered Fraction
jgi|Golor2|4388029|fgenesh1_pg.22_#_15	GT90.hmm	1.70E-85	3	248	0.98
jgi|Golor2|4388754|fgenesh1_pg.30_#_81	GT1.hmm	6.90E-42	5	328	0.845549738
jgi|Golor2|4388800|fgenesh1_pg.31_#_28	CBM18.hmm	5.30E-08	1	38	0.973684211
jgi|Golor2|4388800|fgenesh1_pg.31_#_28	AA5_1.hmm	9.10E-165	10	536	0.934280639
jgi|Golor2|4388853|fgenesh1_pg.32_#_20	AA9.hmm	7.00E-52	8	212	0.927272727
jgi|Golor2|4388913|fgenesh1_pg.32_#_80	GT22.hmm	4.10E-82	9	359	0.899742931
jgi|Golor2|4389000|fgenesh1_pg.34_#_13	GT31.hmm	7.50E-07	75	163	0.458333333
jgi|Golor2|4389322|fgenesh1_pg.39_#_25	CE10.hmm	3.10E-37	112	291	0.524926686
jgi|Golor2|4390006|fgenesh1_pg.50_#_45	GT8.hmm	3.20E-45	30	254	0.871595331
jgi|Golor2|4390888|fgenesh1_pg.66_#_19	GH76.hmm	3.50E-94	8	344	0.938547486
jgi|Golor2|4390911|fgenesh1_pg.66_#_42	GH16.hmm	3.10E-20	6	188	0.962962963
jgi|Golor2|4391091|fgenesh1_pg.70_#_6	GH16.hmm	1.00E-22	36	189	0.80952381
jgi|Golor2|4391584|fgenesh1_pg.79_#_16	CBM18.hmm	3.00E-07	2	35	0.868421053
jgi|Golor2|4391584|fgenesh1_pg.79_#_16	CE4.hmm	1.20E-32	8	125	0.9
jgi|Golor2|4391850|fgenesh1_pg.84_#_40	GT41.hmm	2.30E-49	298	518	0.312056738
jgi|Golor2|4392060|fgenesh1_pg.88_#_54	GT48.hmm	1.70E-306	1	733	0.99052774
jgi|Golor2|4392400|fgenesh1_pg.96_#_9	GT8.hmm	2.10E-44	30	254	0.871595331
jgi|Golor2|4392522|fgenesh1_pg.99_#_11	GT3.hmm	4.40E-289	1	637	0.998430141
jgi|Golor2|4392585|fgenesh1_pg.100_#_37	CE10.hmm	2.20E-27	74	208	0.392961877
jgi|Golor2|4393286|fgenesh1_pg.118_#_48	CBM48.hmm	2.30E-09	2	45	0.565789474
jgi|Golor2|4393286|fgenesh1_pg.118_#_48	GH13_8.hmm	2.90E-80	40	274	0.854014599
jgi|Golor2|4393446|fgenesh1_pg.123_#_8	AA2.hmm	2.40E-61	4	254	0.980392157
jgi|Golor2|4393905|fgenesh1_pg.136_#_15	CBM48.hmm	0.00041	16	68	0.684210526
jgi|Golor2|4394479|fgenesh1_pg.155_#_13	GH18.hmm	3.30E-70	4	282	0.939189189
jgi|Golor2|4401484|estExt_Genemark4.C_430212	GH16.hmm	8.30E-29	11	187	0.931216931
jgi|Golor2|4431576|fgenesh1_kg.1_#_21491_#_TRINITY_DN49988_c2_g2_i3	GH5_9.hmm	1.60E-64	111	306	0.637254902
jgi|Golor2|4475262|fgenesh1_kg.4_#_6223_#_TRINITY_DN46330_c0_g1_i2	GT32.hmm	3.90E-10	48	87	0.433333333
jgi|Golor2|4484890|fgenesh1_kg.4_#_15851_#_TRINITY_DN46069_c0_g3_i1	GH78.hmm	4.30E-83	8	502	0.98015873
jgi|Golor2|4491697|fgenesh1_kg.5_#_6181_#_TRINITY_DN51573_c5_g3_i1	AA7.hmm	3.30E-71	3	449	0.973799127
jgi|Golor2|4529082|fgenesh1_kg.8_#_1176_#_TRINITY_DN46911_c0_g1_i1	GH13_40.hmm	3.10E-65	178	360	0.505555556
jgi|Golor2|4533731|fgenesh1_kg.8_#_5825_#_TRINITY_DN48485_c0_g3_i2	GT2.hmm	2.10E-07	2	167	0.982142857
jgi|Golor2|4537882|fgenesh1_kg.8_#_9976_#_TRINITY_DN48485_c0_g3_i2	GT2.hmm	2.10E-07	2	167	0.982142857

Query	Subject	E-value	Start	End	Covered Fraction
jgi|Golor2|4542098|fgenesh1_kg.9_#_1539_#_TRINITY_DN47165_c0_g1_i1	CE10.hmm	3.80E-22	73	199	0.369501466
jgi|Golor2|4553845|fgenesh1_kg.9_#_13286_#_TRINITY_DN50856_c2_g1_i1	GH72.hmm	4.80E-129	3	311	0.987179487
jgi|Golor2|4554353|fgenesh1_kg.9_#_13794_#_TRINITY_DN48458_c0_g2_i4	GT8.hmm	4.00E-40	28	256	0.887159533
jgi|Golor2|4560274|fgenesh1_kg.10_#_4577_#_TRINITY_DN47191_c0_g1_i1	GH13_40.hmm	9.70E-176	2	359	0.991666667
jgi|Golor2|4564664|fgenesh1_kg.10_#_8967_#_TRINITY_DN45357_c0_g1_i1	GH131.hmm	1.20E-61	3	249	0.964705882
jgi|Golor2|4579687|fgenesh1_kg.12_#_3222_#_TRINITY_DN48230_c0_g1_i4	GH5_12.hmm	3.10E-159	2	357	0.65498155
jgi|Golor2|4583217|fgenesh1_kg.12_#_6752_#_TRINITY_DN44574_c0_g2_i4	CE10.hmm	8.40E-27	71	193	0.357771261
jgi|Golor2|4590999|fgenesh1_kg.13_#_2352_#_TRINITY_DN50349_c0_g1_i12	CE1.hmm	1.10E-48	1	224	0.982378855
jgi|Golor2|4600900|fgenesh1_kg.14_#_2522_#_TRINITY_DN50226_c4_g1_i1	GT39.hmm	1.90E-70	2	222	0.986547085
jgi|Golor2|4608843|fgenesh1_kg.15_#_2154_#_TRINITY_DN51573_c5_g3_i1	AA7.hmm	6.00E-74	3	454	0.984716157
jgi|Golor2|4630557|fgenesh1_kg.17_#_4332_#_TRINITY_DN45377_c0_g1_i2	GH125.hmm	2.40E-157	1	402	0.997512438
jgi|Golor2|4642009|fgenesh1_kg.18_#_7517_#_TRINITY_DN47023_c0_g1_i2	GH17.hmm	1.50E-32	12	306	0.945337621
jgi|Golor2|4672607|fgenesh1_kg.22_#_1555_#_TRINITY_DN45850_c0_g1_i2	GH37.hmm	6.70E-146	5	490	0.987780041
jgi|Golor2|4684588|fgenesh1_kg.23_#_4512_#_TRINITY_DN48198_c9_g2_i4	GH47.hmm	5.00E-128	1	446	0.997757848
jgi|Golor2|4703673|fgenesh1_kg.25_#_6820_#_TRINITY_DN47165_c0_g1_i1	CE10.hmm	9.50E-22	73	199	0.369501466
jgi|Golor2|4703955|fgenesh1_kg.25_#_7102_#_TRINITY_DN44574_c0_g2_i4	CE10.hmm	4.50E-26	70	193	0.360703812
jgi|Golor2|4712792|fgenesh1_kg.27_#_364_#_TRINITY_DN48700_c4_g2_i4	CE5.hmm	1.50E-42	2	189	0.989417989
jgi|Golor2|4734347|fgenesh1_kg.29_#_5973_#_TRINITY_DN47917_c0_g1_i1	GH3.hmm	1.10E-60	6	216	0.972222222
jgi|Golor2|4736423|fgenesh1_kg.30_#_204_#_TRINITY_DN48230_c0_g1_i4	GH5_12.hmm	1.40E-231	2	541	0.994464945
jgi|Golor2|4740055|fgenesh1_kg.30_#_3836_#_TRINITY_DN49972_c1_g1_i2	GT24.hmm	5.30E-133	1	248	0.995967742
jgi|Golor2|4797943|fgenesh1_kg.38_#_2497_#_TRINITY_DN45357_c0_g1_i1	GH131.hmm	1.20E-61	3	249	0.964705882
jgi|Golor2|4805005|fgenesh1_kg.39_#_1740_#_TRINITY_DN48236_c3_g1_i2	GT57.hmm	8.10E-89	3	229	0.46985447
jgi|Golor2|4805005|fgenesh1_kg.39_#_1740_#_TRINITY_DN48236_c3_g1_i2	GT57.hmm	2.70E-53	223	480	0.534303534
jgi|Golor2|4844728|fgenesh1_kg.45_#_4312_#_TRINITY_DN45850_c0_g1_i2	GH37.hmm	9.10E-148	5	490	0.987780041
jgi|Golor2|4898271|fgenesh1_kg.54_#_2687_#_TRINITY_DN46911_c0_g1_i1	GH13_40.hmm	3.10E-65	178	360	0.505555556
jgi|Golor2|4902292|fgenesh1_kg.55_#_701_#_TRINITY_DN48398_c6_g4_i2	PL1_10.hmm	2.20E-95	2	176	0.983050847
jgi|Golor2|4910526|fgenesh1_kg.56_#_2736_#_TRINITY_DN48458_c0_g2_i4	GT8.hmm	1.80E-39	28	256	0.887159533
jgi|Golor2|4992673|fgenesh1_kg.70_#_4022_#_TRINITY_DN49390_c4_g3_i1	GT39.hmm	3.20E-64	2	223	0.99103139
jgi|Golor2|4994881|fgenesh1_kg.70_#_6230_#_TRINITY_DN49747_c2_g1_i1	GT66.hmm	1.50E-189	9	597	0.848484848
jgi|Golor2|5015445|fgenesh1_kg.74_#_4009_#_TRINITY_DN46677_c0_g1_i1	GH20.hmm	2.20E-79	7	336	0.976261128
jgi|Golor2|5062682|fgenesh1_kg.84_#_1731_#_TRINITY_DN48868_c0_g1_i2	GH55.hmm	6.40E-215	5	550	0.736486486

Query	Subject	E-value	Start	End	Covered Fraction
jgi|Golor2|5069091|fgenesh1_kg.85_#_3319_#_TRINITY_DN46069_c0_g3_i1	GH78.hmm	3.80E-83	8	502	0.98015873
jgi|Golor2|5069676|fgenesh1_kg.85_#_3904_#_TRINITY_DN46923_c3_g1_i1	GH18.hmm	5.50E-48	4	287	0.956081081
jgi|Golor2|5077703|fgenesh1_kg.87_#_1219_#_TRINITY_DN47878_c1_g1_i3	GH17.hmm	4.70E-12	17	300	0.909967846
jgi|Golor2|5106324|fgenesh1_kg.93_#_1608_#_TRINITY_DN47878_c1_g1_i3	GH17.hmm	1.10E-12	17	300	0.909967846
jgi|Golor2|5132028|fgenesh1_kg.99_#_868_#_TRINITY_DN48398_c6_g4_i2	PL1_10.hmm	2.20E-96	2	176	0.983050847
jgi|Golor2|5166369|fgenesh1_kg.107_#_3218_#_TRINITY_DN49988_c2_g2_i3	GH5_9.hmm	5.30E-118	3	306	0.990196078
jgi|Golor2|5175948|fgenesh1_kg.110_#_2020_#_TRINITY_DN47318_c2_g1_i1	AA7.hmm	9.20E-68	7	188	0.395196507
jgi|Golor2|5191238|fgenesh1_kg.114_#_2972_#_TRINITY_DN49390_c4_g3_i1	GT39.hmm	1.00E-71	2	223	0.99103139
jgi|Golor2|5198561|fgenesh1_kg.116_#_1329_#_TRINITY_DN48868_c0_g1_i2	GH55.hmm	9.40E-286	5	738	0.990540541
jgi|Golor2|5209880|fgenesh1_kg.119_#_1209_#_TRINITY_DN47318_c2_g1_i1	AA7.hmm	1.40E-71	7	187	0.3930131
jgi|Golor2|5224058|fgenesh1_kg.123_#_1136_#_TRINITY_DN48051_c1_g1_i1	CE10.hmm	1.20E-16	69	319	0.73313783
jgi|Golor2|5264189|fgenesh1_kg.134_#_1117_#_TRINITY_DN48626_c1_g1_i1	GH72.hmm	2.70E-134	3	312	0.990384615
jgi|Golor2|5264189|fgenesh1_kg.134_#_1117_#_TRINITY_DN48626_c1_g1_i1	CBM43.hmm	8.50E-18	1	82	0.975903614
jgi|Golor2|5304621|fgenesh1_kg.146_#_3494_#_TRINITY_DN44602_c0_g1_i1	GT2.hmm	6.30E-41	1	168	0.994047619
jgi|Golor2|5341134|fgenesh1_kg.159_#_3022_#_TRINITY_DN48236_c3_g1_i2	GT57.hmm	7.30E-90	3	229	0.46985447
jgi|Golor2|5341134|fgenesh1_kg.159_#_3022_#_TRINITY_DN48236_c3_g1_i2	GT57.hmm	2.30E-30	324	480	0.324324324
jgi|Golor2|5363432|fgenesh1_kg.169_#_1953_#_TRINITY_DN49747_c2_g1_i1	GT66.hmm	9.10E-189	9	597	0.848484848
jgi|Golor2|5392692|fgenesh1_kg.184_#_56_#_TRINITY_DN50338_c11_g1_i7	GH38.hmm	5.30E-66	20	255	0.873605948
jgi|Golor2|5500833|fgenesh1_pm.1_#_15	GT20.hmm	1.50E-147	37	473	0.917894737
jgi|Golor2|5500928|fgenesh1_pm.1_#_110	AA7.hmm	1.30E-15	7	195	0.410480349
jgi|Golor2|5500960|fgenesh1_pm.1_#_142	GH5_9.hmm	1.20E-98	29	306	0.905228758
jgi|Golor2|5501018|fgenesh1_pm.2_#_26	GT1.hmm	2.70E-45	5	379	0.979057592
jgi|Golor2|5501268|fgenesh1_pm.3_#_97	GH18.hmm	1.70E-79	2	287	0.962837838
jgi|Golor2|5501367|fgenesh1_pm.4_#_92	GH13_25.hmm	2.40E-203	3	448	0.993303571
jgi|Golor2|5501516|fgenesh1_pm.6_#_5	AA2.hmm	3.30E-61	4	253	0.976470588
jgi|Golor2|5501665|fgenesh1_pm.7_#_57	GT2.hmm	5.20E-07	2	166	0.976190476
jgi|Golor2|5501741|fgenesh1_pm.8_#_3	GH31.hmm	8.90E-143	7	427	0.983606557
jgi|Golor2|5502115|fgenesh1_pm.12_#_5	GT20.hmm	2.50E-180	10	475	0.978947368
jgi|Golor2|5502541|fgenesh1_pm.16_#_78	CBM18.hmm	2.60E-08	1	38	0.973684211
jgi|Golor2|5502541|fgenesh1_pm.16_#_78	AA5_1.hmm	1.00E-165	10	536	0.934280639
jgi|Golor2|5502738|fgenesh1_pm.19_#_28	GT22.hmm	1.30E-41	14	173	0.40874036

Query	Subject	E-value	Start	End	Covered Fraction
jgi|Golor2|5502738|fgenesh1_pm.19_#_28	GT22.hmm	1.40E-20	223	388	0.424164524
jgi|Golor2|5503123|fgenesh1_pm.24_#_57	CE1.hmm	1.00E-06	10	141	0.577092511
jgi|Golor2|5503143|fgenesh1_pm.25_#_3	GT4.hmm	6.70E-26	4	154	0.9375
jgi|Golor2|5503441|fgenesh1_pm.29_#_55	GT2.hmm	2.00E-07	79	168	0.529761905
jgi|Golor2|5503583|fgenesh1_pm.31_#_41	GT2.hmm	2.40E-38	1	122	0.720238095
jgi|Golor2|5503625|fgenesh1_pm.32_#_32	GT2.hmm	1.30E-06	2	166	0.976190476
jgi|Golor2|5503805|fgenesh1_pm.35_#_32	CE4.hmm	2.30E-26	6	129	0.946153846
jgi|Golor2|5504071|fgenesh1_pm.41_#_1	GH92.hmm	7.60E-153	4	484	0.977596741
jgi|Golor2|5504076|fgenesh1_pm.41_#_6	GH16.hmm	7.80E-40	5	189	0.973544974
jgi|Golor2|5504133|fgenesh1_pm.42_#_3	GH18.hmm	4.00E-32	33	283	0.844594595
jgi|Golor2|5504348|fgenesh1_pm.46_#_22	GT15.hmm	1.60E-91	1	272	0.992673993
jgi|Golor2|5504671|fgenesh1_pm.53_#_13	AA1_3.hmm	5.10E-127	3	299	0.948717949
jgi|Golor2|5504688|fgenesh1_pm.53_#_30	CE1.hmm	6.10E-12	21	213	0.845814978
jgi|Golor2|5504726|fgenesh1_pm.54_#_18	GH31.hmm	3.70E-122	2	403	0.93911007
jgi|Golor2|5505018|fgenesh1_pm.60_#_2	AA3.hmm	3.10E-48	85	407	0.521035599
jgi|Golor2|5505137|fgenesh1_pm.62_#_13	GT22.hmm	1.30E-75	1	386	0.989717224
jgi|Golor2|5505365|fgenesh1_pm.67_#_10	GH81.hmm	4.00E-219	9	621	0.98392283
jgi|Golor2|5505494|fgenesh1_pm.70_#_5	GT34.hmm	1.30E-76	3	245	0.983739837
jgi|Golor2|5505766|fgenesh1_pm.76_#_14	GH81.hmm	5.00E-212	9	621	0.98392283
jgi|Golor2|5505787|fgenesh1_pm.76_#_35	GH16.hmm	5.40E-19	4	189	0.978835979
jgi|Golor2|5505818|fgenesh1_pm.77_#_19	GT4.hmm	5.50E-35	8	150	0.8875
jgi|Golor2|5507239|fgenesh1_pm.117_#_2	CE14.hmm	6.80E-09	4	124	0.967741935
jgi|Golor2|5507366|fgenesh1_pm.121_#_14	AA1_3.hmm	3.00E-112	3	299	0.948717949
jgi|Golor2|5507406|fgenesh1_pm.123_#_1	GH38.hmm	9.80E-88	2	255	0.940520446
jgi|Golor2|5507483|fgenesh1_pm.125_#_8	CE10.hmm	1.60E-37	73	187	0.33431085
jgi|Golor2|5507519|fgenesh1_pm.126_#_14	GT22.hmm	3.60E-93	10	389	0.974293059
jgi|Golor2|5507560|fgenesh1_pm.127_#_17	GH15.hmm	2.40E-73	17	359	0.947368421
jgi|Golor2|5507560|fgenesh1_pm.127_#_17	CBM20.hmm	5.80E-24	1	89	0.977777778
jgi|Golor2|5507570|fgenesh1_pm.128_#_6	GH16.hmm	4.80E-19	4	189	0.978835979
jgi|Golor2|5507711|fgenesh1_pm.133_#_11	AA4.hmm	3.90E-17	21	191	0.325670498
jgi|Golor2|5507719|fgenesh1_pm.133_#_19	CE10.hmm	1.50E-11	73	251	0.521994135

Query	Subject	E-value	Start	End	Covered Fraction
jgi|Golor2|5507738|fgenesh1_pm.134_#_8	GT48.hmm	9.50E-73	7	237	0.311231394
jgi|Golor2|5507738|fgenesh1_pm.134_#_8	GT48.hmm	6.00E-148	334	733	0.539918809
jgi|Golor2|5507843|fgenesh1_pm.138_#_2	CE4.hmm	4.70E-17	6	117	0.853846154
jgi|Golor2|5508073|fgenesh1_pm.148_#_6	CE4.hmm	2.30E-26	6	129	0.946153846
jgi|Golor2|5508169|fgenesh1_pm.151_#_16	GT34.hmm	4.40E-69	4	243	0.971544715
jgi|Golor2|550851|CE507472_13440	CE1.hmm	6.40E-07	82	207	0.550660793
jgi|Golor2|5530833|MIX21209_5749_83	GT59.hmm	9.60E-121	2	404	0.995049505
jgi|Golor2|5541818|MIX32194_716_23	GT1.hmm	1.30E-47	85	368	0.740837696
jgi|Golor2|5549432|MIX39808_49710_55	CBM18.hmm	3.00E-07	2	35	0.868421053
jgi|Golor2|5549432|MIX39808_49710_55	CE4.hmm	5.30E-32	8	125	0.9
jgi|Golor2|5602867|MIX93243_3503_12	GT2.hmm	4.40E-15	79	163	0.5
jgi|Golor2|5656176|MIX146552_1573_95	GH5_9.hmm	6.90E-105	2	305	0.990196078
jgi|Golor2|5700542|MIX190918_10037_82	CE10.hmm	5.40E-34	75	205	0.381231672
jgi|Golor2|5733047|MIX223423_48_19	GT4.hmm	1.30E-13	5	149	0.9
jgi|Golor2|5794841|MIX285217_7205_90	GT22.hmm	5.40E-77	9	331	0.827763496
jgi|Golor2|5803743|MIX294119_4946_53	GT62.hmm	7.90E-98	2	267	0.98880597
jgi|Golor2|5824163|estExt_fgenesh1_pg.C_2390001	GT28.hmm	3.80E-06	29	124	0.605095541
jgi|Golor2|5824436|estExt_fgenesh1_pm.C_10038	CE10.hmm	5.80E-28	69	200	0.384164223
jgi|Golor2|5825927|estExt_fgenesh1_pm.C_160032	GT39.hmm	5.00E-70	2	222	0.986547085
jgi|Golor2|5826397|estExt_fgenesh1_pm.C_230014	GT4.hmm	8.70E-14	5	150	0.90625
jgi|Golor2|5827217|estExt_fgenesh1_pm.C_370032	GH93.hmm	1.00E-54	2	272	0.879478827
jgi|Golor2|5831497|estExt_fgenesh1_pm.C_1710008	CE10.hmm	3.30E-28	70	200	0.381231672
jgi|Golor2|6697|gm4.6697_g	GH18.hmm	2.70E-20	4	205	0.679054054
jgi|Golor2|670729|CE627350_17877	GT20.hmm	3.20E-159	33	474	0.928421053
jgi|Golor2|697252|CE653873_12337	CE16.hmm	1.20E-66	1	266	0.992509363
jgi|Golor2|782315|CE738936_11633	GT32.hmm	1.70E-06	3	75	0.8
jgi|Golor2|829220|CE785841_6391	GT2.hmm	2.00E-38	1	123	0.726190476

C. *B. graminis f. sp. hordei* genes encoding predicted CAZY proteins

Query	Subject	E-value	Start	End	Covered Fraction
jgi|Blugr1|19164|BGHDH14_bghG009379000001001	CBM21.hmm	0.00017	14	51	0.345794393
jgi|Blugr1|19175|BGHDH14_bgh00800	GT2.hmm	2.90E-31	25	168	0.851190476
jgi|Blugr1|19213|BGHDH14_bghG008100000001001	GT2.hmm	4.00E-36	1	168	0.994047619
jgi|Blugr1|19223|BGHDH14_bgh06427	CE12.hmm	9.40E-15	2	202	0.952380952
jgi|Blugr1|19244|BGHDH14_bgh05865	GT69.hmm	4.60E-67	1	238	0.991631799
jgi|Blugr1|19307|BGHDH14_bgh02627	CE10.hmm	6.50E-08	93	206	0.331378299
jgi|Blugr1|19326|BGHDH14_bgh05559	GT24.hmm	2.30E-132	1	248	0.995967742
jgi|Blugr1|19377|BGHDH14_bgh00180	CE10.hmm	3.40E-09	78	218	0.410557185
jgi|Blugr1|19387|BGHDH14_bgh02286	AA11.hmm	9.60E-71	1	186	0.968586387
jgi|Blugr1|19401|BGHDH14_bgh01040	GH132.hmm	1.70E-88	17	300	0.933993399
jgi|Blugr1|19412|BGHDH14_bgh00737	GH18.hmm	8.00E-19	4	211	0.699324324
jgi|Blugr1|19467|BGHDH14_bgh00576	GT4.hmm	1.00E-39	10	151	0.88125
jgi|Blugr1|19519|BGHDH14_bgh00447	CE1.hmm	1.60E-07	82	207	0.550660793
jgi|Blugr1|19616|BGHDH14_bgh00772	GH55.hmm	1.50E-301	8	739	0.987837838
jgi|Blugr1|19635|BGHDH14_bgh04852	GT41.hmm	1.50E-48	305	519	0.303546099
jgi|Blugr1|19709|BGHDH14_bgh00219	GH17.hmm	2.10E-11	156	311	0.498392283
jgi|Blugr1|19714|BGHDH14_bgh06298	GH17.hmm	3.00E-11	202	311	0.350482315
jgi|Blugr1|19721|BGHDH14_bgh00731	GH16.hmm	4.00E-24	53	185	0.698412698
jgi|Blugr1|19728|BGHDH14_bgh05070	GH17.hmm	2.10E-12	27	311	0.91318328
jgi|Blugr1|19737|BGHDH14_bgh05662	CE1.hmm	2.40E-09	13	208	0.859030837
jgi|Blugr1|19803|BGHDH14_bgh00726	GH16.hmm	2.20E-22	38	188	0.793650794
jgi|Blugr1|19804|BGHDH14_bgh00678	GH3.hmm	3.10E-48	5	215	0.972222222
jgi|Blugr1|19873|BGHDH14_bgh01145	GT32.hmm	1.20E-15	6	87	0.9
jgi|Blugr1|19878|BGHDH14_bgh00783	GH76.hmm	7.00E-113	10	346	0.938547486
jgi|Blugr1|19883|BGHDH14_bgh05093	CE16.hmm	1.10E-63	1	266	0.992509363
jgi|Blugr1|19899|BGHDH14_bgh00590	GT59.hmm	2.50E-51	2	188	0.46039604
jgi|Blugr1|19923|BGHDH14_bgh00755	CE1.hmm	5.40E-18	2	143	0.621145374
jgi|Blugr1|19940|BGHDH14_bgh06477	GT39.hmm	1.50E-69	2	223	0.99103139
jgi|Blugr1|19969|BGHDH14_bgh04733	GH128.hmm	1.50E-62	4	224	0.982142857
jgi|Blugr1|19983|BGHDH14_bgh00311	AA5_1.hmm	2.20E-171	8	536	0.937833037
jgi|Blugr1|20095|BGHDH14_bgh02555	GT50.hmm	1.20E-92	1	261	0.992366412
jgi|Blugr1|20266|BGHDH14_bgh00674	AA1_2.hmm	2.40E-154	3	339	0.988235294
jgi|Blugr1|20289|BGHDH14_bghG005334000001001	CBM6.hmm	0.00084	8	61	0.384057971
jgi|Blugr1|20299|BGHDH14_bgh05717	CBM21.hmm	1.90E-32	3	107	0.971962617
jgi|Blugr1|20315|BGHDH14_bgh01441	GH16.hmm	1.00E-22	24	176	0.804232804

Query	Subject	E-value	Start	End	Covered Fraction
jgi|Blugr1|20316|BGHDH14_bgh00719	GH16.hmm	2.20E-31	18	176	0.835978836
jgi|Blugr1|20355|BGHDH14_bgh05777	AA2.hmm	1.20E-15	14	114	0.392156863
jgi|Blugr1|20355|BGHDH14_bgh05777	AA2.hmm	5.40E-13	20	253	0.91372549
jgi|Blugr1|20437|BGHDH14_bghG005727000001001	GT1.hmm	1.40E-53	94	369	0.719895288
jgi|Blugr1|20557|BGHDH14_bgh00762	GH47.hmm	5.20E-158	2	446	0.995515695
jgi|Blugr1|20634|BGHDH14_bgh02441	GT8.hmm	5.40E-43	26	256	0.894941634
jgi|Blugr1|20659|BGHDH14_bgh00782	GH76.hmm	6.60E-108	11	346	0.93575419
jgi|Blugr1|20715|BGHDH14_bgh01096	GT34.hmm	4.20E-72	1	243	0.983739837
jgi|Blugr1|20728|BGHDH14_bgh00732	GH16.hmm	6.60E-17	4	189	0.978835979
jgi|Blugr1|20812|BGHDH14_bgh02744	GT48.hmm	0	1	733	0.99052774
jgi|Blugr1|20813|BGHDH14_bgh00774	GH72.hmm	4.00E-135	3	311	0.987179487
jgi|Blugr1|20813|BGHDH14_bgh00774	CBM43.hmm	2.80E-19	1	82	0.975903614
jgi|Blugr1|20829|BGHDH14_bgh02379	AA2.hmm	4.10E-57	6	253	0.968627451
jgi|Blugr1|20931|BGHDH14_bgh00673	AA1_3.hmm	2.40E-135	2	312	0.993589744
jgi|Blugr1|20971|BGHDH14_bgh02672	GT66.hmm	6.80E-191	9	597	0.848484848
jgi|Blugr1|20984|BGHDH14_bgh05834	CE10.hmm	4.70E-18	65	316	0.736070381
jgi|Blugr1|20986|BGHDH14_bgh05832	GT39.hmm	1.60E-72	2	223	0.99103139
jgi|Blugr1|21004|BGHDH14_bgh02251	GT39.hmm	3.90E-73	2	223	0.99103139
jgi|Blugr1|21013|BGHDH14_bgh02743	GT34.hmm	5.80E-89	3	245	0.983739837
jgi|Blugr1|21041|BGHDH14_bgh00667	CE1.hmm	2.10E-41	3	194	0.841409692
jgi|Blugr1|21048|BGHDH14_bgh00995	GT8.hmm	2.50E-42	33	255	0.86381323
jgi|Blugr1|21107|BGHDH14_bghG004252000001001	GT21.hmm	1.30E-90	1	233	0.995708155
jgi|Blugr1|21165|BGHDH14_bgh01243	GT15.hmm	4.80E-121	1	272	0.992673993
jgi|Blugr1|21177|BGHDH14_bgh00229	GT3.hmm	3.10E-305	1	637	0.998430141
jgi|Blugr1|21211|BGHDH14_bghG006215000001001	GH37.hmm	4.90E-150	5	489	0.985743381
jgi|Blugr1|21266|BGHDH14_bgh00634	GH18.hmm	4.40E-79	3	286	0.956081081
jgi|Blugr1|21274|BGHDH14_bgh02654	GH135.hmm	2.10E-77	1	202	0.848101266
jgi|Blugr1|21279|BGHDH14_bgh01639	GH114.hmm	3.30E-73	1	190	0.994736842
jgi|Blugr1|21310|BGHDH14_bgh00442	CBM50.hmm	0.00055	1	39	0.95
jgi|Blugr1|21384|BGHDH14_bgh06024	GT22.hmm	5.70E-94	3	388	0.989717224
jgi|Blugr1|21422|BGHDH14_bgh05042	GH16.hmm	2.40E-20	13	189	0.931216931
jgi|Blugr1|21498|BGHDH14_bgh00764	GH47.hmm	3.20E-161	1	446	0.997757848
jgi|Blugr1|21533|BGHDH14_bgh01996	CE10.hmm	1.90E-14	71	316	0.718475073
jgi|Blugr1|21539|BGHDH14_bgh00659	AA2.hmm	4.80E-62	4	254	0.980392157
jgi|Blugr1|21545|BGHDH14_bgh00758	GH38.hmm	7.60E-87	2	255	0.940520446
jgi|Blugr1|21602|BGHDH14_bgh06022	CBM18.hmm	4.70E-05	5	35	0.789473684
jgi|Blugr1|21602|BGHDH14_bgh06022	CE4.hmm	1.70E-27	7	125	0.907692308
jgi|Blugr1|21602|BGHDH14_bgh06022	CBM18.hmm	4.30E-06	6	36	0.789473684

Query	Subject	E-value	Start	End	Covered Fraction
jgi|Blugr1|21639|BGHDH14_bgh02278	AA5_1.hmm	3.50E-170	5	536	0.943161634
jgi|Blugr1|21670|BGHDH14_bgh00715	GT2.hmm	1.80E-37	1	123	0.726190476
jgi|Blugr1|21747|BGHDH14_bgh00736	GH17.hmm	3.00E-34	12	306	0.945337621
jgi|Blugr1|21765|BGHDH14_bghG004450000001001	GH63.hmm	2.80E-33	319	565	0.431578947
jgi|Blugr1|21808|BGHDH14_bgh00122	GH18.hmm	1.50E-55	3	282	0.942567568
jgi|Blugr1|21813|BGHDH14_bgh00059	GH18.hmm	4.60E-56	3	283	0.945945946
jgi|Blugr1|21830|BGHDH14_bgh05372	GH18.hmm	9.20E-54	4	288	0.959459459
jgi|Blugr1|21905|BGHDH14_bgh05368	GT62.hmm	1.70E-95	5	268	0.981343284
jgi|Blugr1|21932|BGHDH14_bghG003071000001001	GT2.hmm	1.20E-15	79	164	0.505952381
jgi|Blugr1|21946|BGHDH14_bgh00857	CBM18.hmm	2.10E-07	2	35	0.868421053
jgi|Blugr1|21946|BGHDH14_bgh00857	CE4.hmm	1.70E-32	8	125	0.9
jgi|Blugr1|21971|BGHDH14_bgh04744	GH81.hmm	3.00E-213	7	621	0.987138264
jgi|Blugr1|21988|BGHDH14_bghG003125000001001	GT76.hmm	6.00E-100	3	407	0.992628993
jgi|Blugr1|22015|BGHDH14_bgh02707	CE10.hmm	5.90E-25	46	182	0.398826979
jgi|Blugr1|22016|BGHDH14_bgh02104	GT4.hmm	7.10E-35	11	149	0.8625
jgi|Blugr1|22106|BGHDH14_bgh00780	GH76.hmm	7.70E-54	40	337	0.829608939
jgi|Blugr1|22129|BGHDH14_bgh03496	GT62.hmm	6.30E-108	2	267	0.98880597
jgi|Blugr1|22151|BGHDH14_bgh00571	GT28.hmm	1.10E-10	29	125	0.611464968
jgi|Blugr1|22247|BGHDH14_bgh00778	GH76.hmm	2.00E-76	19	337	0.888268156
jgi|Blugr1|22260|BGHDH14_bgh02742	GT32.hmm	1.60E-19	3	89	0.955555556
jgi|Blugr1|22313|BGHDH14_bgh00734	GH17.hmm	4.40E-17	16	300	0.91318328
jgi|Blugr1|22323|BGHDH14_bgh00584	GT22.hmm	2.00E-81	5	381	0.966580977
jgi|Blugr1|22386|BGHDH14_bgh03501	GT68.hmm	5.00E-06	196	344	0.422857143
jgi|Blugr1|22406|BGHDH14_bgh06353	GH93.hmm	3.80E-56	2	273	0.882736156
jgi|Blugr1|22406|BGHDH14_bgh06353	GH74.hmm	5.40E-06	48	143	0.407725322
jgi|Blugr1|22465|BGHDH14_bgh00729	GH16.hmm	1.10E-25	54	187	0.703703704
jgi|Blugr1|22487|BGHDH14_bgh01555	GH132.hmm	3.40E-91	20	295	0.907590759
jgi|Blugr1|22515|BGHDH14_bgh00588	GH18.hmm	4.90E-56	3	285	0.952702703
jgi|Blugr1|22626|BGHDH14_bgh05828	GT22.hmm	9.50E-74	1	386	0.989717224
jgi|Blugr1|22662|BGHDH14_bgh01321	GT90.hmm	2.40E-77	6	244	0.952
jgi|Blugr1|22760|BGHDH14_bgh00779	GH76.hmm	5.90E-76	24	335	0.868715084
jgi|Blugr1|22777|BGHDH14_bgh03179	CE10.hmm	8.30E-28	52	208	0.457478006
jgi|Blugr1|22814|BGHDH14_bgh00197	CBM48.hmm	2.90E-10	2	49	0.618421053
jgi|Blugr1|22814|BGHDH14_bgh00197	GH13_8.hmm	4.80E-138	1	274	0.996350365
jgi|Blugr1|22866|BGHDH14_bgh05397	GH74.hmm	1.10E-07	33	109	0.326180258
jgi|Blugr1|22891|BGHDH14_bgh02974	GH128.hmm	8.60E-66	4	223	0.977678571
jgi|Blugr1|22908|BGHDH14_bgh06910	GH31.hmm	7.20E-156	2	427	0.995316159
jgi|Blugr1|22912|BGHDH14_bgh00795	GH92.hmm	3.20E-137	2	491	0.99592668

Query	Subject	E-value	Start	End	Covered Fraction
jgi|Blugr1|22913|BGHDH14_bghG005039000001001	CE10.hmm	3.10E-26	75	188	0.331378299
jgi|Blugr1|22942|BGHDH14_bgh00086	GH5_9.hmm	8.20E-119	2	306	0.993464052
jgi|Blugr1|22946|BGHDH14_bgh00768	GH47.hmm	2.10E-141	1	444	0.993273543
jgi|Blugr1|22965|BGHDH14_bgh04548	AA4.hmm	8.70E-22	9	247	0.455938697
jgi|Blugr1|22984|BGHDH14_bgh00809	GT2.hmm	8.10E-08	2	167	0.982142857
jgi|Blugr1|22993|BGHDH14_bgh00680	GH5_9.hmm	2.00E-117	2	305	0.990196078
jgi|Blugr1|23038|BGHDH14_bgh03781	CE3.hmm	1.40E-53	1	194	0.994845361
jgi|Blugr1|23130|BGHDH14_bgh05640	GH16.hmm	8.60E-24	35	185	0.793650794
jgi|Blugr1|23138|BGHDH14_bgh00591	CE4.hmm	3.00E-25	7	128	0.930769231
jgi|Blugr1|23193|BGHDH14_bgh02161	CE10.hmm	4.10E-31	64	193	0.37829912
jgi|Blugr1|23227|BGHDH14_bgh03005	CE1.hmm	1.40E-07	32	193	0.709251101
jgi|Blugr1|23245|BGHDH14_bgh06777	GH17.hmm	5.30E-24	19	311	0.938906752
jgi|Blugr1|23309|BGHDH14_bgh04624	CE10.hmm	1.30E-49	94	291	0.57771261
jgi|Blugr1|23336|BGHDH14_bgh02330	CE10.hmm	2.20E-45	97	334	0.695014663
jgi|Blugr1|23427|BGHDH14_bgh04916	CE1.hmm	7.50E-06	24	208	0.810572687
jgi|Blugr1|23587|BGHDH14_bgh02390	GH125.hmm	8.00E-153	1	402	0.997512438
jgi|Blugr1|23591|BGHDH14_bgh05283	CE4.hmm	7.30E-17	6	115	0.838461538
jgi|Blugr1|23622|BGHDH14_bgh00315	GH13_40.hmm	1.40E-177	2	359	0.991666667
jgi|Blugr1|23739|BGHDH14_bgh00776	GH72.hmm	1.10E-128	5	311	0.980769231
jgi|Blugr1|23770|BGHDH14_bgh01629	CE14.hmm	1.90E-10	4	124	0.967741935
jgi|Blugr1|23801|BGHDH14_bgh00739	GH18.hmm	1.60E-76	3	286	0.956081081
jgi|Blugr1|23834|BGHDH14_bgh00377	CE10.hmm	9.80E-25	71	193	0.357771261
jgi|Blugr1|23921|BGHDH14_bgh02562	GH63.hmm	1.10E-15	356	562	0.361403509
jgi|Blugr1|23934|BGHDH14_bgh00585	GT57.hmm	2.70E-90	3	233	0.478170478
jgi|Blugr1|23934|BGHDH14_bgh00585	GT57.hmm	1.20E-52	222	480	0.536382536
jgi|Blugr1|23936|BGHDH14_bgh05545	GH20.hmm	1.20E-82	4	336	0.985163205
jgi|Blugr1|23954|BGHDH14_bgh00567	GT68.hmm	3.60E-07	228	345	0.334285714
jgi|Blugr1|24001|BGHDH14_bghG001634000001001	GT20.hmm	2.20E-197	10	475	0.978947368
jgi|Blugr1|24036|BGHDH14_bghG001669000001001	GT1.hmm	3.30E-49	5	378	0.976439791
jgi|Blugr1|24058|BGHDH14_bgh06688	GH5_12.hmm	9.60E-223	2	542	0.996309963
jgi|Blugr1|24086|BGHDH14_bgh02071	GT62.hmm	1.90E-122	4	268	0.985074627
jgi|Blugr1|24093|BGHDH14_bgh05574	GT32.hmm	3.80E-10	48	87	0.433333333
jgi|Blugr1|24140|BGHDH14_bgh00325	GT2.hmm	5.30E-15	79	163	0.5
jgi|Blugr1|24141|BGHDH14_bgh00324	GT2.hmm	1.80E-13	79	167	0.523809524
jgi|Blugr1|24147|BGHDH14_bgh00747	GH125.hmm	6.90E-152	1	402	0.997512438
jgi|Blugr1|24152|BGHDH14_bghG001852000001001	GT32.hmm	3.10E-19	7	89	0.911111111
jgi|Blugr1|24168|BGHDH14_bgh02561	GT15.hmm	1.10E-126	1	272	0.992673993
jgi|Blugr1|24178|BGHDH14_bgh00226	CE5.hmm	4.90E-43	1	188	0.989417989

Query	Subject	E-value	Start	End	Covered Fraction
jgi|Blugr1|24188|BGHDH14_bgh00580	GT58.hmm	4.50E-140	1	364	0.997252747
jgi|Blugr1|24210|BGHDH14_bgh00720	GH16.hmm	2.80E-23	7	188	0.957671958
jgi|Blugr1|24246|BGHDH14_bgh06810	GH5_9.hmm	3.40E-105	2	305	0.990196078
jgi|Blugr1|24263|BGHDH14_bgh00682	CE10.hmm	4.70E-32	74	205	0.384164223
jgi|Blugr1|24288|BGHDH14_bgh00323	GT20.hmm	6.00E-160	19	474	0.957894737
jgi|Blugr1|24305|BGHDH14_bgh00738	GH18.hmm	7.90E-17	24	195	0.577702703
jgi|Blugr1|24374|BGHDH14_bgh02741	GT31.hmm	3.30E-07	68	181	0.588541667
jgi|Blugr1|24484|BGHDH14_bgh04794	AA9.hmm	3.40E-60	2	220	0.990909091
jgi|Blugr1|24558|BGHDH14_bghG000584000001001	GT2.hmm	6.50E-07	2	166	0.976190476
jgi|Blugr1|24620|BGHDH14_bghG000646000001001	GH74.hmm	9.90E-05	94	170	0.326180258
jgi|Blugr1|24643|BGHDH14_bgh00497	GT20.hmm	2.60E-146	12	473	0.970526316
jgi|Blugr1|24659|BGHDH14_bghG000684000001001	GH78.hmm	5.60E-78	6	502	0.984126984
jgi|Blugr1|24660|BGHDH14_bghG000684000002001	GH13_25.hmm	1.30E-211	2	448	0.995535714
jgi|Blugr1|24726|BGHDH14_bgh06932	CE10.hmm	9.90E-44	76	334	0.75659824
jgi|Blugr1|24784|BGHDH14_bgh00303	GH15.hmm	2.30E-38	64	240	0.487534626
jgi|Blugr1|24873|BGHDH14_bgh00470	GH23.hmm	0.00084	37	98	0.451851852
jgi|Blugr1|24976|BGHDH14_bgh03765	CE10.hmm	1.00E-30	39	208	0.495601173
jgi|Blugr1|24981|BGHDH14_bgh04640	GT90.hmm	2.00E-68	15	248	0.932
jgi|Blugr1|24994|BGHDH14_bgh06259	AA3.hmm	1.30E-88	86	409	0.522653722
jgi|Blugr1|25080|BGHDH14_bghG006289000001001	CBM21.hmm	0.00088	13	52	0.364485981
jgi|Blugr1|25123|BGHDH14_bgh00775	GH72.hmm	8.70E-115	4	311	0.983974359
jgi|Blugr1|25154|BGHDH14_bgh00587	GT57.hmm	2.50E-172	12	479	0.970893971
jgi|Blugr1|25158|BGHDH14_bghG006074000001001	GH92.hmm	4.50E-154	4	490	0.989816701
jgi|Blugr1|25178|BGHDH14_bgh00300	GT2.hmm	1.70E-06	2	166	0.976190476
jgi|Blugr1|25275|BGHDH14_bgh00763	GH47.hmm	1.50E-134	1	446	0.997757848
jgi|Blugr1|25276|BGHDH14_bgh03319	GT4.hmm	5.40E-14	6	150	0.9
jgi|Blugr1|25297|BGHDH14_bgh01272	GT90.hmm	2.00E-73	3	248	0.98
jgi|Blugr1|25338|BGHDH14_bghG000061000002001	GH13_40.hmm	9.20E-171	2	360	0.994444444
jgi|Blugr1|25349|BGHDH14_bgh00227	CE5.hmm	7.70E-35	2	186	0.973544974
jgi|Blugr1|25355|BGHDH14_bgh00811	GT2.hmm	2.10E-07	2	167	0.982142857
jgi|Blugr1|25425|BGHDH14_bgh00234	GT35.hmm	8.80E-278	2	674	0.997032641
jgi|Blugr1|25458|BGHDH14_bgh00582	GT22.hmm	7.40E-91	2	389	0.994858612
jgi|Blugr1|25464|BGHDH14_bgh00572	GT33.hmm	3.70E-148	3	424	0.990588235
jgi|Blugr1|25511|BGHDH14_bgh00773	AA11.hmm	1.90E-64	1	188	0.979057592
jgi|Blugr1|25511|BGHDH14_bgh00773	CBM18.hmm	0.00099	2	35	0.868421053
jgi|Blugr1|25562|BGHDH14_bgh00329	GH18.hmm	3.50E-65	6	283	0.935810811
jgi|Blugr1|25568|BGHDH14_bgh05045	GT31.hmm	2.00E-05	74	163	0.463541667
jgi|Blugr1|25574|BGHDH14_bgh00353	GH131.hmm	2.50E-62	51	249	0.776470588

Query	Subject	E-value	Start	End	Covered Fraction
jgi|Blugr1|25579|BGHDH14_bgh06450	GH76.hmm	2.10E-79	20	341	0.896648045
jgi|Blugr1|25584|BGHDH14_bghG000349000001001	GH76.hmm	1.00E-70	19	341	0.899441341
jgi|Blugr1|25590|BGHDH14_bgh05043	GT4.hmm	1.60E-26	4	133	0.80625
jgi|Blugr1|25604|BGHDH14_bgh05252	GH76.hmm	1.20E-78	13	342	0.918994413

D. *B. graminis f. sp. tritici* genes encoding predicted CAZY proteins

Query	Subject	E-value	Start	End	Covered Fraction
jgi|Blugra1|1008|BGT96224_1964T0	GH132.hmm	1.50E-90	17	295	0.917491749
jgi|Blugra1|1049|BGT96224_1259T0	GH16.hmm	2.80E-24	53	187	0.708994709
jgi|Blugra1|1172|BGT96224_5431T0	GH74.hmm	1.40E-07	35	109	0.317596567
jgi|Blugra1|1173|BGT96224_199T0	GH74.hmm	0.0009	24	106	0.35193133
jgi|Blugra1|1199|BGT96224_3142T0	CE1.hmm	3.70E-07	84	193	0.480176211
jgi|Blugra1|1242|BGT96224_14T0	GT62.hmm	1.50E-95	5	268	0.981343284
jgi|Blugra1|1308|BGT96224_1212T0	AA1_3.hmm	9.20E-136	2	312	0.993589744
jgi|Blugra1|1328|BGT96224_1290T0	GH47.hmm	4.40E-54	279	446	0.374439462
jgi|Blugra1|1375|BGT96224_2940T0	GT31.hmm	3.10E-07	68	185	0.609375
jgi|Blugra1|1532|BGT96224_1084T0	GT20.hmm	4.20E-146	12	473	0.970526316
jgi|Blugra1|1546|BGT96224_4859T0	GH78.hmm	2.10E-78	7	502	0.982142857
jgi|Blugra1|1547|BGT96224_4880T0	GH13_25.hmm	4.00E-13	278	416	0.308035714
jgi|Blugra1|1547|BGT96224_4880T0	GH13_25.hmm	1.80E-211	2	448	0.995535714
jgi|Blugra1|1621|BGT96224_857T0	GT35.hmm	9.10E-278	2	674	0.997032641
jgi|Blugra1|1658|BGT96224_1327T0	GT2.hmm	2.10E-07	2	167	0.982142857
jgi|Blugra1|1662|BGT96224_852T0	CE5.hmm	5.10E-35	2	186	0.973544974
jgi|Blugra1|1674|BGT96224_4918T0	GH13_40.hmm	7.00E-171	2	360	0.994444444
jgi|Blugra1|1691|BGT96224_A20375T0	GT34.hmm	1.40E-88	3	245	0.983739837
jgi|Blugra1|1710|BGT96224_A20497T0	GT39.hmm	3.50E-73	2	223	0.99103139
jgi|Blugra1|1831|BGT96224_4300T0	AA9.hmm	2.10E-60	2	220	0.990909091
jgi|Blugra1|1871|BGT96224_721T0	GH5_9.hmm	1.00E-114	2	306	0.993464052
jgi|Blugra1|18|BGT96224_4851T0	GH47.hmm	2.00E-141	1	444	0.993273543
jgi|Blugra1|1902|BGT96224_1489T0	GT8.hmm	7.30E-43	27	255	0.887159533
jgi|Blugra1|1906|BGT96224_ASP21312T0	GT76.hmm	3.00E-69	3	277	0.673218673
jgi|Blugra1|1914|BGT96224_1306T0	GH76.hmm	8.50E-108	11	346	0.93575419
jgi|Blugra1|1926|BGT96224_4746T0	CE10.hmm	2.60E-30	40	193	0.448680352
jgi|Blugra1|1932|BGT96224_4169T0	GT90.hmm	8.00E-68	15	248	0.932
jgi|Blugra1|1946|BGT96224_380T0	AA3.hmm	5.80E-88	86	409	0.522653722
jgi|Blugra1|1982|BGT96224_1269T0	GH18.hmm	1.70E-76	3	286	0.956081081
jgi|Blugra1|2016|BGT96224_1283T0	GH38.hmm	7.30E-87	2	255	0.940520446
jgi|Blugra1|2051|BGT96224_A21067T0	CE1.hmm	5.30E-48	1	223	0.977973568
jgi|Blugra1|2119|BGT96224_937T0	GT2.hmm	5.30E-15	79	163	0.5
jgi|Blugra1|2121|BGT96224_936T0	GT2.hmm	1.50E-13	79	167	0.523809524
jgi|Blugra1|2152|BGT96224_1298T0	GH55.hmm	4.50E-298	9	738	0.985135135
jgi|Blugra1|2169|BGT96224_1215T0	GH5_9.hmm	1.80E-118	2	305	0.990196078

Query	Subject	E-value	Start	End	Covered Fraction
jgi|Blugra1|2197|BGT96224_5424T0	GT32.hmm	3.10E-19	7	89	0.911111111
jgi|Blugra1|2208|BGT96224_2800T0	GT15.hmm	5.00E-125	1	272	0.992673993
jgi|Blugra1|2220|BGT96224_851T0	CE5.hmm	1.30E-42	1	188	0.989417989
jgi|Blugra1|2224|BGT96224_A21024T0	CE10.hmm	7.70E-09	94	216	0.357771261
jgi|Blugra1|222|BGT96224_2398T0	GT62.hmm	1.90E-122	4	268	0.985074627
jgi|Blugra1|2268|BGT96224_2589T0	AA11.hmm	1.50E-70	1	186	0.968586387
jgi|Blugra1|2307|BGT96224_1202T0	AA2.hmm	7.50E-62	4	254	0.980392157
jgi|Blugra1|2314|BGT96224_2335T0	CE10.hmm	1.40E-13	71	309	0.697947214
jgi|Blugra1|2346|BGT96224_2582T0	AA5_1.hmm	9.80E-169	5	536	0.943161634
jgi|Blugra1|2373|BGT96224_1169T0	CE4.hmm	6.20E-25	7	128	0.930769231
jgi|Blugra1|2381|BGT96224_1150T0	GT33.hmm	2.00E-147	3	424	0.990588235
jgi|Blugra1|2386|BGT96224_1161T0	GT22.hmm	4.60E-92	2	389	0.994858612
jgi|Blugra1|2487|BGT96224_825T0	CBM48.hmm	1.60E-10	2	49	0.618421053
jgi|Blugra1|2487|BGT96224_825T0	GH13_8.hmm	1.20E-137	1	274	0.996350365
jgi|Blugra1|251|BGT96224_1168T0	GT59.hmm	9.70E-51	2	185	0.452970297
jgi|Blugra1|2563|BGT96224_1254T0	GH16.hmm	7.50E-23	7	188	0.957671958
jgi|Blugra1|2584|BGT96224_1149T0	GT28.hmm	2.50E-11	28	125	0.617834395
jgi|Blugra1|2590|BGT96224_4877T0	GH63.hmm	2.70E-31	319	565	0.431578947
jgi|Blugra1|2606|BGT96224_927T0	GH13_40.hmm	1.50E-177	2	359	0.991666667
jgi|Blugra1|2642|BGT96224_3115T0	GH128.hmm	9.90E-66	4	223	0.977678571
jgi|Blugra1|2645|BGT96224_1213T0	AA1_2.hmm	6.10E-154	3	339	0.988235294
jgi|Blugra1|2691|BGT96224_2673BT0	GH125.hmm	3.10E-147	41	402	0.89800995
jgi|Blugra1|2698|BGT96224_ASP20650T0	CE4.hmm	1.00E-16	6	115	0.838461538
jgi|Blugra1|2711|BGT96224_5010T0	GH93.hmm	1.60E-56	2	273	0.882736156
jgi|Blugra1|2711|BGT96224_5010T0	GH74.hmm	1.40E-06	48	143	0.407725322
jgi|Blugra1|2751|BGT96224_1324T0	GT2.hmm	2.10E-07	2	167	0.982142857
jgi|Blugra1|2778|BGT96224_A20597T0	AA4.hmm	6.40E-22	9	241	0.444444444
jgi|Blugra1|2804|BGT96224_A20581T0	GH63.hmm	5.30E-15	356	562	0.361403509
jgi|Blugra1|2835|BGT96224_A20467T0	CBM50.hmm	0.00056	1	39	0.95
jgi|Blugra1|2930|BGT96224_A20075T0	GT15.hmm	4.10E-125	1	272	0.992673993
jgi|Blugra1|2985|BGT96224_4797T0	GT22.hmm	6.10E-83	5	381	0.966580977
jgi|Blugra1|3027|BGT96224_935T0	GT20.hmm	8.80E-160	33	474	0.928421053
jgi|Blugra1|307|BGT96224_4938T0	CBM18.hmm	1.50E-05	5	35	0.789473684
jgi|Blugra1|307|BGT96224_4938T0	CE4.hmm	2.20E-27	7	125	0.907692308
jgi|Blugra1|307|BGT96224_4938T0	CBM18.hmm	8.50E-05	6	36	0.789473684
jgi|Blugra1|3097|BGT96224_1262T0	GH16.hmm	7.00E-17	4	189	0.978835979
jgi|Blugra1|3106|BGT96224_4835BT0	GH37.hmm	1.30E-149	5	489	0.985743381
jgi|Blugra1|3116|BGT96224_983T0	CE10.hmm	1.30E-24	71	193	0.357771261

Query	Subject	E-value	Start	End	Covered Fraction
jgi|Blugra1|3160|BGT96224_1220T0	CE10.hmm	3.30E-32	74	204	0.381231672
jgi|Blugra1|31|BGT96224_2034T0	GH114.hmm	2.90E-73	1	190	0.994736842
jgi|Blugra1|3261|BGT96224_853T0	GT3.hmm	1.40E-305	1	637	0.998430141
jgi|Blugra1|3277|BGT96224_1699T0	GT15.hmm	5.70E-121	1	272	0.992673993
jgi|Blugra1|328|BGT96224_2663T0	AA2.hmm	3.30E-57	5	253	0.97254902
jgi|Blugra1|3354|BGT96224_1159T0	GT58.hmm	5.80E-140	2	364	0.994505495
jgi|Blugra1|3362|BGT96224_A21303T0	GT69.hmm	3.80E-66	1	238	0.991631799
jgi|Blugra1|3379|BGT96224_2429T0	GT4.hmm	7.10E-35	11	149	0.8625
jgi|Blugra1|3457|BGT96224_2890T0	GT66.hmm	2.10E-184	9	597	0.848484848
jgi|Blugra1|3579|BGT96224_1720BT0	GT90.hmm	3.60E-74	3	248	0.98
jgi|Blugra1|3634|BGT96224_2941T0	GT32.hmm	1.50E-19	3	89	0.955555556
jgi|Blugra1|365|BGT96224_2483T0	CE10.hmm	8.50E-31	64	193	0.37829912
jgi|Blugra1|3663|BGT96224_939T0	GH18.hmm	1.40E-65	6	283	0.935810811
jgi|Blugra1|3666|BGT96224_959BT0	GH131.hmm	1.10E-38	119	249	0.509803922
jgi|Blugra1|3677|BGT96224_4510T0	GT31.hmm	2.60E-05	74	163	0.463541667
jgi|Blugra1|3734|BGT96224_5071T0	GT4.hmm	6.20E-14	6	150	0.9
jgi|Blugra1|3735|BGT96224_1288T0	GH47.hmm	4.20E-135	1	446	0.997757848
jgi|Blugra1|3840|BGT96224_81T0	GH20.hmm	6.00E-84	4	336	0.985163205
jgi|Blugra1|3854|BGT96224_87T0	GT24.hmm	3.80E-132	1	248	0.995967742
jgi|Blugra1|385|BGT96224_1299T0	AA11.hmm	1.80E-64	1	188	0.979057592
jgi|Blugra1|385|BGT96224_1299T0	CBM18.hmm	0.00099	2	35	0.868421053
jgi|Blugra1|3875|BGT96224_4921T0	GT20.hmm	1.10E-196	12	475	0.974736842
jgi|Blugra1|3950|BGT96224_1305T0	GH76.hmm	6.50E-54	46	338	0.815642458
jgi|Blugra1|395|BGT96224_2624T0	CE10.hmm	6.40E-46	97	334	0.695014663
jgi|Blugra1|3967|BGT96224_3459T0	GT62.hmm	1.60E-108	2	267	0.98880597
jgi|Blugra1|4006|BGT96224_5017T0	CE16.hmm	4.80E-65	1	266	0.992509363
jgi|Blugra1|4012|BGT96224_1307T0	GH76.hmm	5.40E-113	10	346	0.938547486
jgi|Blugra1|4016|BGT96224_1620T0	GT32.hmm	2.20E-15	6	87	0.9
jgi|Blugra1|4112|BGT96224_445T0	CE12.hmm	3.70E-14	2	202	0.952380952
jgi|Blugra1|4222|BGT96224_1276T0	GH125.hmm	2.90E-128	1	330	0.81840796
jgi|Blugra1|4257|BGT96224_1316T0	GH92.hmm	5.40E-137	2	491	0.99592668
jgi|Blugra1|4258|BGT96224_ASP21259T0	CE10.hmm	4.00E-25	75	188	0.331378299
jgi|Blugra1|4353|BGT96224_196T0	CE10.hmm	1.90E-19	62	316	0.744868035
jgi|Blugra1|4355|BGT96224_195T0	GT39.hmm	9.90E-73	2	223	0.99103139
jgi|Blugra1|435|BGT96224_3280T0	CE10.hmm	1.50E-27	53	208	0.454545455
jgi|Blugra1|4387|BGT96224_ASP20929T0	CE14.hmm	1.20E-09	4	124	0.967741935
jgi|Blugra1|4399|BGT96224_A20844T0	GH5_9.hmm	1.10E-104	2	305	0.990196078
jgi|Blugra1|4411|BGT96224_1164T0	GT57.hmm	4.80E-89	3	229	0.46985447

Query	Subject	E-value	Start	End	Covered Fraction
jgi|Blugra1|4411|BGT96224_1164T0	GT57.hmm	3.60E-53	222	480	0.536382536
jgi|Blugra1|4441|BGT96224_4348T0	GT41.hmm	1.40E-48	303	519	0.306382979
jgi|Blugra1|4495|BGT96224_1261T0	GH16.hmm	2.80E-24	39	185	0.772486772
jgi|Blugra1|4504|BGT96224_129T0	CE1.hmm	1.70E-10	13	208	0.859030837
jgi|Blugra1|4514|BGT96224_397T0	GH17.hmm	1.00E-11	172	311	0.446945338
jgi|Blugra1|4538|BGT96224_98T0	GT32.hmm	3.50E-10	48	87	0.433333333
jgi|Blugra1|4612|BGT96224_4927T0	CBM21.hmm	3.20E-32	3	107	0.971962617
jgi|Blugra1|4631|BGT96224_1869T0	GH16.hmm	3.60E-22	35	176	0.746031746
jgi|Blugra1|4632|BGT96224_1253T0	GH16.hmm	2.00E-31	18	176	0.835978836
jgi|Blugra1|4682|BGT96224_4832T0	GT21.hmm	4.00E-90	1	233	0.995708155
jgi|Blugra1|4742|BGT96224_E5689T0	CBM21.hmm	0.00046	13	74	0.570093458
jgi|Blugra1|4854|BGT96224_3463T0	GT68.hmm	2.90E-06	196	344	0.422857143
jgi|Blugra1|4915|BGT96224_A20801T0	GH15.hmm	3.80E-73	39	360	0.889196676
jgi|Blugra1|4915|BGT96224_A20801T0	CBM20.hmm	9.70E-22	9	88	0.877777778
jgi|Blugra1|4938|BGT96224_A20858T0	GT1.hmm	1.40E-54	94	369	0.719895288
jgi|Blugra1|4977|BGT96224_1280T0	CE1.hmm	2.70E-19	2	213	0.929515419
jgi|Blugra1|4991|BGT96224_4825T0	CE10.hmm	2.60E-49	93	291	0.580645161
jgi|Blugra1|504|BGT96224_4249T0	GH128.hmm	1.70E-61	4	224	0.982142857
jgi|Blugra1|5050|BGT96224_1287T0	GH47.hmm	9.50E-158	2	446	0.995515695
jgi|Blugra1|5079|BGT96224_1063T0	GH23.hmm	0.00084	37	98	0.451851852
jgi|Blugra1|5176|BGT96224_194T0	GT22.hmm	1.40E-73	1	386	0.989717224
jgi|Blugra1|5206|BGT96224_3794T0	AA7.hmm	2.20E-12	66	209	0.312227074
jgi|Blugra1|531|BGT96224_5233T0	GT39.hmm	2.80E-69	2	223	0.99103139
jgi|Blugra1|5382|BGT96224_1303T0	GH72.hmm	6.80E-129	5	311	0.980769231
jgi|Blugra1|5398|BGT96224_A20420T0	GH18.hmm	5.00E-79	2	286	0.959459459
jgi|Blugra1|5421|BGT96224_1249BT0	GT2.hmm	6.40E-29	16	123	0.636904762
jgi|Blugra1|542|BGT96224_395T0	GH17.hmm	4.50E-09	201	311	0.353697749
jgi|Blugra1|5437|BGT96224_755T0	GH18.hmm	1.70E-44	74	282	0.702702703
jgi|Blugra1|5440|BGT96224_697T0	GH18.hmm	1.90E-56	3	283	0.945945946
jgi|Blugra1|5475|BGT96224_16T0	GH18.hmm	5.50E-41	4	211	0.699324324
jgi|Blugra1|550|BGT96224_396T0	GH17.hmm	2.90E-06	201	311	0.353697749
jgi|Blugra1|5569|BGT96224_644T0	CE10.hmm	3.50E-44	76	334	0.75659824
jgi|Blugra1|5582|BGT96224_3642T0	CE3.hmm	1.70E-53	1	194	0.994845361
jgi|Blugra1|5599|BGT96224_583T0	GH17.hmm	4.70E-22	19	311	0.938906752
jgi|Blugra1|5639|BGT96224_1767T0	GT90.hmm	8.30E-80	6	244	0.952
jgi|Blugra1|5689|BGT96224_1264T0	GH17.hmm	1.00E-17	16	300	0.91318328
jgi|Blugra1|5697|BGT96224_1166T0	GH18.hmm	2.20E-55	3	283	0.945945946
jgi|Blugra1|5764|BGT96224_1266T0	GH17.hmm	2.80E-34	11	306	0.948553055

Query	Subject	E-value	Start	End	Covered Fraction
jgi|Blugra1|5797|BGT96224_4507T0	GH16.hmm	1.00E-20	13	189	0.931216931
jgi|Blugra1|5851|BGT96224_4876T0	GT2.hmm	6.50E-07	2	166	0.976190476
jgi|Blugra1|5883|BGT96224_1268T0	GH18.hmm	2.60E-16	23	195	0.581081081
jgi|Blugra1|5952|BGT96224_2849T0	CE10.hmm	2.90E-08	82	207	0.366568915
jgi|Blugra1|5974|BGT96224_634T0	GH31.hmm	5.20E-154	2	427	0.995316159
jgi|Blugra1|5993|BGT96224_1291T0	GH47.hmm	2.20E-164	1	446	0.997757848
jgi|Blugra1|6013|BGT96224_123T0	GH16.hmm	5.40E-23	35	185	0.793650794
jgi|Blugra1|6049|BGT96224_4874T0	GT2.hmm	1.20E-15	79	164	0.505952381
jgi|Blugra1|6052|BGT96224_1145T0	GT68.hmm	4.40E-07	228	345	0.334285714
jgi|Blugra1|6065|BGT96224_4508T0	GT4.hmm	1.90E-26	4	132	0.8
jgi|Blugra1|6087|BGT96224_2713T0	GT8.hmm	1.60E-42	27	255	0.887159533
jgi|Blugra1|6160|BGT96224_1267T0	GH18.hmm	1.10E-19	4	203	0.672297297
jgi|Blugra1|6194|BGT96224_4878T0	GT2.hmm	1.20E-35	1	168	0.994047619
jgi|Blugra1|6243|BGT96224_4674T0	GH76.hmm	5.60E-78	28	341	0.874301676
jgi|Blugra1|6249|BGT96224_4872T0	GT22.hmm	1.50E-41	3	147	0.370179949
jgi|Blugra1|6250|BGT96224_4872BT0	GT22.hmm	3.30E-47	183	388	0.526992288
jgi|Blugra1|6308|BGT96224_1257T0	GH16.hmm	8.80E-23	52	188	0.71957672
jgi|Blugra1|6309|BGT96224_4784T0	GH3.hmm	3.10E-48	5	215	0.972222222
jgi|Blugra1|6503|BGT96224_2914T0	CE10.hmm	9.00E-23	43	182	0.407624633
jgi|Blugra1|6525|BGT96224_1581T0	GT34.hmm	4.20E-72	1	243	0.983739837
jgi|Blugra1|661|BGT96224_4961T0	GH81.hmm	2.20E-214	7	621	0.987138264
jgi|Blugra1|687|BGT96224_1362T0	CBM18.hmm	2.10E-07	2	35	0.868421053
jgi|Blugra1|687|BGT96224_1362T0	CE4.hmm	2.40E-32	8	125	0.9
jgi|Blugra1|736|BGT96224_1043T0	CE1.hmm	1.90E-07	83	207	0.546255507
jgi|Blugra1|770|BGT96224_914T0	GT2.hmm	3.60E-06	2	166	0.976190476
jgi|Blugra1|779|BGT96224_1531T0	GH132.hmm	2.00E-88	17	300	0.933993399
jgi|Blugra1|811|BGT96224_1300T0	GH72.hmm	1.40E-134	3	310	0.983974359
jgi|Blugra1|811|BGT96224_1300T0	CBM43.hmm	3.30E-19	1	82	0.975903614
jgi|Blugra1|812|BGT96224_383T0	GT48.hmm	0	1	733	0.99052774
jgi|Blugra1|81|BGT96224_2874T0	GH135.hmm	7.50E-60	1	138	0.578059072
jgi|Blugra1|822|BGT96224_1154T0	GT4.hmm	6.40E-40	5	151	0.9125
jgi|Blugra1|832|BGT96224_5324T0	GH76.hmm	9.80E-62	24	248	0.625698324
jgi|Blugra1|882|BGT96224_1165T0	GT57.hmm	4.90E-172	12	479	0.970893971
jgi|Blugra1|883|BGT96224_4860T0	GH92.hmm	5.60E-155	4	490	0.989816701
jgi|Blugra1|906|BGT96224_543T0	GH5_12.hmm	3.20E-223	2	541	0.994464945
jgi|Blugra1|934|BGT96224_4865T0	GT1.hmm	3.60E-48	5	378	0.976439791
jgi|Blugra1|959|BGT96224_2794T0	GT50.hmm	3.90E-92	1	261	0.992366412

E. *E. necator* genes encoding predicted CAZY proteins

Query	Subject	E-value	Start	End	Covered Fraction
jgi|Erynec1|1034|EV44_g2684T0	GT3.hmm	3.20E-302	1	637	0.998430141
jgi|Erynec1|1048|EV44_g5822T0	GH5_12.hmm	5.10E-229	2	541	0.994464945
jgi|Erynec1|1065|EV44_g0001T0	CE10.hmm	7.00E-34	75	187	0.328445748
jgi|Erynec1|1070|EV44_g1334T0	CE1.hmm	3.50E-07	56	143	0.383259912
jgi|Erynec1|108|EV44_g0434T0	GT4.hmm	1.40E-25	3	138	0.84375
jgi|Erynec1|1105|EV44_g2177T0	GH92.hmm	1.90E-126	2	452	0.916496945
jgi|Erynec1|1188|EV44_g0348T0	GH125.hmm	7.80E-159	2	402	0.995024876
jgi|Erynec1|1198|EV44_g1807T0	GT39.hmm	2.90E-73	1	223	0.995515695
jgi|Erynec1|1227|EV44_g0104T0	CBM18.hmm	1.30E-06	1	38	0.973684211
jgi|Erynec1|1227|EV44_g0104T0	AA5_1.hmm	1.30E-167	5	536	0.943161634
jgi|Erynec1|1244|EV44_g2124T0	AA2.hmm	8.80E-57	6	253	0.968627451
jgi|Erynec1|1277|EV44_g0168T0	GT15.hmm	1.60E-120	1	272	0.992673993
jgi|Erynec1|1292|EV44_g0468T0	GT22.hmm	8.30E-76	1	386	0.989717224
jgi|Erynec1|1306|EV44_g2227T0	GH3.hmm	2.80E-49	7	215	0.962962963
jgi|Erynec1|1320|EV44_g5671T0	CE1.hmm	5.50E-09	8	128	0.528634361
jgi|Erynec1|1338|EV44_g6140T0	GT50.hmm	5.20E-91	1	262	0.996183206
jgi|Erynec1|133|EV44_g0078T0	CE16.hmm	7.70E-67	1	266	0.992509363
jgi|Erynec1|1357|EV44_g1647T0	GT39.hmm	1.20E-69	2	223	0.99103139
jgi|Erynec1|148|EV44_g2102T0	GT2.hmm	2.10E-07	2	167	0.982142857
jgi|Erynec1|1501|EV44_g0305T0	GH131.hmm	9.00E-65	3	249	0.964705882
jgi|Erynec1|1514|EV44_g5129T0	GT90.hmm	1.10E-71	3	247	0.976
jgi|Erynec1|153|EV44_g0565T0	CE10.hmm	6.00E-26	75	188	0.331378299
jgi|Erynec1|1546|EV44_g1116T0	GH13_40.hmm	4.10E-173	2	360	0.994444444
jgi|Erynec1|1574|EV44_g2261T0	CE10.hmm	1.50E-08	69	207	0.404692082
jgi|Erynec1|1580|EV44_g1062T0	CE1.hmm	2.30E-46	1	224	0.982378855
jgi|Erynec1|1632|EV44_g1765T0	CE1.hmm	3.40E-09	83	208	0.550660793
jgi|Erynec1|1669|EV44_g0174T0	GH55.hmm	2.60E-300	10	739	0.985135135
jgi|Erynec1|1749|EV44_g0082T0	AA7.hmm	1.20E-67	5	195	0.414847162
jgi|Erynec1|1794|EV44_g4782T0	GT39.hmm	3.10E-71	2	223	0.99103139
jgi|Erynec1|1883|EV44_g3609T0	CE6.hmm	0.00092	51	92	0.414141414
jgi|Erynec1|1902|EV44_g3001T0	GT2.hmm	2.70E-08	2	166	0.976190476
jgi|Erynec1|2080|EV44_g0331T0	CE10.hmm	5.40E-23	73	193	0.351906158
jgi|Erynec1|2081|EV44_g0443T0	GH17.hmm	4.60E-12	18	300	0.906752412
jgi|Erynec1|2107|EV44_g0394T0	GT59.hmm	2.50E-123	2	404	0.995049505
jgi|Erynec1|2221|EV44_g6279T0	CE10.hmm	3.90E-43	94	334	0.703812317
jgi|Erynec1|2279|EV44_g4379T0	GT21.hmm	1.50E-82	1	233	0.995708155
jgi|Erynec1|227|EV44_g0133T0	CBM18.hmm	3.60E-06	5	36	0.815789474
jgi|Erynec1|227|EV44_g0133T0	CE4.hmm	1.60E-29	7	125	0.907692308
jgi|Erynec1|2359|EV44_g1084T0	CE1.hmm	5.60E-10	24	207	0.806167401
jgi|Erynec1|2443|EV44_g3019T0	GH18.hmm	2.10E-16	56	241	0.625
jgi|Erynec1|2482|EV44_g5210T0	GT58.hmm	1.30E-139	2	364	0.994505495
jgi|Erynec1|2562|EV44_g0234T0	GH132.hmm	4.90E-93	16	302	0.943894389
jgi|Erynec1|2726|EV44_g6318T0	AA7.hmm	1.30E-27	10	202	0.419213974
jgi|Erynec1|2761|EV44_g5255T0	CBM48.hmm	0.00025	16	69	0.697368421
jgi|Erynec1|2807|EV44_g0218T0	GH76.hmm	3.80E-97	11	347	0.938547486
jgi|Erynec1|2811|EV44_g0588T0	GT32.hmm	1.90E-10	49	87	0.422222222
jgi|Erynec1|2834|EV44_g0453T0	GT20.hmm	1.00E-154	33	474	0.928421053
jgi|Erynec1|2863|EV44_g0044T0	CBM18.hmm	0.00064	7	35	0.736842105
jgi|Erynec1|2863|EV44_g0044T0	GH16.hmm	3.40E-23	12	185	0.915343915
jgi|Erynec1|2884|EV44_g0237T0	GH18.hmm	1.50E-43	3	164	0.543918919
jgi|Erynec1|2900|EV44_g2849T0	GT22.hmm	6.90E-98	3	388	0.989717224

Query	Subject	E-value	Start	End	Covered Fraction
jgi|Erynec1|2954|EV44_g0045T0	GT8.hmm	4.20E-48	23	255	0.902723735
jgi|Erynec1|295|EV44_g0185T0	GH5_9.hmm	2.70E-117	2	306	0.993464052
jgi|Erynec1|3035|EV44_g0536T0	GH76.hmm	3.50E-109	10	347	0.941340782
jgi|Erynec1|3077|EV44_g2493T0	CE10.hmm	4.30E-25	61	200	0.407624633
jgi|Erynec1|3106|EV44_g4550T0	GT90.hmm	1.60E-83	3	248	0.98
jgi|Erynec1|3151|EV44_g5322T0	GT35.hmm	1.60E-277	3	674	0.995548961
jgi|Erynec1|3159|EV44_g0215T0	CE5.hmm	6.50E-40	1	187	0.984126984
jgi|Erynec1|321|EV44_g0150T0	GH92.hmm	3.00E-155	4	490	0.989816701
jgi|Erynec1|3258|EV44_g0153T0	GH5_9.hmm	1.10E-119	2	305	0.990196078
jgi|Erynec1|3266|EV44_g4732T0	GT57.hmm	4.40E-86	3	229	0.46985447
jgi|Erynec1|3266|EV44_g4732T0	GT57.hmm	1.40E-53	222	480	0.536382536
jgi|Erynec1|3373|EV44_g0566T0	GH18.hmm	5.80E-18	29	203	0.587837838
jgi|Erynec1|3392|EV44_g4896T0	GT15.hmm	9.20E-126	1	272	0.992673993
jgi|Erynec1|3404|EV44_g0309T0	CE1.hmm	1.50E-18	6	140	0.59030837
jgi|Erynec1|3422|EV44_g0003T0	GH81.hmm	5.00E-221	10	622	0.98392283
jgi|Erynec1|3471|EV44_g0312T0	GT24.hmm	1.80E-130	1	248	0.995967742
jgi|Erynec1|3480|EV44_g0165T0	GH72.hmm	3.40E-115	4	310	0.980769231
jgi|Erynec1|3574|EV44_g0157T0	GH72.hmm	8.60E-128	3	311	0.987179487
jgi|Erynec1|3598|EV44_g5096T0	GT34.hmm	1.90E-86	3	245	0.983739837
jgi|Erynec1|3600|EV44_g0554T0	GH16.hmm	3.50E-22	24	188	0.867724868
jgi|Erynec1|3670|EV44_g6148T0	GH47.hmm	1.60E-140	1	444	0.993273543
jgi|Erynec1|3683|EV44_g2595T0	CE10.hmm	9.10E-16	58	313	0.747800587
jgi|Erynec1|3738|EV44_g0418T0	GH76.hmm	6.90E-113	7	345	0.944134078
jgi|Erynec1|3742|EV44_g5601T0	GT4.hmm	3.90E-17	8	105	0.60625
jgi|Erynec1|3796|EV44_g1235T0	GH16.hmm	1.90E-32	18	176	0.835978836
jgi|Erynec1|3804|EV44_g2170T0	GT69.hmm	8.20E-68	1	238	0.991631799
jgi|Erynec1|3846|EV44_g0581T0	AA1_3.hmm	7.30E-129	2	303	0.96474359
jgi|Erynec1|3958|EV44_g0260T0	GH18.hmm	7.40E-11	193	283	0.304054054
jgi|Erynec1|3999|EV44_g6244T0	GT1.hmm	1.90E-51	6	379	0.976439791
jgi|Erynec1|39|EV44_g5603T0	GT2.hmm	7.30E-06	2	166	0.976190476
jgi|Erynec1|4035|EV44_g4409T0	GT2.hmm	1.30E-15	79	164	0.505952381
jgi|Erynec1|4037|EV44_g5385T0	CE1.hmm	2.10E-13	9	143	0.59030837
jgi|Erynec1|4050|EV44_g0404T0	GH16.hmm	4.20E-21	39	188	0.788359788
jgi|Erynec1|4097|EV44_g0073T0	GH47.hmm	1.50E-164	2	446	0.995515695
jgi|Erynec1|4108|EV44_g0179T0	AA9.hmm	5.20E-53	3	218	0.977272727
jgi|Erynec1|4210|EV44_g0008T0	GH132.hmm	6.90E-88	33	299	0.877887789
jgi|Erynec1|421|EV44_g0875T0	GH20.hmm	2.80E-83	7	336	0.976261128
jgi|Erynec1|4232|EV44_g0477T0	GT2.hmm	4.00E-39	1	109	0.642857143
jgi|Erynec1|4314|EV44_g0980T0	GT76.hmm	5.80E-102	4	407	0.99017199
jgi|Erynec1|4328|EV44_g1323T0	GH13_25.hmm	1.70E-212	2	448	0.995535714
jgi|Erynec1|4331|EV44_g0411T0	GH78.hmm	6.80E-86	8	502	0.98015873
jgi|Erynec1|4352|EV44_g0353T0	CE10.hmm	2.80E-28	68	193	0.366568915
jgi|Erynec1|4366|EV44_g0412T0	GH16.hmm	1.80E-22	5	188	0.968253968
jgi|Erynec1|4410|EV44_g0102T0	GH76.hmm	3.60E-53	71	329	0.720670391
jgi|Erynec1|4434|EV44_g1472T0	GT31.hmm	3.00E-07	75	185	0.572916667
jgi|Erynec1|4555|EV44_g6510T0	GH5_9.hmm	6.40E-101	2	305	0.990196078
jgi|Erynec1|4592|EV44_g2959T0	GH37.hmm	6.10E-150	5	489	0.985743381
jgi|Erynec1|4610|EV44_g5226T0	GH38.hmm	7.40E-84	2	255	0.940520446
jgi|Erynec1|4637|EV44_g6498T0	GH125.hmm	1.60E-162	1	402	0.997512438
jgi|Erynec1|465|EV44_g2210T0	AA2.hmm	8.80E-16	10	114	0.407843137
jgi|Erynec1|465|EV44_g2210T0	AA2.hmm	2.20E-13	28	253	0.882352941
jgi|Erynec1|4742|EV44_g5285T0	GT32.hmm	7.80E-08	3	78	0.833333333
jgi|Erynec1|4777|EV44_g3149T0	GT4.hmm	4.10E-13	8	147	0.86875
jgi|Erynec1|4851|EV44_g0456T0	GH16.hmm	1.10E-23	24	188	0.867724868
jgi|Erynec1|4886|EV44_g0510T0	GT90.hmm	4.50E-70	15	248	0.932

Query	Subject	E-value	Start	End	Covered Fraction
jgi|Erynec1|4887|EV44_g0350T0	CE5.hmm	1.30E-39	1	189	0.994708995
jgi|Erynec1|4906|EV44_g6100T0	GT8.hmm	1.20E-31	122	256	0.521400778
jgi|Erynec1|4933|EV44_g4375T0	GH3.hmm	1.00E-61	7	216	0.967592593
jgi|Erynec1|4934|EV44_g3318T0	GT2.hmm	1.20E-07	79	168	0.529761905
jgi|Erynec1|4936|EV44_g1295T0	GH16.hmm	3.00E-41	4	189	0.978835979
jgi|Erynec1|5063|EV44_g0039T0	GH47.hmm	4.40E-133	1	446	0.997757848
jgi|Erynec1|5085|EV44_g1514T0	GH18.hmm	5.20E-67	5	290	0.962837838
jgi|Erynec1|5115|EV44_g6515T0	AA3.hmm	6.20E-87	85	416	0.535598706
jgi|Erynec1|512|EV44_g0601T0	GH18.hmm	1.30E-52	4	282	0.939189189
jgi|Erynec1|5183|EV44_g0307T0	GH17.hmm	1.30E-39	2	310	0.990353698
jgi|Erynec1|5187|EV44_g4424T0	GT2.hmm	4.20E-15	79	163	0.5
jgi|Erynec1|5188|EV44_g2609T0	GT2.hmm	1.40E-13	79	167	0.523809524
jgi|Erynec1|5189|EV44_g0509T0	GT32.hmm	1.50E-22	3	87	0.933333333
jgi|Erynec1|5244|EV44_g0161T0	GT15.hmm	1.30E-124	1	272	0.992673993
jgi|Erynec1|5298|EV44_g6129T0	CBM21.hmm	1.30E-32	3	106	0.962616822
jgi|Erynec1|5404|EV44_g0730T0	GH47.hmm	9.20E-165	2	446	0.995515695
jgi|Erynec1|5440|EV44_g0083T0	GH15.hmm	6.40E-77	17	360	0.950138504
jgi|Erynec1|5440|EV44_g0083T0	CBM20.hmm	5.50E-20	3	89	0.955555556
jgi|Erynec1|5444|EV44_g2812T0	GH18.hmm	8.90E-82	2	286	0.959459459
jgi|Erynec1|5459|EV44_g5583T0	AA7.hmm	1.60E-11	58	208	0.327510917
jgi|Erynec1|5490|EV44_g0788T0	GT32.hmm	1.40E-19	4	88	0.933333333
jgi|Erynec1|5532|EV44_g5780T0	CBM18.hmm	1.10E-06	1	38	0.973684211
jgi|Erynec1|5532|EV44_g5780T0	AA5_1.hmm	3.50E-168	7	536	0.939609236
jgi|Erynec1|5568|EV44_g1625T0	AA2.hmm	9.40E-64	6	254	0.97254902
jgi|Erynec1|5616|EV44_g0442T0	GT90.hmm	4.90E-72	3	248	0.98
jgi|Erynec1|5645|EV44_g0116T0	GH72.hmm	2.10E-135	3	311	0.987179487
jgi|Erynec1|5645|EV44_g0116T0	CBM43.hmm	3.30E-16	1	83	0.987951807
jgi|Erynec1|5646|EV44_g4995T0	GT48.hmm	0	1	733	0.99052774
jgi|Erynec1|5671|EV44_g0363T0	CE10.hmm	8.40E-41	83	334	0.736070381
jgi|Erynec1|5713|EV44_g0449T0	GH76.hmm	1.20E-113	11	348	0.941340782
jgi|Erynec1|5722|EV44_g0019T0	GH76.hmm	3.50E-77	10	340	0.921787709
jgi|Erynec1|5729|EV44_g5784T0	GH13_40.hmm	3.50E-175	2	359	0.991666667
jgi|Erynec1|5776|EV44_g0089T0	GH17.hmm	9.20E-13	85	309	0.720257235
jgi|Erynec1|5781|EV44_g0034T0	GH74.hmm	4.30E-06	41	111	0.300429185
jgi|Erynec1|5781|EV44_g0034T0	GH74.hmm	0.00018	37	111	0.317596567
jgi|Erynec1|5839|EV44_g1121T0	GT57.hmm	2.90E-171	2	479	0.991683992
jgi|Erynec1|5851|EV44_g0515T0	CE5.hmm	2.90E-35	1	187	0.984126984
jgi|Erynec1|5853|EV44_g0156T0	GH16.hmm	1.70E-15	20	176	0.825396825
jgi|Erynec1|5942|EV44_g0096T0	GH128.hmm	3.10E-69	4	223	0.977678571
jgi|Erynec1|6020|EV44_g1993T0	GT20.hmm	7.90E-148	10	473	0.974736842
jgi|Erynec1|6064|EV44_g0542T0	CE5.hmm	3.60E-41	1	189	0.994708995
jgi|Erynec1|6079|EV44_g0111T0	CE10.hmm	4.00E-45	93	292	0.583577713
jgi|Erynec1|6091|EV44_g0016T0	GH63.hmm	2.40E-29	319	565	0.431578947
jgi|Erynec1|6103|EV44_g0372T0	GH76.hmm	1.20E-92	19	341	0.899441341
jgi|Erynec1|6139|EV44_g2641T0	GH31.hmm	3.90E-155	2	427	0.995316159
jgi|Erynec1|616|EV44_g5728T0	GH17.hmm	3.30E-35	10	306	0.951768489
jgi|Erynec1|6227|EV44_g1802T0	CE10.hmm	5.40E-42	76	334	0.75659824
jgi|Erynec1|622|EV44_g5173T0	CE10.hmm	1.90E-44	93	333	0.703812317
jgi|Erynec1|6298|EV44_g5073T0	GT34.hmm	5.50E-71	2	244	0.983739837
jgi|Erynec1|6353|EV44_g2816T0	CE10.hmm	9.80E-29	73	204	0.384164223
jgi|Erynec1|6418|EV44_g0229T0	CE10.hmm	3.00E-23	74	212	0.404692082
jgi|Erynec1|6461|EV44_g0012T0	GT32.hmm	5.70E-20	6	89	0.922222222
jgi|Erynec1|6484|EV44_g5913T0	GT26.hmm	0.00081	24	91	0.391812865
jgi|Erynec1|663|EV44_g1238T0	GH114.hmm	1.30E-71	1	190	0.994736842
jgi|Erynec1|715|EV44_g0319T0	GH65.hmm	1.80E-62	3	371	0.989247312

Query	Subject	E-value	Start	End	Covered Fraction
jgi|Erynec1|715|EV44_g0319T0	CBM32.hmm	8.00E-07	13	122	0.879032258
jgi|Erynec1|723|EV44_g2744T0	GT66.hmm	5.40E-192	9	596	0.847041847
jgi|Erynec1|744|EV44_g0976T0	GT4.hmm	2.90E-34	11	149	0.8625
jgi|Erynec1|745|EV44_g0333T0	CE10.hmm	1.20E-37	48	187	0.407624633
jgi|Erynec1|754|EV44_g2189T0	GH16.hmm	5.70E-17	4	189	0.978835979
jgi|Erynec1|838|EV44_g2925T0	GT2.hmm	5.20E-42	1	168	0.994047619
jgi|Erynec1|843|EV44_g0384T0	GT31.hmm	3.30E-06	75	162	0.453125
jgi|Erynec1|867|EV44_g4711T0	CBM48.hmm	1.40E-08	3	45	0.552631579
jgi|Erynec1|867|EV44_g4711T0	GH13_8.hmm	1.20E-139	1	274	0.996350365
jgi|Erynec1|925|EV44_g0516T0	AA1_2.hmm	1.80E-156	3	338	0.985294118
jgi|Erynec1|92|EV44_g1109T0	GT20.hmm	8.60E-202	7	475	0.985263158
jgi|Erynec1|939|EV44_g2782T0	CE4.hmm	1.80E-16	7	118	0.853846154
jgi|Erynec1|94|EV44_g0095T0	GT33.hmm	7.80E-146	3	424	0.990588235
jgi|Erynec1|957|EV44_g3028T0	GT28.hmm	4.10E-14	28	123	0.605095541
jgi|Erynec1|95|EV44_g2252T0	GT22.hmm	3.20E-94	2	389	0.994858612
jgi|Erynec1|969|EV44_g0568T0	GT2.hmm	9.20E-08	2	167	0.982142857
jgi|Erynec1|985|EV44_g3003T0	GH16.hmm	1.60E-21	52	176	0.656084656
jgi|Erynec1|993|EV44_g0005T0	GT22.hmm	1.20E-80	4	360	0.915167095